About project A1

3.1.1 Title: Exploring HIOS structure formation by molecular simulations

3.1.2 Principal investigator

Prof. Dr. Joachim Dzubiella (*17.05.1975, German)

Helmholtz-Zentrum Berlin für Materialien und Energie (HZB)
Hahn-Meitner-Platz 1
14109 Berlin, and
Institut für Physik
Humboldt-Universität zu Berlin (HUB)
Newtonstr. 15
12489 Berlin
Phone:+49(030) 8062-42902
E-Mail: joachim.dzubiella@helmholtz-berlin.de

3.2 Project history

3.2.1 Report

3.2.1.1 State-of-the-art and objectives of the proposal

The optical and electronic properties of hybrid inorganic-organic systems (HIOS) are highly sensitive to morphological changes of conjugated organic molecules (COMs) on the inorganic semiconductor surface, for instance, by modifications of the molecular orientation or packing structure of the COMs induced by a different surface termination [1-3]. The theoretical understanding of the self-assembly, nucleation, and growth processes of COMs in HIOS is thus of fundamental importance to eventually control and design HIOS to obtain the desired functional properties. The detailed *molecular-level* structure of those materials is usually difficult to probe experimentally due to a limited length and time resolution. The aim of this project was to employ *classical* all-atom molecular dynamics (MD) computer simulations of COMs on inorganic semiconductor surfaces in order to interpret and guide experimental results by giving fundamental insight into the atomic and molecular scale structures and kinetics (0.1-10 nm; 0.001-100 ns) in HIOS. In particular, it was to address the structural and kinetic behavior of a single up to a few hundreds of COMs on atomistically-resolved ZnO surfaces with varying surface termination. In the computer simulations, individual molecular parts of the COMs and surfaces can be easily modified to investigate the influence of local polarity, atomic defects, dipolar groups, as well as (sub)nanometer-sized steps and barriers on the diffusion, nucleation, and aggregation behavior of COMs. Furthermore, within the hierarchical-scale modeling framework proposed in this CRC, this project was supposed to provide equilibrium unit cell structures and coarse-grained interactions as input for electronic and larger-scale structure calculations in other CRC projects, respectively.

There are already a few examples in literature on very insightful MD simulations of COMs in bulk and at interfaces. For instance, the diffusion of pentacene on fixed crystalline pentacene layers was studied, where interesting anisotropic diffusion patterns were identified [4]. MD simulations were used to explore in detail the energetic deposition of an incident pentacene molecule colliding with the pentacene (010) step edge displaying sensitive dependence on molecular orientation [5]. The dynamics of the adsorption of pentacene molecules on SiO_2 and crystalline pentacene layers was investigated where a significant contribution to film growth kinetics was attributed to molecular insertion events into the topmost layer of the pentacene thin film [6]. Similar simulations of a pentacene monolayer on amorphous silica revealed metastable structures consistent with experiments [7]. A detailed examination of Ehrlich-Schwöbel energy barriers for a single diindenoperylene (DIP) or p-sexiphenyl (*p*-6P) descending a step edge was performed using MD simulations of various force fields [8]. Finally, in organic self-assembled monolayers (SAMs) using oligothiophenes (1P)

on gold [9] the COMs were found to be predominantly arranged in the familiar herringbone structure. Different deposition and substrate-molecule binding conditions captured regimes of experimentally observed growth morphology. Prediction of possible structural changes were made by modifying the molecular backbone of the COM in the MD simulation [9]. Other groups focused on the calculation of the bulk structures of COMs by MD simulations, such as the columnar (liquid crystal) phases of densely packed coronene derivatives [10] or their transition between herringbone and hexagonal mesophases [11] using AMBER and GROMACS force fields [12,13]. Those simulations confirmed experimental candidates of helical microphases of coronene derivatives deduced from X-ray scattering [14].

To the best of our knowledge, however, previous work did not attempt to simulate COMs *self-nucleating and self-assembling* on atomistically-resolved ZnO surfaces as was proposed in this project. Only two contributions pushed forward by Zannoni and co-workers [15,16] indicated that this seems possibly feasible, at least for pentacene and sexithiophene molecules on other surfaces or in bulk: Muccioli *et al.* [15] demonstrated that in progressive pentacene deposition on a C60 crystal the molecules *self-assembled* into crystal nuclei resembling the bulk crystal structure but with deviations that might have originated from surface distortions or force field imbalances. Pizzirusso *et al.* [16] showed for the first time by temperature jumps from an already ordered high temperature (liquid crystal) phase of sexithiophene that the latter spontaneously rearranged into an ordered solid crystal-like structure at room temperature, consistent with experimental densities and global orientations. Regarding COMs on ZnO, we are only aware of the pioneering study of the group of Mattoni *et al.*, who has analyzed the anisotropic diffusion of Zinc-Phthalocyanine (ZnPc) molecules on the (10-10) surface by a combination of force-field simulations and transition state theory [17]. In particular, it was shown that ZnPc on ZnO tends to diffuse and aggregate perpendicular to the polar [0001] direction. It was also demonstrated that the thiophene-based polymers tend to align along the same direction [18,19].

Hence, the major objective was to theoretically understand HIOS assembly bottom-up from ‘simple’ to very complex systems, that is, starting from the adsorption of a single COM onto inorganic semiconductor surfaces up to the self-assembly of a few hundreds of COMs. In particular, the molecular shape, structural, and kinetic behavior on atomistically-resolved ZnO surfaces with varying termination, and possible defects and step edges, was aimed to be explored. In HIOS, where the inorganic substrate surfaces are typically polar, theoretical challenges appear due to highly anisotropic electrostatic interactions. The thereby formed energy landscape defines an underlying template for the COMs to attach in a predefined fashion and nucleate. Therefore, it enables a controlled engineering of both inorganic surfaces and organic molecules with adapted polarity towards property optimization. However, growth of thin films from COMs deposited from the gas phase is an intrinsically nonequilibrium phenomenon governed by a subtle competition between kinetics and thermodynamics [23]. Precise control of the nucleation and growth and thus of the properties of hybrid interfaces becomes possible only after an understanding of the first kinetic steps is achieved. Given such a complex surface energy landscape, a natural question is, how does it influence the time scale of diffusion and with thus possibly the nucleation rates of the COMs? Can it impose anisotropic kinetic barriers which lead to anisotropic transport and nucleation features far from equilibrium? How is the diffusion of a single COM, which precedes nucleation, exactly connected to the energy landscape? These were questions also to be addressed in the beginning of this project A1. However, a necessary prerequisite for growth at interfaces for a certain COM is the simulation ability to reproduce the bulk crystal structure for the COMs and to identify the appropriate classical Hamiltonian for it. Hence, the very beginning of the project needed to focus on the modeling of the organic side of HIOS. We proposed to simulate those COMs which are relevant for this CRC but at the same time can be used for benchmarking and model validation, and for which some polymorphs are already known from experiments [20-22], such as coronene, diindenoperylene (DIP), or oligophenylenes.

Among these fundamental questions, another major objective was to interpret and guide the experiments in this CRC using the molecular insight from the MD simulations. Single molecule configurations were supposed to be compared to scanning tunneling microscopy (STM) to identify orientational order on the ZnO surface [Grill (A2)]. Structures of crystal nuclei and crystallites themselves obtained by MD simulations should provide candidates to be tested against experiments [A5 (Henneberger), A8 (Koch, B3 (Blumstengel), B9 (Stähler/Wolf)], in particular to interpret lattice constants, tilt angles, and molecular orientations in unit cells obtained from X-ray diffraction in A9 (Kowarik). A systematic parameter change (e.g., temperature, coverage, type of COM, force field) in the MD simulations was proposed to finally guide the structural exploration in these experiments and the molecular design of interesting COM architectures [A3 (Hecht)], and give a fundamental understanding of the dominant interactions governing HIOS self-assembly.

Finally, within the hierarchical-scale modeling framework in this CRC, equilibrated unit cell structures and coarse-grained interactions were to be provided for electronic [A4 (Heimel), B4 (Knorr/Scheffler/Rinke), B7 (May)] and large-scale structure calculations [A7 (Klapp) to confine parameter space, respectively. Vice versa, our project benefits from electronic calculations for force-field refinement [A4 (Heimel), B4

(Knorr/Scheffler/Rinke)] of COM-COM and COM-ZnO interactions and from large-scale simulations [A7 (Klapp)] to obtain equilibrium polymorph candidates.

3.2.1.2 Results and applied or newly developed methods

As motivated above, a necessary prerequisite for the study of the nucleation and growth of COMs in HIOS by MD simulations is the identification of a reasonable classical force-field for a particular COM, accurate enough to reproduce experimental bulk crystal structures and, if possible, the whole temperature-dependent phase behavior. This is a challenging task due to the multiple intra-atomic degrees of freedom and strongly attractive dispersion and electrostatic interactions (compared to the thermal energy k_BT). In particular, it would be desirable to have a system of COMs that self-assembles into the right crystal structure 'from scratch', that is, without any pre-assumptions on the lattice structural candidates or other crystal parameters. Then in the next stages of this project, this could be used as a 'working model' for the self-assembly in the presence of an inorganic 'external field'. In our first achievement in this CRC [24], we presented MD simulations of molecular crystals of the COM para-sexiphenyl (*p*-6P), which constitutes a popular basic and prototypical molecule for optoelectronic applications. After validating single-molecule properties with *ab-initio* calculations (such as molecular lengths and minimum energy twist angles), we demonstrated that gradually performed simulated temperature annealing led to the spontaneous self-assembly of p-6P molecules from the fully isotropic state into the correct room-temperature solid crystal. The latter has only a few percent deviation from the experimental unit-cell structure. A detailed investigation of the single crystal in anisotropic Gibbs ensemble simulations then yielded experimentally consistent structures and solid to liquid-crystal phase behavior over a wide temperature range, providing molecular insight into nanometer-scale structural and dynamic properties of self-assembled p-6P crystals. This study thus introduced a working model for p-6p and thus paved the way for future investigations of the computational description of nucleation and growth mechanisms of novel *p*-polyphenylene derivatives in the bulk as well as at functional interfaces or heterojunctions. Simulations snapshots of the crystals for various temperatures are shown in Figure 1. The calculated unit cell lengths and angles are compared to experimental values in the Table of the bottom of the figure and show overall very satisfactory agreement, if compared to other predictive methods (a discussion with references can be found in [24]).

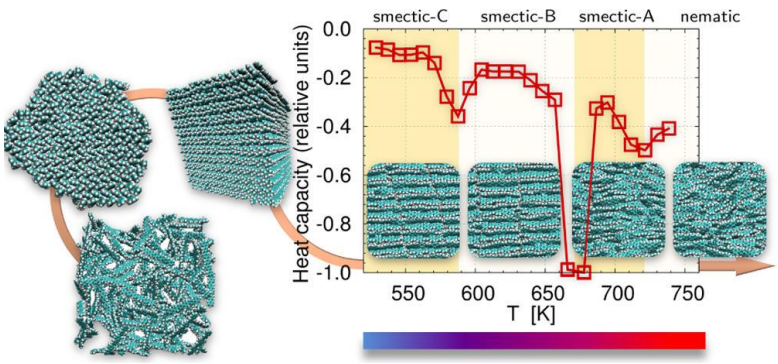

Figure 1: Illustration of p-6p self-assembling to a realistic bulk structure from the high-temperature isotropic phase (bottom left) to a room-temperature herringbone crystal 'droplet' (left) [24]. The unit cell periodically repeated and heated results in the exploration of the full phase diagram with transitions signified by a heat capacity drop (right plot). Bottom: Table (copied&pasted from [24]) comparing calculated and experimental unit cell parameters.

Table 2. Crystallographic Data of *P*-6p Calculated in the Room-Temperature Herringbone Phase from *Npt* Equilibration Simulations at T = 300 K. The Error Of These Values From Block Averaging Is Less Than 1%. The Middle Row Denotes The Standard Deviation of These Values Due to Thermal Fluctuations. The Bottom Row Shows the Experimental Results for the B-Phase.[4]

	a [nm]	b [nm]	c [nm]	α [deg]	β [deg]	γ [deg]	Φ [deg]	θ_H [deg]	ρ [g/cm^3]	φ_{C-C} [deg]
simulation	0.827	0.548	2.668	90.1	101.4	89.8	17.7	61.7	1.295	15.7
standard deviation	0.016	0.013	0.03	5.5	6.0	3.3	6.0	13.7	0.02	7.9
experiment	0.809	0.557	2.624	90	98.2	90	18	66	1.3	20

In our second achievement [25], we have studied the long-time self-diffusion of a single conjugated organic para-sexiphenyl (p-6P) molecule physisorbed on the inorganic ZnO (10-10) surface by means of all-atom MD computer simulations. We used a stochastic integration Langevin-based scheme, where an auxiliary bath friction allows fast dissipation of energy and thus a well-defined canonical equilibrium in these single-molecule simulations. The bath friction can be subtracted from the total friction and the long-time self-diffusion for a COM on ZnO determined the first time. We find strongly anisotropic diffusion processes in

which the diffusive motion along the polar [0001] direction of the surface is many orders of magnitudes slower at relevant experimental temperatures than in the perpendicular direction. The observation can be rationalized by the underlying charge pattern of the electrostatically heterogeneous surface which imposes direction-dependent energy barriers to the motion of the molecule. Furthermore, the diffusive behavior is found to be normal and Arrhenius-like, governed by thermally activated energy barrier crossings. The detailed analysis of the underlying potential energy landscape shows, however, that in general the activation barriers cannot be estimated from idealized zero-temperature trajectories but must include the conformational and positional excursion of the molecule along its pathway. Furthermore, the corresponding (Helmholtz) free energy barriers are significantly smaller than the pure energetic barriers with implications on absolute rate prediction at experimentally relevant temperatures. Our findings suggest that adequately engineered substrate charge patterns could be possibly harvested to select desired growth modes of hybrid interfaces for optoelectronic device engineering. We note that the calculated diffusion constants, which range over many orders of magnitude in a relevant temperature regime, cf. Figure 2, have a large error (up to plus/minus 1000%). The reason is that transport coefficients depend exponentially on energy barriers. As we show, the latter sensitively depend on model details (such as surface vibrations or accuracy of electrostatics in periodic boundary conditions) which challenges currently employed theoretical techniques.

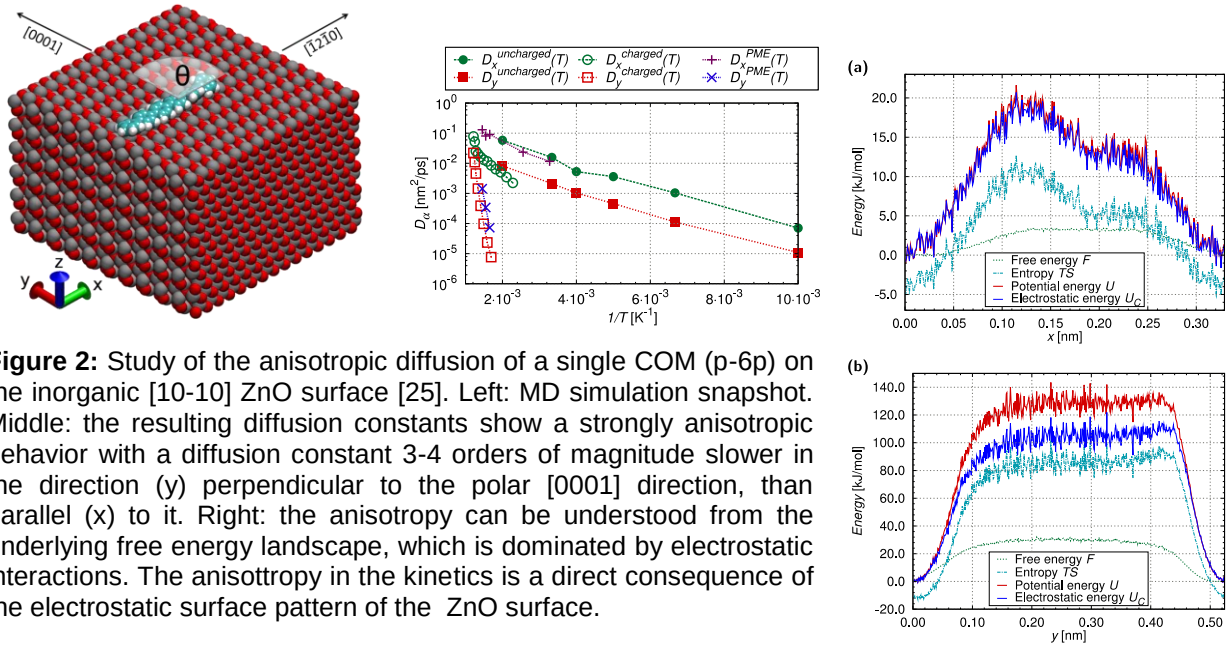

Figure 2: Study of the anisotropic diffusion of a single COM (p-6p) on the inorganic [10-10] ZnO surface [25]. Left: MD simulation snapshot. Middle: the resulting diffusion constants show a strongly anisotropic behavior with a diffusion constant 3-4 orders of magnitude slower in the direction (y) perpendicular to the polar [0001] direction, than parallel (x) to it. Right: the anisotropy can be understood from the underlying free energy landscape, which is dominated by electrostatic interactions. The anisottropy in the kinetics is a direct consequence of the electrostatic surface pattern of the ZnO surface.

Given the highly anisotropic diffusion and directed motion of the COMs on the ZnO surface, the next urgent question concerns the crossing of a COM over a step-edge, cf. Figure 3. If the step-edge is perpendicular to the 'quick' direction of the COM, the crossing is the rate-limiting step in molecule surface transport. However, the physical mechanisms behind the crossing process, such as details of the free energy landscape, the path of crossing, the detailed influence of the electrostatic pattern, or the appropriate reaction-coordinates for a theoretical description are not well understood. In Figure 3, we present preliminary results from simulations of *p*-6P crossing a one-atom-high step edge on ZnO. In this simulation, we switched-off the electrostatic charges to first probe the intrinsic (steric) effects of the atomic step. Already here, a free energy barrier with fine structure can be observed. Details, such as the investigation of the distribution of crossing paths is currently underway. With electrostatic surface-COM interactions switched on, we expect very different behavior with much larger barriers and altered crossing pathways. The investigations is currently performed, and we are confident that the results will be submitted for publication within the first funding period.

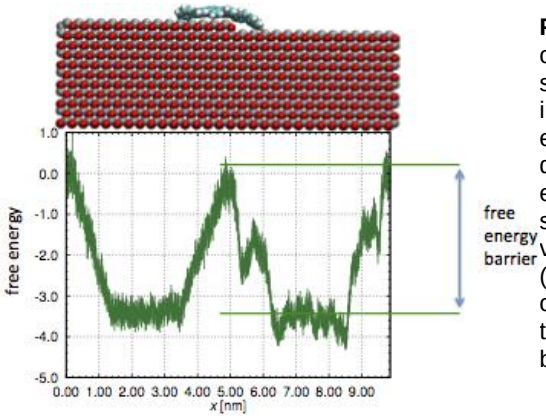

Figure 3: The COM p-6p is crossing a one-atomic step-edge on the [10-10] ZnO surface. Top: simulations snapshot caught in the act of crossing. Bottom: The free energy profile of the COM along the direction perpendicular to the edge. A free energie barrier with a main peak and a side peak to cross the edge is clearly visible. In these simulations, the static (partial) charges of the ZnO are switched-off. Inclusion of electrostatics is expected to have substantial effects on the (kinetic) barrier.

Finally, together with project A7 (Klapp), we have developed coarse-graining methods in order to introduce properly defined effective potentials between particles, where the intramolecular degrees of freedom are integrated out [26]. We have performed this on the highly symmetric COM coronene in an electrostatically neutral (all partial charges switched off) toy version, in order to keep the already challenging problem as simple as possible. The focus was thus on the understanding, how, in particular, the angularly-resolved potentials can be best mapped on coarse-grained effective analytical potentials for the use in mesoscopic simulations.

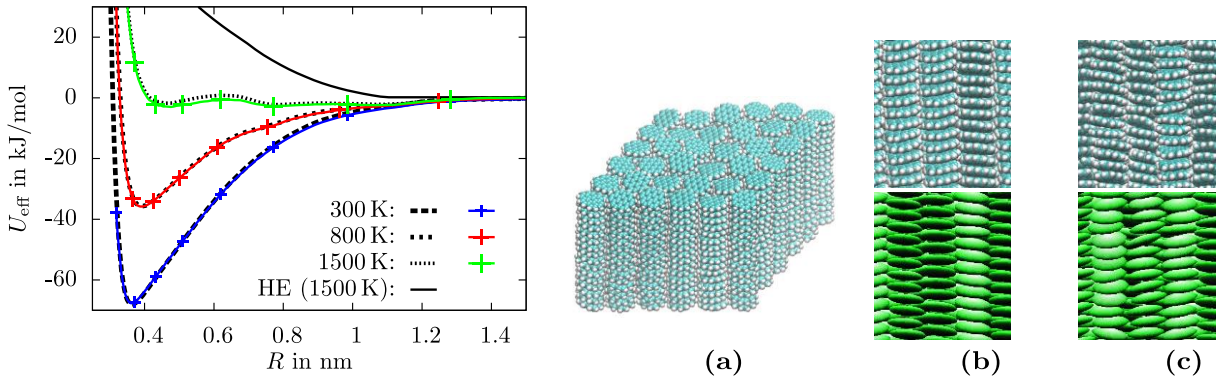

Figure 4: Coarse-graining of the COM coronene [26]. Left: from steered (solid lines) and umbrella (dashed lines) MD simulations, we calculate the angle-averaged potential for various temperatures. For comparison the angle-averaged hard ellipsoidal (HE) potential for 1500 K is added (solid line). This potentials are fit to a Gay-Berne parametrization for smooth, structureless disks, with which an efficient simulation of crystal structural growth is warranted. Right: Simulations snapshots comparing crystal structures from all-atom simulations (green atomically resolved molecules) and coarse-grained (CG) simulations (light green discs). a) Initial hexagonal columnar nematic state of the present system. (b) and (c): Snapshots of the hexagonal nematic regime after 3 ns at b) 300 K and (c) 700 K within the atomic model and the CG model.

In [26], we have presented such an approach for calculating coarse-grained angle-resolved effective pair potentials for uniaxial molecules. For integrating out the intramolecular degrees of freedom we apply umbrella sampling and steered dynamics techniques in atomistically-resolved molecular dynamics (MD) computer simulations. Throughout this study we focus on coronene molecules, which can be regarded as disk-shaped uniaxial particles. To develop the methods we neglect any electrostatic charge contributions. The resulting coarse-grained pair potential reveals a strong temperature and angle dependence. In the next step we fit the numerical data with various Gay-Berne-like potentials to be used in more efficient simulations on larger scales. The quality of the resulting coarse-grained results is evaluated by comparing their pair and many-body structure as well as some thermodynamic quantities self-consistently to the outcome of atomistic MD simulations of many particle systems. We find that angle-resolved potentials are essential not only to accurately describe crystal structures but also for fluid systems where simple isotropic potentials start to fail already for low to moderate packing fractions. A further outcome is that the molecular flexibility can significantly influence the effective pair potential.

3.2.1.3 Problems and difficulties (and future challenges)

A few unforeseen problems and difficulties arose during the execution of this project which slowed down the publications in this project. For this reason, only two COMs, *p*-6p and coronene were studied so far in this project as opposed to the larger number of suggestions for COMs in the original proposal. Actually, every individual COM has specific interaction features which cannot be generalized and have to be analyzed individually. Due to the time delay, we could also not yet start to investigate the self-assembly of many COMs on ZnO surfaces, as originally proposed.

First, the PI underestimated the sensitivity of the results to the underlying force-field, in particular to the classical partial point charges which are assigned to the individual COM atoms. The simulations are all performed in vacuo, where the dielectric screening of electrostatic is small or vanishing, and changes of charges of only a few percent of the elementary charge (*e*) can lead to large effects in the resulting crystal structures of COMs. Additionally, the PI was not entirely aware before, that the prediction of classical charges by of quantum-mechanical (QM) calculation is relatively inaccurate in that respect and only parameter windows of trust in the range of plus/minus 0.2 e could be delivered. In essence, this led to

empirical adjustments and checks of the force field performance along the way of the project which had time delays before the first publications as a consequence.

Secondly, and related to the first point, the PI underestimated the action of explicit polarizability and π-π interactions between the COMs which cannot be included easily in MD simulations. Fortunately, these effects are small in the prototypical p-6p COM and, as we showed, of negligible importance for crystal structure prediction. However, for the higher conjugated coronene, these effects are of importance and led to adjustments in the joint project with A7. Since this inclusion of electrostatics turned out very subtle, we decided to investigate the already challenging [25] coarse-graining only of an electrostatically neutral coronene molecule. The issue of explicit polarizability is also relevant for the ZnO-COM interaction. The polar surface can induce dipole moments in the physisorbed COM and alter the binding energy and conformations (see the literature in our work [26]). Here, stronger collaboration to projects on first-principle calculations and method improvement in the classical MD is required.

Finally, the PI underestimated the time scales in the MD simulations: the absolute strength of the COM-COM interaction potentials in the relevant temperature regime (between 0 and 1000 K) is large. Both van der Waals and electrostatic multipole attraction lead to potential energies on the order of about 10 k_BT (the thermal energy) and more. This implies that the time scales of inter-molecular arrangements are slow and comparable to the total typically accessible simulation time of hundreds of nanoseconds for systems of about a hundred of COMs. Hence, temperature annealing for crystal growth in bulk [24] has to be performed very slowly and thoroughly to avoid kinetic traps. For HIOS, where the bulk crystals grow in the additional 'external field' of the inorganic surface, preliminary simulations indicate that this problems is even worse due to different (metastable) crystal orientations and local deformations assumed on the surface and large energy barriers between them. In future, where we have learned from our findings in the first funding period, we will resort to optimized Replica-Exchange MD simulations (REMD) for HIOS with which a proper equilibrium sampling shall be achieved.

Under the bottom line, a classical description of HIOS nucleation and growth by our pioneering all-atom simulations faces a couple of theoretical modelling challenges which can only be tackled by further tightening the collaborations with QM and experimental partners, as fortunately provided directly within this CRC. With both bottom-up (QM→ MD) or top-down (experimental observations → MD) benchmarking, as we did in our work [24], the performance of MD force fields for COMs needs to be evaluated. A grand challenge would be to optimize MD simulations towards including explicit polarizability of COMs in HIOS, but at the same time to be efficient enough to sample long or good enough to obtain (ergodic) equilibrium statistics. This may be achievable by combining recent efforts in the development of polarizable force field and the REMD methods for efficient equilibrium sampling for the application in HIOS. A promising tool for this could be the TINKER software (http://dasher.wustl.edu/tinker/) and feeding the output into further developed coarse-grained methods, such as kinetic Monte-Carlo (kMC) (cf. project A7).

3.2.1.4 Cooperations to other projects within this CRC

We have had plenty of discussions with the members of project A4 (Heimel) on the QM calculations and refinement of partial charges and force field parameters. Additionally, A4 provided energy minimization calculations for single p-6P COMs to compare those minimized structures to validate our classical force field calculations. This resulted so far in one joint publication [24]. Future joint publications are very likely, in particular for the delivery and validation of force field parameters for 'mutated' phenylenes (where single molecular groups of a p-6p have been replaced by others) or atomic/electronic details of ZnO surface potentials.

A strong cooperation was established with project A7 (Klapp) on the coarse-graining of COMs for the efficient description of organic film growth. So far this resulted in one joint publication [26]. More joint publications are very likely due to tight relation of methods and aims of the projects A1 and A7. Because of this relation, these two projects are planned to be merged into one project (A7) in the second funding period (see the continuation proposal for project A7 in this CRC 951).

Furthermore, we have had many inspiring discussions with other scientists in this CRC such as Kowarik (A9), Koch (A8), Henneberger (A5), and Blumstengel (B3) on COM growth modes, Hecht (A3) on the possibility of COM synthesis and mutations, and Draxl (B11) on QM validation of force field refinement. We are confident that the ideas from these and further ongoing discussions will propagate into and deepen in the second funding period, where the COM growth in HIOS will be investigated more intensely in the merged project A7 (Klapp/Dzubiella).

3.2.1.5 Comparison to works outside this CRC

Our work [24] is the first work in the published literature that systematically demonstrated the self-assembly of COM crystals 'from scratch' in classical MD simulations. Only two contributions before that pushed forward by Zannoni and co-workers [15,16] indicated that this seems possibly feasible, at least for pentacene and sexithiophene molecules, as discussed in the state-of-the-art section above. The authors hypothesized that possibly a slower, that is, gradual cooling, as employed eventually by us, may likely lead to the correct room-temperature solid crystal, but whether that is really the case still awaits disclosure.
Our work [26] is the first study of the long-time self diffusion of single COMs in HIOS and its interpretation by free energy landscapes and electrostatic surface patterns. We are only aware of the study of the group of Mattoni *et al.* [17], as discussed in the state-of-the-art section above.
We are not aware on any classical MD or coarse-grained studies at relevant temperatures (300-800 K) on step-edge crossing or nucleation of COMs on ZnO surfaces.

References

[1] S. Blumstengel, S. Sadofev, and F. Henneberger, New J. Phys. **10,** 065010 (2008).
[2] N. Koch, J. Phys.: Condens. Matter **20**, 184008 (2008).
[3] T. Trevethan, A. Shluger, and L. J. Kantorovich, J. Phys.: Condens. Matter **22**, 084024 (2010).
[4] R. Cantrell and P. Clancy, Surface Science **602**, 3499 (2008).
[5] J. E. Goose and P. Clancy, J. Phys. Chem. C **111**, 15653 (2007).
[6] J. E. Goose, A. Killampalli, P. Clancy, and J. R. Engstrom, J. Phys. Chem. C **113**, 6068 (2009).
[7] R. G. Della Valle *et al*., ChemPhysChem **10**, 1783 (2009).
[8] J. E. Goose, E. L. First, and P. Clancy, Phys. Rev. B **81**, 205310 (2010).
[9] M. Haran, J. E. Goose, N. P. Clote, and P. Clancy, Langmuir **23**, 4897 (2007).
[10] D. Andrienko, V. Marcon, and K. Kremer, J. Chem. Phys. **125**, 124902 (2006).
[11] V. Marcon et al., J. Chem. Phys. **129**, 094505 (2008).
[12] D. A. Case *et al*., AMBER 9, University of California, San Francisco (2006); J. Computat. Chem. **26,** 1668-1688 (2005); Wang et al., J. Comp. Chem. 25, 1157 (2004).
[13] B. Hess, C. Kutzner, D. van der Spoel, D. E. and Lindahl, GROMACS 4, J. Chem. Theory Comput. **4**, 435-447 (2008).
[14] X. Feng *et al*., Nature Materials **8**, 421 (2009).
[15] A. Pizzirusso, M. Savini, L. Muccioli, and C. Zannoni, Mater. Chem. **21**, 125 (2011).
[16] L. Muccioli, and G. D'Avino, and C. Zannoni, Adv. Mater. **23**, 4532 (2011).
[17] C. Melis, L. Colombo, and A. Mattoni, J. Phys. Chem. C **115**, 18208 (2011).
[18] C. Melis, P. Raiteri, L. Colombo, and A. Mattoni, ACS Nano **5**, 9639 (2011).
[19] M. I. Saba, C. Melis, L. Colombo, G. Malloci, and A. Mattoni, J. Phys. Chem. C **115**, 9651 (2011).
[20] K. N. Baker *et al.*, Polymer **34**, 1571 (1993).
[21] S. Kowarik, A. Gerlach, S. Sellner, F. Schreiber, L. Cavalcanti, and O.Konovalov, Phys. Rev. Lett. **96**, 125504 (2006).
[22] J. Monteath Robertson and J. G. White, Nature **154**, 605 (1944).
[23] Z. Zhang and M. G. Lagally, Science **276**, 377 (1997).

3.2.2 Project-related publications

a) Published or accepted publications in peer-reviewed journals

[24] K. Palczynski. G. Heimel, J. Heyda, and J. Dzubiella, " **Growth and characterization of molecular crystals of** *para***-sexiphenyl by all-atom computer simulations***", Cryst. Growth Des. (ACS)* **14**, 3791 (2014).

b) Other publications

[25] T. Heinemann, K. Palczynski, J. Dzubiella, and S. Klapp, " **Angle-resolved effective potentials for disk-shaped molecules***", J. Chem. Phys.*, submitted (2014). arXiv:1407.4352 [cond-mat.soft]

[26] K. Palczynski and J. Dzubiella, " Anisotropic electrostatic friction of *p*-sexiphenyl on ZnO surfaces", J. Phys. Chem. C, submitted (2014). arXiv:1408.4418 [cond-mat.soft]

3.3 Funding

Funding of the project A1 within the Collaborative Research Center started 07/2011. The project A1 will be completed by the end of the current funding period (06/15).

3.3.1 Project staff in the ending funding period

	No.	Name, academic degree, position	Field of research	Department of university or non-university institution	Commitment in hours/week	Category	Funded through:
Available							
Research staff	1)	Dzubiella, Prof. Dr., Group leader	Soft condensed Matter Theory	Helmholtz Center Berlin and HUB Physics	10		
Non-research staff							
Requested							
Research staff	2)	Karol Palczynski	Soft condensed Matter Theory	Helmholtz Center Berlin and HUB Physics		PhD	
Non-research staff							

Job description of staff (supported through available funds):

1) Prof. Dr. Joachim Dzubiella

Principal Investigator for this project. He has been responsible for planning of the project. He has advised the PhD-student and supervised the simulations. He has helped with data analysis and modeling.

Job description of staff (requested):

2) Karol Palczynski (PhD student)

Palcynski has performed research in this project. In particular, he used atomistic (classical force-field) molecular dynamics (MD) computer simulations to investigate the structure, transport properties, and phase behavior of conjugated organic molecules in bulk and on inorganic ZnO surfaces.

3.1 About project A2

3.1.1 Title: Assembly and local probing of single molecules and defects on ultra-thin ZnO films on metals

3.1.2 Research areas: surface Science, physical Chemistry, condensed matter physics, scanning probe microscopy and single molecule spectroscopy

3.1.3 Principal investigator(s)

Dr. Takashi Kumagai (*19.03.1984)
Fritz-Haber Institute of the Max-Planck Society, Department of Physical Chemistry
Faradayweg 4-6, 14195 Berlin
Phone: +49 (0)30 8413 5110
Fax: +49 (0)30 8413 5106
E-mail: kuma@fhi-berlin.mpg.de

Prof. Dr. Martin Wolf (*03.04.1961)
Fritz-Haber Institute of the Max-Planck Society, Department of Physical Chemistry
Faradayweg 4-6, 14195 Berlin
Phone: +49 (0)30 8413 5111
Fax: +49 (0)30 8413 5106
E-mail: wolf@fhi-berlin.mpg.de

Do all above mentioned persons hold fixed-term positions?
No
If no: Takashi Kumagai
End date 14.4.2016
Further employment is planned until 30.06.2019

3.1.4 Legal issues

This project includes

1.	research on human subjects or human material.	no
	A copy of the required approval of the responsible ethics committee is included with the proposal.	no
2.	clinical trials	no
	A copy of the studies' registration is included with the proposal.	no
3.	experiments involving vertebrates.	no
4.	experiments involving recombinant DNA.	no
5.	research involving human embryonic stem cells.	no
	Legal authorization has been obtained.	no
6.	research concerning the Convention on Biological Diversity.	no

3.2 Summary

Understanding the local geometric/electronic structure at the interface between organic and inorganic materials is of fundamental importance for the precise control of the opto-electronic properties of HIOS. One of the challenging and significant topics is to characterize intrinsic defects at HIOS interfaces in order to unravel their impact on the energy level alignment and charge transfer dynamics. The central objective of this project is obtaining a comprehensive picture of the *geometric/electronic structure* including defects of HIOS interfaces *at the single atom/molecule level*. To achieve this goal we employ scanning probe microscopy (SPM) and directly characterize ZnO surfaces and the adsorption behavior of organic molecules

under ultra-high vacuum (UHV) conditions. Our experimental setup is able to measure simultaneously scanning tunneling microscopy (STM) and non-contact atomic force microscopy (nc-AFM) in the temperature range from 5 to 300 K. During the first funding period, we have focused ultrathin ZnO films grown on single crystalline metal supports as a model system. The atomically well-defined structure of the ultrathin ZnO films allows us to explore the fundamental aspects of the local geometric/electronic structures including defects and coupling (interaction) of organic molecules with the surface.
This project was initially headed by Leonhard Grill from 2/2011 to 7/2013, and since 8/2013 by Takashi Kumagai and Martin Wolf (current applicants). After a long-standing trial-and-error approach to prepare ultrathin ZnO film, the Grill group established a reproducible method to prepare the atomically-smooth ZnO layer growth on Ag(111). In addition, the initial adsorption stage of a model organic molecule on the ultrathin ZnO layers and a bare Ag(111) surface and STM resolved the different adsorption behavior between them. Subsequently a local structure and electronic properties of the ZnO layers were examined successfully with low-temperature STM/AFM by Kumagai and Wolf. While ZnO layer growth is initially dictated by the arrangement of the underlying metal substrate, it changes to the bulk structure for thicknesses above 3 or 4 layers. This ensures portability of our results to ZnO/molecule semiconductor interface in practical HIOS. In addition, the local work function changes, which plays a crucial role in energy level alignment, was explored using field-emission resonance measurement with STS and contact potential difference measurement with nc-AFM. These results clearly demonstrate the high capability of SPM techniques to reveal fundamental aspects of geometric/electronic structure at HIOS interfaces. Furthermore, the atomistic model of the ZnO layer was also theoretically examined with density functional theory (DFT) calculations in collaboration with B4 (Körzdörfer/Scheffler/ Rinke).
In the new funding period we continue exploiting the full capability of STM/AFM techniques in order to obtain fundamental insights into the local geometrical/electronic structure at HIOS interfaces. The manipulation of single atom/molecules will also be used to modify the local environment of individual molecules, in particular, to position organic molecules above local defects (e.g. oxygen defects) on ultrathin ZnO films. Additionally, we will employ tip-enhanced Raman spectroscopy (TERS) under UHV conditions to characterize the HIOS interfaces. TERS allows us not only to measure the local vibration spectroscopy (providing a direct insight into the local structure and chemical origin of the local defects in the ZnO surface and ZnO/molecules system), but also to study the coupling of localized plasmon polariton with exciton at the interfaces. Furthermore, the opto-electronic properties will be explored directly by irradiating the SPM junction with light as well as detecting light emission from molecules in the STM junction (induced by the tunneling current). While the experiment with the atomically-defined ultrathin ZnO layers will provide the most fundamental insights into the local geometric/electronic structure and opto-electronic properties at HIOS interfaces, we will expand our scope to the characterization of *bulk* ZnO materials that are widely explored in the CRC. In particular, we will investigate the interface structure and property of ZnO films with/without Ga doping prepared by MBE in collaboration with A5 (Henneberger). On the other hand, as organic semiconductor materials we plan to systematically investigate the series of laddertype oligo(p-phenylene)s (LOPPs) whose electronic properties are optimized for the combination with ZnO as HIOS. The LOPP molecules will be provided from A3 (Hecht). We will study a completely isolated single molecule and individual molecules in assembly structures on the different ZnO surfaces, i.e. ultrathin layers and MBE films with/without the dopant. The assembly structure of the molecule is also a key issue because the intermolecular interaction and packing geometry on the surface may substantially influence to the opto-electronic properties. We will develop strategies using non-covalent intermolecular interactions that can be controlled by molecular dipole moments. The direct observation of molecular assembly by STM/AFM will provide valuable feedback for molecular design in project A3 (Hecht).

We plan close collaboration with the projects A3 (Hecht) for the synthesis of LOPP molecules, A5 (Henneberger) for the investigation of doped ZnO materials and B4 (Körzdörfer/Scheffler/Rinke) for theoretical understanding. We will also have close exchange and potential collaborations with A8 (Koch) on the comprehensive understanding of energy level alignment, B7 (Neher) for the local work function measurement of self assembled monolayers, and B9 (Stähler) and B11 (Draxl) for the understanding of the carrier dynamics

3.3 Project progress to date

3.3.1 Report and state of understanding

In the first funding period we have focused first on ultrathin ZnO films grown on single-crystalline metal supports. Ultrathin (few monolayer thick) oxide films grown on metal supports, which have an atomically well-defined structure, are of general interest as a model system to investigate the elementary processes in

heterogeneous catalysis at the atomic scale [1]. The growth of ultrathin films has also helped to obtain a fundamental insight into the initial growth stages of inorganic crystals. The first obstacle in this project was to establish a reliable preparation procedure of the well-defined and high-quality ZnO films. Several methods have been explored in the first funding period by the Grill group. First, a recipe (at that time unpublished) by the Wöll group (Karlsruhe Institute of Technology) was explored to grow ZnO films on brass substrates when heating them in an oxygen atmosphere. Hence, Cu/Zn single crystals (with a stoichiometry Cu:Zn of 90:10) have been used as substrates in the initial phase of this project. It has been decided to use two low-index orientations, (100) and (111), in order to obtain flat surfaces (the latter orientation had been used previously by the Wöll group). After usual cleaning process under UHV conditions, these substrates were heated at temperatures between 420 K and 670 K for a few minutes while molecular oxygen (O_2) was dosed into the UHV chamber at a vapour pressure between 10^{-7} and 10^{-5} mbar. During this procedure the Zn atoms of the substrate diffuse upwards to the surface where they react with the oxygen molecules and form a ZnO film (without the presence of oxygen the Zn atoms would desorb then at these elevated temperatures). If a rather high heating temperature was used, a copper oxide film (Cu_2O for instance from a comparison with literature data) appears in the STM images due to the desorption of Zn atoms and a Zn-depleted layer appears. At lower temperatures, ZnO films were grown, which however are unfortunately disordered, and therefore not very suitable as a model substrate for further investigations because the undefined structure make it extremely difficult to provide detailed insights into the geometric/electronic structure by means of SPM. Due to this finding (note that no ordered ZnO structure could ever be produced), this strategy has been abandoned after about one year.

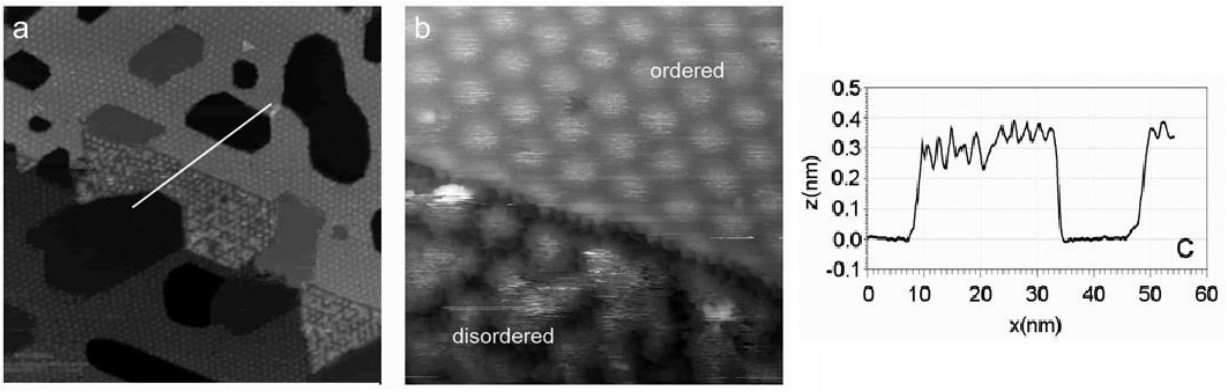

Figure 1(a) A typical overview image of ZnO layers grown on Ag(111) (V_s = 1 V, I_t = 100 pA, 110 × 110 nm², room temperature) and (b) small-scale (V_s = 1 V, I_t = 100 pA, 17 × 17 nm², at room temperature) STM images of the ZnO/Ag(111) surface with ordered and disordered regions (as indicated). (c) Height profile across the surface (as indicated by the white line in (a)), revealing the slightly different apparent heights of the ordered (about 3.6 Å) and disordered (about 3.1 Å) ZnO films.

After this experience, the group has attempted a different approach that has been pioneered by S. Shaikhutdinov and H.-J. Freund (Department of Chemical Physics, Fritz-Haber-Institute Berlin). ZnO /Ag(111) was chosen as a model system because the growth of atomically well-defined films has been observed previously and its structure was also characterized by surface X-ray diffraction (SXRD) and scanning tunneling microscopy (STM) [2], where the ZnO was deposited onto a Ag(111) surface by pulsed laser deposition. However, we employed the reactive deposition method developed by Shaikhutdinov and Freund, in which Zn is deposited onto the surface under oxygen pressure. This method has also been used successfully to grow ultrathin ZnO films on Pd(111) [3], and more recently Pt(111) [4] and Ag(111) [5]. After several trial-and-error for a few months, atomically-smooth ZnO films could be grown and imaged by STM (Figure 1a-b), revealing the characteristic Moiré pattern that corresponds to ZnO(0001)-(7×7)/Ag(111)-(8×8) coincidence structures (as reported before [2]). In addition to these highly ordered ZnO layers, disordered areas have also been found (Figure1a-b), which might be a disordered ZnO overlayer that still gives rise to protrusions as in a Moiré pattern (Figure1b). Their precise origin is not clear yet, but it might be due to the relatively high base pressure (10^{-9}-10^{-8} mbar) of the preparation chamber for the reactive deposition. It is important to note that the apparent height of these disordered areas is slightly lower than for the ordered ZnO layer (Figure1c), suggesting that they correspond to a modified structure. Fourier transformed images of the ordered and disordered areas show the same dominating periodicities, thus indicating equivalent lattices on average. However, in the case of the disordered structure the background intensity is clearly higher, which is the result of the protrusions that deviate from the perfect Moiré pattern and introduce defects in the structure. Interestingly, the disordered patterns are highly localized in specific areas on the surface (Figure1a) and individual defects can therefore be excluded as origin because they should be randomly

distributed over the surface. Furthermore, the boundaries between ordered and disordered areas are very straight with typical angles of 30° multiples between them, which points to a correlation with the substrate structure that exhibits threefold symmetry. In addition to these results, also first molecular adsorption experiments have been done and 6T molecules could be adsorbed and imaged in a stable fashion both on the metallic and ZnO covered areas (as discussed in Figure 2e below).
After successfully reproducing the growth of atomically-smooth ZnO films, Leonhard Grill left the FHI to the University of Graz and the current applicants continued these activities. In order to optimize the film growth and avoid potential contamination problems with the initial setup, a new reaction chamber with a base pressure of 3×10^{-10} mbar, equipped with a Zn source and oxygen dosing valve, was constructed and implemented at a low-temperature STM/AFM machine. Interestingly, the disordered area previously observed by the Grill group were not observed, and it is found that the film morphology can be varied by the preparation conditions, mainly oxygen pressure during the reactive deposition (the atomically-smooth ZnO layer does not grow at a relatively low oxygen pressure). Figure 2a shows a typical STM overview image of ZnO layers on Ag(111) prepared in the new setup, where the oxygen pressure of 10^{-5} mbar was used during the reactive Zn deposition and the sample was post-annealed up to 670 K. The atomically-smooth ZnO layers are observed reproducibly with a characteristic Moiré pattern (Figure 2b). It was revealed from previous SXRD study by J. Kirshcner group (MPG für Mikrostrukturphysik, Halle) that the ultrathin ZnO(0001) films are reconstructed to graphene-like flat geometry to suppress its dipole moment [2], which is considerably different from the bulk. However, the transition from the graphene-like to bulk ZnO(0001) structure was observed even at 3 or 4 monolayer (ML) thickness (Figure 2d). Therefore, the knowledge from relatively thick films can bridge the argument of physical properties between the ultrathin film and bulk surface. The roughened morphology in Figure 2c of the film is similar to the bulk surface that is observed in nominally undpoed ZnO(0001) surface by R. Berndt (Christian-Albrechts-Universität zu Kiel) [20]. The typical STM image of thicker ZnO layers (Figure 2c) is indeed characterized by less ordered (absence of Moiré pattern) and more defective morphology (small black dots). Controlling the defective ZnO surface still remains an important and general question relating significantly with the opto-electronic properties. On the other hand, we found that it is not trivial issue to assign the film thickness directly by the STM apparent height because of the strong contribution from the electronic state of ZnO layers. By measuring STM and AFM at the same time (using tuning fork sensor [6]) we could assign the thickness reasonably and revealed the exclusive growth of more than 2 ML ZnO layers on Ag(111). The preferential growth of hydrogen-free bilayer ZnO on Ag(111) and lack of monolayer growth was further examined in a collaboration with B4 (Körzdörfer/Scheffler/Rinke) and the Freund group at FHI, respectively. DFT calculations predicted the thermodynamical stability of hydrogen-free bilayer ZnO and the STM simulation reproduced nicely the Moiré pattern arising from ZnO(0001)-(7×7)/Ag(111)-(8×8) coincidence structures and the apparent height in STM. These conclusions are also very much consistent with the complementary experiment of LEED, AES, and FT-IR spectroscopy measured in the Freund group. The part of the above results are published in Ref. 22.

One key challenge in this project is to investigate the interaction between ZnO layers and organic semiconductor materials on a single molecule level and to establish the controlled coupling and energy level alignment at the organic/inorganic interface [27], which is central for HIOS explored in this CRC. The adsorption behavior of organic molecules is of particular interest since oxide surfaces can be inhomogeneous, leading to various molecular configurations [7]. At the most basic level one can study the adsorption of individual molecules on ultrathin films which has been done in the last years not only for oxide films [8,9,10] but also for alkali halide films [11,12].
In the first funding period we obtained some initial results for molecular adsorption on ultrathin ZnO films. We have selected α-sexithiophene (6T) molecules as a model, which is an important compound in organic electronics [13]. Different optoelectronic devices have been realized with sexithiophene (and polythiophene) molecules in the last years [14], and its growth properties have also been studied in thin films [15]. The Grill group investigated the initial adsorption steps in the coverage regime below one molecular monolayer. 6T molecules were deposited from a Knudsen cell onto the sample including ZnO layers and bare Ag(111) at room temperature. Figure 2e show a typical STM image after the deposition. 6T molecules appear as rods, similar to adsorption on other surfaces [16] and in general to the appearance of flat lying linear molecules in STM images [17]. However, adsorption does not occur homogeneously on the entire surface, but exclusively on the Ag(111) areas whereas the ZnO surface areas remain uncovered at low coverage regime. This behavior, similar to molecular adsorption on NaCl films [11,18], indicates a smaller diffusion barrier on the ZnO film as compared to the metallic areas. Accordingly, molecules that land on the oxide areas diffuse on the surface and adsorb on the silver areas (the sample was kept at room temperature during molecular deposition). When increasing the molecular coverage, the molecules are forced to adsorb on the ZnO monolayer as soon as the silver areas are saturated with a monomolecular film (Figure 2e). The molecules appear on the oxide areas as flat lying rods, thus very similar to the silver surface. It turned out that the 6T molecules are rather disordered on the ZnO layer, although in some areas small-range order is found. On

the Ag(111) areas three preferred molecular orientations are visible. On the other hand, Kumagai and Wolf started investigating the series of laddertype oligo(p-phenylene)s (LOPPs), which was developed by A3 (Hecht), whose electronic properties are optimized for the combination with ZnO materials [21]. We found that the LOPP molecules have been successfully deposited onto metal surfaces in UHV without any thermal decomposition.

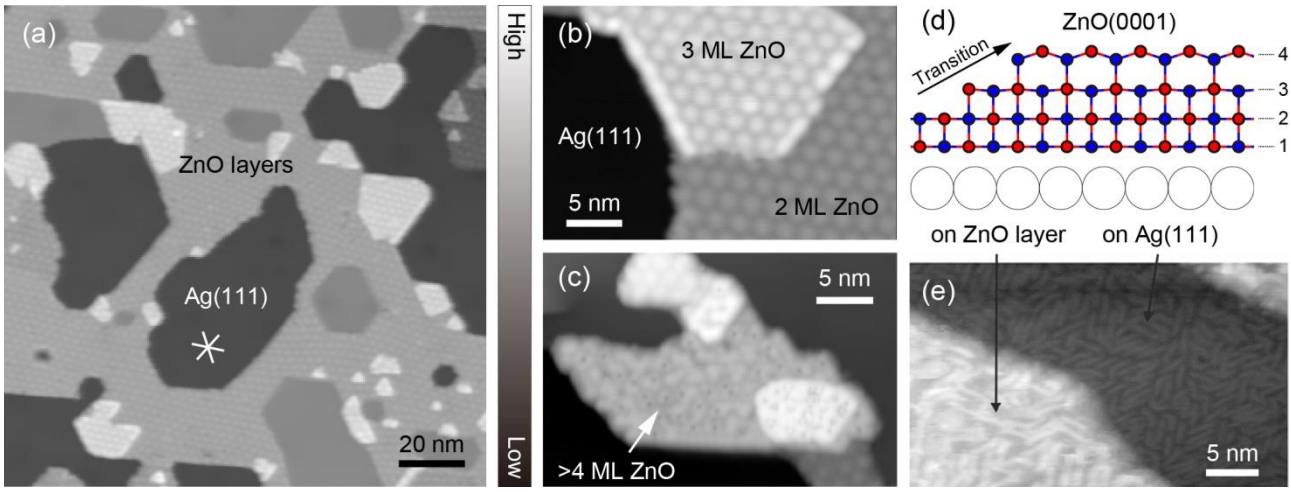

Figure 2 (a) A typical overview image of ZnO layers grown on Ag(111) reproduced in the new setup and measured at 5 K (V_s = 1 V, I_t = 0.1 nA). After the reactive deposition, the sample was post-annealed up to 670 K to obtain the atomically-smooth ZnO layer. (b) The 2 and 3 ML ZnO layers show characteristic Moiré pattern. (c) The morphology of the ZnO layer changes at a higher thickness (> 4 ML), which is less ordered and more defective (small black dots are visible). (d) Schematic illustration of the ZnO layer growth on Ag(111). The ZnO layer grows as an atomically-flat graphene-like structure at lower thickness (1-3 ML), but the transition to the bulk ZnO(0001) structure occurs above ~4 ML. (e) A typical STM image after the deposition of 6T molecules onto the ZnO layer on Ag(111) (V_s = 1 V, I_t =100 pA, at 170 K). At high coverage, the molecules adsorb both on the ZnO layer and bare Ag(111) surface with a different morphology.

We also investigated the local electronic state and work function of ZnO layers using STS at 5 K. The different resonance states are clearly observed depending on the thickness and the two-dimensional STS mapping allows to distinguish between them. Figure 3a shows STS spectra measured over 2 and 3 ML thick ZnO layers, and the bare Ag(111), where the ZnO resonance is observed in the empty state. Figures 3e and f show the STS mapping at the resonance voltage for 2 and 3 ML ZnO layers, respectively. The energetic difference of the ZnO resonance state allows resolving the island size, edge effects and local defects (marked by the red circle). On the other hand, the local work function was directly studied by the field-emission resonance (FER) of ZnO layers. Figure 3b shows the FER spectra measured over 2 and 3 ML ZnO layers, and the bare Ag(111) (STS measured with the feedback loop). The series of the FER is clearly observed for Ag(111), while it is shifted over the ZnO layers (the first peak on the ZnO layers corresponds to the electronic resonance). It is known that the FER state is associated with work function and the shift of the resonance corresponds to local work function changes [19]. The downward shift of the first resonance state for ZnO layers compared to the bare Ag(111) surface represents the reduction of work function, and the reduction is larger in 3 ML than that of 2 ML ZnO layer. This result is also consistent with the contact potential difference (CPD) measurement with nc-AFM (Figure 3c-d). Figure 3c shows the parabolic voltage dependence of the electrostatic force (frequency shift in the resonance oscillation of the tuning fork) measured over 2 ML ZnO layer with nc-AFM. Since the electrostatic forces are attractive, the resonant frequency shift is always negative, and the maximum position in the frequency shift represents the compensated V_{CPD}. As seen in Figure 3d (V_{CPD} as a function of gap distance), the reduced CPD is observed for ZnO layers when it is measured close to the surface (if the distance increases, the local work function change is averaged out). Both FER spectra and CPD measurement are able to map out the local work function.

Figure 3g and h show the mapping of first FER state for 2 and 3 ML ZnO layers, respectively, where the local modification of the work function is clearly observed. These results provided microscopic insights into the geometric/electronic structure of ultrathin ZnO layers on metal substrates. In order to obtain further understanding of the atomistic structure and local electronic states and publish these results we collaborate closely with the theory project B4 (Körzdörfer/Scheffler/Rinke).

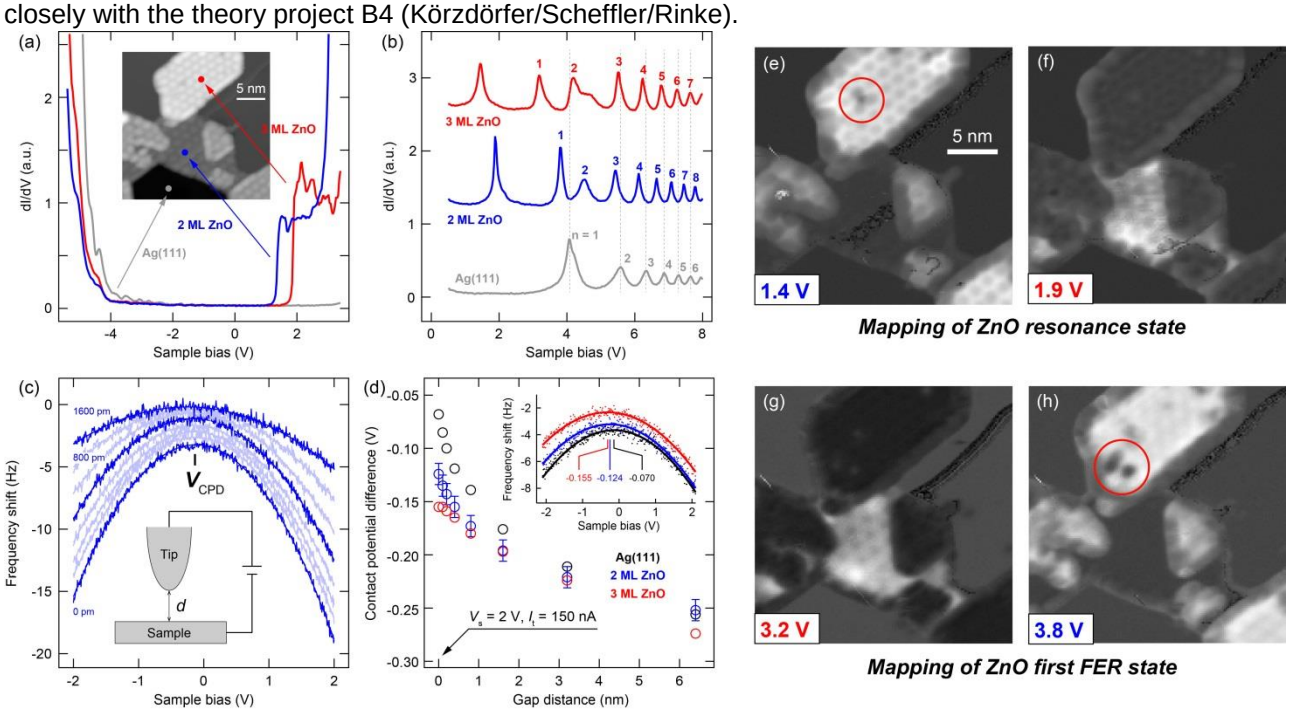

Figure 3 STS, FER, and CPD measurement at 5 K. (a) STS spectra measured over 2-3 ML ZnO layers and a bare Ag(111) without the STM feedback loop. The inset shows the STM image of a partially covered Ag(111) area. (b) FER spectra measured over 2 and 3 ML ZnO layers. The feedback loop of STM was activated during the measurement to record the dI/dV single with a wider range. (c) Parabolic voltage dependence of the electrostatic force measured over 2 ML ZnO layer with nc-AFM. The frequency shift in the resonance oscillation of the tuning fork was recorded at the fixed tip position (the feedback loop was off during the measurement). (d) The gap distance dependence of local contact potential difference measured over Ag(111) (black circles), 2 ML ZnO layer (blue circles), and 3 ML ZnO layer (red circles). The inset shows the parabolic voltage dependence of the electrostatic force measured over Ag(111) (black), 2 ML ZnO layer (blue), and 3 ML ZnO layer (red), where the different V_{CPD} is observed. (e)-(f) STS mapping at the resonance voltage of 2 (1.9 V) and 3 ML (1.4 V). (g)-(h) FER mapping at the resonance voltage of 2 (3.2) and 3 ML (3.8 V). The local modifications, most probably due to the defect in the ZnO layer, of the electronic resonance and work function are highlighted by the red circle.

In the new funding period, we plan to exploit tip-enhanced Raman spectroscopy (TERS) to characterize the local structure and coupling of localized plasmon polariton and exciton at HIOS interfaces, which are strongly related to the central objective of this CRC. Kumagai and Wolf have developed TERS under UHV conditions and demonstrated the performance using graphene nanoribbons (GNRs) fabricated on Au(111) [24] The 0.74 nm wide armchair GNRs by means of on-surface polymerization method [22] under UHV conditions are directly observed by STM and the characteristic vibration modes appear in both, the far- and near-field (tip-enhanced) Raman spectra at room temperature, whereby the Raman scattering is enhanced by up to 4×10^5 in the near-field [24].

References

[1] S. Shaikhutdinov, H.-J. Freund, Annu. Rev. Phys. Chem. 63, 619–633 (2012).
[2] C. Tusche, H. L. Meyerheim, and J. Kirschner, PRL 99, 026102 (2007).
[3] G. Weirum et al. Phys. Chem. C 114, 15432 (2010).
[4] Y. Martynova et al. J. Catal. 301, 227 (2013).
[5] Q. Pan, Q et al. Catal. Lett. 144, 648 (2014).
[6] F.J. Giessibl, APL 76, 1470 (2000).
[7] S. W. Wu, G. V. Nazin, X. Chen, X. H. Qiu, and W. Ho, Phys. Rev. Lett. 93, 236802 (2004).
[8] X. H. Qiu, G. V. Nazin, and W. Ho, Science 299, 542 (2003).
[9] E. Cavar et al. Phys. Rev. Lett. 95, 196102 (2005).

[10] N. Nilius, Surf. Sci. Rep. 64, 595 (2009).
[11] J. Repp, G. Meyer, S. Stojkovic, A. Gourdon, and C. Joachim, Phys. Rev. Lett. 94, 026803 (2005).
[12] R. Bennewitz, J. Phys. : Condens. Matter 18, R417 (2006).
[13] S. Duhm, Q. Xin, N. Koch, N. Ueno, and S. Kera, Org. Electron. 12, 903 (2011).
[14] N. Koch, ChemPhysChem 8, 1438 (2007).
[15] A. Moser et al. Chem. Phys. Lett. 574, 51 (2013).
[16] M. Oehzelt, S. Berkebile, G. Koller, J. Ivanco, S. Surnev, and M. G. Ramsey, Surf. Sci. 603, 412 (2009).
[17] M. Oehzelt et al. ChemPhysChem 8, 1707 (2007).
[18] C. Bombis et al. Angew. Chem. Int. Ed. 48, 9966 (2009).
[19] H.-C. Ploigt, C. Brun, M. Pivetta, F. Patthey, W.-D. Schneider, Phys. Rev. B 76, 195404 (2007).
[20] H. Zheng, J. Kröger, R. Berndt, Phys. Rev. Lett. 108, 076801 (2012).
[21] B. Kobin, L. Grubert, S. Blumstengel, F. Henneberger, and S. Hecht, J. Mater. Chem. 22, 4383 (2012).
[22] J. Cai et al. Nature 466, 470 (2010).

3.3.2 Project-related publications

[23] A. Shiotari, B.-H. Liu, S. Jaekel, L. Grill, S. Shaikhutdinov, H.-J. Freund, M. Wolf, T. Kumagai, J. Phys. Chem. C, in press.
[24] A. Shiotari, T. Kumagai, M. Wolf, J. Phys. Chem. C 118, 11806–11812 (2014).
[25] T. Kumagai, F. Hanke, S. Gawinkowski, J. Sharp, K. Kotsis, J. Waluk, M. Persson, and L. Grill, Nature Chemistry 6, 41–46 (2014).
[26] J.C. Deinert, D. Wegkamp, M. Meyer, C. Richter, M. Wolf, and J. Stähler, Phys. Rev. Lett. 113, 057602 (2014).
[27] O. Hofmann, J.-C. Deinert, Y. Xu, P. Rinke, J. Stähler, M. Wolf and M. Scheffler, J. Chem. Phys. 139, 174701 (2013).

3.4 Research plan

3.4.1 Overview

In this project we investigate the local geometric and electronic structures of HIOS interfaces *at the single atom/molecule level* using scanning probe techniques (STM, AFM, and TERS). The ZnO, which is the material of choice in this CRC, is a promising wide-gap semiconductor as a material for opto-electronic devices. We will focus on the *local* structural characterization of the ZnO interface including defects, and the adsorption and energy level alignment of organic semiconductor molecules. Although the defects at HIOS interfaces are known to act as a trapping center for charge carriers and thus have a significant impact on the opto-electronic functions, the underlying microscopic mechanism is not yet understood. We will extend our studies of well-defined ultrathin ZnO layers on metal substrates because the well-defined surface morphology will provide a unique opportunity to obtain microscopic insights into the local geometric/electronic structure and chemical interaction of organic molecules with ZnO as well as the formation and properties of defects. By studying such model systems, we hope to obtain an in-depth understanding of the electronic properties of HIOS interfaces and how they can be optimized in view of opto-electronic functions. The well-defined geometric/electronic structure is also suitable to explore both the fundamental aspects of TERS (the enhancement factor and selection rules) as well as the coupling mechanism between localized plasmon polariton and interfacial excitons. In the new funding period we also plan to investigate the surface structure and electronic properties of ZnO films with different doping levels (concentration? Carrier density up to ???) prepared by molecular beam epitaxy in collaboration with A5 (Hennerberger). The sample allows variation of the carrier density from insulating to nearly metallic behavior (up to ~10^{21} e^-/cm^{-3})

On the organic semiconductor side, we plan to investigate vacuum-comparable ladder type oligo(p-phenylene)s (LOPPs; Figure 4) in a collaboration with A3 (Hecht), which is a prominent compound to attain outstanding optoelectronic functions with a combination of ZnO materials. The selection of molecule is governed by mainly their optical properties, thus the electronic excitation fits to the spectral range of ZnO. The exciton transition of ladder-type quarter-phenyl is almost in resonance with that of ZnO and the additional linker between aryl-aryl moieties suppresses their free rotation, leading to a sharp resonance in absorption and emission spectra. It was already revealed by A3 (Hecht) that the absorption coefficient of LOPPs is considerably larger than that of the reactive oligo(*p*-phenylene)s without rigidified backbone such as p-sexiphenyl compounds and the fluorescence quantum yield reaches unity in solution. We will study the adsorption structure and chemical interaction of LOPP molecules with the ZnO surface by STM (STS), AFM, and TERS in order to provide microscopic understanding about the energy level alignment.

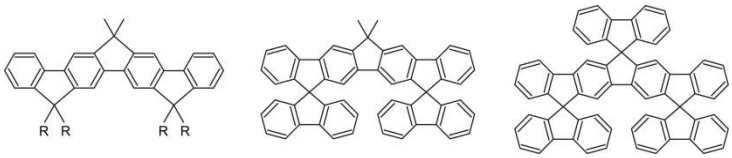

R = CH_3, CF_3

Figure 4 Chemical structure pf LOPP molecules to be investigated in this project.

The controlled assembly of molecular components is a key to design nano-, meso-, and even macroscale properties and functions. Non-covalent intermolecular interaction through molecular dipole mainly determines assemble structure and relative orientation of adsorbed molecules with regard to each other as well as to surfaces. Such an interaction will be controlled by substituting the side group of organic molecules. We will examine in LOPP molecules with several different substituents as shown in Figure 4. During the first funding period the LOPP molecules have been successfully deposited onto metal surfaces under UHV conditions without thermal decomposition. In the new funding period we will investigate the adsorption geometry and electronic state of LOPP molecules on the ZnO surfaces in detail. Although the electronic structure of adsorbed molecules can be examined directly by STS, the chemical identification and structural details of organic molecules on material surfaces remains a rather general research subject to be solved. TERS has a sufficient potential to provide to address such an important question. Moreover, our low temperature SPM combined with optical system enables us to investigate directly opto-electronic functions of LOPPs/ZnO interfaces at the single molecule level.

3.4.2 Methods

High-performance scanning probe microscopy is an essential prerequisite for the project. We employ an UHV system equipped with low-temperature STM/AFM (operation temperature from 5 K up to room-temperature). The use of the tuning fork sensor allows us to measure STM and nc-AFM at the same time. The low temperature SPM is combined with the optical system and a controlled irradiation of the SPM junction is possible. Furthermore, we have developed a tip-enhanced Raman spectroscopy (TERS) system operating under UHV conditions at room temperature [24, 27] and plan to develop a new low-temperature TERS system, which will be available end of 2015. The TERS setup, in principle, is able to collect photons emitted from the SPM junction and thus photoluminescence of a single molecule induced by the tunnelling electron can be detected. This would allow studying directly the opto-electronic functions at HIOS interfaces at the single atom/molecule limit. All UHV systems are equipped with standard options for *in situ* sample preparation: sputter gun, sample heating (cooling), Knuden cell evaporators (for molecular deposition) and gas inlet.

Our instruments allows;

- Sample preparations and thin film growth under UHV conditions.
- Imaging of atomic structure of conductive surfaces.
- Imaging of single molecules by STM/nc-AFM; characterization of the conformation and adsorption site.
- Local electronic spectroscopy (STS); characterization of local density of state, electronic structure of single molecules
- Atom/molecule manipulation using the force acting between SPM tip and adsorbates.
- Local work function measurement; field-emission resonance spectroscopy with STM, Kelvin-probe microscopy with nc-AFM.
- Force spectroscopy by nc-AFM.
- Direct observation of local photochemistry/physics; Controlled irradiation of SPM junction with various wavelengths from UV to NIR, and observation of photo-induced processes by STM/AFM
- Local Raman (vibration) spectroscopy by TERS; chemical identification of adsorbates and defects, characterization of local geometric structure.
- Direct observation of the coupling between localized plasmon polariton and exciton at interfaces.
- Photoluminescence spectroscopy of single molecules.
- Single-molecule chemistry: Chemical reactions can be induced in single molecules by various driving forces, i.e. tunneling electron, electric field in STM junction, mechanical force from the tip apex, laser-illumination with different wavelengths.

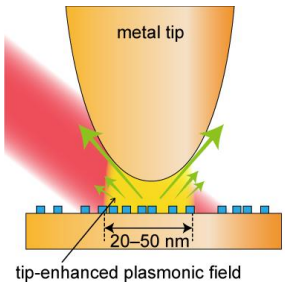

Figure 5 Schematic illustration of TERS. The incident light (red) excite the localized plasmon polariton (yellow) that couples with adsorbates (blue), resulting in the enhanced Raman scattering (green arrows).

It should be noted that UHV-TERS is still an immature experimental technique and involves lots of challenging subjects. Kumagai and Wolf have developed the technique. Figure 5 illustrates the concept of TERS. The irradiation of SPM junction with a resonant wavelength of localized plasmon excitation generates the enhanced field in the proximity of the

SPM tip.
Then the strong field couples with Raman scattering of adsorbates on the surface, resulting in enhancement of the scattering. Since the enhancement is onfined in the SPM junction, in principle, TERS is able to measure local Raman (vibration) spectroscopy. Although the spatial resolution is still controversy, the TERS spectra from a single molecule has recently been reported at low temperature [28].

References

[27] B. Pettinger, P. Schambach, C.J. Villagómez, N. Scott, Annu. Rev. Phys. Chem. 63, 379 (2012)
[28] R. Zhang et al. Nature 498, 82 (2013).

3.4.3 Work program

1. Characterization of local geometric/electronic structure and defects in the ZnO surface: It is of fundamental importance in the precise control of HIOS properties to understand local geometric/electronic structure and defects. The defects substantially affect the electronic structure, thus opto-electronic properties of HIOS interfaces. However, the local characterization remains a challenging subject and the detailed physics and chemistry is yet imperfectly understood. The ultrathin ZnO layers on metal support provides a unique opportunity to study such issues. As shown above, we have observed the transition from the atomically-flat graphene-like structure to bulk-like one with increasing the thickness of ZnO layer on Ag(111). The STM image of such a thicker layer exhibit less ordered morphology and local defects (the black dots), which may be associated directly with the defect formation in the bulk. Although a chemical identification of such defects is extremely difficult with STM and AFM, TERS will be a powerful method to characterize them and would provide unprecedented insights into their structure and origin. On the other hand, the change in the electronic property of the ZnO surface have been observed by dosing hydrogen [26]. We plan to examine the geometric/electronic modification caused by the incorporation of hydrogen into ZnO films. This will be implemented by dosing molecular or atomic hydrogen onto the ZnO layer, or during the reactive deposition (coexistence of oxygen). The local structural/electronic variation will be investigated by STM/STS, nc-AFM and TERS measurements.

2. Investigation of ZnO films prepared by MBE with different doping level: We also investigate ZnO films (few hundreds nm thick) prepared by MBE in A5 (Henneberger) [29]. Two different films will be explored, which are heavily-doped ZnO films with Ga and covered with pure ZnO films (Figure 6). In order to measure atomic structure of these novel materials with SPM, it will be essential to establish a reliable cleaning procedure under UHV conditions. Conventional cleaning process (ion sputtering and/or annealing) and passivation with inert molecules after MBE growth will be examined in a close collaboration with A5 (Henneberger). Once the atomically-defined surface is obtained, the geometric/electronic structure will be characterized in detail using our SPM techniques.

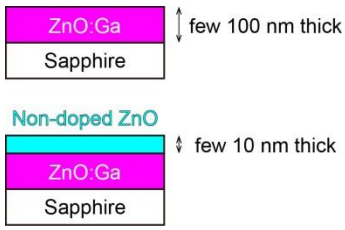

Figure 6 Schematic illustration of ZnO film prepared by MBE.

3. Characterization of local geometric/electronic structure of LOPP molecules on ZnO surfaces: We will study the adsorption structure and electronic state of LOPP molecules on ultrathin ZnO layers on metal supports and ZnO films prepared by MBE. The optical- and electrochemistry of the series of LOPP molecules have been investigated in A3 (Hecht) and desirable properties such as sharp and intense optical transitions were observed [21]. However, the opto-electonic properties will be significantly affected by the adsorption onto the surface because of the strong coupling with ZnO. We plan to investigate the geometric/electronic structure of individual LOPP molecules adsorbed on ZnO surfaces in order to obtain the microscopic insight. The completely isolated single molecule and individual molecules within the molecular assembly will be explored. STS measurement will provide a direct insight into energy level alignment of LOPP molecules on different ZnO surfaces, i.e. ultrathin layer, doped and undoped films, and the mechanism will be also examined by work function measurement for individual molecules. Moreover, the detailed adsorption geometry and chemical state will be studied by TERS. The assembly structure of organic molecules are a primary interest for organic-semiconductor. We will directly observe the molecular assembly of LOPP molecules on surfaces using STM/nc-AFM, and also characterize the electronic state of individual molecules in the assembly. As shown above, the adsorption behavior of organic molecules are considerably different between a metal and ZnO layers. We will focus on how the geometric and electronic structure is different depending on the surface morphology and property.

4. Investigation of local interaction between organic molecules and defects in the ZnO surface: We will investigate interaction between organic molecules and local defects in a controlled fashion using SPM manipulation. Although the local environment at the atomic scale has a significant impact on a molecular state as well as a molecular function [24], it is yet imperfectly understood. SPM, in principle, can manipulate a local defect on ZnO surface as well as molecules and we will try following two different approaches; First,

we attempt to manipulate intrinsic defects in the ZnO surface, which are observed, for instance, in the thicker layer of ZnO layers on Ag(111). Second, we plan to intentionally create defects by ion bombardment or adsorb metal adatoms on a ZnO surface, which will be examined for ultrathin ZnO layers and ZnO films prepared by MBE.

5. Investigation of opto-electronic properties of LOPP molecules on the ZnO surface: *STM-induced photoluminescence*; By exciting photon emission with the tunnelling electrons in the STM junction, the optical properties of molecules in the junction can be probed directly at the single molecule level. The luminescence spectrum will depend on the electronic structure and thus on the local interaction of the molecules with the ZnO surface as well as with neighbouring molecules. Our TERS setup, in principle, is able to collect such light emission from the STM junction. We plan to investigate the STM-induced luminescence of LOPP molecules on different ZnO surfaces, which will be a key interest to address directly the opto-electronic functions at HIOS interfaces. *Photo-degradation*; it is a fundamental importance for opto-electronic application of LOPP molecules to understand the stability against light-irradiation on the ZnO surface. The irradiation may induced additional defects at HIOS interfaces, i.e. dissociation of molecules. Such a local defect formation potentially has a significant impact on the opto-electronic properties. Even if molecules are stable in solution or molecular crystals, the modification of electronic state and the coupling with the ZnO surface may change the stability. In order to obtain the microscopic insight, we will investigate the interaction of LOPP molecules with light using our combined SPM and laser system with various wavelengths (from UV to near IR region).

Timeline

Year 1-2:
- Investigation of local defects in ultrathin ZnO layers on Ag(111)
- Investigation of surface structure of ZnO films with/without Ga doping.
- Investigation of the influence of hydrogen/water dosing to the ZnO surfaces.
- Deposition of LOPP molecules on the ZnO surfaces
- Construction of a new low-temperature TERS system.

Year 2-4:
- TERS measurement of ultrathin ZnO films on Ag(111).
- Characterization of local geometric/electronic structure of LOPP molecules on the ZnO surfaces.
- Investigation of local interaction between organic molecules and defects using SPM manipulation.

Year 3-4:
- TERS measurement of LOPP molecules on ZnO surfaces.
- Investigation of opto-electronic properties of the ZnO surfaces and ZnO/LOPPs.

References

[29] S. Sadofev, S. Kalusniak, P. Schäfer, F. Henneberger, Appl. Phys. Lett. 102, 181905 (2013).

3.5 Role within the Collaborative Research Centre

This project will contribute to this CRC by studying the geometric/electronic structure of HIOS interfaces at the single atom/molecule level. It is of pivotal importance in this CRC to obtain detailed knowledge about the mechanism that governs the energy level alignment at HIOS interfaces, which determines energy/charge transfer dynamics, thus the opto-electronic functions. While UPS and 2PPE spectroscopy employed in A8 (Koch) and B9 (Stähler) will provide direct insights into the (laterally averaged) electronic structure of ZnO/molecule interfaces, our STS results will offer a complementary (local) information at the single atom/molecule level. The investigation of doped ZnO films prepared by MBE in A5 (Henneberger) will further contribute to the central objectives of the CRC. In our project organic chemistry is required to synthesize vacuum-processable LOPP molecules. A3 (Hecht) will perform this important task and we will have a close exchange and feedback to optimize the chemical structure and electronic properties of LOPP molecules on ZnO surface. *These molecules will be studied in … (I'd like to get some feedback which project plans to investigate LOPP molecules.)* We will also have close discussions and collaborate with A8 (Koch) for the comprehensive understanding of energy level alignment, with B4 (Körzdörfer/Scheffler/Rinke) for theoretical analysis, with B7 (Neher) on local work function measurement of self-assembled monolayers, and with B9 (Stähler) and B11 (Draxl) on understanding of the carrier dynamics.

We plan specifically directed collaboration with other projects within this CRC.
- The novel molecules synthesized in A3 (Hecht) will be examined.
- The epitaxially-grown ZnO materials with a desired dopant concentration fabricated in A5 (Henneberger) will be examined.

- DFT calculations in B4 (Körzdörfer/Scheffler/Rinke) will assist our understanding of the geometric and electronic structure of the ZnO surface.

3.6 Delineation from other funded projects

The proposed project is not funded by the DFG or other sources and is clearly separated from other funded projects of the principal investigators, which all employ very different experimental techniques like time-resolved laser spectroscopy and address problems of ultrafast dynamics.

3.7 Project funds

3.7.1 Previous funding

The project has been funded within the Collaborative Research Centre since 07/2011.

3.7.2 Funds requested

Funding for	2015/2		2016		2017		2018		2019/1	
Staff	Quantity	Sum	Quantity	Sum	Quantity	Sum	Quantity	Sum	Quantity	Sum
E13	1	31800	1	63600	1	63600	1	63600	1	31800
Total		31800		63600		63600		63600		31800
Direct costs	Sum		Sum		Sum		Sum		Sum	
Small equipment, Software, Consumables	5000		10000		10000		10000		5000	
Other	0		0		0		0		0	
Total	5000		10000		10000		10000		5000	
Major research equipment	Sum		Sum		Sum		Sum		Sum	
€ 10.000 - 50.000	0		0		0		0		0	
> € 50.000	0		0		0		0		0	
Total	0		0		0		0		0	
Total	36800		73600		73600		73600		36800	

(All figures in Euro)

3.7.3 Staff

	No.	Name, academic degree, position	Field of research	Department of university or non-university institution	Commitment in hours/week	Category	Funded through:
Available							
Research staff	1	Takashi Kumagai, PhD, Research group leader	Physics, Surface science	FHI, Physical Chemistry	15		MPG
	2	Martin Wolf, Prof. Dr., Director	Physics, Surface science	FHI, Physical Chemistry	5		MPG
	3	Hannes Böckmann	Physics, Surface science	FHI, Physical Chemistry	8		MPG
Non-research staff	4	Sven Kubala, Technician		FHI, Physical Chemistry	8		MPG
Requested							
Research staff	5	N.N., Postdoc	Physics, Surface science	FHI, Physical Chemistry		39	
Non-research staff							

Job description of staff (supported through available funds):

1) Takashi Kumagai: Principal investigator; Scientific and organizational coordination of the project, instruction and supervision of the project staff, co-operation in experiments and data analysis, publication.
2) Martin Wolf: Principal investigator; scientific administration, supervision of PhD students, publication of results
3) Hannes Böckmann: PhD student on tip-enhanced Raman spectroscopy (TERS) and development of new instrumentation. Within his thesis work he will participate in the TERS experiments on ZnO samples with different doping levels (see work program)
4) Sven Kubala: Technician with a broad experience in all technical aspects of surface and vacuum science. He will in troubleshooting, development and maintenance of the instrumentation.

Job description of staff (requested):

5) *N.N.*: Postdoctoral researcher; will perform the following tasks: sample preparation (ultrathin ZnO films & HIOS systems), low-temperature STM/AFM studies of local defects, single molecule manipulation and scanning tunneling spectroscopy (STS) and TERS experiments. The project outlined above requires a very broad but also very specific knowledge of different techniques and methods, including sample preparation and organic film growth in UHV as well the handling of low-temperature STM/AFM setup. These tasks include also improvements of the setup as well as a demanding list of topics outlined in work program. This can only be performed in an effective way by an experienced (postdoctoral) researcher as a graduate student would need much more time to learn all different techniques and perform these tasks.

3.7.4 Direct costs for the new funding period

	2015/2	2016	2017	2018	2019/1
Funds available	5000	10000	10000	10000	5000
Funds requested	4500	9000	9000	9000	4500

(All figures in Euro)

Consumables for 2015/2

Materials for STM, sample holders	EUR	500
Materials for thin film growth, crystals and substrates	EUR	1000
Optical components for TERS/Photoluminescence	EUR	1500
Small UHV parts	EUR	1500

Consumables for 2016

cf. 2015/2	EUR	9000

Consumables for 2017

cf. 2015/2	EUR	9000

Consumables for 2018

cf. 2015/2	EUR	9000

Consumables for 2019/1

cf. 2015/2	EUR	4500

3.7.5 Major research equipment requested for the new funding period

No funding for instrumentation is requested**.**

3.7.6 Student assistants

No funding requested

3.1 About project A3

3.1.1 Title: Design of functional molecular building blocks for covalent and non-covalent assembly at semiconductor surfaces

3.1.2 Research areas: Molecular chemistry

3.1.3 Principal investigator

Prof. Stefan Hecht, Ph.D. (*06.01.1974, German)
Humboldt-Universität zu Berlin, Department of Chemistry (HU Chem)
Brook-Taylor-Str. 2, 12489 Berlin
Phone: +49 (0)30 2093 7365
Fax: +49 (0)30 2093 6940
E-mail: sh@chemie.hu-berlin.de

Does the above mentioned person hold a fixed-term position?
Yes

3.1.4 Legal issues

This project includes

1.	research on human subjects or human material.	no
	<If applicable:> A copy of the required approval of the responsible ethics committee is included with the proposal.	
2.	clinical trials	no
	<If applicable:> A copy of the studies' registration is included with the proposal.	
3.	experiments involving vertebrates.	no
4.	experiments involving recombinant DNA.	no
5.	research involving human embryonic stem cells.	no
	<If applicable:> Legal authorization has been obtained.	
6.	research concerning the Convention on Biological Diversity.	no

3.2 Summary

The central goal of this project continues to be the design and synthesis of functional molecular building blocks to achieve control over the assembly structure and the resulting energetics at inorganic/organic interfaces. Based on knowledge gained during the initial funding period, this project will follow a synthetic organic chemist's approach thereby tailoring the electronic and geometrical structure as well as the assembly properties of the molecules to tune the electronic coupling and resulting optical and electronic properties of the prepared HIOS. The main objective is the design and preparation of the organic components, from which structurally and compositionally well-defined HIOS will be prepared within the CRC. Based on this "Aufbau" principle, the project is divided into two subprojects, one dealing with the design of suitable molecular building blocks for the organic as well as the HIOS interfacial layer and the other with their assembly on semiconductor substrates, in particular ZnO and GaN as well as Si surfaces.

1st Subproject "Molecular Design": Focus will be on the further development of proper conjugated building blocks based on the successful design of ladder-type oligo(para-phenylene)s in the initial funding period. Key properties that will be optimized include: HOMO-LUMO gap, HOMO/LUMO alignment with respect to the semiconducting surface, exciton migration (Stokes-shift), luminescence quantum yield, thermal and photochemical stability, among others. In addition, the HIOS interfacial layer that mediates the coupling between both organic and inorganic semiconductors will be tuned by introducing either static molecular dipoles in controlled orientation and strength or photoswitchable dipolar molecules. The latter should allow for convenient tuning of the coupling and hence hybridization by an external light stimulus thereby introducing an additional element of control over HIOS properties, in particular to transiently modulate the work function of the inorganic semiconductor.

2nd Subproject “Molecular Assembly”: While work on physisorbed mono- and multilayers will continue, focus in this funding period will be on chemisorbed monolayers. For this purpose, new anchor groups with high binding strength and selectivity, allowing for targeting of specific surface reconstructions of ZnO and GaN will be developed. If necessary, the stability of these self-assembled monolayers will be enhanced by covalent crosslinking within the monolayer (topochemical reaction) or post-assembly grafting to the surface.

This project will synthesize a multitude of molecular building blocks, which together with various experimental as well as theoretical projects within the CRC will be used to generate high quality HIOS. Their resulting properties will be correlated with the structures of the molecular building blocks and assemblies thereof to derive general design principles for the bottom-up construction of HIOS with advantageous features, for example efficient and tunable interfacial charge transport and emission.

3.3 Project progress to date

3.3.1 Report and state of understanding

Over the course of the initial funding period the project has been designing and synthesizing a large variety of organic components, from which structurally and compositionally well-defined HIOS were prepared within the CRC following two different organic growth strategies, namely non-covalent and covalent assembly:

Non-covalent assembly

In the first initial subproject conjugated organic molecules with specific optical and electronic properties to match the inorganic ZnO substrate were targeted. The following requirements were identified:

- the absorption (HOMO-LUMO gap) of the organic component should be efficient (high extinction coefficient ε) and resonant to ZnO emission ($\lambda_{max} = \lambda_{em}(ZnO)$) to assure for efficient interfacial inorganic $\rightarrow$ organic FRET,
- the emission quantum yield of the organic component should be close to unity ($\Phi \rightarrow 1$) to assure for efficient luminescence,
- the absorption and emission spectra of the organic component should be separated by only a small Stokes shift ($\Delta\lambda \rightarrow 0$) to assure for efficient FRET within the organic layer (large exciton diffusion),
- the frontier orbital levels (HOMO and LUMO) should ideally be positioned at similar energies as their inorganic counterparts, i.e. valence band and conduction band of ZnO, to avoid (photoinduced) charge separation,
- the molecule should be thermally and photochemically stable to assure compatibility with vacuum deposition (evaporation) on the one hand and avoid photodegradation on the other hand,
- the compound should grow in closed thin films on the desired substrate, and
- the compounds’ self-assembly on the substrate should be tuned by introducing proper substituents.

Faced with these stringent criteria and the challenge to prepare respective molecules the PhD student in charge, Björn Kobin, developed and continously improved ladder-type oligo(*para*-phenylene)s (LOPPs). By varying and optimizing the important structural parameters, namely rigidity, chain length, substitution pattern, and in-plane curvature of the π-system (Fig. 1), LOPPs such as **L4P-sp$_3$** or **bent-L4P-sp$_2$** ideally suited for their use in conjunction with ZnO were prepared and studied.[4] Specifically, by annulation of the adjacent, otherwise twisted phenyl rings, the intensity of the optical transitions increased dramatically, while the Stoke’s shift decreased significantly. By adjusting the chain length to a ladder-type tetra(*para*-phenylene) the desired optical features were achieved; however, the rapid (photo)bleaching of the methylated derivative **L4P** sparked a detailed investigation of the LOPP’s photochemically induced degradation pathways and a critical revisiting of the fluorenone defect [6]. As a result spiro-annulated derivatives such as **L4P-sp$_3$** moved into the center of attention not only due to their superior photostability but also advantageous thin-film growth properties. To counteract the slight red-shift of the spiroannulation, we synthesized the bent isomer **bent-L4P-sp$_2$**, which due to its in-plane curvature exhibits less pronounced π-conjugation and hence a slight blue shift to perfectly match the ZnO for resonant energy transfer. Subsequently, in collaboration with A5 (Henneberger) and B3 (Blumstengel) as well as A8 (Koch) it became clear that despite the identical HOMO-LUMO gap, the relative offset compared to the ZnO led to charge separation that could only be prevented by a buffer layer, which also reduced the energy transfer efficiency [ref?Manuskript]. Therefore, we investigated the influence of methylene-bridge fluorination and indeed the LUMO level could be reduced by the required amount of ca. 1 eV [5] proving the general validity of our approach. Since these fluorinated derivatives display an extremely rapid photodegration we have now shifted our attention on trifluoromethylation of the aromatic core, while maintain the spiroannulation.

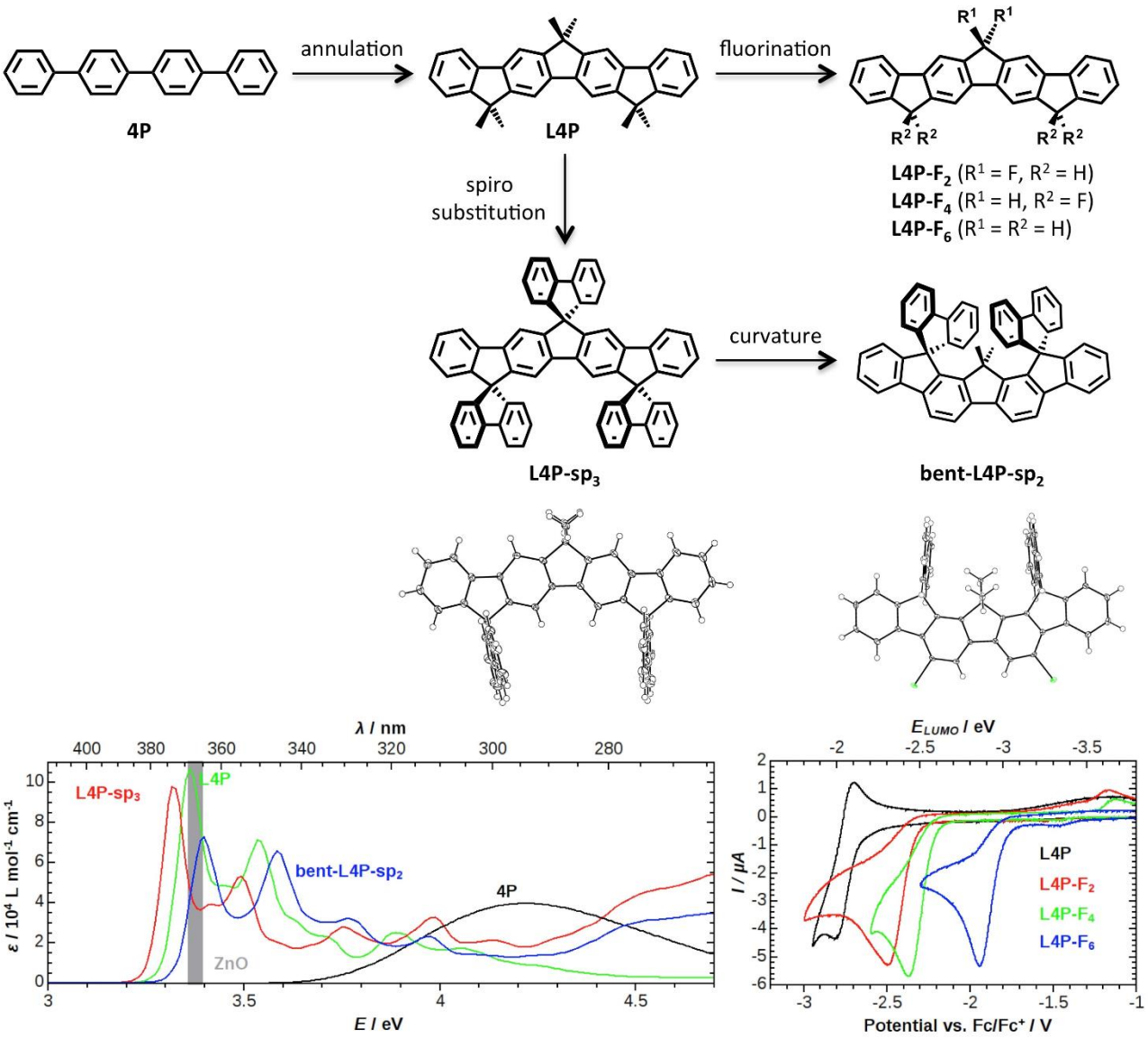

Fig. 1: Structural evolution of π-conjugated organic molecules with favorable optical properties: Rigidification of **4P** leads to ladder-type quarterphenyl **L4P** (for narrow and intense absorption and emission bands separated by a small Stokes' shift), which can either be fluorinated in the bridge to yield **L4P-F$_n$** (for lower MO-levels and introduction of dipoles) or spiro-substituted to yield **L4P-sp$_3$** (for improved photochemical stability). Finally, introduction of in-plane curvature leads to **bent-L4P-sp$_3$** with a slight blue-shifted absorption spectrum perfectly resonant to ZnO. Below the chemical formulae the molecular structures of **L4P-sp$_3$** and a **bent-L4P-sp$_3$** derivative as obtained by single crystal X-ray diffraction are shown. At the bottom, absorption spectra of **4P**, **L4P**, **L4P-sp$_3$**, and **bent-L4P-sp$_2$** (in CH_2Cl_2 solution, slight red-shifted absorption in the solid state; gray bar: emission of ZnO quantum well at low temperature) as well as cyclic voltammetry results for **L4P**, **L4P-F$_2$**, **L4P-F$_4$**, and **L4P-F$_6$** (0.1 M Bu_4NPF_6 in DMF; dE/dt = 1 V/s) including estimated LUMO energy levels are shown. More details can be found in refs. 4 and 5.

Furthermore, it should be mentioned that the LOPPs' substitution pattern has been optimized to assure their deposition onto the inorganic semiconductor substrate either from vacuum (by evaporation) or from solution. By omitting solubilizing side chains to limit the molecular weight and by avoiding thermally sensitive substituents, the LOPPs could be evaporated thereby aiding HIOS preparation but also greatly facilitating their initial high-level purification by means of gradient sublimation (sublimation apparatus was purchased and successfully established in the initial funding period). It should be noted that in many cases high-quality crystals could be grown, either from solution or by gradient sublimation, and their packing behavior has been analyzed [see for example 5].

In collaboration with a variety of groups within the CRC, most importantly A5 (Henneberger), B3 (Blumstengel), and A8 (Koch), the LOPPs in combination with ZnO have been implemented into new HIOS with superior properties. For example, resonant coupling of the organic and inorganic components could be achieved, enabling efficient light harvesting and emission, but also lasing could be demonstrated. See their reports for more details.

In addition to establishing and optimizing LOPPs for the use in HIOS with ZnO, sexiphenyl derivatives have been explored to investigate structural factors that govern their self-assembly on semiconductor surfaces. For this purpose, we first deviced a synthetic route to access non-symmetrically substituted (but otherwise unsubstituted) sexiphenyl rigid rods. Such compounds possessing a dipole along their molecular axis had thus far not been known as their insoluble nature precluded their synthesis and purification by conventional techniques. Recently, we could overcome this issue and prepare these compounds via a soluble desymmetrized precursor, which was planarized to the insoluble products in the final step of the synthesis (Fig.2) [7]. Once again gradient sublimation turned out to be the method of choice for purifying the desired products.

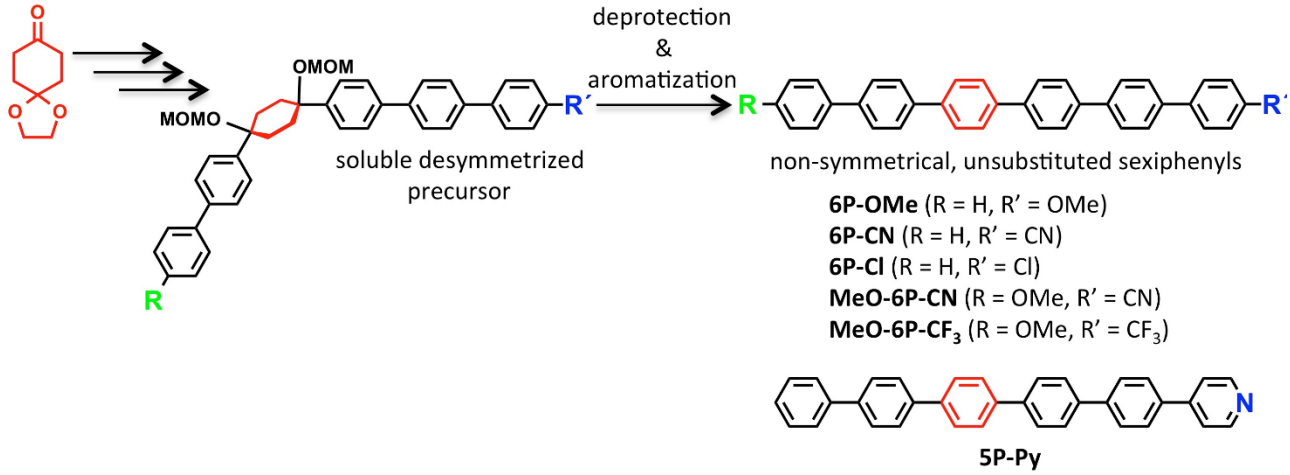

Fig. 2: Synthesis of insoluble non-symmetrical sexiphenyl derivatives: Introduction of biphenyl and terphenyl substituents to a monoketal-protected 1,4-cyclohexanedione unit (red) gives the soluble desymmetrized key precursors, which after deprotection of the methoxymethyl (MOM) groups and oxidation yield the desired sexiphenyl derivatives carrying various donor and acceptor functionalities at their termini and no solubilizing groups. More details can be found in ref. 7.

Within the CRC these new dipolar sexiphenyl derivatives have been investigated, for example with regard to their self-assembly on various surfaces in project A8 (Koch) or in the case of **5P-Py** as elongated π-conjugated pyridine derivatives on ZnO in project B9 (Stähler/Wolf). Furthermore, symmetrically fluorinated sexiphenyls have been investigated with regard to their self-assembly and growth behavior by projects A9 (Kowarik) and B3 (Blumstengel).

Covalent assembly

In the second subproject we worked towards the covalent connection of molecular monomer units to prepare π-conjugated polymers directly on semiconducting substrates, in particular ZnO. For this purpose we and A2 (Grill) wanted to adapt our on-surface polymerization technique [1] to thin ZnO films grown on metal substrates to enable STM imaging. For this purpose we prepared a few aromatic dihalide monomers, for example diiodoterfluorene (**3F-I_2**), which displays a lower activation temperature than the bromine analogue (**3F-Br_2** [2]) as observed in our hierarchical 2D network growth via sequential activation [12]. However, A2 (Grill) encountered significant problems in establishing reliable conditions for extended ZnO thin film growth and Leonhard Grill accepted a chair at the University of Graz and moved. Hence, we looked for an alternative collaboration partner outside the CRC and became involved with the group of Prof. Marek Szymonski (Krakow), who is an expert in STM on semiconducting substrates. His student Marek Kolmer investigated dibromodianthracene monomers [3] as well as our **3F-I_2** on reduced rutile substrates TiO2 and could show that on-surface polymerization to polyfluorene (**PF**) chains indeed occurs (Fig. 3). The exact mechanism and the origin of the polymerization's tolerance for hydrogen-termination (in contrast to a conventional radical dimerization process) are currently subject of experimental and theoretical investigations.

In collaboration with A5 (Henneberger) there have been polymerization experiments with **3F-I$_2$** and related monomers on ZnO, which rely on optical spectroscopy for monitoring growth of the π-conjugated **PF**. The growth conditions are currently being optimized to subsequently prepare **PF**@ZnO in-situ and characterize the resulting HIOS by various spectroscopy and microscopy techniques.

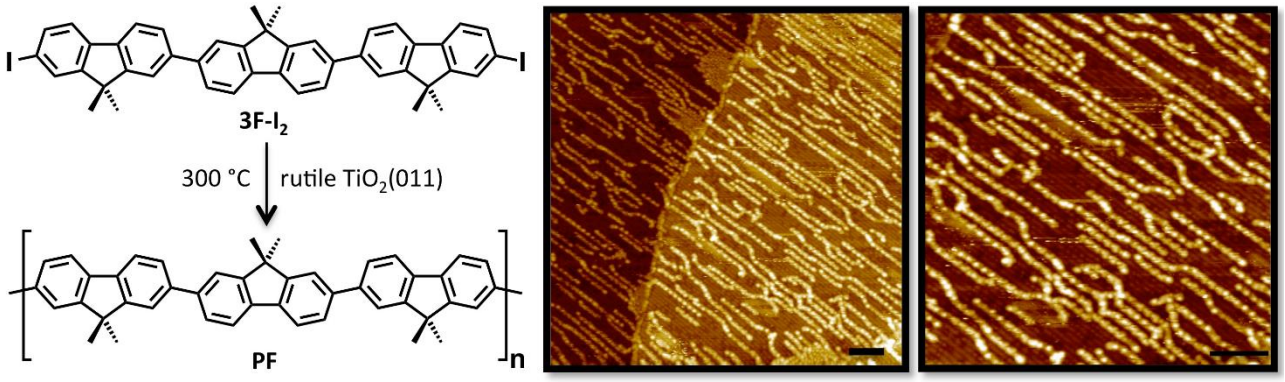

Fig. 3: On-surface polymerization on a semiconducting transition metal oxide substrate: Heating α,ω-diiodoterfluorene **3F-I$_2$** on a reduced rutile TiO2 (011) surface leads to formation of polyfluorene **PF** as evidenced by STM imaging of individual polymer chains at 7 K (scale bars = 10 nm). This work was done in collaboration with the group of Prof. M. Szymonski (Krakow).

Additional research activities relevant for the second funding periode

In addition to the above described work on non-covalent and covalent assembly carried within the framework of the CRC, there have been relevant activities with regard to develop concepts to modulate charge transport in devices by light. By blending properly designed photochromic diarylethene derivatives into a polymeric semiconductor matrix of regioregular poly(3-hexylthiophene) photoaddressable transistors have been prepared in collaboration with Prof. Samori (Strasbourg). Our approach relies on the dispersed switch molecules to act as photoswitchable hole traps and therefore block charge transport in one form, while not interfering with charge transport in the other form. Since the interconversion between these two forms can be conveniently triggered photochemically, the transistor operation can be controlled by light (Fig. 4).

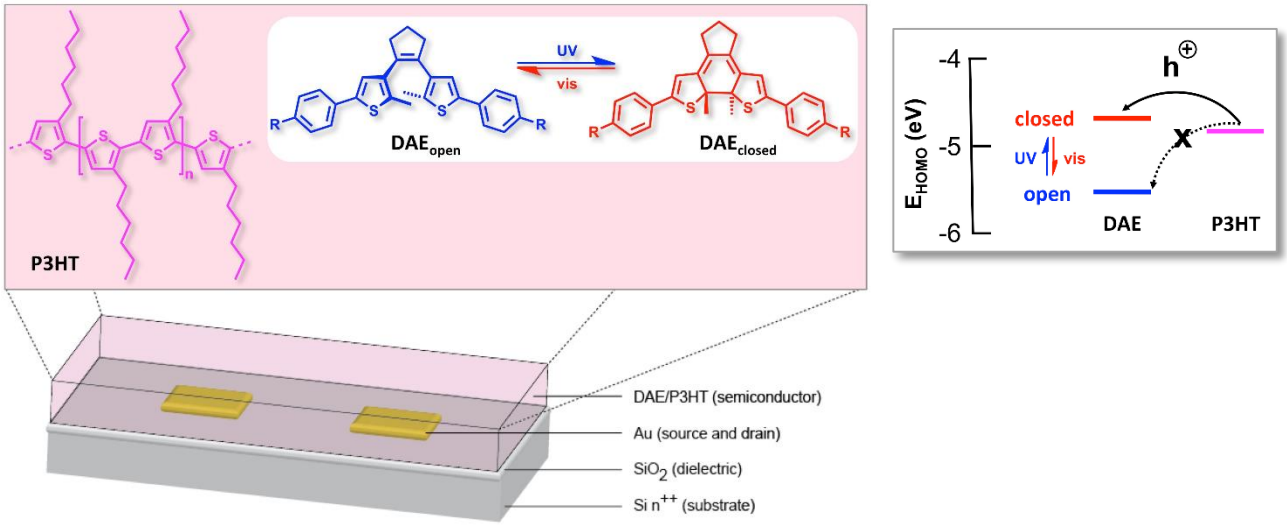

Fig. 4: Light-gated charge transport in organic thin film transistors via switchable hole traps: Upon UV-irradiation of diarylethene (DAE) photoswitches, blended into the polymeric semiconductor matrix (P3HT), the formed ring-closed isomer **DAE$_{closed}$** exhibits a dramatically reduced ionization potential (high-lying HOMO level) and acts as hole trap thereby blocking charge transport (OFF state), while visible light regenerates the initial ring-open isomer **DAE$_{open}$** and restores the original ON state. This work was done in collaboration with the groups of Prof. Samori (Strasbourg) and Norbert Koch (A8). More information can be found in refs. 9 and 10.

Since the initial proof of concept, various aspects have been studied and improved, in particular the blending of the small switch molecules in the organic matrix. However, it should be pointed out that the approach

relies on a bulk phenomenon and an organic-organic interface, similar to molecular approaches consisting of donor-switch-acceptor triads [11]. Therefore, a conceptually different and potentially more general and powerful approach to reversibly photomodulate the energetics at an inorganic semiconductor surface and the resulting HIOS is highly desirable and will be developed in the upcoming funding period. For this purpose dihydropyrene (DHP) derivatives will be the photochromes of choice since they display … [refs]. Initial experience with this often neglected yet highly promising class of photochromes has successfully being built up by Yves Garmshausen during his Diploma Thesis.

References

[1] L. Grill, M. Dyer, L. Lafferentz, M. Persson, M. V. Peters, and S. Hecht, Nat. Nanotechn. **2,** 687 (2007).
[2] L. Lafferentz, F. Ample, H. Yu, S. Hecht, C. Joachim, and L. Grill, Science **323**, 1193 (2009).
[3] M. Kolmer, A. A. Ahmad Zebari, J. S. Prauzner-Bechcicki, W. Piskorz, F. Zasada, S. Godlewski, B. Such, Z. Sojka, and M. Szymonski, Angew. Chem. Int. Ed. **52**, 10300 (2013).

3.3.2 Project-related publications

[4] B. Kobin, L. Grubert, S. Blumstengel, F. Henneberger, and S. Hecht, “Vacuum-processible ladder-type oligophenylenes for organic-inorganic hybrid structures: Synthesis, optical and electrochemical properties upon increasing planarization as well as thin film growth”, J. Mater. Chem. **22**, 4383 (2012).
[5] B. Kobin, L. Grubert, S. Mebs, B. Braun, and S. Hecht, “Gradual fluorination of ladder-type quarterphenyl”, Isr. J. Chem. **54**, 789 (2014).
[6] B. Kobin, F. Bianchi, S. Halm, J. Leistner, S. Blumstengel, F. Henneberger, and S. Hecht, “Green emission in ladder-type quarterphenyl: Beyond the fluorenone-defect”, Adv. Funct. Mater., published online DOI: 10.1002/adfm.201402638.
[7] Y. Garmshausen, J. Schwarz, J. Hildebrandt, B. Kobin, M. Pätzel, and S. Hecht, “Making nonsymmetrical bricks: Synthesis of insoluble dipolar sexiphenyls”, Org. Lett. **16**, 2838 (2014).
[8] M. Höfner, B. Kobin, S. Hecht, and F. Henneberger, “Strong coupling and laser action of ladder-type oligo(p-phenyl)s in a microcavity”, Chem. Phys. Chem., published online DOI: 10.1002/cphc.201402492.
[9] E. Orgiu, N. Crivillers, M. Herder, L. Grubert, M, Pätzel, J. Frisch, E. Pavlica, D. T. Duong, G. Bratina, A. Salleo, N. Koch, S. Hecht, and P. Samorì, “Optically switchable transistor via energy-level phototuning in a bicomponent organic semiconductor”, Nat. Chem. **4**, 675 (2012).
[10] J. Frisch, M. Herder, P. Herrmann, G. Heimel, S. Hecht, and N. Koch, “Photoinduced reversible changes in the electronic structure of photochromic diarylethene films”, Appl. Phys. A **113**, 1 (2013).
[11] S. Castellanos, A. A. Vieira, B. M. Illescas, V. Sacchetti, C. Schubert, J. Moreno, D. M. Guldi, S. Hecht, and N. Martín, “Gating charge recombination rates through dynamic bridges in tetrathiafulvalene-fullerene architectures”, Angew. Chem. Int. Ed. **52**, 13985 (2013).
[12] L. Lafferentz, V. Eberhardt, C. Dri, C. Africh, G. Comelli, F. Esch, S. Hecht, and L. Grill, "Controlling on-surface polymerization by hierarchical and substrate-directed growth", Nat. Chem. **4**, 215 (2012).
[13] C. Bronner, S. Stremlau, M. Gille, F. Braußе, A. Haase, S. Hecht, and P. Tegeder, “Aligning the band gap of graphene nanoribbons by monomer doping”, Angew. Chem. Int. Ed. **52**, 4422 (2013).

3.4 Research plan

3.4.1 Objective

This project primarily aims at designing and preparing organic molecular building blocks with specific optolectronic properties that can be integrated into structurally and compositionally well-defined HIOS when grown on inorganic semiconductor surfaces, in particular on ZnO and GaN (as well as Si). The resulting HIOS will be fabricated and evaluated with regard to their hybrid characteristics in collaboration with other group in the CRC.

…potentially list…

3.4.2 Methods

Work in this project largely involves the preparation of organic molecules via multi-step synthetic routes followed by extensive purification of the target compounds and their structural characterization. In addition, the compounds’ optical and electronic properties in solution and thin film as well as their thermal stabilities and structure formation in the crystalline solid will be investigated. Furthermore, binding studies will be carried out. Hence, methods utilized in this project include:

- Organic synthesis (aromatic and heteroaromatic syntheses, cross-coupling reactions, side-chain introduction, oligomer syntheses via divergent and convergent routes, among others),
- Purification methods (preparative high-performance liquid chromatography (HPLC) or gel permeation chromatography (GPC), recrystallization, zone and plate sublimation),
- Structure elucidation in solution by nuclear magnetic resonance (NMR) and mass spectrometry,
- Structure elucidation in the solid by Xray diffraction (single crystal or powder),
- Thermal stability by thermal gravimetric analysis (TGA) and phase behaviour by differential scanning calorimetry (DSC),
- Optical properties in solution and thin film (UV/vis absorption, emission),
- Electrochemical properties in solution (cyclic voltammetry),
- Isothermal titration calorimetry (ITC) and NMR for binding studies.

Note that HIOS preparation using the molecular building blocks synthesized in this project will be carried out in several collaborating projects throughout the CRC (as detailed below in 3.4.3). The involved PhD students will closely interact with these projects to discuss the results and improve the organic components.

3.4.3 Work plan

The project is divided into two subprojects, one concerned primarily with the design of suitable π-conjugated systems and (switchable) dipolar mediator units and constructs thereof while the other one is exploring assembly strategies to prepare (mostly) covalently and regioselectively bound HIOS. As both approaches have different requirements on the needed molecular components, the work plan, which will be carried out by (at least) two graduate students independently, is detailed for each subproject below:

First subproject:

Molecular Design

Conjugated molecular systems for organic layers in HIOS: In particular, we will be focusing on organic semiconductors in combination with ZnO and GaN as well as Si surfaces. Important parameters include electronic and optical properties as well as assembly behavior and processability. Work started during the initial funding period with the focus to develope and optimize lead structures for organic semiconductors, in particular LOPPs, allowing for resonant energy transfer in conjuction with ZnO, we will now also include donor and acceptor molecules to tune charge transfer at HIOS interfaces. Compound classes that will be investigated include LOPPs as well as (oligo)triarylamine and oligo(thiophene) donors (Fig. 5). By carefully chosing their molecular conformation and the point of attachment, their relative orientation to the surface normal will be controlled. Of course, the attachment implies the use of covalent anchoring groups as detailed in the other subproject. In addition to covalent attachment we will continue to investigate the self-assembly behavior in physisorbed layers, in particular the influence of the relative orientation of molecular dipole and molecular axes.

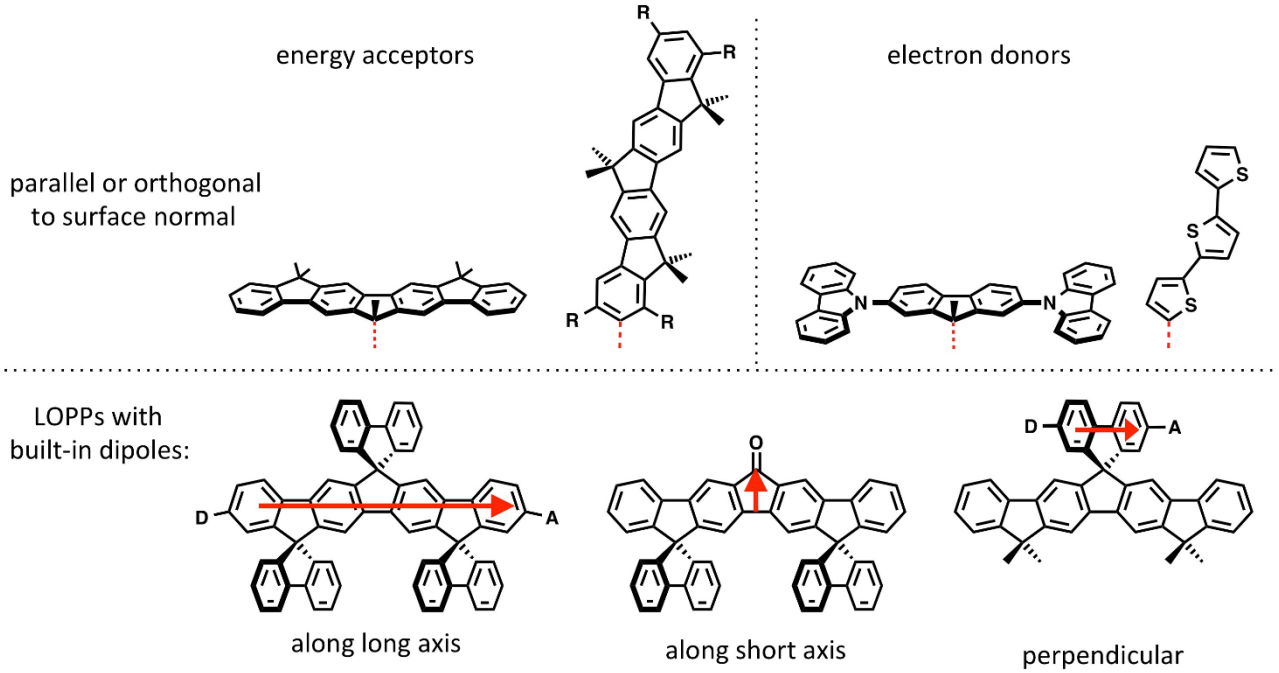

Fig. 5: Overview of π-conjugated systems to be investigated: LOPPs as well triarylamine and oligo(thiophene) donors with defined orientation in covalently bound layers (red dashed line marks point of covalent attachment, and LOPP-based rigid-rods with dipoles oriented along the long and short axes of the molecule as well as orthogonally to them for controlling self-assembly on polar ZnO and GaN surfaces.

Mediating coupling at HIOS interfaces: In the initial funding period, our work was primarily aiming at tailoring the organic layer to be complementary to the inorganic layer, which in some cases was modified by a self-assembled monolayer to tune the work function of the ZnO [ref. AFM?]. In contrast, we now want to mediate the coupling at the HIOS interface by investigating the role of static dipoles, which are covalently connecting both HIOS layers (Fig. 6).

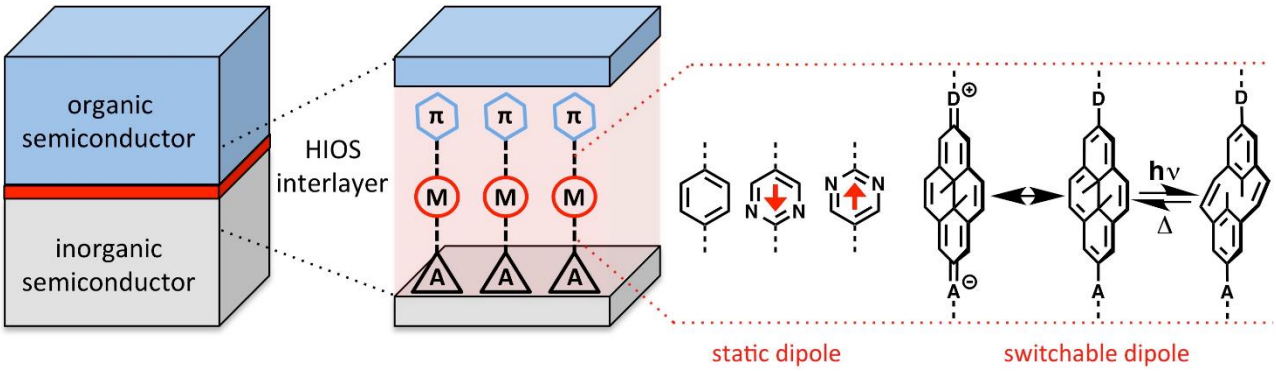

Fig. 6: Concept of HIOS interlayer with static and dynamic coupling: By covalently connecting the desired conjugated systems (π) to anchoring groups (A) via a mediator (M), the latter mediates the coupling either by a static dipole, which can be adjusted in orientation and strength, or a dynamic dipole, which can be reversibly generated by an external light-stimulus.

Once, the influence of the dipole strength and orientation on the coupling has been investigated, we will take a step further and introduce switchable dipoles instead to mediate the HIOS interfacial coupling by an external stimulus, in this case light. Detail specifics about dihydropyrene switches…

Timeline. Within the first two years, various conjugated molecular systems (see Fig. 5) will be synthesized and characterized. Furthermore, they will be attached to various mediator moieties and anchoring groups. Subsequently, dihydropyrenes carrying donor and acceptor functionalities will be synthesized and their switching behavior analyzed. Constant feedback from the collaborative projects within the CRC about the utility of the prepared organic materials for HIOS preparation, work will focus on the most promising oligomers and their further synthetic optimization.

Second subproject:

Molecular Assembly

The second subproject deals with the development of new covalent surface functionalization chemistry on ZnO and GaN. For this purpose, we will first compare the binding of various simple ligands (pyridines, phenols, etc.) as well as chelate ligands (phosphonates vs. phosphates, sulfonates vs. sulfates, bisphosphonates, etc.) and investigate the impact of enviromental conditions (solvent, pH, temperature) on binding. Based on the derived intrinsic binding characteristics, ligands will be designed to bind strongly to ZnO (or GaN) yet to discriminate between the non-polar and the non-polar surfaces. For this purpose, rigid scaffolds possessing the right ligands in the correct distance and angle will be designed (Fig. 7).

…detailed ligand design and experimental description…

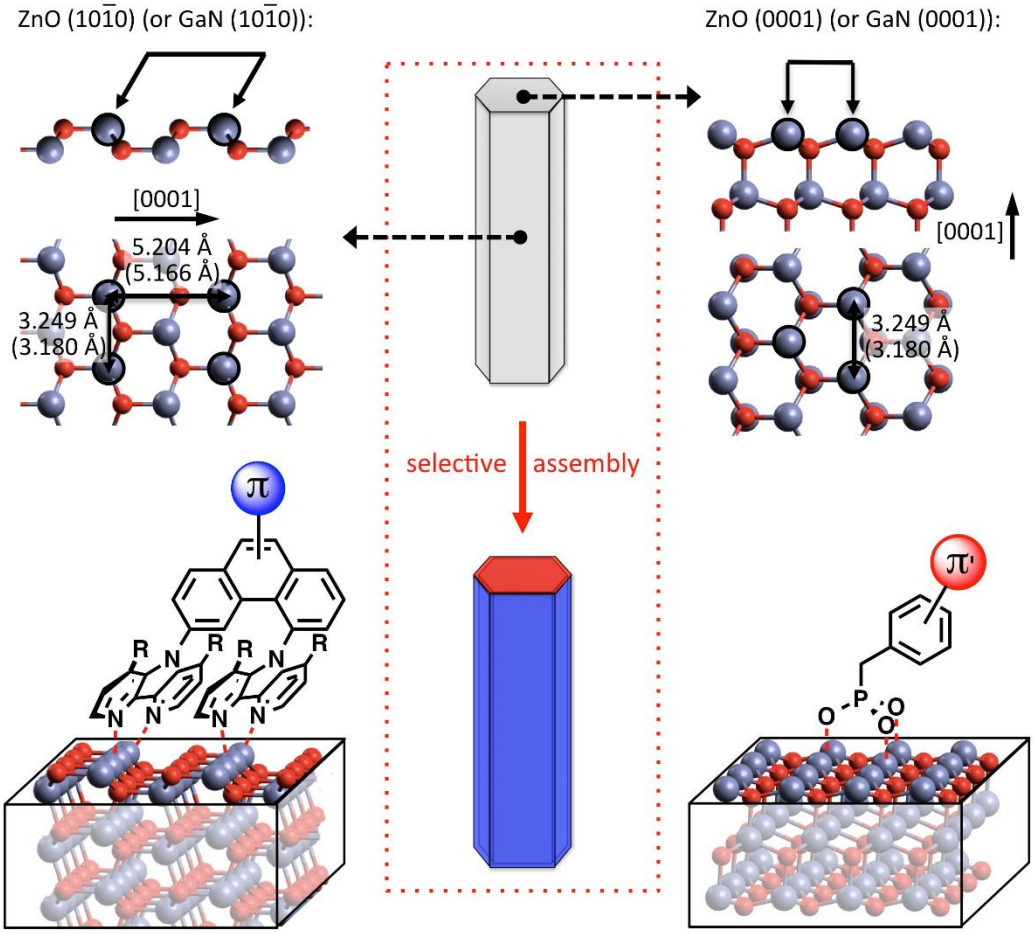

Fig. 7: Design of face-selective ligands for the polar and non-polar ZnO (and GaN) surfaces: Exploiting the different symmetry and periodicity of the non-polar and polar ZnO (and GaN) surfaces to construct selective ligands with a rigid structure to recognize either the rectangular or trigonal Zn-atom pattern. Ultimately, mixing the two components with a ZnO (or GaN) nanorod should enable multicomponent self-assembly into a defined HIOS architecture, for example a light-harvesting and terminally emitting nanorod. Note that numbers in parentheses refer to the distances of the respective GaN surfaces.

Timeline. Initial binding studies will occupy the first year, afterwards the ligand will be prepared and tested …

3.5 Role within the Collaborative Research Centre

This project develops new strategies to create a significant part of the HIOS' organic materials basis (in addition to other standard organic components available either commercially or via Z1) and therefore it is strongly connected to various projects in project areas A and B of the CRC. This project's expertise in the choice and design of molecular components, their preparation and structure optimization will continue to be a

significant advantage of the CRC. Hence, we tackle new syntheses and novel target structures to provide unique organic building blocks for the construction of superior HIOS as a prerequisite for the fundamental studies of their structure and properties within the CRC.

Our interactions within the CRC relate to several different lines of expertise of the collaborating projects, namely: the preparation of HIOS, their structural characterization, the resulting electronic and optical property investigations, as well as interactions with computation and theory. Hence, the following collaborations are planned or already ongoing:

- Preparation of non-covalent self-assemblies on various ZnO surfaces (first subproject) with A2 (Kumagai/Wolf, evaporation, ZnO), A5 (Henneberger, OMBD/MBE, ZnO), A8 (Koch, evaporation, ZnO),
- Investigation of the thus generated HIOS' structure and growth with A2 (Kumagai/Wolf, STM, ZnO), A8 (Koch, AFM/XPS, ZnO), A11 (Christiansen), and Z2 (Kowarik, X-ray diffraction, ZnO),
- Electronic and optical characterization of the prepared HIOS with A8 (Koch, UPS, ZnO), A11 (Christiansen, nanoparticles), B3 (Blumstengel, photoluminescence/excitation spectroscopy, ZnO), B9 (Stähler, 2PPE, ZnO)…
- Intense interaction with quantum chemistry performed in A4 (Heimel) to aid molecular design.

It should be pointed out that the interaction is bidirectional and hence results from the collaborating groups will be taken into account in the next molecular design to yield efficient feedback loops and continuous optimization of the organic components to finally achieve attractive HIOS properties.

3.6 Delineation from other funded projects

The principle investigator of the project is participating in the CRC 658 "Elementary processes in molecular switches at surfaces" (final funding period until 06/2017) and is currently also funded by an ERC Starting Grant (Consolidator Phase) "Light4Function" (until 12/2017). While in the CRC 658 project diarylethenes and spiropyrans are being used to photomodulate the charge transport through carbon nanotubes and graphene, one relevant subproject of the ERC project aims at photomodulating charge transport in organic transistors consisting of blends of diarylethenes in commercial organic semiconductor matrices. None of these projects involves inorganic semiconductors. In contrast, the project proposed herein is based on completely different compound classes and specifically involves the design and synthesis of novel organic semiconductors (mostly LOPPs), novel organic dipole switches (DHPs), as well as completely new ligands for selective covalent functionalization of inorganic semiconductor surfaces.

3.7 Project funds

3.7.1 Previous funding

The project has been funded within the Collaborative Research Centre since 07/2011.

3.7.2 Funds requested

Funding for	2015/2		2016		2017		2018		2019/1	
Staff	Quantity	Sum	Quantity	Sum	Quantity	Sum	Quantity	Sum	Quantity	Sum
PhD student, 67%	2	39.400	2	78.800	2	78.800	2	78.800	2	39.400
Student assistant	1	3.000	1	6.000	1	6.000	-	-	-	-
Total		42.400		84.800		84.800		78.800		39.400
Direct costs	Sum		Sum		Sum		Sum		Sum	
Consumables	6.000		12.000		12.000		12.000		6.000	
Other	-		-		-		-		-	
Total	6.000		12.000		12.000		12.000		6.000	
Major research equipment	Sum		Sum		Sum		Sum		Sum	
€ 10.000 - 50.000	-		-		-		-		-	
> € 50.000	-		-		-		-		-	
Total	-		-		-		-		-	
Total	48.400		96.800		96.800		90.800		45.400	

(All figures in Euro)

3.7.3 Staff

	No.	Name, academic degree, position	Field of research	Department of university or non-university institution	Commitment in hours/week	Category	Funded through:
Available							
Research staff	1	Hecht, Stefan, Prof.	Organic Chemistry	HU Chem	5		HUB
	2	Kobin, Björn, (Dr.)	Organic Chemistry	HU Chem	10		HUB
	3	Pätzel, Michael, Dr.	Organic Chemistry	HU Chem	5		HUB
	4	Kathan, Michael, M.Sc.	Organic Chemistry	HU Chem	20		HUB
Non-research staff	5	Schwarz, Jutta, Chem-Technician		HU Chem	10		HUB
	6	Voigtländer, Daniela, Admin. Assistant		HU Chem	5		HUB
Requested							
Research staff	8	Garmshausen, Yves, Dipl.-Chem.	Organic Chemistry	HU Chem		2/3 E13	
	9	Liesfeld, Pauline, (M.Sc.)	Organic Chemistry	HU Chem		2/3 E13	
Non-research staff	10	N.N.	Organic Chemistry	HU Chem		SHK	

Job description of staff (supported through available funds):

1) S. Hecht: Scientific and organisational management of the project, supervision of PhD students and staff scientists, planning and managing collaborations, discussion of experiments, interpretation and dissemination of results.
2) B. Kobin: Responsible for electrochemistry (cyclovoltammetry) measurements and analytical methods, support for PhD students.
3) M. Pätzel: Additional experimental support for PhD students by supervision of related undergraduate activities (research tutors, internships).
4) M. Kathan: Design and synthesis of various scaffolds and anchoring groups and exploration for selective covalent surface functionalisation.
5) J. Schwarz: Synthetic support by preparation of advanced starting materials and precursor molecules.
6) D. Voigtländer: Administrative support (ordering/purchasing, accounting, contracting).

Job description of staff (requested):

7) Y. Garmshausen: This PhD student will focus on developing new π-conjugated molecular building blocks with specific optoelectronic properties and control their coupling to the underlaying inorganic semiconductor substrates. He will synthesize various triads consisting of a suitable anchoring group for covalent surface mounting, a static or switchable coupling unit to mediate the interfacial communication, and a suitable π-conjugated active moiety for absorption/emission or charge injection/extraction. He will characterize the individual components as well as the dyads and triads with regard to their structure as well as optoelectronic and switching properties. He will interact closely with the collaborating projects A5 (Henneberger), A8 (Koch), B3 (Blumstengel), B7 (Neher) and B9 (Stähler). During the initial funding periode and within the framework of his PhD dissertation work he has thus far been involved in the synthesis of various non-symmetrically substituted sexiphenyl derivatives for HIOS.

8) P. Liesfeld: This PhD student will focus on developing new anchoring scaffolds for selective covalent assembly on specific inorganic semiconductor surfaces. She will design various ligand target structures and synthesize them by connecting rigid aromatic bridge moieties with suitable (bifunctional) anchoring groups. In addition, she will investigate their binding properties at different inorganic semiconductor surfaces with regard to their structure, energetics, and dynamics. She will closely interact with the collaborating projects A2 (Kumagai/Wolf), A4 (Heimel), and A11 (Christiansen) regarding the preparation and characterization of the targeted HIOS. Within the framework of her Master thesis she is currently working in the group of Prof. Fischer (UC Berkeley) on the on-surface synthesis of various conjugated nanostructures.

3.7.4 Direct costs for the new funding period

	2015/2	2016	2017	2018	2019/1
Funds available	3.000	6.000	6.000	6.000	3.000
Funds requested	6.000	12.000	12.000	12.000	6.000

(All figures in Euro)

Consumables for 2015/2

Chemicals for syntheses	EUR	2250
Catalysts (Pd-complexes, ligands)	EUR	500
(Deuterated) solvents (NMR, UPLC, GPC)	EUR	1250
Silica gel for column chromatography	EUR	1000
Syringes, needles, septa	EUR	500
Glassware	EUR	500

Consumables for 2016, 2017, and 2018

Chemicals for syntheses	EUR	4500
Catalysts (Pd-complexes, ligands)	EUR	1000
(Deuterated) solvents (NMR, UPLC, GPC)	EUR	2500
Silica gel for column chromatography	EUR	2000
Syringes, needles, septa	EUR	1000
Glassware	EUR	1000

Consumables for 2019/1

Chemicals for syntheses	EUR	2250
Catalysts (Pd-complexes, ligands)	EUR	500
(Deuterated) solvents (NMR, UPLC, GPC)	EUR	1250
Silica gel for column chromatography	EUR	1000
Syringes, needles, septa	EUR	500
Glassware	EUR	500

The consumables necessary for both synthetically working PhD students amount to 6000 Euros per year for each person. These costs are associated primarily with the purchase of expensive fine chemicals and catalysts, as well as (deuterated) solvents and silica gel for chromatographic separations.

3.7.5 Major research equipment requested for the new funding period

No funding for instrumentation is requested.

3.7.6 Student assistants

	2015/2	2016	2017	2018	2019/1
Quantity	1	1	1	-	-
Commitment in hours/week	10	10	10	-	-
Sum	3.000	6.000	6.000	6.000	3.000
Tasks	The student assistant (1st semester Master student) will be supervised directly by one of the involved PhD students (Y. Garmshausen) and become increasingly familiar with the project to eventually succeed her/his mentor as PhD student in the end of 2017. Specifically, she/he will synthesize various starting materials and intermediates for the different triad moieties.				

3.1 About project A4

3.1.1 Title: Surface-selective functionalization of inorganic semiconductors

3.1.2 Research areas:

307-02 Theoretische Physik der kondensierten Materie
302-03 Chemische Festkörper- und Oberflächenforschung / Theorie und Modellierung
303 Physikalische und Theoretische Chemie

3.1.3 Principal investigator

Dr. Techn., Heimel, **Georg** (*24.02.1975, Austria)
Institut für Physik
Humboldt-Universität zu Berlin
Newtonstr. 15
12489 Berlin
Germany
Phone: +49 (0)30 2093 7537
Fax: +49 (0)30 2093 7443
E-mail: georg.heimel@physik.hu-berlin.de

Does the above mentioned person hold a fixed-term positions? no
Georg Heimel:
End date 30.6.2015
Further employment is planned until 30.6.2019

3.1.4 Legal issues

This project includes

1.	research on human subjects or human material.	no
2.	clinical trials	no
3.	experiments involving vertebrates.	no
4.	experiments involving recombinant DNA.	no
5.	research involving human embryonic stem cells.	no
6.	research concerning the Convention on Biological Diversity.	no

3.2 Summary

In the first funding period of CRC 951 “HIOS”, project A4 employed methods of first-principles electronic structure theory to assess the possibility of stabilizing ZnO surfaces, whose atomistic structure and stoichiometry notoriously depend on preparation conditions and environmental factors, with covalently attached, self-assembled monolayers (SAMs) of organic molecules. At the same time, these SAMs were envisioned to allow tuning the work function of the ZnO surfaces and, thereby, the energy alignment between the inorganic-semiconductor band edges and the transport states in a subsequently deposited organic semiconductor.

Suitable SAM molecules were indeed identified and their properties predicted, facilitating the interpretation of experiments performed by partners within the CRC, which demonstrated that the intended function could be achieved. After identifying deep-rooted conceptual inconsistencies in the commonly accepted literature approach to predicting surface structures and stoichiometries, project A4 invested significant resources into reformulating the theory, which then allowed revising existing predictions for bare ZnO surfaces and, importantly, providing unprecedented insight into the structure and stoichiometry of SAMs on ZnO surfaces. Not only could reliable predictions for the thermodynamically most stable structures now be given, but calculated reaction/diffusion barriers also shed light onto kinetics. Experimentally accessible quantities were then computed for the established systems. Further methodological developments that now allow treating

spatially extended band-bending regions on both sides of a HIOS interface and supporting calculations for sub-projects on a more coarse-grained level of theory complement the achievements of A4 in the first period. Building upon this experience and fully capitalizing on the methodological developments, the first goal for the second funding period is to now approach the technologically more relevant scenario of predicting the atomistic structure and stoichiometry of SAMs on ZnO surfaces also in solution. In particular, the possibility for the surface-selective functionalization of ZnO will be assessed by exploring the competitive binding of different chemical anchoring groups to different ZnO crystal faces in different solvents with a combined first-principles and thermodynamic approach. Extending the range of considered materials in response to experimental efforts within the CRC, these investigations will be continued also on GaN surfaces once a working methodology is in place. Computing a series of properties will yield experimentally testable predictions.

The second goal of project A4 for the second funding period is to further raise the complexity of the investigated SAMs. In addition to simply modifying the work function of the underlying inorganic semiconductor, multiple functionalities will now be integrated into the SAM itself in order to provide an atomistically defined HIOS system for the targeted study of interfacial hybrid charge-transfer excitons within the CRC. In particular, A4 will computationally explore the possibility for covalently linking an organic-semiconductor segment to a functional chemical unit that is grafted onto both ZnO and GaN surfaces with suitable anchoring groups. As functional units, both dipolar heterocycles and molecular switches are envisioned, which should allow tuning both the energy levels of the organic-semiconductor segment as well as its electronic coupling to the inorganic part, while maintaining a predictable interface geometry.

A combination of quantum-chemistry, periodic (hybrid) density-functional theory calculations (with vdW corrections), solvation models for the two, and thermodynamics will be employed to achieve these goals.

Molecular design will be coordinated with ***A3*** (*Hecht*) and methodological approaches with ***A10*** (*Tkatchenko/Scheffler*) as well as ***B4*** (*Körzdörfer/Scheffler/Rinke*). A4 will provide support for quantum-chemical calculations in ***B6*** (*May*) and will provide input from first-principles calculations on both molecules and surfaces for ***A7*** (*Klapp/Dzubiella*). Established structures will be forwarded to ***B11*** (*Draxl*). A close feedback loop will be established with ***A8*** (*Koch*), ***A11*** (*Christiansen*), ***B3*** (*Blumstengel*), ***B9*** (*Stähler*) and ***B7*** (*Neher*) to continuously assess and refine the theoretical methods employed in A4 and to provide guidance for both the design and the interpretation of the experiments performed there.

3.3 Project progress to date

3.3.1 Report and state of understanding

At the outset of the previous (and first) funding period of project A4 in this CRC 951 “HIOS” was the observation that the stoichiometry, structure, and properties of zinc-oxide (ZnO) surfaces notoriously depend on preparation and environmental conditions. The scientific question was if and, if so, how ZnO surfaces could be stabilized and their work functions tuned with covalently attached self-assembled monolayers (SAMs) of organic molecules. Addressing this question, A4 employed first-principles electronic-structure methods to:

(i) design and quantum-chemically characterize SAM-forming molecules;
(ii) determine the atomistic surface structure and stoichiometry of ZnO surfaces and SAMs;
(iii) predict a series of experimentally observable quantities to connect to other projects in the present CRC;
(iv) develop the computational methods necessary for conducting the theoretical studies listed above.

In the following, results, current efforts and – if applicable – encountered problems will be summarized for each of these four objectives and contrasted to anticipations formulated in the initial proposal.

ad i) Molecular design: In consultation with projects *A3* (*Hecht*) as well as *A8* (*Koch*) and B7 (*Neher*), who respectively synthesized and experimentally studied SAMs, the decision was made to first focus on phosphonic acid as chemical linker to the ZnO surfaces. To realize the molecular dipole moments required for work-function modification, a systematic series of phosphonic acids was mutually agreed upon with A4 contributing in particular the concept of pyrimidine-based dipolar heterocycles [31] – instrumental to realizing the more challenging scenario of low ZnO work functions. Hybrid density functional theory (DFT) was employed to compute the structures of all molecules, which allowed comparison with X-ray reflectivity measurements conducted in project *A9* (*Kowarik*). For the molecular dipole moment, careful convergence

test were performed, revealing Jensen's DFT-optimized, polarization-consistent basis set [1] as the optimal compromise between accuracy and computational cost. Together with the PI's previous observations on mutual depolarization of dipolar molecules in close-packed layers [2], a comprehensive picture of ZnO work-function tuning with SAMs could be established, as published in Ref. [32].
As envisioned in the proposal for the first funding period, supporting quantum-chemical calculations were also performed on individual organic-semiconductor molecules, notably *para*-sexiphenyl, coronene and hexabenzocoronene. Results, typically obtained at the hybrid-DFT level with the B3LYP exchange-correlation (XC) functional and the correlation-consistent, polarized, valence triple-ζ basis set (cc-pVTZ), served to derive atomic charges needed to parameterize classical force-fields employed in project *A1* (*Dzubiella*) and to benchmark resulting molecular structures and potential-energy surfaces. Results were duly published in Ref. [33]. Additionally, molecular quadrupole moments were forwarded to project *A7* (*Klapp*).

ad ii) Surfaces and SAMs: As proposed in the project description for the first funding period, these efforts started out by setting up the three bare ZnO surfaces studied in the present CRC 951, that is, the polar zinc-terminated (0001) and oxygen-terminated (000-1) as well as the non-polar mixed-terminated (10-10) surfaces, in all their previously proposed stoichiometries and reconstructions [3-9]. Relying, as announced, on the plane-wave DFT code VASP, a computational working methodology was subsequently established and convergence of key quantities with respect to all numerical parameters was carefully checked.

After relaxing all known reconstructions with these settings, first-principles thermodynamics was employed to construct phase diagrams which, according to literature [3-9], should yield the structure and stoichiometry of each ZnO surface as a function of temperature as well as H_2 and O_2 partial pressures. As envisioned, the structural phase diagrams of the bare ZnO surfaces could indeed be reproduced. Project A4 subsequently extended established knowledge by computing also the diffusion barriers of the adsorbates that define the various ZnO surface structures (typically OH^-, O^{2-}, or H^+) with the climbing-image nudged elastic-band (CL-NEB) method [10]. This was done to support experimental projects ***A5*** (*Henneberger*), ***A8*** (*Koch*), ***B3*** (*Blumstengel*), and ***B9*** (*Stähler/Wolf*) in developing preparation protocols for ZnO surfaces in ultra-high vacuum (UHV), *i.e.*, to see if different structures can readily interconvert or are kinetically hindered so as to persist under conditions, where steady-state thermodynamics predicts them to be unstable.

Further pursuing the proposed research plan, the next step was to employ first-principles thermodynamics again to now also assess the relative stabilities of SAMs as a function of temperature and the partial pressures of all adsorbates. It was during attempts of executing this last and, purportedly, almost trivial step that what initially seemed mere ambiguities in the method started to manifest themselves. Repeated attempts to resolve these ambiguities eventually led to the realization that, in fact, deep-rooted, conceptual inconsistencies lie at the very core of the theoretical framework underpinning first-principles thermodynamics, a well-recognized method widely applied to a broad variety of systems [3-9,11-19]. For project A4, this equally important and inconvenient finding represented a veritable show-stopper: In the absence of atomistically resolved experimental data on the structure of SAMs on ZnO surfaces, reliable structure prediction is a mandatory prerequisite for computing SAM properties. Without reliable structures that are likely to actually represent the situation encountered in experiment, calculating any properties is close to meaningless. Consequently, significant resources were invested into first understanding its shortcomings and, subsequently, into reformulating the theory. As detailed below (see **ad iv**), an elegant solution was eventually developed, which made progress along the originally formulated research plan possible again, albeit with some delay.

Back on track, the newly developed method could finally be put to its intended use, *i.e.*, the assessment of the thermodynamic stability against H_2, O_2, and H_2O of various chemical linkers that covalently bond functional molecules to ZnO surfaces. Staying with the (10-10) surface, where the lack of three-fold symmetry makes phosphonic acids a less obvious choice, the focus was first put on carboxylic acids, which match the two-fold surface symmetry, have been extensively employed in literature [20-22], and were used in ***B5*** (*Kühn/Elsässer*). Fig. 1 shows results for acetic acid, the molecule originally proposed as starting point.

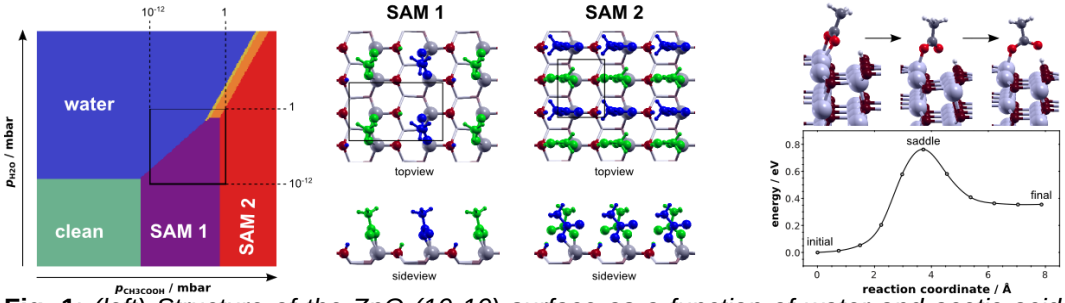

Fig. 1: *(left) Structure of the ZnO (10-10) surface as a function of water and acetic acid partial pressure in gas phase at T = 400 K with p_{H2} and p_{O2} fixed at 10^{-12} mbar. (centre) Structures of SAM 1 and SAM 2 with two inequivalent CH_3COOH molecules, green and blue, per (2x2) and (1x2) super cell, respectively. (right) Reaction path and barrier for rotating the molecules in SAM 1 towards their positions in SAM 2.*

With a working methodology in place and with major obstacles overcome, further calculations along the lines outlined above are currently under way on different ZnO surfaces, different chemical linkers such as phosphonic acids, and more complex SAM molecules.

ad iii) Link to experiment: Also here, A4 proceeded as proposed in the original project. Because X-ray photoelectron spectroscopy (XPS) turned out to be by far the most commonly employed experiment for characterizing ZnO surfaces, notably also in project ***A8*** (*Koch*), a strong focus was placed on this technique. To support experiment in determining the likely structure and stoichiometry of the bare ZnO surfaces emerging from the employed preparation protocol, oxygen 1s core-level shifts (relative to bulk O1s) were computed for all previously predicted and structurally distinct surface reconstructions [3-9]. To enable direct comparison with experiment, tabulated values for electron mean free paths were employed to construct actual spectra for various electron take-off angles at the experimentally employed photon energy (*hv* = 620 eV).

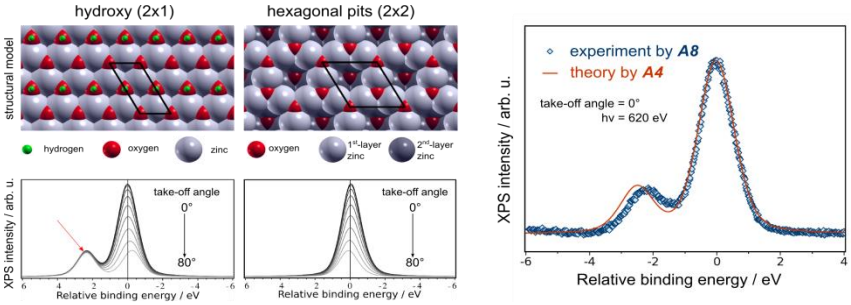

Fig. 2: *(left) Structural model and calculated O1s XPS spectra for two possible reconstructions of the O-terminated ZnO (000-1) surface. Unit cells are indicated in black and the OH-shoulder is marked by a red arrow. (right) comparison between theory and experiments performed in project **A8** (Koch).*

Fig. 2 shows the example of the O-terminated (000-1) surface, published in Ref. [37]. Excellent agreement between theory and experiment, both in surface core-level shift and spectral weight, suggests the structure shown in the leftmost panel, a (1x2) unit cell with every second surface oxygen carrying an adsorbed H-atom [4], to well represent the surface under experimental conditions. As revised phase diagrams for the structure of bare and SAM-covered ZnO surfaces emerge from ongoing work, similar core-level calculations and, additionally, hybrid-DFT calculations on surface electronic structure and work function are being undertaken.

ad iv) Tools and methods: As already highlighted in sub-section **ad ii)** above, applying atomistic electronic-structure theory to compute interface properties is only meaningful if the surface/SAM structure and, in particular, the stoichiometry, is known on the atomistic level as well. As experimental structure/stoichiometry determination at the required level of detail is cumbersome (if possible at all), A4 originally proposed to employ the well-established method of "first-principles thermodynamics", which is routinely used to predict the structure and stoichiometry of a broad variety of surfaces in particle exchange with various molecules in gas phase [3-9,11-19]. In the course of the project, however, it became apparent that deep-rooted, conceptual flaws plague this theory, precluding any further work. To appreciate how – after investing considerable resources – A4 overcame this critical point, a brief introduction to first-principles thermodynamics is required: The basic premise of this theory is that the most stable surface, composed of N_i units of species i with chemical potential μ_i, minimizes the excess Gibbs free energy γ per unit area A.

$$\gamma = 1/A \cdot (G_{surf} - \Sigma_i \mu_i N_i) \qquad (1)$$

The Gibbs free energies G_{surf} are typically approximated by DFT-calculated, zero-Kelvin, ground-state total energies E_{surf}. In the exemplary but highly relevant case of solid ZnO in particle exchange with an

atmosphere composed of the elements hydrogen and oxygen, μ_{ZnO} is furthermore approximated by the DFT-calculated energy e_{ZnO} per ZnO formula unit in the bulk. Eq. (1) then reads:

$$\gamma = 1/A\cdot(E_{surf} - e_{ZnO}N_{ZnO} - \mu_{H2}N_{H2} - \mu_{O2}N_{O2}) \qquad (2)$$

Plotting γ for each of a comprehensive set of surfaces varying in structure and numbers N_i of constituent components as a (linear) function of μ_{H2} and μ_{O2} then reveals the most stable surface under the conditions corresponding to a particular choice for the values of these chemical potentials as that with the lowest γ. To connect to experiment, the axes μ_{H2} and μ_{O2} of the resulting phase diagrams are then converted into respective partial pressures p_{H2} and p_{O2} at temperature T through

$$\mu_i(T,p_i) = E_i + \mu_{TD}(T,p_i) \qquad (3)$$

where E_i is, consistently, the DFT-calculated, zero-Kelvin, ground-state electronic energy of species i and the thermodynamic part, $\mu_{TD}(T,p_i)$, is well-known from statistical physics for ideal gases.

The important development in A4 is best explained on the (deceivingly) simple example of the non-polar, mixed-terminated ZnO (10-10) surface. The phase diagram constructed through the procedure outlined above is shown in Fig. 3a. At room temperature, the surface is predicted to be covered with water monolayer for all reasonable partial pressures p_{H2} and p_{O2} between 10^{-12} mbar and 1 bar [23]. Given this finding, however, the question inevitably arises why one would chose H_2 and O_2 as gaseous reservoirs in evaluating Eq. (2) and not simply water, which is equally part of ambient atmosphere and UHV residual gas.

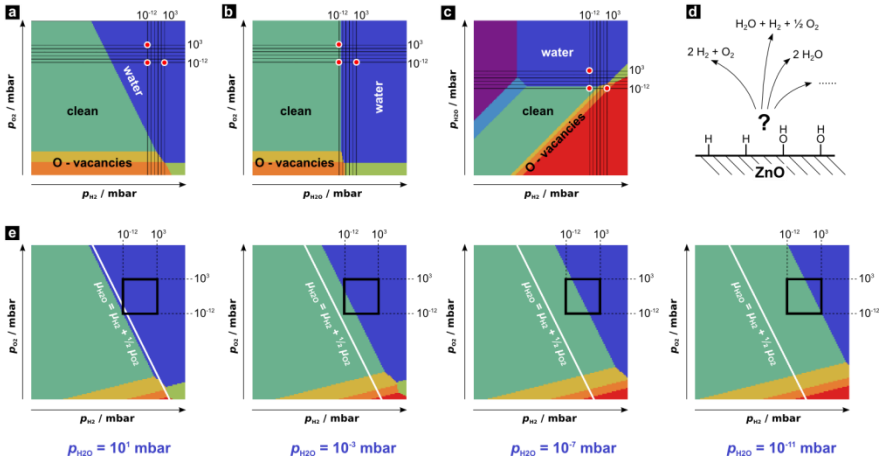

Fig. 3: *(a,b,c) Phase diagrams of the ZnO (10-10) surface at T = 300 K. Red dots highlight the difference between the predictions. (d) Illustration of the ambiguity in how to count ad-atoms on ZnO surfaces for evaluating the surface energy. (e) Revised phase diagrams for T = 600 K and 4 different water partial pressures. The white diagonal marks the equilibrium line for water dissociation into H_2 and O_2.*

One can do so, of course, but only together with a second reservoir because, otherwise, arbitrary surface stoichiometries could not be tested. Choosing H_2O and O_2 leads to the phase diagram in Fig. 3b, while the choice of H_2O and H_2 yields the phase diagram shown in Fig. 3c. As highlighted by the red dots, the predictions of first-principles thermodynamics seem to depend on the choice for the gas-phase reservoirs: Compared to Fig. 3a, the clean ZnO surface becomes accessible in Fig. 3b and, in Fig. 3c, oxygen vacancies are additionally reachable. This ambiguity is highly unsatisfactory and, clearly, introducing yet another molecular species, that is, the SAM molecules of interest to the CRC, will not improve matters.

The first step to resolve these ambiguities was to treat H_2O as separate and independent gas-phase species in Eq. (3). The inconvenient consequence of this extension is that, now, N_{H2}, N_{O2} and N_{H2O} are not uniquely defined (Fig. 3d). It is the principal achievement of A4 to have established a general solution to this problem: A unique vector $\boldsymbol{N} = (N_{H2},N_{O2},N_{H2O})$ can be found by demanding that it be orthogonal to the stoichiometric vector $\boldsymbol{v} = (-2,-1,2)$ of the water reaction $2\,H_2 + O_2 \rightarrow 2\,H_2O$, *i.e.*, that $\boldsymbol{v}\cdot\boldsymbol{N} = 0$. This lifts the stoichiometry-dependent bias introduced by other "adsorbate-counting" schemes. The results of this novel procedure are illustrated in Fig. 5e for the exemplary temperature of T = 600 K. The most notable difference is that, now, whether there is or is not water on the surface actually depends on how much water is in the atmosphere. The fact that no previous theory could predict this intuitive finding highlights the importance the methodological developments in A4 for a wide range of topics also beyond CRC 951. The theory, published as Ref. [34], can easily be generalized to multiple molecular species that reactively interact on surfaces and it is now used in A4 to test the stability of SAMs on ZnO surfaces against H_2, O_2, and H_2O (as shown in Fig. 1).

Also the final methodological development in A4 emerged as a critical prerequisite for further studies only in the course of the first funding period, where it was understood that band bending on both sides of a HIOS interface would heavily impact the energy-level alignment between organic and inorganic semiconductors. Notably, defects give rise to a continuous density of states tailing deep into the fundamental gap of organic semiconductors and its filling/depletion due to electronic equilibration with a reservoir of charge (*e.g.*, the substrate supporting the HIOS structure) leads to band-bending like effects even in the absence of doping [35]. The full phenomenology of this organic band bending could be explained with a self-consistent, electrostatic model [36] developed in A4 and also ***A8*** (*Koch*), and it has since been expanded to allow also coupling of the organic with an inorganic semiconductor treated semi-classically in the depletion-region approximation. In collaboration with ***B4*** (*Knorr/Scheffler/Rinke*) this electrostatic model was coupled to atomistic DFT calculations of the immediate HIOS interface. The resulting multi-scale procedure, published as Ref. [38], now allows accounting for extended space-charge regions in slab-type electronic structure calculations of doped semiconductor surfaces, whose spatial extent precludes explicit quantum-mechanical treatment in slab-type DFT calculations.

References

[4] F. Jensen, J. Chem. Phys. **115**, 9113 (2001).
[5] L. Romaner, G. Heimel, C. Ambrosch-Draxl, and E. Zojer, Adv. Funct. Mater. **18**, 3999 (2008).
[6] M. Valtiner, M. Todorova, G. Grundmeier, and J. Neugebauer, Phys. Rev. Lett. **103**, 065502 (2009).
[7] R. Wahl, J. Lauritsen, F. Besenbacher, and G. Kresse, Phys. Rev. B **87**, 085313 (2013).
[8] B. Meyer, H. Rabaa, and D. Marx, Phys. Chem. Chem. Phys. **8**, 1513 (2006).
[9] O. Dulub, U. Diebold, and G. Kresse, Phys. Rev. Lett. **90**, 016102 (2003).
[10] D. J. Cooke, A. Marmier, and S. C. Parker, J. Phys. Chem. B **110**, 7985 (2006).
[11] G. Kresse, O. Dulub, and U. Diebold, Phys. Rev. B **68**, 245409 (2003).
[12] B. Meyer, Phys. Rev. B **69**, 045416 (2004).
[13] G. Henkelman and H. Jónsson, J. Chem. Phys. **113**, 9901 (2000).
[14] D. Torres, P. Carro, R. C. Salvarezza, and F. Illas, Phys. Rev. Lett. **97**, 226103 (2006).
[15] D. Loffreda, Surf. Sci. **600**, 2103 (2006).
[16] P. Raybaud, D. Costa, M. Corral Valero, C. Arrouvel, M. Digne, P. Sautet, and H. Toulhoat, J. Phys.: Condens. Matter **20**, 064235 (2008).
[17] D. B. Rasmussen, T. V. Janssens, B. Temel, T. Bligaard, B. Hinnenmann, S. Helveg, and J. Sehested, J. Catal. **293**, 205 (2012).
[18] P. Carro, R. C. Salvarezza, D. Torres, and F. Illas, J. Phys. Chem. C **112**, 19121 (2008).
[19] K. Reuter and M. Scheffler, Phys. Rev. B **65**, 035406 (2001)
[20] K. Reuter and M. Scheffler, Phys. Rev. Lett. **90**, 046103 (2003)
[21] K. Reuter and M. Scheffler, Phys. Rev. B **68**, 045407 (2003)
[22] A. Marmier and S. C. Parker, Phys. Rev. B **69**, 115409 (2004).
[23] Y. Vaynzof, D. Kabra, L. Zhao, P. K. H. Ho, A. T. S. Wee, and R. H. Friend, App. Phys. Lett. **97**, 033309 (2010).
[24] J. S. Park, B. R. Lee, J. M. Lee, J.-S. Kim, S. O. Kim, and M. H. Song, Appl. Phys. Lett. **96**, 243306 (2010).
[25] A. Lendz, L. Selegård, F. Söderlind, A. Larsson, P. O. Holtz, K. Uvdal, L. Ojamäe, and P.-O. Käll, J. Phys. Chem. C **113**, 17332 (2009).
[26] B. Meyer, D. Marx, O. Dulub, U. Diebold, M. Kunat, D. Langenberg, and C. Wöll, Angew. Chem. Int. Ed. **43**, 6641 (2004).
[27] N. H. Moreira, A. Dominguez, T. Frauenheim, and A. Luisa da Rosa, Phys. Chem. Chem. Phys. **14**, 15445 (2012).
[28] K. A. Persson, B. Waldwick, P. Lazic, and G. Ceder, Phys. Rev. B **85**, 235438 (2012).
[29] I. E. Castelli, K. S. Thygesen, and K. W. Jocobsen, Top. Catal. **57**, 265 (2014).
[30] M. Valtiner, X. Torrelles, A. Pareek, S. Borodin, H. Gies, and G. Grundmeier, J. Phys. Chem. C **114**, 15440 (2010).
[31] S. Rangan, A. Batarseh, K. P. Chitre, A. Kopecky, E. Galoppini, and R. A. Bartynski, J. Phys. Chem. C **118**, 12923 (2014).
[32] B. Baur, G. Steinhoff, J. Hernando, O. Purrucker, M. Tanaka, B. Nickel, M. Stutzmann, and M. Eickhoff, Appl. Phys. Lett. **87**, 263901 (2005).
[33] C. G. Van de Walle and J. Neugebauer, Phys. Rev. Lett. **88**, 066103 (2002).

3.3.2 Project-related publications

[34] V. Obersteiner, D. A. Egger, G. Heimel, and E. Zojer, "Impact of Collective Electrostatic Effects on Charge Transport through Molecular Monolayers", J. Phys. Chem. C **118**, 22395 (2014).
[35] I. Lange, S. Reiter, M. Pätzel, A. Zykov, A. Nefedov, J. Hildebrandt, S. Hecht, S. Kowarik, C. Wöll, G. Heimel, and D. Neher, "Tuning the Work Function of Polar Zinc Oxide Surfaces using Modified Phosphonic Acid Self-Assembled Monolayers", Adv. Funct. Mater., DOI: 10.1002/adfm.201401493
[36] K. Palczynski, G. Heimel, J. Heyda, and J. Dzubiella, Cryst. Growth. Des. **14**, 3791 (2014).
[37] P. Herrmann and G. Heimel, "Structure and Stoichiometry Prediction of Surfaces Reacting with Multicomponent Gases", Adv. Mater., accepted (2014).
[38] H. Wang, P. Amsalem, G. Heimel, I. Salzmann, N. Koch, and M. Oehzelt, "Band-Bending in Organic Semiconductors: the Role of Alkali-Halide Interlayers", Adv. Mater. **26**, 925 (2014).
[39] M. Oehzelt, N. Koch, and G. Heimel, "Organic semiconductor density of states controls the energy level alignment at electrode interfaces", Nature Comm. **5**, 4174 (2014).
[40] N. Abedi and G. Heimel, "Correlating Core-Level Shifts and Structure of Zinc.Oxide Surfaces", submitted
[41] O. Sinai, O. T. Hofmann, M. Scheffler, P. Rinke, G. Heimel, and L. Kronik, "A multi-scale approach to the electronic structure of doped-semiconductor surfaces", almost submitted

3.4 Research plan

Experience in the first funding period has shown that knowledge of the atomistic structure at HIOS interfaces is a crucial prerequisite not only for computing further properties, but also for understanding and interpreting experimental results. Having invested significant resources in developing a sound theoretical model for predicting the structure and stoichiometry of complex surfaces in particle exchange with an environment of multiple, reactive molecular species, A4 intends to now majorly capitalize on these developments. Firmly based on the insights already gained on the properties of SAMs on ZnO, the research plan for the second funding period naturally breaks into two main areas of activity, which are outlined consecutively below.

3.4.1 From the vacuum into solution

Work in the first funding period was conducted with an UHV-scenario in mind, where inorganic-semiconductor surfaces would, after pre-treatment/preparation, be allowed to reactively interact with a controlled atmosphere (comprising, amongst others, functional SAM molecules) until a steady-state surface structure develops, whose properties are then investigated *in-situ*. This experimental approach is certainly conducive to understanding fundamental, surface-scientific aspects but, for practical applications, SAMs on any substrate are almost exclusively produced *ex-situ*, that is, by immersing it into a solution containing the SAM molecules; experimental efforts in the present CRC are no exception. With a reliable theoretical method for predicting surface structures in the UHV scenario now available, the natural next step for A4 is, therefore, to extend these newly developed tools towards treating also the solution scenario. The goal of this first area of activity in A4 can thus be formulated as:

> *The development and subsequent application of a first-principles approach for predicting the stability, structure, and stoichiometry of inorganic-semiconductor surfaces reactively interacting with solvents and solutions of functional SAM molecules.*

Reaching this ambitious goal represents a formidable challenge indeed and has never, to the best of our knowledge, been seriously pursued despite the undisputable relevance of potentially obtainable result [24]. The most closely related concept are Pourbaix diagrams used in the context of corrosion and catalysis [25,26]. In contrast to the electrochemical setup envisioned there, however, no counter-electrode and no external electrical circuit is present in the case of inorganic semiconductor sample immersed in solution. Therefore, both the solution and the inorganic semiconductor have to remain charge neutral individually.

Bare ZnO surfaces. Efforts to predict surface structure and stoichiometry under these conditions, will start with systems investigated experimentally in ***B7*** (*Neher*) and **A8** (*Koch*), that is, various ZnO surfaces in ethanol and THF solutions, respectively. The former scenario in particular will serve to develop a working methodology, which is best outlined by considering the differences between UHV and solution:

- The most apparent difference is clearly that now also EtOH is available as molecular species that can interact with the ZnO surfaces. Leaving SAM molecules out of the picture for now, the ground-state total energies need to be calculated also for a series of EtOH adsorption patterns, varying in surface coverage and degree of intermixing with co-adsorbed H^+, OH^-, O^{2-}, and H_2O. Experience with MeOH adsorption gained in the first funding period will guide the choice of structures. Slab-type DFT

calculations will be performed with the VASP code in this step to obtain the values for E_{surf} required to evaluate Eq. (1). Owing to the large number of structures that need to be considered, the PBE functional will be employed with Tkatchenko-Scheffler vdW corrections, further developed in ***A10*** (*Tkatchenko/Scheffler*).

- The second difference to the UHV scenario is that the values for E_{surf} so obtained might change in the presence of a solvent due to, *e.g.*, screening of strongly polar Zn-O bonds. The importance of these potential differences in ground-state total energies, ΔE_{surf}, will be assessed by performing two additional single-point calculations for each tested surface structure, with and without solvent, using the plane-wave pseudopotential code JDFTX, which has been specifically developed to that purpose.
- The third difference is the choice for the number and type of species considered in the sum $\Sigma_i \mu_i N_i$ entering Eq. (1). As Fig. 3 underlines, it is also the most critical. To understand this point, it is insightful to consider Eq. (1) as the energy balance of a reaction, where all atoms in the surface region are "put back" into their respective reservoirs. This reaction must, of course, obey element conservation (all atoms in the surface region must go into some reservoir) and, additionally, charge conservation (both the inorganic semiconductor and the solution always remain charge-neutral individually). Even under these constraints, several combinations of molecular species are conceivable as reservoirs and the energy balance represented by Eq. (1) evidently depends on that choice.
  In order to evaluate the stability of a given surface structure only with respect to processes that are likely occur, we will first consider EtOH, H_2O, O_2, EtO^-, OH^- and $H3O^+$ as molecular species in addition to ZnO as solid species. This choice conveniently suppresses the (unlikely) water reaction $2\ H_2 + O_2 \rightarrow 2\ H_2O$ but fully takes into account that ethanol is never 100 % dry, that it is never 100 % free of dissolved oxygen, and that the reactions $EtO^- + H_2O \rightarrow EtOH + OH^-$ and $2\ H_2O \rightarrow OH^- + H3O^+$ therefore occur. Realistically assuming both to be in thermodynamic equilibrium, *i.e.*, that

$$\mu_{EtO\text{-}} + \mu_{H2O} = \mu_{EtOH} + \mu_{OH\text{-}} \quad (4.a)$$
$$2\,\mu_{H2O} = \mu_{OH\text{-}} + \mu_{H3O+} \quad (4.b)$$

  allows reducing the number of independent chemical potentials in Eq. (1) to just those of EtOH, O_2, and H_2O. At each triple of values (μ_{EtOH}, μ_{O2}, μ_{H2O}), the most stable surface structure can (and will) then be determined *via* Eq. (1) as that with the lowest value of γ.
- The fourth and last important difference to the UHV scenario lies in the way these chemical potentials are converted into quantities that can be directly controlled in experiment to achieve a desired surface structure. Assuming dissolved O_2 to be in equilibrium with the atmosphere above the solution, μ_{O2} is conveniently related to the oxygen partial pressure *via* Eq. (3). μ_{EtOH} and μ_{H2O}, however, are determined by molecules in the liquid phase, where Eq. (3) no longer holds. Instead, the chemical potentials of EtOH and H_2O can only be related to their respective mole fractions x_i in solution by inverting

$$\mu_i = E_i + \Delta G_i + k_B T \ln(f_i \cdot x_i) \quad (5)$$

  with ΔG_i the Gibb's free energy of solvation in the standard state and f_i the activity coefficient. The accuracy of the results and, therefore, the predictive power of the proposed procedure, clearly hinges on the accuracy of both ΔG_i and f_i. For that reason, the best method currently available for quantitatively predicting these values will be employed: a combination of the TURBOMOLE quantum-chemistry package with the conductor-like screening model for real solvents (COSMO-RS) as implemented in the software package COSMOtherm. Finally, by combining Eq. (5) with Eqs. (4) and the condition of charge-neutrality in solution, also the mole fractions of the remaining species, $x_{EtO\text{-}}$, $x_{OH\text{-}}$ and x_{H3O+} will be obtained.

The procedure outlined above will first be developed in detail and will then be applied to predict the surface structures and stoichiometries of various ZnO crystal faces as a function of water and oxygen content in both EtOH and THF solutions. Results will already yield important insights into the difference between working with regular solvents in laboratory atmosphere and using dry solvents in the glove-box.

SAMs on ZnO surfaces. In a second step, more structures will consecutively be added, including now also SAM-forming molecules as additional species on the surface(s) and in solution. Focusing on the selectivity of different chemical anchoring groups towards different ZnO crystal faces, the starting point will be the relatively simple chemical structure shown in Fig. 4 which, nevertheless, well represents the basic elements of the SAMs previously studied in the CRC and those planned for the second funding period. New anchoring

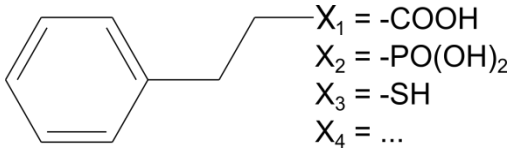

Fig. 4: *SAM molecules to be initially studied in this first area of activity. X denotes the anchoring group to the ZnO*

groups will be developed jointly with ***A3*** (*Hecht*) in the course of the second funding period. This work is expected to yield viable predictions as to which concentration of potentially SAM-forming molecules in which solvent with which oxygen and water content at which temperature is needed to achieve a close-packed SAM on a given ZnO surface. As in the first funding period, connection to experimental characterization methods, *e.g.*, XPS and work-function measurements performed in ***A8*** (*Koch*), ***B7*** (*Neher*) and ***B9*** (*Stähler*) will be sought by computing the respective properties on the (hybrid) DFT level.

Stability of the bulk inorganic semiconductor. Common anchoring groups for SAMs on oxides (*cf.* Fig. 4) are acids that, by definition, dissociate to some degree and, thereby, notably increase the concentration and, according to Eq. (5), the chemical potential of H_3O^+ ions in all but the driest solvents. Importantly, if the *pH*-value of the solution is thus pushed below a critical limit, ZnO is known get etched [27] – a scenario that was, in fact, observed and successfully avoided in joint work with ***B7*** (*Neher*) [32]. Once ideal preparation conditions for a given SAM have been identified in terms of μ_{O2} and μ_{H2O}, also the corresponding chemical potential of H_3O^+ will be computed *via* the case-by-case equivalents of Eqs. (4) and Eq. (5). To test the stability of ZnO against etching, the Gibb's free energy balance will then be calculated for all reactions of the type

$$ZnO + n\cdot H_2O \rightarrow p\cdot P + a\cdot H_3O^+ + b\cdot O_2 \qquad (6)$$

where the product P is one of Zn^{2+}, $ZnOH^+$, ZnO_2, HO_2Zn^-, $(HO)_3Zn^-$, O_2Zn^{2-} and $(HO)_4Zn^{2-}$.The chemical potentials of this dissolved species at a small concentration (typically chosen as 10^{-6} mole/liter [26]) need to be calculated only once in each considered solvent *via* Eq. (5) and the stoichiometric coefficients *n*, *p*, *a* and *b* are uniquely defined through element and charge conservation. Should any of these reactions prove exothermic, then ZnO must be deemed unstable under the given circumstances and different preparation conditions and/or different SAM molecules must be established in a close feedback loop with experiment and synthesis. It is important to note, however, that conditions close to the edge of ZnO dissolution are actually desirable because, there, the dynamic equilibrium between desorption and re-adsorption must be expected to both heal defect on the surfaces and to facilitate the formation of highly ordered SAMs.

Towards surface-selective functionalization of inorganic nanostructures. Accumulating the results of the procedure outlined above for different docking groups and different ZnO crystal faces opens up the intriguing possibility of studying the competitive adsorption of two or more SAM molecules in the same solution. Because each docking group has a different adsorption energy on each crystal face and causes a different energy of solvation for the SAM molecule(s), it is conceivable that on one crystal face only one molecular species adsorbs and the other(s) stay in solution while, on a different crystal face, a different molecular species preferentially adsorbs, again with the other(s) staying in solution. Immersing into such a solution ZnO nanostructures that expose multiple crystal faces, *e.g.*, nanowires or nanoparticles, would then lead to a surface-selective functionalization of that nanostructure in that each crystal face will be covered with a SAM of a different species (Fig. 5). Assessing the feasibility of this unprecedentedly targeted concentration of multiple functionalities not only on ZnO but also on GaN nanowires is the long-term vision driving work in project A4.

Fig. 5: *Envisioned scenario for surface-selectively functionalized*

3.4.2 Integrating functionality in multi-purpose SAMs

The main thrust in the first funding period was to employ SAMs for the passivation of ZnO surfaces and to concomitantly tune their work function. This allowed optimizing the energy alignment of the transport levels in a subsequently deposited organic semiconductor with respect to the ZnO bands for charge injection/collection. Project A4 exclusively studied the interfacial region comprising the ZnO surface and the SAM itself, but not the organic-semiconductor part (Fig. 6a), which was physisorbed onto the SAM in experiment with unknown registry, orientation and order. In light of the CRC's concerted effort in the second funding period – to study the nature, energetics and dynamics of optical excitations across the hybrid inorganic/organic interface – this rather ill-defined situation is hardly ideal and greater control over the orientation and location of the organic semiconductor with respect to the inorganic surface as well as over mutual electronic coupling is certainly desirable. To support these efforts and to provide dearly required insight at the atomistic level, the goal for project A4 in this second area of activities can thus be formulated as:

> *To computationally explore the possibility for creating a highly defined and tunable HIOS interface for the targeted study of hybrid optical excitations.*

To achieve this goal, the organic semiconductor will be covalently linked to the functional element in the SAM (Fig. 6b), which must be suitably adapted to still allow tuning the energy-level alignment between organic and inorganic semiconductor as well as the mutual electronic coupling. Work in this area clearly depends on targeted molecular design conducted in ***A3*** (*Hecht*) and efforts will, therefore, be closely coordinated. Potential candidates for realizing dipolar moieties within the SAM will be based on the heterocycles developed in the first funding period [31,32]. Their insertion between anchoring group and organic chromophore (Fig. 6c) must, therefore, be expected to shift its energy levels with respect to the inorganic semiconductor band edges by a comparable amount and their directionality dictates the direction of this shift [28,31].

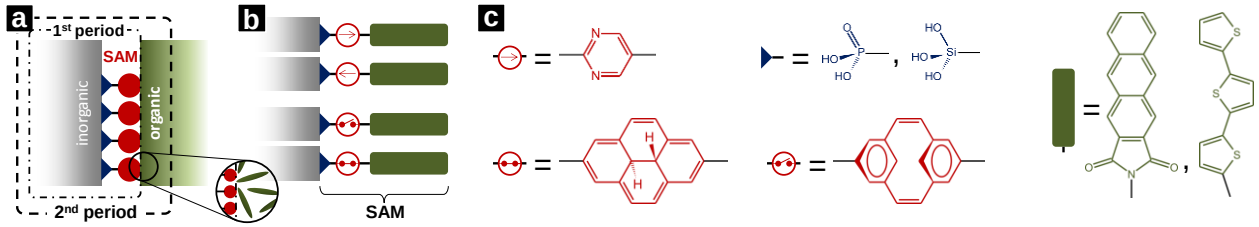

Fig. 6: *(a) Schematic of the HIOS regions studied in A4; inset highlights poorly controlled contact at the SAM/organic-semiconductor (green blobs) interface. (b) Schematic of multi-functional SAMs that allow tuning the band offset between inorganic semiconductor (grey) and organic chromophores (green) by built-in dipolar groups (top) and mutual electronic coupling by built-in switches (bottom). (c) Potential molecular structures with blue triangle indicating starting points for chemical docking groups on ZnO and GaN, respectively.*

While this principle would allow tuning the energy of hybrid excitons with charge-transfer character across the HIOS interface, it is important to recall that the SAMs employed in the first funding period inevitably affected also the electronic coupling between inorganic and organic semiconductors and, thereby, the oscillator strength of such hybrid charge-transfer excitations, as well as their formation/dissociation dynamics. To provide a means for studying the impact of this coupling in an equally controlled manner, dipolar units in the SAM will be replaced by a molecular switch between docking group and organic chromophore, providing a continuous π-electron pathway in the "closed" state and efficient decoupling in the "open" state (Fig. 6c).

Extending the range of materials studied in A4 and, thereby supporting experimental efforts, such SAMs will first be studied on GaN surfaces employing, as also indicated in Fig. 6c, silanes as initial choice for the chemical anchoring group [29]. ZnO, however, will continue to play an important role and phosphonic acids will be employed as initial choice there.

Methods. The size and complexity of the systems targeted in this second area of activity poses significant challenges to electronic-structure theory. A4 will start by characterizing all molecules proposed in Fig. 6 as well as new suggestions continuously developed by ***A3*** (*Hecht*) with quantum-chemical methods, using the GAUSSIAN09 and TURBOMOLE software packages. In particular, hybrid DFT will be used to determine ground-state properties such as dipole moment and molecular structure. For the dihydropyrene molecular switch, the reaction path and barrier in the ground state, required to assess the stability of open and closed forms as well as the rate of switching, will first be calculated with the CL-NEB method for an isolated molecule in the gas phase. Wave-function stability analysis at the transition state will be performed to check for potential symmetry-broken, spin-unrestricted solutions at the point of bond making/breaking. On this basis, TDDFT will then be employed to assess also the reaction path and barrier for switching in the optically excited state.

Past experience on ZnO surfaces will then serve to bind these SAMs onto slabs in reasonable starting geometries and optimize their ground state structure using VASP with the PBE functional and vdW corrections developed in ***A10*** (*Tkatchenko/Scheffler*). On GaN, several surface-bonding patterns will be tested based on literature suggestions for the GaN surface structure and stoichiometry [30]. Comparing, as in the first funding period, calculated XPS core-level shifts with those measured in ***A8*** (*Koch*) will allow assessing the plausibility of the chosen surface-bonding motifs. The relevant physical quantities for the dipolar SAMs, that is, the alignment of the organic energy levels with the band edges in the inorganic semiconductor, will then be computed at the hybrid DFT level. For the molecular switch, the most critical question is whether it still does switch in a densely packed SAM on the surface. A4 thus plans to invest the significant computational effort of calculating the ground-state reaction path and barrier between open and closed forms using the CL-NEB method also on the surface. Results from the gas phase will serve to guide

these efforts. Again, the quantities of physical interest are the energy alignments between inorganic-semiconductor band edges, the frontier orbitals on the molecular-switch section of the SAM, and those on the organic-semiconductor segment. This information will be projected out from the density of states computed at the hybrid DFT level. As work progresses in the in the first area of activities and initial results have been produced in the second, efforts will slowly be merged to assess the possibility for solution-processing also of multi-functional SAMs on GaN.

3.4.3 Timeline and project structure

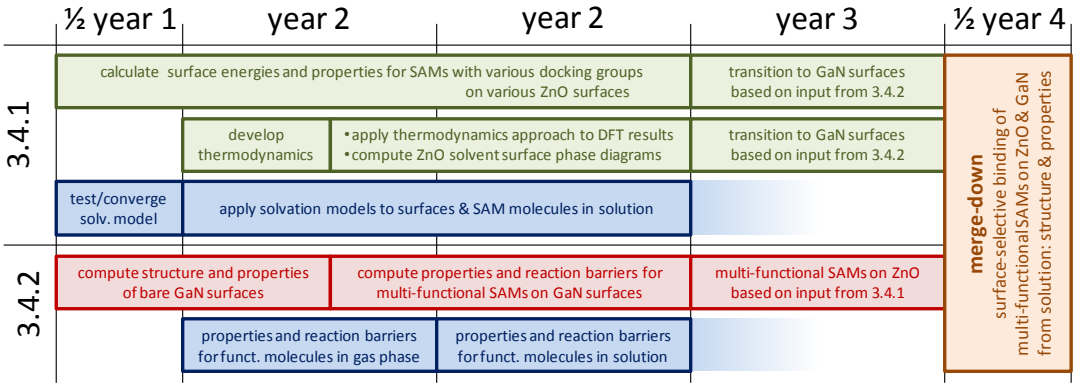

Fig. 7: *Based on established experience with ZnO, Ph.D. student 1 (green) will first learn the techniques for first-principles surface calculations and then routinely run them while fully developing and then continuously applying the thermodynamic theory required to construct solution-based surface phase diagrams. Ph.D. student 2 (red) will learn the techniques on GaN surfaces and then apply them to multi-functional SAMs, which will be studied on ZnO in year 3, when Ph. D. student 1 will apply the developed methods to GaN in return. The PI (blue) will perform quantum-chemical calculations in gas phase and solution, as well as slab-type DFT calculation in solution. Finally merging all results (brown) will provide a comprehensive picture.*

3.5 Role within the Collaborative Research Centre

Project A4 fulfills a threefold role in CRC951 “HIOS”: It is lies at the interface between physics and chemistry, it is part of the lowest, first-principles rung in the hierarchy of theoretical methods, and attempts to provide an interface also between theory and experiment.

As mentioned above, efforts in molecular design will be closely coordinated with ***A3*** (*Hecht*). Project A4 will employ further refinements to accurate vdW corrections developed in ***A10*** (*Tkatchenko/Scheffler*) and will support ***B4*** (*Körzdörfer/Rinke/Scheffler*) in improving surface phase diagrams. Furthermore, A4 will continue to provide molecular parameters (atomic charges, dipole- and quadrupole moments, *etc.*) as well as surfaces structures and atomic charges for ***A7*** (*Klapp/Dzubiella*), where input from first-principles is required to parameterize atomistic and coarse-grained interaction potentials. Collaboration is also envisioned with **B6** (*May*), where quantum-chemical calculations on the (TD)DFT level will be performed for neutral and charged organic-semiconductor mono- and dimers in their ground and excited states to extract parameters needed for the model Hamiltonians employed there to compute the dynamics of hybrid charge-transfer excitations. Structures determined in A4 for the multi-functional SAMs addressed in 3.4.2 will be forwarded to ***B11*** (*Draxl*), where they will serve as starting points for the calculations of interfacial hybrid excitons.

On the experimental side, A4 will provide guidance for projects ***A8*** (*Koch*), ***A11*** (*Christiansen*) and ***B3*** (*Blumstengel*) in finding preparation conditions for functionalizing GaN surfaces and nanowires, while feedback from experiment will help to assess the reliability of theoretical methods and to better account for real-world scenarios. Results on multifunctional SAMs on ZnO will help interpreting and designing experiments performed in ***B3*** (*Blumstengel*), ***B7*** (*Neher*) and ***B9*** (*Stähler*) on hybrid charge-transfer excitons.

3.6 Delineation from other funded projects

No other funded projects available.

3.7 Project funds

3.7.1 Previous funding

The project has previously been funded within the Collaborative Research Centre 951 HIOS since July 2011.

3.7.2 Funds requested

Funding for	2015/2		2016		2017		2018		2019/1	
Staff	Quantity	Sum	Quantity	Sum	Quantity	Sum	Quantity	Sum	Quantity	Sum
PhD student, 75%	2	44.100	2	88.200	2	88.200	2	88.200	2	44.100
Total		44.100		88.200		88.200		88.200		44.100
Direct costs	Sum		Sum		Sum		Sum		Sum	
Small equipment, Software, Consumables	0		0		0		0		0	
Other	0		0		0		0		0	
Total	0		0		0		0		0	
Major research equipment	Sum		Sum		Sum		Sum		Sum	
€ 10.000 - 50.000	0		0		0		0		0	
> € 50.000	0		0		0		0		0	
Total	0		0		0		0		0	
Total	44.100		88.200		88.200		88.200		44.100	

(All figures in Euro)

3.7.3 Staff

	No.	Name, academic degree, position	Field of research	Department of university or non-university institution	Commitment in hours/week	Category	Funded through:
Available							
Research staff	1	Georg Heimel, Ph.D., PI	Theoretical Physics	Institut für Physik	15		Grundausstattung of HU Berlin
Non-research staff							
Requested							
Research staff	2	N.N., M.Sc., PhD Student	Theoretical Physics	Institut für Physik		PhD student	
	3	N.N., M.Sc., PhD Student	Theoretical Physics	Institut für Physik		PhD student	
Non-research staff							

Job description of staff (supported through available funds):
1. Georg Heimel
The PI will coordinate all organizational and scientific matters of the project, perform all quantum-chemical and solvent-related calculations (see Fig. 7 in section 3.4.3), and will mentor the two Ph.D. students. This involves introducing them to the subject matter of HIOS, to scientific computing, to first-principles electronic-structure theory in general, and to the techniques required for project A4 in particular. Furthermore, the PI will provide guidance in performing scientific research as well as in its presentation and publication.

Job description of staff (requested):
2. N.N.
As highlighted in green in Fig. 7 (section 3.4.3), the main task of the first Ph.D. student will be to pursue work in the area of activity outlined in section 3.4.1. This involves mastering the techniques of first-principles electronic-structure calculations and their application to a large number of different systems. Additionally, the first Ph.D. student must rapidly develop a keen sense for the thermodynamic/statistical-physics model needed to post-process the first-principles results and should program software to efficiently perform this analysis.

3. N.N.
As highlighted in red in Fig. 7 (section 3.4.3), the main task of the second Ph.D. student will be to pursue work in the area of activity outlined in section 3.4.2. He or she will have to quickly learn the tools of theoretical science, apply them, and gain a deep understanding of the complex GaN surfaces. Furthermore, the second Ph.D. student will have to develop the skills required for calculating reaction paths and barriers with the CL-NEB method and for computing properties, such as XPS core-level shifts, from first-principles.

3.7.4 Direct costs for the new funding period

No direct cost is requested. All required software is either free of charge (JDFTx) or the required licenses are already available at the HU Berlin (Gaussian09, Turbomole, COSMOtherm, VASP).

3.7.5 Major research equipment requested for the new funding period

No funding for major research equipment is requested. Calculations will be run on the 8-node, 32 CPU, 384-core, 2 TB RAM computing cluster financed by the DFG in the first funding period of CRC 951 “HIOS”.

3.1 About project A5 (Henneberger)

3.1.1 Title: Inorganic-oxide/organic hybrid structures: Structure and Function

3.1.2 Research areas: Molecular Beam Epitaxy, Photonics, Plasmonics

3.1.3 Principal investigator

Prof. Fitz Henneberger (*04.12.1951)
Humboldt-Universität zu Berlin, Institute of Physics
Newtonstr. 15, 12489 Berlin
Phone: +49 (0)30 2093 7670
Fax: +49 (0)30 2093 6886
E-mail: fh@physik.hu-berlin.de

Do the above mentioned persons hold fixed-term positions? Yes
End date:
Further employment is planned until.

3.1.4 Legal issues

This project includes

1.	research on human subjects or human material.	no
	A copy of the required approval of the responsible ethics committee is included with the proposal.	
2.	clinical trials	no
	<If applicable:> A copy of the studies' registration is included with the proposal.	
3.	experiments involving vertebrates.	no
4.	experiments involving recombinant DNA.	no
5.	research involving human embryonic stem cells.	no
	<If applicable:> Legal authorization has been obtained.	no
6.	research concerning the Convention on Biological Diversity.	no

3.2 Summary

The project will continue the efforts of the first funding period with focus points realigned by the gained knowledge and understanding.

First, the efforts towards control of the aggregation mode of representative conjugated organic molecules on ZnO and other oxide-semiconductor surfaces will be continued. Encouraging results for sexiphenyl and its fluorinated derivatives showed a way for achieving well-oriented molecular assemblies and uniform thin-film morphologies. In collaboration with A7 (Dzubiella/Klapp) we aim at an in-depth understanding of these findings enabling us the transfer of these concepts to other molecule classes (oligo-perylenes, -acenes, thyophenes) serving as functional building blocks in various projects of the CRC.

Second, as demonstrated by extra project work, ZnO, when heavily doped n-type, is capable of low-loss surface plasmon polaritons, tuneable from the mid infrared up the telecommunication wavelength range. We plan to resonantly couple and hybridize these excitations with infrared molecular resonances of vibronic and/or electronic origin. These new electromagnetic/molecular eigenstates are associated with functional features not available otherwise. Vibrational energy and charge can be coherently transported, molecular light emission be switched or exciton dissociation for current generation be triggered (to name just a few). Preliminary identified organic materials suited for these purposes are fused tetraanthracenylporphyrin, F6TCNNQ:5T, ethylen-bissuccinimid, and PMMA. B5 (Wörner/Elsässer) will contribute to these studies with time-resolved and non-linear THz/infrared spectroscopy.

Third, we will fabricate hybrid ZnO/organic multi-layer stacks and demonstrate their function. One target are hybrid microcavity structures based on ladder-type oligo-(p-phenylenes) for vertical-cavity surface-emitting laser action and strong exciton-photon coupling. By the photon-mediated hybridisation of Frenkel- and Wannier-Mott excitons, relaxation bottlenecks can be avoided providing improved lasing parameters (threshold, bandwidth). A second goal is the realization of infrared hybrid metamaterials by combining n-ZnO with suitable molecular materials (e.g. ,….). We will study the modified emission characteristics of molecules embedded in the stack, the occurrence of negative refraction, as well as the presence of an anisotropic index hyperbola. B10 (Busch) will join these experimental efforts by developing the required in-depth description and numerical modelling.

The experimental core facility that enables us to tackle the above issues is a tandem MBE apparatus where both ZnO and other oxide-semiconductors - when needed heavily doped - as well as the conjugated organic material can be deposited in a continuous UHV regime. Suitable organic molecules are developed in collaboration with A3 (Hecht) or supplied by Z1 (Hecht). Extensive use of the analytical tools provided by Z2 (Kowarik/Koch) will be made. The project will continue to provide tailored HIOS specimen for other CRC projects, in particular A8 (Koch), B2 (Ballauff/Benson/Lu), B3 (Blumstengel), B7 (Neher), and B13 (List-Kratochvil).

3.3 Project progress to date

3.3.1 Report and state of understanding

In the previous funding period we have extensively worked on three topical aspects as proposed by the then project application as well as triggered by findings which were not available at project start. In what follows an outline of the results is presented and conclusions are drawn for the next funding period.

A) Aggregation of organic molecules on pristine ZnO surfaces

Enabled by the availability of a tandem MBE apparatus we have uncovered the aggregation mode of various prototypical conjugated organic molecules on selected surfaces of ZnO in an all-UHV regime. For the non-polar $(10\bar{1}0)$ surface, an electrostatically based mechanism for the alignment of long molecules with a highly axial π-electron system (para-sexiphenyl, penta-phenylene-venylene) has been identified [P1]. The quadrupole moment (and even higher-order multi-poles) of these molecules couple to the strong inhomogeneous dipolar field created by the Zn-O surface dimers dictating an orientation along the dimer rows where the electrostatic substrate-molecule interaction is maximized. The alignment energies can become as large 0.5 eV. Molecules with a less axial π-electron system like pentacene are not expected to exhibit the electrostatically driven alignment [P1] and, indeed, this has been experimentally confirmed by Witte and coworkers [1]. Motivated by this finding, we have investigated the effect of chemical modification on the molecular assembly. In a close collaboration with A3 (Hecht) and A9 (Kowarik), combining in-situ AFM as well as real-time X-ray scattering measurements, para-sexiphenyl (6P) and its symmetrically terminally fluorinated derivative (6P-4F) have been compared [P2]. Both molecules grow in a highly crystalline mode on ZnO$(10\bar{1}0)$, however, with a distinctly different morphology. While 6P films are characterised by the formation of two different phases composed of three-dimensional nanocrystallites and, consequently, a rather rough surface morphology, layer-by-layer growth and phase purity in case of 6P-F_4 prevails leading to smooth terraced thin films. Our current conjecture is that the fluorination increases the molecular surface diffusivity favouring “flat-land” aggregation. These results might provide a path towards highly uniform molecular films as demanded in many practical applications, however, further consolidation is needed, both by theoretical studies as well as by including other molecular derivatives in the analysis.

ZnO can be grown by MBE with very good crystalline quality at temperatures as low as 50 to 100 °C [2]. Those temperatures are compatible with organic molecules allowing for the fabrication of HIOS with multiple inorganic/organic interfaces, all potentially well-defined in an all-UHV approach. In a first step, we have investigated the regrowth of ZnO on sub-monolayer 6P films deposited on either (0001) or $(10\bar{1}0)$ oriented ZnO templates [P3]. As revealed by high-resolution transmission electron microscopy [Z2 (Kirmse)], the ZnO-on-6P interface is remarkably abrupt and the ZnO layer exhibits a rather uniform columnar structure with a *c*-axis orientation perpendicular to the interface, but an almost random twist of the unit cell within the film plane. The ZnO columns extend over the whole film thickness and have a cross-section of some 10 nm. The ordering is thus remarkably better then achieved by able by other methods (sol-gel, spray pyrolysis,…) where the morphology is dominated by ZnO grains with strong fluctuations of size, shape, and orientation [3, 4]. The 6P nano-columns are electronically unimpaired by the overgrowth as demonstrated by absorption

and photoluminescence data. Though yet no epitaxial relation with respect to the ZnO template or the 6P layer is found, these results are highly encouraging and we will continue the efforts in the next funding period as detailed below.

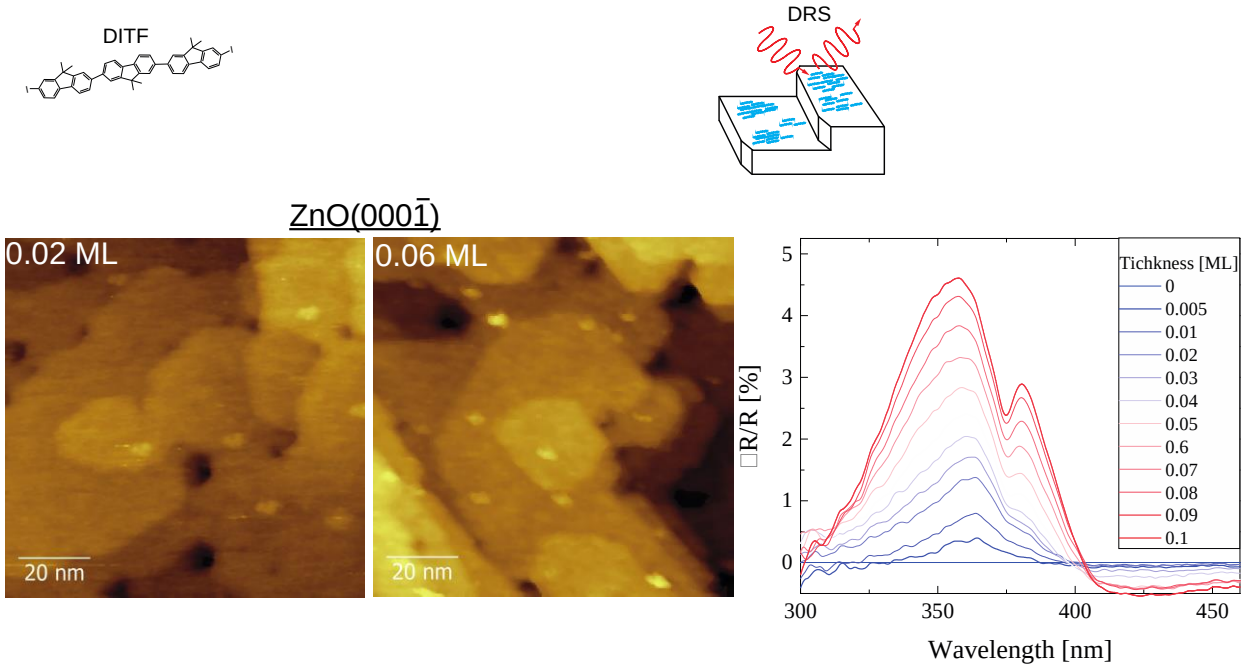

Fig. 1: DITF on ZnOGa Left: STM images demonstrating terrace structures on the (10$\bar{1}$0) surface (growth temperature not yet optimized) and single molecular entities atop. Right: DSR spectra showing the appearance of the HOMO-LUMO signature with sensitivity far below monolayer coverage. The long-wavelength feature is due to phase-perturbation of the ZnOGa reflection. Coverage observed in STM and DRS is fully consistent.

On the methodological side, we have advanced our in-situ characterization tools by improving our AFM/STM setup as well as by implementing differential reflection spectroscopy (DRS) [5] for obtaining real-time information on morphology and electronic structure of the growing molecular film. The gain achieved by these measures is exemplified in Fig. 1 for a study on DIFT (diiodoterfluorene) undertaken in the context of on-surface polymerization together with A3 (Hecht). The use of a heavily n-type doped ZnOGa substrate has enabled the identification of single molecules in STM and the DRS exhibits resolution far below a molecular monolayer.

In the first funding period, we have also extended our oxide MBE know-now. Nucleation procedures have been developed that allow for the growth of a-plane ZnO on r-plane sapphire and m-plane ZnO on MgO(001), respectively. Besides providing extra interfaces for the molecular assembly, these achievements enable the fabrication of non-polar quantum well structures, essential for light-emitting applications due to the absence of strain-induced built-in electric fields. In addition, we have included NiO_2 and Er_2O_3 [P4] in the growth portfolio and also set up regimes for the ultra-heavy n-type doping of ZnO by Ga as described next.

B) ZnO as a tuneable metal

It is known for quite some time that ZnO can be heavily doped n-type making it a candidate for use as transparent electrode [6]. Motivated by two additional reasons, we have devised a systematic and reproducible approach towards Ga-doped ZnO [P5]. First, it turned out during the first funding period [P6,P7] that doping is an essential degree-of-freedom for HIOS energy-level control. Second, high free-carrier concentrations in semiconductors are of usability in infrared plasmonics [7]. A critical issue in this context is the search for growth and doping methods that allow for the generation of ultra-high carrier concentrations without deteriorating substantially the crystalline structure of the material. With core support we have targeted that issue by MBE. For properly adjusted MBE parameters, ZnOGa can be grown in a layer-by-layer

mode up to Ga molecular fractions as large of 7 % without substantial degradation of the material's structure. The doping efficiency is close to 100 % so that free-electron concentrations as large as $n = 10^{21}$ cm^{-3} can be reached (Fig. 2). Beyond that point, the incorporation of electronically active Ga is hampered by the formation of polarity inversion domains [P8].

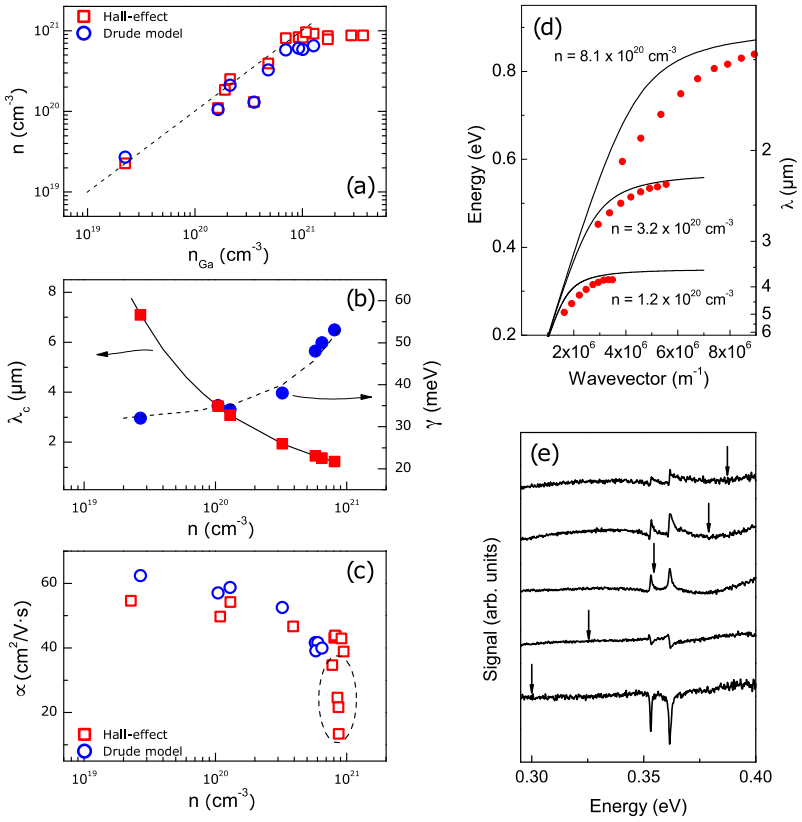

Fig. 2: MBE-grown n-type ZnGaO (substrate: a-plane sapphire, film thickness: 400 nm). a) Free-electron concentration versus Ga incorporation derived from Hall measurements as well as from infrared reflection and transmission spectra. b) Drude damping (γ) and positive-to-negativ crossover wavelength (λ_c) of the permittivity's real part. c) Mobility versus free-electron concentration again from Hall and optical data. d) Tunable SPPs of air/ZnOGa interfaces. Shown is the energy-versus-(in-plane)wavevector dispersion relations at three different doping levels. Dots: experiment (ATR). Curves: calculation. e) ATR signatures of the symmetric and antisymmetric CH_3 stretching vibrations of a C40 monolayer deposited on ZnOGa. The arrows mark the position of the ATR minimum related to the spectrally broader SPP feature set by the

The doping is accompanied by the emergence of a metallic infrared reflection edge moving systematically to shorter wavelengths with increase of the adjusted free-electron concentration. Reflection and transmission spectra are very well reproduced when describing the infrared response of ZnOGa by the Drude permittivity. The shortest wavelengths for the crossover from positive to negative real part attained so far is $\lambda_c = 1.23$ μm, i.e., the telecommunication window is completely included in the currently available metallic range. The Drude damping of only some 10 meV is fully consistent with mobility data obtained from Hall measurements. The experimental values of $\mu = 40$ - 60 cm^{2}V^{-1}s^{-1} are close to the intrinsic mobility limit predicted for ZnO by account of LO-phonon and ionized impurity scattering. As a consequence, the losses defined by the imaginary part of the permittivity are at least one order of magnitude lower than for conventional metals in the infrared spectral range.

Based on these material achievements, we have demonstrated surface plasmon polaritons (SPPs), both at dielectric/ZnOGa interfaces as well as at interfaces between differently doped ZnOGa films [P9]. These latter metal/metal-type SPPs are characterized by a finite frequency in the long-wavelength limit and are thus accessesible under free-space excitation. The surface plasmon frequency of conventional metals is deep in the ultraviolet range. Thus, when targeting infrared wavelengths, their SPPs become almost entirely photon-like and, as a result, localization on the sub-wavelength scale is lost. In contrast, this localization is inherent to the SPP of ZnOGa and, moreover, the surface plasmon frequency can be even tuned to a requested target frequency by the doping level. ZnOGa is thus an ideal candidate for coupling SPPs to infrared excitations in matter. In a proof-of-concept experiment, we have demonstrated resonant coupling to molecular vibrations [P10]. Monolayers of the n-alkane tetracontane (C40) deposited on the ZnOGa surface generate distinct signatures in total-attenuated-reflection (ATR) spectra at the frequencies of the symmetric and asymmetric stretching vibrations of the CH_3 group. Their line shape undergoes profound changes from absorptive to dispersive and even anti-resonance character in dependence on the detuning to the surface plasmon frequency. Similar observations for Au required expensive size-adjusted nanostructures generating field hot spots for detecting the molecular resonances [8,9], whereas a planar field geometry is fully sufficient for creating a phase-sensitive coupling to the SPPs of ZnOGa. The infrared detection of molecular vibrations by, e.g., surface-enhanced Raman scattering [10] or direct absorption [11] is of immense practical interest.

Classical ATR sensors rely on the spectral shift of the SPP resonance introduced by the refraction index of the molecular material and demand thus relatively thick molecular films [12]. Contrary, the resonance coupling enabled by ZnOGa provides direct signatures of the vibrational resonances and is thus capable of sensing much lower amounts of molecular material. Though of considerable impact for sensing applications [13,14], we will not pursue this aspect further in the CRC. Instead, we will target the hybridization of these infrared SPPs with vibrational and electronic excitations of molecular materials in the strong-coupling regime. As described below, we expect novel optoelectronic functionalities carried by these so far undemonstrated organic/inorganic hybrid states. Finally, we emphasize that the availability of high-quality ZnO films with fully controllable free-electron concentration up to a strongly degenerate regime is also of essence beyond the use in infrared plasmonics. Besides utilization as conductive electrode in device geometries or in a methodological context (e.g. STM), it allows for studying systematically the role of the doping level on the aggregation of organic molecules and to adjust interfacial properties.

c) Inorganic/organic multilayer stacks: hybrid cavities and metamaterials

The inorganic/organic MBE tandem enables the combination of these materials beyond a single-interface geometry maintaining UHV conditions. We are not aware of any similar approach targeting functional inorganic/organic multilayer systems on that level. In what follows we present two examples demonstrating project progress during the first funding period in this direction.

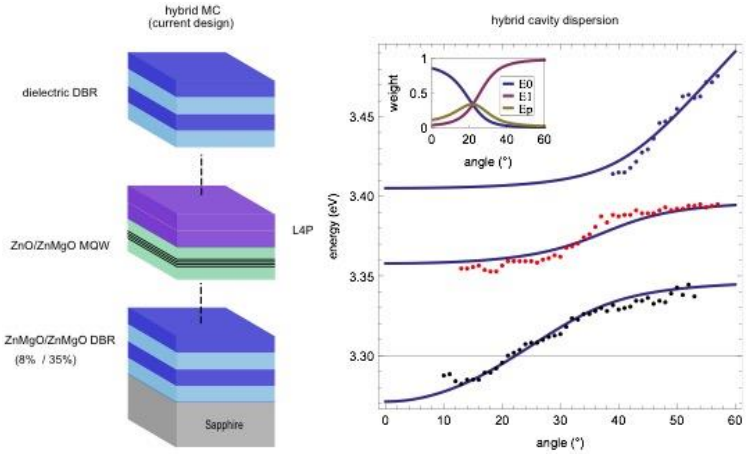

Fig. 3: Strong coupling in a hybrid ZnO/L4P-sp2 microcavity. Left: cavity design. Right: hybrid polariton dispersion derived from angle-dependent reflection measurements (dots), curves: calculation in a three-oscillator model, dashed lines mark positions of Wannier-Mott and Frenkel excitons. Inset: weights of the three states composing the hybrid polariton state along the middle branch.

Inorganic/organic hybrid microcavities: In a proposal made way back in 1997 [15], such cavities were theoretically analysed and it was shown that the merger of the strong optical coupling provided by the organic Frenkel exciton with the efficient relaxation pathways of the extended inorganic Wannier-Mott exciton should result in an unprecedented figure-of-merit for light emission, unattainable by sole organic or inorganic microcavities. Despite continuous efforts over past years, no demonstration of the predicted precedence succeeded. In a very recent effort, the observation of hybrid polaritons combining photons and Frenkel and Wannier-Mott excitons has been claimed for a cavity consisting of ZnO nanocrystals and NTCDA [16]. However, there are various inconsistencies, both in the experimental data as well as in their interpretation, arousing severe doubts. Unambiguity is caused by a lack in structure definition and a pure cavity quality by using, e.g., metallic mirrors. The approach developed in A5 overcomes these issues by taking advantage of the fact that the hetero-system ZnO/ZnMgO allows for fabrication of distributed-Bragg-reflection (DBR) mirrors [17]. These mirrors can be monolithically and resonantly combined with a ZnO-based multiple quantum well (MQW) structure serving, like originally proposed [16], as the active inorganic part. Provided by A3 (Hecht), spiro-annulated ladder-type quarterphenyl (L4P-sp2) with spectrally sharp optical transition matching the MQW exciton resonance was employed for the organic component. In a first step, vertical-cavity surface emitting laser (VCSEL) action and strong coupling at ultraviolet wavelengths has been demonstrated for the sole organic material in dielectric DBR microcavities [P11]. The hybrid cavity for which data are presented in Fig. 3 is designed such that the MQW exciton feature is high-energy shifted about one LO-phonon energy of ZnO (60 meV) relative to the (0,0) transition of L4P-sp2 whereas the first (0,1) vibronic replica is already located outside the DBRs' stop band. On the one hand side, the separation between the two exciton species is thus smaller than the molecular line broadening defining practically inorganic/organic resonance conditions – a case never achieved before – while, on the other hand, very rapid relaxation

towards the energetically lowest polariton states by LO-phonon emission is assured. Angle-dependent measurements of the cavity's reflection spectrum unveil the targeted three-branched polariton dispersion. Analysis within a standard three-coupled-oscillator model provides that these hybrid polaritons are indeed constituted in the relevant spectral regions by photons, inorganic and organic excitons at almost equal weight. The data collected in Fig. 3 present thus directed evidence for a photon-mediated hybridization of Frenkel and Wannier-Mott excitons. Based on the availability of suitable microcavity structures, issues that can be addressed next are the emission properties of these hybrid excitations, their relaxation dynamics as well as many-body effects and laser action under high-excitation levels.

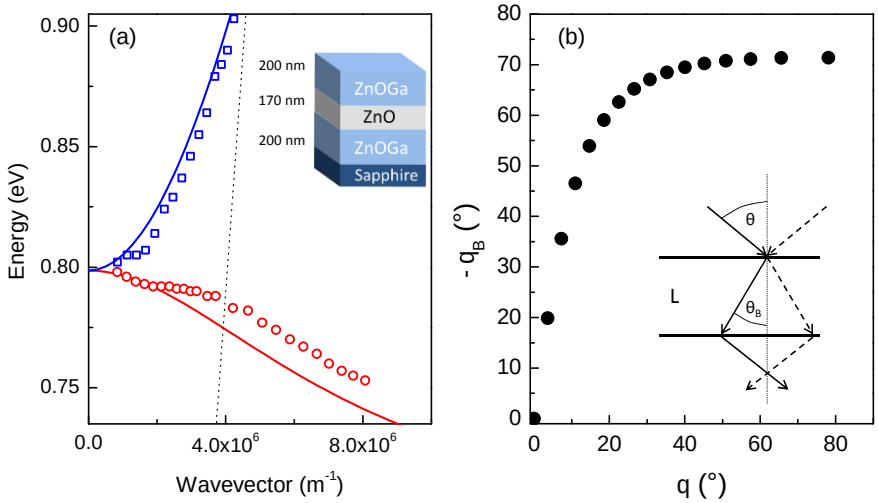

Fig. 4: Strong coupling of SPPs and cavity photons. a) Dispersion relations in TE and TM polarization (symbols: from reflection measurements, curve: calculated). The coupling in TM polarization leads to a negative group velocity. Inset: cavity design. b) Negative refraction under free-space illumination.

ZnOGa-based infrared metamaterials: Negative refraction and/or a negative group velocity are among the essential characteristics defining the functionality of metamaterials [18]. Metal-insulator-metal (MIM) film layers have the potential of producing anomalous electromagnetic dispersion. A recent demonstration of negative refraction on Au/SiO2/Ag slot-waveguides at visible wavelengths [19] is insofar limited as it is not addressable from free-space. On the other hand, the cavity photon modes of the MIM hybridize with the plasmonic excitations when their frequency is comparable with the surface plasmon frequency of the isolator/metal interface, with the result of a negative in-plane group velocity under appropriate conditions. For traditional metals, this concept is not practicable as their surface plasmon frequency is too large. However, employing ZnOGa as the metal, that frequency can be brought into resonance with the photon modes of submicron-sized cavities. Fig. 4 shows the first-time realization of this kind of photon-plasmon hybridization and the resultant negative refraction by an all-ZnO film structure. In a next step, a molecular emitter can be placed inside the cavity and the effect of the anomalous photonic density-of-states on its emission characteristics be studied. Moreover, the structure shown in Fig. 4 is the first step towards realization of hyperbolic metamaterial consisting of many alternating layers of ZnO/ZnOGa. In the next funding period, we will extend these encouraging initial studies as expounded below.

In addition to the above central topics, A5 has prepared tailored HIOS for numerous other projects of the CRC and has been involved in collaborations on

- doping and interfacial energy level tuning with A8 (Koch), B3 (Blumstengel), and B4 (Knorr/Scheffler/Rinke) [P6,P7,P12]
- synthesis, characterization, and photodegradation of ladder-type oligophenylenes with A3 (Hecht), and Blumstengel (B3) [P13,P14]
- charge-separation versus energy transfer in HIOS with A3 (Hecht), A8 (Koch), and Blumstengel (B3) [P15,P16]
- surface excitons in ZnO-based HIOS with B3 (Blumstengel) and B5 (Kühn/Elsässer) [P17,P18]

References

[1] M. E. Helau et al., J. Phys. C **24**, 445012 (2012).
[2] S. Blumstengel, S. Sadofev, H. Kirmse, and F. Henneberger, Appl. Phys. Lett. 98, 031907 (2011).
[3] E. Katsai et al., Appl. Phys. Lett. **94**, 43501 (2009).
[4] A. C. Cruickshang et al., Chem. Materials **23**, 3863 (2011).

[5] R. Forker and T. Fritz, Phys. Chem. Chem. Phys. **11**, 2129 (2009).
[6] K. Ellmer, Nature Photonics **6**, 809 (2012).
[7] A. Boltasseva and H. A. Atwater, Science **290**, 331 2011.
[8] F. Neubrech et al., Phys. Rev. Lett. **101**, 157403 (2008).
[9] V. Giannini, Y. Francescato, H. Amrania, C. C. Phillips, and S. A. Maier, NanoLett. **11**, 2835 (2011).
[10] S. M. Nie and S. R. Emory, Science **275**, 1102 (1997).
[11] H. Wang, J. Kundu, and N. J. Halas, Angew. Chem. **4**6, 9040 (2007).
[12] J. Homala, Chem. Phys. **108**, 462 (2008).
[13] H. Matsui, W. Badalawa, A. Ikehata, and H. Tabata, Adv. Optical Mater. **1**, 297 (2013).
[14] M. Abb et al., Nano Lett. **14**, 346 (2014).
[15] V. Agranovich, H. Benisty, and C. Weisbuch, Solid State Commun. **102**, 631 (1997).
[16] M. Slootsky, X. Liu, V. M. Menon, and S. R. Forrest, Phys. Rev. Lett. **112**, 076401 (2014).
[17] S. Kalusniak, S. Sadofev, S. Halm, and F. Henneberger, Appl. Phys. Lett. **98**, 011101 (2011).
[18] R. Dolling et al., Science **312**, 892 (20006).
[19] H. J. Lezec, J. A. Dionne, and H. A. Atwater, Science **316**, 430 (2007).
[20] R. Deng et al. , J. Lum. **134**, 240 (2013).
[21] Peŕez-Gonzaĺez et al., Nano Lett. **10**, 3090 (2010); P. Vasa et al., ACS Nano **4**, 7559 (2010).

3.3.2 Project-related publications

a) Publications published or accpeted

[P1] F. della Sala, S. Blumstengel, and F. Henneberger, “Electrostatic-field-driven alignment of organic ologomers on ZnO surfaces”, Phys. Rev. Lett. **107**, 146401 (2011).
[P2] M. Sparenberg, A. Zykov, P. Beyer, L. Pithan, C. Weber, Y. Garmshausen, F. Carlà, S. Hecht, S. Blumstengel, F. Henneberger, and S. Kowarik, “Controlling the growth mode of para-sexiphenyl (6P) on ZnO by partial fluorination”, J. Phys. Chem. Chem. Phys., in press.
[P3] S. Blumstengel, H. Kirmse, M. Sparenberg, S. Sadofev, F. Polser, and F. Henneberger, “Texture and morphology of ZnO grown nanocrystalline p-sexiphenyl thin films“, J. Cryst. Growth **402**, 187 (2014).
[P4] A. Kuznetzov, S. Sadofev, P. Schäfer, S. Kalusniak, and F. Henneberger, Appl. Phys. Lett. **105**, 191111, (2014).
[P5] S. Sadofev, S. Kalusniak, P. Schäfer, and F. Henneberger, “Molecular beam epitaxy of n-Zn(Mg)O as a low-damping plasmonic material at telecommunication wavelengths”, Appl. Phys. Lett. **102**, 181905 (2013).
[P6] R. Schlesinger, Y. Xu, O.T. Hofmann, S. Winkler, J. Frisch, J. Niederhausen, A. Vollmer, S. Blumstengel, F. Henneberger, P. Rinke, M. Scheffler, and N. Koch, „ Controlling the work function of ZnO and the energy-level alignment at the interface to organic semiconductors with a molecular electron acceptor “, Phys. Rev. B **87**, 155211 (2013).
[P7] Y. Xu, O.T. Hofmann, R. Schlesinger, S. Winkler, J. Frisch, J. Niederhausen, A. Vollmer, S. Blumstengel, F. Henneberger, N. Koch, P. Rinke, and M. Scheffler, „Space-charge transfer in hybrid inorganic-organic systems“, Phys. Rev. Lett. **111**, 226802 (2013).
[P8] S. Sadofev, S. Kalusniak, P. Schäfer, H. Kirmse, and F. Henneberger, “Free-electron concentration and polarity inversion domains in plasmonic (Zn,Ga)O}”, phys. stat. sol (b), in print.
[P9] S. Kalusniak, S. Sadofev, and F. Henneberger, “ZnO as a tunable metal: New types of surface plasmon polaritons”, Phys. Rev. Lett. **112**, 137401 (2014).
[P10] S. Kalusniak, S. Sadofev, and F. Henneberger, “Resonant interaction of molecular vibrations and suface plasmon polaritons: The weak coupling regime”, Phys. Rev. B ### (2014).
[P11] M. Höfner, B. Kobin, S. Hecht, and F. Henneberger, Chem. Phys. Chem. published online DOI:10.1002/cphc.201402492.
[P12] N. Kedem, S. Blumstengel, F. Henneberger, H. Cohen, G. Hodes, and D. Cahen, „ Morphology-, synthesis- and doping-independent tuning of ZnO work function using phenylphosphonates “, Phys. Chem. Chem. Phys. **16**, 8310 (2014).
[P13] B. Kobin, L. Grubert, S. Blumstengel, F. Henneberger, and S. Hecht, " Vacuum-processible ladder-type oligophenylenes for organic-inorganic hybrid structures: Synthesis, optical and electrochemical properties upon increasing planarization as well as thin film growth ", J. Mater. Chem., **22**, 4383 (2012).
[P14] B. Kobin, F. Bianchi, S. Halm, J. Leistner, S. Blumstengel, F. Henneberger, and S. Hecht: "Green Emission in ladder-type quarterphenyl: beyond the fluorenone-defect" Adv. Funct. Mater. published online DOI: 10.1002/adfm.201402638.
[P15] F. Bianchi, S. Sadofev, R. Schlesinger, B. Kobin, S.Hecht, N. Koch, F. Henneberger, and S.

Blumstengel, “Cascade energy transfer versus charge separation in ladder-type oligo(p-phenylene)/ZnO hybrid structures for light-emitting applications, submitted.
[P16] R. Schlesinger, F. Bianchi, S. Blumstengel, C. Christodoulou, R. Ovsyannikov, B. Kobin, K. Moudgil, S. Barlow, S. Hecht, S. R. Marder, F. Henneberger, N. Koch, “Efficient light emission from inorganic/organic semiconductor hybrid structures by energy level tuning”, submitted.
[P17] S. Kühn, S. Friede, S. Sadofev, S. Blumstengel, F. Henneberger, and T. Elsässer, “Surface excitons on a (000-1) thin film“, Appl. Phys. Lett. **103**, 191909 (2013).
[P18] S. Friede, S. Kühn, S. Sadofev, S. Blumstengel, F. Henneberger, and T. Elsässer, “Nanoscale transport at the interface of ZnO and a molecular monolayer“, submitted.

b) Other publications

c) Patents

F. Henneberger, H. Riechert, and N. Koch, Electromagnetic radiation generating arrangement, has electron hole pairs from charge carrier injection zone of semiconductor cylinders entering organic material in which pairs excite emission of electromagnetic radiation by recombination, Patent Number(s): DE102010019660-A1 ; WO2011134464-A1 ; EP2564445-A1 ; US2013092908-A1.

3.4 Research plan

Project A5 will continue the efforts of the first funding period with focus points realigned by the knowledge and understanding described above.

A) Control of HIOS structure and morphology

Here, we intend both to add new oxide semiconductors to our MBE portfolio as well as to deepen the study of molecular assembly on these surfaces.

(i) NiO, Er_2O_3, and $(InSn)_2O_3$ will be in the focus on the inorganic side. Contrary to ZnO, NiO is natively p-type and has been intentionally doped by Li up to $p = 10^{19}$ cm^{-3} [20]. It may thus serve as hole injector into organic materials and even surpass the frequently used MoO_3 because of its low electron affinity assuring much better electron blocking. However, NiO films currently described in literature suffer from considerable structural disorder resulting in a very low hole mobility. We will attempt to improve material quality by an MBE-approach. MgO - a commercially available substrate - and NiO_2 have the same (rocksalt) crystal structure and almost identical ionic radii. The phase-pure MBE growth of the ZnMgO ternary has been mastered years ago. By combining these prerequisites, we have the reasonable hope for obtaining suitable p-type material, even with injection barriers tunable by composition. Er_2O_3 can be employed as electron blocker as well. It further emits at 1.5 µm and is thus interesting in the context of infrared plasmonics. For the same reason, we plan the MBE growth of $(InSn)_2O_3$. Because of its cubic crystal structure, polarity inversion is not an issue here and LO-phonon scattering should be weaker than in ZnO. Assuring layer homogeneity, still higher free-electron concentrations at even reduced Drude damping might be generated and the operational range shifted markedly beyond a photon energy of 1 eV. Moreover, $(InSn)_2O_3$ fits structurally to Er_2O allowing for better integration of the infrared light emitter. The electrical functionality of NiO and Er_2O_3 layers will be verified and employed in B3 (Blumstengel), B7 (Neher) and B12 (List-Kratochvil), while the energy-level tuning for relevant organic molecules will be investigated in A8 (Koch).

(ii) Sexiphenyl and its fluorinated versions have turned out to represent model molecules for studying the electrostatically driven aggregation and morphology on dipolar surfaces, such as ZnO($10\bar{1}0$). While the experimental studies have revealed a substantial potential for achieving low-roughness, highly uniform molecular films, the underlying physical processes are not yet satisfactorily understood. How does the fluorination affect Ehrich-Schwöbel barriers and the anisotropy of diffusion rates? What is the role of step edges? How does the interplay between molecule-molecule and molecule substrate interaction control the molecular morphology beyond the sub- and single-monolayer regime. Based on the methodological know-how developed by A1 (Dzubiella) and A7 (Klapp) in the first funding period, the new combined project A7 (Dzubiella/Klapp) will tackle these questions in-depth. A5 will join these activities by performing dedicated experiments suggested by the improved understanding. In addition to 6P-F_4, the asymmetric version 6P-F2 with a permanent dipole moment will be included in the analysis.

(iii) The preliminary work on the on-surface polymerization of ZnO surfaces will be continued with A3 (Hecht) where suitable molecules (…) will be designed and synthesized. A5 will be also strongly linked to A2 (Kumagai/Wolf) complementing our in-situ structural analysis by low-temperature STM and AFM techniques. In this context, we will also include ladder-type oligophenylenes in our investigations and prepare (highly conductive) ZnO templates for use in A2 (Kumagai/Wolf).

Access to the analytical methods provided by Z2 (Koch/Kowarik) will be mandatory for all the project goals described above. A5 will supply tailored MBE films and quantum well structures for various other projects [A8 (Koch), B3 (Blumstengel), B7 (Neher), B11 (List-Kratochvil)]. Specimen with controlled free-electron concentration up to the strongly degenerate regime will be provided for studying the influence of doping on the molecular attachment, a central subject of B4 (Scheffler, Körzdörfer, Rinke).

Methods: MBE and OMBD in a tandem setup, RHEED, LEED, AFM, STM, KPM, DRS, all in-situ, photoluminescence and absorption, required X-ray and TEM techniques provided by Z2 (Kowarik/Koch).

Timeline: MBE of NiO_2 and InSnO (development of suitable growth protocols 06/15-12/15, then film growth as required), 6P-Fx (06/15-12/16, decision on further molecules)

B) Infrared hybrid plasmonics

In the first funding period, we have established an MBE regime for growing low-loss ZnOGa films for use in infrared plasmonics and demonstrated new types of surface SPPs with tunable dispersion relations. In a next, logic step, we intend to couple these SPPs to molecular excitations and to test plasmonic functions. The working program is four-parted.

(i) So far, the infrared properties of n-type ZnO were analyzed in terms of a Drude permittivity. While this level of understanding was sufficient for conceptualizing experiments, a more adequate physical description is still needed, also for optimizing material properties. The Drude formula relies on complete screening of the Coulomb interaction, an assumption questionable at the free-electron densities realized in doped semiconductors. B10 (Busch) will elaborate the theory of such electron gases while A5 will conduct experiments suggested by the progress in physical insight. Time-resolved and non-linear measurements performed in collaboration with B5 (Wörner/Elsässer) will play an essential role in this context. One goal of these efforts is to extend the metallic range to shorter wavelengths, i.e., by replacing ZnO by another semiconductor with better-suited parameters. As mentioned above, we will start with $(InSn)_2O_3$ as it looks promising in this regard.

(ii) In the first funding period we have demonstrated resonant but weak coupling of SPPs to stretching vibrations of the CH_3 group in a molecular material. Now, we will target strong coupling where molecular vibrations and SPPs form a hybrid state. In this way, the otherwise uncorrelated molecular vibrations are locked into a collective phonon-type excitation. This new electromagnetic/vibrational eigenstate is not only interesting from a fundamental point-of-view, but also of direct relevance for opto-electronic functionality. Intra-molecular relaxation rates are modified or vibrational energy can be transported for triggering electronic processes (e.g., exciton dissociation), to name just two examples. Our estimates show that the strong-coupling regime is attainable by using molecular vibrations with stronger optical dipole moments such as those of carbonyl groups.

(iii) In addition to the vibrational hybridization, we also intend to demonstrate strong coupling of SPPs to electronic excitations. Unlike attempts to couple molecular excitons to surface plasmons of nanostructures made from traditional metals in the visible range (plexitons [21]), we are aiming at single-carrier excitations of charged molecules, i.e., cat- or anions. The optical transitions that couple to the SPPs of ZnOGa (or InSnO) are hence LUMO-LOMO* or HOMO-HOMO* representing the direct molecular analog to the free-carrier transition of the inorganic semiconductor. In this way, a generic hybrid plasmonic state is created. Similarly as for the vibrational hybridization, novel opto-electronic functionality is resulting, but now in the electronic domain, i.e., charge can be coherently transported in molecular films. Project success is critically related to the availability of molecules with strong absorption cross-section in the infrared spectral range. Candidates are molecules used as dopants in molecular opto-electronics such as …. This and similar molecules will be designed and synthesized in A3 (Hecht) and A8 (Koch).

(iv) Finally, we plan to implement and test specific realizations of plasmonic enhancement and switching in HIOS. One question to be addressed is whether and to what extend molecular transitions in the visible spectral range can be intensified by two infrared plasmons (two-plasmon enhancement).

Traditional J-aggregates perfectly fit to the SPPs of ZnOGa. A further goal will be the enhancement of hybrid charge-transfer exciton transitions, typically located at infrared wavelengths. This may help to identify these otherwise weakly absorbing excitations as planned in B3 (Blumstengel), B7 (Neher), and B9 (Stähler). Moreover, the surface plasmon frequency can be also tuned into resonance with the exciton binding energy of molecular materials typically some 100 meV. In this way, hybrid charge-transfer excitons can be split-off creating separated electrons and holes for current generation or, in case of direct excitons, the light emission can be switched off by plasmonic excitation. B5 (Wörner/Elsässer) will be the partner in these time-resolved or non-linear studies.

Methods: MBE and OMBD in a tandem setup, Fourier transform and Raman spectroscopy, attenuated total reflection, (ns) time-resolved infrared spectroscopy, infrared pump-probe techniques provided by B5 (Wörner/Elsässer)

Timeline: better understanding of the semiconductor's infrared response (07/15-07/17), strong vibrational-SPP coupling (07/15-12/15), strong charge-SPP coupling (01/16-12/16), switching experiments (01/17-06/19), demonstration of plasmonic functions (01/16-06/19)

c) Functional HIOS multi-layers

Again, we will continue and advance encouraging work of the first funding period. The structural design of the stacks will be improved and operation with respect to the target function tested and refined.

(i) The inorganic-on-organic MBE process will be one of the focus points. For the targeted photonic or plasmonic function of the inorganic layers, a degree of disorder below the optical wavelength is tolerable. However, in order to minimize scattering losses, we intend to implement nucleation procedures that increase the structural uniformity of the ZnO layer atop the organic material. So far, the active organic layer in the hybrid cavities has been fabricated off-MBE by spin casting. While sufficient for proof-of-concept experiments, significant operational improvement can be expected in an all-UHV regime. For the fabrication of hybrid metamaterials, continuous UHV deposition this is even a demand. Growth protocols enabling the deposition of highly reproducible inorganic/organic layer structures have thus to be implemented. We will solve this issue stepwise and increase the number of layers as enabled by progress.

(ii) Photon-mediated hybridization of Frenkel and Wannier-Mott excitons in ZnO/L4P-sp2 cavities already succeeded. Based on this milestone, we will now concentrate on the photonic properties of such cavities. First, the relaxation dynamics across the hybrid polariton dispersion will be unveiled by wavelength selective short pulse excitation. We expect the absence of relaxation bottlenecks limiting the performance of purely organic microcavities. In the next step, the role of many-body effects (polariton-polariton scattering, electron-hole-plasma formation), characteristic of inorganic semiconductors at high-excitation levels, will be elucidated for the hybrid system.c This data and measurements of the optical gain will enable us to identify the leading processes giving rise to laser action, eventually demonstrated under intense optical pumping and optimized. In addition, we will study the optical non-linearity provided by hybrid cavities through change of its mode spectrum under illumination with a strong optical beam.

(iii) We will attempt to fabricate hybrid infrared metamaterials utilizing the plasmonic features of oxide semiconductors. In a first step, an organic emitter will be placed between to resonant plasmonic layers of ZnOGa. The occurrence of negative refraction on such a cavity, still with a passive medium inside, could already be demonstrated (Fig. 4). Adding infrared emitter molecules (…), we expect substantial changes of the emission characteristics by coupling to the SPPs, see B10 (Busch). Increasing the number of layers will eventually lead to a hyperbolic metamaterial. The presence of a refractive-index hyperbola will tested by reflection and transmission experiments, again in collaboration with B10 (Busch).

A5 will also grow inorganic/organic few-layer stacks with additive interfaces for the investigation of charge separation processes and hybrid charge-transfer excitons in B3 (Blumstengel) and B7 (Neher).

Methods: MBE and OMBD in a tandem setup, photoluminescence and photoluminescence excitation spectroscopy, including ps-time resolution and high-excitation levels, method of variable stripe length, short-pulse pump-probe spectroscopy, infrared measurement with the methods described B).

Timeline: optimization of hybrid layer growth (07/15-06/18), relaxation processes in hybrid cavities (07/15-06/16), high-excitation effects (01/16-12/16), laser action (07/16-06/17), final optimization of the laser

process (07/18-06/19), molecular emitter in plasmonic environment (07/15-12/16), hyperbolic stacks and functionality (01/17-06/19)

3.5 Role within the Collaborative Research Centre

A5 is linked to various other projects of the CRC. The assemblage of conjugated organic molecules on oxide-semiconductor surfaces will be studied in close collaboration with A7 (Dzubiella/Klapp) where the processes controlling morphology and structure of the molecular layers will be treated with the adequate theoretical methodology. Access to the tools for structure characterization supplied by Z2 (Koch/Kowarik) is mandatory for A5, also for the targeted growth of new oxide-semiconductors. Continuing fruitful cooperation of the first funding period, the molecular materials required for the goals of A5 will be developed and synthesized by A3 (Hecht) or, if synthesis protocols are known, by Z1 (Hecht). The efforts on plasmon-related hybridization and functionality will be joined by B5 (Wörner/Elsässer) contributing the PIs' expertise on infrared excitations as well as the experimental techniques for studying their dynamics. B10 (Busch) will foster these activities by developing the required in-depth description. The electrical functionality of NiO and Er_2O_3 layers will be tested and employed in B3 (Blumstengel), B7 (Neher) and B12 (List-Kratochvil), while the energy-level tuning for relevant organic molecules will be investigated in A8 (Koch). A5 will also fabricate HIOS building blocks for the device structures targeted in B3 (Blumstengel and B12 (List-Kratochvil),

If possible and adequate, A5 will provide MBE-made HIOS layers and stacks wherever required in the CRC [to be detailed ….] . A7 [Rabe/Kirstein] will be supported by supply of the time-resolved photoluminescence setup available in A5.

3.6 Delineation from other funded projects

To be detailed

3.7 Project funds

3.7.1 Previous funding

The project has been funded within the Collaborative Research Centre since 07/2011.

3.7.2 Funds requested

Funding for	2015/2		2016		2017		2018		2019/1	
Staff	Quantity	Sum	Quantity	Sum	Quantity	Sum	Quantity	Sum	Quantity	Sum
PhD student, 75%	2	45.500	2	90.900	2	90.900	2	90.900	2	45.500
Total		45.500		90.900		90.900		90.900		45.500
Direct costs	Sum		Sum		Sum		Sum		Sum	
Small equipment, Software, Consumables										
Other										
Total										
Major research equipment	Sum		Sum		Sum		Sum		Sum	
€ 10.000 - 50.000										
> € 50.000										
Total										
Total										

(All figures in Euro)

3.7.3 Staff

	No.	Name, academic degree, position	Field of research	Department of university or non-university institution	Commitment in hours/week	Category	Funded through:
Available							
Research staff							
Non-research staff							
Requested							
Research staff							
Non-research staff							

Job description of staff (supported through available funds):

<laufende Nummer gemäß obenstehender Tabelle> <Name>
<Aufgabenbeschreibung>

Job description of staff (requested):
2 Doctoral student: to be detailed

3.7.4 Direct costs for the new funding period

	2015/2	2016	2017	2018	2019/1
Funds available					
Funds requested					

(All figures in Euro)

< Kategorie> for <Jahreszahl/2>

<Bezeichnung und Begründung der Antragsposition>	EUR	<sum>
<Bezeichnung und Begründung der Antragsposition>	EUR	<sum>

<category> for <year>

<Bezeichnung und Begründung der Antragsposition>	EUR	<sum>
<Bezeichnung und Begründung der Antragsposition>	EUR	<sum>

<etc.>

3.7.5 Major research equipment requested for the new funding period

€ 10.000 - 50.000 for <Jahreszahl/2 bzw. Jahreszahl>

<Bezeichnung des Gerätes (ggf. Typenbezeichnung und Leistungsklasse) und wissenschaftliche Notwendigkeit>	EUR	<sum>
<Bezeichnung des Gerätes (ggf. Typenbezeichnung und Leistungsklasse) und wissenschaftliche Notwendigkeit>	EUR	<sum>

> € 50.000 for < Jahreszahl/2 bzw. Jahreszahl>

<Bezeichnung des Gerätes (ggf. Typenbezeichnung und Leistungsklasse) und wissenschaftliche Notwendigkeit>	EUR	<sum>
<Bezeichnung des Gerätes (ggf. Typenbezeichnung und Leistungsklasse) und wissenschaftliche Notwendigkeit>	EUR	<sum>

3.7.6 Student assistants

	2015/2	2016	2017	2018	2019/1
Quantity					
Commitment in hours/week					
Sum					
Tasks					

3 About project A6

3.1.1 Title: HIOS based on nanotubular J-aggregates

3.1.2 Research areas: Physical Chemistry, Experimental Physics of Condensed Matter

3.1.3 Principal investigators

PD Dr. Kirstein, Stefan (*19.10.1960, German)
Humboldt-Universität zu Berlin
Department of Physics, Physics of Macromolecules
Newtonstr. 15, 12489 Berlin
Phone: +49 (0)30-2093-7821
Fax: +49 (0)30-2093-7632
E-mail: kirstein@physik.hu-berlin.de

Prof. Dr. Rabe, Jürgen P. (*20.11.1955, German)
Humboldt-Universität zu Berlin
Department of Physics, Physics of Macromolecules
Newtonstr. 15, 12489 Berlin
Phone: +49 (0)30-2093-7788
Fax: +49 (0)30-2093-7632
E-mail: rabe@physik.hu-berlin.de

Do the above mentioned persons hold fixed-term positions? no

3.1.4 Legal issues

This project includes

1.	research on human subjects or human material.	no
2.	clinical trials	no
3.	experiments involving vertebrates.	no
4.	experiments involving recombinant DNA.	no
5.	research involving human embryonic stem cells.	no
6.	research concerning the Convention on Biological Diversity.	no

3.2 Summary

The project will continue the exploration of highly ordered, regular and uniform tubular cyanine dye aggregates as an organic scaffold in aqueous solution to build nanostructures of higher complexity and functionality through the combination with inorganic nanomaterials. This strategy to grow HIOS structures complements the building principle of other projects where the inorganic substrate serves as the scaffold to build organic structures on it. The unique feature of the system investigated here is the fact that the molecular packing is *a priori* not defined by an underlying substrate but only due to the intermolecular van der Waals forces and dispersion forces between the dye molecules. This results in self-assembly into well-ordered aggregate structures that are characterized by very strong exciton coupling and therefore shall be utilized here to elucidate energy and/or charge transfer between the organic and the inorganic semiconducting materials.

In the first funding period it was shown that these aggregates are stable enough to use them as a scaffold to synthesize *in-situ* inorganic nanomaterials at the surface or to attach nanomaterials via electrostatic attraction without affecting the aggregate's structure. Silver nanowires were grown inside the nanotubes and studied in detail. An interesting and unexpected chemical instability of the resulting wires was found, which also limits however their attraction for further applications in plasmonics. CdS nanocrystals were synthesized at the aggregate's surface as well as a transparent silica shell was obtained by room temperature synthesis. Using polyelectrolytes as a gluing material we succeeded in adsorbing acid capped CdTe nanoparticles and could show effective resonance energy transfer between the particles and the dye aggregate.

In the forthcoming funding period in one sub-project we intend to study long-range energy transfer between two donor-acceptor couples mediated by Frenkel excitons within the organic J-aggregate. These studies are of fundamental interest for all applications that create or annihilate extended and mobile excitons at localized states. The principal idea is to create an exciton state within the aggregate locally by energy transfer from attached semiconducting nanoparticles that act as donors in a Förster-resonance couple. The excitation will then diffuse within the aggregate and be eventually transferred to nanoparticles or dyes that act as acceptors and emit light. The excitation and de-excitation is limited to the size of the Förster radius of the donor-acceptor couples and hence much smaller than the expected dimensions of exciton diffusion, which was estimated in the literature to be above 200 nm. The major goal is to find suitable combinations of materials and an optimized build-up of the structures to demonstrate such an exciton-mediated long range coupling between two HIOS structures.

In a second sub-project it is planned to use the sol-gel method to synthesize a silica shell around the tubular aggregates to stabilize the structure against chemical and mechanical damage, to create an isolating layer, and to find new ways to attach inorganic and organic materials. The silica shell leaves the aggregate structure unaffected but shows a very regular and uniform super structure that is very suitable for application of advanced 3D image reconstruction techniques. A systematic study has to be performed to clarify the connection between the silica super structure and the molecular organization of the aggregates. A detailed structure determination is of great importance for the molecular dynamics simulations and theoretical calculations performed in B6 (May). The 3D-image reconstruction and tomography by cryo-TEM shall be carried out at the Joint Lab of Structural Research at IRIS Adlershof and the Research Center of Electron Microscopy, with the support of C. Böttcher at Freie Universität Berlin, who is already experienced with these systems from previous collaborations.

3.3 Project progress to date

3.3.1 Report and state of understanding

State of the art before the project started

At the beginning of the project it was known that the tubular J-aggregates of the amphipilic cyanine dye, 3,3′-bis(2-sulfopropyl)-5,5′,6,6′-tetrachloro-1,1′-dioctylbenzimidacarbocyanine (C8S3), formed in aqueous solution by spontaneous self-assembly, could be used as templates to grow silver nanowires. The wires are growing within the void space of the tubes by reduction of silver ions from $AgNO_3$ salt and it was supposed that this is due to oxidation of the dyes. The resulting nanowires have a diameter of 6.5 ±0.5 nm and length exceeding micrometers. The protocol for the wire synthesis was elaborated although not understood in detail. [1] E.g., it was always found that nanowires are grown in coexistence with the growth of nanoparticles outside of the tubular aggregates. The growth kinetics of the wires was only coarsely looked at by spectroscopic investigation of the oxidation of the dyes within the aggregates [2]. It was clear, that growth occurs over time scales of one to two days and that for longer times the presence of excess of silver ions leads to the growth of nanostructures that exceed the void volume of the initial tubular J-aggregates. However, there was no detailed chemical or structure analysis of the real 6.5 nm wires available at this time. The growth of the wires was found to be accompanied by new absorption bands which were attributed to plasmon resonances of the silver structures. Also, no direct assignment of these bands to plasmon resonances of the nanowires was available.

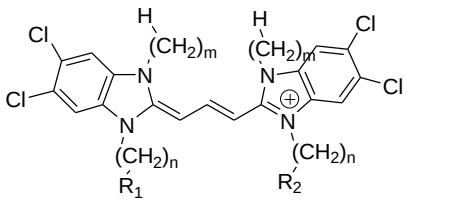

C8S3: m = 3; n = 3; $R_1 = SO_3Na$ $R_2 = SO_3^{\ominus}$

Based on these findings a major goal of this project was to explore the growth mechanism of these silver wires in order to better control their synthesis and make them available for studies of plasmon resonances between silver nanowires and organic molecular aggregates. With the reduced resources approved for the project (one instead of two PhD students), we focused to the following:

- Understanding of the nucleation and growth processes of noble metal, especially silver, wires in tubular aggregates in aqueous solution.
- Application of the principal of synthesis to the production of wires of other noble metals or semiconducting materials.

In parallel, using core and external funding, the route to synthesize inorganic materials at or within the tubular aggregates by in-situ chemistry under ambient conditions in aqueous solutions was extended to other materials. We succeeded to synthesize semiconducting materials as well as silica on the aggregates and

made use of electrostatic adsorption to build complex structures of aggregates and semiconducting nanoparticles.

Major achievements

a) Growth and structure of Ag nanowires

The growth of the silver nanowires after addition of $AgNO_3$ to an aggregate solution was studied systematically and in detail using cryo-TEM and TEM analysis [22] in collaboration with Z2 (F. Polzer, H. Kirmse). Because of the slow growth kinetics it was possible to extract samples at different time steps between first appearance of seeds and aggregates fully filled with silver wires. Typical growth states are presented in Fig. 1. Some remarkable new and fundamental observations were made by these experiments:

- The spatial position of the majority of initially formed seeds discriminates between growth of particles at outer surface of the aggregate or wires at inner space. Both structures do not coexist at one aggregate; whatever growth faster is favored for further growth, similar to an Ostwald ripening process.
- Wires are growing piece-wise from isolated seeds within the aggregate until they completely fill the tube, which can only be explained if strong and fast transmission of Ag ions or Ag nuclei through the membrane of the the amphiphilic dyes is allowed.
- Addition of NaCl dissolves the previously formed wires and converts them into AgCl crystallites. This effect is called oxidative etching [3,4] and discloses the chemical instability of the wires but also the permeability of the aggregate membrane.

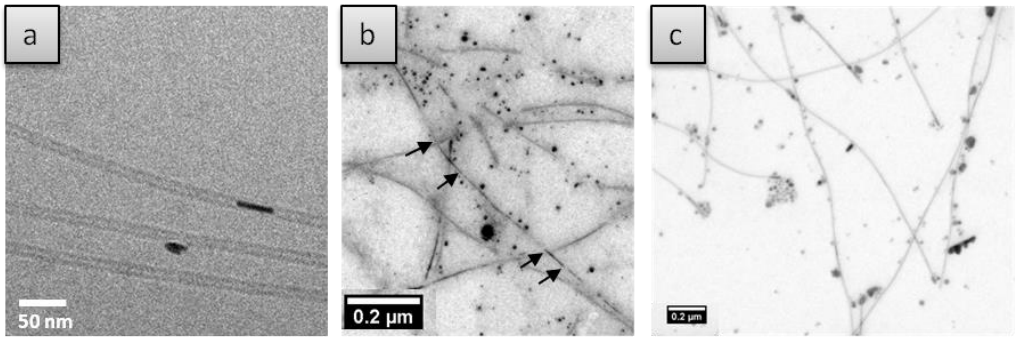

Figure 1: cryo-TEM (a) and TEM (b,c) images representing typical situations after three different time steps of the growth of silver nanowires within the tubular J-aggregate template. a) First formation of seeds, after 3 minutes of growth time (one inside, one outside of the aggregates). b) Fragments of wires in coexistence with particles outside the aggregates, after approx. 2h of growth time. For some pieces of wires the endpoints are marked by arrows. c) Aggregates completely filled with silver nanowires after approx. 24 h growth time.

The crystal structure and the chemical composition of the silver nanowires was elucidated further by means of EDX measurements and high resolution TEM (Z2, H. Kirmse). It was confirmed that the wires consist of silver and crystalline domains were found that have extensions that fit to the 6.5 nm diameter of the nanowires. Serendipitously we found crystalline pieces of wires that extend over more than 100 nm in length, as shown in Fig. 2 with almost monocrystalline structure but showing twin boundaries as expected for the growth of quasi one-dimensional metal structures [3].
The crystal structure was analyzed further by selected area electron diffraction (SAED, Fig. 3). A typical diffraction pattern shows few blurred spots that partially can be assigned to a distorted silver [110] plane, but some of them have to be addressed to a super structure like a Moiree pattern of differently oriented crystal fragments which are in strong correlation to each other due to twin boundaries. Those effects have been reported elsewhere [4] for silver nano-platelets and nano-rods. However, the position of these peaks varies between different images and is still under investigation.

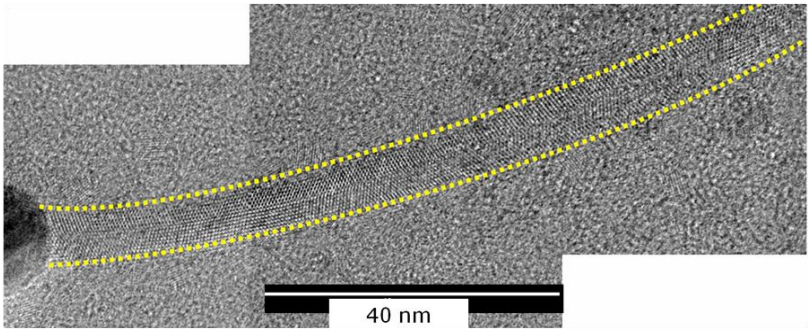

Figure 2: HRTEM image of a single crystalline domain of a silver nanowire. A particle is seen on the left and the wire extends over several images over a length of more than 120 nm. At least one twin boundary is visible in parallel to the long crystal axis.

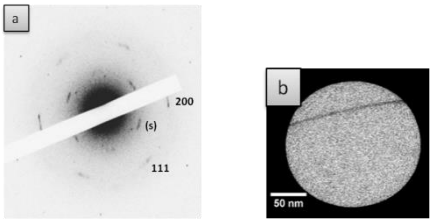

Figure 3: SAED of single Ag nanowire. a) Diffraction pattern with Ag diffraction and super structure peaks (s) indicated separately (see text). The sharp spots are artifacts. b) Image of single Ag nanowire as seen by the diffraction spot. The spot size is about 200 nm.

b) Spectroscopy of plasmon resonances

A spectroscopic investigation of single silver nanowires was carried out with the principal idea to visualize the nanowires using optical dark field microscopy and to measure the scattered spectra when illuminated with white light from a mercury lamp. If possible, plasmon conduction along a wire should be verified by excitation of the wire at one end with light of appropriate wavelength, and monitoring the out-coupling of the plasmon at the other end. From simple theoretical calculations for an infinitely long wire it was expected that plasmons could be excitable at least in transverse mode in the wavelength range of 350 to 380 nm (Fig. 4b). Finite length nanowires exhibit additionally longitudinal modes depending on their lengths. The experiments, however, suffered from a strong damping of the plasmons and rather small signals with respect to the background noise. Another difficulty in a bulk scattering experiment was to separate the signals of the nanowires from spherical nanoparticles, as can be seen in Figure 4a, since the nanoparticles found in parallel caused scattering signals that exceeded the signal of the wires. The plasmon transmission experiments on single nanowires on a substrate were carried out in cooperation with B1 (Benson). The setup and the experimental parameters were very similar to those selected for successful measurements of plasmon transmission in larger silver nanowires [5]. For the ultrathin wires investigated here the experiments did not allow to investigate the length-dependence of the plasmon properties, partly due to the small signals but also due to the difficulty to control and stabilize the length of the nanowires (see a) above). Both limit the attraction of the nanowires for plasmonics. On the other hand, it appears that the plasmonic signatures of the silver nanoparticles are rather strong and therefore attractive for enhancing the local fields at the surface of the molecular nanotubes.

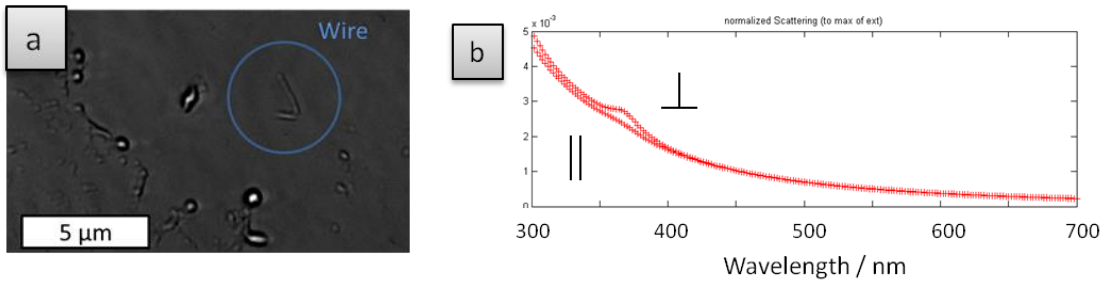

Figure 4: a) Dark field microscope image of single silver nanowire and b) theoretically calculated plasmon resonance scattering.

c) In-situ synthesis of semiconducting nanostructures at the amphiphilic J-aggregates

A breakthrough of the project was the finding that semiconducting nanoparticles can be grown by in-situ synthesis on the surface of the amphiphilic J-aggregates without destroying the structure and morphology [19]. In Figure 5 cryo-TEM images of CdS nanoparticles are shown that were grown on the tubular

aggregates. These particles have a typical size of 3 to 4 nm and are closely attached to the aggregate. The principle of the chemical synthesis is based on the addition of a metal salt to release the metal ions (Me^{2+}, where Me = Cd, Zn, or Ni) which will be enriched at the aggregates surface due to electrostatic attraction. Addition of a sulfur source (thiactamide in this case) and the presence of ammonium hydroxide as a precipitation agent results in the growth of CdS (Zns, NiS, respectively) nanoparticles at the aggregate surface. Typically, a shell of nanoparticles is formed around the tubular structures without significantly affecting the aggregates morphology. The crystal structure is analyzed by electron diffraction revealing a sphalerite structure. The coverage of CdS particles can be tuned by varying the concentration of the sulphur source. Efficient energy transfer from nanoparticles to the dye aggregates is proven by the complete quenching of CdS emission.
The recipe was applied also to the growth of metal oxides such as ZnO, however with less success. Nanoparticles were formed, but not only in the vicinity of the aggregates and most of the tubular aggregates were transformed into planar sheet-like structures. The problem was that reaction at room temperature was too slow and at elevated temperatures the aggregates were destroyed.

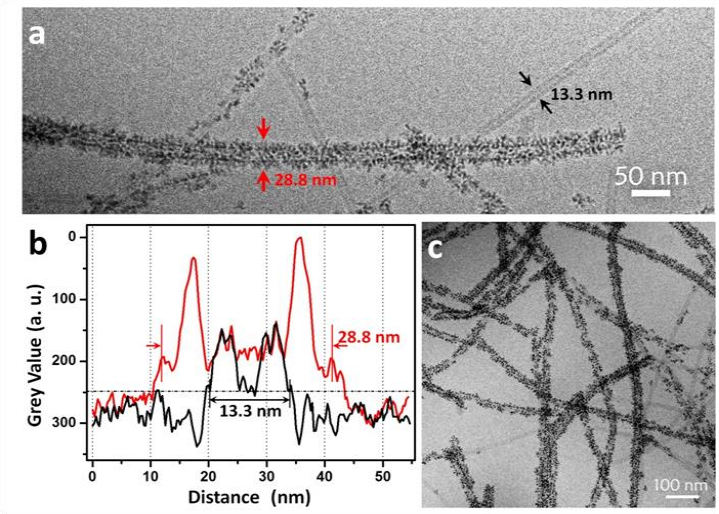

Figure 5. (a) Cryo-TEM image of nanohybrids consisting of CdS nanocrystals decorating on the outer surface of C8S3 J-aggregate nanotubes. (b) Line scans across the J-aggregate/CdS hybrid (red) and bare J-aggregate nanotube (black) showing the diameters of nanohybrid and J-aggregate are 28.8 nm and 13.3 nm, respectively. (c) Large area cryo-TEM image of J-aggregate/CdS nanohybrids (taken from [19]).

d) <u>FRET experiments between QDots and J-aggregate</u>

As an alternative strategy to prepare nanohybrid structures comprising cyanine dye J-aggregates decorated with semiconducting quantum dots we employed electrostatic adsorption of negatively charged CdTe nanoparticles (QDs, capped with 3-mercaptopropionic acid (MPA)). Prior to adsorption of the particles the aggregates were decorated with a thin layer of a polycations (PDADMAC) in order to reverse the sign of the surface charge. QDs with different emission wavelengths (i.e., 535 and 665 nm) were successfully assembled on the supramolecular J-aggregate where the J-aggregates are left structurally unaffected, as shown in Figure 6. [20] The structural organization of these nanohybrids is unprecedented and the concept of fabrication can easily be extended to combine the J-aggregates with other inorganic materials given that they have a chemical coating that provides negative surface charges.

Strong energy transfer from the QDs to the aggregate was measured by quenching of donor emission (Figure 7) and energy transfer from the aggregate to the QDs was detected by enhanced acceptor emission (Figure 8). The direction of energy transfer was adjusted by the size and hence optical properties of the QDs. A remarkable asymmetry of the transfer efficiency was observed, as it was up to 100% for the case of transfer from the QDs, while it achieved 20% in the case of transfer to the QDs. For the case of FRET from the particles to the aggregates the time decay resembles the structural duality observed by cryo-TEM. A fast decay is caused by strong coupling of the particles very close to the aggregates surface, while the slower decay is due to the particles that are loosely bound. These results show that the (at least partial) homogeneity of the samples allows direct interpretation of energy transfer efficiencies without deconvolution of distance distributions. This is considered as a major advantage against work done before by other groups that have investigated resonance energy transfer in J-aggregate/QD systems using films of blends of the materials [6] or via layer-by-layer (LBL) technique [7].

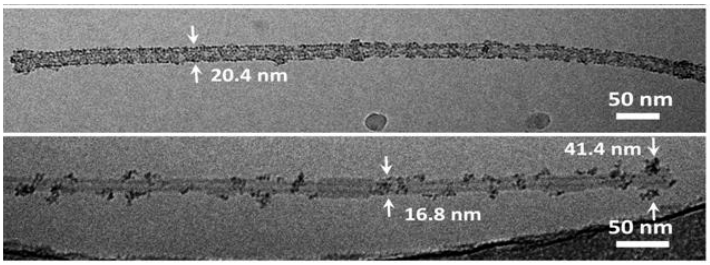

Figure 6: Representative cryo-TEM images of J-aggregate/QD-535 nanohybrids formed by electrostatic self-assembly method. Both images are taken from the same sample showing coexistence of different structural motifs. (Scale bar = 50 nm) (taken from [20])

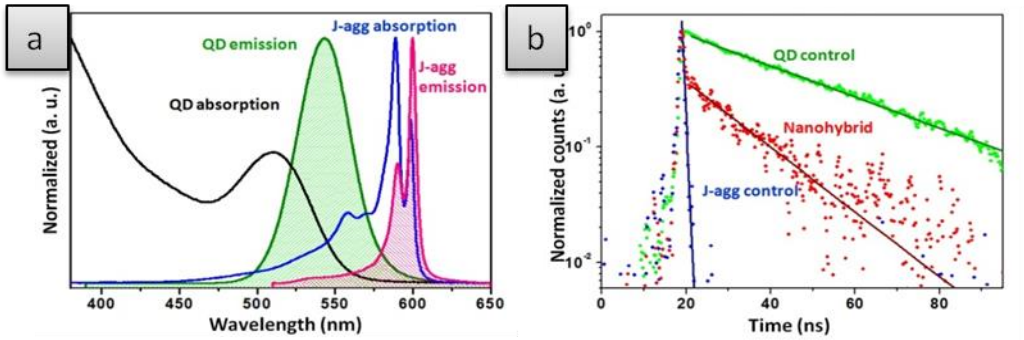

Figure 7: Optical spectra of J-aggregate/QD-535 nanohybrids to illustrate FRET from QD-535 to the J-aggregate. (left) Absorption and emission spectra of C8S3 J-aggregate nanotubes (λ_{ex} = 535 nm) and QDs (λ_{ex} = 380 nm); the spectra are normalized to the maximum value. (right) Normalized time-resolved decay of PL emission at 535 ± 10 nm in J-aggregate/QD-535 nanohybrids, QD-535, and J-aggregate control, which is a pure J-aggregate solution. (taken from [20])

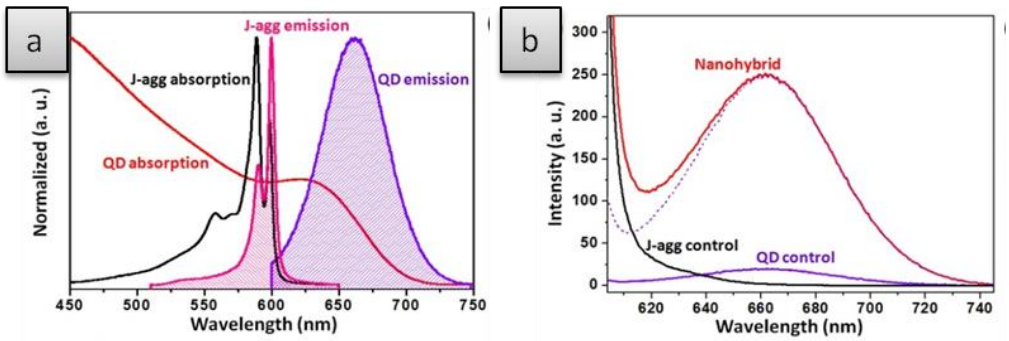

Figure 8: Optical characterizations of J-aggregate/QD-665 nano hybrids to explore resonance energy transfer from J-aggregate to QD-665. (left) The absorption and emission spectra of C8S3 J-aggregate (λ_{ex} = 500 nm) and QD-665 (λ_{ex} = 600 nm). (right) PL spectra of the J-aggregate/QD-665 nano hybrids, QD-665, and C8S3 J-aggregate. The excitation wavelength was set to λ_{em} = 589 nm, which is the peak of J-band absorption. By subtracting the contribution of J-aggregate, the sole emission spectrum of QD-665 in the hybrid system was obtained (purple dashed line). (taken from [20])

e) Silica coverage of J-aggregates

As part of our constant effort to find ways to stabilize the J-aggregates against mechanical destruction and photobleaching we investigated the coverage with silica. A sol-gel method was successfully applied using electrostatic attraction between the charged aggregates surface and oppositely charged precursors [8,9]. In this case the cationic species, such as $[Si(OH)_3(NH_3)]^+$ hydrolyzed from ATPES, is attracted by the negative surface potential opf the aggregates and forms an ultrathin silica layer. Further condensation of hydrolysis products of TEOS, e. g. $[Si(OH)_4]$, leads then to the formation of silica nanoshell specifically on parts of the J-aggregate surface that was previously covered by APTES. The reaction scheme is shown in Fig. 9 and the resulting coverage for a certain concentration range is demonstrated in Fig. 10. The thickness of the silica shell can be varied by the relative concentrations and was grown up to 8 nm [23]. The silica shell leaves the structure of the aggregates unaffected as can be easily probed by the absorption spectra. Preliminary results indicate that the silica shell reduces photo oxidation of the dyes.

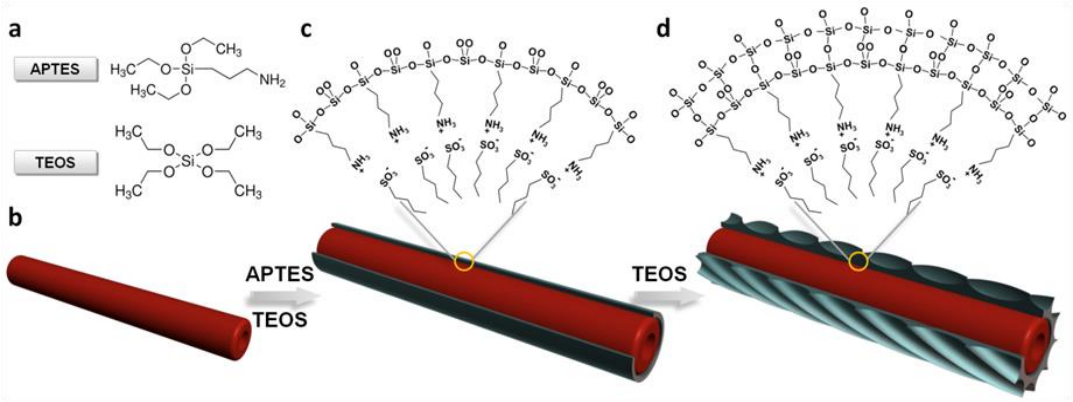

Figure 9: Sketch of electrostatically driven silication mechanism of silica nanoshell-coated J-aggregate. (a) Molecular structures of the constituents: APTES, and TEOS; (b) sketch of J-aggregate nanotube, (c) electrostatic adsorption of APTES on J-aggregates; (d) condensation of TEOS on J-aggregate nanotubes, (taken from [23])

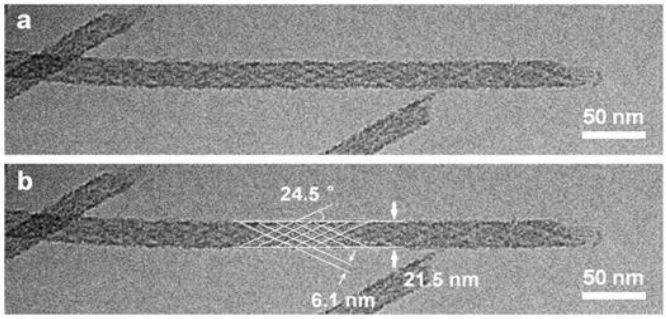

Figure 10: a,b) Cryo-TEM image of silica nanoshell coated J-aggregates. In b) lines are drawn as guidelines to the eye to indicate the helical or net-like structure of the silica. c) Absorption spectra of J-aggregate before and after addition of the silica. (taken from [23])

A regular and periodic super structure of the silica was observed and is shown in Figure 10. This structure indicates a helical winding of bands of silica around the tubular aggregates. This structural motif could be caused by the helical super structure of the underlying aggregate. It appears well pronounced on cry-TEM images. This coverage is unprecedented and opens many interesting questions, not only specifically for this system but also in general for other similar systems. Besides the synthetical and technical questions of how to control better thickness and structure of this shell the main scientific interest is about its ability to protect the aggregate with a transparent, isolating, and impermeable shell against mechanical damage photobleaching. The ability to add other functional groups to the silica groups opens a new route to the preparation of stable complex functional HIOS units.

References

[42] D.M. Eisele, H. von Berlepsch, C. Böttcher, et al., J. Am. Chem. Soc. **132**, 2104 (2010).
[43] D.M. Eisele, C.W. Cone, E.A. Bloemsma et al., Nature Chem. **4**, 655 (2012).
[44] Y. Xia, Y. Xiong, B. Lim, S.A. Skrabalak, Angew. Chem. Int. Ed. **48**, 60-103 (2009).
[45] B. Wiley, T. Herricks, Y. Sun, Y. Xia, Nano Lett., **4**, 1733 (2004).
[46] T. Kiesner, "Untersuchungen zu Oberflächenplasmonen", Bachelor Thesis, HU Berlin, 2013.
[47] Walker, B. J.; Bulovic, V.; Bawendi, M. G. Nano Letters **10**, 3995-3999 (2010).
[48] Q. Zhang, T. Atay, J. Tischler, et al., Nature Nanotechnology **2**, 555-559 (2007).
[49] S. Che, A.E. Garcia-Bennett, T. Yokoi et al., Nature Materials **6**, 801 (2003).
[50] Y. Qiao, H. Chen, Y. Lin, et al., J. Phys. Cem. C **115**, 7323 (2011)
[51] E. Hennebicq, G. Pourtois, G. D. Scholes, et al., J. Am Chem. Soc., **127**, 4744 (2005).
[52] Katie A. Clark, Emma L. Krueger, and David A. Vanden Bout, J. Phys. Chem. Lett. **5**, 2274 (2014).
[53] H. Najafov, et al., Nature Materials, **9**, 938 (2010).
[54] F. Würthner, T.E. Kasier, C.R. Sarah-Möller, Angew. Chem. Int. Ed., **50**, 3376, (2011).
[55] N. Chevalier, M. Nasse, J. Woehl et al., Nanotechnology, **16**, 613 (2005).
[56] H. von Berlepsch, K. Ludwig, S. Kirstein, C. Böttcher, Chem. Phys. **385**, 27 (2011).
[57] D.M. Eisele, D.H. Arias, X. Fu, et al., PNAS **111,** E3367 (2014)
[58] P.J. Meadows, E. Durjadin, S.R. Hall, S. Mann, Chem. Commun. **2005**, 3688
[59] K.L. Gurunatha, E. Durjadin, J. Phys. Chem.B, **117**, 3489 (2013)

3.3.2 Project-related publications

[60] Y. Qiao, F. Polzer, H. Kirmse, E. Steeg, S. Kirstein, J.P. Rabe, "*In situ* synthesis of semiconductor nanocrystals at the surface of tubular J-aggregates", J. Mater. Chem. C **2**, 9141-9148 (2014).
[61] Y. Qiao, F. Polzer, H. Kirmse, E. Steeg, S. Kühn, S. Friede, S. Kirstein, J.P. Rabe, „*Coupled Nanotubular J-Aaggregates and Quantum Dots for Efficient Resonance Excitation Energy Transfer*", ACS Nano, submitted.
[62] J. Megow, M.I.S. Röhr, M.S. am Busch, T. Renger, R. Mitric, S. Kirstein, J.P. Rabe, V. May, "Site-dependent van der Waals interaction explains e3xciton spectra of double-walled tubular dye-aggregates", subm. to ArXiv by 15.11.2014, to be published in Nano Lett.
[63] E. Steeg, F. Polzer, H. Kirmse, Y. Qiao, J.P. Rabe, S. Kirstein, „Nucleation and Growth of Ag Nanostructures Mediated by J-Aggregates of Amphiphilic Dyes", subm. to ArXiv by 15.12.2014, to be published in Langmuir
[64] Y. Qiao, F. Polzer, H. Kirmse, S. Kirstein, J.P. Rabe, „Tubular J-aggregates covered by transparent silica nanoshell", subm. to ArXiv by 15.12.2014, to be published in Langmuir (Letter)

3.4 Research plan

3.4.1 Main objectives

The unique feature of the system investigated in this project is the possibility to utilize the tubular J-aggregates to fabricate HIOS sample based on ordered organic material that exhibits extended Frenkel excitons with high coupling strength. In the previous funding period this system was mostly used to fabricate silver nanowires as the inorganic component and it was intended to study electronic coupling effects between excitons of the organic dyes and plasmon resonances within the silver. Although the silver nanowires became an interesting research object by themselves, due the delicate growth behaviour and the surprisingly found dynamical chemical instability, our focus was changing from the plasmonic excitations to energy transfer systems. From preliminary experiments we have learned that functional HIOS structures from quantum dots and tubular J-aggregates can be made with unprecedented structural integrity. The successful MD simulation of the structure delivers a base for theoretical calculations of the electronic structure but needs detailed experimental structure analysis. It was a serendipitous finding that high resolution structure determination becomes feasible with aggregates covered by silica. Since this coverage also is expected to mechanically and chemically stabilize the delicate organic aggregates and allows inclusion or addition of further functional inorganic materials, this topic is seen to be a second hot topic for further investigation. The proposal is therefore split into two parts.

3.4.2 Sub-project A: Exciton mediated energy transfer between HIOS Förster-couples.

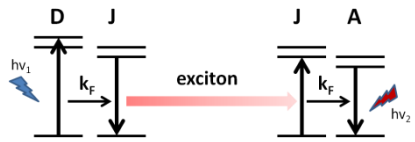

In this sub-project the main effort is directed to the formation and investigation of a HIOS device that allows coupling between two Förster-transfer couples via migration of Frenkel-excitons .Light is absorbed by a Donor-particle (usually a CdTe particle, selected by size and optical absorption and emission energy to fit as a donor for energy transfer into the tubular J-aggregates of C8S3) and transferred to the J-aggregate. Since the energy transfer only occures over distances given by the Förster radius R_{0D}, this leads to an excitation of the aggregate within an area of this size. Typical values fo R_0 are of the order of 3 … 5 nm, as was measured in previous experiments [qioa-II]. The same situation holds for an acceptor attached to the aggregate, which collects excitation energy from an area of the size of R_{0A}. In this case it is not clear to what extend an exciton delocalization would broaden this collection area, a questions that is investigated theoretically in B6 (May). In other words, the energy transfer units create very local probes for excitation and emission of the J-aggregates. Since the dimension of this probe is less than 10 nm, it should allow to measure or to monitor exciton diffusion within the J-aggregates.
The range of exciton diffusion or migration is a topic of research interest for all systems of conjugated molecules, starting from organic crystals [10], over conjugated polymers [11] to molecular aggregates [12]. It is an important question for applications of organic layers such as LEDs or solar cells, since exciton diffusion is one crucial step in the operation of the devices. However, in most disordered systems the excitonic couplings are weak which causes diffusion lengths of order of 10 to 50 nm. However, for J-aggregates this length was supposed to be much larger, supported by early experiments of fluorescence quenching as well as by theoretical estimates [13]. In a very recent work by vanden Bout et al., exciton diffusion lengths

exceeding 200 nm were observed for the J-aggregates of C8S3. Even larger extensions were found for aggregates in a state were several tubes are attached to each other forming a rope-like bundle. The experiment done there was direct excitation with a circular laser spot and measurement of the elongation of the emissive spot, which was ascribed to the exciton diffusion. These measurements required deconvolution of the data by the excitation spot of the microscope, which is of the same order of magnitude or even larger than the diffusion length. These findings are promising for the long-range coupling of Förster-transfer couples as it is proposed here. Additionally, the locality of the Förster-process should enable us to measure the exciton diffusion length with unprecedented accuracy.
The key prerequisites for a successful accomplishment of this experiment and how we think we can fulfil them are listed as follows. These conditions directly lead to the work program to be done.

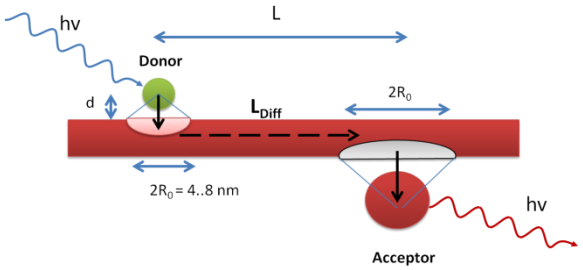

Figure 11: Sketch of principle HIOS structure for the study of extended coupling between two Förster-transfer couples via exciton migration within a J-aggregate. Excitation and emission of light is observed from a donor and acceptor unit, respectively. The aggregate is excited and de-excited via Förster-transfer solely. The Förster couples act as local probes with extensions of a few nanometer.

- The diffusion length L_{Dif} must be larger than the typical Förster radius of the Förster couples. From the data published by vanden Bout et al. [12] we are convinced that this major condition is fulfilled. It also shows that bundles of aggregates are of high interest. From our experience we know that bundles can easily be induced by increasing the ionic strength of the solution.
- Donor emission and acceptor absorption have no direct spectral overlap and the aggregate plus acceptor must not be directly excited when donor is excited. Careful selection of donor and acceptor species is required. Donors are identified (QD-535) and emitters also have been used previously fulfilling these criteria (PDADMAC labelled with Alexa-631 dye). They have to be combined and careful reference experiments must be conducted.
- The transfer efficiency within the Förster couples must be very high, best close to 100%.
  In our previous experiments we achieved almost 100% transfer efficiency for semiconducting particles as donors, when attached close to the aggregates. We had also very high efficiencies for dye molecules brought to close distance by means of labeled polyelectrolytes (60%). The efficiency can be controlled by the distance between donor/acceptor and dye tube.
- The mean distance between donor and acceptor must be controllable in the range of 20 to 2000 nm.
  The distance variation can be achieved by statistics or by direct positioning of donors. A control of a mean distance can be obtained using a mixture between donor / acceptor particles and optically inactive particles, such as silica particles. The concentration defines then the mean distance. An alternative would be to use an optical probe made of an AFM tip covered by donor particles and observe the donor emission while moving the across the acceptor decorated aggregate [14].
- The attachment of the donor / acceptor groups must not disturb the structure and hence the optical properties of the aggregates.
  It was found that adsorption of polyelectrolytes and colloidal particles change structure only slightly. Very promising is the silication of the aggregates which leaves the structure almost unaffected.
- The acceptor / donor groups must be electrically isolated from the aggregate to avoid charge transfer effects.
  From the selection of the positioning of the energy levels for many systems an electron transfer can be excluded. Otherwise, an isolation layer is planned to be formed by a silica shell. Oppositely, if charge transfer effects are wanted, it can be achieved by using a molecular thin gluing layer.

Work plan (divided into work packages (WP)):

WP-A1: For the control of the mutual distance of the Förster-couples the density of donors as well as that of acceptors has to be optimized. Series with different concentrations but also mixtures with optically inactive particles have to be used. The characterization is via static and time resolved spectroscopy and structure

has to be controlled by cryo-TEM. The combination of both, donors and acceptors at the aggregates has to be achieved. As acceptors dye-labelled polyelectrolytes shall be used, which then serve as a glue for the attachment of the Qdots. In parallel samples with bundles of aggregates have to be prepared and characterized. They are spectroscopically different, which could give access to other donor/acceptor probes.

WP-A2: The samples with both Förster-couples present shall be investigated by means of time-resolved spectroscopy. Great care has to be taken to the analysis using the respective reference samples. Also distances between donor/ acceptor must be varied according to the limits identified in WP-A1.

WP-A3: Besides the statistical approach where donor/acceptor particles are present in statistical mixture, donors shall be brought to a sample with acceptors present, using an AFM tip decorated by respective particles. These experiments are performed on top of an optical microscope combined with CCD spectrometer. These experiments should at least allow identification of an inhomogeneous emitter distribution on the aggregates. The experiments may be accompanied by fluorescence lifetime imaging microscopy which allows separating aggregate-emission from particle emission by their very different life times. Such experiments can be done in collaboration with the BAM.

3.4.3 Sub-project B: Silica coverage for stabilization, isolation, and structure analysis

Objectives:
In this subproject the silication of tubular J-aggregates of the cyanine dye C8S3 shall be investigated with respect to its application for a detailed structure analysis and in view of its applicability as a protective layer. The pronounced super-structure found in the silica layer by cryo-TEM (Figure 10) is well suited for further analysis by advanced image analysis. Under the assumption of a helical super structre a full 3D image reconstruction is possible. This was demonstrated for the pure C8S3 aggregate earlier [13] and is shown in Figure 12a,b. To reveal the internal structural details a sophisticated averaging algorithm is used, that uses small pieces of aggregates that are overlayed by adjustment of the position in order to minimize phase averaging effects. The same procedure was applied to images of silica covered aggregate, Figure 12c and 12d. The first attempts show at least two structural motifs that differ mostly by their symmetry. The high contrast and the high degree of regularity of the structures are very prospective for a detailed analysis by this method. For detailed theoretical treatment the knowledge of the detailed structure is indispensible. Big progress in theoretical understanding was made because it was possible to simulate the tubular aggregate structure by molecular dynamics simulations [21]. Calculations of the electronic structure were performed and are planned to be extended to include semiconducting nanostructures in B6 (May) It should be emphasized that the structure model for the theoretical calculations is based on the structure analysis carried out using cryo-TEM images in combination with 3-dimensional image reconstruction as shown in Figure 15.

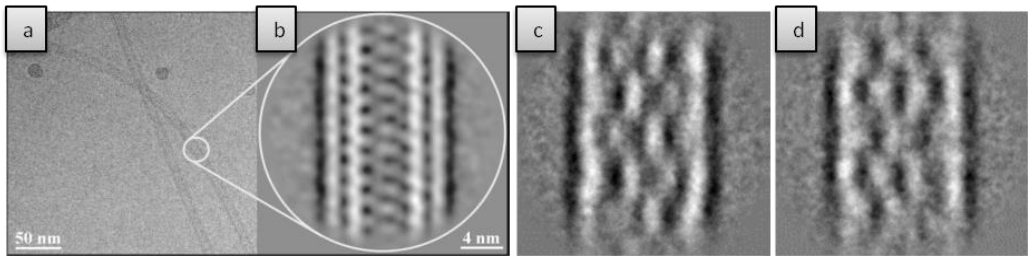

Figure 12: a) cryo-TEM image of tubular J-aggregates of C8S3; (from [ ]). b) magnification of part of the aggregate with image improved by advanced averaging methods; c,d) same image treatment as in b, but for aggregates covered by silica shell as shown in Figure 6. (courtesy of C. Böttcher). The images are obtained for different aggregates.

One goal is the clarification if there is transcription of the aggregate structure to the silica structure and how other parameters influence the silica structure. A structure transfer from the aggregate to the silica layer would allow us to draw conclusions back to the aggregate structure on length scales that is not accessible by any other method. The high stability of the silica also should allow the performance of tomographic 3D imaging, what is much more challenging for plain organic structures [14].
The sol-gel polycondensation of APTES and TEOS for silication is a method that also was applied to J-aggregates of tetra(4-sulfonatophenyl)porphyrin [15,16], where the thickness of the shell was varied by the APTES/TEOS concentrations. Further functionalisation with gold nanoparticles is demonstrated showing plasmon interactions [16]. This route shall be followed to add nanostructures to the silica shell. This is promising, because the silica shell should be isolating and thus prevents any type of charge transfer. Additionally, the silica super structure may help to localize semiconducting and metallic nanoparticles in a

regular way with well-defined distance distribution. Other synthetic methods to attach particles shall also be tested, such as using 3-Mercaptoproyltrimethoxysilan (MEPTES) instead of APTES to provide thiol groups for attachment of gold particles.
An important property of the silica shell is its protection against mechanical damaging and chemical degradation. Both effects shall be investigated in more detail, with respect to thickness and structural appearance of the silica layer.

Work plan (divided into work packages (WP)):
WP B1: Improvement of synthesis of silica shell around aggregates. The silica shell shall be varied by systematic variation of concentration ratios, different reagents (MEPTES instead of APTES) and also for different dye aggregates. The amphiphilic dyes are available with different chemical side groups which results in different aggregate morphologies. The use of different structures and morphologies allows the study structure transcription towards the silica shell. All synthetic work has to be analyzed by cryo-TEM and absorption spectroscopy. The synthesis has to be optimized with respect to high uniformity of the samples to make them suitable for the 3D image reconstruction. The image reconstruction is exclusively done at the Fu (C. Böttcher), the synthesis and optical characterisation can be done at HU.

WP B2: Addition of inorganic species to the silica shell. The synthetic route has to be modified in order to either include or attach other organic and inorganic species. Electrostatic and covalent binding of metal nanoparticles, semiconducting nanoparticles, or organic species shall be realized. An important parameter is control of particle density, shell thickness, and particle location on structures silica shells. These samples will be delivered to sub-project A for energy transfer studies.

WP B3: The mechanical and chemical stabilization effect of the silica shell shall be probed. The protection against photobleaching of the aggregates shall be investigated for various structurally different silica shells. Bleaching experiments shall be performed in a fluorescence spectrometer and with isolated aggregates using fluorescence microscopy in combination with emission spectroscopy. A typical penetration depth of oxigen will provide hints if the silica shell is closed or has porosity that is not seen by cryo-TEM images. The mechanical stiffening of the aggregates shall be probed using nanomanipulation techniques by AFM. Therefore, the aggregates shall be moved on a sample using an AFM tip. Bending and breakage can be observed that give hints on the stiffness and stability, at least in a qualitative description.

The work packages are organized with respect to the following **timeline:**

	Year 1	**Year 2**	**Year 3**	**Year 4**
Project A	A1 (Structure optimization)		A2 (Coupled FRET)	A3 (Local methods)
Project B	B1 (Synthesis / 3D structure model)		B2 (Additional particles)	B3 (Protection / mechanical properties)

3.5 Role within the Collaborative Research Centre

- The collaboration with **B6** (May) will be continued and deepened. They will perform calculations of energy transfer dynamics based on the geometry of our samples and we will vary experimental parameters that are required for improvement of theory.
- With the group of **B3** (Blumstengel) and **A5** (Henneberger) the time resolved fluorescence spectroscopy experiments will be performed.
- Synthetic expertise of the group **B2** (Ballauff, Benson, Lu) will lead to strong exchange for the silica shell synthesis.
- The expertise in surface characterization by scanning probe methods will be shared with various projects by direct collaboration, such as **B2** (Ballauff/Benson/Lu), **B3** (Blumstengel), and **A3** (Hecht).
- The project **Z2** (Kowarik / Koch) will be essential for their TEM and cryo-TEM resources.

3.6 Delineation from other funded projects

Project	Project title	Comment
DFG: CRC 765	Multivalenz als chemisches Organisations- und Wirkprinzip: Neue Architekturen, Funktionen und Anwendungen (TP C3)	investigates forces on mutli-valent chemical bonds; has no relation to A6
SALSA, the Graduate School of Analytical Sciences Adlershof	?	?
Helmholtz Energie Allianz	?	?
DFG, DAAD: IRTG1524:	Self-Assembled Soft Matter Nano-Structures at Interfaces	Manipulation of DNA and other macromolecules on solid substrates; has no direct relation to A6.

3.7 Project funds

3.7.1 Previous funding

The project has been funded within the Collaborative Research Centre since July 2011.

3.7.2 Funds requested

Funding for	2015/2		2016		2017		2018		2019/1	
Staff	Quantity	Sum	Quantity	Sum	Quantity	Sum	Quantity	Sum	Quantity	Sum
<category, percentage>										
PhD student, 75%	2	44.100	2	88.200	2	88.200	2	88.200	2	44.100
Total										
Direct costs	Sum		Sum		Sum		Sum		Sum	
Small equipment, Software, Consumables	6.000		12.000		12.000		12.000		6.000	
Total										
Total	6.000		12.000		12.000		12.000		6.000	

(All figures in Euro)

3.7.3 Staff

	No.	Name, academic degree, position	Field of research	Department of university or non-university institution	Commitment in hours/week	Category	Funded through:
Available							
Research staff	1	Rabe, Jürgen P., Prof. Dr.	Macromolecular Physics	HU Berlin, Physics Dept.	5		GA(HU)
	2	Kirstein, Stefan, PD Dr.	Macromolecular Physics	HU Berlin, Physics Dept.	10		GA(HU)
	3	Christoph Böttcher, PD Dr.	Electron Microscopy	FU Berlin, Research Center of Electron Microscopy	5		GA(FU)
Non-research staff	4	Poblenz, Evi		HU Berlin, Physics Dept.	3		GA(HU)
	5	Jürgen Gatzmann		FU Berlin, Research Center of Electron Microscopy	3		GA(FU)
Requested							
Research staff	6	N.N., PhD student	Macromolecular physics	HU Berlin, Physics Dept.			
	7	N.N., PhD student	Physics / Chemistry	HU Berlin, Physics Dept			
Non-research staff							

Job description of staff (requested):

1. Jürgen P. Rabe: Scientific and organizational leadership of the project.
2. Stefan Kirstein: Scientific and organizational leadership of the project, instruction of technician.
3. Christoph Böttcher: Scientific support for cryo-TEM analysis, instruction of technician.
4. Evi Poblenz:Technical support and assistance for laboratory work.
5. Jürgen Gatzmann: Technical support and assistance for the image analysis.
6. N.N: One PhD student (sub-project A) works on the preparation, structural characterization and spectroscopic investigation of the energy transfer units. The investigation is done in solution as well as on single aggregates using scanning probe techniques.
7. N.N.: One PhD student (sub-project B) works on the silica shell coverage of the aggregates and the further functionalisation. The work includes structure analysis performed at FU under supervision of C. Böttcher and extended systematic studies on synthesis using different parameters at HU.

3.7.4 Direct costs for the new funding period

	2015/2	2016	2017	2018	2019/1
Funds available	1000	2000	2000	2000	1000
Funds requested	6000	12000	12000	12000	6000

(All figures in Euro)

For years 2015/2 and 2019/1

Small equipment	EUR	
Optical and opto-mechanical components (filters, mounts, mirrors), lamp for spectrometer	EUR	3000
Consumables		
Chemicals for synthesis and cleaning, dye, nanoparticles	EUR	2000
TEM grids, lab disposables	EUR	1000

For years 2016 to 2018

Small equipment	EUR	
Optical and opto-mechanical components (filters, mounts, mirrors), lamp for spectrometer	EUR	5000
Consumables		
Chemicals for synthesis and cleaning, dye, nanoparticles	EUR	3000
TEM grids, lab disposables	EUR	1000
AFM tips	EUR	3000

3.1 About project A7

3.1.1 Title: Exploring HIOS structure formation by atomistically-resolved and coarse-grained computer simulations

3.1.2 Research areas: Theoretical physics, statistical physics of soft matter

3.1.3 Principal investigators

Prof. Dr. Sabine Klapp (*21.11.1968, German)

Institut für Theoretische Physik, Sekr. EW 7-1,
Technische Universität Berlin
Hardenbergstrasse 36, 10623 Berlin
Phone: +49 (30) 314 23763
Fax: +49 (30) 314 21130
E-mail: klapp@physik.tu-berlin.de

Prof. Dr. Joachim Dzubiella (*17.05.1975, German)

Helmholtz-Zentrum Berlin für Materialien und Energie (HZB)
Hahn-Meitner-Platz 1
14109 Berlin, and
Institut für Physik
Humboldt-Universität zu Berlin (HUB)
Newtonstr. 15
12489 Berlin
Phone:+49 (030) 8062-42902
E-Mail: joachim.dzubiella@helmholtz-berlin.de

Do the above mentioned persons hold fixed-term positions? no

3.1.4 Legal issues

This project includes

1.	research on human subjects or human material.	no
	A copy of the required approval of the responsible ethics committee is included with the proposal.	no
2.	clinical trials	no
	A copy of the studies' registration is included with the proposal.	no
3.	experiments involving vertebrates.	no
4.	experiments involving recombinant DNA.	no
5.	research involving human embryonic stem cells.	no
	Legal authorization has been obtained.	no
6.	research concerning the Convention on Biological Diversity.	no

3.2 Summary

This project, merged from previous projects A1 (Dzubiella) and A7 (Klapp), aims at understanding the equilibrium structure and non-equilibrium growth of conjugated organic molecules (COMs) in HIOS on time- and length scales beyond those accessible in ab-initio calculations. To this end, we will combine classical all-atom Molecular Dynamics (MD) simulations based on semi-empirical force fields and coarse-grained simulation techniques such as (kinetic) Monte Carlo (MC) based on effective Hamiltonians and energy barriers.

In the ongoing funding period we have successfully developed, in close collaboration with project A4 (Heimel), a robust atomistic model for oligo-paraphenylene crystal growth as well as techniques to extract the diffusion behavior of single COMs on ZnO surfaces. In parallel, we have gained substantial experience with kinetic Monte Carlo (kMC) simulations which allowed us to quantitatively reproduce multilayer growth of C_{60} experimentally studied in A9 (Kowarik). Further, we have developed coarse-grained potentials for anisotropic COMs to study crystallisation (cooperation A1/A7) on larger scales as well as generic features of monolayer equilibrium structures subject to a heterogeneous charge pattern.
Building on these grounds, we will now move towards various new, HIOS-specific challenges, including improvement of sampling methods in all-atom simulations to tackle the slow relaxation characterizing HIOS growth, study of electrostatically guided COM transport, advancement of growth simulations for anisotropic multilayer films, and development of refined coarse-grained potentials for COMs with varying polarity. The main structural questions concern the spatially-varying tilt angle, nuclei, island shapes and morphologies, the impact of different surface modifications and the COM polarity. We will focus on the COMs sexiphenyl (p-6P), its fluorinated versions p-6P-2F and p-6P-4F to study polarity effects, and the ladder-type quarterphenyl L4P on ZnO surfaces.
For an accurate description of surface properties and for an exchange of structural data we will further tighten our connections to our quantum-theoretical partners in this CRC, particularly A4 (Heimel), A10 (Tkatchenko)], and B12 (Knorr/Richter)]. The structural growth modes will be compared to our experimental partners in this CRC [A5 (Henneberger), Z2 (Kowarik/Koch)].

3.3 Project progress to date

3.3.1 Report and state of understanding

The functional material properties of HIOS such as the work function (determing electron transport) and the charge carrier mobility are highly sensitive to morphological changes of the COMs at the inorganic semiconductor surface [1-4]. In particular, the functionality depends on the orientation of the anisotropic molecules relative to the surface („tilt angle“), the smoothness of the film, and the degree of crystallinity. The theoretical understanding of the self-assembly, nucleation, and growth processes of COMs in HIOS is thus of fundamental importance to eventually control and design „tunable“ HIOS for optoelectronics [4,5]. Ab-initio methods to explore the (electronic) structure of HIOS play a key role in predicting certain properties (such as Schwöbel barriers [6]), but are currently still limited to rather small numbers of moelcules. Moreover, they typically focus on the ground state (T=0). This motivates to complement the ab-initio calculations (performed in various other projects in this CRC) with many-particle computer simulations of HIOS based on classical force-fields. In principle, these techniques not only allow to access structural properties at larger length- and time scales, they are also capable of describing the formation of ordered phases, nucleation and surface growth at T>0. In practice, classical simulations of HIOS are still very challenging [5] due to the strong anisotropy and complicated internal character (e.g., the charge distribution) of the COMs and the typically patterned character of the semiconductor surfaces, a prime example being ZnO(10-10). Therefore, a comprehensive molecular-level understanding of structural and growth properties of HIOS is still missing [5].

In the first funding period of this CRC, projects A1 (Dzubiella) and A7 (Klapp) have made several important contributions in this area by using state-of-the-art methods from classical statistical physics, focusing, however, on different levels of resolution. In particular, the aim of project A1 (Dzubiella) was to develop classical all-atom molecular dynamics (MD) computer simulations of COMs on inorganic semiconductor surfaces in order to interpret and guide experimental results by giving fundamental insight into the atomic and molecular scale structures and kinetics (0.1 - 10 nm; 0.001 - 100 ns) in HIOS. In parallel, project A7 (Klapp) focused on investigating structure formation and growth on a mesoscopic scale (10 nm - 100 nm, 100 ns - 1 ms), using coarse-grained (non-atomistic) potentials which take into account only main ingredients such as shape and electrostatic features of the molecules. A bridge between projects A1 and A7 was established concerning the derivation of a coarse-grained potential for the COM coronene by systematically integrating out atomistic degrees of freedom.

A detailed report on the results of project A1 (Dzubiella) is given elsewhere in this CRC proposal. Briefly, the key achievements of project A1 are:

- Establishment of a working model for MD simulations of realistic crystal growth of p-polyphenyl COMs [P1], **in cooperation with A4 (Heimel)**
- Development of MD simulation methods to extract and characterize the anisotropic long-time self-diffusion behavior of p-polyphenyl COMs on the ZnO (10-10) surface [P3]

- Advancement of coarse-graining strategies for COM bulk systems **in cooperation with A7 (Klapp)** [P8] (see report on A7 below)

We now report on project A7 (Klapp). Here, the overall goal was to achieve a theoretical description of collective phenomena in systems of COMs in presence of typical surface properties of inorganic semiconductors such as electrostatic defects and topological fields. Within this area, the two main objectives were, on one hand, the investigation and clarification of universal, coarse-grained molecular features (such as shape, presence of dipole- or quadrupole moments) determining the morphology of the organic component of HIOS, and, on the other hand, advancing coarse-graining strategies from the atomistic to the mesoscale level for specific HIOS together with project A1 (Dzubiella).

The achievements of A7 (Klapp) can be summarized as follows:

1. Growth processes of the fullerene C60 on surfaces
Using kinetic Monte Carlo (kMC) simulations, we have investigated non-equilibrium multilayer growth of systems of the organic molecule C_{60} (fullerene), **together with project A9 (Kowarik)** [P2,P10], where time-resolved X-ray experiment were carried out. Indeed, the kMC simulations were not planned in the original proposal of project A7 which was rather focused on equilibrium phenomena. Therefore, the corresponding simulation programmes had to be newly developed. It turned out that the kMC calculations can provide a quantitative description of the multilayer growth [P2] (see Figure 1).

In particular, by comparing experimental and kMC results for various target quantities involving relevant length scales in lateral and vertical direction over a range of temperatures, we have been able to determine, for the first time, a consistent set of energy parameters characterizing intra- and interlayer transport in such systems [P2]. These parameters are the binding energy, the barrier of free diffusion, and the Schwöbel barrier. Analyzing these energy parameters we found that C_{60} forms an important intermediate case between atoms and colloids. This behaviour is intimately related not only to the size of C_{60} (~1nm), but also to the fact that the range of the effective interaction stemming from atom-atom van der Waals interactions is significantly smaller than in atoms.

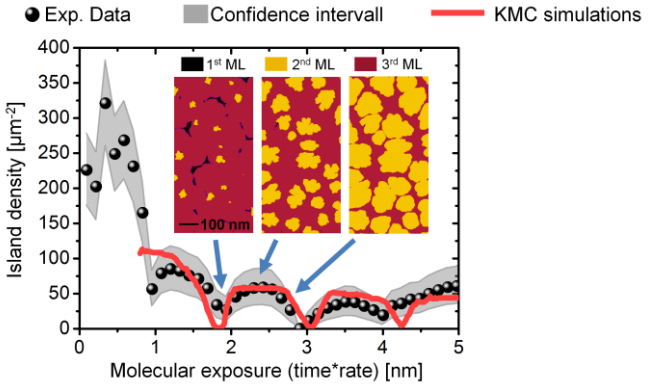

Figure 1: Comparison of experimental and kMC data (cooperation A7/A9) for the time-dependence of the island density in C_{60} multilayer growth. Included are simulation snapshots representing the morphology at specific times [P2].

As a "byproduct" of the growth simulations, we have investigated in detail the single-particle and collective dynamics during the surface growth of C_{60} [P10]. Quantities considered include the single-particle mean-squared displacement (MSD) and various layer-averaged correlation functions. We have monitored these quantities as functions of time, i.e., the stage of the growth process, and have related them to the surface morphology. It turns out that the specific morphological features of C_{60} growth (which, in turn, are related to the relative magnitude of the energy parameters) have profound impact on the MSD: The latter rather behaves as it is known from colloidal surface growth. We have also identified pronounced differences to the well-investigated case of atomic growth [P10].

In summary, our results in [P2,P10] provide a fundamental understanding of non-equilibrium growth processes in a "simple" organic system. We now plan to use this experience for approaching the growth of anisotropic HIOS systems in the next funding period. This research has also stimulated investigations of growth processes in other anisotropic (magnetic) systems [P6].

2. Self-assembly of 6P on ZnO (10-10)
The second part of project A7 (Klapp) was devoted to the development of a coarse-grained Hamiltonian H_{eff} describing an ensemble of p-6P molecules at a ZnO (10-10) surface [P9]. The latter is characterised by a "electrostatic" stripe-like pattern formed by alternating stripes of positive and negative surface charges. Our aim in [P9] was not to derive H_{eff} by systematic coarse-graining (in contrast to our study [P8]); rather we attempted to focus on relevant key ingredients for the many-particle behaviour.
Specifically, we modelled intermolecular interactions via a uniaxial Gay-Berne potential (describing steric and van-der-Waals interactions) combined with the electrostatic potential between two linear quadrupoles.

Similarly, the molecule-substrate interactions include a coupling between a linear molecular quadrupole and the electric field generated by the line charges characterizing ZnO(10-10). As shown in [P9] there are various, non-neglible higher-order multipole moments of 6P which are relevant for the molecule-surface coupling. Here we have merged these effects into a fictive quadrupole. As far as possible, parameters have been set according to DFT calculations [6].
To validate our approach, we have performed equilibrium (lattice-) Monte Carlo simulations with continuous rotational degrees of freedom to investigate orientational ordering in the condensed state. We were able to reproduce various experimentally observed features [P9] such as the alignment of individual molecules with the line charges on the surface, the formation of a standing nematic phase with a herringbone structure, as well as the formation of a lying nematic phase (see Figure 2 in Sec. 3.4). Thus, the model can serve as a starting point for investigations of island formation and growth planned in the next funding period.

3. Systematic coarse-graining of anisotropic molecular interactions

In a joint effort of projects A1 and A7, we have developed coarse-graining methods in order to introduce properly defined effective potentials between particles, where the intramolecular degrees of freedom are integrated out [P8] in a systematic fashion based on the partition sum [P7]. We have performed this procedure on the highly symmetric COM coronene in an electrostatically neutral (all partial charges switched off) toy version, in order to keep the already challenging problem as simple as possible. The focus was thus on the understanding, how, in particular, the angularly-resolved potentials can be best mapped on coarse-grained effective analytical potentials for the use in mesoscopic simulations. For integrating out the intramolecular degrees of freedom we applied umbrella sampling and steered dynamics techniques in atomistically-resolved MD computer simulations.

The resulting coarse-grained pair potential reveals a strong temperature and angle dependence (see Fig. 4 in the report on A1 elsewhere in this CRC proposal). In the next step we have fitted the numerical data with various Gay-Berne-like potentials to be used in more efficient simulations on larger scales. The quality of the resulting coarse-grained results is evaluated by comparing their pair and many-body structure as well as some thermodynamic quantities self-consistently to the outcome of atomistic MD simulations of many particle systems. We find that angle-resolved potentials are essential not only to accurately describe crystal structures but also for fluid systems where simple isotropic potentials start to fail already for low to moderate packing fractions. A further outcome is that the molecular flexibility can significantly influence the effective pair potential.
So far, the joint study [P8] of A1 and A7 has focussed on coarse-graining van-der-Waals and intramolecular interactions. Clearly, a future challenge is to include the effect of electrostatics. We note that this is a non-trivial task already on the atomistic level since the partial charges are not static; rather, one needs to take into account polarizability, particularly in the crystalline phase.

Cooperations to other projects within this CRC

In the first funding period project A1 (Dzubiella) developed a collaboration with project A4 (Heimel) on refinement of partial charges and force field parameters for atomistic simulations based on quantum DFT calculations [P1]. In particular, A4 provided energy minimization calculations for single p-6P COMs to compare those minimized structures to validate corresponding atomistic calculations [24]. At the same time, project A7 (Klapp) established a fruitful collaboration with the experimental project A9 (Kowarik) on growth phenomena; in particular, this has led to the proposal of a consistent set of energy parameters describing multilayer growth of C60 [P2]. Moreover, the two projects A1 and A7 jointly worked on coarse-graining of COMs for the computationally efficient description of organic film growth [P8]. This study and many intense discussions stimulated a bunch of further research ideas of the two PIs regarding growth processes in anisotropic COMs, including ideas of exchanging information between atomistic and mesoscale simulations. Therefore, the two PIs have decided to merge the two projects into one project (A7) in the second funding period.

On top of the collaborations already mentioned, both A1 and A7 have had many inspiring discussions with other scientists in this CRC such as Koch (A8), Henneberger (A5), and Blumstengel (B3) on COM growth modes, Hecht (A3) on the possibility of COM synthesis and mutations, and Draxl (B11) on QM validation of force field refinement. We are confident that the discussions will deepen in the second funding period, where the COM growth in HIOS will be investigated in the merged project A7 (Klapp/Dzubiella).

Comparison to work outside this CRC

Both A1 (Dzubiella) and A7 (Klapp) have made substantial methodological advancements, which allowed us already in the first funding period to focus on HIOS-related questions which were essentially out of reach before. To start with A1, Ref. [P1] is the first work in the published literature that systematically demonstrated the self-assembly of oligophenyl COM crystals 'from scratch' in classical MD simulations. Further, [P3] is the first study of the long-time self diffusion of single COMs in HIOS and its interpretation by free energy landscapes and electrostatic surface patterns. MD studies of that type did not exist so far. See also the final report A1 for more details.
Likewise in A7, the model developed for the HIOS system 6P/ZnO [P9] is the first one allowing for large-scale computer simulations. Further, in [P2] we have proposed a consistent energy parameter set which is, contrary to previous works, capable of describing growth of several layers for a range of temperatures. Finally, the joint study [P8] has provided a systematic recipe to treat the combined effect of angle- and temperature dependency of effective potentials.

References

[27] S. Blumstengel, S. Sadofev, and F. Henneberger, New J. Phys. **10,** 065010 (2008).
[28] N. Koch, J. Phys.: Condens. Matter **20**, 184008 (2008).
[29] T. Trevethan, A. Shluger, and L. J. Kantorovich, J. Phys.: Condens. Matter **22**, 084024 (2010).
[30] G. Hlawacek and C. Teichert, J. Phys.: Condens. Matter **25**, 143202 (2013).
[31] P. Clancy, Chem. Mater. **23**, 522 (2011).
[32] Della Salle, Blumstengel, Henneberger, PRL
[33] G. Hlawacek, P. Puschnig, P. Frank, A. Winkler, C. Ambrosch-Draxl, and C. Teichert, Science **321**, 107 (2008).
[34] D. Choudhary, P. Clancy, R. Shetty, and F. Escobedo, Adv. Func. Mat. **16**, 1768 (2006)
[35] J.S. Raut and K. Fichthorn, J. Chem. Phys. **110**, 587 (1999).
[36] T. Hjelt and I. Vattulainen, J. Chem. Phys. **112**, 4731 (2000).
[37] M. Sparenberg, A. Zykov, P. Beyer, L. Pithan, C. Weber, Y. Garmshausen, F. Carla, S. Hecht, S. Blumstengel, F. Henneberger, S. Kowarik, preprint
[38] P.K. Jana and A. Heuer, J. Chem. Phys. **138**, 124708 (2013).
[39] L.Tumbek, C. Gleichweit, K. Zojer, and A. Winkler, Phys. Rev. B **86**, 085402 (2012).
[40] B. Hess, C. Kutzner, D. van der Spoel, D. E. and Lindahl, GROMACS 4, J. Chem. Theory Comput. **4**, 435-447 (2008).
[41] T. Potocar et al., Phys. Rev. B **83**, 075423 (2011).

3.3.2 Project-related publications

a) Published or accepted publications in peer-reviewed journals

[P1] K. Palczynski. G. Heimel, J. Heyda, and J. Dzubiella, " Growth and characterization of molecular crystals of para-sexiphenyl by all-atom computer simulations", Cryst. Growth Des. (ACS) **14**, 3791 (2014).
[P2] S. Bommel, N. Kleppmann, C. Weber, H. Spranger, P. Schäfer, J. Novák, S.V. Roth, F. Schreiber, S.H.L. Klapp, and S. Kowarik, "Unravelling the multilayer growth of the fullerene C60 in real-time", Nature Communications, in press (2014), doi: 10.1038/ncomms6388.
[P3] K. Palczynski and J. Dzubiella, “Anisotropic electrostatic friction of p-sexiphenyl on ZnO surfaces”, J. Phys. Chem. C, in press (2014). doi:10.1021/jp507776h.
[P4] I. Kalcher and J. Dzubiella, "NaCl crystallization in apolar nanometer-sized confinement studied by atomistic simulations", Phys. Rev. E 88, 062312 (2013)
[P5] P. Setny, R. Baron, P. Kekenes-Huskey, J. A. McCammon, and J. Dzubiella, "Solvent fluctuations in hydrophobic cavity ligand binding" Proc. Natl. Acad. Sci USA (PNAS) **110**, 1197-1202 (2013).
[P6] K. Lichtner and S.H.L. Klapp, „Spinodal decomposition of a binary magnetic fluid confined to a surface“, Phys. Rev. E **88**, 032301 (2013).
[P7] S.H.L. Klapp, D.J. Diestler, and M. Schoen, „Why are effective potentials soft?“, J. Phys.: Condens. Matter **16**, 7331 (2004).

b) Other publications

[P8] T. Heinemann, K. Palczynski, J. Dzubiella, and S. H. L. Klapp, " Angle-resolved effective potentials for disk-shaped molecules", J. Chem. Phys., submitted (2014); arXiv:1407.4352 [cond-mat.soft].
[P9] N. Kleppmann and S.H.L. Klapp, "A scale-bridging modeling approach for anisotropic organic molecules at patterned semiconductor surfaces," J. Chem. Phys., submitted (2014); arXiv:1407.6265 [cond-mat.mtrl-sci].

[P10] N. Kleppmann and S.H.L. Klapp, "Particle-resolved dynamics during multilayer growth of C60“, Phys. Rev. B, submitted (2014): arXiv: 1410.8763 (cond-mat.mes-hall)

3.4 Research plan

Combining various classical simulation techniques established in the first funding period, we now aim at a synergistic treatment of several new key questions: Identifying the impact of COM polarity and electrostatic surface patterns, developing refined sampling (replica-exchange) methods to deal with slow relaxation typical of HIOS, and advancing kMC simulations of anisotropic multilayer growth. Our investigations shall result in a scale-bridging understanding, starting from the single-molecule kinetics towards the full phase formation of different COMs.
In particular, we will investigate p-6P, p-6P-2F and p-6P-4F to study polarity effects, and the ladder-type quarterphenyl L4P at ZnO surfaces with various terminations. The oligophenyl-based COMs chosen here are relevant for applications (and studied in other projects in this CRC) while at the same time, they still show a high symmetry and are well-defined from a molecular force-field perspective. In particular, they are relatively weakly conjugated, and their structural and phase behavior is describable by our nonpolarizable force-field for p-polyphenyls [P1].

From a conceptual point of view, our goals are to develop and improve our methods to

- **(i) study the influence of COM polarity, step edges, and various electrostatic surface patterns on COM nucleation at the atomistic level**
- **(ii) calculate anisotropic transport coefficients as an input for the coarse-grained models**
- **(iii) address anisotropic multilayer growth by coarse-grained kinetic MC simulations**

These tasks will be performed in parallel by two PhD students who will primarily focus on parts (i) (fully atomistic calculations) and (iii) (fully mesoscopic simulations). Part (ii) will form the bridge between the atomistic and mesoscopic simulations as described below.

3.4.1. Description of planned research in project parts (i)-(iii)

Project part (i): Atomistic simulations

Starting from our achievements so far, the next urgent topics to address in our microscopic study of HIOS growth by all-atom MD simulations [14] are A) the heterogeneous nucleation and growth of a few dozen of COMs on ZnO surfaces, and B) the kinetic COM step-edge and molecular terrace crossing mechanisms. The latter are also directly related to the derivation of coarse-grained transport parameters for project part iii) Since our previous results have shown a strong sensitivity to electrostatics, a strengthened focus of our proposed research direction will be moved to the study of surface electrostatic patterns and COM polarity. Switching from p-6p to p-6p-2F and p-6p-4F, for instance, introduces local dipoles into the COM and changes the overall polarity to strongly dipolar and quadrupolar, respectively.

A) Having established an MD working model for oligophenyl-based COMs with accurately represented COM-COM interactions [P1], we are now in the position to study the nucleation of a few COMs on ZnO surfaces. One challenge faced in our previous simulations so far had been the slow relaxation of appearing structures apparently leading to kinetically trapped states within our MD simulations time scale of about tens of nanoseconds (unpublished). The reason is that the effective pair potential between the COMs is roughly one order of magnitude larger than the thermal energy k_BT. We will tackle this problem now by performing replica exchange MD (REMD) simulations [14] with which proper equilibrium sampling can be ensured. Preliminary results for COM clustering in the bulk are presented in Fig. 2, showing MD snapshots of a few selected equilibrium clusters, along with the ensemble-averaged free energy G(n) corresponding to the cluster probability distribution $G(n) = -k_BT \ln P(n)$. From the latter, we observe stable clusters for a critical number $n^*>4$ molecules in agreement with literature [15], exemplifying the reasonable output of the REMD simulations. We are currently investigating these results and the accompanying thermodynamics (entropies) and structures in more detail. In the next period, REMD simulations will then be applied to COM clustering on various ZnO surfaces. Expected results will describe the influence of the surface pattern on the critical stable cluster size, structures of nucleation seeds, the ensemble of appearing cluster structures, and the free energy of the heterogeneous nucleation. Repeating the study for a selection of the other proposed COMs will lead also to an understanding of the influence of COM polarity and geometry on nucleation.

B) The kinetic aspects determining the COM growth modes are the anisotropic diffusion processes of the COMs on the electrostatically patterned surfaces and their crossing of terrace-like steps of the ZnO surface

and/or those of nucleated COM clusters. Having established a p-polyphenyl working model [P1] as well as methods to study the long-time diffusion of COMs [P3], we are now in the position to sample the behavior of step edge crossing in MD simulations of COMs in more detail. Preliminary simulations (see final report A1, Fig.3) of a single COM crossing a completely apolar (10-10) ZnO step edge (by switching off all charges of the Zn and O atoms) already reveals a complex free energy landscape and barriers, as well as complicated crossing pathways, such as a parallel alignment of the COM to the edge and a subsequent flip-over mechanism for climbing. For a fully charged (10-10) surface, the parallel alignment will be energetically strongly penalised [P3] and other pathways with significantly altered free energy barriers must occur. Due to the high kinetic barriers, advanced MD free energy sampling methods have to be applied, such as umbrella sampling. In another line of works, we recently applied the theory of diffusion-controlled reactions to crystal cluster growth [P4] and for the calculation of diffusivity profiles along appropriate reaction coordinates [P5]. In the next funding period, these methods will be extended and applied to the diffusive crossing of terrace-like steps of varying height and directions on ZnO surfaces and those created from small COM clusters studied in part i) A). Expected results will describe the free energy barriers of crossing and the dominant reaction pathways and modes, with which a better understanding of the molecular kinetics as well as input parameters for the coarse-grained modelling can be obtained. The study will be repeated for a selection of the other proposed COMs to explore the influence of COM polarity and geometry.

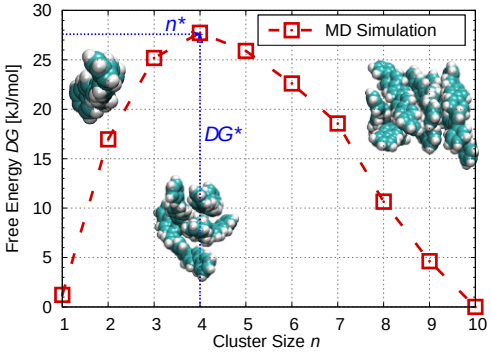

Figure 2 Cluster nucleation free energy at T = 630 K of p-6P clustering in REMD bulk simulations. The free energy is calculated from the cluster probability distribution $\Delta G=-k_B T \ln(P(n))$ to find a cluster with size n. A critical cluster size n*=4 can be identified in accordance with literature [15]. The nucleation free energy barrier estimated from our MD is about 27 kJ/mol.

Both parts, A and B, will lead to a deeper understanding of the influence of the steric topology and the charge pattern of the ZnO surface on the nucleation structure and kinetics of COMs. This research will thus help to interpret growth modes observed in experiments [A5 (Henneberger) and Z2 (Kowarik/Koch)] and how to control them. The results will deliver equilibrium surface cluster structures as input for refining first principle calculations [A4 (Heimel) and A10 (Tkatchenko)] as well as transport coefficients and energy barriers for coarse-graining, see goals ii) and iii) for details. For the refinement of ZnO-COM interaction potentials, first principle calculations (A4 and A10) will deliver problem-specific partial charges and van der Waals interactions.

Project part ii) Bridging atomistic and coarse-grained simulations

This part represents the „bridge“ between the atomistic calculations in part (i) and the coarse-grained simulations in (iii). As will be described below, both equilibrium and non-equilbrium (growth) simulations are planned in iii). All of these require as an input an *effective* interaction Hamiltonian H_{eff} describing, at a coarse-grained (beyond atomistic) level, molecule-molecule and molecule-substrate interactions. Moreover, the non-equilibrium simulations of monolayer growth require estimates for the single-molecule transport coefficients such as hopping times and energy barriers on the ZnO surfaces.

In Ref. [P9] we have suggested an interaction Hamiltonian of the form $H_{eff} = H_{mol-mol} + H_{mol-subs}$ for the system 6P on ZnO(10-10). The molecule-molecule part, $H_{mol-mol}$ involves sterical, van-der-Waals (Gay-Berne-like) and electrostatic (quadrupolar) interactions, while the molecule-substrate part, $H_{mol-subs}$, contains a quadrupole-field and an attractive term [P9]. These terms have been formulated in an *ad-hoc* fashion, in close exchange with the PIs of A1 (Dzubiella), A5 (Henneberger), and B3 (Blumstengel). In future we plan to refine the interaction potentials, one issue being to improve the modelling of the van-der-Waals parts in $H_{mol-subs}$ [with A10 (Tchatchenko)] as well as the anisotropic molecule-molecule interactions in $H_{mol-mol}$. Here we will benefit from our previous work on the systematic coarse-graining of anisotropic molecules [P8]. Moreover, similar to our study of 6P [P9], we need to identify „relevant“ features (shape, multipole moments) to define coarse-grained models for more complex COMs such as fluorinated (thus, dipolar) versions of 6P as well as ladder-type molecules. This will be done in close exchange with A4 (Heimel) and A2 (Hecht).

For the planned non-equilibrium simulations, which will be performed using a lattice-based kMC algorithm with continuous rotational degrees of freedom [see project part (iii)], we additionally need the following input quantities:

- *Translational diffusion barriers*: These include the energy barrier(s) E_D related to the translational diffusion of an *isolated molecule* over the chosen surface in lateral directions or over a step edge formed by the substrate material, and the „Schwöbel" barrier(s) E_S related to translational diffusion over a *molecular* step edge. Contrary to E_D, E_S clearly involves interaction effects between the COMs and is thus particularly relevant in multilayer growth.

  So far, there are only few studies addressing calculations of these barriers in organic molecular systems [7-10]. In atomic systems, one typically one assumes an Arrhenius-like relation between the tracer diffusion coefficient, D, and the above-mentioned energy barriers. This relation also involves the „attempt frequency" □□as a prefactor. Similar relations have been suggested for organic molecules [7-10]. However, the precise identification of energy barrier and prefactor is often difficult since they appear as a product. Moreover, in a real molecular systems, both E_D and E_S are expected to be *direction-dependent*, therefore one has an entire set of diffusion/Schwöbel barriers rather than a single number. For example, on a stripe-patterned surface such a ZnO(10-10) one expects strongly different diffusion along and perpendicular to the stripes, as it has been already demonstrated atomistically in A1 (Dzubiella) [P3]. The latter study has provided explicit values for the long-time diffusion constants, parallel and perpendicular to the stripes. In fact, the surface diffusion was shown to stem from activated barrier hopping with time scales identified with □$_D$ exp(-β E_D), which is the kinetic prefactor needed in the kMC simulations in part iii). The energy barriers E_D were calculated [P3]. In forthcoming MD work, see the report to A1 and goal (i) above, the energy barriers corresponding to surface step edges and molecular terraces E_s will be calculated. The barrier E_D (lateral diffusion or surface-step crossing of an isolated molecule) will be used in the kMC simulations for monolayer growth to gauge the required energy barriers for in-plane diffusion. The MD result for E_S (climbing of COMs from the ZnO surface onto the monolayer or vice versa) will be of interest for the multilayer kMC simulations. We note, however, that the precise separation between diffusion and interaction effects in kMC remains to be sorted out.

- *The rotational diffusion barrier E_R and corresponding attempt frequency.* Typically, one assumes the rotational kinetic barrier ~ □$_R$ exp(-β E_R) to be much higher than that for translational diffusion due to the strong steric frustration effects expected in a dense system. Indeed, in our previous work [P3] we observed very restricted orientational motion of p-6P on the (10-10) ZnO surface due to very large barriers E_R. More precise estimates will be developed from the atomistic calculations where rotational degrees of freedom are included in the diffusion and step edge crossing, and their kinetic behavior will be further quantified.

- *The rate of adsorption*: Here, we will take input from experiment.

Project part (iii) Coarse-grained simulations

Simulations of multilayer growth of organic molecules at semiconductors are in their infancy [5]. Here we put forward our understanding by investigating A) the equilibrium structure and phase behavior of COMs in the monolayer, B) energetic ground states of both, mono- and multilayers, and C) non-equilibrium (growth).

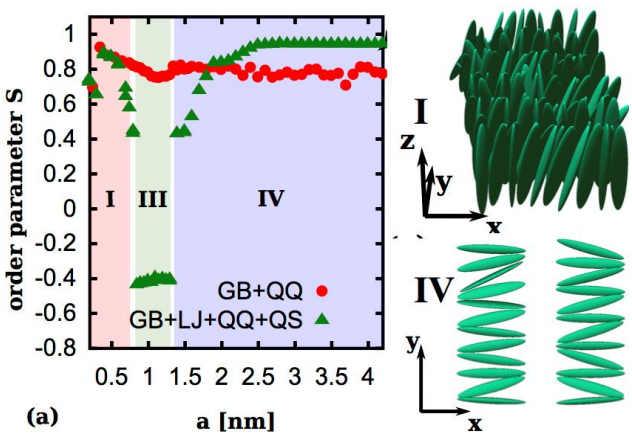

Figure 3 a) Equilibrium MC results for the orientational (nematic) order parameter of 6P at ZnO (10-10) as function of lattice constant [P9]. In the low density phase (IV) the molecules tend to order according to the electrostatic surface pattern, while at high densities (I) an upright ordering with quadrupolar T-like ordering becomes stable (see snapshots).

A) As a very first step, we will generalize the equilibrium lattice-MC simulations performed in [P9] (see Figure 3) for a monolayer of 6P molecules on ZnO(10-10) to **off-lattice situations.** We note that in [P9] the orientations were modelled as *continuous* degrees of freedom; only the positions have been discretized. Relaxing this constraint will allow for a better identification of packing effects, an easier comparison of structural data (e.g., structure factor, crystalline units cells) with atomistic MD simulations and experiments, and thus, to a more refined validation of the effective Hamiltonian. We

consider these equilibrium calculations as an indispensable prerequisite for understanding nucleation and growth. Further, the structural data (together with corresponding ones from project part (i)] serve as an input into quantum-optical calculations in B12 (Knorr/Richter).

B) In parallel to A), we will perform **ground state calculations** in the dense state, again based on the effective Hamiltonain suggested in [P9] and suitable variants designed for the other COMs under investigation. Specifically, based on our experience for the monolayer ordering behavior (e.g., the formation of an upright nematic phase with quadrupole-induced herringbone-like ordering [P9]) and observations from experiment [11] we will *guess* certain lattice candidate structures and calculate their energy (for a periodically replicated system) as function of a suitable parameter, e.g. the „tilt angle“. The idea is to get a rough insight into the complex interplay of (electrostatic and van-der-Waals) molecule-molecule interactions under spatial confinement, on the one side, and molecule-substrate interactions, on the other side. For example, an important question is how far the ordering induced by the substrate pattern reaches into the material from an energetic point of view. Besides providing a guideline for the outcome of finite-temperature simulations, these groundstate calculations will also help to interprete parallel experiments in the CRC [e.g., A5 (Henneberger), Z2 (Kowarik/Koch)], see e.g. Ref. [11].

C) **Non-equilibrium simulations**: We intend to generalize the kMC simulations performed for C_{60} in the first funding period towards more complex HIOS systems. Importantly, we aim at an algorithm where the molecule's orientation is treated as a *continuous* degree of freedom. This is motivated by experimental observations [11] demonstrating that the main orientation of a molecular layer is not only tilted, but also can vary from layer to layer. The assumption of continuous rotations contrasts earlier kMC studies (see, e.g., [5,8,9,12]) where the orientations are typically discretized according to edges of a cubic lattice (6-state model), i.e., each molecules can only ly on the surface or stand perfectly upright. In another recent kMC study involving 6P, the rotational degree of freedom was even neglected completely [13].
Our kMC algorithm employed for C_{60} [P2] is based on a list (and corresponding rates) of all possible events, and on a stochastic time step determined by the sum of all rates (n-fold way). With continuous degrees of freedom this list would become infinitely long. We therefore perform a metropolis-like kMC involving three processes, that is, 1. pure translational diffusion, 2. pure rotation, 3. flux (the latter drives the system into non-equilibrium). Here, the time step Δt is constant, and stochasticity comes in through the acceptanc probabilities for each process.

To begin with we will use the algorithm to investigate nucleation and growth in sub-monolayer situations. In the simplest case (no anisotropy in the kinetic coefficients, no surface step edges) the translational diffusion occurs with probability $P_D = \nu_D \Delta t \exp[-\beta E_D] \min\{\exp[-\beta \Delta H_{mol-mol}],1\}$ involving the diffusion barrier E_D (from all-atom MD), the attempt frequency η_D and the difference in interaction energies, $\Delta H_{mol-mol}$, between final and initial state. The rotational motion occurs with probability $P_R = \nu_R \Delta t \exp[-\beta E_R] \min\{\exp[-\beta \Delta H_{mol-mol}],1\}$ and adsorption with $P_A = \nu_A \Delta t$, if the lattice site is free. A preliminary results from corresponding kMC simulations is shown in Fig. 4, where we estimated E_D through the molecule-substrate part of our effective Hamiltonian [P9]. The snapshot already reflects the competition between lying ordered islands (favored by the substrate) and standing nematic islands (packing effects). In the next step, anisotropic surface diffusion has to be built in (using direction dependent barriers E_D). From a physical point of view, further questions concern the occurrence of herringbone structures, island distributions and critical cluster size, and correlations between islands.

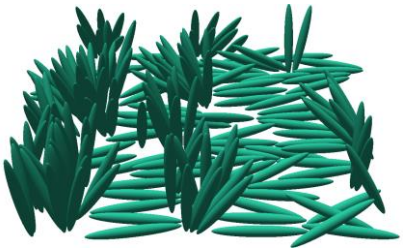

Figure 4 Preliminary kMC result for submonolayer growth of 6P on ZnO(10-10) based on H_{eff} [P9]. Parameters are E_R=0, and $\nu_A << \nu_R << \nu_D$. One observes formation of both, lying and standing islands.

Having explored the monolayer situation, we will attempt to grow a second (third, ..) layer. Clearly, this is not a straightfoward task to do in a system with continuous degrees of freedom, due to the (possible) lack of a well-defined crystal structure. To our knowledge, multilayer growth in kMC hasn't even been done for rotationally discrete systems. As a first step, we will assume that molecular orientations in the first layer *freeze* after layer completion, i.e., there is no intralayer relaxation. This will allow to handle growth of the second layer as growth on a rough (yet passive) substrate, an assumption which has to be tested (possibly in comparsion with MD simulations). Another challenge in the multilayer simulations is to find appropriate coarse-grained diffusion barriers E_D, E_S, and to identify their relation to the results from all-atom MD simulations in part (i).

3.4.2. Work programme

Initially, the two requested PhD students will focus on project parts (i) and (iii); the joint investigations planned within the interface project part (ii) will start in the second year.

First year
- (i) REMD simulations of tens of p-6p molecules on various ZnO surfaces to study critical nucleation and onset of growth; investigation of the in-plane diffusion of p-6P-2F and p-6P-4F and L4P on planar ZnO surfaces [P3].
- (iii) Off-lattice (MC) simulations of monolayers of 6P/ZnO(10-10), development of coarse-grained models for other COMs.

Second year
- (i) MD and umbrella sampling simulations and theoretical description of the diffusive crossing of step-edges and molecular terraces of p-6p on various ZnO surfaces.
- (ii) Determination of kinetic input parameters for monolayer diffusion (translational/rotational).
- (iii) Refinement of the existing kMC code for monolayers, investigations of 6P and derivates. Start of ground-state calculations.

Third year
- (i) REMD investigation of the influence of COM type and polarity on nucleation.
- (ii) Determination of kinetic input parameters and pathways for step-edge diffusion.
- (iii) Development of a kMC code for multilayer growth, ground state calculations for monolayers.

Fourth year
- (i) MD and umbrella sampling investigation of the influence of COM type and polarity on step edge and terrace crossing.
- (ii) Refinement of kinetic input parameters, investigations of different COMs and surfaces.
- (iii) kMC calculations for various types of COMs/surfaces, possibly parallel MD calculations to explore relaxation effects.

3.5 Role within the Collaborative Research Centre

This project adds to the CRC a theoretical understanding of the morphology and growth of HIOS at an atomistic and coarse-grained level. It is therefore complementary to the other theoretical projects which focus on electronic and optical aspects of HIOS. At the same time, the project provides models to interprete experimental results for morphology and growth as well as candidate crystal structures as input for first-principle calculations. Specifically, the following cooperations are planned:

- A4 (Heimel): Force-field parameters from DFT, geometrical single-molecule structure from atomistic MD
- A5 (Henneberger): Interpretation of experimental results for equilibrium/non-equilibrium HIOS structures
- A10 (Tchatchenko): Refinement of classical force-fields for molecule-surface interactions, particularly van-der-Waals contributions
- B6 (May): Advice concerning atomistic MD techniques (force-fields) to relax small oligophenylene COM assemblies at ZnO clusters
- B12 (Knorr/Richter): Delivery of structural input for quantum-optical calculations of disordered COM systems on surfaces.
- Z2 (Kowarik/Koch): Interpretation of time-dependent structures from scattering experiment

3.6 Delineation from other funded projects

There is no overlap with other, already funded or planned projects of the two PIs.

- DFG-CRC 910 *Control of self-organizing nonlinear systems*, Project B2 (Klapp): *Feedback control of dynamical structures and transport in driven colloidal systems* (2011-2014, planned until 2018, under review)

- DFG-IRTG 1524 *Self-assembled soft matter nanostructures at interfaces*, Project C5 (Klapp): *Field-driven self-assembly and transport of Janus particles at interfaces (2014-2018).*
- DFG-RTG 1558 *Nonlinear Collective Dynamics in Condensed Matter and Biological Systems,* Project B1 (Klapp): *Dynamical behavior and self-assembly of exotic magnetic colloids* (2014-2018).
- DFG Project KL1215/8-1 (Klapp) *Computer simulations and theory of hybrid materials composed of magnetic particles in liquid-crystalline matrices* (2013-2015).
- DFG Project DZ-74/6 *Theoretical investigation of electrostatic effects on the critical solution temperature of thermosensitive statistical copolymers (*2013-2016*)*
- DFG Project DZ-74/7 *Theoretical investigation of the role of water in hydrophobic key-lock binding kinetics (*2014-2017*)*

3.7 Project funds

3.7.1 Previous funding

Project A7 has been funded within the CRC since 07/2011. Project A1 has been funded within the CRC since 07/2011 and will be terminated 06/2015.

3.7.2 Funds requested

Funding for	2015/2		2016		2017		2018		2019/1	
Staff	Quantity	Sum	Quantity	Sum	Quantity	Sum	Quantity	Sum	Quantity	Sum
category, percentage										
PhD student, 75%	2	44.100	2	88.200	2	88.200	2	88.200	2	44.100
Total										
Direct costs	Sum		Sum		Sum		Sum		Sum	
Small equipment, Software, Consumables	1000		2000		2000		2000		1000	
Total	45.100		90.200		90.200		90.200		45.100	
Major research equipment	Sum		Sum		Sum		Sum		Sum	
€ 10.000 - 50.000										
> € 50.000										
Total										
Total										

(All figures in Euro)

3.7.2 Staff

	No.	Name, academic degree, position	Field of research	Department of university or non-university institution	Commitment in hours/week	Category	Funded through:
Available							
Research staff	1)	Klapp, Prof. Dr.	Theo. Phys./ Stat. Phys.	TU Berlin, Institute of Theor. Physics	5h		
	2)	Dzubiella, Prof. Dr.	Theo. Phys./ Stat. Phys	Helmholtz Center Berlin and HUB Physics	5h		
	3)	Kraft, Alexander, M.Sc.	Theo. Phys./ Stat. Phys.	TU Berlin, Institute of Theor. Physics	5h		
Non-research staff	4)	Orlowski, Peter, Dipl.-Phys., System Administrator		TU Berlin, Institute of Theor. Physics	1h		
Requested							
Research staff	5)	n.n.	Theo. Phys./ Stat. Phys.	TU Berlin, Physics		PhD	
	6)	n.n.	Theo. Phys./ Stat. Phys.	Helmholtz Center Berlin and HUB Physics		PhD	
Non-research staff							

Job description of staff (supported through available funds):

1) Prof. Dr. Sabine Klapp (PI)
Scientific coordination of the project together with J. Dzubiella, including supervision of scientific staff; exploration of concepts, goals and selection of methods; coordination of cooperations within the CRC.

2) Prof. Dr. Joachim Dzubiella (PI)
Scientific coordination of the project together with S. Klapp, including supervision of scientific staff; exploration of concepts, goals and selection of methods; coordination of cooperations within the CRC.

3) Kraft, Alexander, Dipl.-Phys.
Scientific cooperation on growth phenomena, particularly in non-equilibrium.

4) Orlowski, Peter, Dipl.-Phys.
System administration and maintenance of computers.

Job description of staff (requested):

5) n.n. (PhD student)
Coarse-grained simulations planned in project part (iii), including equilibrium and kinetic Monte-Carlo of effective Hamiltonians. Exchange with PhD student 6) on input data via the interface project part (ii).

6) n.n. (PhD student)
Atomistic (classical force-field) MD simulations planned in project part (i) to investigate the structure, transport properties, and growth of COMs in bulk and on inorganic ZnO surfaces. Exchange with PhD student 5) on input data via the interface project part (ii).

3.7.3 Direct costs for the new funding period

Klapp/TUB	2015/2	2016	2017	2018	2019/1
Funds available	500	1,000	1,000	1,000	500
Funds requested	1,000	2,000	2,000	2,000	1,000

(All figures in Euro)

Dzubiella/HZB:	2015/2	2016	2017	2018	2019/1
Funds available	500	1,000	1,000	1,000	500
Funds requested	1,000	2,000	2,000	2,000	1,000

Consumables for 2015-2018 (each year)

Small computer equiments, spare components, and consumables required specifically for this project	EUR	2,000

3.7.4 Major research equipment requested for the new funding period

No major research equipment requested.

A8 (Koch)

In Bearbeitung

3.1 About project A9

3.1.1 Title: A9: Controlling HIOS growth: in-situ and real-time x-ray scattering

3.1.2 Principal investigator

Prof. Dr. Kowarik, Stefan (*21.08.78, deutsch)
Humboldt-Universität zu Berlin, Institut für Physik, Newtonstr. 15 12489 Berlin
Phone: +49 (0)30 2093 4818
Fax: +49 (0)30 2093 7760
E-mail: stefan.kowarik@physik.hu-berlin.de

3.2 Project history

3.2.1 Report

At the beginning of the funding period there had been no real-time studies on the growth kinetics of molecules on ZnO surfaces. In the funding period we have made great progress in the structural characterisation as well as optimisation of HIOS heterostructures. In particular we have measured crystal structures of HIOS and interface structures where we resolved surface induced phases. Methodically we have made significant advances in X-ray scattering by not only including real-time specular X-ray scattering but also the diffuse scattering in the analysis. This has led to a productive collaboration with the project of S. Klapp on real-time growth modelling, which at the current stage has yielded results for spherical molecules. The tuning and optimisation of HIOS growth through chemically modifying the molecular entities (without changing their optical properties) was of particular interest and we have made use of newly synthesized molecules in the CRC.

This report is structured along the following questions which were posed in the goals section of the proposal:

a. What is the crystal structure and (buried) interface structure for given growth parameters?

In a close collaboration with project Z1 / A3 Hecht and A5 Henneberger we focused on the prototypical molecule 6P and its synthesized derivatives 6P-F_2, 6P-F_4 and 6P-CN to investigate the growth and crystal structure and to undestand if one can design HIOS thin-films by chemically tuning functional molecules.

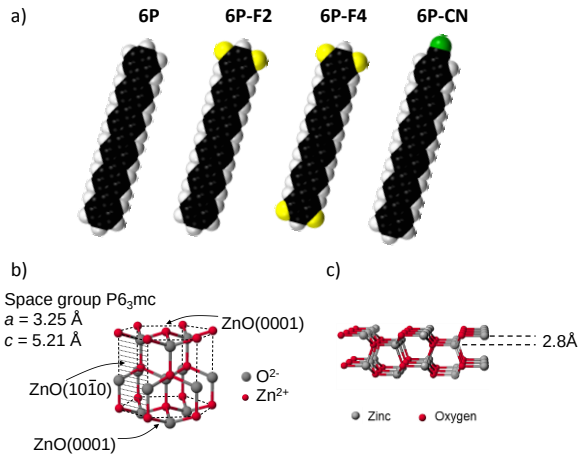

Fig. 1: a) Schematic molecular structures of 6P, 6P-F_2, 6P-F_4 and 6P-CN. c) Sketch of the ZnO crystal structure. d) Side view of the (10-10) ZnO surface.

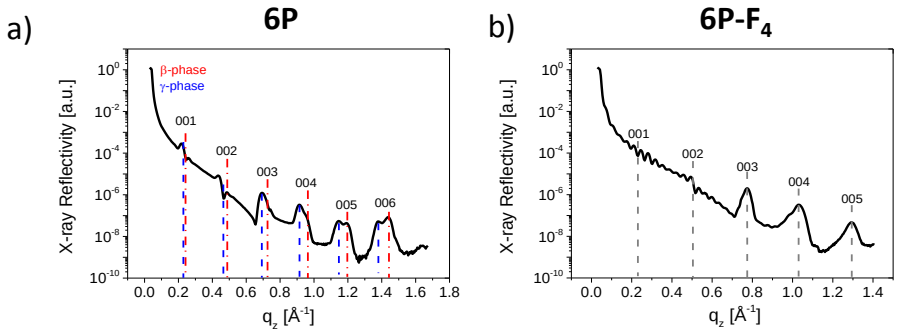

Fig. 2: a) and b) out-of-plane crystal structure of 6P and 6P-F_4 measured by XRR.

For all four molecules we found a nearly upright standing orientation of the molecules on the mixed-terminated ZnO (10-10) surface as exemplarily shown in the X-ray reflectivity measurements in Figure 2 a) and b) for 6P and 6P-F_4. As shown in Figure 2 a) a polymorphism is found for 6P which grows in the so called *β*- and a *γ*-phase. Our analysis has shown that by changing the substrate temperature the ratio between these phases can be modified. Whereas they are equally developed at room temperature (equal peak heights in Figure 2a) at elevated temperatures the *γ*-phase begins to dominate. Another novel possibility to receive phase pure films is through fluorination of 6P. As shown exemplarily in Figure 2 b) a phase pure crystal thin-film is achieved if 6P-F_4 is used. The same is found by using 6P-F_2, but 6P-CN again exhibts two phases. For applications of HIOS systems the chemical tunability of polymorphism through fluorination is of crucial importance since functional properties such as charge carrier mobility depend on the crystal structure as well as the grain boundaries between crystallites, so that films with high phase purity is desirable.

b. How are anisotropic molecules oriented, does the orientation change at a critical film thickness, and does polymorphism occur?

As stated above we found that the chosen prototypical molecule 6P and its chemical derivatives prefer a more or less upright standing orientation on ZnO (10-10) surfaces independent of the substrate temperature, with 6P and 6P-CN exhibiting polymorphism. However the exact orientation, i.e. the molecular tilt angle can be tuned through chemical modification and the tilt angle also changes between molecules directly at the interface and molecules in thick films. In our *in situ* and real-time X-ray reflectivity measurement we have found changes in the molecular tilt angle with film thickness. As an example the (004) out-of-plane Bragg reflection for 6P-F_4 films for the first three MLs is shown in Figure 3. A surface induced structure that differs from the bulk is responsible for the shifting reflection, and the decreasing lattice constant as shown in Figure 3. This means that 6P molecules stand more upright in the first layers, a trend that has been observed also for the 6P derivatives as well as in many systems such as pentacene or diindenoperylene.

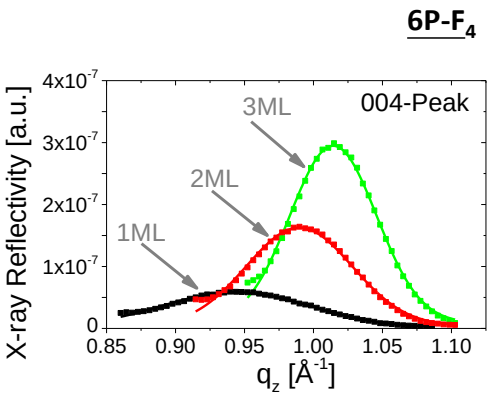

	d [nm]
1 ML	2.64 ± 0.12
2 ML	2.46 ± 0.06
3 ML	2.42 ± 0.03

Fig. 3: (004) Out-of-plane Bragg reflection of 6P-F4 films for the first three MLs.

c. Which atomic processes occur and can rate equation models explain the experimental data by fitting sticking coefficient, interlayer transport, and Ehrlich Schwöbel barrier?

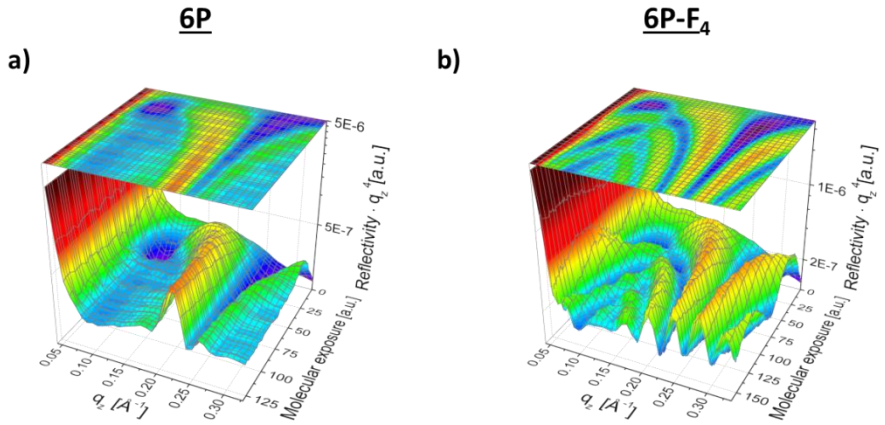

Fig. 4: Evolution of the X-ray reflectivity during the growth of 6P and 6P-F_4 films at room temperature on ZnO (10-10).

To analyse the growth and to investigate if the chemical tuning of 6P changes the growth mode of the organic part of HIOS we performed real-time X-ray reflectivity measurements. Figure 4 shows the results in which a smooth layer-by-layer growth corresponds to stronger film thickness oscillations that persist up to large film thicknesses, while rough 3d growth results in quick damping of growth oscillations. As clearly shown in Figure 4 chemical tuning of 6P to 6P-F_4 drastically changes the organic thin-film growth.

The fluorination of 6P in the four “corner” positions (6P-F_4) changes intermolecular electrostatic interactions through the introduction of two local dipole moments at both molecular termini. Therefore a flat-lying chemically modified 6P molecule diffusing on the surface of an island exposing fluorine atoms at its boundary will experience a substantially altered binding energy as compared to 6P where the islands are presenting hydrogen at their periphery. As a consequence, the activation energy for molecules diffusing on islands as well as the Ehrlich-Schwoebel barrier, both critical parameters in a kinetically controlled growth process, will differ. Our result of 6P-F_4 layer-by-layer growth therefore suggests that both Ehrlich Schwoebel as well as diffusion barrier are reduced by terminal fluorination.

We have further performed growth studies for molecules with asymmetric modification, that is 6P-F_2 and 6P-CN with a built in dipole moment. In the case of 6P-CN the incorporated dipole moment of the –CN group is even larger than for the fluorinated molecules. As shown in Figure 5 we do not find a trend of improved growth with increasing dipole moment, but 6P-F_2 exhibits the best growth while 6P is growing in a more layer by layer fashion than 6P-CN (note that these experiments were performed at higher substrate temperature, explaining the improved growth of 6P when compared to Figure 4).

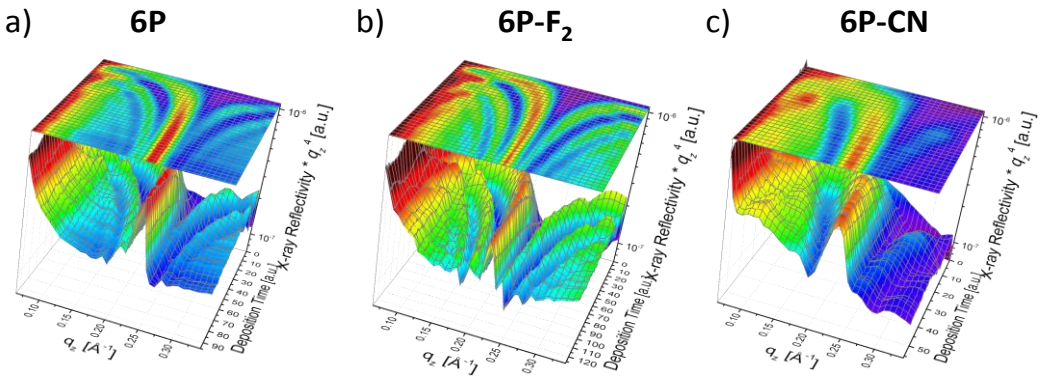

Fig. 5: Evolution of the X-ray reflectivity during the growth of 6P, 6P-F_2 and 6P-CN films at elevated substrate temperature (100°C) on ZnO (10-10).
A complete set of energy parameters (Ehrlich Schwoebel barrier, diffusion barrier, and binding energy) has been determined in collaboration with A7 (Klapp). This marks a significant technological advance as we have been able to not only measure the reflectivity, but also the diffuse scattering. However, currently only the spherical system C60 is accessible to the KMC simulations so that this can only be applied to rod-shaped HIOS molecules in the future.

d) Which growth mode (layer-by-layer, Stranski-Krastanov, Volmer-Weber) occurs and how does it depend on growth parameters and the inorganic surface (polar vs. non-polar ZnO/GaN surface orientation, self-assembled monolayer passivation of the surface)?

For a quantitative analysis of the growth mode of the different molecules we have fitted the X-ray reflectivity shown in Figure 4 and Figure 5 using two independent methods. On the one hand, we take cuts at fixed q_z values of ½, ⅔, and ¾ · q_{Bragg} and analyse as a function of time the resulting growth oscillations, a technique that is frequently used in growth of inorganic and organic materials. On the other hand, we take cuts through the 3D data at fixed times t and use the Parratt formalism to determine the electron density distribution of the films at each point in time. The resulting layer coverage and roughness curves from an analysis of the Trofimov and Parratt fits is shown in Figure 6. All performed experiments conclusively show that terminal fluorination of 6P causes a transition from a 3D, Stranski-Krastanov growth for the parent 6P to an almost 2D, layer-by-layer growth mode for 6P-F4 on ZnO(10-10).
Due to the low number of collaboration partners in the CRC using GaN, we have not studied this surface. Also, due the lack of an epitaxial relation between molecules and ZnO treated by sputtering and annealing we have not further investigated other ZnO surfaces. SAM surfaces have not been used as a substrate but have been studied in collaboration with B7 (Neher), where X-ray measurements provided detailed insight in the SAM layer thickness.

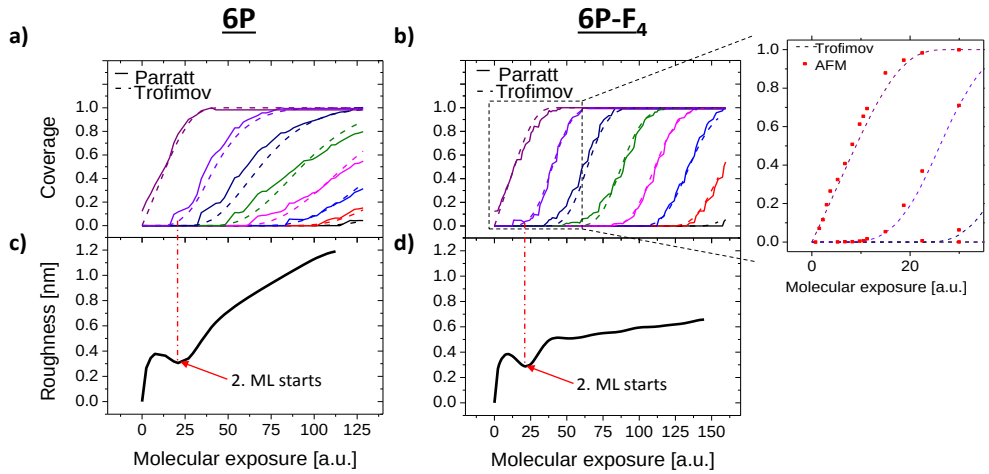

Fig. 6: Comparison of the calculated layer coverages by using the Trofimov model and fits of the in situ XRR curves based on the Parratt formalism for 6P (a) and 6P-F_4 (b). Enlargement in (b) demonstrates excellent

agreement in layer coverage curves between AFM data and the Trofimov model. c) and d) calculated RMS roughness during the film growth.

e) Can the large scale surface roughness and in-plane correlation length / island size be rationalized through scaling laws?

We have used the island size scaling approach to study the nucleation behaviour of 6P and 6P-F_2. For this film thickness series on silica (which for our application behaves similar to other oxidic surfaces such as sputtered annealed ZnO, where we do not find epitaxy) have been prepared and studied by AFM. From the island size scaling the critical nucleus size *i* has been determined, which is defined as largest unstable cluster, that is *i*+1 molecules form a stable island nucleus. Surprisingly in the first ML no influence of the dipole on *i* has been found with *i* ranging between 2 -3 for both molecules. However the smoother growth mode for the fluorinated compound indicates that this may change for the second layer. We are therefore currently finishing the determination of *i* for growth of molecules in the second layer, which will give further insight into the mechanism improving the growth mode for fluorinated compounds.

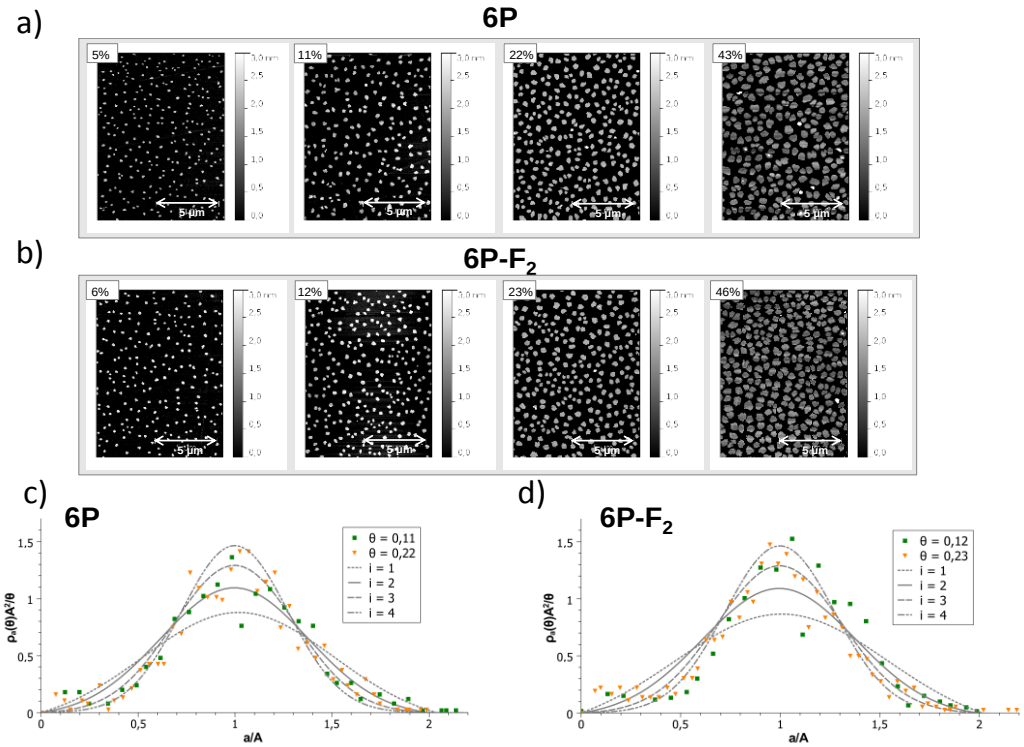

Fig. 7: a) and b) AFM images showing nucleation of 6P and 6P-F_2. c) island size scaling allows us to extract the critical cluster size.

3.2.2 Project-related publications

[65] M. Sparenberg, A. Zykov, P. Beyer, L. Pithan, C. Weber, Y. Garmshausen, F. Carlà, S. Hecht, S. Blumstengel, F. Henneberger, S. Kowarik, "Controlling the growth mode of para-sexiphenyl (6P) on ZnO by partial fluorination" Physical Chemistry Chemical Physics (2014), DOI: 10.1039/c4cp04048a.
[66] I. Lange, S. Reiter, M. Pätzel, A. Zykov, A. Nefedov, J. Hildebrandt, S. Hecht, S. Kowarik, C. Wöll, G. Heimel, and D. Neher, "Tuning the Work Function of Polar Zinc Oxide Surfaces using Modified Phosphonic Acid Self-Assembled Monolayers" Advanced Functional Materials, DOI: 10.1002/adfm.201401493 (2014).
[67] S. Bommel, N. Kleppmann, C. Weber, H. Spranger, P. Schäfer, J. Novak, S.V. Roth, F. Schreiber, S.H.L. Klapp, S. Kowarik, "Unravelling the multilayer growth of the fullerene C60 in real-time" Nature Communications, DOI: 10.1038/ncomms6388 (2014).

Further publications with the above mentioned results on dipolar molecules and island size scaling are in preparation, as is usual for a PhD project that has been running for 2 ½ years and will be completed by mid 2015.

3.3 Funding

Funding of the project within the Collaborative Research Centre started 2010/7. The project will be completed by the end of the current funding period in 6/2015.

3.3.1 Project staff in the ending funding period

	No.	Name, academic degree, position	Field of research	Department of university or non-university institution	Commitment in hours/week	Category	Funded through:
Available							
Research staff	1	Zykov, Anton	Exp. phys.	Institute of physics	40	PhD	Sfb951
	2	Kowarik, Stefan, Prof. Dr.	Exp. phys.	Institute of physics	5	other	HU Berlin
Non-research staff							
Requested							
Research staff							
Non-research staff							

Job description of staff:
1. Anton Zykov:
Performed growth runs with organic UHV MBE apparatus on laboratory X-ray diffractometers. Used complementary measurements (AFM, X-ray microscopy) to study the structure of HIOS. Was responsible for preparation and execution of synchrotron experiments.

2. Stefan Kowarik:
Designed experiments and helped with data analysis, participated in synchrotron experiments.

3.1 About project A10

3.1.1 Title: Van der Waals Effects on Dynamics and THz Spectroscopy of HIOS

3.1.2 Research areas:

307-02 Theoretische Physik der kondensierten Materie
302-03 Festkörper- und Oberflächenforschung / Theorie und Modellierung
303 Physikalische und Theoretische Chemie

3.1.3 Principal investigator(s)

Dr. Alexandre Tkatchenko (*07.02.1980, Mexican)
Theory Department, Fritz-Haber-Institut der Max-Planck-Gesellschaft
Phone: +49 30 8413 - 4802
Fax: +49 30 8413 - 4701
E-mail: tkatchenko@fhi-berlin.mpg.de

Prof. Dr. Matthias Scheffler (*25.06.1951, German)
Theory Department, Fritz-Haber-Institut der Max-Planck-Gesellschaft
Phone: +49 30 8413 - 4711
Fax: +49 30 8413 - 4701
E-mail: scheffler@fhi-berlin.mpg.de

Do the above mentioned persons hold fixed-term positions? yes
Name: Alexandre Tkatchenko
End date: 31.08.2016
Further employment is planned until 30.06.2019

3.1.4 Legal issues

This project includes

1.	research on human subjects or human material.	no
2.	clinical trials	**no**
3.	experiments involving vertebrates.	**no**
4.	experiments involving recombinant DNA.	**no**
5.	research involving human embryonic stem cells.	no
6.	research concerning the Convention on Biological Diversity.	no

3.2 Summary

The binding between (large) organic molecules and inorganic substrates is driven to a large extent by van der Waals (vdW) interactions, in combination with other covalent and non-covalent forces. Even in the presence of strong covalent linker groups to the surface, accurate treatment of vdW interactions can have a qualitative influence on the structure, stability, and sometimes even the electronic properties of HIOS. It has been already convincingly demonstrated during the first funding period of CRC 951 that vdW interactions play an important role in determining the adsorption geometry of organic molecules on ZnO and other substrates (*Rinke/Scheffler*). However, all previous studies of realistic HIOS relied on an *a posteriori* pairwise-additive treatment of vdW interactions. Surprisingly, such inherently approximate treatment is sometimes able to properly describe structures and stabilities of HIOS. However, it is well known that vdW interactions arise from instantaneous fluctuations of the electron density. Therefore, they should be treated *self-consistently* by explicit many-body methods based on robust quantum-mechanical description of the system. The aspect of self-consistency refers to the fact that the vdW potential (functional derivative of the vdW energy) should be included in the Kohn-Sham exchange-correlation potential and this allows vdW interactions to have a direct influence on the electron density, electronic orbitals, and other related properties of a given system.

In small or weakly polarizable molecular systems, the effect of vdW self-consistency is typically tiny, leading to negligible modifications of their stability, dynamics, and electronic properties. However, unexpectedly large self-consistency effects can be found for binding properties and electrostatic moments of systems with higher polarizability density. Specifically, in the context of this project, vdW interactions have been observed to cause complex and sizeable electronic charge redistributions in the vicinity of inorganic surfaces, along with a visible shift of the Fermi level. As a result, vdW interactions can *directly* (i.e. at fixed geometry) modify workfunctions of HIOS by up to 0.3 eV in the case of rather small molecules, revealing a non-trivial connection between electrostatics and long-range electron correlation effects. However, this important influence of ubiquitous vdW interactions beyond structure and stability has not been prominently recognized up to date. In summary, the role of self-consistent vdW interactions in the electronic, vibrational, and time-dependent phenomena in HIOS remains to be critically assessed, and this is one of the main goals of this proposal.

We have recently developed an efficient method that explicitly includes many-body effects to all orders in the dipole approximation (DFT+MBD) for accurate description of vdW interactions in realistic materials. Since substantial collective couplings are observed in HIOS, the effect of many-body vdW interactions in their optical, electronic, and other response response is expected to be quite prominent. These couplings can be observed, for example, by linear and non-linear THz spectroscopy done in the project B5 (*Wörner/Elsässer*). In this project, we will develop, implement, and apply the self-consistent DFT+MBD method to study static and time-dependent electronic and vibrational properties for a hierarchy of HIOS. As substrates, we will consider pristine and doped ZnO, and we will compare with the adsorption on “model semiconductors” Si and Ge. For the organic part, we will consider coronene, oligophenyls, pyridine, and oligofluorenes.This will allow us to study the effect of self-consistent vdW interactions for molecules covering the entire visible spectral range for light emission and absorption. Our theoretical calculations will be directly compared with experimental results obtained by projects B5 (*Wörner/Elsässer*), A5 (*Henneberger*), B9 (*Stähler*) and others. Our work will be performed in close contact with other theoretical projects lead by B4 (*Körzdörfer/Scheffler/Rinke*), A7 (*Dzubiella/Klapp*), and A4 (*Heimel*).

3.3 Research rationale

3.3.1 Current state of understanding and preliminary work

Ubiquitous in nature, van der Waals (vdW) interactions are the result of quantum-mechanical fluctuations of the electron density, $n(\mathbf{r})$, and play a critical role in the formation, stability, and function of a wide variety of systems, ranging from simple noble-gas dimers to complex hybrid organic/inorganic interfaces [1,2,3]. Since the long-range vdW energy, E_{vdW}, typically represents only a tiny fraction (~0.001%) of the total electronic energy, the vdW influence on $n(\mathbf{r})$ and electronic properties, such as multipolar moments and orbital energy levels, is commonly assumed to be rather small, if not negligible. For this reason, many of the widely used methodologies for incorporating vdW interactions within the framework of density-functional theory (DFT), are generally approximated by an *a posteriori* perturbation of the total energy, and are therefore only accounted for after $n(\mathbf{r})$ has been obtained via the self-consistent solution of the non-linear Kohn-Sham (KS) equations. Obviously, this is an approximation, and its validity has been rigorously assessed only for very few systems [4,5,6]. While self-consistent vdW effects are indeed expected to produce modest structural and density changes in small gas-phase dimers, a rigorous investigation of these electron density modifications, as well as a thorough analysis of larger and more complex systems, such as inorganic surfaces and organic/inorganic interfaces, has still not been performed to date.

Considering now the influence of vdW interactions on the structure and stability of HIOS, we also found a few surprises when applying advanced vdW-inclusive DFT methods to these systems. For example, vdW interactions can often lead to a more substantial contribution to adsorption energies of strongly-bound molecules on metals than they do when molecules are purely physisorbed. This situation is illustrated in Figures 1 and 2. Figure 1 shows the equilibrium vertical heights and adsorption energies for benzene – the fundamental building block of many molecules within CRC 951 – on a range of transition metals. Surprisingly, vdW interactions stabilize the adsorption on reactive transition metals Pt, Pd, Rh, Ir substantially more than in the case of much less reactive coinage metals Cu, Ag, Au. In addition, Figure 2 shows that the adsorption geometries of large organic molecules on Pt(111) and Pd(111) can be largely modified by the inclusion of vdW interactions, even in the presence of covalent oxygen-metal bonds with the substrate. For systems studied within CRC 951, these results strongly suggest that vdW interactions will play

a significant role for determining the structure and stability of molecule/semiconductor interfaces, even in the presence of strong electrostatic effects. Our recent comprehensive investigation of 25 organic/metal interfaces demonstrate that only an accurate inclusion of vdW interactions allows one to account for the remarkable stability of large molecules on inorganic surfaces as observed, e.g., in desorption experiments [8].

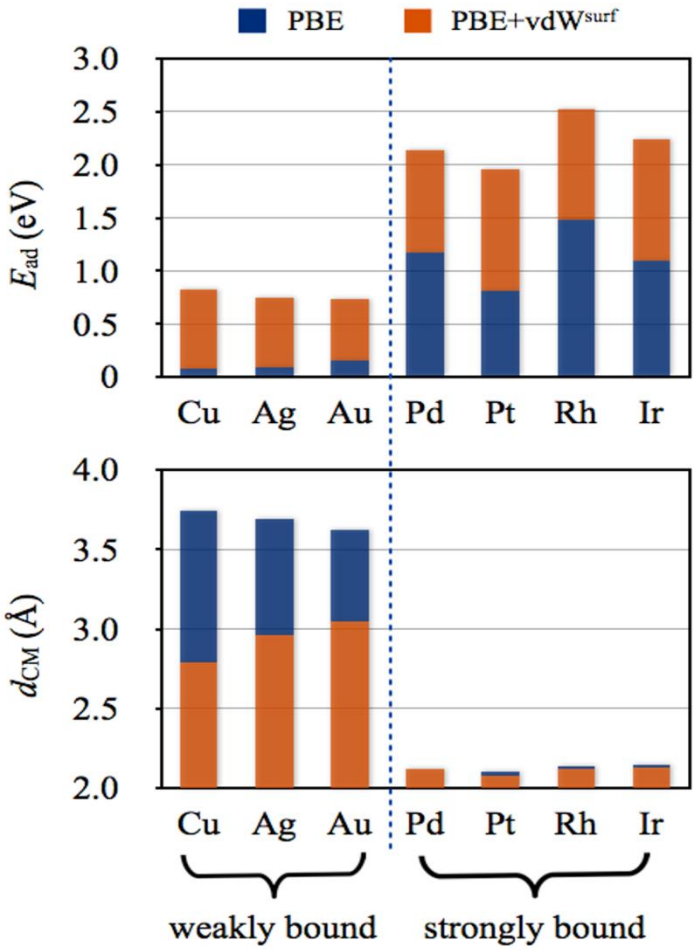

Figure 1. Adsorption energies E_{ad} (in eV) and the average distance between carbon and the first metal layer d_{CM} (in Å) for benzene (C_6H_6) on the (111) surfaces of Cu, Ag, Au, Pd, Pt, Rh, and Ir from pure PBE functional and vdW-inclusive PBE+vdW^{surf} methods [8].

In the last few years, substantial evidence has been accumulated suggesting that vdW interactions are not only important for the structure and stability of a multitude of systems. Other important static and dynamic properties, including reaction barriers, vibrational spectra, and elastic response are also largely affected by vdW interactions [8,9]. In particular, we have recently demonstrated that pairwise-additive vdW interactions can have a strong influence also on the electronic properties of HIOS, modifying workfunctions by up to 0.3 eV, and significantly altering charge transfer between organic molecules and inorganic substrates. The self-consistent inclusion of vdW interaction into DFT exchange-correlation functionals also leads to much better agreement of calculated workfunctions of surfaces with and without organic adsorbates with reliable experimental references [8]. Therefore, accurate first-principles predictions of electronic properties of HIOS require a fully self-consistent treatment of vdW interactions.

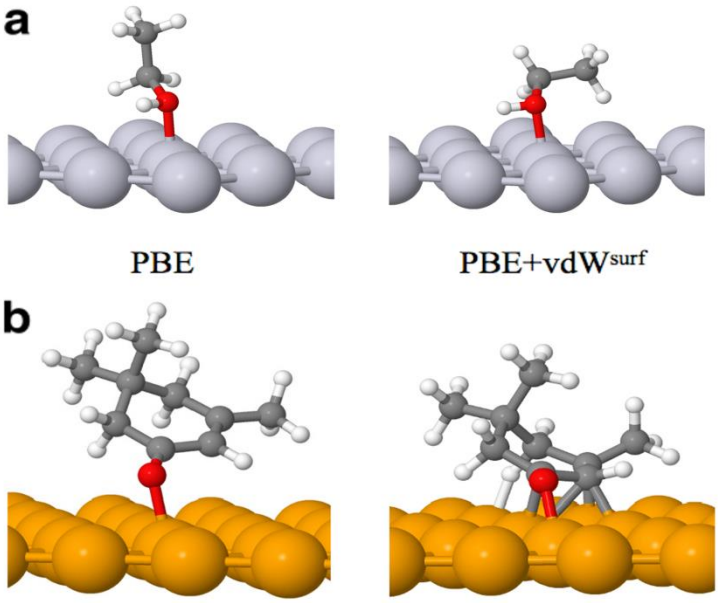

Figure 2. Most stable adsorption structures of ethanol (C_2H_5OH) at Pt(111) (a) and of isophorone ($C_9H_{14}O$) at the Pd(111) surface (b) optimized by pure PBE and PBE+vdW^{surf} methods. Gray, white, red, light gray, and yellow represent C, H, O, Pt, and Pd atoms, respectively. See Ref. [8] for more details.

Our studies have also shown that the widely employed pairwise-additive treatment of vdW interactions is sometimes insufficient for reliable predictions of properties in large inhomogeneous systems, such as most HIOS [10,12,13]. This realization lead us to develop the so-called DFT+MBD method that models vdW interactions in an explicit many-body fashion, where the dipolar correlations of a given system are captured to infinite order [12,13,14]. A schematic description of the MBD method is shown in Figure 3. DFT+MBD calculations have allowed us to identify a wealth of novel phenomena in complex materials, for example revising our understanding of stability and mobility of point defects in semiconductors [15], and predict the appearance of hybrid terahertz (THz) modes coupling plasmonic and phononic excitations at finite temperature in the aspirin crystal [16]. Our preliminary work on applying the DFT+MBD method to HIOS indicates that we are able to achieve quantitative accuracy in the modeling of the structure and adsorption energies of organic molecules on metal surfaces.

For large organic molecules and their oligomers of interest in the CRC 951, vdW interactions often constitute the largest contribution to the molecule¯surface potential upon adsorption on an inorganic substrate (ZnO, Si, or Ge). A rough estimate is that vdW interactions contribute about ~ 1 eV per benzene ring for an organic molecule interacting with a semiconductor surface. This is clearly a substantial contribution which, for large enough molecules, can amount to adsorption energies even larger than typical covalent bonds. Furthermore, the intricate coupling between the localized electronic states of the organic layer and the substrate electronic bands also leads to the emergence of non-trivial many-body correlations that can be further understood by analyzing the collective plasmon-like dipolar excitations obtained from the DFT+MBD calculations. Since the vdW contribution to the total energy can exceed a few eV for large molecules, vdW effects fall within the energy scale of many relevant phenomena of interest in HIOS, such as optical excitations and exciton formation. However, our understanding of these effects is only starting to be developed.

Since efficient many-body methods for vdW interactions have been developed only recently, very little is currently known about the non-trivial contributions of many-body vdW effects to the structural and energetic properties of HIOS. However, the role of many-body interactions on vibrational, electronic, and optical properties is even less well understood. A complete understanding of the structure and energetic properties demands a fully self-consistent implementation of the DFT+MBD method, which will require deriving the MBD potential (functional derivative of the MBD energy with respect to the electron density). The calculation of optical and non-linear vibrational properties (e.g., measured in project B5 (*Wörner/Elsässer*)) will require to go further to the implementation of the MBD kernel (second functional derivative of the MBD energy). These are some of the very challenging goals that we aim to address in this proposal. These developments will be largely complementary to other theoretical efforts and the experimental measurements carried out

within CRC 951.

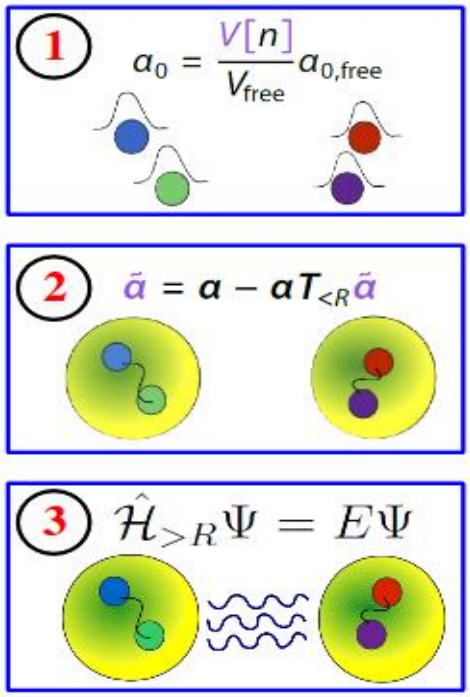

Figure 3. Schematic diagram illustrating the computation of the long-range vdW correlation energy *via* the MBD method. The first step is to map the response of realistic material to a system of atomic response functions (ARFs) by using its electron density, computed using semilocal DFT. The second step is to account for short-range many-body screening effects that are crucial in condensed materials by solving the Dyson-like response equation with a short-range potential. The final step is to couple the ARFs by a long-range dipole potential and solve the Schrödinger equation for coupled ARFs. See Ref. [13] for further details.

References

[1] D. Langbein, *Theory of van der Waals Attraction* (Tracts in Modern Physics vol 72) (Berlin: Springer, 1974)
[2] V. A. Parsegian, *van der Waals Forces: A Handbook for Biologists, Chemists, Engineers and Physicists* (Cambridge: Cambridge University Press, 2005)
[3] J. F. Dobson and T. Gould, J. Phys.: Condens. Matter **24**, 073201 (2012).
[4] T. Thonhauser, V. R. Cooper, S. Li, A. Puzder, P. Hyldgaard, and D. C. Langreth, Phys. Rev. B **76**, 125112 (2007).
[5] M. Mura, A. Gulans, T. Thonhauser, and L. Kantorovich, Phys. Chem. Chem. Phys. **12**, 4759 (2010).
[6] E. Bremond, N. Golubev, S. N. Steinmann, and C. Corminboeuf, J. Chem. Phys. **140**, 18A516 (2014).
[7] V. Blum, R. Gehrke, F. Hanke, P. Havu, V. Havu, X. Ren, K. Reuter, and M. Scheffler, Comput. Phys. Commun. **180**, 2175 (2009).

3.3.2 Project-related publications

[8] W. Liu, A. Tkatchenko, and M. Scheffler, Acc. Chem. Res. (2014); dx.doi.org/10.1021/ar500118y.
[9] L. Kronik and A. Tkatchenko, Acc. Chem. Res. (2014); dx.doi.org/10.1021/ar500144s.
[10] A. Tkatchenko, “Current Understanding of van der Waals Effects in Realistic Materials”, Adv. Func. Mat. (2014), in press.
[11] A. Tkatchenko, L. Romaner, O. T. Hofmann, E. Zojer, C. Ambrosch-Draxl, and M. Scheffler, MRS Bulletin **35**, 435 (2010).
[12] A. Tkatchenko, R. A. DiStasio Jr., R. Car, and M. Scheffler, Phys. Rev. Lett. **108**, 236402 (2012).
[13] A. Ambrosetti, A. M. Reilly, R. A. DiStasio Jr., and A. Tkatchenko, J. Chem. Phys. **140**, 18A508 (2014).
[14] R. A. DiStasio Jr., V. V. Gobre, and A. Tkatchenko, J. Phys.: Condens. Matter **26**, 213202 (2014).
[15] W. Gao and A. Tkatchenko, Phys. Rev. Lett. **111**, 045501 (2013).
[16] A. M. Reilly and A. Tkatchenko, Phys. Rev. Lett. **113**, 055701 (2014).
[17] A. Tkatchenko and M. Scheffler, Phys. Rev. Lett. **102**, 073005 (2009).

[18] V. G. Ruiz, W. Liu, E. Zojer, M. Scheffler, and A. Tkatchenko, Phys. Rev. Lett. **108**, 146103 (2012).
[19] N. Ferri, R. A. DiStasio Jr., A. Ambrosetti, R. Car, M. Scheffler, and A. Tkatchenko, "*Electronic Properties of Molecules and Surfaces with a Self-Consistent Interatomic van der Waals Density Functional*", to be submitted to Phys. Rev. Lett.

3.4 Research plan

The proposed research can be divided into two parts: (i) the derivation and implementation of a self-consistent DFT+MBD functional into electronic structure codes, (ii) Application of the DFT+MBD method to HIOS. These two parts are largely complementary, since applications and developments will benefit from each other. In addition, applications can be started immediately since an *a posteriori* version of DFT+MBD is already fully implemented. Two PhD students will be employed to carry out the proposed research, and it is planned that both students will strongly collaborate with each other, and with other students and researchers within the CRC.

Workpackage 1 (WP1, PhD student 1): Derivation and implementation of self-consistent DFT+MBD functional

It is well known that vdW interactions are quantum-mechanical phenomena that arise from correlated electron density fluctuations in molecules and materials. To move beyond the traditionally employed second-order pairwise additive approximations, our group has recently developed the so-called MBD (many-body dispersion) method [12,13,14]. The essential idea of the MBD method is to map the response of a given nucleoelectronic system into an auxiliary system of coupled atomic response functions (ARF), by using the Tkatchenko-Scheffler (TS) prescription to determine the parameters of the ARFs from the electron density (see Figure 3) [17]. In the TS method, the vdW parameters are functionals of the electron density $n(\mathbf{r})$, hence they respond to changes in the electron density induced by hybridization, static charge transfer, and other electron redistribution processes. The MBD method has been already implemented in several computer codes and has been mainly applied to small and large molecular systems. Applications of DFT+MBD to surfaces and adsorption are still missing, but are expected to be most interesting from scientific perspective.

By using the DFT+MBD method or approximations thereof, we have demonstrated that vdW interactions can have large contributions in the structure, stability, vibrational, elastic, and electronic properties of large realistic systems. However, it has also become apparent that one needs to go beyond an *a posteriori* treatment of vdW interactions, where the vdW energy is simply added to the DFT energy after the self-consistent Kohn-Sham calculation has been finished. We here propose to derive and implement a fully self-consistent DFT+MBD method, where the potential $V_{MBD}[n(\mathbf{r})]$ is added to the Kohn-Sham exchange-correlation potential and the DFT+MBD energy is obtained as a result of a fully self-consistent calculation. The $V_{MBD}[n(\mathbf{r})]$ potential is calculated as,

$$V_{\mathrm{MBD}}[n(\mathbf{r})] = \frac{\delta E_{\mathrm{MBD}}[n(\mathbf{r})]}{\delta n(\mathbf{r})}$$

Since the analytical expression for $E_{MBD}[n(\mathbf{r})]$ is quite involved, its functional derivative is not trivial. We have already carried out the derivation of MBD forces [13], and we will follow a similar strategy in this work, following the chain rule with respect to $n(\mathbf{r})$ akin to the force derivatives,

$$\mathbf{F}_{\mathrm{MBD}} = \frac{1}{2\pi}\int_0^\infty \mathrm{d}\omega\, \mathrm{Tr}\left[(\mathbf{1}-\mathbf{AT})^{-1}(\nabla\mathbf{AT})\right]$$

where $\mathbf{F}_{MBD}$ is the force (negative gradient of the energy), **A** is the polarizability matrix, **T** is the dipole interaction matrix (rows and columns refer to spatial positions **r** and **r'**), ω is the frequency of the electric field, and Tr is the double integral over **r** and **r'**.

The main challenge in the derivation and implementation of the self-consistent DFT+MBD functional consists in involved chain rules that have to be carried out to achieve full self-consistency (see three-step MBD procedure outlined in Figure 3). We have recently implemented a fully self-consistent version of the pairwise Tkatchenko-Scheffler density functional [19], and this implementation already contains several terms that will be utilized for the DFT+MBD implementation. The most time consuming part is finding a good

compromise between analytical simplification of MBD potential and its efficient numerical implementation. The computation of $V_{MBD}[n(\mathbf{r})]$ has to be done at every iteration of a self-consistent KS-DFT calculation. This can lead to substantial computational cost. Therefore, much of the effort will be dedicated to the numerical optimization of the MBD algorithm and the Hirshfeld partitioning used to define the dependence of V_{MBD} on $n(\mathbf{r})$. The efficient implementation of DFT+MBD is even more critical for enabling calculations on large periodic systems, such as HIOS.

The implementation of $V_{MBD}[n(\mathbf{r})]$ will enable fully self-consistent DFT+MBD calculations and assess the role of many-body vdW interactions on the electronic properties of HIOS. However, the calculations of spectroscopic and time-dependent properties of HIOS requires to go beyond the MBD potential and derive the MBD kernel,

$$K_{\mathrm{MBD}}[n(\mathbf{r}), n(\mathbf{r}')] = \frac{\delta^2 E_{\mathrm{MBD}}[n(\mathbf{r})]}{\delta n(\mathbf{r}) \delta n(\mathbf{r}')}$$

The derivation of the K_{MBD} kernel will allow us to efficiently calculate phonons, and infrared, THz, and Raman spectra by using density-functional perturbation theory (DFPT). It will also enable TDDFT calculations where the influence of many-body vdW interactions on dynamical electronic properties is fully included. This opens up an avenue for efficient calculations of linear and non-linear IR and THz spectroscopies of complex HIOS.

All the proposed developments will be implemented in the full-potential all-electron FHI-aims code [7]. The FHI-aims code is being developed at FHI, and already includes *a posteriori* implementations of DFT+TS and DFT+MBD methods, as well as the fully self-consistent DFT+TS method. The DFPT method has also been recently implemented in the FHI-aims code, enabling efficient integration with the MBD kernel.

The implementation of the K_{MBD} kernel will also allow us to carry out time-dependent DFT (TDDFT) simulations of non-linear spectroscopies, such as IR and THz, as well as optical absorption spectra. These calculations will be directly compared to experimental measurements in projects B5 (*Wörner/Elsässer)* and B9 (*Stähler*).

<u>Workpackage 2 (WP2, PhD student 2): Application of DFT+MBD to determine structure, stability, and static electronic properties of HIOS</u>

While non-self-consistent DFT+MBD method has been already applied to a wide variety of molecular materials, here we will extend its range of applications to HIOS. In fact, many-body effects in the vdW energy are expected to be most relevant in polarizable and inhomogeneous systems. Interfaces between organic and inorganic materials satisfy both of these requirements. Therefore, the first step will be to utilize the existing DFT+MBD implementation in FHI-aims and apply it to HIOS of interest in CRC 951. As inorganic substrates, we will consider Si, Ge, and ZnO. For the organic part, we will consider coronene, oligophenyls, pyridine, and oligofluorenes. This will allow us to study the effect of vdW interactions for molecules covering the entire visible spectral range for light emission and absorption. We will calculate the optimum structures and stabilities for single molecules, monolayers, and bilayers for all molecules of interest. Our main goal here is to understand the systematics of molecular adsorption on semiconductor surfaces. This will provide us with a reliable database of structures and energetics for HIOS, which can then be used as an input to develop effective potentials (force fields) in projects A7 (*Dzubiella/Klapp*). Our higher-level calculations can also be compared to pairwise vdW treatments in projects A4 (*Heimel*) and B4 (*Körzdörfer/Scheffler/Rinke*). One particularly important goal of these theory projects is to achieve a dynamical description of HIOS, and our calculations can serve as a benchmark of structures and energetics for static geometries. In fact, we will utilize structures obtained in other theoretical projects as a starting point for DFT+MBD optimizations.

After completing the derivation and implementation of $V_{MBD}[n(\mathbf{r})]$ in the first part of WP1, we will proceed to study the electronic properties of abovementioned HIOS. Our goal is to understand how the electron density, workfunctions, charge transfer, and interface level alignment are influenced when treating many-body vdW interactions in a fully self-consistent manner. Based on our preliminary results with self-consistent TS functional, we have considerable evidence that vdW interactions can play a large role when aiming at a quantitative description of electronic properties of molecule/metal interfaces. Building on this work, we expect similarly significant vdW effects in the electronic properties of molecule/semiconductor interfaces.

Workpackage 3 (WP3, Both PhD students): Application of DFT+MBD to dynamics and vibrational spectroscopy of HIOS

We have already demonstrated that many-body vdW interactions can lead to appearence of novel low-energy THz phonon modes in organic molecular crystals [16]. These modes arise from a subtle collective coupling between low-energy vibrations and neutral plasmonlike electronic excitations. Here, we aim to systematically investigate such collective coupling in HIOS. We will start by modeling thin films of organic material by building single crystals of organic molecules employed in CRC 951 (coronene, oligophenyls, pyridine, and oligofluorenes), and studying their linear and non-linear IR and THz spectra. These results will be compared with the experimental measurements in project B5 (*Wörner/Elsässer*). As a second step, we aim to understand how the bulk THz peaks depend on the thickness of the molecular layer on top of a semiconductor surface (Si, Ge, and ZnO). To achieve this goal, we will employ HIOS structures obtained in projects A7 (*Klapp/Dzubiella*) and B4 (*Körzdörfer/Rinke/Scheffler*).

Obviously, since many molecules of interest are rather flexible, thermal fluctuations can have an important role in the vibrational spectroscopy of HIOS. Our final goal in WP3 is to compute fully anharmonic spectra of HIOS by calculating autocorrelation functions from molecular dynamics trajectories with DFT+MBD method.

Workpackage 4 (WP4, Both PhD students): Development and application of DFT+MBD to HIOS based on doped ZnO

During the first funding period of CRC 951, highly-doped ZnO has emerged as a novel material exhibiting a range of interesting optoelectronic properties. However, achieving accurate and efficient theoretical treatment of doped ZnO remains a formidable challenge. Clearly, there are issues to be solved on different scales of hierarchical modeling.

The first issue is how to reliably describe the structure, stability, and electronic properties of HIOS based on doped ZnO as an inorganic material. Increasing the level of doping drives ZnO from being a semiconductor to exhibiting metallic properties. Treating vdW interactions between molecules and ZnO for different levels of doping requires assessing existing DFT+MBD method for vdW interactions and possibly extending it to be able to accurately treat localized and delocalized electronic fluctuations on equal footing. The key assumption behind the MBD method is the projection of valence excitations of real system to an auxiliary system composed of ARFs. We have assesed the validity of this approximation for many organic molecules and even narrow-gap semiconductors as Ge. However, metallic systems with delocalized single-particle excitations represent a challenge for the current implementation of MBD. A pragmatic solution would be to compute the dielectric function of highly-doped ZnO and renormalize the polarizability of Zn and O ions to match the solid dielectric response, as successfully demonstrated in Ref. [18]. However, here we aim to go beyond this simple approximation and extend the definition of polarizability in the MBD method to delocalized single-particle states. This may be achieved by utilizing information contained in the gradient of the electron density and/or the local kinetic energy density. This work can potentially lead to a new level of fundamental understanding of the connection between electron density and polarizability for systems characterized by increasingly delocalized electronic states.

The final step within WP4 will be to apply our developments to understand how the adsorption properties of molecules on ZnO depend on the degree of doping. In particular, we will calculate adsorption structures, stabilities and vibrational spectra and compare those to adsorption on pristine (undoped) ZnO, calculated in WP2. The results of our calculations will be compared to experimental measurements done in project A5 (*Henneberger*).

3.5 Role within the Collaborative Research Centre

As already stated above, vdW interactions are a crucial ingredient for the correct description of HIOS. Our project will provide improved understanding of these ubiquitous quantum-mechanical effects in complex HIOS. We will collaborate strongly with the project B5 (*Wörner/Elsässer*), by directly comparing our calculated linear and non-linear THz spectra with experimental measurements. Our developments for accurate calculations on doped ZnO can be (directly or indirectly) compared to experimental measurements done in A5 (*Henneberger*) and B9 (*Stähler*). Furthermore, we will provide reference data for vdW interactions in HIOS that will be used in theoretical projects B4 (*Körzdörfer/Rinke/Scheffler*), A7 (*Klapp/Dzubiella*), and A4 (*Heimel*). Our accurate calculations can be used to develop novel coarse-grained potentials that will have an immediate impact beyond the CRC to developments of improved effective potentials for molecules interacting with inorganic substrates.

Furthermore, to setup our DFT+MBD calculations, we will utilize the HIOS structures generated in projects A4, A7, and B4.

Obviously, there is a strong potential for important contributions of our research results and findings within the CRC.

3.6 Delineation from other funded projects of the principal investigator(s)

The proposed research is clearly delineated from all the other funded projects of the Pis.

(i) ERC StG „VDW-CMAT“ (EU): In this project, the first PI is developing improved methodologies for the treatment of vdW interactions in complex materials. Only static properties of molecular and solid state systems are addressed. In the CRC 591, we propose to study interfaces between molecules and solids and also extend our work to dynamic response properties. These subject are not covered by the ERC grant.

(ii) DFG grant „Chemical Compound Space“ (Germany): In this project, machine learning techniques are developed and applied for efficient prediction of molecular electronic properties. Therefore, no overlap exists with the current project.

(iii) DOE EFRC grant „IMASC“ (USA): In this grant we propose to apply first-principles calculations to understand and design new catalysts based on mesoporous nanomaterials. There is no overlap with the current proposal.

(iv) Einstein Foundation Berlin (Germany) – Einstein Research Project ETERNAL: Exploring Thermoelectric Properties of Novel Materials: In this grant, promising thermoelectric materials are identified from first principles. There is no overlap with the current proposal.

(v) DFG – German Research Foundation, Cluster of Excellence 314: Unifying Concepts in Catalysis (UniCat), coordinator: M. Driess; M. Scheffler - first funding period November 2007 - October 2012, new funding period until October 2017. There is no overlap with the current proposal.

(vi) NSF – The National Science Foundation, Partnership for International Research and Education (PIRE): Electron Chemistry and Catalysis, director: S. Scott; M. Scheffler - since 2005.There is no overlap with the current proposal.

(vii) Max Planck - EPFL Center for Molecular Nanoscience and Technology - Max Planck Society and the École Polytechnique Fédérale de Lausanne, directors: K. Kern, T. Rizzo; board members: B. Deveaud-Plédran, J. Hubbel, A. Wodtke, M. Scheffler - since 2013. There is no overlap with the current proposal.

(viii) Vetenskapsrådet – Swedish Research Council: “Catalysis on the atomic scale”, organizer: E. Lundgren; S. Levchenko, M. Scheffler - since 2011. There is no overlap with the current proposal.

3.7 Project funds

3.7.1 Previous funding

No previous funding has been received. This is a new application within CRC 951.

3.7.2 Funds requested

Funding for	2015/2		2016		2017		2018		2019/1	
Staff	Quantity	Sum	Quantity	Sum	Quantity	Sum	Quantity	Sum	Quantity	Sum
PhD student, 75%	2	44.100	2	88.200	2	88.200	2	88.200	2	44.100
Total		44100		88200		88200		88200		44100
Direct costs	Sum		Sum		Sum		Sum		Sum	
Other	2000		4000		4000		4000		2000	
Major research equipment	Sum		Sum		Sum		Sum		Sum	
€ 10.000 - 50.000	0		0		0		0		0	
> € 50.000	0		0		0		0		0	
Total	0		0		0		0		0	
Total	46100		92200		92200		92200		46100	

(All figures in Euro)

3.7.3 Staff

	No.	Name, academic degree, position	Field of research	Department of university or non-university institution	Commitment in hours/week	Category	Funded through:
Available							
Research staff	1	Alexandre Tkatchenko, Dr., PI	Theoretical physics	Frtiz-Haber-Institut der MPG	10		MPG/ ERC
	2	Matthias Scheffler, Prof. Dr., PI	Theoretical physics	Frtiz-Haber-Institut der MPG	5		MPG
Non-research staff							
Requested							
Research staff	1	Johannes Hoja, M.Sc., PhD student	Theoretical chemistry	Frtiz-Haber-Institut der MPG		PhD student	
	2	N.N, M.Sc. PhD student	Theoretical physics	Frtiz-Haber-Institut der MPG		PhD student	
Non-research staff							

Job description of staff (supported through available funds):

1. Alexandre Tkatchenko
The PI will coordinate all organizational and scientific matters of the project and will provide direct mentoring to the two Ph.D. students. This involves introducing them to the subject matter of HIOS, to scientific computing, to first-principles electronic structure theory and many-body methods in general, and to the techniques required for project A10 in particular. Furthermore, the PI will provide guidance in performing scientific research as well as in its presentation and publication.

2. Matthias Scheffler
The PI will aid in organizational and scientific matters of the project. Regular meetings will be scheduled with the first PI and the two PhD students to discuss progress and decide on future research directions.

Job description of staff (requested):
3. Johannes Hoja
Johannes Hoja will be responsible for the derivation and implementation of the fully self-consistent DFT+MBD method, including the potential and kernel of the MBD energy. Since these developments will be time consuming, Johannes will also participate in applying the existing implementation of a non-self-consistent DFT+MBD method to study vibrational spectroscopy (infrared and THz response) of HIOS. The results obtained will be directly compared to the experimental measurements in project B5.

4. N.N.
This student will carry out DFT+MBD calculations to study structure, stability, and electronic properties of HIOS. He will assemble a database of accurate structures and stabilities of HIOS to be used as input for other theoretical projects (A4, A7, B4). He/she will collaborate with Johannes Hoja on vibrational spectroscopy of HIOS. Finally, the student will also derive and implement the extension of the DFT+MBD method for highly-doped ZnO surfaces.

3.7.4 Direct costs

	2015/2	2016	2017	2018	2019/1
Funds available	2000	4000	4000	4000	2000
Funds requested	2000	4000	4000	4000	2000

(All figures in Euro)

3.7.5 Major research equipment requested

No major equipment is requested. All calculations will be carried out on available computer clusers at FHI (more than 2,000 cores), and at Max Planck supercomputer facilities in Garching (~ 10,000 cores)

3.1 About project A11

3.1.1 Title: Interface-dominated hybrid 3D nano-architectures with tailored opto-electronic properties

3.1.2 Research areas: 307-01 Experimentelle Physik der kondensierten Materie

3.1.3 Principal investigator

Christiansen, Silke, Prof. Dr., 22.04.1966, German
Helmholtz-Zentrum Berlin für Materialien und Energie
Hahn-Meitner-Platz 1
14109 Berlin
+491796894182
Phone: +49 (0)1796894182
E-mail: silke.christiansen@helmholtz-berlin.de

Do the above mentioned persons hold fixed-term positions? no

3.2 Summary

During the first funding period of the CRC 951, detailed knowledge about the properties and interactions of two-dimensional (2D) semiconductor-based HIOS was obtained. For planar systems, mainly with ZnO as an inorganic component in combination with a variety of organic materials for different HIOS approaches, detailed methods to tune the band alignment, simulate and test charge transport and transfer processes were successfully developed and implemented. To further expand possible HIOS systems, the proposed project A11 aims at the transfer of the existing expertise in 2D ZnO layers and patterned coinage metal layers to ***new inorganic materials***, namely differently doped silicon (Si) and gallium nitride (GaN) as well as metallic nano-particles, preferably arranged in ***three-dimensional*** (3D) ***HIOS nano-architectures***. On the organic side ***conjugated polymers*** such as oligothiophenes and oligofluorenes as well as energy and interface adapted molecules will be explored for the novel inorganic constituents. Furthermore, the integration and evaluation of ***2D- and 3D HIOS*** in ***functional opto-electronic devices*** is envisaged.
One of the main tasks of A11 will be the design and fabrication of the aforementioned inorganic constituents and their arrangement with organics in well determined composite 3D HIOS nano-architectures that promise enhanced functionality through three-dimensionality and the organic-inorganic interface tuning. The inherently enlarged interfacial area and the great number of crystal facets in crystalline, inorganic 3D nano-structures in contact with organic materials are critical for the successful application of HIOS in devices. Consequently, they need to be understood and thus investigated systematically by the CRC to answer many open questions of great scientific interest. In this context, designed 3D nano-architectures will be optimized with respect to photonic and plasmonic mode generation to amplify the coupling between organic and inorganic materials. To realize these sophisticated 3D HIOS, a ***powerful infrastructure*** of top-down and bottom-up ***nano-patterning*** and ***deposition techniques*** is available. Using a versatile combination of ***advanced electrical, optical, compositional*** and ***structural analysis techniques*** fundamental processes such as e.g. charge transport, optical absorption and emission as well as band alignment in planar 2D references and ultimately of nano-structured composite HIOS will be investigated. The thereby gained knowledge will be applied to materials and ultimately device ***testing*** in an integrated ***device environment***. It is a primary goal of A11 to validate that HIOS findings can be adapted to functional systems and to point out ways to ***exploit hybrid materials in applications***.
In ***cooperation*** with other ***HIOS projects*** the knowledge acquired in the first funding period for ZnO based HIOS will be used to choose and design molecular groups and polymers that can chemically be attached to A11's novel material classes and permit ***efficient charge transfer*** at the ***hybrid interfaces***. As a sensitive monitor for the properties of hybrid interfaces, ***two-dimensional HIOS diodes*** based on GaN and Si will be studied in detail. Correlated optical and electrical studies on these devices will reveal the crucial physical properties of the interface and how interfaces determine charge transport processes and, thus, the performance of the test devices. In this regard, one research focus will reside on the examination of the ***actual band alignment*** in a device environment at HIOS interfaces, which can be ***tuned*** by ***different polymers*** with their respective doping strength and by ***deliberately designed molecules*** as interlayers

forming additional interfacial dipoles. A11 aims at realizing ***extreme band-line up conditions***, and in particular an ***inversion layer formation*** at the inorganic material surfaces of differently doped n- and p-type inorganic semiconductors. To reach this goal additional band ***matching*** of ***contact layers*** for the different HIOS will be an important additional development task. Furthermore, the ***stability*** of the ***HIOS interfaces*** and ***surfaces*** is crucial. ***Degradation mechanisms***, like oxidation of the inorganic semiconductor or the light soaking induced degradation of the organic component, will have an immense effect on band alignment and electrical transport properties. It is one of the goals of A11 to ***chemically stabilize*** the Si and GaN surfaces by ***specifically selected molecules*** or ***inorganic, atomically thin layers***. Complementing the 2D reference structures, and exploiting the achievements of collaborators in the CRC on the novel nano-structured materials, ***3D HIOS devices*** will be investigated. Large aspect ratios creating huge interfaces and the opportunity to address specially chosen facets make 3D nano-architectures an even better monitor for opto-electronic properties and stability optimization. This calls for the development of ***(crystal face-) selective binding of*** self-assembled monolayer ***interface modification agents***, which is jointly targeted together with various other projects of the current CRC. One of the prime challenges will be to assess and consequently control the opto-electronic properties of these 3D HIOS at the nanoscale. To tackle these challenges the use of ***in-situ nano-manipulation*** and ***nano-probing*** in combination with ***correlated microscopy/spectroscopy techniques*** will permit opto-electrical readout even of individual functional nano-HIOS as well as microscopic and macroscopic hybrid devices.

3.3 Research rationale

3.3.1 Current state of understanding and preliminary work

Application of hybrid inorganic-organic interfaces in functional devices

The discovery of conductive molecules and polymers in 1977[1] initiated the exciting new research area of organic electronics. Closely related, the field of hybrid inorganic-organic opto-electronic devices emerged, attempting the successful combination of advantages of both material classes such as the cheap and easy fabrication of organics and superior electronic properties of inorganics. Soon after, charge selective interfaces have been demonstrated in different hybrid systems[2]. The synergy of organics and inorganics has been proven to work for rectifying contacts, light emitting diodes and photovoltaic cells. In all of these hybrid device configurations it is possible to utilize the organic component as the active device material and the inorganic part as a charge carrier extraction layer or vice versa. Even the well-known dye sensitized solar cells[3] as well as the incredibly successful perovskite devices[4] rely on a hybrid interface for carrier extraction. While there are different approaches to hybrid opto-electronic applications, often a common inorganic such as an established semiconductor is used in combination with conductive polythiophenes or polyfluorenes. A few examples for applications are:

- ***Rectifying diodes*** combining poly(3-hexylthiophene) (P3HT) with inorganic semiconductors such as TiO2, Si, CdSe or ZnO[5]
- ***Hybrid light emitting diodes*** with poly(9,9-dioctylfluorene-co-9,9-di(4-methoxy) phenylfluorene) (F8DP) and oxidic inorganic extraction layers[6] or in a layer stack with InGaN[7].
- ***Photovoltaic devices*** with inorganic absorbers like Si and highly doped ‘metallic’ poly(3,4-ethylene-dioxythiophene):poly(styrenesulfonate) (PEDOT:PSS) [21] or GaAs and P3HT[8]

Only few mechanisms of these hybrid devices ruled by their inorganic-organic interfaces are fully understood yet, since a lot of parameters critically influence the behavior of any HIOS. In the first funding period, CRC 951 groups (B3, A8) have already shown essentially for ZnO surfaces how heavily the band alignment at the interface as well as the charge transfer of the excitons depends on either the electronic coupling strength of physisorbed molecules or electronic hybridization for chemisorbed molecules.[9] However, up to now in most cases it is not even clear if the organic material is physisorbed or chemisorbed on the semiconductor surface and how this influences charge separation and transport. Also, it is still a question how loss mechanisms such as surface defects or oxidization of the inorganic component and degradation of the organics influence these processes. In this sense the band alignment as well as optical and electrical properties, especially of new HIOS are basically unknown.

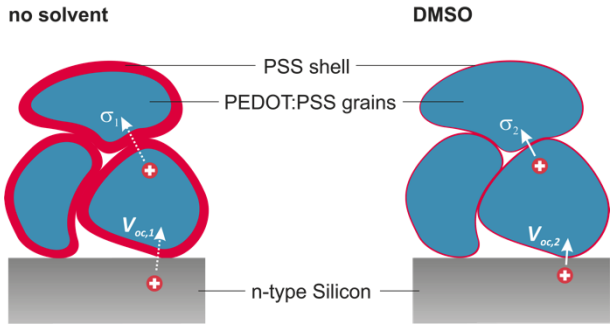

Figure 1 Schematic demonstrating hole transport in PEDOT:PSS layers on a Si substrate surface with and without the solvent DMSO. The charge transport (condutivity σ) well as the charge carrier separation (Voc) is limited by the PSS barrier.[22]

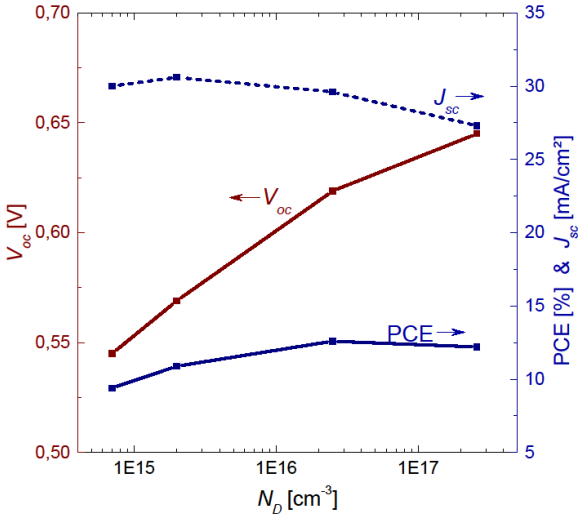

Figure 2 Dependence of n-Si/PEDOT:PSS solar cell device parameters for different substrate doping levels contradicting a Schottky junction formation indicating minority carrier dominated transport mechanism.[21]

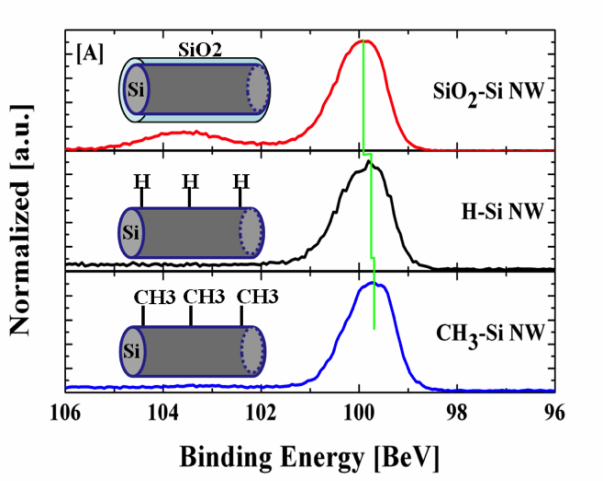

Figure 3 Si2p window of XPS survey for SiO2–Si, H–Si and CH3–Si nanowires. The vertical solid green line indicated a shift of the difference between valence band and Fermi level at the surface with different passivation. [23]

For HIOS consisting of the strong hole conducter PEDOT:PSS and n-type silicon we were able to show that the concentration of the solvent in the polymer as well as the doping of the inorganic semiconductor critically influence the system performance and can be used as a monitor to explain band energy alignments dominated by details of the interface layout. The variation of the DMSO concentration in PEDOT:PSS unveils that charge separation and transport in this HIOS is largely dominated by an insulating PSS shell around conductive PEDOT:PSS grains.[22] Monitoring the electrical properties of n-Si/PEDOT:PSS devices depending on doping concentration of the n-Si substrate showed that the charge transport is not dominated by Schottky injection of majority carriers as commonly assumed and that the defects at the Si surface are not controlling the barrier formation.[21] Nevertheless, it is still unclear if the promising device characteristics originate from actual chemical bond formation at the hybrid interface. Likewise it is yet unknown how to stabilize this system against the fast degradation of a still to be identified mechansim. Specifically selected organic molecules can additionally be attached to the Si surfaces to alter the band alignment by surface dipoles, enhance charge transport or stabilize the interface. We have shown that the large surface area of Si nanowires can be covered by chemisorbed alkyl molecules stabilizing the inorganic surface against oxidation while maintaining a reliable passivation of surface defects comparable to hydrogen termination[23] Moreover, the surface passivation with alkyl type molecules permits a tuning of the band alignment, since for instance the chemisorbed methyl group creates a negative dipole on the Si surface.

Fabrication, Characterization and Implementation of Si und GaN micro-rods and nanowires

Since HIOS are mainly dominated by their interfaces, 3-D nano-architectures are an ideal testing structure for their properties. The project A11 will focus on arrays of nanowires as well as individual ones of group IV semiconductor type such as Si and of group III-nitride type such as (In)GaN with changeable size (lengths, diameter, aspect-ratio), shape (rods, cones and inverted cones) and assembly (arrangement, pitch, disorder parameter, and other controllable variables). There are different techniques for the fabrication of Si and GaN based microrods and nanowires. They can be grown bottom up by metal-particle [24] or self-catalyzed vapor-liquid-solid (VLS) processes[20] or by top down shadow mask assisted wet[23] and dry etching[18,25,26] processes using large area compatible nanolithography with spheres, imprint or metal particles for masking.
Nanowires with diameters on the order of visible wavelengths show strong resonant field enhancements of incident light. The scattering and absorption of these photonic nanostructures can be described by full analytic solution of Maxwell's equations for plane wave incidence analog to Mie theory. [24] Depending on the shape and faceting these resonances can also be excited and trapped insight a nano-architecture. It was shown by the PI that by using a self-catalyzed metal-organic vapor-phase epitaxy (MOVPE) hexagonal GaN nano- and micro-rods with smooth side wall facets can be grown.[18] Cathodo- and micro-photoluminescence measurments carried out on single GaN rods showed whispering gallery modes (WGMs) with quality factors greater than 4000 demonstrating the high morphological and optical quality of the material. It is worth noting, that there is quite a vivid community seeking optical reed out concepts for highly responsive sensing of even individual molecules via the detection of WGM shifts upon molecule attachments on usually dielectric microparticles, which reproducibly permit ad- and desorbing of molecules[10]. First results suggest that the different facets of highly regular GaN micro- and microrods can serve as well as an accessible monitor for HIOS through molecule attachment at side wall facets. The surface of individual semiconductor microrods

and nanowires can also be characterized by micro-Raman. We were able to show that by controlled roughening of the surface of GaN microrods with InGaN/GaN multi-quantum wells (MQW) that constitute the active component of a light emitting diode (LED) the occurrence of surface optical phonon modes can be measured and tuned without affecting the strain states and quantum well peak position[25]. It is still a intriguing question how these surface-tailored microrod LEDs change their emission properties and carrier lifetimes when being decorated at their surfaces with organic molecules.

Using the combination of nanosphere lithography (NSL) surface masking and subsequent reactive ion etching (RIE), it is also possible to fabricate homogeneous arrays of regular microrods and nanowires on large areas.[18] Even on substrates with defects such as multi-crystalline thin film silicon layers or GaN epitaxial layers on lattice mismatched sapphire substrates, microrods or nanowires can be created with entirely predetermined shapes including lengths, diameters, lattice constants, and showing straight sidewalls independently of their crystalline orientation. These wire or rod arrays show a large surface-to-volume ratio with the advantage that the properties of the surfaces or interface become increasingly important and can even dominate bulk properties in respective measurements. For instance the detectability of methyl-bonds on the Si surface using x-ray photo-electron spectroscopy (XPS) for is considerably better for a surface with wires or rods.[23] In addition not only structures but even functional devices with 3D-HIOS can be fabricated, e.g. PEDOT:PSS layers on Si rod or wire surfaces.[11] Even more than on planar devices the crucial mechanisms, e.g. charge transport and separation at the organic-inorganic hybrid interface, interfacial charge recombination losses and hybrid interface stability are not understood yet and are therefore subject to intense research.

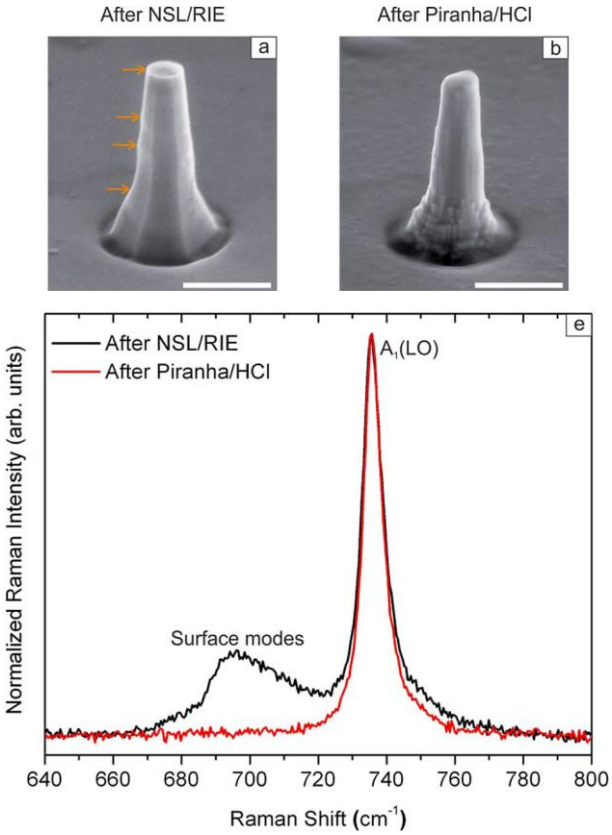

Figure 4 (Top) SEM images of the same extended defect-free nano-LED after combined nano-sphere lithography masking and reactive ion etching and and subsequent piranha/HCl surface layer removal. The arrows highlight the homogeneous surface modulation / faceting at the nanoscale initiating the surface optical phonon modes in the lower graph (black line). These SO modes disappear when the microrod LED surface becomes inhomogeneously rough (red line). The scale bars are 500 nm.[25]

Besides large arrays of nanostructures and their characterization in functional devices, in-situ nano-manipulation and nano-probing in combination with correlated electron microscopy/spectroscopy techniques provide for opto-electrical parameter read-out even of individual functional nano-objects (cf. Fig. 5). Therewith, we were able to study an individual Si nanowire diode, asses its current-voltage (I-V) characteristics in the dark and under controlled illumination (defined and tunable wavelength and power) in a scanning-electron microscope (SEM) and correlate these results with TCAD device simulations.[26] Novel, soft SEM imaging techniques that do not alter or destroy organic materials[12] promise the possibility to prepare and measure single hybrid nanostructures in the same manner.

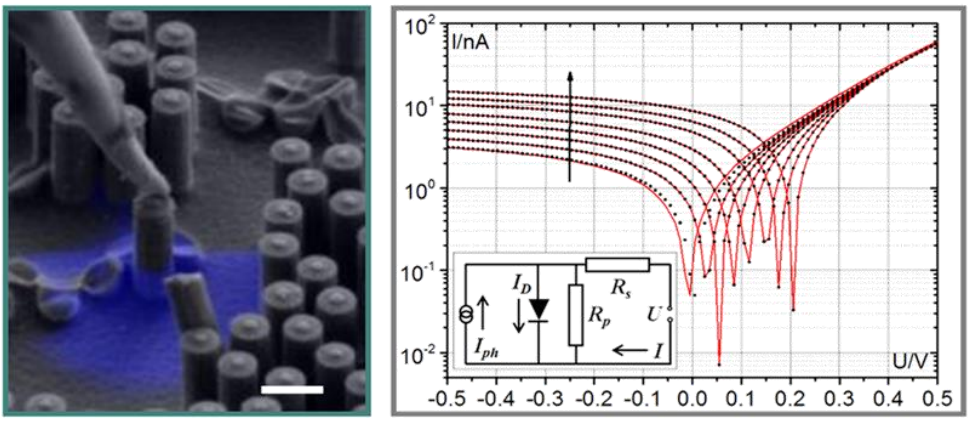

Figure 5 [26] (left) SEM image of an individually contacted Si nanowire (tilted view - 45° tilt angle). A current mapping is superimposed in blue color (scale bar 1 mm). The current is generated through electron beam induced carriers. (right) I–V curves of the single diode under illumination with 700 nm laser light at different power between 500 nWatt and 1900 nWatt.

Here, HIOS devices will be used to further advance these microscopy / spectroscopy techniques for this type of irradiation sensitive materials.

Three-dimensional plasmonic nanostructures

For the most efficient applications of HIOS some device concepts require the management and guidance of incident light to be converted into free charge carriers. In this respect, metals, especially coinage metals, play a particularly important role since their free electron gas oscillations can show a strongly resonant behavior when being excited by visible light. Such material and geometry dependent resonances, called plasmon-polaritons, provide for extreme evanescent light localization as well as for efficient (and if needed directed) scattering. Therewith, fundamental processes dominating HIOS-devices can be improved, since plasmonic structures can provide for (1) increased optical excitation rates, (2) modified radiative and non-radiative decay rates, and (3) altered emission directionality[13]. The tuning of these resonant phenomena by proper choice of the functional metals (e.g. gold, silver, copper or aluminum) and a specially designed geometry delivers the necessary degrees of freedom for spectrally matching in principle any organic/inorganic coupling. While the plasmonic enhancement and coupling to organic molecules has been shown with one dimensional and planar structures during the first funding period by (A6,B6), 3D geometries of plasmonic nanostructures give the opportunity to realize more directional emission, tailored light concentration and even modification of the polarization state of light via optical rotation in chiral nano-objects and, thus, enhancing the chiro-optical response of chiral molecules.[14]

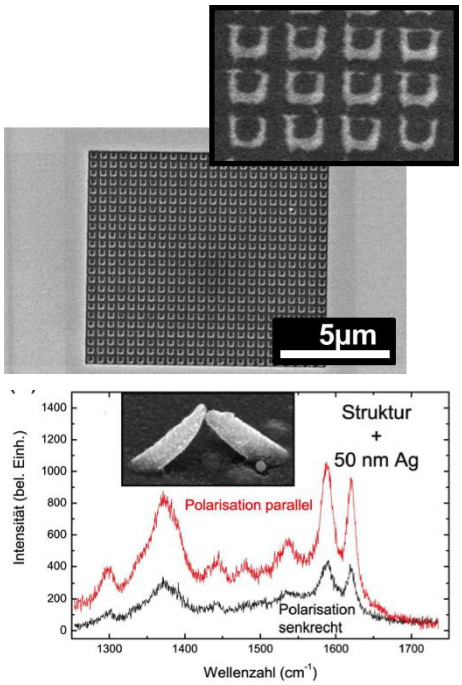

Figure 6 (upper) SEM micro-graphs of aluminum split-ring arrays on a Si wafer substrate [19], (lower) Raman spectra of methyl violet on a pre-patterned Si wafer with EBID antennas coated with 5 nm silver for a polarization along (red) and perpendicular to (black) the dimer axis[27]

3D plasmonic nanostructures can be fabricated by a variety of dedicated top-down and bottom-up techniques and combined methods available for A11. For instance electron beam lithography was used to fabricate an array of aluminum split-ring resonators, showing their tunable coupling to typical vibrational modes of graphene.[19] Furthermore, core-shell dimer nano-antennas were fabricated by direct writing using the electron beam induced deposition (EBID) that relies on electron beam induced cracking of precursor molecules which are locally inserted into the vacuum chamber of an SEM. For plasmonic activation such EBID deposits were subsequently coated with silver such that these dimer antennas showed polarization dependent hot-spots efficiently exciting typical molecular vibrations in the model dye methyl violet.[27] Although complex 3D-nanostructures are already realized by EBID, their coupling to possible organic emitters still has to be demonstrated. Concerning 3D patterning, a very promising technique to be further explored is the precise structuring and deposition using not only conventional focused gallium ion beams, which are not competitive to electrons in terms of resolution and irradiation damage, but also smaller and lighter focused ion beams of helium or neon ions. In this context, imaging with helium ions shows also the advantage of inducing less beam damage in organic materials such as P3HT/PCBM blends[12] in comparison to heavier ions and in particular to electrons while guaranteeing highest imaging performance. Using the combination of imaging and material modification capacities, novel ion microscopy tools can help to answer urgent questions of morphology and structure properties across HIOS interfaces and devices. Ion beam milling of HIOS structures permits in addition the preparation of free-standing lamellae and thus opens the opportunity to study these interfaces even in low voltage transmission electron microscopy and analytics. The proposed project will make such tools accessible for the HIOS consortium to precisely create and modify new hybrid material classes on the nanoscale.

Another option to sensitively tune hybrid interactions at HIOS interfaces are dedicated arrangement of plasmonic building blocks as meta-atoms in two- or three-dimensional functional geometries, called metamaterials in general and hyperbolic metamaterials (HMM) for 2D layered systems. Hyperbolic metamaterials belong to the anisotropic metamaterials showing metallic behavior in-plane ($\varepsilon\parallel < 0$) and strong dielectric behavior out of plane ($\varepsilon\perp < 0$) or vice versa.[15] Such indefinite permittivities can result in enhanced spontaneous emission rates of quantum emitters, like dye molecules.[16] The thereby realized huge Purcell factors render them interesting for design and investigation of HIOS. Besides the strongly increased photonic density of states providing a diverging number of radiative decay channels, the strongly anisotropic HMMs give rise to emission of photons in a preferred direction. Thus, collection efficiencies of single emitters can be dramatically increased.[17]

References

[68] H. Shirakawa, E. J. Louis, A. G. MacDiarmid, C. K. Chiang and A. J. Heeger, J. Chem. Soc., Chem. Commun., 578-580 (1977)
[69] M. Ozaki, D. L. Peebles, B. R. Weinberger, C. K. Chiang, S. C. Gau, A. J. Heeger, and A. G. MacDiarmid, Appl. Phys. Lett. **35,** 1 (1979)
[70] B. O'Regan, and M. Grätzel, Nature **353**, 737 - 740 (1991)
[71] M. Liu, M. B. Johnston, and H. J. Snaith, Nature **501,** 395 (2013)
[72] T. Xu, Q. Qiao, Energy Environ. Sci., **4**, 2700 (2011)
[73] N. Tokmoldin, N. Griffiths, D. D. C. Bradley, and S. A. Haque, Adv. Mater. **21**, 3475 (2009)
[74] C. Zhang, and A. J. Heeger, J. Appl. Phys. **84**, 1579 (1998)
[75] J.-J. Chao, S.-C. Shiu, C.-F. Lin, Solar Energy Materials & Solar Cells **105**, 40 (2012)
[76] S. Blumstengel, H. Glowatzki, S. Sadofev, N. Koch, S. Kowarik, J.P. Rabe, and F. Henneberger, Phys. Chem. Chem. Phys., **12**, 11642 (2010)
[77] F. Vollmer, D. Braun, A. Libchaber, M. Khoshsima, I. Teraoka, and S. Arnold, Appl. Phys. Lett., **80**, 21, 4057 (2002)
[78] S. Jeong, E. C. Garnett, S. Wang, Z. Yu, S. Fan, M. L. Brongersma, M. D. McGehee, and Yi Cui, Nano Lett. **12**, 2971 (2012)
[79] A. J. Pearson, S. A. Boden, D. M. Bagnall, D. G. Lidzey, and C. Rodenburg, Nano Lett. **11**, 4275 (2011)
[80] J. A. Schuller, Nat. Materials **9**, 193 (2010)
[81] V. K. Valev, J. J. Baumberg, C. Sibilia, and T. Verbiest, Advanced Materials **25**, 2517 (2013)
[82] A. Poddubny, I. Iorsh, P. Belov and Y. Kivshar, Nature photonics, **7** (2013)
[83] K. V. Sreekanth, K. H. Krishna, A. De Luca, and Giuseppe Strangi, Sci. Rep. **4** 6340 (2014)
[84] Z. Jacob, I. Smolyaninov, and E. Narimanov, **20**, 8100 (2009)

3.3.2 Project-related publications

[85] S. Schmitt, F. Schechtel, D. Amkreutz, M. Bashouti, S.K. Srivastava, B. Hoffmann, C. Diecker, E. Spiecker, B. Rech, and S.H. Christiansen, " Nanowire Arrays in Multicrystalline Silicon Thin Films on Glass: A Promising Material for Research and Applications in Nanotechnology ", Nano Lett. **12**, 4050 (2012).
[86] G. Sarau, B. Lahiri, P. Banzer, P. Gupta, A. Bhattacharya, F. Vollmer, and S. Christiansen, " Enhanced Raman Scattering of Graphene using Arrays of Split Ring Resonators", Adv. Opt. Mater. **1**, 151 (2013).
[87] C. Tessarek, G. Sarau, M. Kiometzis, and S. Christiansen, "High quality factor whispering gallery modes from self-assembled hexagonal GaN rods grown by metal-organic vapor phase epitaxy", Optics Express, **21,** 2733 (2013).
[88] M. Pietsch, S. Jäckle, and S. Christiansen, "Interface investigation of planar hybrid n-Si/PEDOT:PSS solar cells with open circuit voltages up to 645 mV and efficiencies of 12.6 %", Appl. Phys. A 115, 1109 (2014).
[89] M. Pietsch, M. Bashouti, and S. Christiansen, "The Role of Hole Transport in Hybrid Inorganic/Organic Silicon/Poly(3,4-ethylenedioxy-thiophene):Poly(styrenesulfonate) Heterojunction Solar Cells", J. Phys. Chem. C **117**, 9049 (2013).
[90] M. Bashouti, K. Sardashti, S. Schmitt, M. Pietsch, J. Ristein, H. Haick, and S. Christiansen, "Oxide-free hybrid silicon nanowires: From fundamentals to applied nanotechnology", Progr. Surf. Sci., **88**, 39 (2013).
[91] G. Brönstrup, N. Jahr, Ch. Leiterer, A. Csaki, W. Fritzsche, and S.H. Christiansen, "Optical properties of Individual Silicon Nanowires for Photonic Devices", ACS Nano **4**, 7113 (2010).
[92] G. Sarau , M. Heilmann , M. Latzel and S. Christiansen, "Disentangling the effects of nanoscale structural variations on the light emission wavelength of single nano-emitters: InGaN/GaN multi quantum well nano-LEDs for a case study", Nanoscale **6**, 11953 (2014).
[93] S. W. Schmitt, G. Brönstrup, G. Shalev, S. K. Srivastava, M. Y. Bashouti, G. Döhler, and S. Christiansen, "Probing photo-carrier collection efficiencies of individual silicon nanowires diodes on a wafer substrate", Nanoscale **6**, 7897 (2014).
[94] K. Höflich, M. Becker, G. Leuchs and S. Christiansen, "Plasmonic dimer antennas for surface-enhanced Raman scattering", Nanotechnology **23**, 185303 (2012).

3.4 Research plan

The goal of the CRC on "***Hybrid Inorganic/Organic Systems (HIOS) for Opto-Electronics***" is to understand and improve fundamental processes at hybrid interfaces and to determine the functionality of hybrid optoelectronic devices. For HIOS the following material classes are considered: (1) ***inorganic semiconductors*** that serve as well-established opto-electronic components, (2) ***conjugated organic molecules / polymers*** with their strong light-matter coupling and tunability of electrical as well as optical properties, and (3) ***metal nano-structures*** permitting confinement and enhancement of electromagnetic fields. Project A11 aims at the extension of the already established HIOS from funding period one with specifically designed and fabricated novel 2D and 3D metallic and semiconducting inorganic materials in conjunction with tailor-made organic constituents. ***Photonic silicon*** (Si) and ***gallium nitride*** (GaN) as well as ***plasmonic metal nanostructures*** will be realized with a variety of combined deposition and patterning techniques while the central goal is the integration and evaluation of well-selected cases of hybrid interfaces that are particularly interesting for opto-electronic or nano-optic devices. The proposed study represents a challenging combination of ***fundamental research*** with ***device design*** and ***testing***. Fabrication issues must be as much solved as adaption of characterization techniques to the physical and chemical mechanisms at HIOS interfaces that need to be unveiled. Based on the knowledge-gain device designs and -concepts relying on HIOS will be formulated, characterized and subsequently optimized. Thus, project A11 will mainly contribute two research foci to the CRC:

(1) Development and characterization of inorganic nanostructures for 3D-HIOS
(2) Monitoring of HIOS by application into specially developed functional devices

These two project parts will merge into development and testing of functional 3D-HIOS-devices. In presenting the very front end and back end of the knowledge that shall be accumulated in the CRC, A11 relies and aims for a strong cooperation and feedback-loop with various other project groups.

3.4.1 Materials and Methods

Materials and Structuring: From the three material classes relevant for HIOS we will mainly contribute to the CRC with inorganic materials, especially semiconductor, metal and composite nanostructures relevant for photonic, plasmonic and opto-electronic applications. The first CRC research period focused mainly on the **semiconductor** ZnO. In the second funding period A11 will provide the well established semiconductors **Si** and **GaN** for integration in HIOS. While GaN has a wurtzite crystal lattice, similar to ZnO, Si crystallizes in a diamond cubic lattice. An additional challenge for GaN and Si is the stability of their surfaces against oxidation, a problem non-existent in metal-oxides like ZnO. Wafers with different orientations ({100} and {111} in case of Si and {0001} in case of GaN) and different doping concentrations (n- and p-type Si from 10^{14} to 10^{17} and n-type GaN with 10^{18} cm^{-3}) will serve as planar references. 3D nano-architectures composed of Si and GaN microrods or nanowires can be realized using top-down and bottom-up techniques in the group of the PI. Individual Si and GaN rods and wires and their dense ensembles will be created top-down through micro- / nano-lithography using masking and subsequent reactive ion etching (RIE). Respective masks can be realized by large area nanosphere lithography (NSL) with densely packed polystyrene or quartz spheres or nano-imprint lithography. Bottom-up GaN nano-structures are grown by self-seeded VLS growth on a variety of substrates such as Si, sapphire or graphene. Core-shell nano-structures are realized by epitaxial overgrowth of InGaN/GaN multi-quantum-wells (MQM) on the initial micro- or nanorods by metal organic vapor phase epitaxy (MOVPE). In A11 a precise control of rod/wire geometries and in particular surface facets relevant for the realization of HIOS interfaces. P**lasmonic structures** with tailored properties will be realized by wet-chemical synthesis of **metal particles** (Ag and Au particles, Ag wires, Au flakes) as well as by layer patterning of physical vapor deposition Au-, Ag-, Al-, Cu-layers and atomic layer deposition of Pt, aluminum doped ZnO - AZO. While these processes are mainly established, the ALD process for Pt still needs to be developed during the project duration. Scientifically relevant plasmonic and metamaterial structures for HIOS will be designed by simulation (B2, B10) and correspondingly fabricated by powerful top-down focused ion beam (FIB) patterning with novel small-ion sources (He, Ne) as well as conventional Ga ion beams , electron beam induced deposition (EBID) using locally injected novel precursor compounds, sequential electron beam lithography (EBL), and possibly pick-and-place manipulation (PPM). For this purpose highly developed nano-microscopy tools are available, like (1) a He and Ne ion microscope with highest resolution (~0.5 nm) and large depth of field in combination with a powerful patterning engine providing nanostructuring < 10 nm (available only at few places in Germany), (2) a dual beam instrument with electrons and gallium ions in combination with strong patterning engine for bottom-up EBID/IBID nanofabrication and top-down focused ion beam milling, (3) a scanning electron microscope with integrated atomic force capability for pick-and-place manipulation. As **organic component** we will mainly apply high conductive **conjugated polymers** as well as strong acceptor and donor **molecules**

inducing a dipole at hybrid interfaces. As we have already extensively worked with the hole conductor PEDOT:PSS, we will extend our work within the CRC also to other polytiophenes and polyfluorenes. In close cooperation with other projects (A3, Z1, A8) we will select polymers and molecules fitting the desired band alignment for the envisioned HIOS device applications.

Characterization: A detailed characterization is key for deeper insights into the ruling interface mechanisms in HIOS. Nanomaterial properties will be investigated in depth using the imaging capabilities of scanning and transmission electron microscopy (SEM and TEM) in correlation with (1) chemical analysis using energy-dispersive X-ray spectroscopy (EDX), (2) structural characterization using electron backscatter diffraction (EBSD) and µ-Raman spectroscopy (Raman) as well as (3) optical/bandstructure investigation using cathodoluminescence (CL) and photoluminescence, and finally (4) topological characterization using atomic force microscopy (AFM). The optical characterization includes ellipsometric measurements on thin films (determining optical material response and accurate film thickness), as well as VIS spectroscopy measurements of transmittance and reflectance not only for large samples but also for areas < 5x5 µm² via a fiber-coupled optical microscope. Therewith, effective material properties of nanostructured materials can be deduced in collaboration with other groups of the CRC and a full numeric description of the respective systems can be established.
The second pillar of characterization represents a complete optoelectronic assessment of HIOS devices. The properties of individual functional layers, inorganic semiconductors and conjugated polymers, will be determined by 4-point and Hall measurements (resistivity, mobility, doping) as well as profilometry (thickness, roughness), absorption and scattering behavior via visible light (VIS) spectroscopy and photoluminescence (carrier lifetime, band gap). For monitoring HIOS in functional devices it is essential to design and electrically test suitable contacting schemes for the individual layers (like Ohmic contacts by proper metals). Charge transport in HIOS-diodes will be monitored by dark and illuminated (with a class AAA sun simulator) current density-voltage (J-V) measurements and correlated to known models (drift-diffusion, Schottky, tunneling etc.) For hybrid photovoltaic cells also internal and external quantum efficiency will shed light on the separation of excitons/carriers at the HIOS. Capacity-voltage measurements of HIOS in devices will provide critical parameters like barrier formation due to band alignment, doping concentration and surface/interface defect densities and distributions. Long-term stability tests of the devices, and therefore the dominating HIOS interface, will be performed in a protected glove box environment as well as with light-soaking benches (LSB). Supplementary to macroscopic device characterization, the HIOS in nano-device concepts will be analyzed in-situ by advanced SEM techniques including electron beam induced current (EBIC) to monitor any junction within the cell and a four-point nanoprobing set-up for nanoscale electrical characterization. With these specialized tools is possible to contact and test even single nanowire based HIOS.

3.4.2 Work programm

(1) <u>Development and characterization of inorganic nanostructures for 3D-HIOS</u>

The following tasks include the fabrication of the broad inorganic material basis for HIOS in combination with detailed characterization in terms of material quality (SEM/TEM imaging correlated with EDX, EBSD, CL, PL, EELS, possibly Raman and AFM) as well as concerning the tailored photonic/plasmonic properties (ellipsometry, VIS spectroscopy, EELS).

(1.a) Si and GaN nanowires: Large areas (~ 1cm²) of nanowires having hexagonal lattice symmetry will be fabricated using RIE on different Si and GaN substrates in combination with NSL. The size of the spheres (typically around 1µm) sets the lattice constant and assigns an upper limit to the accessible diameters, which can be tuned via subsequent plasma shrinking down to several hundreds nanometer. Furthermore, differently In-doped GaN rods possibly enwrapped with InGaN/GaN MQMs will epitaxially be grown by MOVPE .

Year 1: dry etching for different Si and GaN substrates established, MOVPE growth of tailored MQM around epitaxial GaN rods realized

Year 2: accessible diameters adapted to desired photonic responses (B10), fully characterized photonic Si/GaN substrates with tailored nano-optical response available

Year 3: fully characterized single InGaN/GaN MQM nanodevices with enhanced light absorption and con trolled mode formation available

(1.b) Plasmonic 3D structures: Starting from either WCS, PVD, ALD or CVD three-dimensional nanostructures from coinage metals or highly doped semiconductors will be realized based on the powerful top-down FIB patterning with novel small-ion sources (He, Ne) possibly combined with bottom-up EBID growth for individual devices. Large area fabrication will start from PVD with EBL or optical lithographic techniques.

Year 1: wet-chemical synthesis of large Au flakes (~1000 µm²) and atomic layer deposition of Pt established
Year 2: parameter for nanofabrication with He/Ne ions established and first large area plasmonic decorations with functional geometries from EBL available for HIOS
Year 3: tailored 3D nanostructures from He/Ne-FIB milling with numerically guided resonant behavior and possibly chiro-optical activity for certain HIOS realized

(1.c) Hyperbolic Metamaterials: Planar HMM will be realized by sequential physical deposition of e.g. Ag and SiO_2, and can thereby efficiently be combined with one or even several interlayers of molecules to enhance the molecular optical excitation rates as well as to favor the desired decay channel and direction of emission. Later, HMM can be fabricated even on non-planar substrates by in-situ ALD growth on any pre-structured surface. All geometries will be numerically guided and optimized in strong collaboration with B10.
Year 1: planar HMM with Ag/SiO_2 or another metal/oxide of numerically derived geometries are available
Year 2: ALD of Pt established (oxides are typically available) and HMM on non-planar substrates realized
Year 3: Numerically promising (possibly nanostructured) HMM with incorporated organics available.

(2) <u>Monitoring of HIOS by application into specially developed functional devices</u>

To test optoelectronic properties of HIOS in applications they have to be incorporated into functional structures. Based on existing knowledge and our previous work we will start with developing and monitoring hybrid rectifying junctions on differently doped planar Si and GaN wafers, as well as applying them with suitable contact schemes to photovoltaic cells and light emitting diodes. As a crucial technicality for future use of HIOSs in applications we will also focus on monitoring the stability of HIOS in a device environment and test different novel concepts for stabilization.

(2.a) Junction formation in planar HIOS based on silicon: This task aims at developing and testing organic selective contacts for n- and p- doped Si. Detailed optoelectronic measurements under variation of doping of the Si as well as the polymers will be utilized to monitor the junction formation. Analogue to the already established diode junction of a highly hole conducting polymer (PEDOT:PSS) introduction of an inversion layer in the band alignment to n-type silicon, we aim at combining p-type silicon with an electron conducting polymer.
Year 1: integration of new p-conducting polymers (P3HT) in existing device concept with n-type Si, design and realization of device concept and contacting scheme for HIOS-diodes based on p-type silicon, establishment of solution processing and layer formation of the different polymers
Year 2: determination of the junction type and band alignment in HIOS-diodes under variation of the work function of the polymer by doping (e.g. F6TCNNQ for P3HT or PSS in PEDOT) and the Si substrate doping concentration with various optoelectronic measurements
Year 3: monitoring of charge generation, transport and separation by applying the developed HIOS-diodes into photovoltaic cells, realization of a hybrid photovoltaic diode with hole and electron selective contacts dismissing any inorganic semiconductor/metal contact.

(2.b) Development of GaN based devices with functional HIOS: Starting with our knowledge on all-inorganic GaN devices (rectifying diodes, LEDs) we will transfer the concepts to application in HIOS devices, strongly relying on the results of other groups in the CRC of preferable organic polymers and molecules for desired band alignment and charge transfer.
Year 1: development of device structure and contacting schemes for HIOS devices based on GaN, preparation of planar GaN with InGaN MQWs for highly efficient non-radiative Förster resonant energy transfer (FRET) to organic molecules (in cooperation with B3).
Year 2: optoelectronic testing of rectifying and Ohmic contacts by organic molecules on GaN, integration of inter-molecules for preferable charge transport and band alignment (in cooperation with A3, A4, A8, B11, B13).
Year 3: fabrication of first functional HIOS devices based on (In)GaN (possibly LEDs or photovoltaic cells).

(2.c) Stability and band alignment tuning by inter-molecules and atomically thin layers: Stability under basic device environment conditions is a known issue for HIOS. Degradation mechanisms in the organic material and/or the HIOS interface have to be identified and stabilized. Therefore, we will test incorporation of chemisorbed molecules thin inorganic tunneling layers on stability and band alignment of the devices.
Year 1: identification of degradation mechanisms in PEDOT:PSS/n-Si junctions by electrically monitoring of diodes and organic layers under different environmental conditions (light vs. dark, air vs. inert).
Year 2: depending on the results from the first year development of concepts to stabilize the interface by chemisorbed conductive molecules (cooperation A8, Z1) and atomically thin tunneling layers (ALD) or encapsulation schemes for the HIOS diodes

Year 3: extension of stability concepts to other HIOS developed within the CRC, also based on GaN; exten sive analysis of the band alignment of HIOS with inter-molecules or interlayers, with the goal to achieve strong inversion (cooperation A8).

Development, Fabrication and Nano-testing of 3D-HIOS devices

In **year 4** the achievements of the first three years in the main parts of project A11 with the knowledge acquired in other CRC 951 projects will be used to develop and test first 3D-HIOS devices. These will incorporate photonically active nanostructured inorganic semiconductors and possibly plasmonic structures. This ambitious goal involves many challenges that need to be tackled. As silicon is the most investigated material, we will build large area HIOS diodes (~1cm^2) based on silicon nanowires analogue to project part (2.a). Processes will be developed such that the solution processed polymers can penetrate the nano-array. Because of the large interface area of nanowire assembles, the defect density on the silicon surface plays an even more important role and the effect on junction formation will be intensively monitored. The same holds true concerning stability of the hybrid interface. Single nanowires of Si and GaN will be decorated with polymers and molecules based on findings of the first three projects years and tested with our opto-electrical nano-contacting in-situ SEM setup providing the unique opportunity to test the previously developed HIOs in interface dominated nano-devices.

3.5 Role within the Collaborative Research Centre

The project A11 'Interface-dominated hybrid 3D nano-architectures with tailored opto-electronic properties' with its front end focus on a broad range of inorganic nano-material synthesis and assembly as well as back end integration of HIOS into functional devices will benefit from, interact with and support the following other projects in the CRC 951.
(I) Design and fabrication of photonic and plasmonic inorganic 3D-nanostructures for a broad spectral range (UV to NIR) of resonances adapted to various organic and inorganic materials:

- Nanostructured plasmonics HIOS (B1, Z2)
- Plasmonic structures on solution processed goldflakse (B2)
- Plasmonic nanostructures based on degenerately doped ZnO (A5, B10, Z2)
- GaN and Si single nanowires and assemblys and 2D references (A3, B13, A8, B7, B3)

The new project and partner A11 will provide sophisticated and precisely designed 3D nano-architectures of a variety of inorganic material classes. Thus, we will supply a new level of material complexity to the CRC offering the design and transfer of knowledge already gained to novel HIOS for even more specific applications and thus even better understanding of hybrid configurations.

(II) Implementing and understanding of HIOS with arrays and individual 3D nanostructures in comparison to planar 2D systems into functional devices:

- Band alignment and tuning of HIOS with different polymers and molecules (A8)
- Integration of novel conductive molecules and polymers (Z1)
- Electronic properties of organic polymers and molecules in conjunction with faceted GaN micro- and nano-rods and InGaN quantum wells (B3, Z2)
- Charge transfer at heterojunctions of organic polymers with Si and GaN layers and nano-structures (B7, Z2)

Project A11 will very much rely on the fundamental knowledge acquired in the first and upcoming second funding period by the other CRC project groups, particularly also on the selective binding schemes predicted from simulations (A4, B11), and test these for specially selected HIOS in a device monitoring environment.

Finally, A11 will contribute to the CRC and support other project groups with our broad spectrum of sophisticated correlated microscopy/spectroscopy with the ability of optoelectronic testing of nano-objects and -devices as well as novel 3D nanofabrication methods making even more precious HIOS possible.

3.6 Delineation from other funded projects of the principal investigator

Ongoing Projects:
Seventh Framework Program (EU)
(I) Universal SEM as a multi-nano-analytical tool (**UnivSEM**), 01/04/2012 - 31/03/2015
Delineation: The aim of the UnivSEM project is to develop a novel multimodal tool combining: (I) a vision capability by integrating SEM, SPM and optical microscopy (OM), (II) chemical analysis by TOF-SIMS, EDX, (III) structural characterization by EBSD, (IV) non-destructive optical analysis by confocal Raman spectroscopy and CL. Through this strongly technological approach UnivSEM is completely distinct from the fundamental research strategy of HIOS.
(II) A Nanoscale Artificial Nose to easily detect Volatile Biomarkers at Early stages of Lung Cancer and Related Genetic Mutations (**LCAOS**), 01/04/2011 - 31/03/2015
Delineation: The LCAOS project aims at the earliest possible detection of lung cancer (LC) using volatile biomarkers by applying artificial noses based on cross-selective and sensitive sensor arrays from 3D silicon nanowire (Si NW) based field effect transistors (FETs). The LCAOS project focuses on the direct application of fully inorganic device systems which distinguishes its research goals clearly from HIOS.

DFG Research Unit
Dynamics and Interactions of Semiconductor Nanowires for Optoelectronics (**FOR 1616**), 2012 -
Delineation: The part project E2 of FOR1616 aims at the design of (In)GaN nanorod (NR) based solarcells. The project relies on the development of fully inorganic nanowire based approaches for solar cells on the basis of (In)GaN and, thus, differs clearly in the scientific goals pursued as the material basis investigated.

DFG Cluster of Excellence
Engineering of Advanced Materials (**EAM**) - Hierarchical Structure Formation for Functional Devices, **Research area C:** Photonic and Optical Materials, 2007-2017
Delineation: The research area C of the EAM includes the theoretical and experimental investigation of photonic crystals and metamaterials to enable the control of light onto the nanoscale. In that respect major research topics include photonic crystal fibers and their use as optical tweezers as well as spectroscopic nanoprobes. Thus, the PI project within research area C of the EAM concentrates exclusively onto optical phenomena and differs distinctly in the scientific goals.

Upcoming projects:
DFG priority program
Tailored Disorder - A science- and engineering-based approach to materials design for advanced photonic applications, 2015 – 2018 and/or 2018-2021 possible
Delineation: The priority program “Tailored Disorder” aims at the investigation of photonic properties of materials with deliberately introduced structural and/or compositional disorder from a fundamental scientific perspective. The project proposals to be written for the SPP have to explore photonic properties of biological blueprints originating from disorder or, theoretically, identify and optimize design rules for the development of new structures showing tailored disorder resulting in the desired photonic functionality. Summing up, the SPP concentrates exclusively onto optical phenomena of various material systems.

BMBF Verbundprojekt
MatPhochS: 2015 - 2018 possible
Delineation: The proposed BMBF project MatPhochs aims at the fabrication of plasmonic/photonic nano-composite materials for the photo-electrochemical reduction of carbon dioxide to carbon based solar fuels. The materials investigated include metal oxides like cuprous oxide and iron oxides. Such electrodes are optimized for efficient light capture and guiding by nanostructuring and the introduction of plasmonically acting metals, will be encapsulated and functionalized..In conclusion, MatPhochS differs not only in the scientific goals pursued but also in the materials investigated from the proposed CRC project A11.

3.7 Project funds

3.7.1 Previous funding

The project is currently not funded and no funding proposal has been submitted.

3.7.2 Funds requested

Funding for	2015/2		2016		2017		2018		2019/1	
Staff	Quantity	Sum	Quantity	Sum	Quantity	Sum	Quantity	Sum	Quantity	Sum
PhD student, 75%	2	44.100	2	88.200	2	88.200	2	88.200	2	44.100
Total		44.100		88.200		88.200		88.200		44.100
Direct costs	Sum		Sum		Sum		Sum		Sum	
Small equipment, Software, Consumables	15.000		30.000		30.000		30.000		15.000	
Total	15.000		30.000		30.000		30.000		15.000	
Total	59100		118200		118200		118200		59100	

(All figures in Euro)

3.7.3 Staff

	No.	Name, academic degree, position	Field of research	Department of university or non-university institution	Commitment in hours/week	Category	Funded through:
Available							
Research staff	1	Silke Christiansen, Prof. Dr., Institutsleiterin	Material science	Helmholtz-Zentrum Berlin für Materialien und Energie (HZB)	8h		Direct costs
	2.	Katja Höfllich, Dr.	Physics	HZB	10h		Helmholtz-Postdoc-Programm
	3.	Christian Tessarek, Dr.	Physics	HZB in collaboration with Max Planck Institut (MPL)	4h		EU LCAOS
	4.	already selected currently graduating, Postdoc	Physics	HZB	10h		Direct costs
	5.	N.N., Postdoc	Physics	HZB	10h		Direct costs
Non-research staff	6.	Holger Kropf		HZB	4h		Direct costs
	7.	Harald Stapel		HZB	4h		Direct costs
Requested							
Research staff	8.	N.N.	Physics	HZB		PhD student	
	9.	N.N.	Physics	HZB		PhD student	

Job description of staff (supported through available funds):

1 Silke Christiansen
Scientific and organizational management of the project, supervision of scientific staff and PhD students, discussion and dissemination of results.
2 Katja Höfllich
Support and supervision of PhD-student [8.] concerning plasmonic 3D nanostructure development and fabrication, especially electron microscopy and stucturing
3 Christian Tessarek
Growth and characterization of GaN nanostructures in a MOCVD
4 already selected currently graduating, Postdoc
Nanosphere lithography and reactive ion etching of Si and GaN, support and supervison of both PhD students [8. and 9.] concerning 3D-devices concepts.
5 N.N., Postdoc
Support and supervison of PhD student [9.] regarding HIOS-device concepts, contacting and optoelectrical device characterization.
6 Holger Kropf
Structuring of metals and semiconductors with focusd ion beam.
7 Harald Stapel
Imaging and standard analytics with electron microscopy.

Job description of staff (requested):

8 N.N., PhD student
Fabrication and characterization of photonic and plasmonic 3-D semiconductor and metal nanostructures, especially advanced analytics and structuring in new generation of electron microscopes
9 N.N., PhD student
Development, fabrication and optoelectronic characterization of HIOS-devices with 2-D and 3-D interfaces based on Si and GaN and highly conductive polymers and specific interfacial molecules.

3.7.4 Direct costs

	2015/2	2016	2017	2018	2019/1
Funds available	7.500	15.000	15.000	15.000	7.500
Funds requested	15.000	30.000	30.000	30.000	15.000

(All figures in Euro)

Small equipment, Software, Consumables for 2015/2, 2019/1

Softwarelicences, Optoelectronic simulations of nanostructures and devices	EUR	2.500
Small equipment, for electrical characterization and solution processing	EUR	2.500
Consumables (chemicals, clean room equipment, feed materials and so on)	EUR	10.000

Small equipment, Software, Consumables for 2016, 2017, 2018, 2019

Softwarelicences, Optoelectronic simulations of nanostructures and devices	EUR	5.000
Small equipment, for electrical characterization and solution processing	EUR	5.000
Consumables (chemicals, clean room equipment, feed materials and so on)	EUR	20.000

3.7.5 Major research equipment requested

none

3.7.6 Student assistants

	2015/2	2016	2017	2018	2019/1
Quantity	2	2	2	2	2
Commitment in hours/week	20	20	20	20	20
Sum	12.000	24.000	24.000	24.000	12.000
Tasks	Support of the PhD students. Running standard processes for 3D inorganic nanostructures for HIOS.				

3.1 About project B1

3.1.1 Title: Plasmonic nanoantennae as efficient input/output ports for fundamental opto-electronic elements based on organic/inorganic interfaces

3.1.2 Principal investigators

Dr. rer. nat. Thomas Aichele
*31. 12. 1974
German
Humboldt-Universität zu Berlin
Institut für Physik
Newtonstraße 15
12489 Berlin
Phone: +49 (0)30 2093 4824
Fax: +49 (0)30 2093 4718
E-Mail: thomas.aichele@physik.hu-berlin.de

Prof. Dr. rer. nat. Oliver Benson
*9. 2. 1965
German
Humboldt-Universität zu Berlin
Institut für Physik
Newtonstraße 15
12489 Berlin
Phone: +49 (0)30 2093 4711
Fax: +49 (0)30 2093 4718
E-Mail: oliver.benson@physik.hu-berlin.de

3.2 Project history

3.2.1 Report

Preliminary remarks

PI Dr. Aichele left Humboldt-Universität by 31.10.2011. The project was continued by the other PI.

State of the art at beginning of project

The project was based on results concerning coupling of single molecules to surface plasmon polaritons (in short: surface plasmons). Several groups had investigated the optimization of excitation and radiative decay rate, signal-to-noise ratio, photostability and weak transitions to dark states by coupling a single molecule to optical antennae [1-3] utilising surface plasmons. Coupling to nanoscopic light emitters was achieved on a variety of structures, such as quantum dots [4], molecules [1-3,5], diamond defect centres [15] and up-conversion crystals [14].

In combination with donor/acceptor pairs of emitters, surface plasmons also acted as transducers to mediate and enhance the energy transfer between two optically active constituents [7]. Exploring the fundamental level of the interaction of molecules with plasmonic structures initiated the new research field of *molecular plasmonics* [8]. Apart from the most widely studied effect of surface enhanced Raman scattering (SERS), novel experiments were motivated, e.g., by improving the energy transfer between donor and acceptor layer in an organic light emitting diode [9] or by potential photovoltaic applications [10]. Besides, organic molecules were considered as frequency converters for surface plasmons [11].

Due to the ease of fabrication and synthesis most experimental studies with surface plasmons had been performed on gold structures and in the red/near-infrared regime. Nevertheless, theoretical and experimental

studies predicted plasmonic resonances down to ~350 nm in optical antennae made of aluminium or silver [12,13].

In order to study arrangements of nanoantennae and single emitters, these systems have to be brought together in a controlled fashion. In Refs. [4] and [5] this was achieved by preparing the antenna at the tip of an scanning probe microscope, which was then scanned over the emitter, while in [6], conjugated organic molecules were attached to the metal nanoparticle via molecular spacers. In this project, we aimed at nanomanipulation of nanoparticles with the tip of an Atomic Force Microscope (AFM).

Project objectives

The goal of this project was to study plasmon-enhanced transfer processes at HIOS interfaces. Three processes should be studied: (i) Transfer of photons to/from organic molecules, i.e. enhancement of fluorescence and absorption via plasmonic antenna structures; (ii) plasmonic enhancement of exciton transfer across inorganic-organic interfaces in the incoherent, possibly coherent regime; (iii) transfer of energy between separated organic molecules along plasmonic wires. A peculiar approach in this project was the construction of precisely arranged model systems of individual conjugated organic molecules coupled to plasmonic antennae and waveguides. Three objectives were defined:

1.) Enhancement of exciton transfer across an inorganic/organic interface
2.) Optimise the architecture for plasmonic enhancement in HIOS
3.) Energy transport along hybrid nanowires

The work plan of the project was organised in three parts with 2-3 tasks each. In the following we will discuss the work performed so far according to this work plan.

Part 1 of work plan – Characterization of single molecules on semiconductor surfaces

The goal of WP1 was to retrieve optimum conditions for the experiments in subsequent work packages, where spatially isolated molecules with good stability, defined orientation and distance to the hybrid interface were required.

Task 1.1 – Single molecule spectroscopy

In this task we set up a completely new experiment on an optical table which combines atomic force microscopy (AFM) and optical microscopy. A new AFM (NT-MDT) was purchased and assembled on top of a home-built scanning confocal microscope. Different laser sources (two Ti:Sa and a pumplaser at 532nm) were connected and single-pass frequency doubling of the Ti-Sa-laser radiation was established. Detectors with single molecule sensitivity and spectrometers were installed. Fig. 1 shows a schematic of the setup.

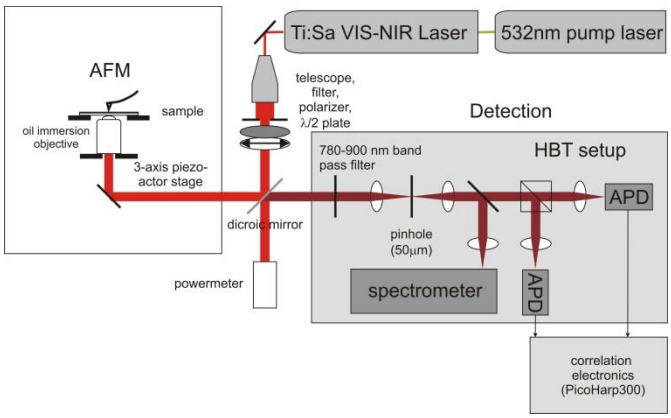

Figure 1: Schematics of the new setup built in this project. A home-built confocal microscope is combined with a commercial AFM (ND-MDT). The optical path has single photon sensitivity and allows for time-resolved single photon counting (HBT setup). Dark field imaging of single plasmonic structures is possible as well.

Three techniques were developed to fabricate dilute molecular samples: (1) spin coating, (2) sublimation, (3) molecular deposition. Technique (3) was developed together with **B3 (Blumstengel)**. Results with these samples are introduced in 3.2. The first two were utilized to fabricated stable dibenzoterrylene (DBT) samples in an anthracene host matrix as a model system following [16]. Figure 2 shows AFM and confocal microscopy measurements on the DBT samples with the new setup.

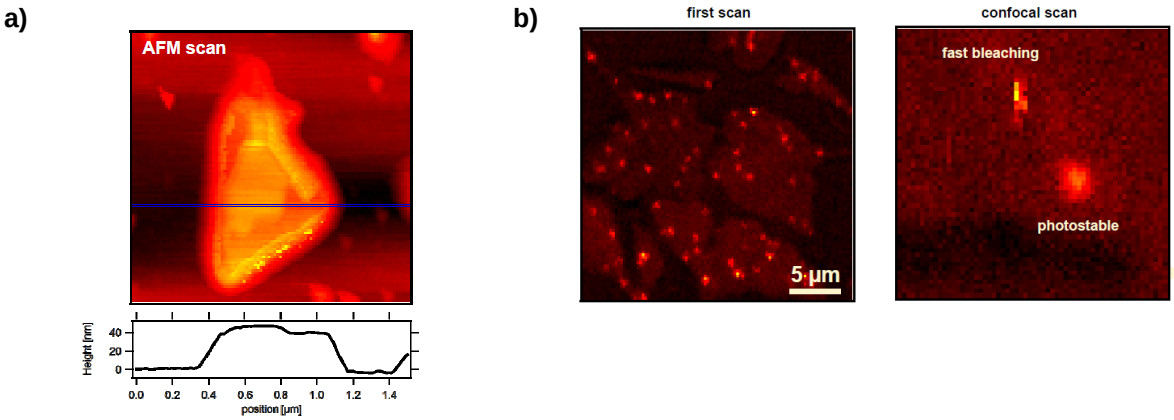

Figure 2: a) Atomic force microscopy scan of a single anthracene crystal. b) Confocal images of single DBT molecules in anthracene. In the right-most zoomed-in image bleaching of a molecule can be observed. Stable molecules remained active for days.

Excellent single molecule sensitivity was obtained. A single photon counting setup in Hanbury Brown-Twiss configuration was used to determine the normalized photon autocorrelation function $g^{(2)}(\tau)$. Antibunching from single molecules was detected.

A next important goal of this task was to exploit if AFM-nanomanipulation could be applied to organic molecules in order to establish a deterministic method for functionalization of plasmonic antenna. For this reason we tried to pick-up individual anthracene crystals with an AFM probe. It turned out that the anthracene host crystals was too soft and that its surface adhesion was to large to allow for lifting. However pushing and "carving" was very well possible. Further attempts are on the way to improve this manipulation method.

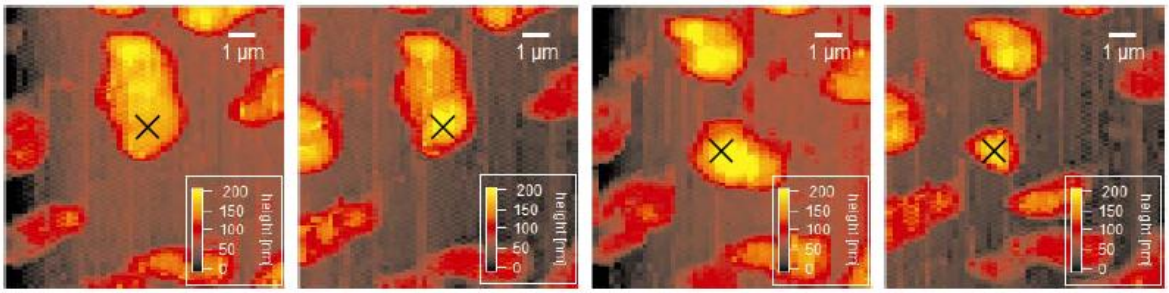

Figure 3: Nano-"carving" of an anthracene crystal containing single molecules. The images are AFM scans in tapping mode, while "carving" was performed in AFM contact mode. The cross marks nominal identical positions. Sub-micron crystals could be fabricated in this way.

The results obtained in Task 1.1 have been combined in a publication (Kewes et al., "Key components for nano-assembled plasmon-excited single molecule non-linear devices") that is presently under review in Optics Express.

Task 1.2 – Molecules on semiconductors

In this task molecules should be detected on ZnO. At first single molecule sensitivity of the new setup had to be achieved. For this we used molecules emitting in the visible. In parallel plasmonic antennae with resonances at shorter wavelengths were tested. It was decided to investigate primarily coupling of molecules to these antennae before studying systems that match the transition in ZnO structures. For this reason this task was postponed.

Part 2 of work plan – Coupling of single molecules to plasmonic nanoantennae

This part was dedicated to the characterization of the conjugated organic molecule coupled to an optical nanoantenna, at this stage still isolated from any inorganic semiconductor. Several approaches to achieve coupling between the two components (metal and organic molecule) were studied. The design (size, shape,

lithographical preparation process) of the plasmonic structures should be accompanied by numerical simulations of the electromagnetic field (Finite Difference Time Domain method, FDTD).

Task 2.1 – Coupling of conjugated organic molecules to metallic nanospheres.

This task was performed together with the partners at Helmholtz-Zentrum (**project B2(Ballauff/Benson/Lu)**). 14 nm spherical gold nanoparticles were synthesized via the Turkevich method [17] while a silica shell surrounding the spherical gold nanoparticles was attached via a modified Stöber process [18].

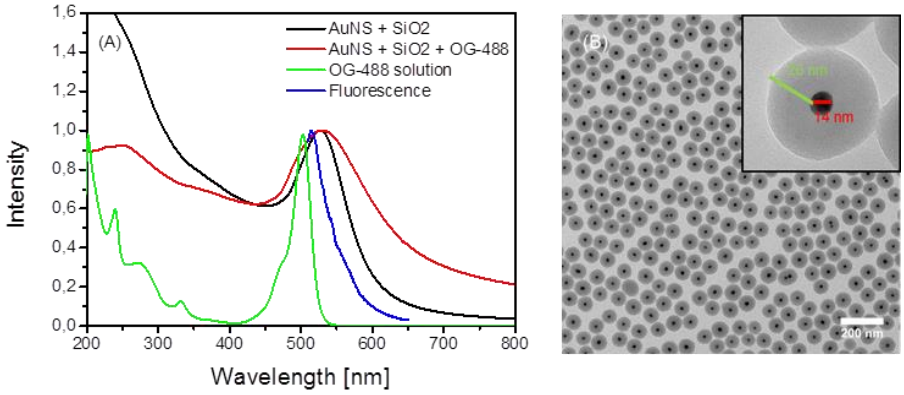

Figure 4: ***a) UV/VIS and fluorescence spectra (blue curve) of gold-silica core-shell nanoparticles with and without Oregon Green 488 (OG-488) dye molecules. b) TEM image of fluorescent gold-silica core-shell nanoparticles.***

In order to obtain coupling of organic molecues to the plasmonic gold-silica core-shell nanoparticles various dyes were used. Close spatial and spectral overlap was an important parameter. The plasmonic dipole mode of gold nanoparticles absorbs light at 524 nm. Bright fluorescent dye molecules emitting light in this wavelength regime are fluorescein and its more stable derivative Oregon Green 488. These dyes were incorporated successfully. Unreacted dye molecules were washed away by repetitive centrifugation until the supernatant showed no fluorescence. Figure 4a shows a UV/VIS and the fluorescence of gold-silica nanoparticles with Oregon Green 488 molecules. The respective TEM image is given in Fig. 4b.
The functionalized core-shell particles were also used in project **B2(Ballauff/Benson/Lu)** where the key focus is to explore spaser action.

Task 2.2 – Coupling of conjugated organic molecules to bowtie antenna structures

In this task design and fabrication of plasmonic antenna (possibly with resonances at short wavelengths) should be performed together with measurements on coupled (organic molecules and antanna structures) systems.

Due to a down period of an electron beam lithography system in the clean room the e-beam writing of antanna structures was significantly delayed. We decided to continue by (1) performing measurements on structures provided by other partners, (2) to investigate tuning possibilities of available plasmonic antennae, and (3) to exploit novel routes of assembling coupled structures.

The following Fig. 5 a) shows an SEM image from Al rod-like antenna structures provided by the group of Prof. R. Bratschitsch, Universität Münster. In the same figure (b) measured dark-field scattering spectra are plotted. It is apparent that resonances down to a wavelength of 440nm could be observed.

a)

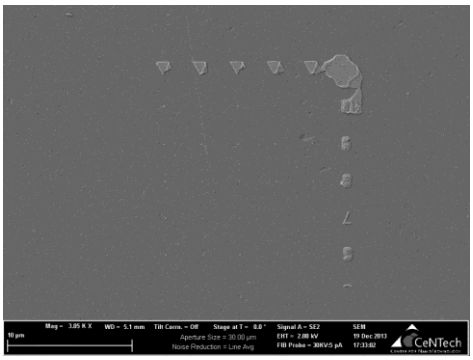

b)

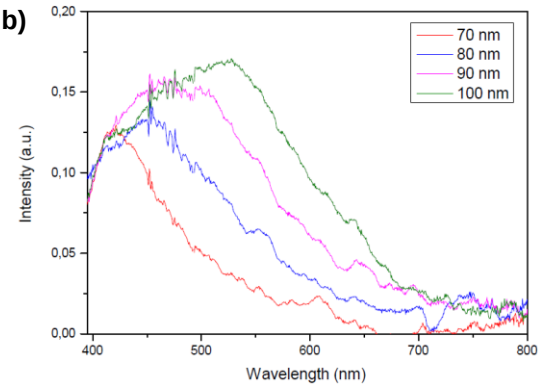

Figure 5: a) Scanning electron-beam microscopy (SEM) image of rod-type Al antenna. The tiny antenna structures of varying size are ordered in an array and are hardly visible in this image (sample was provided by Prof. R. Bratschitsch). b) Dark-field scattering spectra of individual antennae of different lengths.

First results of measurements on theses structures are described in the report on part 3 of the work plan.

An important issue when coupling molecules to resonant plasmonic antenna is the matching of the antennae resonances to the emission wavelength of the molecules. For this reason we studied a new method to tune plasmonic Au dipole antennae in a reproducible way [19]. The method was discovered while taking dark-field scattering spectra. A high scattering intensity can melt the Au particle. Then, the dipole force and radiation pressure of the excitation laser shapes the antennae into ellipsoids. Tuning and enhanced directional emission is obtained in this way. Figure 6 shows examples of tunable plasmonic antennae fabricated in this way.

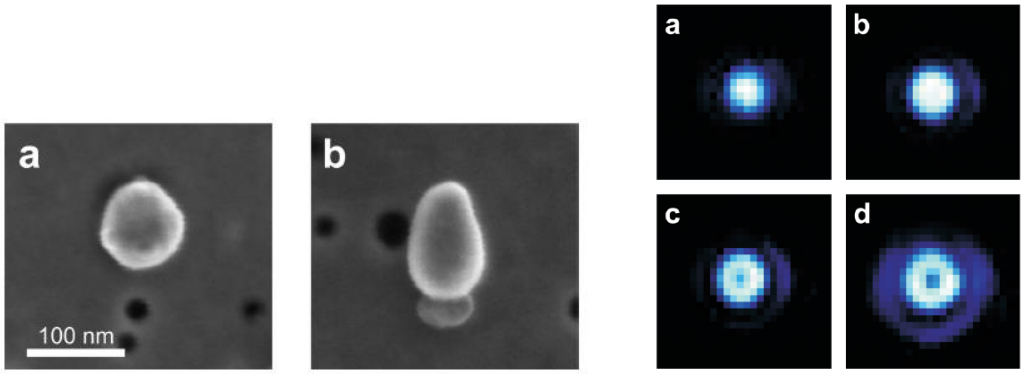

Figure 6: Left a) and b): SEM images of gold nanoparticles on a glass substrate. a) Unmelted spherical gold nanoantenna. b) Melted gold nanoantenna
Right a)-d): Change of the photoluminescence emission pattern of a gold nanantenna during melting with increasing laser intensity. a) Image of unmelted nanoantenna. b) The emission pattern starts to widen until (c) the emission pattern forms a donut. d) With further increasing laser intensity, the donut pattern becomes more distinct.

The novel tuning method may also be applicable to other metal systems. The experimental studies were accompanied by extensive numerical studies also in cooperation with project **B10(Busch)**. A joint paper was published in Nano Letters [19].

Finally, in this task we also investigated methods to bring dye-funcionalized nanoparticles to plasmonic structures in a controlled way. The studied approach uses trapping of the particles in a AC-trap after electrospray injection. The setup is described in [20]. After trapping and optical characterization the particles can be deposited on almost any – even very fragile – structures. A local electrostatic potential can lead the charged particles directly to metallic antennae. Optical pre-characterization allows for a selection of optimum particles (e.g. highest desity of molecules, maximum of emission wavelength etc.). In this way the problem of the inhomogeneity of the particles can be overcome. A paper utilizing the principle of this method was published in Applied Phys. Lett. [20].

Closely related work that was publisched in Scientific Reports [21] concerned a novel fabrication method for laser-written structures as templates for three-dimensional plasmonic structures.

Part 3 of work plan – Transfer processes across an inorganic/organic interface mediated by nanoantennae

In this part plasmonically mediated energy and exciton transfer processes should be investigated.

Task 3.1 – Assembly of inorganic/organic/metal hybrid structures

As discussed in Task 1.2 the coupling of molecules to ZnO structures via plasmonic antennae was postponed. This concerns exciton transfer across organic-inorganic interfaces. First results on plasmonically mediated energy transfer are discussed in the following.

Task 3.2 – Time-resolved spectroscopy of plasmon-mediated excition transfer processes

A first candidate to study energy transfer processes and their modification via a plasmonic antenna is a FRET pair. Together with project **B3 (Blumstengel)** we identified a suitable pair (SP3-L4P:L6P) and fabricated a test structure. The design of the test structure is shown in Fig. 7

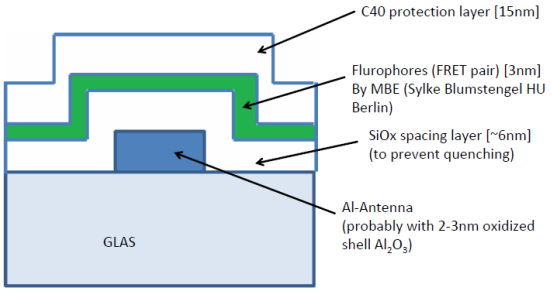

Figure 7: Design of the test structure to study plasmon-modified energy transfer. An Al antenna covered with SiOx as a spacer to prevent quenching is covered with a SP3-L4P:L6P. C40 is finally used as protective layer.

We intentionally selected a non-optimal 10:1 blend in order to obtain only partial energy transfer without a plasmonic antenna. In order to characterize modifications of the FRET process we performed fluorescence lifetime images (FLIM). An area around the antennae was scanned and for each pixel the fluorescence lifetime was determined. Then pixels in the supposedly plasmonically field-enhanced region were compared to pixels further away from antennae. We also selected two spectral windows corresponding to the acceptor absorption and fluorescence maximum, respectively. The measurements are shown in Fig. 8.

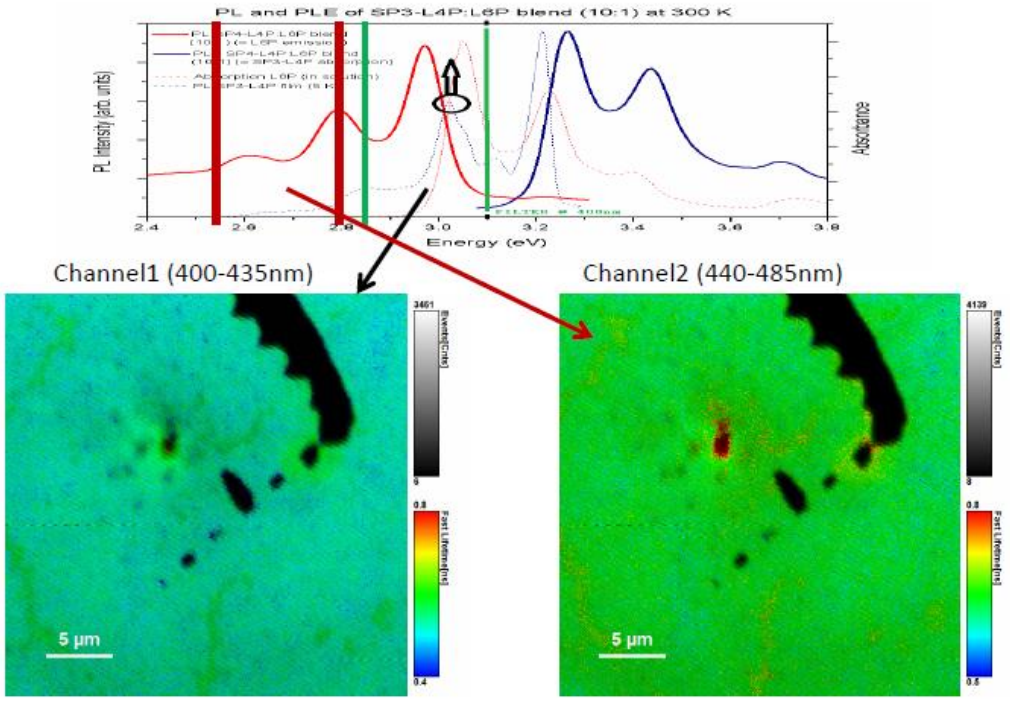

Figure 8: Top: Absorption and fluorescence spectra of the FRET pair SP3-L4P:L6P. Coloured lines indicate the selected spectral windows for the FLIM measurements. Bottom: Measured FLIM images for the two selected spectral windows. The square array (tilted by 45°) can be recognized as well as the markes (compare Fig. 5a).

In the first preliminary results hot spots with a modified lifetime could be identified. However, the results are not yet conclusive. One reason is the inhomogeneity of the SP3-L4P:L6P film. Also the spacer layer may have had a fluctuating thickness. The experiments are presently ongoing with improved sample preparation.

Task 3.3 – Conjugated organic molecules coupled to propagating surface plasmons

As a long-term goal of the project coupling between remote emitters mediated via a plasmonic wire shall be obtained. As novel plasmonic waveguide silver nanowires within photo-catalytically active nanotubular dye aggregates (cooperation with project **A6(Kirstein/Rabe)**) was suggested. However, as a result of A6 it was

found that it is difficult to obtain sufficiently long wires with low damping. Studies on these wires could therefore not be performed in this task.

Instead we studied coupling of organic molecules to dielectric and plasmonic wires. For this the fabrication and manipulation techniques developed in Task 1.1 were exploited. Few (down to a single) organic DBT molecules in anthracene crystals were coupled to a chip that contained dielectric waveguides and including a dielectric-plasmonic coupler. Figure 9 shows first results of the experiments.

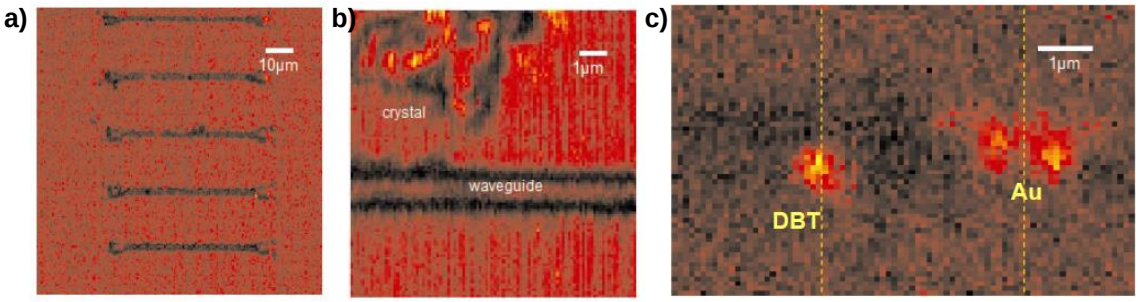

Figure 9: Scattering and fluorescent confocal images of molecules coupled to dielectric and plasmonic waveguides. a) Scattering confocal image of a part of the fabricated sample with 5 dielectric waveguides. Every second waveguide contains a short plasmonic waveguide in the middle. b) Zoom-in into a). Next to the waveguide an anthracene crystal can be recognized. c) Fluorescent confocal image of an area close to the short plamonic waveguide. Flurescence from a single (?) DBT molecule can be seen together with fluorescence from the Au plasmonic wire.

The experiments are presently ongoing, but the first promising results show that it is possible to couple fluorescence from single molecules to dielectric and plasmonic waveguides. Coupling between two single molecules via propagating surface plasmons seem feasible.

The results obtained in this task have been submitted (Kewes et al., “Key components for nano-assembled plasmon-excited single molecule non-linear devices”) and are presently under review in Optics Express.

Summary:

A new setup to study coupling of organic molecules and plasmonic nanostructures was set up and is operating. First preliminary results on coupling of molecules via propagating surface plasmons were obtained. Indications for plasmon-modified energy transfer between organic molecules have been found. The experiments are ongoing and conclusive results to support the first indications can be expected within the remaining project time.

The new setup will be utilized for investigations planned in project B2 in the new period of the CRC. The various designs and techniques concerning plasmonic antennae will be continued, but as a result of the studies here will be performed at longer wavelengths. Funding by the Einstein foundation, Berlin, for a follow-up project was already granted.

In addition to the peer-reviewed journals there are two completed Bachelor theses (see 3.2.2). One PhD theses (A. Kuhlicke) will be completed by the end of this project duration.

References

[1] A. Kinkhabwala, et al., Nature Photonics **3**, 654 (2009).
[2] K. Vasilev, et al., J. Chem. Phys. **120**, 6701 (2004).
[3] T. D. Neal, et al., Appl. Phys. Lett. **89**, 221106 (2006).
[4] J. N. Farahani, D.W. Pohl, H.-J. Eisler, and B. Hecht, Phys. Rev. Lett. **95**, 017402 (2005).
[5] T. H. Taminiau, et al., Nano Lett. **7,** 28 (2007).
[6] E. Dulkeith, et al., Nano Lett., **5,** 585 (2005).
[7] P. Andrew and W. L. Barnes, Science **306**, 1002 (2004)
[8] See, e.g., recent workshop “Molecular Plasmonics”, May 14-16 2009, Jena, Germany
[9] J. Feng, T. Okamoto, R. Naraoka, and S. Kawata, Appl. Phys. Lett. **93,** 051106 (2008).
[10] V. E. Ferry, L. A. Sweatlock, D. Pacifici, and H. A. Atwater, Nano Lett. **8,** 4391 (2008).
[11] T. K. Hakala, *et al.*, Appl. Phys. Lett. **93,** 123307 (2008).
[12] A. Mohammadi, V. Sandoghdar, and M. Agio, J. Comp. & Theo. Nanosci. **6,** 2024 (2009).
[13] W. Dickson, et al., Phys. Rev. B **76**, 115411 (2007).

[14] S. Schietinger, et al., Nano Lett. **10,** 134 (2010).
[15] S. Schietinger, et al., Nano Lett., **9,** 1694 (2009).
[16] C. Toninelli *et al.* Opt Exp. 18, 6577 (2010).
[17] J. Turkevich, P. C. Stevenson, J. and Hillier, Discussions of the Faraday Society **11**, 55-75 (1951).
[18] A. van Blaaderen and A. Vrij, Langmuir **8,** 2921-31 (1992).

3.2.2 Project-related publications

a) Peer-reviewed journal:

[19] A. Kuhlicke, S. Schietinger, C. Matyssek, K. Busch, and O. Benson, „In Situ Observation of Plasmon Tuning in a Single Gold Nanoparticle“, Nano Lett. 13, 2041-2046 (2013).
[20] A. Kuhlicke, A. W. Schell, J. Zoll, and O. Benson, „Nitrogen vacancy center fluorescence from a submicron diamond cluster levitated in a linear quadrupole ion trap“, Appl. Phys. Lett. 105, 073101 (2014).
[21] A. W. Schell, J. Kaschke, J. Fischer, R. Henze, J. Wolters, M. Wegener & O. Benson, Three-dimensional quantum photonic elements based on single nitrogen vacancy-centres in laser-written microstructures, Sci. Rep. 3, 1 (2013).

b) other publications

[22] Robert Koslowski, „Wellenleitung von Oberflächenplasmonen entlang lithographischer Goldstrukturen, Bachelorarbeit, Humboldt-Universität zu Berlin, 2011
[23] Thomas Kiesner, „Untersuchungen zu Oberflächenplasmonen“, Thomas Kiesner, Bachelorarbeit, Humboldt-Universität zu Berlin, 2013

3.3 Funding

Funding of the project within the Collaborative Research Centre started Juli 2011. The project will be completed by the end of the current funding period.

3.3.1 Project staff in the ending funding period

	No.	Name, academic degree, position	Field of research	Department of university or non-university institution	Commitment in hours/week	Category	Funded through:
Available							
Research staff	1	Oliver Benson, Prof. Dr., Professor	Nano Optics	HU Berlin	10		
	2	Oliver Neitzke, PhD student	Nano Optics	HU Berlin	26,7		
Non-research staff	3	Klaus Palis, Dipl. Ing.		HU Berlin	4		
	4	Christine Rosinska		HU Berlin	4		
	5	Regina Rheinländer, Secretary		HU Berlin	4		
Requested							
Research staff							
Non-research staff							

1. Oliver Benson: Scientific and organizational management of the project, supervision of PhD students, analysis, discussion and dissemination of results.

7. Oliver Neitzke: Characterization of the employed samples using spectroscopy and correlation measurements; preparation of antenna/inorganic/organic structures using AFM nanomanipulation; study the transport of energy/exciton exchange over inorganic/organic films mediated by nanoantennas; study plasmonic transport along metal/organic nanowires; analysis of experimental results.
4. Klaus Palis: Development of and advisory service for electronic components
5. Christine Rosinska: Development and technical support for fine mechanical devices.
6. Regina Rheinländer: Administrative tasks.

3.1 About project B2

3.1.1 Title: Coherent scattering, amplification, and lasing of metal/organic hybrid structures on the nanoscale

3.1.2 Research areas: Experimental Physics

3.1.3 Principal investigators

Ballauff, Matthias, Prof. Dr. (13.07.1952), German
EM-ISFM Soft Matter and Functional Materials
Helmholtz-Zentrum Berlin für Materialien und Energie GmbH (**HZB**)
Hahn-Meitner-Platz 1, 14109 Berlin
Phone: +49 (0)30 8062-43071
E-Mail: matthias.ballauff@helmholtz-berlin.de

Benson, Oliver, Prof. Dr. (09. 02. 1965), German
Humboldt-Universität zu Berlin (**HUB**)
Institut für Physik, Nanooptik
Newtonstraße 15, 12489 Berlin
Phone: +49 (0)30 2093 4711
E-Mail: oliver.benson@physik.hu-berlin.de

Lu, Yan, Dr. (02.09.1976), Chinese
EM-ISFM Soft Matter and Functional Materials
Helmholtz-Zentrum Berlin für Materialien und Energie GmbH (**HZB**)
Hahn-Meitner-Platz 1, 14109 Berlin
Phone: +49 (0)30 8062-43191
E-Mail: yan.lu@helmholtz-berlin.de

3.1.4 Legal issues

This project includes

1.	research on human subjects or human material.	no
2.	clinical trials.	no
3.	experiments involving vertebrates.	no
4.	experiments involving recombinant DNA.	no
5.	research involving human embryonic stem cells.	no
6.	research concerning the Convention on Biological Diversity.	no

3.2 Summary

In this project we will reveal the interaction of organic molecules within metal-organic hybrid structures on (sub-)nanometer dimensions. Our approach aims at a comprehensive understanding from a single molecule level up to high-density molecular layers. Ultimate control of fabrication via chemical synthesis of layered and core-shell structures as well as single-molecule deposition & single-particle manipulation will be combined with ultra-sensitive spectroscopy and time-resolved photon counting. Rigorous quantitative modelling of the structures will be performed in close cooperation with theory groups. We have defined 3 main objectives for the continuation of our project that are based on the present status of research in metal-organic hybrid structures and on our own results of the first CRC funding period. We will (1) analyze and demarcate collective coherent effects in active organic/plasmonic hybrid nano-structures. This is motivated in particular by the debate on published reports on spasing in metal-organic nanostructures. As second objective we will (2) strive for a quantitative experimental and theoretical understanding of molecule-plasmon coupling in confined geometries from single molecules to spasers. This shall shed light on the physics of molecule-metal coupling in the regime of a distance of few nanometers approaching the molecular scale where many common approximations fail. Finally we will (3) explore routes towards novel dielectric nanolasers which have recently been suggested as alternative to spasers, but yet preserving their advantages of low modal volume and fast response. The project will continue as joint effort between the HZB and the HUB, bringing together extensive expertise in synthesis of metal-organic hybrid structures and spectroscopy of nanophotonic systems.

3.3 Research rationale

3.3.1 Current state of understanding and preliminary work

Motivation of the project

A spaser (Surface Plasmon Amplification by Stimulated Emission of Radiation) as suggested by Bergman and Stockman in 2003 [1] is a hybrid structure consisting of a metal core acting as resonator for localized surface plasmons surrounded by a gain medium. Organic molecules may provide sufficient gain, and many metal-silica core-shell systems with embedded dye molecules have been investigated [2]. In 2009 spasing in a metal-organic silica core-shell structure was reported by Noginov et al. [3]. This work was the main motivation for the project B2. Since then only one report showing spaser behavior for metal nanoparticles with dye molecules as gain medium was published (Meng et al. [4]). Meng et al. adsorbed gold nanorods with a thin silica shell on a glass substrate and spin-coated a polymer film highly doped with rhodamine on top. Besides regular spontaneous emission a strong amplified spontaneous emission (ASE) signal was observed. However, with gold nanoparticles embedded a third emission peak appeared which was associated with spasing. Meanwhile, other groups tried to mitigate optical losses with similar approaches without achieving spaser action [2,5]. In the first funding period **HUB** and **HZB** concentrated on 5 tasks which are described in the following. Key results are underlined.

(1) Synthesis of active core-shell and layered nanostructures

The principle design of the spaser architecture followed the first reported spaser by Noginov and co-workers in 2009 [3] where non-linear emission by pumping gold nanospheres with a dye-loaded silica shell was reported. At **HZB** 14 nm spherical gold nanoparticles were synthesized [23] via the Turkevich method. A silica shell was attached surrounding the spherical gold nanoparticles via a modified Stöber process. An amine functionalized silane derivative, (3-aminopropyl) triethoxysilane, has been further covalently bound with amine reactive dyes and co-condensed in the silica network surrounding the spherical gold nanoparticles [6]. Efficient non-radiative energy transfer from the dye molecules to gold requires close spatial and spectral overlap [1]. For this reason fluorescein and its more stable derivative Oregon Green 488 were incorporated successfully, and unreacted dye molecules were separated by repetitive centrifugation until the supernatant showed no fluorescence. More efficient plasmon generation and energy coupling between the dye molecules and the gold core may be achieved with a well-defined spacer layer, as demonstrated by the numerical calculations performed at **HUB** [7] (see section **(5)**). Accordingly, gold-silica core-shell nanoparticles with a double silica shell were synthesized by **HZB**. The first shell consisted of pure silica, whereas the second shell was incorporated with dye-molecules. Figure 2 shows a scheme of these particles, UV/VIS and fluorescence of gold-silica nanoparticles with Oregon Green 488 molecules measured at **HZB**. The respective TEM image was measured in cooperation with project **Z2** (Kowarik/Koch).

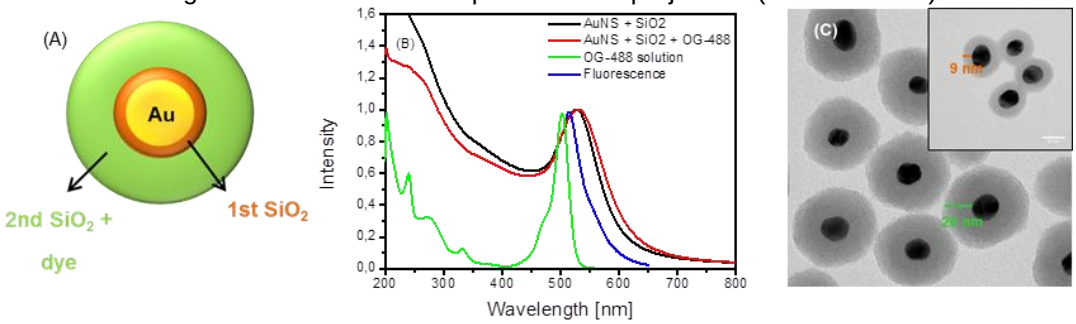

Figure 2: (A) Scheme of core-double-shell gold-silica nanoparticles with a spacer layer. (B) UV/VIS and fluorescence of such nanoparticles with and without Oregon Green 488 (OG-488) dye molecules. (C) TEM image of fluorescent gold-silica core-double-shell nanoparticles, the inset shows the single shell nanoparticles.

A more promising shape for a spaser is a nanorod which has a stable polarization along the major axis [8]. The localized surface plasmon resonance of this longitudinal mode strongly corresponds with the aspect ratio of the nanorod. Gold-silica core-shell nanorods were synthesized at **HZB** via the seed mediated growth mechanism [9] with a direct silica deposition method to create a spacer layer around the gold nanorod [10]. A second dye-incorporated silica shell was formed by using the Stöber method. Bright and stable dyes used are Alexa Fluor 532 and Atto Rho101. The aspect ratio of the gold nanorods was reduced accordingly and the longitudinal localized plasmon resonance was shifted to match spectrally the emission of these dyes.

A different approach was to first synthesize metal-silica core-shell nanoparticles with the silica shell being a spacer layer as described in the previous sections. The gain medium consisted of the same amine-reactive dye molecules which are covalently bound to an amine functionalized polymer (poly(allylamine)

hydrochloride (PAH)). Unreacted dye molecules were separated via dialysis before the dye-functionalized polymers were lyophilized. The silica surface inhibits negatively charged silanol groups which allow for the adsorption of the polycationic dye-functionalized PAH. More layers can be adsorbed via the layer-by-layer approach [11] by alternating adsorption of the anionic poly(acrylic acid) (PAA) and PAH. Zeta potential measurements proved the alternating surface charges after each addition of different polyelectrolytes indicating that respective polyelectrolytes were attached successfully (Figure 3).

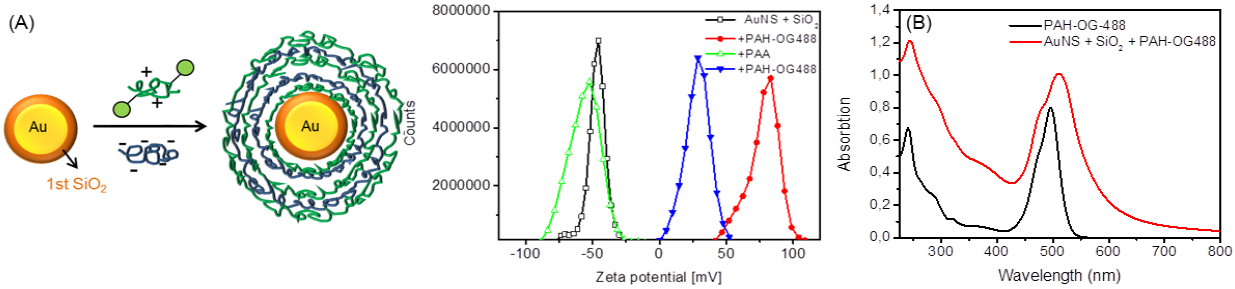

Figure 3: (A) Scheme of layer-by-layer approach and zeta potential measurements after alternating polyelectrolyte adsorption. (B) Absorption spectra of triple layer PAH-OG488 polyelectrolyte on spherical gold nanoparticles.

Attachment of layers was confirmed by UV/VIS measurements showing strong absorption peaks of the dye after coating with three layers of dye-functionalized PAH (Figure 3). The approach is very promising as a large amount of dye molecules can be adsorbed near the gold core with a precisely controlled distance. This is advantageous compared to the approach of gold-silica core-shell particles with dye molecules randomly embedded in the silica shell. As proposed by Bergman and Stockman [1], **HZB** also established a route to attach CdTe quantum dots to spectrally resonant gold nanorods. Quantum dots (provided by the group of Prof. Eychmüller at TU Dresden) are more photostable than dyes, in particular when excited under high pump power conditions. To attach the quantum dots, **HZB** synthesized a thermo-responsive polymeric shell (poly(N-isopropylacrylamide), (pNIPA)) around the gold nanorods. The quantum dots showed fluorescence quenching when in close spatial correlation with the gold nanorods and reduced fluorescent life times.

(2) Implementation of setups to study spaser and nanolaser structures

To study optical properties of spasers a new experimental setup was constructed at **HUB**. The setup provides the capability to perform studies on ensembles or on single spaser particles/structures. Analytic tools like dark-field spectroscopy can be combined with atomic force microscopy and fluorescence studies with a confocal microscope on the same individual particles. Two frequency-doubled Tsunami Titan-Sapphire Laser (Ti:Sa) systems were installed for excitation to provide high peak intensities. Capability of fast measurement of possible non-linear rises of the fluorescence intensity as a function of pump intensity (laser input-output curves) was implemented. This is a mandatory feature as the relatively poorly resolved laser threshold behavior measured by others [3,4] led to a debate in the community. The high repetition-rate of the Ti:Sa Lasers of about 80 MHz, led to quenching via population of long-lived triplet states. Also the short pulses of around 150 fs were insufficient to create inversion. Therefore, an alternative laser source (Nd:YAG laser with 25 ps pulses at 10 Hz repetition rate) at the Max-Born Institute (MBI), Berlin, was used. A similar, but simpler setup was installed there. This setup allowed for the observation of the threshold-like signatures as discussed in the following section **(4)**. With the various new setups all samples synthesized by **HZB** and also various plasmonic waveguides and coupler fabricated via electron beam lithographyby **HUB** [23,24] were investigated.

(3) Characterization of optical properties of spaser structures on the level of single particles

The left panel of Figure 4 shows an exemplary measurement at **HUB** on a sample synthesized by **HZB**. It could be correlated to scattering spectra (dark field microscopy) and topology (AFM) as well. The setups at **HUB** were optimized so that investigation of single metal-organic nanostructures was possible. As another example the middle panel of Figure 4 shows the change of the photoluminescence (PL) emission pattern of a gold nanoparticle while its shape was modified by laser melting [25]. The combination of an optical microscopy setup with atomic force microscopy (AFM) also allowed for an ultimate characterization of plasmonic nanostructures [26]. The right panel of Figure 4 shows a measurement where a fluorescent scanning probe containing a single fluorescent emitter was scanned across an Ag plasmonic wire. From the measurement of the lifetime of the emitter a mapping of the local density of states was possible. This is crucial information to quantify the possible coupling enhancement of organic molecules in the near-field of plasmonic nanostructures. The developed method can be applied to almost any nanostructure.

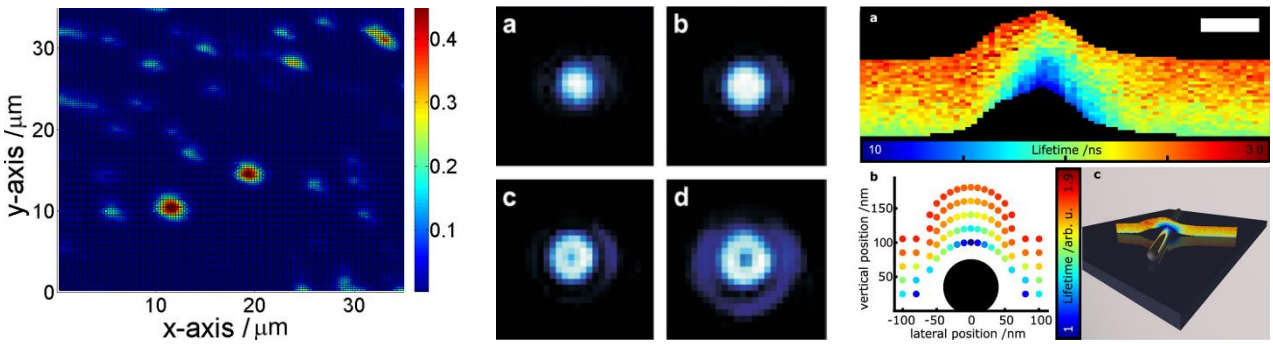

Figure 4: Left panel: Confocal scan of core-shell particles spin-coated onto a glass slide. Middle panel: Change of the photoluminescence emission pattern of a gold nanoparticle (appr. 80 nm in diameter) when its shape is modified via laser melting. Melting power increases from a-d and the shape changes from a sphere to an ellipsoid. Right panel: (a) Color-coded lifetime data as a function of height and position perpendicular to a silver nanowire. Height and position axis are scaled equally and the scale bar is 100 nm. (b) Numerical simulation corresponding to the data in (a). (c) Artists view clarifying the geometry of silver wire and data in panels a,b.

(4) Observation of 'spaser-like' features from metal organic nanostructures

In addition to PL maps photon statistics and lifetime measurements as well as spectral information were acquired. Figure 5 (left) shows a series of lifetime measurements with increasing excitation time and thus increased bleaching of the sample. A reduction in lifetime is observed, indicating that emitters further away from the gold core of the core-shell particles are bleaching faster as their mean-time in the excited state is longer. Figure 5 (right) shows a measurement of the PL of an ensemble of core-shell particles in solution over time as well as the stepwise increased pump-power measured simultaneously. No non-linear PL increase was observed, however strong bleaching was found (indicated by the exponential PL reduction when the pump is set to a constant level).

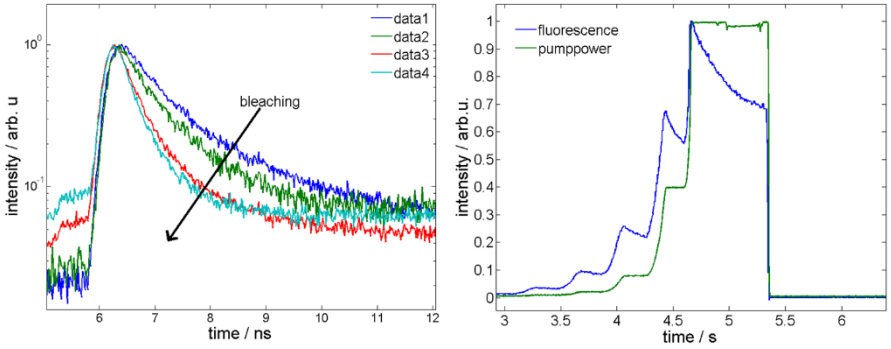

Figure 5: Left: Series of lifetime measurements on individual core-shell particle that reveal a reduction of the lifetime with increased bleaching. Right: measurement of PL intensity and pump power over time.

The results led **HUB** to a construction of a new setup at MBI as mentioned in **(2)**. With this setup **HUB** investigated core-shell particles as well as samples consisting of plasmonic nanoparticles coated with films of gain media (following the results reported in Meng et al. [4]). In the measured fluorescence spectra signatures of gain-media inversion, amplified spontaneous emission (ASE) peaks as well as laser-like peaks and random-lasing effects (Figure 6) were found.

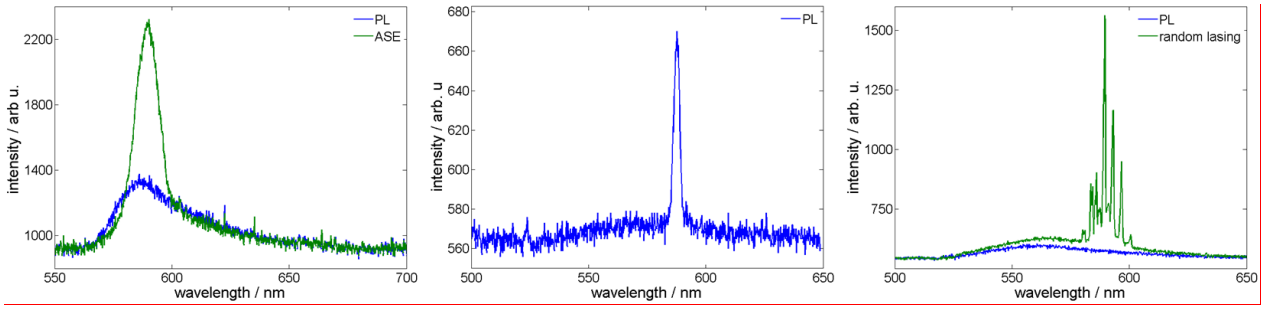

Figure 6: Laser and laser-like signatures. Left: Standard PL and ASE from a R6G doped PVA film. ASE positions varied with film thickness. Middle: Glass substrate coated with Core-Shell particles showing a laser-like peak at high pump intensities with relatively poor signal-to-noise ratio. The peak actually results from glass PL due to ablation. Right: Standard PL and random-lasing effects, due to multiple scattering effects on inclusions in the dye-doped PVA film.

It is important to notice that similar effects were observed in reference samples even without plasmonic particles. It was found that seemingly laser-like peaks in the PL spectra can emerge just due to an increase of a non-linear signal versus the noisy background when the pump power is increased. A careful analysis of ASE revealed that ASE peaks on samples with gain-media films (also without metal particles) were sensitive to the layer thickness and disappeared for thin films. This effect is well known from studies on organic films where waveguiding effects produce pronounced ASE peaks [12,13]. Based on these results **HUB** analyzed the data provided in the studies by Meng et al. [4], where spasing was claimed. It was found that their results could also be explained by ASE and waveguiding modified by scattering of incorporated metal particles. Finally, it was found that generally small inclusions appear in PVA-films doped with organic molecules as gain-media. Presumably these inclusions are sufficient to lead to the random-lasing signatures as observed in the measurements at **HUB**.
It was concluded that although **HUB** and **HZB** were able to observe similar features as the ones reported by Noginov et al. [3] and Meng et al. [4], there is so far no unambiguous proof of spasing in such metal-organic nanostructures.

(5) Theoretical considerations concerning spaser and nanolaser structures
Extensive theoretical work was performed by **HUB** together with **B10** (Busch) to derive a more realistic description of spasers. While existing theoretical work predicted a very strong feedback of the gain medium with the resonant mode in surface plasmon lasers [8] and thus a low spaser threshold, experimental realizations reported on high demands for the pump lasers and material quality. In order to understand this mismatch and to develop strategies to optimize the spaser design several theoretical papers were critically analyzed. It was noticed that the spaser models render the relaxation of pumped gain medium by a single global decay rate (or lifetime) of the excited state. With the awareness of the well-known effect of strong fluorescence-quenching [14–17] that can significantly limit plasmonic nanoantenna performance [18], **HUB** and **B10** explicitly incorporated this effect into a theoretical model to see how it affects the spaser performance. A semi-classical model based on Mie theory was developed [7]. Indeed this model demonstrated that the effect of gain-medium quenching close (~ 5 nm) to the plasmonic core will significantly increase the spaser threshold. Thus, the model gives clear and quantitative guidelines to optimize the spaser design, especially by incorporation of an emitter-free spacing layer between gain-medium and plasmonic core or by the use of alternative materials (with high refractive index and low imaginary part of the dielectric permittivity) like silicon that do not cause such strong quenching effects.

References

[1] D. Bergman and M. Stockman, Phys. Rev. Lett. **90**, 027402 (2003).
[2] B. Peng, et al., ACS Nano **6**, 6250 (2012).
[3] M. A. Noginov, et al., Nature **460**, 1110 (2009).
[4] X. Meng, et al., Nano Lett. **13**, 4106 (2013).
[5] A. De Luca, et al., ACS Nano **5**, 5823 (2011).
[6] A. Van Blaaderen and A. Vrij, Langmuir **8**, 2921 (1992).
[7] G. Kewes, R. Rodríguez-Oliveros, K. Höfner, A. Kuhlicke, O. Benson, and K. Busch, arXiv:1408.7054 (2014).
[8] M. I. Stockman, Journal of Optics **12**, 024004 (2010).
[9] B. Nikoobakht and M. A. El-Sayed, Chem. Mater. **15**, 1957 (2003).
[10] I. Gorelikov and N. Matsuura, Nano Lett. **8**, 369 (2008).
[11] G. Schneider, et al., Nano Lett. **6**, 530 (2006).
[12] M. McGehee, et al., Phys. Rev. B **58**, 7035 (1998).
[13] R. Xia, et al., Org. Electron. **4**, 165 (2003).
[14] C. S. Yun, et al., J. Am. Chem. Soc., **127**, 3115–3119 (2005).
[15] G. Colas des Francs, et al., Opt. Express **16**, 17654 (2008).
[16] R. Carminati, et al., Opt. Commun. **261**, 368 (2006).
[17] A. Moroz, Opt. Commun. **283**, 2277 (2010).
[18] S. Schietinger, et al., Nano Lett. **9**, 1694 (2009).
[19] K. J. Russell, et al., Nat. Photonics **6**, 459 (2012).
[20] C. Toninelli, et al., Opt. Express **18**, 6577 (2010).
[21] L. Mangolini, J. Vac. Sci. Technol. B Microelectron. Nanom. Struct. **31**, 020801 (2013).

3.3.2 Project-related publications

b) Peer-reviewed publications

[22] O. Benson, “Assembly of Hybrid Photonic Architectures from Nanophotonic Constituents”, Nature **480**, 193-199 (2011).

[23] S. Wu, A. W. Schell, M. Lublow, J. Kaiser, T. Aichele, S. Schietinger, F. Polzer, S. Kühn, X. Guo, O. Benson, M. Ballauff, and Y. Lu, "Silica-coated Au/Ag Nanorods with Tunable Surface Plasmon Bands for Nanoplasmonics with Single Particles", Colloid Polym. Sci. **291**, 585 (2013).
[24] G. Kewes, A. W. Schell, R. Henze, R. Simon Schönfeld, S. Burger, K. Busch, and O. Benson, "Design and Numerical Optimization of an Easy-to-fabricate Photon-to-plasmon Coupler for Quantum Plasmonics", Appl. Phys. Lett. **102**, 051104 (2013).
[25] A. Kuhlicke, S. Schietinger, C. Matyssek, K. Busch, and O. Benson, "In Situ Observation of Plasmon Tuning in a Single Gold Nanoparticle during Controlled Melting", Nano Lett. **13**, 2041 (2013).
[26] A. W. Schell, P. Engel, J. F. M. Werra, C. Wolff, K. Busch, and O. Benson, "Scanning Single Quantum Emitter Fluorescence Lifetime Imaging: Quantitative Analysis of the Local Density of Photonic States", Nano Lett. **14**, 2623 (2014).
[27] A. Ott, S. Ring, G. Yin, W. Calvet, B. Stannowski, Y. Lu, R. Schlatmann, M. Ballauff, "Efficient Plasmonic Scattering of Colloidal Silver Particles Through Annealing-Induced Changes", Nanotechnology **25**, 455706 (2014).

c) Other publications

[28] A. W. Schell, J. Wolters, G. Kewes, et al., "Assembly of Quantum Optical Hybrid Devices via a Scanning Probe Pick-and-Place Technique", IEEE CLEO conf., San Jose, CA, May 06-11 (2012)

3.4 Research plan

(a) Objectives

We have defined 3 objectives for the continuation of our project that are based on the present status of research in metal-organic hybrid structures and on our own results of the first CRC funding period (see **3.3.1**).

1) Analysis and demarcation of collective coherent effects in active organic/plasmonic hybrid nano-structures
High-gain and high-density in metal-organic samples as well as a high pumping power supports a variety of collective coherent phenomena. Amplified spontaneous emission, random lasing, and spasing have been reported or claimed. However, the experimental evidence – in particular for spasing – is weak and even doubtful. Based on our results of the first funding period our strategy is to investigate and verify these phenomena in well-controllable and specially synthesized structures.

2) Quantitative experimental and theoretical understanding of molecule-plasmon coupling in confined geometries from single molecules to spasers
Our novel theoretical description and our extensive studies of different spaser architectures in the first funding period showed that ultimate control of the geometry down to the molecular scale is crucial to realize true spasers. We will strive for full control and understanding of molecule-metal coupling in hybrid systems.

3) Exploring routes towards nanolasers
Recently, dielectric nanolasers with ultra-small mode volumes have been discussed as potential alternatives to purely metal-based spasers. An advantage lies in the significantly lower damping even in geometries where the mode volume can well compare with spaser modes. We will adapt this novel approach in our project in addition to work on 'pure' spasers.

(b) Work plan

In order to achieve our goals **HZB** and **HUB** will bring together expertise in synthesis of compound metal-organic hybrid structures and spectroscopy of nanophotonic systems, respectively. The 3 work packages – each subdivided in different tasks – reflect the structure of our objectives. Extensive photophysical and photochemical studies of compound metal-organic systems as well as stability and gain enhancement of conjugated organic molecules will be performed. Different active organic/plasmonic hybrid nano-structures will be synthesized via wet chemistry methods. Numerical studies will complement the experimental efforts.

WP1 – Coherent effects in active organic/plasmonic hybrid nano-structures
In this work package we will focus on collective coherent effects mediated via metal particles in organic films. In order to separate different contributions, such as scattering, plasmon resonances, random feed-back or spasing, we will rely on a well controllable architecture of our samples: Gold metal rods with a silica spacer layer will be embedded in a dye-doped polymer film. Well-controllable parameters of the samples are (1) shape & aspect ratio of particles, (2) particle density, (3) density of dye molecules, (4) thickness of polymer film, and (5) thickness of spacer layer. Together with the new implemented setups we will be able to study the transition from single particle effects (plasmon enhanced fluorescence, perhaps single particle spasing) to collective effects (plasmon enhanced amplified spontaneous emission, random lasing).

Task1.1 Molecular films and core-shell nanoparticles in a well-controllable architecture
A first task concerns the synthesis of gold-silica core-shell nanorods embedded in a polymer film. Gold nanorods of different aspect ratios with the variable silica spacer layer will be synthesized by **HZB**. In order to control the particle density and thus the mean distance between the particles, the core-shell gold-silica nanorods will be spin-coated on a glass substrate. 3 different dyes (Alexa Fluor 532, rhodamine B and rhodamine 6G), will be embedded in the polymer film of polyvinyl alcohol (PVA). The gold nanorod aspect ratio shall match the emission of the dyes accordingly with various silica shell thicknesses as shown in Figure 7.

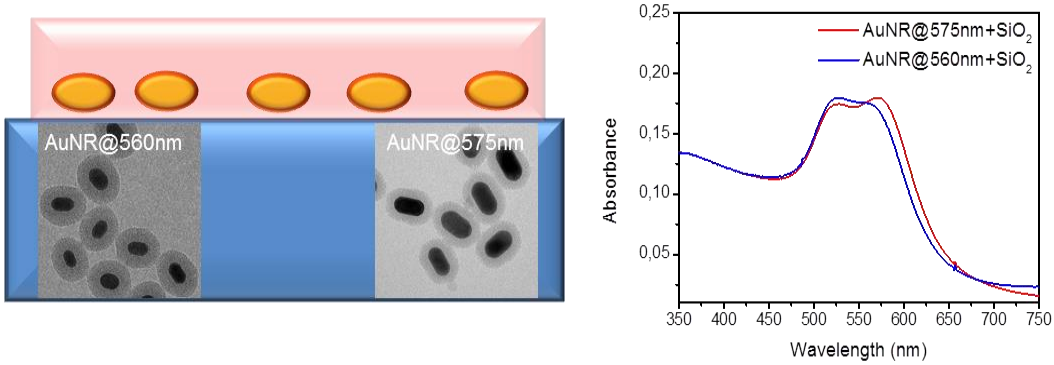

Figure 7: Scheme of gold nanorods on a glass substrate and embedded in a dye doped polymer film, showing also TEM images of the core-shell gold-silica nanorods. UV/VIS of gold-silica nanorods with different aspect ratios.

Task1.2 Investigation of random lasing and amplified spontaneous emission versus spasing in metal-organic films and particles
The experiments will be performed with a setup described in **3.3.2 (2)**. In this task we install several improvements concerning stability, sensitivity, and control of pump power. There is an extensive debate on previously published results concerning spaser action in organic-metal particles [3] and metal-organic films [4]. A main concern is that with the typically high pump powers and high densities of organic dye molecules it is easy to observe collective effects such as amplified spontaneous emission, wave guiding, and random lasing. As an example we showed a measurement performed with our setup in section **3.3.1** (Figure 6). By controlling the experimental parameters (film thickness, film composition, density of molecules and metal particles) and careful measurements as a function of pump power, repetition rate, and excitation volume we will be able to unambiguously separate spasing from other coherent and/or non-linear effects. The contribution of different collective coherent phenomena (spasing, random lasing) will also play a role in other plasmonic systems, e.g. the one studied in **A5** (Henneberger).

A key goal of this work package is to separate the different collective coherent phenomena that occur in metal-organic particles and films and to unambiguously clarify the difference from single particle spasing.

WP2 – From single molecule-plasmon coupling to spasing in optimized geometries
In the first funding period we learned that the spaser design published 2009 by Noginov et al. [3] has severe drawbacks, also reflected by the missing report on a reproduction of similar results in literature. In this work package we will investigate modified plasmon resonators that allow for a step-by-step optimization until spasing action can be observed. The approaches in the different tasks are based on our experimental and in particular our theoretical results (see also 3.3.1 and [7]) of the first funding period.

Task2.1 Numerical analysis of advanced spaser geometries
We will follow a plasmonic cavity design that was reported in [19]. It consists of a guided gap plasmon between a noble metal film and a metal nanowire (shown in Figure 8).

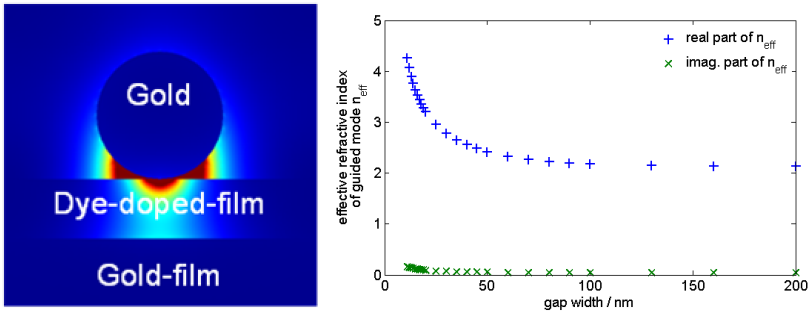

Figure 8: Guided modes of plasmonic gap mode between a gold film and a gold nanowire calculated with FEM. Left: Electromagnetic field intensity distribution of a guided plasmon mode at a frequency corresponding to 650 nm photon wavelength in air, a nanowire diameter of 75 nm and a gap width of 35 nm. Right: Effective refractive index n_{eff} of guided gap modes (same frequency like left figure) as a function of gap width. High real parts correspond to a high energy concentration inside the gap, high imaginary parts correspond to increased propagation losses.

The gain medium can be placed inside the gap. The enhanced fluorescence in [19] showing a Fabry-Perot-like modulated spectrum is a clear spectral signature of gain-to-cavity coupling. This coupling can then be optimized until spasing is reached eventually. Starting with numerical finite element simulations **HUB** will investigated possible designs on the basis of gold nanostructures (nanowires) and high quality films. High quality refers to mono-crystalline metal films that can be realized, e.g., by gold flakes. Figure 8 shows the principle design of the spaser structure to be investigated in this task together with first preliminary calculations of properties of a guided gap-plasmon mode.
Adjusting the gap width, the amount of guided power in the gap can be controlled, which gives a qualitative estimate for the efficiency of gain-to-plasmon coupling. Appropriate emitter-free spacing layers have to be considered and implemented (task 2.2) that separate the gain medium from the gold.

Task2.2 Synthesis of organic-plasmonic structures – from single molecules to spaser geometries
Similar as in work package WP1 synthesis of optimized metal-organic structures is a key issue in the work package WP2. In this task there are two approaches:

Approach A: Core-shell gold-silica nanorods on Layer-by-Layer adsorbed polymer films
A system consisting of adsorbed polyelectrolytes on a gold substrate will be prepared via the layer-by-layer approach at **HZB** and **HUB**. This allows for excellent control of the polymer film thickness. Then, the gold-silica core-shell nanorods will be spin-coated on the top. Film thicknesses will be determined by ellipsometry in cooperation with project **A6** (Kirstein/Rabe). Dye molecules, such as Alexa Fluor 532 and Atto Rho101, will be used. Core-shell gold-silica nanorods that match the emission of the two dyes will be fabricated by **HZB**. Synthesis will go hand-in-hand with the simulations (task 2.1) and the experiments (task 2.3).

Approach B: Molecular beam deposition of stable organic molecule layers
This novel approach aims at the fabrication of molecule layers with ultra-low densities allowing for single molecule studies. Utilizing molecular beam deposition (in collaboration of **HUB** with **B3** (Blumstengel)), we will grow layers of stable organic molecules in host matrices with controllable density. In the first funding period we have realized single molecule studies on dibenzoterylene (DBT) embedded in an anthracene host matrix [20]. Samples have been fabricated via spin-coating or by sublimation. A goal of the molecular deposition technique is to fabricate very thin layers of the host matrix and to embed molecules at a very low density. The technique allows in principle for deposition on various substrates, e.g. on substrates with gold films or gold flakes. In this way, structures like the one shown in Figure 8 (in task 2.1) can be fabricated, but complementary to approach A with a very low density.

Task2.3 Exploring coupling regimes of organic molecules to plasmon structures
This task concentrates on the experimental studies of the systems described in task 2.1 and 2.2. **HUB** and **HZB** will explore two extreme regimes of coupling. One is the high-density regime aiming at spasing action. The high-density samples will be optimized as described above to observe coherent gain and eventually spasing. Aside from an excellent control of the parameters (spaser resonance, spaser mode, spacer layers) the wave-guide-like character of the spaser structure will facilitate outcoupling of coherent plasmons to adjacent plasmon waveguides. In order to achieve this, plasmon waveguides on metal films will be investigated in cooperation with project **A11** (Christiansen). Electron beam lithography and focussed ion beam milling are available fabrication tools.
The other regime concerns single or few molecules coupled to a plasmonic structure. With stable single molecule samples as fabricated in task 2.2 modification of the photo-physics when coupling to the plasmonic near-field can be studied in detail. Appropriate configurations can be obtained either by randomly distributing

the gold nanorods (e.g. by spin-coating) on a low-density molecule sample and select nanorods with one or few molecules in the near-field. Alternatively atomic force microscopy (AFM) nanomanipulation as developed in the first funding period in project **B1** (Aichele/Benson) will be used. Modification of the lifetime, radiative emission rate, and the quantum efficiency of single molecules coupled to the plasmonic near-field will be quantified by time-resolved single photon counting. The wave-guide-like extended mode of the gold nanorods is also ideally suited to study collective effects between two or few molecules sharing a common plasmon mode. The studies will be of high relevance for the theory projects **B10** (Busch) and **B12** (Knorr/Richter). The system may be regarded as a model system to study transfer processes between molecules and nanoplasmonic structures as investigated in **B6** (May). Even a 'simple', but well controllable geometry, i.e. a single molecule close to metal surface, will provide valuable information on the energy level alignment occurring at organic-metal hybrid interfaces.

A key goal of this work package is to investigate the coupling of organic molecules to the plasmonic near-field from the regime of single or few-molecule coupling up to coherent amplification in spasing action.

WP3 – Organic/dielectric nanolasers

While the potential relevance of the spaser concept is out of question, spasers inevitably suffer from high thresholds that could only be reduced when demanding fabrication requirements have been employed. As described in **3.3.1** we have developed in the first funding period a theory together with project **B10** (Busch) for nanoscopic spasers. It turned out that in principle any sphere supporting Mie-modes can be analyzed with this theory. Figure 9 illustrates our model and provides an example of the numerical results. In this work package we will explore the potential of spherical silicon nanoparticles as novel organic-dielectric nanolasers.

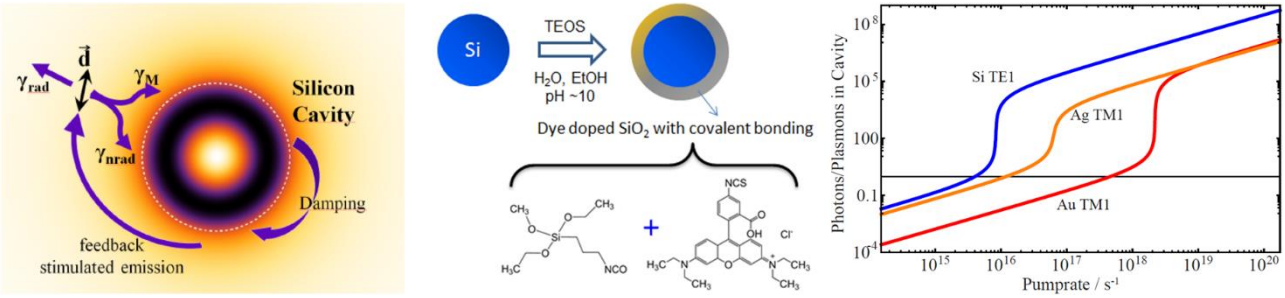

Figure 9: Left: Schematic of a spherical dielectric nanolaser. A Si particle is covered with a layer of organic molecules as gain material. Individual molecules are treated as dipoles with dipole moments d. Different rates (radiative decay, non-radiative decay, and emission in the laser mode) determine the dynamics. Middle: Route for synthesis of a nanolaser. Right: Calculated stationary solution of nanolaser rate equations. Input-output curves for comparable gold (red), silver (orange) and silicon (blue) cavities coated with 1 nm of 2000 homogeneously distributed and randomly oriented dipolar emitters for the bright dipolar cavity-mode are shown.

Task3.1 Synthesis of organic-dielectric nanolasers core-shell structures

A crucial first task concerns the synthesis of core-shell nanostructures with silicon cores as resonator. Chemical methods to synthesize crystalline silicon nanoparticles of 200 nm in diameter are still difficult to realize, while nanoparticles produced by physical methods suffer from high polydispersity [21]. Preliminary studies at **HZB** showed that by gradient centrifugation, at the right concentrations and centrifugation speed, commercial available silicon samples with huge polydispersity could be separated into narrow ranged size fractions. The layer-by-layer approach will be applied by **HZB** for dye-functionalization with PAH-bound dye molecules on the silicon surface, which can act as gain medium for the silicon cavities. This procedure can be followed by zeta potential measurements. Furthermore, due to a thin native silica layer on the surface, silane chemistry is possible. This enables to synthesize silicon-silica core-shell structures with dyes embedded as shown in the middle panel of Figure 9.

Task3.2 (HUB) Coherence properties of spasers and nanolasers

In this task **HUB** will study the performance of the dielectric nanolasers fabricated by **HZB** in task 3.1. The extensive optical characterisation will be performed with the same setups used in the previous tasks. A key figure of merit is the threshold of the nanolasers in comparison with spaser structures of similar dimensions. There will also be an intense cooperation with project **B10** (Busch) in order to evaluate the theoretical description of nanolasers and to refine it according to the experimental results. A goal is to develop a model

that predicts quantitatively the behaviour of dielectric nanolasers. In the regime of few excitations we will look for signatures of non-classicality also in cooperation with project **B12** (Knorr/Richter).

Task3.3 Coupling of spasers and dielectric nanolasers to integrated waveguides
A final task of this work package will address the possibility to utilize spasers and dielectric nanolasers as local sources for coherent plasmons. Whereas the outcoupling of plasmons from a spaser to integrated waveguides has already been addressed in task **2.3** a similar approach may utilize dielectric nanolasers. Excitations in the tightly confined mode of a nanolaser may be efficiently converted in plasmonic excitations of a plasmonic waveguide in the near-field of the nanolaser. Assembly of spaser or nanolaser particles lithographically written waveguides will be done by the AFM nanomanipulation as developed in project **B1** (Aichle/Benson) of the first funding period. Appropriate plasmon waveguide structures will be investigated again with project **A11** (Christiansen). The design of plasmonic waveguide structures and couplers for different wavelengths will also be relevant for the ZnO structures in project **A5** (Henneberger).

A key goal of this work package is to realize novel organic-dielectric nanolasers and to evaluate their performance against spasers.

3.5 Role within the Collaborative Research Centre

- There will be a continuation of the close collaboration with the theory project **B10** (Busch) on modelling of spaser properties and coupling of molecules to various plasmonic structures.
- Cooperation with theory will be complemented by **B12** (Knorr/Richter) providing a full quantum calculation of the emission of molecular-metal-hybrids.
- The system of few molecules coupled to nanoplasmonic structures is an experimental counterpart of similar systems studied theoretically in **B6** (May).
- Together with **B3** (Blumstengel) we will develop a method to fabricate well controllable molecular films with varying densities using the molecular deposition technique.
- Plasmonic ZnO structures are studied in **A5** (Henneberger) as well. Designing and fabricating appropriate plasmonic hybrid architectures will be performed in cooperation due to the scalability of the plasmonic structures with respect to the wavelength. Also collective coherent phenomena (amplified spontaneous emission, random lasing) may occur in the ZnO system as well and have to be demarcated from true spasing.
- In project **A11** (Christiansen) there is expertise in fabrication techniques such as lithography and focussed ion beam milling. In addition Si samples and monocrystalline metal flakes can be provided.
- Film deposition techniques and characterisation of layered hybrid systems will be performed in cooperation with **A6** (Kirstein/Rabe).
- The project **Z2** (Kowarik/Koch) will provide techniques such as cryo-TEM, TEM, XRD, AFM, and SEM to characterize the structure of the hybrid systems studied in this project.
- **Z1** (Hecht) will provide advice concerning appropriate molecules for the studies.

3.6 Delineation from other funded projects

funding agency: project number	**project title**	**comment**
PI O. Benson:		
DFG: CRC 787	Semiconductor Nanophotonics (TP C2)	semicond. quantum dots as light emitters for quantum inforamtion, no relation to B2
DFG: FOR1493	Integrated Quantum Optics and Nanophotonics with Defect Centers in Nanodiamonds	quantum optics and photonic with defect centers in diamond, no relation to B2
DFG: BE2224/15	Three-dimensional quantum photonic elements based on single emitters in laserwritten microstructures…	fabrication and investigation of laser-written photonic structures functionalized with defect centers in diamond, no relation to B2
Einstein Foundation, Berlin	Active plasmonic nano-antennas for generating, detecting, and converting quantum light (ActiPlAnt)	fabrication and investigation of antenna structures for enhancing light collection and non-linear effects, no relation to B2
BMBF: Q.com-H	Optische Quantenschnittstellen zwischen Quanten-punkten und Atomen (QcomHHUB)	semicoductor nanostructures for quantum repeaters, no relation to B2

Pis M. Ballauff & Y. Lu:		
DFG: BA 758/29-3	Hydrogele als aktive Trägerpartikel für Katalysatoren	Using microgels as template for the immobilization of metal nanoparticles and proteins, no relation to B2
DFG: BA 758/27-1	Complexation behavior between polyelectrolyte stars and charged colloids	Investigation of complexation behaviour of polyelectrolyte stars with charged colloids, no relation to B2
DFG: BA 758/28-1	Biofunctional Self-Organized Nano-Structures of Ionic/Non-Ionic Amphiphilic Copolymers, Biopolymers-Biomacremolecules and Nanoparticles…	Studies of biofunctional self-organized nano-structures, no relation to B2
Sino-German center: GZ 962	Exploration on mechanism of morphological transitions of macromolecular self-assemblies and their bio-interest	Studies of the morphological transition of macromolecular self-assemblies, no relation to B2
CSC-DAAD	The design, fabrication, and photocatalytic utility of nanostructured TiO_2 and Au nanoparticles immobilized in thermoresponsive microgels	Investigation of the photocatalytic activity of TiO_2 nanoparticles with plasmonic Au nanoparticles, no relation to B2

3.7 Project funds

3.7.1 Previous funding

The project has been funded within the Collaborative Research Centre since July 2011.

Funds requested

Funding for	2015/2		2016		2017		2018		2019/1	
Staff	Quantity	Sum	Quantity	Sum	Quantity	Sum	Quantity	Sum	Quantity	Sum
PhD student, 75%	2	44.100	2	88.200	2	88.200	2	88.200	2	44.100
Total		44.100		88.200		88.200		88.200		44.100
Direct costs	Sum		Sum		Sum		Sum		Sum	
Small equipment, Software, Consumables	8000		16000		16000		16000		8000	
Other	0		0		0		0		0	
Total	8000		16000		16000		16000		16000	
Major research equipment	Sum		Sum		Sum		Sum		Sum	
€ 10.000 – 50.000	30.000		0		0		0		0	
Total	30.000		0		0		0		0	
Total	82.100		104.200		104.200		104.200		82.100	

(All figures in Euro)

3.7.2 Staff

	No.	Name, academic degree, position	Field of research	Department of university or non-univ. institution	Commitment in hours/week	Category	Funded through:
Available							
Research staff	1	Matthias Ballauff, Prof. Dr.	Colloid physics	HZB and HU Berlin, Physics Dept.	7.5		Grund-ausst.
	2	Oliver Benson, Prof. Dr.	Nano Optics	HU Berlin, Physics Dept.	7.5		Grund-ausst.
	3	Dr. Benjamin Sprenger	Nano Optics	HU Berlin, Physics Dept.	10		Grund-ausst.
	4	Yan Lu, Dr., Group leader	Colloid chemistry	HZB	10		Grund-ausst.
	5	Jie Cao, PhD student	Colloid chemistry	HZB	5		CSC
	6	Annegret Günter, Dr., Postdoc	Colloid physics	HZB	5		BMBF
Non-research staff	7	Klaus Palis, Dipl. Ing., Engineer		HU Berlin, Physics Dept.	5		Grund-ausst.
	8	Regina Rheinländer, Secretary		HU Berlin, Physics Dept.	5		Grund-ausst.
	9	Nikoline Hansen, Dr., Secretary		HZB	5		Grund-ausst.
Requested							
Research staff	10	NN, PhD student	Colloid Chemistry	HZB			
	11	NN, PhD student	Nano Optics	HU Berlin, Physics Dept.			

Job description of staff (supported through available funds):

1. Matthias Ballauff: Scientific and organisational leadership of the project, design and coordination of the experiments, discussion of the results.
2. Oliver Benson: Scientific and organisational leadership of the project, design and coordination of the experiments, discussion of the results.
3. Benjamin Sprenger: Support concerning the design & characterization of opt. setups.
4. Yan Lu: Scientific and organisational leadership of the project, design and coordination of the experiments, discussion of the results.
5. Jie Cao: Support for the morphology investigation of the organic/plasmonic hybrid nano-structures (including TEM, SEM measurements).
6. Annegret Günter**:** Support for the charact. of the Si based nanostructures (including DLS).
7. Klaus Palis: Development of and advisory service for electronic components.
8. Regina Rheinländer: Administrative tasks.
9. Nikoline Hansen: Administrative tasks.

Job description of staff (requested funds):

10. N.N.: One PhD student works on the fabrication of active organic/plasmonic hybrid nano-structures and organic-dielectric nanolasers core-shell structures based on silicon particles. In addition, the assembly of metal core/organic shell structures within the molecular films on the planar surface will be developed. The ensembles in solution and the optical properties will be investigated in HZB and HUB, respectively.
11. N.N.: One PhD student will be responsible for all optical investigations (spectroscopy, photon counting, time-resolved, measurements) performed at HUB. He or she will also carry out numerical simulations of the plasmonic structures.

3.7.3 Direct costs for the new funding period

	2015/2	2016	2017	2018	2019/1
Funds available HUB: Funds available HZB:	1000 1000	2000 2000	2000 2000	2000 2000	1000 1000
Funds requested	8000	16000	16000	16000	8000

(All figures in Euro)

For years **2015/2 and 2019/1**

Small equipment		
Optical and opto-mechanical components (mirrors, splitters, filters, holdrers, …)	EUR	4000 per half year
Consumables		
Optical fibers, mirror coating, chemicals, special electronic components	EUR	1000 per half year
Chemicals (chemicals for synthesis, solvents, dye, silicon nanoparticles, etc.)	EUR	2000 per half year
Analysis (cuvettes for light scattering, TEM and cryo-TEM grids, membrane for ultrafiltration, centrifugation tubes)	EUR	1000 per half year

For years **2016, 2017 and 2018**

Small equipment		
Optical and opto-mechanical components (mirrors, splitters, filters, holdrers, …)	EUR	8000 per year
Consumables		
Optical fibers, mirror coating, chemicals, special electronic components	EUR	2000 per year
Chemicals (chemicals for synthesis, solvents, dye, silicon nanoparticles, etc.)	EUR	4000 per year
Analysis (cuvettes for light scattering, TEM and cryo-TEM grids, membrane for ultrafiltration, centrifugation tubes)	EUR	2000 per year

3.7.4 Major research equipment requested for the new funding period

€ 10.000 - 50.000 for year **2015/2**

EMCCD camera (Andor DU897-UCS-BV) allows for imaging of fluorescence particles down to the level of single molecules. A camera for wide-field imaging with such sensitivity is not available in the labs.	EUR	30.000

3.1 About project B3

3.1.1 Title: Electronic coupling in inorganic/organic semiconductor hybrid structures for opto-electronic function

3.1.2 Research areas: Experimental physics of condensed matter

3.1.3 Principal investigator

Dr. Blumstengel, Sylke (*28.2.1966, German)
Humboldt-Universität zu Berlin, Institut für Physik
Newtonstrasse 15, 12489 Berlin
Phone: +49 (0)30 20937825
Fax: +49 (0)30 20937886
E-mail: sylke.blumstengel@physik.hu-berlin.de

Do the above mentioned persons hold fixed-term positions? yes
End date: 30.6.2015
Further employment is planned until 30.6.2019.

3.1.4 Legal issues

This project includes

1.	research on human subjects or human material.	no
	If applicable: A copy of the required approval of the responsible ethics committee is included with the proposal.	
2.	clinical trials	no
	If applicable: A copy of the studies' registration is included with the proposal.	
3.	experiments involving vertebrates.	no
4.	experiments involving recombinant DNA.	no
5.	research involving human embryonic stem cells.	no
	If applicable: Legal authorization has been obtained.	
6.	research concerning the Convention on Biological Diversity.	no

3.2 Summary

The first funding period focused on the interplay between exciton and charge transfer in HIOS composed of ZnO quantum well (QW) structures and newly-designed ladder-type oligo-phenyls (LOPPs). Due to the large electron affinity of ZnO, most common organic molecules form a type-II interface with ZnO detrimental when targeting at light-emitting applications. Therefore, several strategies were developed in collaboration [Henneberger(A5), Koch(A8)], including energy level adjustment by molecular interlayers and cascade energy transfer, to achieve efficient light emission from the organic layer when excited via Förster-type resonant energy transfer (FRET) from the inorganic part. The expertise gained will be applied in the next funding period to develop HIOS building blocks for light-emitting devices. On the inorganic side, the materials basis will be expanded to InGaN/GaN nanostructures [A11 (Christiansen)] as well as to *p*-type oxides like NiO to complement *n*-type ZnO. LOPPs as well as fluorene-based copolymers will serve as organic emitter materials. Two different working principles will be explored, namely injection and FRET-based devices. Device design and fabrication, especially nanostructuring will be performed in collaboration with B13 (List-Kratochvil). Optical spectroscopy (cw and time-resolved) in conjunction with electrical characterisation will be employed to elucidate fundamentals relevant for device performance.
As second topic, electronic excitations at interfaces between ZnO and organic semiconductors will move into the focus. During the first funding period it was established that excitons dissociate with high efficiency at various ZnO/organic interfaces. Generation of free charges is believed to proceed via the formation of an intermediate charge transfer complex. So far, almost no knowledge exists on the nature and dynamics of this charge separated state. This topic will be addressed by means of linear optical spectroscopy with spatial and temporal resolution, by optical pump probe spectroscopy as well as by electroluminescence (EL) and

photocurrent measurements. Molecules of interest are LOPPs, oligothiophenes and perylene derivatives. As the expected signatures will be weak, the experiments will also be performed at ZnO/organic multiple interfaces resorting on expertise in growth of ZnO on molecular layers developed during the first funding period [A5 (Henneberger)]. Furthermore, small molecules like naphthalene derivatives which are expected to interact more strongly with the ZnO surface than the above mentioned molecules will be employed. In situ measurements of the optical constants of molecular (sub)monolayers on ZnO in combination with photoluminescence (PL) spectroscopy will be performed to study coupling with surface excitons and to detect signatures of a possible hybridisation at the interface.

3.3 Project progress to date

3.3.1 Report and state of understanding

The following goals were defined in the initial funding period proposal:

(i) Providing fundamental understanding of the electronic processes governing HIOS opto-electronic function.

(ii) Development and testing of strategies for tuning structural and electronic properties of HIOS to optimize coupling of optical excitations amongst the constituents, and ultimately, to achieve the hybridisation of excitons.

(iii) Elaboration of design schemes to implement HIOS in opto-electronic/photonic devices for light/laser emission, optical nonlinearity, and light-electrical energy conversion.

The focus of the first funding period was on goal (i) and (ii). While there are still fundamental questions unanswered and research on task (i) and (ii) will continue, task (iii) will be given more space in the second funding period.

Task (i):

State of the art at the beginning of the first funding period

Electronic processes relevant for HIOS function are exciton and/or charge transfer across the inorganic/organic (i/o) semiconductor interface. The occurrence of these transfer processes had already been experimentally verified in our own previous work as well as by other groups when the project started [1-4]. The work in the first funding period targeted at an in-depth understanding of the interplay between exciton and charge transfer processes in order to learn how to realise efficient HIOS for light-emitting applications.

Results of the first funding period

Energy vs. charge transfer in ZnO/LOPP HIOS (cooperation with A3)

To achieve high performance functional elements for light-emitting applications, both, the inorganic/organic exciton conversion efficiency by FRET as well as the luminescence yield of the organic layer should ideally reach 100%. On the inorganic side, we focused on ZnO/ZnMgO QW structures. In collaboration with A3(Hecht) considerable effort was devoted to design suitable LOPP matching spectrally ZnO. These molecules feature narrow absorption bands with high oscillator strength as well as very high PL quantum yields [28]. All these properties predestine these molecules as perfect FRET partners for ZnO. Two representatives of the LOPP family are shown in Fig. 1a. The transition energies of the molecules can be fine-tuned via attachment of different substituents at the bridging carbon atoms so that the $S_{0,\square=0} \rightarrow S_{1,\square=0}$ transition can be moved into resonance with the ZnO QW PL to ensure effcient excitonic FRET. By attaching spiro groups, the photostability [28], film forming properties and solid state luminescence yield are enhanced. Therefore, this molecule is chosen for FRET experiments. Combined time-resolved PL and PL excitation (PLE) spectroscopy indeed indicate FRET efficiencies reaching 80% at low temperature (at 5 K) in L4P-Sp3/ZnO/ZnMgO HIOS of optimized design (see inset of Fig. 1b). However, as seen in Fig. 1b, the PL yield of the HIOS is very low, much lower than the yield of the isolated components. The QW PL is quenched due to FRET but no light appears in the spectral range of the molecular emission. In collaboration with A8(Koch),

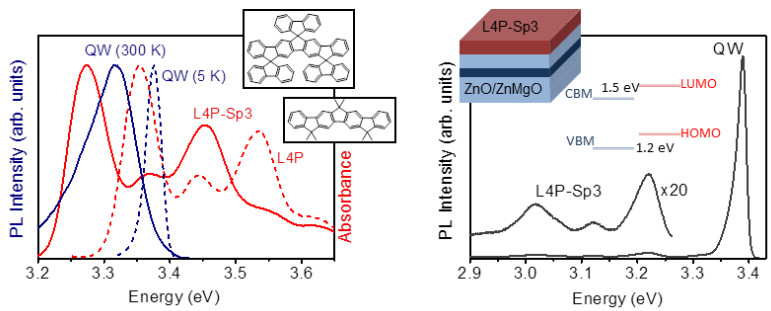

Fig. 1 a) Spectral overlap of the absorption spectra of L4P diluted in PMMA (red dashed) and a L4P-Sp3 thin film (red solid) with ZnO PL spectra recorded at room (blue solid) and low (5 K) (blue dashed) temperature. b) Low temperature (5 K) PL spectrum of the HIOS schematically depicted in the inset and i/o energy level off sets as measured

an unfavorable type-II energy level alignment between the L4P-Sp3 frontier molecular levels and the ZnO band edges at the hybrid interface (see inset of Fig. 1b) was identified as the major loss channel. In such a configuration, an excited molecule will transfer an electron to the ZnO conduction band resulting in quenching of the molecular emission. Indeed, time-resolved PL data show that the efficiency of the process can reach 90%. Thus 9 out of 10 excitons generated via FRET in the organic layer do not decay radiatively. Such HIOS is certainly unsuited for light-emitting applications. Unfortunately, the same situation is also encountered at other large band gap semiconductor (GaN)/molecule interfaces [5]. Furthermore, due to the very large electron affinity of ZnO, the problem cannot simply be healed by choosing other molecules with larger electron affinity. Therefore, substantial effort of the first funding period was devoted to shape the i/o interface such that unwanted exciton dissociation is turned off.

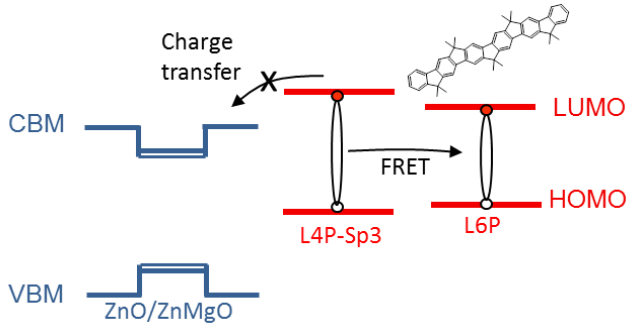

Fig. 2 Competition between charge transfer at the i/o interface and secondary FRET within the organic layer composed of a blend of L4P-Sp3 and L6P. The structure of L6P is shown as well.

One successful approach is the introduction of a secondary FRET step within the organic layer [30]. The challenge was to find a suitable system where the secondary FRET step is faster than charge transfer at the i/o interface (see Fig. 2). A newly designed ladder-type sexiphenyl (L6P) which spectrally perfectly matches L4P-Sp3 fulfills this condition: In the cascade HIOS featuring a L4P-Sp3:L6P blend, the secondary FRET step occurs with an efficiency close to 100 % rendering exciton dissociation negligible at the i/o interface and recovering the molecular PL yield. Raising the temperature, the efficiency of the primary i/o FRET step drops from nearly 80% to 32% at room temperature. This result appears disappointing on a first glance; however, it has to be interpreted in the context of the radiative properties of QW excitons: while the radiative decay rate intrinsically decreases with increasing temperature, nonradiative recombination is thermally activated resulting generally in low PL yields of inorganic semiconductor QW structures at room temperature. Our results indicate that via FRET a substantial fraction of excitons which would otherwise decay non-radiatively in the QW can be recovered by transfer to the organic layer resulting in a much higher total PL yield of the cascade HIOS compared to the isolated systems. Employing a secondary FRET step is one way to achieve highly efficient HIOS for light emission. However, a perhaps more versatile approach is to tune the alignment of the energy levels of the frontier molecular orbitals with respect to the band edges of the inorganic semiconductor according to the desired function of the HIOS. This will be discussed in the next section.

Work **outside the Sfb** was devoted to uncover the role of exciton dimensionality (i.e. free vs. localized) on the FRET efficiency and the use of cascade energy transfer to produce white light emission [6,7]. These studies were performed on planar GaN-based HIOS. FRET in 3D nanostructures composed of InGaN/GaN nanorods covered by a polyfluorene layer was demonstrated [8]. Furthermore, energy transfer of triplet excitons in tetracene and pentacene generated via singlet fission to PbS nanoparticles was studied to enhance the light harvesting efficiency in photovoltaic cells [9,10]. Charge transfer at ZnO/polymer interfaces was studied addressing in particular the role of intermediate charge transfer states [11]. Furthermore, the effect of defects in the ZnO near surface region and of adsorption induced interface states on the energy level alignment and charge transfer at ZnO/organic (fullerene, PTCDI, perylene) interfaces was elaborated [12-14].

Task (ii):

State of the art at the beginning of the first funding period

To achieve HIOS with advanced functionality either for efficient light emission or charge carrier generation after light absorption, the electronic structure of the i/o interface must be optimized. While strategies for tuning of the work function of metals were established at the start of the first funding period, no knowledge existed how to tune semiconductor surfaces. It was known that the energy offsets between the frontier molecular orbitals and the valance band offsets depend on the orientation of the molecules on the surface [15], whereby the change can be as large as 1 eV. For practical application of HIOS tuning over larger energy ranges independent on the structure of the molecular film and the crystal face of the inorganic semiconductor system was highly demanded.

Results of the first funding period

1) Tuning of the energy offsets at the i/o interface

In collaboration with A5(Henneberger), A8(Koch), B4(Scheffler/Rinke) it was demonstrated that by adsorption of the donor molecule 2,3,5,6-tetrafluoro-7,7,8,8-tetracyanoquinodimethane (F4TCNQ) the work

function of ZnO can be massively increased by up to 2.8 eV [31,32]. These studies were managed by A8(Koch) and B4(Scheffler/Rinke) and are discussed in the respective reports.

Another approach pursued with an external collaboration is the attachment of SAMs with dipole-bearing moieties on ZnO via phosphonic acid anchor groups [33]. The molecules used in the study are depicted in Fig. 3. The electron-donating methoxy tail group results in a positive dipole, pointing away from the surface, which decreases the work function, while the electron-withdrawing cyano tail group introduces a negative dipole, which increases the work function. The tuning range of epitaxial ZnO(000-1) surfaces extends from -300 meV … 500 meV. Furthermore, by mixing the molecules a continuous shift of the work function is possible. The tuning range achieved with those molecules is, however, too small to achieve a type-I energy level alignment of ZnO with common conjugated organic molecules which is needed to construct HIOS with high luminescence yield.

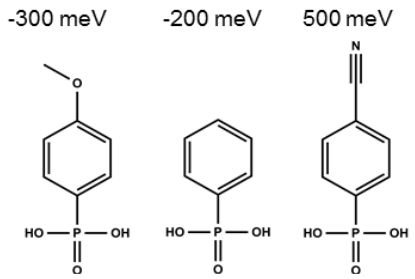

Fig. 3 Chemical structure of SAMs and achieved work function shift of the exitaxial ZnO(000-1) surface.

In collaboration with A2(Hecht), A5(Henneberger), A8(Koch) it was discovered that a much more substantial lowering of the work function of ZnO by 1.5 eV can be achieved by adsorption of a monolayer of the donor molecule $[RuCp^*mes]_2$ [NK7]. Inserting a interlayer of this molecule between ZnO and L4P-Sp3, the HOMO (LUMO) level of L4P-Sp3 can indeed be tuned into resonance with the VBM (CBM) of ZnO [A8(Koch)]. In the following, the effect of the tuning of the energy levels on exciton and charge transfer is described.

2) Effect of a $[RuCp^*mes]_2$ interlayer on exciton and charge transfer [34]

To reveal the effect of the energy level tuning, ca. one monolayer of $[RuCp^*mes]_2$ is deposited on a part of a ZnO/ZnMgO QW structure which is subsequently overgrown with a thin layer (3 nm) of L4P-Sp3 (see Fig. 4a and inset of 4b). Incorporation of Mg into ZnO widens the band gap of ZnO so that ZnMgO/L4P-Sp3 is expected to form a type-I interface as schematically depicted in Fig. 4a. Combined time-resolved PL and PLE spectroscopy proofed that the high FRET efficiency is maintained in the HIOS with the $[RuCp^*mes]_2$ interlayer while at the same time the electron transfer efficiency is strongly reduced to 45% resulting in a substantial recovery of the molecular PL yield by a factor of 7 (see Fig. 4b). However, there is still a substantial fraction of excitons quenched at the i/o interface not expected the present energy level alignment hinting at the presence of interface states. Though the principle feasibility of the approach is shown further work is required to identify and eliminate interface states acting as electron acceptors.

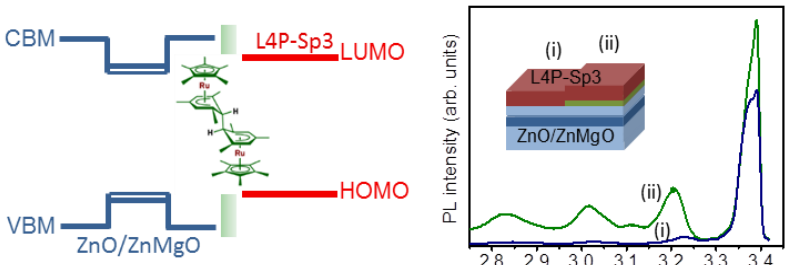

Fig. 4a) Schematic energy level alignment at the interface of a ZnO/ZnMgO QW and L4P-Sp3 containing a $[RuCp^*mes]_2$ interlayer. b) PL spectra of HIOS without (i) and with interlayer (ii). The HIOS layout is shown in the inset.

Outside the Sfb, intensive research activity is devoted to the question how to shape the interface between ZnO (or other transparent conductive oxides) with conjugated molecules or polymers to achieve highly efficient charge separation for photovoltaic applications. These experiments were performed mostly on sol-gel or ALD ZnO thin films and focused on the effect of energy offsets, various surface treatments and the intentional introduction of surface states on the charge generation efficiency [12,14,16]. Work function tuning of ZnO by dipole-bearing phosphonic acid interlayers was shown in parallel to our work [17]. Furthermore, the function of fullerene interlayers on charge transfer between ZnO and polymers was explored [11].

Task (iii):

State of the art at the beginning of the first funding period

Targeted functions of HIOS are either light emission or charge carrier generation after light absorption. Hybrid light-emitting diodes (LED) utilizing a FRET excitation scheme was (and is) not realized yet. However, a related finding had been reported: namely luminescence of colloidal nanocrystals could be excited by electrical pumping of InGaN/GaN nanorod *p-i-n* junctions [18]. Furthermore, hybrid LEDs based on organic/inorganic *p-n* junctions had been demonstrated displaying however poor performance. Examples are polymer/ZnO nanorod and molecule/InGaN/GaN QW light emitting diodes (LEDs) [19,20]. For implementation of HIOS in devices, overgrowth of the organic layer with an inorganic semiconductor is necessary which are typically prepared under conditions not compatible with organic molecules. ZnO is an exception and the principle feasibility of growth of ZnO/organic/ZnO HIOS was shown [21].

Results of the first funding period

1) ZnO-based light-harvesting and light-emitting devices

During the first funding period, a UHV system was completed with a metal deposition chamber in order to produce functional HIOS elements. Our first efforts concentrated on layered HIOS which can either harvest or emit light. To be completed.

Outside the Sfb, ZnO/organic junctions are intensively investigated whereby ZnO serves either as charge collection layer in photovoltaic cells or as injecting contact in LEDs [12,16]. Related work important for the next funding period regards the progress in realization of purely inorganic LEDs with ZnO as emitter material. As widely accepted by now, reliable *p*-doping of ZnO is not possible. Therefore, ZnO has to be combined with another *p*-type semiconductor to realize bipolar heterojunctions. GaN appears as a natural choice, and indeed progress has been made to realize electroluminescence (EL) *p*-GaN/*n*-ZnO heterojunctions with the emission originating either from the ZnO and/or GaN side of the diode [22-24]. Alternatively, also *p*-NiO/*n*-ZnO LEDs are demonstrated [25].

New methods and results obtained in collaboration with and by other projects of the CRC important for projected goals of the second funding period:

In collaboration with A5 (Henneberger) and Z2 (Kirmse), overgrowth of nanocrystalline *p*-sexiphenyl (6P) films by molecular beam epitaxy (MBE) was studied and it was shown that the ZnO-on-6P interface is well-defined and abrupt on a monolayer level [35] as described in the report of A5 (Henneberger). The experimental basis was expanded A5 (Henneberger) and it is now possible to measure *in situ* optical constants of (sub)monolayer organic films while deposited on semiconductor (or other) surfaces by differential reflectance spectroscopy. This will be needed to assess the electronic and optical properties of molecules in direct contact with an underlying semiconductor surface. So far recorded thin film spectra of PTCDI served as input for modelling of intermolecular interactions performed by B4 (Körzdörfer) und B6 (May) [36]. The presence of surface excitons on ZnO(000-1) and ZnO(10-10) was uncovered in collaboration with A5 (Henneberger), B5 (Kühn/Elsässer) [37] and by B9 (Stähler/Wolf) [26], respectively. The coupling of such surface excitons with adjacent molecules will be explored in the next funding period. Efficient *n*-doping of ZnO with Ga up to a level of 10^{20} cm^{-3} maintaining high carrier mobilities of ca. 50 cm^2/Vs was realized by A5 (Henneberger) [27].

Changes with respect to plans defined for the first funding period:

Preparation of hybrid microcavities and exploration of photon-mediated coupling of Frenkel and Wannier-Mott excitons could not be realized due to lack of capacities as ½ requested PhD was not granted. The topic is part of a PhD thesis funded otherwise and supervised by A5 (Henneberger).

References

[95] G. Itskos et al., Phys. Rev. B **76**, 035344 (2007).
[96] S. Chanyawadee et al., Phys. Rev. B **77**, 193402 (2007).
[97] S. Blumstengel et al., Phys. Rev. Lett. **97**, 237401 (2006).
[98] S. Blumstengel et al., Phys. Rev. B **77**, 085323 (2008).
[99] G. Itskos et al., Appl. Phys. Lett. 102, 063303 (2013).
[100] J.J. Rindermann et al., Phy.Rev.Lett. **107**, 236805 (2011).
[101] G. Itskos et al., Nanotechnology **20** , 275207 (2009).
[102] R. Smith et al., Nano Lett., 13, 3042 (2013).
[103] M. Tabachnyk et al., Nature Mater. 13, 1033 (2014).
[104] N.J. Thompson et al., Nature Mater. **13**, 1039 (2014).
[105] Y. Vaynzof et al., Phys.Rev.Lett. **108**, 246605 (2012).
[106] P. Schulz et al., Adv. Funct. Mater. (2014).
[107] P. Winget et al., Adv. Mater. **26**, 4711 (2014).
[108] C. Strothkämper et al., J. Phys. Chem. C **117**, 17901 (2013).
[109] S. Blumstengel et al., Phys. Chem. Chem. Phys. **12**, 11642 (2010).
[110] K.P. Musselman et al., Adv. Funct. Mater. **24**, 3562 (2014).
[111] S.R. Cowan et al., Adv. Funct. Mater. **24**, 4671 (2014).
[112] S. Chanyawadee, et al., Adv. Mater. **22**, 602 (2010).
[113] J.H. Na et al. , Appl. Phys. Lett. **94**, 213302 (2009).
[114] C.Y. Lee, et al., Nanotechnol. **20**, 425202 (2009).
[115] S. Blumstengel et al., Adv. Mater. **21**, 4850 (2009).
[116] D. J. Rogers et al., Appl. Phys. Lett. **88**, 141918 (2006).
[117] X.-M. Zhang et al., Adv. Mater. **21**, 2767 (2009).
[118] J. J. Dong et al., Appl. Phys. Lett. **100**, 171109 (2012).

[119] H. Long et al., Appl. Phys. Lett. **95**, 013509 (2009).
[120] J.C. Deinert et al., Phys. Rev. Lett. **113**, 057602 (2014).
[121] S. Sadofev et al., Appl. Phys. Lett. **102**, 181905 (2013).

3.3.2 Project-related publications

[122] B. Kobin, L. Grubert, S. Blumstengel, F. Henneberger, and S. Hecht, " Vacuum-processible ladder-type oligophenylenes for organic-inorganic hybrid structures: Synthesis, optical and electrochemical properties upon increasing planarization as well as thin film growth ", J. Mater. Chem., **22**, 4383 (2012).
[123] B. Kobin, F. Bianchi, S. Halm, J. Leistner, S. Blumstengel, F. Henneberger, and S. Hecht: "Green Emission in Ladder-type Quarterphenyl: Beyond the Fluorenone-Defect" Adv. Funct. Mater. published online DOI: 10.1002/adfm.201402638.
[124] F. Bianchi, S. Sadofev, R. Schlesinger, B. Kobin, S.Hecht, N. Koch, F. Henneberger, and S. Blumstengel, "Cascade energy transfer versus charge separation in ladder-type oligo(p-phenylene)/ZnO hybrid structures for light-emitting applications, submitted.
[125] R. Schlesinger, Y. Xu, O.T. Hofmann, S. Winkler, J. Frisch, J. Niederhausen, A. Vollmer, S. Blumstengel, F. Henneberger, P. Rinke, M. Scheffler, and N. Koch, „ Controlling the work function of ZnO and the energy-level alignment at the interface to organic semiconductors with a molecular electron acceptor ", Phys. Rev. B **87**, 155211 (2013).
[126] Y. Xu, O.T. Hofmann, R. Schlesinger, S. Winkler, J. Frisch, J. Niederhausen, A. Vollmer, S. Blumstengel, F. Henneberger, N. Koch, P. Rinke, and M. Scheffler, „Space-charge transfer in hybrid inorganic-organic systems", Phys. Rev. Lett. **111**, 226802 (2013).
[127] N. Kedem, S. Blumstengel, F. Henneberger, H. Cohen, G. Hodes, and D. Cahen, „ Morphology-, synthesis- and doping-independent tuning of ZnO work function using phenylphosphonates ", Phys. Chem. Chem. Phys. **16**, 8310 (2014).
[128] R. Schlesinger1, F. Bianchi1, S. Blumstengel1, C. Christodoulou1, R. Ovsyannikov2, B. Kobin3, K. Moudgil4, S. Barlow4, S. Hecht3, S. R. Marder4, F. Henneberger1, N. Koch1 "Efficient light emission from inorganic/organic semiconductor hybrid structures by energy level tuning", submitted.
[129] S. Blumstengel, H. Kirmse, M. Sparenberg, S. Sadofev, F. Polzer, and F. Henneberger, „ Texture and morphology of ZnO grown on nanocrystalline p-sexiphenyl thin films ",J. Cryst. Growth **402**, 187 (2014).
[130] J. Megow, T. Körzdörfer, T. Renger, M. Sparenberg, S. Blumstengel, F. Henneberger, and V. May, ''Calculating optical absorption spectra of thin polycrystalline films: Structural disorder and site-dependent molecular electronic polarization", https://www.physik.hu-berlin.de/sfb951/publications.
[131] S. Kühn, S. Friede, S. Sadofev, S. Blumstengel, F. Henneberger, and T. Elsässer, "Surface excitons on a ZnO (000-1) thin film", Appl. Phys. Lett. **103**, 191909 (2013).

3.4 Research plan

The projected research is a continuation of the work initiated in the first funding period. Based on the knowledge generated the activities will be bundled into two subprojects.

Subproject 1: Development of HIOS building blocks for light-emitting applications

Goals and work plan:
In the first funding period we have identified an intrinsic non-radiative loss channel present at the i/o interface and developed strategies for its deactivation paving thus the way for HIOS with high FRET efficiency and luminescence yield. In the next funding period, the activity will be pursued further targeting finally at the realisation of electrically driven FRET-based HIOS light emitters. Achieving of this goal will require concerted action of several projects. Main partners will be A5(Henneberger) [provides (Zn, Mg,Cd)O heterostructures], A8(Koch) [energy level adjustment], A11 (Christiansen) [provides GaN/InGaN heterostructure, support in device characterization] and B13(List-Kratochvil) [nanostructuring, support in device characterization]. Project B3 will dedicate substantial efforts to achieve a thorough understanding of the physics governing the function of individual components of HIOS light emitters.
The design and working principle of a FRET-based light-emitter is as follows: The HIOS is built of an inorganic semiconductor QW with a layer of conjugated organic molecules in close proximity. This FRET couple is integrated in a *p-i-n* configuration to allow for electrical pumping of the QW. Current commercial state-of-the-art lighting utilizes blue emission from InGaN/GaN-based LEDs radiatively exciting inorganic phosphor material(s) providing the longer wavelength emission and leading to generation of light of the desired color. In contrast, here we intend to use non-radiative FRET to pump an organic emitter layer. This

approach promises among others higher color conversion efficiencies, lower power consumption, better color rendering and downsizeability.
Two principle designs are sketched in Fig. 6. In the two-dimensional (2D) structure (Fig. 6a), a *p*(*n*)-type layer is overgrown with an intrinsic layer on top of which an array of molecular islands is deposited. The structure is completed with a *n*(*p*)-type layer. Recombination of carriers will take place in the intrinsic (QW) layer and after the FRET step light is emitted from the organic inclusion and if needed for color tuning also partially from the QW. The 3D structure is based on multiple QW (MQW) nanorod LED arrays covered by a layer of organic molecules. Again, excitons generated in the QWs are transferred to the organic layer via FRET supported by exciton diffusion.

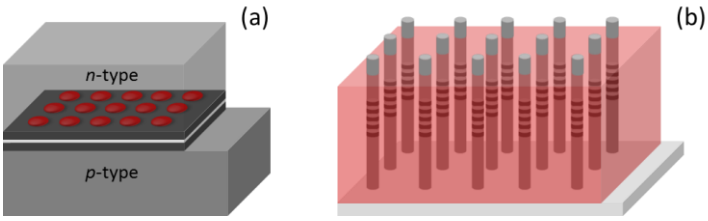

Fig. 6 Schematic depiction of (a) 2D and (b) 3D FRET-based HIOS building blocks for light-emitting devices. Different shades of gray represent inorganic semiconductor layers with different function while the organic molecular inclusion (a) or coating (b), respectively, is depicted in red.

Alternatively, also injection-based HIOS light emitters are possible. Here, the organic layer is sandwiched between two inorganic semiconductor layers providing electron and holes. Such structures can reversely also serve for charge generation after light absorption. Compared to conventional organic LEDs or photovoltaic cells, these structures offer the advantage of full transparency and ease of fabrication as they can be even realized with one type of semiconductor given that the interfacial energy level alignment is properly adjusted.
The proposed structures consist of many interfaces and rely on the interplay of several subcomonents. The function of each will be essential for the performance of the device. The realization of the structures requires advancement of growth and nanostructuring techniques. The contributions of B3 are listed in the following.
Task 1: Planar electroluminescent ZnO-based *p*-*i*-*n* or *p*-*n* heterojunctions.
As ZnO cannot reliably *p*-doped we extend our material basis to *p*-GaN and other transparent conductive oxides such as *p*-NiO to produce 2D bipolar heterojunctions. Such ZnO-based heterojunction LEDs are reported in the literature. Furthermore, our group has developed recently experience in epitaxial growth of *n*-ZnO on *p*-GaN and first purely inorganic LEDs are prepared. GaN/ZnO forms a type-II interface. Detailed knowledge on the interface formation does not exist yet and the origin of the electroluminescence (EL) is so far not resolved. Therefore, research is required to learn how via introduction of carrier blocking, confinement or polarity inversion layers, the recombination zone in the structure can be shifted to the desired position. The same holds also n-ZnO/p-NiO heterojunctions. For support in characterization of such purely inorganic heterojunctions we will rely on the expertise present in A11 (Christiansen).
Task 2: Energy and charge transfer at the i/o interface
Targeted HIOS light-emitters rely on efficient FRET and high luminescence yield of organic layer. We will evaluate exciton and charge transfer in HIOS designs compatible with electrical pumping by means of optical spectroscopy and test new strategies developed by A4(Heimel), A(8) Koch, A(11) Christiansen to optimize i/o interfaces via surface functionalization. In the first funding period, we have learned how to properly shape the i/o interface of ZnO-based HIOS for an requested opto-electronic function. However, the structures are not fully optimized yet and fundamental open questions remain, namely: How does strain-induced quantum confined Stark effect present in polar quantum structures affects FRET? What is the role of length-scales? Can exciton diffusion assist energy transfer? What is the underlying mechanism of the temperature dependence of the FRET efficiency? Is it possible to switch off non-radiative bypasses present at HIOS interfaces even with properly adjusted energy levels and related to that, what is the role of surface/interface states? How is excitonic coupling and charge transfer modified under high-excitation conditions? Can energy transfer assisted optically pumped lasing be achieved in the organic layer?
Our knowledge on i/o FRET and charge transfer will be applied to GaN-based HIOS which are much less explored yet. Energy level adjustment will certainly be also an issue here. Furthermore, especially in the case of InGaN/GaN nanorods surface band bending and exciton dead layers may hamper efficient excitonic coupling with the surrounding molecular layer as revealed by B8 (Riechert/Grahn) and surface passivation will most likely be required. The dimensions of the nanorods must be properly adjusted as FRET is a short range process and assistance of exciton diffusion is required to achieve efficient energy transfer to the organic layer.
Similarily, interfacing of organic molecules with NiO is barely explored yet. NiO is believed to act as a hole collecting layer. We will study charge transfer at NiO/organic interfaces.
Task3: Electrically driven HIOS
Finally, electrically driven HIOS will be prepared utilizing optimized building blocks and EL generation demonstrated on a proof-of-concept level. Combined with optical spectroscopy and electrical

characterization also of individual components we will uncover the origin of EL and excitation pathways (injection, exciton diffusion, radiative vs. non-radiative energy transfer).

Materials and methods

Materials: The 2D structure can be produced by embedding the i/o FRET couple either between a bottom *p*-GaN layer and a top *n*-ZnO layer or between a bottom *n*-ZnO layer and a top *p*-NiO layer. MBE-grown QW structures based on (Zn,Cd,Mg)O are provided by by A5 (Henneberger). Using either *a*-plane, *r*-plane Al_2O_3, MgO substrates, polar 000-1)- and non-polar (10-10) and (11-20) structures can be prepared, respectively. The layers can be *n*-doped with Ga. Planar or nanorod (Ga,In,Al)N will be provided by A11 (Christiansen). *p*-Gan is commercially available while *p*-NiO will be prepared by e-beam deposition. As organic emitter molecules, LOPPs have proven successful and we will continue to use these molecule and develop them further A3(Hecht). Examples are LTPPT-Sp3 to decrease the optical gap and fluorinated LOPPs to increase the electron affinity. For solution processing, commercially available polyfluorenes with matching optical gap will be employed. Furthermore, molecules covalently linked to the semiconductor surfaces will be tested. These molecules are prepared by A3(Hecht) with theoretical support by A4(Heimel) whereby it is planned to incorporate even dipolar units to adjust interfacial energy levels. Alternatively, tuning of energy levels will be performed either with vacuum deposited donor and acceptor interlayers (so far $[RuCp^*mes]_2$ and HATCN) or dipole-bearing self-assembled monolayers.

Preparation of HIOS components: For sample preparation, an UHV deposition system consisting of growth chambers for organic molecules by organic molecular beam deposition (OMBD) and contacts (metals, MoO_3, etc.) and a glove box are available. Both can be connected via a HV transfer vessel to the MBE system dedicated to ZnO growth to assure preparation of well-defined interfaces.

Deposition of molecular nano-islands (2D structure): The size of the nano-islands must match the exciton diffusion length in ZnO or GaN which is ca.100-200 nm. Such islands can be prepared with selected molecules employing a Vollmer-Weber growth mode. A more versatile method is the use of nanoproximity masks [provided by B13(List-Kratochvil)] allowing nanostructuring on the required length scale.

Deposition of the top inorganic semiconductor layer (2D structure): Building on knowledge acquired in the first funding period *n*-type ZnO top layers with high structural quality and carrier mobility can be produced on nano-scale organic inclusions. If shape and size are properly chosen, even epitaxial lateral overgrowth with coalescence might be achieved. Growth regimes for preparation of well-defined NiO-on-organic interfaces need to be elaborated. The structural properties will be checked by TEM in collaboration with Z2(Koch/Kowarik).

Preparation of molecular coating of InGaN/GaN nanorods (3D structure): Molecular layers will be prepared by OMBD or spin coating. Alternatively, covalent linkage of molecules via anchor groups will be tested.

Methods: Energy and charge transfer will be studied by combined cw PL and PL excitation spectroscopy as well as time-resolved PL measurements with ps…ns resolution also in confocal geometry and as a function of temperature. Tracking the transient emission on both donor and acceptor wavelength will allow for extraction of the kinetics, time constant, and efficiency of the transfer process as well as of the electronic coupling strength. The effect of quantum confined Stark effect on FRET will be evaluated by comparing HIOS utilizing polar and non-polar QW structures. FRET will also be investigated under high-excitation conditions, i.e., in a regime where stimulated emission occurs. ASE spectra will be studied in waveguide configurations and gain spectra by the variable-stripe-length method. The role of length scales will be assessed by changing the physical size of the molecular nano-islands. FRET from InGaN/GaN nanorods to a molecular coating will be studied in two configurations; either with GaN rods containing MQW layers (see Fig. 6b) or core-shell nanorods where the InGaN QW and the top GaN barrier form a cylindrical coating around an inner GaN rod. Especially the latter will be useful when investigating the effect of surface functionalization and geometric size on the PL yield of the nanorods in the near surface region and the FRET efficiency. To evaluate the contribution of exciton diffusion, the MQW nanorods are better suited. These experiments will be accompanied by FRET studies in planar InGaN/GaN structures. Theoretical support in interpreting the experiments will be provided by B12 (Knorr/Richter). Electrical measurements will be performed on the two structure types depicted in Fig. 6a and b completed by contacts as well as in sandwich-type injection based HIOS. *p-i-n* InGaN/GaN nanorods on conductive substrates will be developed by A11 (Christiansen). Those will be either filled with the molecular acceptor layer or in case that a covalently linked molecular layer yields better results by a transparent material (for instance PMMA). Contacts and nanostructuring will be developed in collaboration with A11 (Christiansen) and B13 (List-Kratochvil). Electrical characterization will include current-voltage, brightness-voltage and EL measurements.

Timeline

Year 1 Investigation and optimization of FRET in ZnO/LOPP-based HIOS, verification of FRET in planar and nanorod InGaN/GaN. Choice of suitable acceptor molecules for InGaN/GaN structures.

Year 2 Study effect of surface functionalisation on FRET efficiency and PL yield in GaN-based HIOS. Preparation of organic nano-islands and inorganic overgrowth. FRET in 2D structure (Fig. 6a). Electrical characterization and realization of EL in injection-based HIOS.
Year 3 Optimisation of 3D structure (Fig. 6b) with regard to FRET efficiency and PL yield. Choice of material combination, p-GaN/n-ZnO or n-ZnO/p-NiO for planar structure (Fig. 6a). Realization of electrically pumped light-emission in 2D structure.
Year 4 Realization of electrically pumped light-emission in 3D structure, FRET under high excitation conditions, amplified spontaneous emission.

Subproject 2: Electronic excitations at HIOS interfaces

Goals and work plan:
Above described excitonic coupling via FRET is based on dipole-dipole interaction which is long-ranged acting over of several nm distance. In subproject 2, the focus is on shorter range interactions requiring overlap of wavefunctions of organic and inorganic semiconductor and on charge transfer across the i/o interface.
Time-resolved PL measurements performed in the first funding period established that Frenkel excitons optically excited in the organic layer are quenched with high efficiency at the ZnO interface. These measurements provide, however, no information about the fate of the separated charges. In the literature, it is discussed that generation of separated charges occurs via an intermediate coulombically bound electron-hole pair state with the electron residing on the inorganic and the hole on the organic side. This state is in the following termed hybrid charge transfer exciton (HCTE). It is widely acknowledged that this intermediate state critically determines the efficiency of charge separation. However, the actual nature as well as relaxation and recombination pathways of HCTEs are largely unknown. So far reported experiments (pump-probe spectroscopy, (photo)current-voltage measurements) provide only indirect information and are furthermore performed on very complex interfaces. Direct spectroscopic signatures were only very recently observed within the CRC [B7 (Neher)] in EL experiments. In the second funding period substantial efforts within the CRC will be directed towards understanding and control of charge transfer process at i/o interfaces. This involves complementary experiments undertaken by B7 (Neher), B9 (Stähler) and this project in close interaction with projects B4(Körzdörfer/Scheffler/Rinke), B6 (May) and B11 (Draxl) providing a theoretical description and projects A3 (Hecht), A4 (Heimel) and A8 (Koch) developing molecules and strategies for functionalization of the i/o interface, respectively.
The contribution of B3 will be optical spectroscopy combined with EL and photocurrent measurements performed on ZnO/organic interfaces prepared under UHV conditions systematically varying the semiconductor surface: By using differently terminated epitaxial ZnO surfaces ((0001), (000-1), (10-10) and (11-20)), alloying with Mg or Cd, hydroxylation/hydrogenation, doping, adsorption of donor/acceptor or dipolar molecular interlayers (physisorbed or covalently bonded), the effect of the energy offsets between frontier molecular orbitals with respect to valance and conduction band, the presence of surface and interface states, band bending and associated charge accumulation layers on charge transfer and HCTE will be evaluated. Additionally, we will take a closer look at the optical properties of molecule directly in contact with the semiconductor surface. Especially, we will study interaction with surface excitons found in ZnO(000-1) as well as ZnO(10-10) and search for signatures of hybridization of molecular orbitals. We will study PL properties of such hybridized states and evaluate the effect on the charge transfer process. In parallel, B11 (Draxl) will develop a theoretical description (wave functions and spectra) of interfacial hybrid excitations.

Materials and methods:
Materials: On the inorganic side, the focus will be on MBE-grown (Zn,Mg,Cd)O [provided by A5 (Henneberger)]. Alloying of ZnO with Mg and Cd will be employed complementary to introduction of molecular interlayers to tune the energy levels at the hybrid interface. Epitaxial (0001), (000-1), (10-10), (11-20) surfaces will be obtained by using proper substrates. On the organic side, we will use beside the LOPPs (and its newly developed siblings, see above) also oligothiophes (parent molecules as well as functionalized by attaching anchor groups also with dipole bearing units A3 (Hecht)). Furthermore, we will employ perylene derivatives (PTCDI, PTCDA) as well as NTCDA. Those molecules possess larger electron affinities than LOPPs or oligothiophenes and typically adsorb flat on surfaces allowing maximal coupling with the ZnO underlay. Especially the smaller NTCDA which spectrally also matches ZnO will be promising to study the interaction with surface excitons and hybridization.
Preparation of HIOS: Facilities and growth techniques described above will be used for HIOS growth. For optical experiments, we will fabricate bilayer but also multilayer structures as oscillator strength and PL yield of HCTE will be extremely weak. To study optical spectra of molecules at the i/o interface and detect signatures of hybridization, submonolayers will be grown on different ZnO surfaces and investigated *in situ* and *ex situ*. The coverage has to be kept ideally low enough to avoid aggregation that might blur the effect of

the interaction with the ZnO surface. For *ex situ* experiments, the submonolayers will be capped immediately after deposition by a transparent cover to avoid postgrowth dewetting and aggregate formation. For photocurrent and EL measurements, a (Zn,Mg,Cd)O layer will be grown on heavily doped ZnGaO. Subsequently, the organic layer(s) will be deposited and the structure completed by a suitable top contact (e.g. MoO_3/Ag).

Methods:

Time-resolved PL in the visible spectral range in ps..ns time domain will be performed to measure Frenkel exciton lifetimes as a function of thickness of the organic layer and to obtain the characteristic time and efficiency of exciton dissociation at the i/o interface. These measurements will be used on the one hand to identify suitable material couples and on the other hand to evaluate the impact of the ZnO surface termination, the band gap and the effect of molecular interlayers.

Integrated and gated (i.e. delayed) PL and EL measurements will yield emission spectra of HTCEs and time-resolved PL in the NIR in ps..ns time domain information of the dynamics of the state again as a function of a specific ZnO surface. The complementary HTCE absorption spectrum will be obtained via the external quantum efficiency (EQE) measurements of photogenerated charge carriers. Photoreflectivity and photo-induced absorption will be provide absorption spectra of molecular polarons as well as information on the recombination dynamics on long time-scales (□s…ms). Field and temperature dependence of the photocurrent will be evaluated for indications of HTCE formation and the presence of trap states. Furthermore, we will measure PL, EL (molecular and HCTE) and/or the photocurrent in external magnetic fields to obtain information about the recombination pathway of HTCE and the role of triplet states. Complementary Kelvin probe AFM will be performed to measure the work function change of pristine epitaxial ZnO surfaces induced by hydroxylation/hydrogenation as well as by adsorbed donor/acceptor or dipole bearing molecular monolayers.

In situ differential reflectance spectroscopy and *ex situ* PL measurements (cw and time-resolved) of molecular submonolayers will allow to study interaction of molecular submonolayers with ZnO surface excitons and interfacial hybridization.

Timeline

Year 1 Overview time-resolved PL study (VIS) of various molecules-ZnO surface couples, measurement of HTCE spectra via PL, EL and EQE measurements. Kelvin probe AFM of epitaxial ZnO.

Year 2 Dynamics of HCTE and polarons. Field and temperature dependence of photocurrent. Modelling of photocurrent. DRS and PL of molecular submonolayers on different ZnO surfaces.

Year 3 Study of effect of interface functionalization on HTCE formation and charge transfer. Kelvin probe AFM of functionalized ZnO surfaces. Continuation of DRS and PL of molecular submonolayers on different ZnO surfaces. Interaction with surface excitons.

Year 4 Magnetic field dependence of PL, EL, photocurrent. Hybrid exciton formation across the i/o interface. Correlation with theory.

3.5 Role within the Collaborative Research Centre

Project B3 will provide a contribution to the understanding of the fundamental processes governing HIOS function. It will assess the success of strategies developed in project area A to tailor the i/o interface with the aim to optimize HIOS for light-emission and charge carrier generation. The project will employ optical spectroscopy as well as electrical characterization techniques, whereby the focus is on HIOS prepared entirely under UHV conditions. Developed HIOS will be implemented in light-emitting devices and function demonstrated on a proof-of-concept level.

To develop HIOS building blocks for light-emitting applications, close collaboration with A5 (Henneberger), A11 (Christiansen) and B13 (List-Kratochvil) will be essential. We will exchange materials and expertise in fabrication and characterization techniques. Optimization of the i/o interface will be tackled in collaboration with (Koch) (energy-level adjustment), A11 Christiansen (surface passivation) and with theoretical support by A4 (Heimel) and B4 (Körzdörfer/Rinke/Scheffler) whereby the task of this project will be the evaluation of the impact on the opto-electronic function of the interface. FRET studies performed in this project will provide experimental input for theoretical modelling pursued in B12 (Knorr/Richter) and profit from their predictions. Projects B4 (Körzdörfer/Rinke/Scheffler), B6 (May), B7 (Neher), B9 (Stähler), B11 (Draxl) unites the common zest to understand interfacial electronic excitations and charge transfer. B7 (Neher), B9 (Stähler) and this project use complementary experimental techniques to reveal the nature and follow pathways of electronic excitations while B4 (Körzdörfer/Rinke/Scheffler), B6 (May) and B11 (Draxl) will provide theoretical description. Novel molecules synthesized in A3 (Hecht) will be tested with regard to their electronic coupling with ZnO and GaN nanostructures. Finally, this project will prepare highly diluted host-guest organic thin films by OMBD for B2 (Ballauff, Benson, Lu) required to study interactions with plasmonic metal nanostructures.

3.6 Delineation from other funded projects

There are no other funded projects.

3.7 Project funds

3.7.1 Previous funding

The project has been funded within the Collaborative Research Centre since July 2011. Preliminary work cited in 3.3.1 was partially funded by DFG within the CRC 448 (ended in December 2009).

3.7.2 Funds requested

Funding for	2015/2		2016		2017		2018		2019/1	
Staff	Quantity	Sum	Quantity	Sum	Quantity	Sum	Quantity	Sum	Quantity	Sum
<category, percentage>										
PhD student, 75%	2	44.100	2	88.200	2	88.200	2	88.200	2	44.100
Total										
Direct costs	Sum		Sum		Sum		Sum		Sum	
Small equipment, Software, Consumables										
Other										
Total										
Major research equipment	Sum		Sum		Sum		Sum		Sum	
€ 10.000 - 50.000	0		0		0		0		0	
> € 50.000	0		0		0		0		0	
Total	0		0		0		0		0	
Total										

(All figures in Euro)

3.7.3 Staff

	No.	Name, academic degree, position	Field of research	Department of university or non-university institution	Commitment in hours/week	Category	Funded through:
Available							
Research staff	1	Blumstengel, Sylke, Dr.	Physics	HU Phys	20		
	2	Sadofev, Sergey, Dr.	Physics	HU Phys	5		
Non-research staff	3	Fahnauer, Dagmar		HU Phys	4		
	4	Renger, Elfriede		HU Phys	4		
Requested							
Research staff	7	N.N., PhD student		HU Phys			
	8	N.N., PhD student		HU Phys			
Non-research staff							

Job description of staff (supported through available funds):
1. S. Blumstengel:
Scientific and organisational management of the project, supervision of scientific staff and PhD students, planning of experiments, data analysis, discussion and dissemination of results
2. S. Sadofev:
MBE growth of ZnO-based heterostructures. Support in realisation of purely inorganic LEDs.
3. D. Fahnauer:
Fabrication of mechanical parts required for experimental set-ups
4. E. Renger:
Technical support in sample preparation

Job description of staff (requested):

5. N.N.: Performs experimental work described in subproject 1. This includes design, preparation, electrical and optical characterisation of HIOS building blocks and their optimisation for light-emitting application.
6. N.N.: Performs experimental work described in subproject 2. Tasks include preparation of HIOS for optical and electrical measurements, performance of cw and time-resolved optical spectroscopy of HIOS interfaces, photoconductivity measurements, experiments in magnetic fields and evaluation of experimental data.

3.7.4 Direct costs for the new funding period

	2015/2	2016	2017	2018	2019/1
Funds available	5000	10000	10000	10000	5000
Funds requested	8000	16000	16000	16000	8000

(All figures in Euro)

Consumables for 2015/2 and 2019/2

Materials (Conjugated organic molecules, targets for e-beam evaporation, metals, p-GaN)	EUR	4000
Optical spare parts	EUR	1500
Laser dyes, filters for dye laser	EUR	500
UHV spare parts	EUR	1500
Electronic parts for control experiments	EUR	500

Consumables for 2016, 2017 and 2018

Materials (Conjugated organic molecules, targets for e-beam evaporation, metals, p-GaN)	EUR	8000
Optical spare parts	EUR	3000
Laser dyes, filters for dye laser	EUR	1000
UHV spare parts	EUR	3000
Electronic parts for control experiments	EUR	1000

3.7.5 Major research equipment requested for the new funding period

No funding is requested.

3.7.6 Student assistants

No funding is requested.

3.1 About project B4

3.1.1 Title: First-principles characterization of hybrid inorganic/organic interfaces

3.1.2 Research areas: theoretical physics, computational material science

3.1.3 Principal investigators

JProf. Dr. Körzdörfer, Thomas (*21.11.1980, German)
Institut für Chemie, Universität Potsdam, Karl-Liebknecht-Str. 24-25, 14476 Potsdam-Golm
Phone: +49 (0)331 977 5502
Fax: +49 (0)331 977 5566
E-mail: koerz@uni-potsdam.de

Prof. Dr. Rinke, Patrick (*26.04.1975, German)
Aalto University School of Science, P.O. Box 11100, FI-00076 AALTO, Finland
Phone: +358504433199
Fax: +358-9-855 4019
E-mail: patrick.rinke@aalto.fi

Prof. Dr. Scheffler, Matthias (*26.06.1951, German)
Fritz-Haber-Institut der MPG, Theory Department, Faradayweg 4-6, 14195 Berlin
Phone: +49 (0)30 8413 4711
Fax: +49 (0)30 8413 4701
E-mail: scheffler@fhi-berlin.mpg.de

Does any of the above-mentioned persons hold fixed-term positions? yes
If yes: Thomas Körzdörfer
End date 31.07.2015 (first phase of Junior Professorship)
Further employment is planned until 31.07.2018 (second phase of Junior Professorship)
Employment until 30.06.2019 is guaranteed provided the proposed CRC is funded.

3.1.4 Legal issues

This project includes

1.	research on human subjects or human material.	no
2.	clinical trials	no
3.	experiments involving vertebrates.	no
4.	experiments involving recombinant DNA.	no
5.	research involving human embryonic stem cells.	no
6.	research concerning the Convention on Biological Diversity.	no

3.2 Summary

Experience in the first funding period of the “HIOS” CRC has underlined that an in-depth understanding of electronic and/or optical phenomena in HIOS critically hinges on a reliable description of the atomic and electronic structure. The central objective of this project is to continue and further expand the development of a theoretical/computational framework to achieve such a reliable description using first-principles electronic structure methods.

In the first funding period, we have addressed a broad range of physical phenomena that are of particular interest for HIOS. For example, we have developed a hierarchy of methods to treat charged surfaces and interfaces from first-principles, which allowed us to study the role of bulk-doping for the hydroxylation of the ZnO surface and helped us to identify the ZnO doping concentration as a new and important control

parameter for interfacial charge transfer. In addition, we have studied the role of van der Waals interactions on the adsorption geometry of physisorbed molecules as well as partial charge-transfer in covalently bonded organic molecules at the HIOS interface. Application of these first-principles methods helped to explain experimentally observed work-function modifications and photoelectron spectra of T4-TCNQ and pyridine deposited on ZnO.

Our agenda for the second funding period is twofold. First, we will build on the insight gained in the first funding period for ordered organic monolayers on ZnO, now extending the analysis to organic multilayers. While the interface can induce novel or unusual structures in the first few layers of the organic film, it is expected that subsequent layers adopt a different, more organic bulk-like structure. We will analyze whether such structural changes at the interface are conducive or detrimental for potential devices. In terms of the organic materials, we will mainly focus on molecules studied by the experimental collaborators in projects A8 (Koch), B3 (Blumstengel) and B9 (Stähler) such as perylene- and naphthalene-derivatives (PTCDI, NTCDA), nitriles (F4-TCNQ) and dipolar molecules used for tuning the energy level alignment. The influence of the ZnO bulk doping concentration on the surface phase diagram of ZnO and on the organic films will be studied in collaboration with A4 (Heimel). The emergence of the associated space charge regions in doped organic films will also be investigated. In this context, we also plan to study plasmonic effects and the potential coupling to plasmons and polarons in heavily doped (metallic) ZnO as investigated experimentally in project A5 (Henneberger).

Second, we will go beyond the ideal, static description of the HIOS interface utilized in the first funding period by developing methodologies that allow us to investigate the effects of lattice vibrations and disorder on the ground-state electronic structure. In particular, we plan to study how electron-phonon coupling (EPC) and disorder influence the band structure measured, for example, by photoemission spectroscopy. The coupling to phonons and molecular vibrations leads to a broadening and a shift of experimental peaks, thereby aggravating the identification of molecular states and the level alignment at the interface. To investigate these effects, we will derive expressions for the self-energy based on EPC matrix elements from density-functional perturbation theory. Regarding the development and implementation of accurate and efficient EPC routines, we will closely collaborate with project B11 (Draxl), in which the role of EPC effects for excited states will be studied. Using these methods, we will explore zero-point renormalization, temperature dependence, energy level alignment, and phonon-induced lifetime broadenings of the band structure at the HIOS interface and develop methods that include the effects of disorder on the calculated band structure. In collaboration with experiments (Stähler, Henneberger, Kowarik, Blumstengel and Koch), we will use this methodology to investigate the role of disorder and vibrations on the electronic and atomic structure at the interface. Van-der-Waals contribution to EPC will be analyzed in collaboration with A10 (Tkatchenko/Scheffler). Computed EPC matrix elements will serve as input for energy transfer simulations performed in B12 (Richter/Knorr).

3.3 Project progress to date

3.3.1 Report and state of understanding

The objectives of the first funding period were to combine (i) first-principles methods for the interface and surface electronic structure (including coupling matrix elements between the electronic and the vibrational states of the system) with (ii) a microscopic equation-of-motion approach to calculate the formation and subsequent electron and exciton dynamics due to external optical excitation. Objective (ii) has now been moved into the separate project B12 (Richter/Knorr). We will thus report only on objective (i) – the first-principles part.

Prior to the first funding period, little was known about the microscopic details of organic molecules or molecular films on ZnO. Most experimental and first-principles studies had focused on the structure of the ZnO surface [1,2,3] or the properties of small molecules in the context of catalysis [3]. The earlier ZnO-based first-principles explorations were carried out with density-functional theory applying common local and semi-local density-functionals. These functionals are computationally efficient but suffer from intrinsic deficiencies, such as self-interaction errors (which for instance manifests itself in the underestimation of band gaps), the absence of long-range van der Waals (vdW) interactions and surface polarization effects.

To address these deficiencies, we developed new and efficient approaches that include vdW interactions [7] and systematically studied advanced density-functionals that reduce the self-interaction error (so called hybrid functionals) [8,9]. vdW interactions contribute significantly to the binding energy of organic molecules and films (such as graphene) and are crucial when the interaction with the substrate is weak (e.g. in

physisorption) [8,9,10,11]. Conversely, hybrid functionals significantly increase the band gaps of solids and the ionization energies of molecules by reducing the self-interaction error. For the organic molecules PTCDA, F4TCNQ and PYTON adsorbed on silver, hybrid functionals improve the molecular properties, but not those of the metal and conventional functionals prove to be sufficient [8]. For semiconducting substrates, such as ZnO, the situation is different, because the band edges and the molecular states both vary strongly with the admixture of exact exchange in the hybrid functionals, which affects the relative position of the molecular states to the band edges. For pyridine on ZnO(10-10) this resulted in varying absolute work functions, while work function changes were unaffected and in good agreement with photoemission measurements carried out in project B9 (Stähler/Wolf) [9]. In contrast, the magnitude of charge transfer to molecular acceptors such as F4TCNQ on ZnO(000-1) depends critically on the exact-exchange admixture, if ZnO is treated as intrinsic (i.e. without including bulk doping) [10].

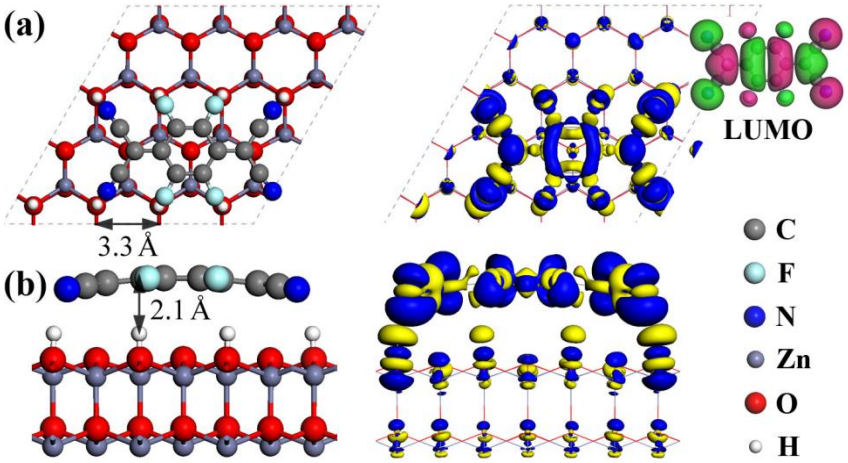

Figure 10

Top (a) and side view (b) of F4TCNQ adsorbed on ZnO(000-1) (2x1)-H (left) and the adsorption-induced electron density rearrangement for n-doped ZnO (right). Electrons flow from the yellow to blue areas upon adsorption.

An important discovery of the first funding period was that the bulk doping concentration of ZnO may have a strong influence on the interface properties, in particular if charge is transferred to molecular acceptors [10,13]. To include bulk-doping effects into our first-principles approaches we developed new methodologies [4,10,12]. Equipped with this, we first investigated the ZnO(000-1) surface and discovered that the bulk doping concentration affects the hydrogen concentration on the surface. n-type doping stabilizes hydrogen deficiency [12]. Hydrogen-rich growth environments might thus be more conducive for the growth of regular surfaces. For F4TCNQ on ZnO(000-1) (see Fig. 1), we showed that the adsorption energy and the electron transfer also depend strongly on the bulk doping concentration of ZnO. The associated work function changes are large, for which the formation of space-charge layers is the main driving force [10]. As a result, large work-function changes can be achieved with little charge transfer for moderate to low doping concentrations in agreement with photoemission measurements in project A8 (Koch) [13]. This work was carried out in collaboration with projects A5 (Henneberger), A8 (Koch) and B3 (Blumstengel). These prominent doping effects are expected to be quite general for charge-transfer interfaces in hybrid inorganic-organic systems as exemplified by recent work by Winget et al. [5] and will be important for device design.

To investigate the optical absorption of hybrid systems we developed a coupled scheme in which the Heisenberg equation of motion technique is parameterized by our DFT calculations. We derived the Bloch equations for these hybrid systems and applied them to ladder-type quarterphenyl (L4P) molecules on the ZnO(1010) surface. We find that the nonradiative dipole-dipole energy transfer causes the formation of coupled excitations, effectively reducing the excitation energy of the optical resonance in the molecular film and inducing a broadening of the associated absorption peak [14]. The coupling to lattice vibrations [6] could not be included at this stage, because the implementation of the required electron-phonon coupling elements took longer than anticipated. It is since finished and we will apply these methods in the next funding period (see Section 3.4.1 B).

[132] M. Valtiner, M. Todorova, G. Grundmeier, J. Neugebauer, Phys. Rev. Lett. **103**, 065502 (2009).
[133] G. Kresse, O. Dulub, and U. Diebold. Phys. Rev. B **68**, 245409 (2003).
[134] C. Wöll, Prog. Surf. Sci. **82**, 55 (2007).
[135] N.A. Richter, S. Sicolo, S.V. Levchenko, J. Sauer, and M. Scheffler, Phys. Rev. Lett. **111**, 045502 (2013).
[136] P. Winget, L. K. Schirra, D. Cornil, H. Li, V. Coropceanu, P. F. Ndione, A. K. Sigdel, D. S. Ginley, J. J. Berry, J. Shim, H. Kim, B. Kippelen, J.-L. Brédas, and O. L. A. Monti, Adv. Mat. **26**, 4711 (2014).
[137] F. Giustino, S. G. Louie, and M. L. Cohen, Phys. Rev. Lett. **105**, 265501 (2006).

3.3.2 Project-related publications

[138] A. Tkatchenko, R. A. DiStasio Jr., R. Car, and M. Scheffler, “Accurate and Efficient Method for Many-Body van der Waals Interactions”, Phys. Rev. Lett. **108**, 236402 (2012).

[139] O. T. Hofmann, V. Atalla, N. Moll, P. Rinke, and M. Scheffler, “Interface dipoles of organic molecules on Ag(111) in hybrid density-functional theory”, New J. Phys. **15**, 123028 (2013).

[140] O. T. Hofmann, J.-C. Deinert, Y. Xu, P. Rinke, J. Stähler, M. Wolf, and M. Scheffler, “Large work function reduction by adsorption of a molecule with a negative electron affinity: Pyridine on ZnO(10-10)”, J. Phys. Chem. **139**, 174701 (2013).

[141] Y. Xu, O. T. Hofmann, R. Schlesinger, S. Winkler, J. Frisch, J. Niederhausen, A. Vollmer, S. Blumstengel, F. Henneberger, N. Koch, P. Rinke, and M. Scheffler, “Space Charge Transfer in Hybrid Inorganic-Organic Systems”, Phys. Rev. Lett. **111**, 226802 (2013).

[142] L. Nemec, V. Blum, P. Rinke, and M. Scheffler, “Thermodynamic equilibrium conditions of graphene films on SiC”, Phys. Rev. Lett. **111**, 065502 (2013).

[143] N. Moll, Y. Xu, O. T. Hofmann, and P. Rinke, “Stabilization of Semiconductor Surfaces through Bulk Dopants”, New J. Phys. **15**, 083009 (2013).

[144] R. Schlesinger, Y. Xu, O. T. Hofmann, S. Winkler, J. Frisch, J. Niederhausen, A. Vollmer, S. Blumstengel, F. Henneberger, P. Rinke, M. Scheffler, and N. Koch, “Controlling the work function of ZnO and the energy-level alignment at the interface to organic semiconductors with a molecular electron acceptor”,
Phys. Rev. B **87**, 155311 (2013).

[145] E. Verdenhalven, B. Bieniek, A. Knorr, P. Rinke, and M. Richter, “Theory of optical excitations in dipole coupled hybrid molecule-semiconductor layers: coupling of a molecular resonance to semiconductor continuum states“, Phys. Rev. B **89**, 235314 (2014).

[146] J. Stähler, O. T. Hofmann, P. Rinke, S. Blumstengel, F. Henneberger, Y. Li, and Tony F. Heinz, “Raman study of 2,7-bis(biphenyl-4-yl-)2’,7’-ditertbutyl-9,9’-spirobifluorene adsorbed on oxide surfaces”, Chem. Phys. Lett. **584**, 74 (2013).

3.4 Research plan

3.4.1 Goals

The main goal of this project is to provide a theoretical understanding of the factors that govern the atomic and electronic structure at the organic/inorganic interface and to further develop and apply electronic structure methods that facilitate a reliable and computationally efficient description of hybrid inorganic/organic systems from first-principles. The long-term vision is to combine the first-principles treatment of bulk doping, covalent and non-covalent bonding at the organic/inorganic interface and in multiple organic layers, band bending, charge-transfer, electron-phonon coupling (EPC), and disorder to achieve a realistic, reliable, and numerically feasible prediction of the electronic band structure of hybrid inorganic/organic systems.

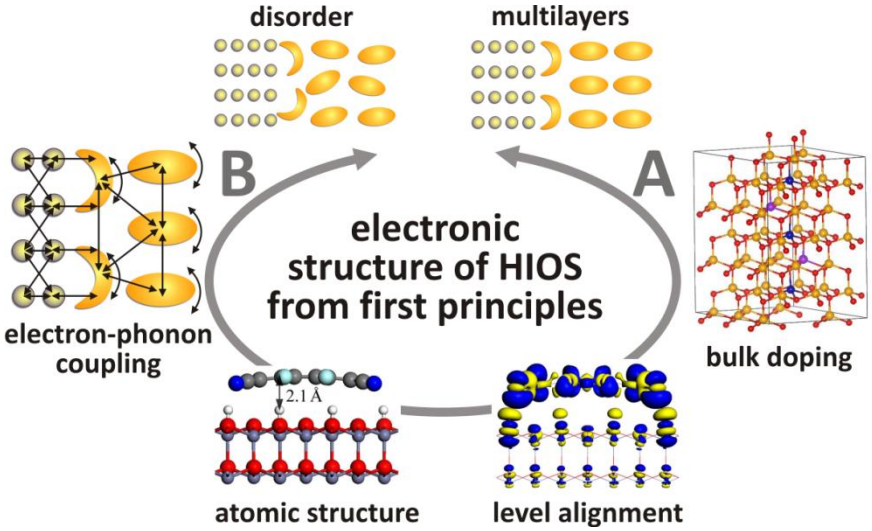

Figure 2:

Outline for the work program in the second funding period. Starting from the results of the first funding period on the atomic and electronic structure of static, single-layered HIOS, will include bulk-doping and organic multilayers (part A) as well as electron-phonon coupling and disorder (part B) in the first-principles description of ZnO/organic interfaces.

Building on the results obtained in the first funding period, we have identified four aspects that are of central importance for a reliable description of HIOS and that were not fully included in our previous work, i.e., bulk-doping, organic multilayers, EPC, and disorder. In the second funding period, we will further develop and apply methods that will allow us to take all these aspects into account. To connect the theoretical description achieved in B4 with experiment, we will continue and extent the collaborations with the projects of A5 (Henneberger) on highly doped ZnO, with A8 (Koch) and A9 (Stähler) on photoelectron and B3 (Blumstengel) optical spectra,of HIOS.

A) Organic multilayers and bulk doping

To comprehend the effect of adsorbates on the non-polar ZnO $(10\bar{1}0)$, an overall understanding of the surface properties is required. Previous studies at 300 and 200K have reported the existence of hydrogen at half and full coverages, respectively. Both significantly affect the electronic properties of the surface [Deinert et al., PRL 119, 057602 (2013), Wang et al., PRL 95, 266104 (2005)]. Preliminary photoemission measurements in project B9 (Stähler) indicate that the actual H coverage is much lower (of the order of 5-20%). With this in mind, the first step will be a systematic study of the surface stability at these low H concentrations before we study adsorbed molecules on the surface. Subsequently, we will investigate the adsorption of self-assembled and a multi-layered organic films on the ZnO $(10\bar{1}0)$ surface in the presence of doping.

Stability of H-terminated ZnO $(10\bar{1}0)$ *surfaces*

Preliminary *ab initio* results on various H-terminated surfaces ranging from 6.25 % to 100 % H obtained at the FHI, indicate that the pristine thermodynamically stable surface retains its stability at very low H concentrations (6.25% H), intermediate (50% H) and full H termination. At low concentrations, H adsorption occurs on individual O-sites, which leads to a metallic behavior at the surface. The next stable regions are semiconducting half and full monolayer configurations with H adsorbed on the Zn and O atoms of ZnO-dimers. These preliminary results beckon for further investigation, in particular in the low coverage regime that is not easily accessible by DFT. To achieve this, we will generate the extensive number of possible surface structures at various low coverages by a combination of DFT calculations with a cluster expansion (CE). In the CE, all possible H adsorption sites are arranged on a two dimensional lattice. The Hamiltonian of the CE is then parameterized with training structures whose energy is calculated in DFT. Once parameterized, arbitrary H configurations can be generated at very low computational cost, because each surface-energy is given by an algebraic sum over a finite number of terms. Therefore, any system state of interest will be defined by the occupation of the sites in the lattice and the total energy of any configuration will be expanded into a sum of discrete interactions between these lattice sites. This enables us to determine the full thermodynamic phase diagram, also allowing for disordered structures [Stampfl et al., Phys. Rev. Lett. **83**, 2993 (1999)].

Global effects of doping at HIOS interfaces

In the first funding period we have discovered the impact of the bulk ZnO doping concentration on HIOS interfaces that include only one organic monolayer [10,13]. We devised an efficient way to combine first-principles calculations with electrostatic models for the space-charge region that builds up in the inorganic semiconductor [4,10]. We will now transfer this concept also to HIOS structures with thicker organic films. For this we will have to devise suitable models for the space-charge region in organic crystals and films in collaboration with A4 (Heimel) [Oehzelt et al., Nature Comm. 5, 4174 (2014)]. With this computational technique we are then equipped to investigate HIOS that comprise thicker organic films.

Building the multi-layered doped organic semiconductor

With the effect of the doped ZnO $(10\bar{1}0)$/individual monolayer calculated, the next step will be the study of a doped multi-layered organic entity in terms of the local geometries of the individual layers and the electronic properties induced at the interface. We will begin with the non-polar ZnO $(10\bar{1}0)$ surface and investigate films of chemi- or physisorbed π-conjugated molecule. We will begin with perylene- and naphthalene-derivatives (PTCDI, NTCDA), nitriles (F4-TCNQ) and oligophenyls. We expect that the geometries of the first few layers are significantly affected by the interface, while subsequent layers adopt a more bulk-like structure. The effects of these structural changes on the electronic properties of HIOS will be explored via a combination of methods: Cascade Genetic Algorithms (GA) [Bhattacharya et al., arXiv: 1409.8522] and force-field Molecular Dynamics (MD) will be utilized to discover the structure of the subsequent layers. We will pay particular attention to the force-field parametrization of surface Zn and O surface, which is usually not included in

standard force-field models [H. Meskine and P. A. Mulheran, Phys. Rev. B 84, 165430 (2011)]. After first performing an extensive GA pre-scanning of structures by means of a computationally inexpensive classical force field MD, the structures with the lowest energy will be used as initial guesses for further GA searches at the *ab initio* level. The effect of doping will be taken into account as described above after the construction of the multi-layered organic slab on ZnO $(10\bar{1}0)$ substrates. Once we have identified stable film structures, we will analyse their electronic structure and their properties in collaboration with A5 (Henneberger), A8 (Koch), A9 (Stähler) and B3 (Blumstengel).

B) Electron-phonon coupling and disorder

EPC and disorder significantly influence the shape and dispersion of electronic bands. These effects are anticipated to be of particular importance for the electronic structure of HIOSs. As EPC is generally expected to be more pronounced in the organic film than in the inorganic material, a correct description of the level alignment critically hinges on the temperature-dependent, phonon-induced band narrowing on either side of the interface. Disorder leads to increased band dispersion, thereby aggravating the identification of molecular states and the level alignment. Hence, we aim to incorporate both EPC and disorder in the first-principles description of hybrid inorganic/organic systems.

Comparison of AHC theory with the frozen phonon approach to calculate EPC matrix elements

EPC can be introduced using Allen-Heine-Cardona (AHC) theory of the frozen phonon (FP) approach (more details on the methods are provided below). Despite being computationally more efficient, AHC theory requires analytic derivatives of the Hamiltonian. These are available for standard DFT approaches such as local-density approximation (LDA), but not for the more accurate hybrid functionals or the *GW* method. However, self-interaction errors and the many-electron effects neglected in LDA can lead to a significant underestimation of the EPC when compared to more accurate GW calculations [G. Antonius et al., PRL 112, 215501 (2014)]. It remains to be clarified whether the underestimation of LDA can be corrected by using hybrid DFT approaches that yield an improved description of the HOMO/LUMO gap. This question will be investigated in our study. In a first step, we will compare the performance of AHC and FP approaches to the calculation of EPC matrix elements for several **organic molecules**. In particular, we will analyze the role of the DFT functional and study whether we can improve the agreement between DFT- and *GW*-calculated EPC energies by using suitable hybrid functionals. *GW*-calculated EPCs will be calculated for comparison. In a second step, we will test and compare the AHC and FP methods for **bulk ZnO** and the non-polar **ZnO surface**. In this context, we will also assess whether the weak coupling regime, in which both the FP and AHC methods have been formulated, is indeed sufficient to describe the EPC in ZnO. If this is not the case, we will investigate ways to improve the approach by going beyond the weak-coupling regime.

E-ph coupling, lifetimes and temperature dependent band normalization at the organic/ZnO interface

We will next focus on the temperature-dependent band structure and energy level alignment at the HIOS interface. Compared to the single molecule and bulk solid cases, several additional challenges arise for HIOS interfaces. We will start our analysis by studying a single pyridine molecule on the ZnO $(10\bar{1}0)$ surface. This will be done in close collaboration in B11 (Draxl). The comparison of both codes for the same test system allows us to optimize efficiency and to test basis-set dependence and other numerical approximations. By identifying leading contributions to the EPC at the interface, we anticipate that it will be possible to reduce the computational effort of future calculations significantly. We will study how the presence of the interface influences the temperature-dependent band renormalization and quasiparticle lifetimes in the organic layer.

E-ph coupling in organic multilayers

Having studied a single molecule on the ZnO surface, we will then focus on the effect of electron-phonon coupling on the band structure in organic multilayers. As a first step, we will focus on the **organic layer only**, comparing the electron-phonon coupling strength and their influence on the quasiparticle spectra for inter- and intra-molecular vibrations. This will allow us to identify the dominant contributions to EPC in organic multilayers. In particular, we will compare inter- and intra-molecular contributions to EPC. Van-der-Waals contributions will be studied in close collaboration with A10 (Tkatchenko). In a second step, we will then analyze EPC at the **HIOS interface**. In order to reduce the numerical costs as far as possible, it will be necessary to take only the most dominant modes into account and to use the most efficient numerical procedures developed in the previous steps.

Inclusion of disorder

Besides electron-phonon interactions discussed so far, the broadening of photoemission spectra of thin organic films is also affected by static disorder. The different nano-scale environments of the organic molecules lead to energy fluctuations of the different sites in the crystallites, which needs to be taken into account to achieve a reliable description of quasiparticle energies of organic thin films directly comparable to photoemission experiment. To achieve this, we will combine the ab-initio calculated band structure and EPC with **dynamical mean field theory (DMFT)**, which allows the calculation of photoemission spectra that include static disorder in the form of spatial fluctuations of the molecular energy levels [Ciuchi et al., PRL 108, 256401 (2012)]. Comparison with the ab-initio results for the phonon-induced band renormalization enables us to directly assess (and optimize) the quality of the model-Hamiltonian underlying the DMFT. The DMFT approach to disorder will be validated by comparing the results to ab-initio band-structure calculations for a limited number (~5-10) of different geometries. The approach will be used to analyze the photoelectron spectra of thin organic films studied by the collaborators in the CRC in direct comparison to experiment. In summary, the results of this study will yield important insights into the role of EPC and disorder on the band structure at the HIOS interface.

3.4.2 Methods

We will predominantly use first-principles DFT and many-body perturbation theory (MBPT) in the *GW* approximation as implemented in the FHI-aims code. This is an efficient all-electron electronic structure code based on numeric atom-centered orbitals developed at the FHI. Production-ready implementations of many of the theoretical methods necessary to perform the proposed work already exist in FHI-aims. This includes: global and range-separated hybrid functionals, dispersion corrections to DFT (the TS pairwise method and the many-body dispersion method), non-periodic *GW* methods at all levels of self-consistency, the charge-reservoir electrostatic sheet technique (CREST) to treat doped semiconductor surfaces, dynamical mean-field theory (DMFT), as well as the density-functional perturbation theory calculation of EPC matrix elements. However, the project also requires advanced methods that still need to be developed, implemented, optimized, and/or tested (see below).

DFT and MBPT methods

FHI-aims has versatile capabilities to perform ground state and excited-state calculations for periodic and non-periodic systems. DFT calculations for systems comprising few thousand atoms can be routinely performed with all types of semi-local, global and range-separated hybrid functionals. A robust parallel implementation of many-body perturbation theory methods (RPA, *GW*) enables calculations for up to several hundred atoms with converged basis sets. Specifically for *GW* (and other many-body perturbation theory methods) the all-electron implementation in FHI-aims has the advantage that it does not introduce pseudo-potential errors. In addition, the FHI-aims *GW* implementation treats the frequency dependence of the self-energy by analytical continuation, which is more accurate than the generalized plasmon pole model used in other codes. Both pseudopotentials and the plasmon pole model may introduce significant errors for ZnO, which makes the FHIaims approach particularly suitable for the tasks of this project. Periodic *GW* and hybrid DFT routines have been implemented and are currently being optimized to be sufficiently fast for this HIOS project (we expect this to be the case within the next 4-6 months). Owing to the locality and compactness of the NAO basis sets, FHI-aims also exhibits a superior convergence behaviour with respect to the number of basis functions. To the best of our knowledge, this combination of attributes, which is vital for the proposed research and for the computational design of hybrid organic/inorganic interfaces, is presently unique to FHI-aims.

Electron-phonon coupling, quasiparticle lifetimes and disorder

We will employ two different approaches to calculate electron-phonon coupling (EPC) from first-principles: the *Allen-Heine-Cardona (AHC) approach* and the *frozen-phonon (FP) method*. In **AHC theory**, the thermal shifts of the electronic energies are described in second-order perturbation theory using the harmonic and adiabatic approximations. Then, the electron-phonon correction $\Delta\epsilon_{n\boldsymbol{k}}$ to the one-particle energy $\epsilon_{n\boldsymbol{k}}$ of the electronic state with wave vector $\boldsymbol{k}$ and band n is given by the sum of two terms, *i.e.*, the phonon-induced self-energy or Fan term, $\Delta^{\mathrm{Fan}}\epsilon_{n\boldsymbol{k}}$, and the Debye-Waller (DW) term, $\Delta^{\mathrm{DW}}\epsilon_{n\boldsymbol{k}}$:

$$\begin{aligned}\Delta\epsilon_{n\boldsymbol{k}} &= \Delta^{\mathrm{Fan}}\epsilon_{n\boldsymbol{k}} + \Delta^{\mathrm{DW}}\epsilon_{n\boldsymbol{k}} \\ &= \sum_{m\neq n,\nu}\int \frac{d\boldsymbol{q}}{\Omega_{\mathrm{BZ}}}\,\frac{2n_{\boldsymbol{q}\nu}(T)+1}{\epsilon_{n\boldsymbol{k}}-\epsilon_{m\boldsymbol{k}+\boldsymbol{q}}}\left|g_{mn,\nu}(\boldsymbol{k},\boldsymbol{q})\right|^2 - \sum_{m\neq n,\nu}\int \frac{d\boldsymbol{q}}{\Omega_{\mathrm{BZ}}}\,\frac{2n_{\boldsymbol{q}\nu}(T)+1}{\epsilon_{n\boldsymbol{k}}-\epsilon_{m\boldsymbol{k}}}\left|g^{\mathrm{DW}}_{mn,\nu}(\boldsymbol{k},\boldsymbol{q})\right|^2\end{aligned}$$

where Ω_{BZ} is the volume of the Brillouin zone and $n_{\boldsymbol{q}\nu}(T)$ is the (temperature-dependent) Bose-Einstein occupation factor of the phonon with wave vector $\boldsymbol{q}$ and branch ν. [6] The EPC matrix element

$$g_{mn,\nu}(\boldsymbol{k},\boldsymbol{q}) = \langle m\boldsymbol{k}+\boldsymbol{q}|\Delta_{\boldsymbol{q}\nu}V|n\boldsymbol{k}\rangle$$

can be calculated from the first-order variations $\Delta_{\boldsymbol{q}\nu}V$ of the self-consistent potential *V*, which can be derived from density-functional perturbation theory (DFPT). The DFPT approach to calculate EPC has been implemented in FHIaims, and the calculation of the Fan- and DW-Terms of AHC theory is currently finalized. Extension to the periodic case as well as optimization and testing is expected to take us another 4-6 months from now. In FHIaims, EPC matrix elements can be calculated directly in a numeral atomic orbital (NAO) basis and then Fourier transformed to a dense sampling of the Brillouin zone in momentum space. Then, ehe **phonon-induced, temperature dependent lifetime broadening** of the electronic band $\epsilon_{n\boldsymbol{k}}$ can then be calculated directly from the imaginary part of the electron self-energy, that is,

$$\Sigma''_{n\boldsymbol{k}} = \pi \sum_{m,\nu} \int \frac{d\boldsymbol{q}}{\Omega_{\mathrm{BZ}}} \left|g_{mn,\nu}(\boldsymbol{k},\boldsymbol{q})\right|^2 \left[\left(n_{\boldsymbol{q}\nu}+f_{m\boldsymbol{k}+\boldsymbol{q}}\right)\delta\left(\epsilon_{n\boldsymbol{k}}-\omega_{\boldsymbol{q}\nu}-\epsilon_{m\boldsymbol{k}+\boldsymbol{q}}\right) + \left(n_{\boldsymbol{q}\nu}+1-f_{m\boldsymbol{k}+\boldsymbol{q}}\right)\delta\left(\epsilon_{n\boldsymbol{k}}+\omega_{\boldsymbol{q}\nu}-\epsilon_{m\boldsymbol{k}+\boldsymbol{q}}\right)\right],$$

where $f_{m\boldsymbol{k}+\boldsymbol{q}}$ is the Fermi-Dirac occupation factor (this needs to be implemented and tested).

In the **frozen-phonon (FP) approach**, the change of the eigenenergies due to atomic displacements along the normal modes is calculated numerically, i.e., from finite differences. If the rigid-ion-approximation (which is inherent to DFPT) is valid, which has recently demonstrated to be the case for crystals [Antonius et al., PRL 112, 215501 (2014)], the FP and AHC approaches are equivalent (see, e.g., [Poncé et al., arXiv: 1408.2752v1]). However, while the FP approach is computationally more demanding than the AHC, it allows one to calculate EPCs from more accurate electronic structure approaches such as hybrid DFT or the *GW* method without the need for analytic derivatives.

The combination of the ab-initio calculated band structure and EPCs with **dynamical mean field theory (DMFT)** allows the calculation of photoemission spectra that include static **disorder** in the form of spatial fluctuations of the molecular energy levels. This approach can be interpreted as a generalization of the dynamical *coherent potential approximation (DCPA)*, which has been used as an effective tool for the description of disorder in bulk materials. The basic idea is the effective single-site approximation, where one embeds a single scattering impurity into an effective medium. The latter is to be determined self-consistently by enforcing the scattering from a single impurity to vanish on average. Disorder can be included as a local modulation of the molecular energy levels with an Gaussian distribution width , which can be determined by comparison of the band broadening in experiment. The DMFT approach also allows the inclusion of EPC, e.g., in the context of a local Holstein-type interaction term. The self-energy $\Sigma(\omega)$ obtained from the self-consistent solution of the DMFT equations in the presence of both disorder and EPC is then used to determine the hole Green's function

$$G(\omega) = Tr[\omega - \epsilon_{\boldsymbol{k}} - \Sigma(\omega)],$$

from which the spectral function is obtained via

$$A(\boldsymbol{k},\omega) = -ImG(\boldsymbol{k},\omega)/\pi.$$

The ground-state structure, band-dispersion, and EPC elements are derived from first-principles and included in the model-Hamiltonian ansatz of DMFT. This combination of ab-initio and semi-empirical methods enables us to study the influence of static disorder and electron-phonon interactions on the band structure of the HIOS interface at the same time. FHIaims already includes a DMFT implementation, which however needs to be significantly extended, optimized, and tested to account for the treatment of EPC and disorder as described above.

3.4.3 Work program

The work program for the second funding period is split up into parts A and B. While part A deals with bulk-doping and organic multilayers, part B focuses on the role of EPC and disorder. Both parts will, however, be worked on in very close collaboration between all members of the project.

Year 1

A) bulk-doping and multilayers

- Extension of the CREST to organic semiconductors, implementation and testing.

- Calculation of the surface-phase diagrams of different ZnO surfaces under variation of the ZnO bulk-doping concentration.
- DFT calculations for multilayered organic thin films: structure and role of van-der-Waals interactions.

B) EPC and disorder

- Method development and coding
- Comparison of the performance of AHC theory and the FP approach to the calculation of electron-phonon matrix elements for single organic molecules; performance of different DFT functionals.
- Calculation of temperature-dependent band-gap normalization and phonon-induced lifetime broadening of photoelectron spectra for single organic molecules and bulk ZnO.

Year 2

A) bulk-doping and multilayers

- Analysis of plasmonic effects and the potential coupling to plasmons and polarons in heavily doped ZnO.
- DFT calculations for multilayered organic thin films: electronic structure and band-bending.

B) EPC and disorder

- Single organic molecule on ZnO: Comparison with implementation in B11 (Draxl), optimization of efficiency and accuracy (basis-set, grids, etc), identification of most important modes (bulk phonons, interfacial and intramolecular vibrations).
- Calculation of the temperature-dependent band normalization and phonon-induced lifetime-broadenings for single organic molecules on ZnO.

Year 3

A) bulk-doping and multilayers

- First-principles description of space-charge regions in organic thin films as a function of ZnO bulk-doping concentration.
- DFT calculations for multilayered organic thin films: electronic structure and band-bending.

B) EPC and disorder

- EPC in organic crystals: Analysis of inter- vs. intra-molecular EPC and the role of van-der-Waals interactions, calculation of temperature-dependent band normalization and phonon-induced lifetime broadening in organic thin films.
- Inclusion of disorder: Implementation and testing of DMFT routines.

Year 4

A) bulk-doping and multilayers

- Towards a full description of the electronic structure of a multilayered organic film on ZnO: structure, bulk-doping, space charge regions, band-bending, EPC, and temperature-dependent level alignment.

B) EPC and disorder

- Towards a realistic theoretical prediction of photoelectron spectra for HIOS systems from first-principles: the role of EPC and disorder.

3.5 Role within the Collaborative Research Centre

This project aims at a fundamental analysis of the atomic and electronic structure at HIOS interfaces, providing a guide for experiment as well as semi-empirical theories that model HIOS systems on a mesoscopic and/or time-dependent phenomena. An active information and knowledge transfer is concerted with the following projects:

- Our study of EPC and phonon-induced lifetime broadening of the ground-state band structure is complementary to the calculations performed in **B11** (Draxl), which focuses on EPC and polarization effects for excited states. In particular, there is a significant overlap between the two projects in terms of the used methods. We will closely collaborate with B11 on the implementation, testing, and optimization of the EPC routines. In particular, we will compare both implementations in terms of accuracy and efficiency, basis-set dependence and other numerical challenges. This will be done for one hybrid inorganic/organic test system, that is, pyridine on the ZnO(1010) surface.

- The work on spectral and temporal opto-dynamics of the HIOS coupling on the meso-scale that was developed in B4 (formerly Knorr/Rinke/Scheffler) will be continued in the new project **B12** (Knorr/Richter). B12 will study the simultaneous influence of EPC and disorder on hybrid excitations and their optical properties, thus, extending the ab-initio treatment of B4 to mesoscopic length scales and including time-dependent aspects. Specifically, B12 will use ab-initio structures and EPC-parameters derived in B4 and develop models on the meso-scale including the interplay of disorder and EPC.
- We will continue the collaboration with **A4** on the bulk-doping dependence of HIOS and the surface phase diagrams for ZnO. Specifically, we will investigate space-charge models for thicker organic layers.
- The analysis of plasmonic effects and the potential coupling to plasmons and polarons in heavily doped ZnO complements the measurements performed in **A5** (Henneberger).
- With **B9** (Stähler) we will continue to investigate the properties of the ZnO(10-10) surface and selected organic molecules adsorbed on it, such as Pyr-5P.
- Our theoretical results for the photoelectron spectra of organic films and HIOS interfaces will be compared to measurements performed in **A8** (Koch), **B3** (Blumstengel), and **B9** (Stähler).
- B4 will provide structural information for **A10** (Tkatchenko/Scheffler), which in return will help to calculate reliable van-der-Waals contribution to the electron-phonon coupling at the HIOS interface.
- In collaboration with A2 we will elucidate the structure of ultrathin ZnO films on metal substrates to decipher about the microscopic structure of HIOS interfaces.

3.6 Delineation from other funded projects

There is **no** overlap with any of the following, already supported projects:

- DFG – Priority Program SPP 1708, Material Synthesis near Room Temperature, Project: *Ionic Liquid Precursors for Multicomponent Inorganic Nanomaterials* , T. Körzdörfer, 2014 - 2017.
- Einstein Foundation Berlin (Germany) – Einstein Research Project ETERNAL: Exploring Thermoelectric Properties of Novel Materials: In this grant, promising thermoelectric materials are identified from first principles, M. Scheffler.
- DFG – German Research Foundation, Cluster of Excellence 314: Unifying Concepts in Catalysis (UniCat), coordinator: M. Driess; M. Scheffler - first funding period November 2007 - October 2012, new funding period until October 2017.
- NSF – The National Science Foundation, Partnership for International Research and Education (PIRE): Electron Chemistry and Catalysis, director: S. Scott; M. Scheffler - since 2005.
- Max Planck - EPFL Center for Molecular Nanoscience and Technology - Max Planck Society and the École Polytechnique Fédérale de Lausanne, directors: K. Kern, T. Rizzo; board members: B. Deveaud-Plédran, J. Hubbel, A. Wodtke, M. Scheffler - since 2013.
- Vetenskapsrådet – Swedish Research Council: “Catalysis on the atomic scale”, organizer: E. Lundgren; S. Levchenko, M. Scheffler - since 2011.

Scientific overlap exists with the following project:
- 07/2014-07/2015: US DOE - ASCR Leadership Computing Challenge (ALCC), Project: *Interfaces in Organic and Hybrid Photovoltaics* (T. Körzdörfer, P. Rinke). This project ends before the start of the second funding period.

3.7 Project funds

3.7.1 Previous funding

The project has been funded within the Collaborative Research Centre since 01.07.2011.

3.7.2 Funds requested

Funding for	2015/2		2016		2017		2018		2019/1	
Staff	Quantity	Sum	Quantity	Sum	Quantity	Sum	Quantity	Sum	Quantity	Sum
PhD student, 75%	1	22.725	1	45.450	1	45.450	1	45.450	1	22.725
Postdoc, 100%	1	32.700	1	65.400	1	65.400	1	65.400	1	65.400
Total										
Direct costs	Sum		Sum		Sum		Sum		Sum	
Small equipment, Software, Consumables	1.000		2.000		2.000		2.000		1.000	
Other										
Total	56.425		111.850		111.850		111.850		56.425	
Major research equipment	Sum		Sum		Sum		Sum		Sum	
€ 10.000-50.000										
> € 50.000										
Total	0		0		0		0		0	
Total	56.425		111.850		111.850		111.850		56.425	

(All figures in Euro)

3.7.3 Staff

	No.	Name, academic degree, position	Field of research	Department of university or non-university institution	Commitment in hours/week	Category	Funded through:
Available							
Research staff	1)	Körzdörfer, Thomas, Dr. rer. nat., JProf.	Electronic structure	Uni Potsdam	10		
	2)	Rinke, Patrick, Dr., Prof.	Electronic structure	Aalto	5		
	3)	Scheffler, Matthias, Dr. rer. nat., Prof.	Electronic structure	FHI	5		
	4)	Shang, Honghui, Dr.	Electronic structure	FHI	30		
	5)	Bieniek, Björn	Electronic structure	FHI	30		
Non-research staff							
Requested							
Research staff	7)	Stournara, Maria, Dr.	Electronic structure	FHI		E 13	
	8)	N.N.	Electronic structure	Uni Potsdam		E 13	
Non-research staff							

Job description of staff (supported through available funds):

1) T. Körzdörfer: Scientific and organizational coordination of the project, exploration of the fundamental theoretical concepts, selection of methods, supervision of PhD students.
2) P. Rinke: Scientific and organizational coordination of the project, exploration of the fundamental theoretical concepts and selection of methods, supervision of PhD students and post-docs.

3) M. Scheffler: Scientific and organizational coordination of the project, exploration of the fundamental theoretical concepts and selection of methods.
4) H. Shang: Development of EPC methodology in FHIaims.
5) B. Bieniek: First-principles description of ultra-thin, metal-supported ZnO films.

Job description of staff (requested):

6) M. Stournara: The post-doc will carry out part A) of the research program outlined above. She will first investigate the structure of the ZnO(10-10) surface in collaboration with B9 (Stähler). Then she will extend the doping methodology to encompass organic multilayers. Subsequently, she will build models for HIOS with organic multilayers on ZnO(10-10) and determine their structure with a cascade genetic algorithm approach.
7) N.N.: The PhD student will carry out part B) of the research program outlined above. In particular, she/he will further develop and apply the electron-phonon coupling routines in FHI-aims to study temperature-dependent band renormalization and phonon-induced lifetime broadenings of organic molecules, bulk ZnO, and hybrid organic/ZnO systems. The student will also implement the treatment of disorder and work towards a realistic theoretical prediction of photoelectron spectra for HIOS systems from first-principles by including both EPC and disorder.

3.7.4 Direct costs for the new funding period

	2015/2	2016	2017	2018	2019/1
Funds available (UP)	500	1000	1000	1000	500
Funds available (FHI)	1000	2000	2000	2000	1000
Funds requested	1000	2000	2000	2000	1000

(All figures in Euro)

Consumables for 2015/2

Computer supplies	EUR	500

Other for 2015/2

Software	EUR	500

Consumables for 2016-2018

Computer supplies	EUR	1000/year

Other for 2015/2

Software	EUR	1000/year

Consumables for 2019/1

Computer supplies	EUR	500

Other for 2019/1

Software	EUR	500

3.7.5 Major research equipment requested for the new funding period

No funding for major research equipment is requested.

3.7.6 Student assistants

	2015/2	2016	2017	2018	2019/1
Quantity	1	1	1	1	1
Commitment in hours/week	10	10	10	10	10
Sum	3.000	6.000	6.000	6.000	3.000
Tasks	The designated candidate, BSc. Lukas Gallandi, is a staff member (Studentische Hilfskraft) in the group of T. Körzdörfer since 03/2013 (currently on a different project). Mr. Gallandi is a an expert in programing, shell scripting, and HTML design, and he will be assisting the project with the optimization of the source code, efficient parallelization, and by maintaining the projects website.				

3.1 About project B5

3.1.1 Title: Ultrafast nonlinear terahertz and infrared spectroscopy on HIOS

3.1.2 Research area: Experimental physics of condensed matter

3.1.3 Principal investigators

Dr., Wörner, Michael (*02.08.1960, German)
Max-Born-Institute for Nonlinear Optics and Short Pulse Spectroscopy
Phone: +49 (0) 30 6392 1470
Fax: +49 (0) 30 6392 1489
E-mail: woerner@mbi-berlin.de

Prof. Dr., Elsässer, Thomas (*28.09.1957, German)
Max-Born-Institute for Nonlinear Optics and Short Pulse Spectroscopy
Phone: +49 (0) 30 6392 1400
Fax: +49 (0) 30 6392 1409
E-mail: elsasser@mbi-berlin.de

Do the above mentioned persons hold fixed-term positions? no

3.1.4 Legal issues

This project includes

1.	research on human subjects or human material.	no
	A copy of the required approval of the responsible ethics committee is included with the proposal.	
2.	clinical trials	no
	A copy of the studies' registration is included with the proposal.	
3.	experiments involving vertebrates.	no
4.	experiments involving recombinant DNA.	no
5.	research involving human embryonic stem cells.	no
	Legal authorization has been obtained.	
6.	research concerning the Convention on Biological Diversity.	no

3.2 Summary

In the first funding period, the project was focused on electronic, in particular excitonic excitations of ZnO-based HIOS, which were studied by a combination of spatially and time-resolving methods. This work resulted in the first observation of surface excitons in hybrid systems and an in-depth analysis of their optical and transport properties. At much lower optical transition energies in the energy range of millielectron volts, one expects an easier formation of hybrid modes of HIOS. Thus, the present proposal aims at exploring coupling mechanisms and nonequilibrium dynamics in HIOS in the energy range between 5 and several hundreds of meV, corresponding to terahertz (THz) frequencies between 1 and 100 THz. Here, many low-energy excitations such as low-energy electronic transitions, plasmons, and phonons are located. Moreover, THz methods provide direct access to nonequilibrium charge dynamics and transport at ultrafast time scales.

In addition to the direct electronic coupling of elementary excitations of organic molecules and an inorganic semiconductor via long-range Coulomb interactions, radiative coupling and damping, i.e., the exchange of "virtual" transversal photons, dominate light-matter interactions at THz frequencies. This leads in turn to a hybridization of inorganic/organic quantum states with novel opto-electronic properties. In particular, the pronounced coupling of electric currents in the two materials which is beyond elementary dipole-dipole coupling schemes should result in a novel type of low-energy hybrid excitations. While such phenomena

have been studied in a number of inorganic systems, among them epitaxial multi-layer graphene, their role for the functional properties of HIOS has remained unexplored.

The project will mainly focus on two classes of HIOS, (i) molecules with strong vibrational resonances on heavily doped ZnO to explore plasmon-phonon excitations in close collaboration with project A5 (Henneberger), and (ii) molecular systems with an electric dipole moment on inorganic semiconductors such as GaAs/AlGaAs heterostuctures. Examples are dipolar oligo-phenylenes [collaboration with A8 (Koch) and A3 (Hecht)], and molecular crystals like acetylsalicylic acid. Depending on the polymorphic crystal type, the van der Waals interactions between the molecules result in a pronounced coupling between collective electronic fluctuations and quantized lattice vibrations, similar to soft-modes in ferrolectrics, leading in turn to phonon-plasmon polaritons around 2 THz. In combination with doped quantum well structures on the inorganic side, HIOS can be manufactured with hybrid modes consisting of intra- or intersubband transitions and phonon-plasmon excitations of the conjugated organic material. For a detailed experimental characterization of THz hybrid modes of HIOS, ultrafast nonlinear THz and infrared (IR) spectroscopy will be the main experimental tool to unravel and characterize the coupling between elementary excitations of the organic and inorganic part in detail. In particular, fully phase-resolved 2-dimensional THz spectroscopy will allow for dissecting the overall nonlinear response into different orders of the driving electric field. The results will be analyzed in close collaboration with A10 (Tkatchenko/Scheffler).

3.3 Project progress to date

3.3.1 Report and state of understanding

The objective of this subproject has been the spatially and temporally resolved investigation of ultrafast processes in HIOS by optical methods to elucidate the evolution of optical excitations and their mutual couplings. Research in the first funding period included optical experiments to characterize the structural heterogeneity of HIOS, steady-state and time-resolved spectroscopy of excitons, and the investigation of spatial transport processes of excitons with the help of time-resolved near-field scanning optical microscopy.

The two compounds investigated initially were hexaphenyl (6P) crystals and an epitaxial ZnO thin film. The fabrication of these compounds was well established at the beginning of the funding period and spatially averaged spectra were known. However, the structural, optical, dynamical and transport properties at the nanoscopic length scale as well as an understanding of broadening mechanisms were not available. With the advancement of the CRC, newly developed compounds and systems became available and were subjected to optical studies. These were L4P-Et-Hex (L4P, ladder-type tetraphenyl, Z1), composite core-shell metallic nanoparticles (B1) and hybrids of tubular J-aggregates and CdSe quantum dots (QD, A6).

For the initial studies 6P was chosen because its growth is well controlled on the relevant substrates. Crystals were grown (by B3) on the (000-1) facet of a $Zn_{92}Mg_8O$ epitaxial layer, where two crystal adsorption geometries co-exist *on the same* substrate: one with the molecular backbone oriented perpendicular and one parallel to the surface. The first kind forms mono-molecular microcrystals (islands) at sub-monolayer coverage; for the second kind three-dimensional growth in needles is preferred. This facilitates a clear comparison of the different coupling for the two geometries to the substrate. The ZnMgO substrate is the barrier material for ZnO quantum wells.
To individually address the two morphologies, a combined confocal and atomic force microscope was developed, permitting to correlate optical, dynamical and morphological information. The orientation of the electric field vector in the focus was controlled to lie perpendicular or along the optic axis by utilizing higher order Gaussian beams in order to efficiently excite either of the two morphologies. Moreover, an optical near-field microscope (NSOM) with a resolution of ~100 nm was applied to obtain correlated optical and topographic information.
An unexpected distinction was found in the fluorescence and excitation spectra of both crystal types. While needles exhibit a well pronounced vibronic progression reflecting high crystalline quality, spectra taken from islands strongly resemble solution spectra pointing to a high degree of disorder. Such static disorder will prevent the formation of narrow exciton-polariton lines in the molecular crystal even at low temperature. Signs of heterogeneity in the intermolecular coupling or microscopic aggregation are also found in the transient fluorescence decay. It exhibits a highly non-exponential shape and the decay dynamics depend on the chosen energy interval ranging from 100 ps (10 GHz) to several ns.
From the position of the conduction band minimum of $Zn_{92}Mg_8O$ and the exciton energy of 6P, the only coupling mechanism is expected to be charge transfer (CT). To estimate the rate, control samples have been prepared on sapphire (islands) and mica (needles) substrates. The shortening of the lifetime for

needles on ZnMgO leads to CT rates on the order of 400 ps (2.5 GHz). However, the change is on the same order as the width of the distribution of lifetimes at different sites for each sample. Moreover, this rate is averaged over the height of the needles which varies between 5-40 nm. The CT rate for islands is even slower, on the order of 1.6 ns (0.6 GHz), and reflects the weak spatial overlap of the molecular orbitals with the semiconductor bands.
By comparison of the rates of recombination, CT and the expected hybridization, it is found that strong coupling could still be dominant with a suitably modified molecule and a quantum well exciton. However, the inhomogeneous broadening and the vibronic interaction leading to linewidths around 100 meV is anticipated to obscure and weaken the coupling even when methods of high spatial resolution are applied at low temperatures.

The coupling strength strongly depends on the spatial separation between the excitons. At 1 nm it can increase to 10 meV for two-dimensional excitons. It is therefore desirable to utilize surface excitations. One such resonance is the surface exciton (SX) that is frequently observed on ZnO nanostructures. To evaluate the suitability of the SX for HIOS, spatially and temporally resolved experiments were carried out on a specially designed ZnO 20 nm thin film structure providing a high surface-to-volume signal ratio [13] (supplied by A5). In this work, the SX has been observed on an epitaxial ZnO single crystal for the first time. It was found that the adsorption of molecules with a carboxylic acid functionality (HJA-149 supplied by Z1 and stearic acid) by a Langmuir-Blodgett technique leads to an enhancement of the SX photoluminescence (PL) (cooperation with A6). Another commonly used anchor group, the phosphonic acid (cooperation with A8), was inactive. To obtain a sub-diffraction spatial resolution, a variable temperature NSOM was constructed. The resolution of ~100 nm in excitation/detection mode with uncoated, etched silica tips was determined by imaging a GaN quantum well structure [1]. The main finding was that the shape of the SX resonance remains broad (~4 meV) and smooth even at local excitation and detection at 5 K [2], which is in stark contrast to GaAs based quantum structures where one-dimensional localization results in narrow PL lines limited by radiative decay. Moreover, time resolved measurements with local excitation and detection showed that the SX migrates about 50 nm during its lifetime of 90 ps, corresponding to a diffusivity of 0.3 cm^2/s. Since the ZnO surface coupled with the molecular monolayer is expected to cause a short range potential roughness of several meV on the sub-nm length scale, the large width is attributed mainly to spectral diffusion on the ps time scale. This type of inhomogeneous broadening appears to be a general property at the surface of highly polar semiconductor materials such as ZnO and GaN. Thus, excitations that come into contact with the surface appear to be unsuitable for the observation of spectral shifts caused by the hybridization with a molecular exciton.

In cooperation with B1 an optical characterization of composite core-shell metallic nanoparticles was carried out [14]. These particles represent a major building block for a plasmon based laser device (SPASER). The main objective was to record optical scattering spectra from individual, unaggregated particles in order to relate the geometry of the synthesized particles to their plasmon resonance. This was accomplished by utilizing a polarizing dark-field micro-spectrometer with high dynamic range and contrast.

In another cooperation with A6 the dynamics of a hybrid system consisting of tubular J-aggregates and CdSe QD of variable sizes were investigated [3]. Changes in the PL decay dynamics were measured using a streak camera with a 10 ps time resolution. The results revealed that the transfer efficiency was at unity for the majority of QD donors, but there was a remaining fraction of weakly coupled QDs reducing the overall transfer efficiency. This finding was in agreement with the structural information obtained from TEM images by Z2.

(a)

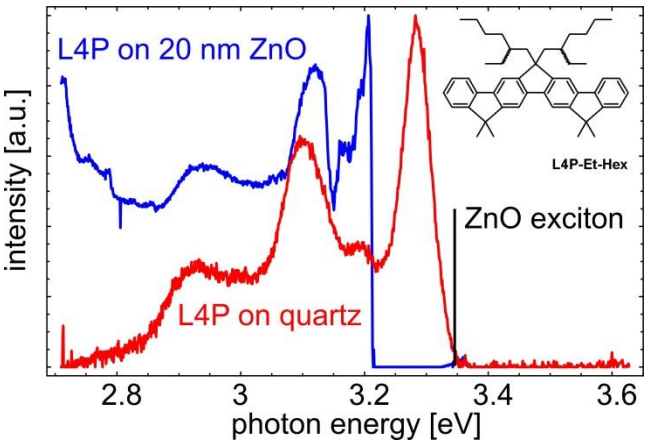

(b)

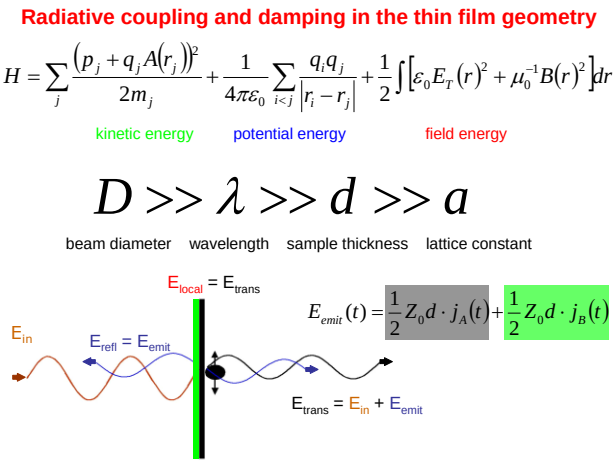

A key goal of CRC 951 is to form hybrid excitations made up of an elementary excitation in the inorganic material (e.g. excitons in ZnO) with that of an organic molecule. Very narrow absorption lines of terrylene molecules embedded in a para-terphenyl crystal have been found at cryogenic temperatures [4]. Under such conditions, the linewidth of the zero-phonon transition connecting the singlet ground and excited states becomes lifetime-limited, so that at low doping concentrations the spectra of different molecules in a small excitation volume no longer overlap. We tried to observe such a zero phonon line of organic molecules also in ZnO-based HIOS. The L4P molecule was designed to resonate with the ZnO exciton [see Fig. 1(a)]. A monolayer of the molecule was deposited on an epitaxial ZnO thin film by the Langmuir Blodgett technique (cooperation with A6) since growth from the vapor phase led to three-dimensional microcrystals. The fluorescence signal from the monolayer is considerably weaker than the photoluminescence of the ZnO thin film. Thus, detection of L4P was only possible off-resonance at the first phonon peak with a signal-to-background ratio of 1:35. Even at low temperatures (8 K), the inhomogeneous linewidth remained 40 meV broad (80 meV at room temperature). Moreover, photo-bleaching occurred even in vacuum at low temperatures. The survival half-time at 50 W/cm (325 nm excitation) was ~40 s.

Our experiments with L4P molecules on ZnO show that it is extremely difficult to observe narrow electronic absorption lines of organic molecules adsorbed on a ZnO surface, a prerequisite to form purely optical hybrid excitations in ZnO-based HIOS. Due to these problems we decided for the next funding period to aim at hybrid modes of HIOS for optical transitions at much longer wavelengths. Thus, the present proposal focuses on exploring coupling mechanisms and nonequilibrium dynamics in HIOS in a complementary energy range at terahertz (THz) frequencies between 1 and 100 THz. In this spectral range a multitude of low-energy excitations such as low-energy electronic transitions, plasmons, phonons, and molecular vibrations are located. In addition, linear and nonlinear THz spectroscopy provide direct access to nonequilibrium charge dynamics and transport at ultrafast time scales. The applicants are among the pioneers of nonlinear, in particular 2-dimensional THz spectroscopy [15-16,18-22].

We expect an easier formation of hybrid modes of HIOS for optical transitions at longer wavelengths as explained in Fig. 1(b). In addition to the direct electronic coupling via long-range Coulomb interactions [second term in the Hamiltonian of Fig. 1(b)], radiative coupling and damping, i.e., the exchange of “virtual” transversal photons [third term], dominates the coupling at THz frequencies leading in turn to a hybridization of inorganic/organic quantum states with novel opto-electronic properties. In a typical experimental geometry the beam diameter D is much larger than the wavelength □ which is in turn much larger than the sample thickness d and in turn the lattice constant a of the involved crystal(s).
Since the local field $E_{local} = E_{ltrans} = E_{in} + E_{emit}$ [driving the elementary excitations in a two-component (layer) system as shown in Fig. 1(b)] is the sum of both the incident field E_{in} and the field emitted by the sample E_{emit} the transverse current in the "green layer" drives the elementary excitations in the "black layer" and vice versa [5]. Thus, a resonant coupling of electric currents in the two materials which is beyond elementary dipole-dipole coupling schemes via the Coulomb interaction should result in a novel type of low-energy hybrid excitations. The applicants have studied such radiative coupling phenomena in a number of inorganic systems [6,7,15,16], i.e., coupling of two or more layers of inorganic materials.

To illustrate this concept, we briefly discuss THz radiative coupling and damping in multilayer graphene. In Ref. [16] we studied the nonlinear dynamics of electrons in epitaxial multilayer graphene grown on the c-face

of the inorganic semiconductor SiC where the graphene layers are rotationally stacked so that they are electrically isolated. Considering graphene layers a big organic molecule with a conjugated □-electron system, epitaxial multilayer graphene resembles strongly a radiatively coupled HIOS. We studied the nonlinear interaction between intense terahertz (THz) pulses and epitaxial multilayer graphene by field-resolved THz pump–probe spectroscopy. Instead of the expected bleaching due to the saturation of interband absorption, the pump–probe signals showed exclusively induced absorption due to electron-hole generation, which decays with time constants of a few picoseconds, much faster than carrier recombination in single graphene layers. The time constants decrease with increasing temperature and increase with increasing energy density deposited. This behaviour originates from the predominant coupling of electrons in the graphene layers to the electromagnetic field via the very strong interband dipole moment while scattering processes with phonons and impurities play a minor role. Interestingly, our results are fully explained by theoretical calculations using a pseudopotential band structure for graphene and light-matter interaction including radiative coupling and damping. The calculations showed that even the refractive index of the SiC substrate has a strong influence on the experimentally observed electron-hole recombination rates via collective radiative damping of all graphene layers and the virtual, i.e., nonresonant, excitations in the SiC substrate. To summarize, in the THz range one expects an extraordinarily strong coupling of elementary excitations of conjugated organic materials with those of an inorganic semiconductor at the interface. Since the role radiative coupling for the functional properties of HIOS has remained unexplored so far, we focus in the present proposal on making and spectroscopically analyzing such radiatively coupled HIOS.

References

[147] S. Friede, S. Kuehn, J. W Tomm, V. Hoffmann, U. Zeimer, M. Weyers, M. Kneissl, and T. Elsaesser, Semicond. Sci. Technol. **29**, 112001 (2014).

[148] S. Friede, S. Kuehn, S. Sadofev, S. Blumstengel, F. Henneberger, and T. Elsaesser, submitted to Nano Letters.

[149] Y. Qiao, F. Polzer, H. Kirmse, E. Steeg, S. Kuehn, S. Friede, S. Kirstein, and J. P. Rabe, in preparation.

[150] C. Hettich, C. Schmitt, J. Zitzmann, S . Kühn, I. Gerhardt, V. Sandoghdar, Science **298**, 385 (2002)

[151] T. Stroucken, A. Knorr, P. Thomas, and S. W. Koch, Phys. Rev. B **53**, 2026 (1996).

[152] P. Gaal, W. Kuehn, K. Reimann, M. Woerner, T. Elsaesser, R. Hey, J. S. Lee, U. Schade, Phys. Rev. B **77,** 235204 (2008).

[153] T. Tyborski, R. Costard, M. Woerner, T. Elsaesser, J. Chem. Phys. 141, 034506 (2014).

[154] S. Kalusniak, S. Sadofev, and F. Henneberger, Phys. Rev. Lett. **112**, 137401 (2014).

[155] M. Braun, von Korff-Schmising, C., M. Kiel, N. Zhavoronkov, J. Dreyer, M. Bargheer, T. Elsaesser, C. Root, T. E. Schrader, P. Gilch, W. Zinth, M. Woerner, Phys. Rev. Lett. **98**, 248301 (2007).

[156] M. Walther, P. Plochocka, B. Fischer, H. Helm, P. Uhd Jepsen, Biopolym. (Biospectros.) 67, 310 (2002).

[157] A. M. Reilly and A. Tkatchenko, Phys. Rev. Lett. **113**, 055701 (2014).

[158] R. A. Kaindl, M. A. Carnahan, D. Hägele, R. Lövenich & D. S. Chemla, Nature **423**, 734 (2003).

3.3.2 Project-related publications

[159] S. Kuehn, S. Friede, S. Sadofev, S. Blumstengel, F. Henneberger, and T. Elsaesser, “Surface excitons on a ZnO (000-1) thin film”, Appl. Phys. Lett. **103**, 191909 (2013).

[160] S. Wu, A. W. Schell, M. Lublow, J. Kaiser, T. Aichele, S. Schietinger, F. Polzer, S. Kühn, and X. Guo, “Silica-coated Au/Ag nanorods with tunable surface plasmon bands for nanoplasmonics with single particles”, Colloid. Polym. Sci. **291**, 585 (2013).

[161] T. Shih, K. Reimann, M. Woerner, T. Elsaesser, I. Waldmüller, A. Knorr, R. Hey, and K. H. Ploog, “Nonlinear response of radiatively coupled intersubband transitions of quasi-two-dimensional electrons”, Phys. Rev. B **72**, 195338 (2005).

[162] P. Bowlan, E. Martinez-Moreno, K. Reimann, M. Woerner, and T. Elsaesser, “Terahertz radiative coupling and damping in multilayer graphene”, New J. Phys. **16**, 013027 (2014).

[163] F. Zamponi, P. Rothhardt, J. Stingl, M. Woerner, and T Elsaesser, “Ultrafast large-amplitude relocation of electronic charge in ionic crystals”, Proc. Nat. Acad. Sci. **109**, 5207 (2012).

[164] P. Bowlan, E. Martinez-Moreno, K. Reimann, T. Elsaesser, and M. Woerner, “Ultrafast terahertz response of multi-layer graphene in the nonperturbative regime”, Phys. Rev. B **89**, 041408 (2014).

[165] C. Somma, K. Reimann, C. Flytzanis, T. Elsaesser, and M. Woerner, “High-field terahertz bulk photovoltaic effect in lithium niobate”, Phys. Rev. Lett. **112**, 146602 (2014).
[166] M. Woerner, W. Kuehn, P. Bowlan, K. Reimann, and T. Elsaesser, “Ultrafast two-dimensional terahertz spectroscopy of elementary excitations in solids”, New J. Phys.**15**, 025039 (2013).
[167] W. Kuehn, K. Reimann, M. Woerner, T. Elsaesser, and R. Hey, “Two-dimensional terahertz correlation spectra of electronic excitations in semiconductor quantum wells”, J. Phys. Chem. B **115**, 5448 (2011).
[168] W. Kuehn, K. Reimann, M. Woerner, T. Elsaesser, R. Hey, and U. Schade, “Strong correlation of electronic and lattice excitations in GaAs/AlGaAs semiconductor quantum wells revealed by two-dimensional terahertz spectroscopy”, Phys. Rev. Lett. **107**, 067401 (2011).

3.4 Research plan

The present proposal for the second funding period aims at exploring coupling mechanisms and nonequilibrium dynamics in HIOS in a complementary energy range at frequencies between 1 and 100 THz. Using linear and nonlinear spectroscopic methods we want to study low-energy excitations such as low-energy electronic transitions, e.g., intersubband or intra-exciton transitions in quantum wells, plasmons, and phonons in both the inorganic and the organic part of the HIOS and as coupled excitations. Since the typical transition dipoles of organic molecules at THz frequencies are quite small we will also put our focus on thin (i.e. a few microns thick) crystalline layers of the organic material to ensure both sufficient amplitude of the (non)linearly emitted THz radiation and enough radiative coupling strength to the respective elementary excitation in the inorganic semiconductor. In addition to monitoring the (non)linear response of the hybrid modes of such HIOS, THz methods provide also direct access to nonequilibrium charge dynamics and transport at ultrafast time scales.

A key goal consists in a detailed experimental characterization of THz hybrid modes of HIOS. Ultrafast nonlinear THz and IR spectroscopy of HIOS will be the main experimental tool to unravel and characterize in detail the coupling between elementary excitations of the organic and inorganic part. In particular, fully phase-resolved two-dimensional (2D) THz spectroscopy allows us to dissect the overall nonlinear response into different orders of the driving electric field. Fully phase-resolved 2D-THz spectroscopy was pioneered by the proposers and corresponds to simultaneously performed photon-echo, spectral hole burning, and pump-probe experiments on the sample. In addition, 2D spectroscopy allows for analyzing spectral correlations between two different optical transitions and, thus, it is an ideal tool to investigate the development of hybrid modes in a HIOS as a function of various parameters. At MBI, we have both a fully equipped nonlinear THz-laboratory, which allows for 2D-THz spectroscopy in vacuum and at cryogenic temperatures, and a second laboratory for performing similar experiments in the mid-infrared (MIR) spectral range. While in the latter we detect the light with MIR detector arrays, the THz laboratory allows for a fully phase-resolved detection of the (non)linearly emitted transients by free-space electro-optic sampling.

The project will mainly focus on two classes of HIOS:

3.4.1 In the first year of the second funding period we would like to investigate molecules with strong vibrational resonances on heavily doped ZnO. The basic idea is to explore plasmon-phonon excitations in close collaboration with project A5 (Henneberger). The latter has recently demonstrated that ZnO doped with Ga can serve as a tunable metal. In a recent article [8], they demonstrated a new type of surface plasmon polaritons by using of the free-electron gas in a heavily doped semiconductor (ZnO:Ga). Varying the doping concentration and/or the angle of incidence and exploiting the concept of using two layers with different concentrations allows for the realization of almost arbitrarily shaped surface-plasmon-polariton dispersion curves in the mid-infrared spectral range, i.e. □ = 1.5 to 6 □m. In a different context, the applicants have investigated single crystals of the strongly polar 4-(diisopropylamino)benzonitrile (DIABN) molecules using both femtosecond x-ray diffraction [9] and VIS pump- MIR probe experiments [the latter probe the CN stretching absorption at 2104 cm^{-1} (□ = 4.8 □m)]. Femtosecond photoexcitation of such organic chromophores in a molecular crystal induces strong changes of the electronic dipole moment via intramolecular charge transfer as is evident from transient vibrational spectra. Changes of diffracted and transmitted x-ray intensity demonstrate an angular rearrangement of molecules around excited dipoles following the 10 ps kinetics of charge transfer and leaving lattice plane spacings unchanged. The idea is now to bring the surface-plasmon-polariton of ZnO:Ga in resonance with the CN stretching absorption at □ = 4.8 □m in crystalline DIABN. The mutual couplings in the hybrid mode of such a HIOS shall be investigated in detail by 2D MIR spectroscopy. Furthermore, optical pumping of a small fraction of DIABN molecules to the

intra-molecular charge transfer state changes their static dipole moment to a large extent followed by intra-crystalline dipole solvation may lead to switching on and off the hybrid mode of such a HIOS.

3.4.2 In a second series of experiments (2nd and 3rd year) we want to investigate molecular systems with an electric dipole moment on inorganic semiconductor structures such as multiple quantum well structures. In these experiments we will focus on elementary excitations located at transition frequencies which are accessible with electro-optic sampling, i.e. 1 - 40 THz. On the inorganic side we will begin with intersubband transitions in GaAs/AlGaAs heterostuctures (external collaboration [15] with Paul-Drude-Institute, Berlin). In a later stage of this subproject we aim also at quantum well structures based on the ZnO material system in close collaboration with project A5 (Henneberger). On the organic side interesting examples examples are dipolar oligo-phenylenes in close collaboration with A8 (Koch) and Z1 (Hecht). Another very interesting class of molecular crystals are drugs like the acetylsalicylic acid [10]. Recently, the authors of Ref. [11] have theoretically shown that depending on the polymorphic crystal type, the van der Waals interactions between the molecules results in a pronounced coupling between collective electronic fluctuations and quantized lattice vibrations (similar to soft-modes in ferroelectrics [17]) leading in turn to phonon-plasmon polaritons around 2 THz. In combination with doped quantum well structures on the inorganic side, HIOS can be manufactured with hybrid modes consisting of intra- or intersubband transitions on the semicondcutor side (e.g. ZnO, GaAs, etc.) with the phonon-plasmon excitations of the conjugated organic material. A10 (Tkatchenko/Scheffler) will be here the direct theoretical counterpart to our nonlinear THz-experiments.

3.4.3 In the last year of the second funding period we would like to come back to the surface exciton in ZnO which was discovered within the CRC during the first funding period [13]. In addition to the well known optical transition of an exciton in visible or ultraviolet spectral range there are also intra-exciton transitions within an existing quasiparticle, e.g. the 1S to 2P transition of the relative motion between the electron and the hole typically having a transition frequency somewhat smaller than the exciton binding energy (i.e. 60 meV in ZnO). Such intra-excitonic excitations were recently found in GaAs/AlGaAs quantum well structures [12]. The plan is now to find an organic molecular crystal with a polar low frequency phonon which is resonant to the intra-exciton transition of the ZnO crystal. Such a situation would offer a switchable HIOS because the hybrid mode of the latter would only exist if surface excitons were previously excited in the sample. In turn a strong THz pulse could be used to switch the excitons into the "dark" 2P state. Switching on and off the hybrid mode of a HIOS opened the door to completely new applications of HIOS in the ultrafast time domain.

3.5 Role within the Collaborative Research Centre

The project B5 focuses on linear and nonlinear spectroscopy on HIOS in the spectral range between 1 to 100 THz. Concerning the assembly of HIOS we aim for the inorganic part at a close collaboration with projects A5 (Henneberger) and A8 (Koch). Concerning the synthesis of organic molecules we will have a close collaboration with Z1 (Hecht). A10 (Tkatchenko/Scheffler) will be the direct theoretical counterpart to our linear and nonlinear THz-experiments. Concerning the physics of radiative coupling we will have intense discussion with B12 (Knorr/Richter).

3.6 Delineation from other funded projects

Michael Wörner receives currently (10/2014 - 09/2016) funding from the DFG through project WO 558/13-2 "Ultraschnelle Umverteilung elektronischer Ladung in ionischen Kristallen mittels Femtosekunden-Röntgenbeugung". In the latter project we use the experimental method femtosecond x-ray diffraction which is quite different from nonlinear terahertz spectroscopy, the major concept of the present proposal.

3.7 Project funds

3.7.1 Previous funding

The project has been funded within the Collaborative Research Centre since 07.2011. Previously, it was funded by DFG under reference number B5 from 07.2011 to 06.2015.

3.7.2 Funds requested

Funding for	2015/2		2016		2017		2018		2019/1	
Staff	Quantity	Sum	Quantity	Sum	Quantity	Sum	Quantity	Sum	Quantity	Sum
Postdoc, 100%	1	31.800	1	63.600	1	63.600	1	63.600	1	31.800
Total		31.800		63.600		63.600		63.600		31.800
Direct costs	Sum		Sum		Sum		Sum		Sum	
Small equipment, Software, Consumables	7.500		15.000		15.000		15.000		7.500	
Other										
Total	7.500		15.000		15.000		15.000		7.500	
Major research equipment	Sum		Sum		Sum		Sum		Sum	
€ 10.000 - 50.000										
> € 50.000										
Total										
Total	39.300		78.600		78.600		78.600		39.300	

(All figures in Euro)

3.7.3 Staff

	No.	Name, academic degree, position	Field of research	Department of university or non-university institution	Commitment in hours/week	Category	Funded through:
Available							
Research staff	1.	Michael Wörner, Dr., department head	Experimental physics	Max Born Institute	15		MBI
	2.	Thomas Elsässer, Prof. Dr., director	Experimental physics	Max Born Institute	5		MBI
	3.	Klaus Reimann, Prof. Dr., scientist	Experimental physics	Max Born Institute	15		MBI
Non-research staff	4.	Peter Scholze, technician		Max Born Institute	15		MBI
Requested							
Research staff	5.	N.N., scientist	Experimental physics	Max Born Institute		postdoc	
Non-research staff							

Job description of staff (supported through available funds):

1. Michael Wörner: Scientific and administrative project management

2. Thomas Elsässer: Scientific and administrative project management

3. Klaus Reimann: Scientific support and discussion

4. Peter Scholze: Making of special equipment in mechanical work shop

Job description of staff (requested):

5. N.N.
The postdoc will carry out the one- and two-dimensional nonlinear experiments on HIOS in the terahertz to mid-infrared spectral range. He/she will analyze the experimental data and is supposed to write the first drafts of manuscripts and conference abstracts. In a later stage he/she will also be involved in the detailed planning of experiments in close collaboration with the other partner projects within the CRC. Mastering the complexity of nonlinear THz experiments requires a researcher at the postdoctoral level.

3.7.4 Direct costs for the new funding period

	2015/2	2016	2017	2018	2019/1
Funds available	5.000	10.000	10.000	10.000	5.000
Funds requested	7.500	15.000	15.000	15.000	7.500

(All figures in Euro)

Funds available: The Max-Born-Institute provides both a fully equipped laboratory for nonlinear THz spectroscopy and a second laboratory for performing similar experiments in the mid-infrared spectral range. In addition to the overhead costs and the salaries of the MBI staff involved in the project, the institute will provide an amount of € 10.000 per year for equipment and running costs. This includes laser warranties, liquid helium for low temperature experiments, and other parts (lenses, laser crystals, etc.) which are subjects to regular wear and tear in our femtosecond spectrometers and have to be replaced at regular intervals.

Funds requested: The current nonlinear THz and MIR spectrometers allow exclusively for experiments in transmission geometry. Thus, for the planned reflection experiments on HIOS systems we need special additional equipment for both femtosecond spectrometers (THz and MIR). From the funds requested we will integrate special setups for performing experiments in reflection geometry under variable angles of incidence. Other HIOS will be investigated using the ATR geometry. For such home-built devices we have to buy special prisms, mirrors, and opto-mechanical components for controlling the setups in our femtosecond spectrometers. In addition, the optics in the spectral range 1 - 100 THz has to be changed almost for every micron of wavelength since the transparency range and dispersion of almost all materials is strongly influenced by their respective Reststrahlen band. Furthermore, the nonlinear crystals for generating electric field transients in the range 1 - 100 THz are also different depending on the exact wavelengths needed. For generating the high electric fields necessary for performing nonlinear THz spectroscopy the nonlinear crystals are operated at their damage threshold making them to an additional subject to regular wear and tear in our femtosecond spectrometers. Thus, for the special additional equipment exclusively used for the planned experiments on HIOS systems we request an amount of € 15.000 per year to be funded through the DFG.

3.7.5 Major research equipment requested for the new funding period

No major research equipment is requested for the new funding period.

3.7.6 Student assistants

No student assistants are requested for the new funding

3.1 About project B6

3.1.1 Title: Theory of transfer processes and optical spectra of molecule, inorganic semiconductor, and metal nano-particle hybrid systems

3.1.2 Research areas: theoretical chemical physics, dynamics and optical properties of nano-systems

3.1.3 Principal investigator

PD Dr. habil. Volkhard May (*22.03.1954, German)
Humboldt-Universität zu Berlin, Institut für Physik, Newtonstr. 15, 12489 Berlin
Phone: +49 (0)30 2093 4821
Fax: +49 (0)30 2093 7666
E-mail: may@physik.hu-berlin.de

Do the above mentioned persons hold fixed-term positions? no

3.1.4 Legal issues

This project includes

1.	research on human subjects or human material.	no
	A copy of the required approval of the responsible ethics committee is included with the proposal.	no
2.	clinical trials	no
	A copy of the studies' registration is included with the proposal.	no
3.	experiments involving vertebrates.	no
4.	experiments involving recombinant DNA.	no
5.	research involving human embryonic stem cells.	no
	Legal authorization has been obtained.	no
6.	research concerning the Convention on Biological Diversity.	no

3.2 Summary

Prospective work shall continue the theoretical analysis of ultrafast excited state dynamics in hybrid systems which are formed by molecular complexes (dye aggregates), semiconductor nano-crystals (NCs), and metal nano-particles (MNPs). Therefore, we further apply the semi-empirical type of description which has been developed in the first founding period and which allows to investigate larger systems but just with an atomic resolution. While the computations were restricted to the study of electronic excitation energy dynamics so far, future work will also cover charge separation processes taking place at a semiconductor molecule interface.

In sub-project 1 we intend to describe photoinduced charge separation at a ZnO organic molecule (oligophenyl) interface as experimentally investigated in B3 (Blumstengel), B7 (Neher) and B9 (Stähler). Using a semi-empirical description, a ZnO cluster with thousands of atoms faced to a complex with some hundreds of molecules will be simulated. To follow charge separation kinetics up to a picosecond time region without electron (hole) reflection at the boundaries of the finite system, such large interface complexes are necessarily to be considered.

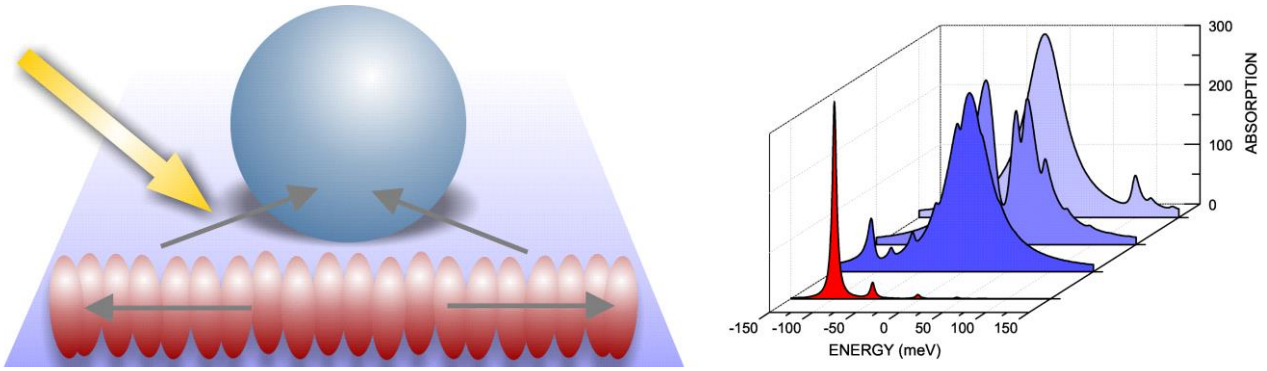

Figure 11: Arrangement of a spherical MNP (blue) in the proximity of a molecular chain (ruby coloured) as considered in [P2,P4,P5,P6] (left panel). The molecule-MNP system is treated as a uniform quantum system covering the electronic excitations of all components and the Coulomb-coupling among them. The scheme has been used to investigate MNP induced changes of optical and transport properties within the molecular system. Right panel: absorption spectrum of a J-aggregate of 10 molecules near a MNP (change of resonance condition; red filled curve: without MNP, increased by 5000).

Depending on the concrete photoexcitation process (wavelength, number of pulses, duration) different scenarios of electron-hole pair formation at the interface will be investigated. Transient spectra as measured in the experiment shall be computed. Own Molecular Dynamics (MD) simulations of the molecular complex on the ZnO clusters offer insight on the overall arrangement of atoms and molecules. These computations are done in collaboration with A4 (Heimel) and A7 (Klapp/Dzubiella). The excited electronic states are determined in the framework of a tight-binding description of ZnO and in using a Frenkel-exciton model as well as a hole transfer description for the molecular complex. Parameters of the ZnO tight-binding model will be taken from literature. Own quantum chemical computations will be carried out to characterize the molecular excitations. Some parameters of the charge separated state are gained by a comparison with ab-initio computations done by B11 (Draxl). The temporal evolution of the charge separation process will be characterized in different levels of sophistication. We will start with the solution of the time-dependent Schrödinger equation governing the dynamics of a Coulomb-correlated electron-hole pair. To have a more realistic description we, then, turn to a density matrix approach. It also allows to account for weak and intermediate electron-phonon coupling in ZnO and for electron vibrational coupling in the molecular system. A description of stronger electron-vibrational coupling, for example, to consider polaron formation will be only undertaken at the end of the second funding period. It requires more sophisticated methodologies like the multi-configuration Hartree technique to propagate coupled electron-vibrational states. When turning to the computation of transient optical spectra a generalization becomes necessary to the description of two interacting electron-hole pairs.

Sub-project 2 shall study the interplay between Frenkel-like excitons formed in a huge tubular dye aggregate (TDA) and Wannier-Mott-like excitons of a semiconductor (CdTe) NC. Related experiments are carried out in A6 (Kirstein/Rabe). The intended computations merge work of the first founding period on electronic excitations in NCs and on excitations in molecular complexes. The molecular structure of the TDA formed by isocyanine type dyes are studied by MD simulations and the electronic excitations are characterized on the basis of own quantum chemical computations. This enables in a direct way the investigation of Frenkel-exciton localization and the influence of structural and energetic disorder. An atomistic description of semiconductor NC electron-hole pair excitations is achieved in the framework of the tight-binding description (as it was already applied in the first funding period). Further on, matrix elements of electronic excitation energy transfer between TDA and NC excitations have to be calculated. They decide on the coupling strength between both sub-systems and thus of the type of energy transfer. To study this in accordance with planned experiments we first concentrate on the independent photoinduced energy transfer dynamics in the TDA. Respective kinetics of the Frenkel-like excitons will be tackled either in the framework of a density matrix description or a mixed quantum-classical approach. As further planed in the experiment these kinetics shall be probed by energy exchange between semiconductor NCs differently placed in relation to the dye aggregate. If one NC acting as an energy donor and one acting as an energy acceptor are attached to the TDA in a defined distance photoinduced excitation of the donor may result in a delayed photoemission of the acceptor. This is due to a finite time of energy transfer along the TDA. By comparing respective experiments of A6 (Kirstein/Rabe) with own simulations details of the transfer can be uncovered. Finally, the theory of molecule MNP coupling as developed in the first founding period will be used to make predictions on plasmon enhancement effects on the Frenkel-exciton Wannier-Mott-exciton interplay.

3.3 Project progress to date

3.3.1 Report and state of understanding

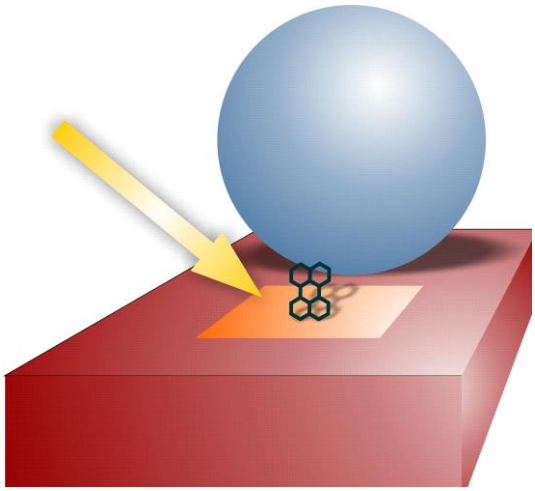

Figure 12: Scheme used in [P8] to describe MNP enhanced interfacial electron transfer. A perylene molecule has been attached to a TiO_2-surface which is additionally decorated with a MNP. Plasmon induced absorption enhancement of the dye may increase the charge injection probability by three orders of magnitude.

Project work of the first funding period concentrated on two sub-projects. One addressed the problem of plasmon enhancement effects of optical properties and excitation energy transfer in molecular complexes. The second sub-project was aimed at a description of exciton formation in NCs coupled to a system of molecules. At the beginning of project work both issues required the solution of a number of methodological problems. The project PI had a longstanding experience in the description of molecular systems and their internal dynamics. However, it was necessary to establish a proper description of MNP plasmon excitations and of Coulomb correlated electron-hole pairs in NCs.

To carry out the required microscopic description of molecules interacting with MNPs (cf. Fig. 1) a respective plasmon Hamiltonian had to be constructed. In [P2] we gave a detailed description how to establish such a Hamiltonian for spherical MNPs and how to introduce the coupling of plasmon excitations to a molecular system. The approach was based on some work in literature on the so-called energy momentum method. However, the derived molecule plasmon coupling is new. The used treatment implied the introduction of a uniform quantum theory of the molecule MNP interaction. Like the molecular system the MNP is characterized by its electronic excitations, here the collective multipole plasmon excitations. If negative and positive charge is totally balanced in the molecule (absence of permanent dipole moments either in the ground or the excited state) the Coulomb interaction between the molecule and the MNP does not include image charge effects. It exclusively covers an excitation energy transfer coupling (similar as the interaction among excited molecules). However, the theoretical description needed to account for the short plasmon life-time. This could be directly realized in the framework of the used density matrix theory.

If the molecule-MNP coupling is weak a molecular excitation is irreversible transferred into a MNP plasmon. The latter quickly decays into an individual electron-hole pair excitation and finally heat is produced. Thus, molecular excitation has been quenched. It is essential for the whole used theoretical methodology that this molecular quenching process is an obligatory part of the theory. If the molecule nano-particle coupling is strong, hybridization appears. The molecular excitation gains oscillator strength to an extreme extend. This explains all effects of molecular absorption and emission enhancement due to nearby placed MNPs [P2,P4,P5,P6] (Ref. [P2] describes for the first time J-aggregate Frenkel exciton oscillator strength rearrangement). Formulated in this way the theory does not need the introduction of a local field (to which an external field has been changed due to the presence of the MNP).

The description of interacting molecule MNP systems has been also applied to suggest plasmon enhancement of heterogeneous (interfacial) electron transfer in [P8] (see also Fig. 3). Furthermore, plasmon enhanced single molecule conductivity [P1] and a novel scheme of plasmon enhanced electroluminescence [P3,P7,P10] has been demonstrated. The work of [P10] also concentrates on an exact density matrix description of a system of many molecules interacting with a single MNP. (Recent work demonstrated for a system of up to 50 molecules the possibility to pump the molecules to such an extent that multiple dipole plasmons are excited although their life-time is extremely short.)

By investigating Wannier-Mott like excitons in semiconducting NCs the project work further entered a field which was new for the group of the PI. As documented in [P9,P13] we are now ready to describe a single Coulomb correlated electron-hole pair in a CdSe NC with some thousands of atoms. Thereby, we followed the methodology of [1-4] (see also Fig. 3). It starts with a tight-binding description of electrons and holes and accounts for the intra electron-hole pair Coulomb coupling by a configuration interaction (CI) scheme. This work has been extended to the computation of the excitation energy transfer coupling to a single molecule close to the NC. The considerations could be based on the use of atomic centered partial transition charges both for the NC and for the molecule. In this way one arrives at a description far beyond any dipole-dipole coupling. Respective rates of Förster (FRET)-like excitation energy transfer have been computed. They demonstrate for the CdSe-NC tetrapyrrole-type molecule systems transfer times in the nanosecond region. Thus, hybrid exciton formation can be excluded for this system. (The special type of molecule has been taken since its excitation energy fits to the NC gap and since data for the excited state have been available from separate quantum chemical computations of [5].) Similar considerations for a NC-NC energy transfer are known from literature (see, for example, the recent work of [6]). A description of a molecule-NC coupling with an atomic resolution can be only found in [7], but ignoring exciton effects. Our treatment improves the

theory in this respect and also considers particular NC geometries. Recently, the work has been extended to NC-excitations which couple to Frenkel-type excitons of a large molecular aggregate [P12,P13]. This represents

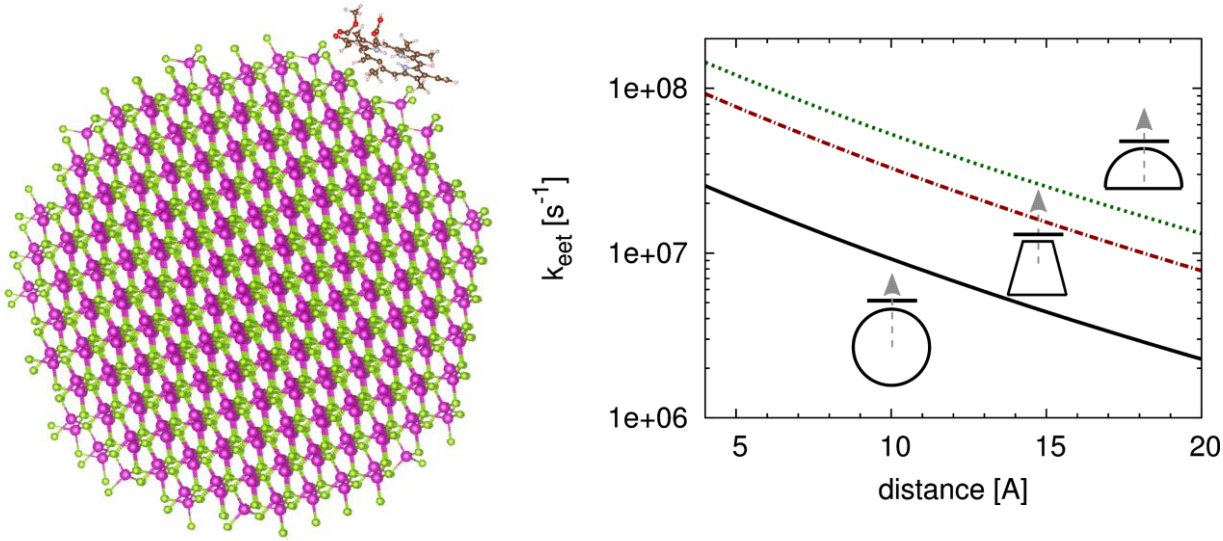

Figure 13: Spherical $Cd_{1159}Se_{1450}$ NC with the tetrapyrrole type Pheophorbide-a molecule close to its surface as investigated in [P9] (left panel). FRET-type energy transfer from the NC to the molecule is possible. Right panel: rate of excitation energy transfer from a thermal distribution of NC-excitons. The rate is drawn versus NC molecule distance as indicated and for different shaped NCs (after [P9]).

essential preparatory work for the new funding period.
It is also necessary to indicate that the newly suggested concept of site-dependent polarization effects in molecular complexes as explained in [P11] is of huge importance for further work. The effect accounts for a change of the molecular excitation energy due to an environmental electronic polarization. In this manner it generalizes what is known for molecular crystals as the gas-to-crystal shift. The considered molecule polarizes its environment and this polarization reacts back to the molecule by changing its wave function and its energy. In the case of a nano-structured system the actual type of the polarizable environment may strongly depend on the molecular position. Accordingly, the excitation energy shift does not remain a constant but becomes site-dependent. Since this shift may overcome the strength of the resonant excitation energy transfer (excitonic) coupling, it strongly affects the spectrum of excitation energies and thus the absorption line-shape. Ref. [P11] offers a reliable scheme to calculate this site-dependent energy shift.
The work on molecule-MNP systems was oriented at planed measurements of B1 (Aichele/Benson). This project has been interrupted, what explains the missing common publications. Work on larger NCs using a semi-empirical tight-binding description has been undertaken to finally simulate photoemission of nano-rods decorated by molecules as to be formed in B8 (Riechert/Grahn). Structure growth techniques were not successfully applied and the project B8 is not continued. Again, a common publication could not be written. However, by concentrating on experiments of A5 (Henneberger), A6 (Kirstein/Rabe), and B3 (Blumstengel) diverse questions were investigated which are of direct interest for the experiments as well as for the work in the new funding period [P11,P12,P13].

References

[1] S. Schulz, S. Schumacher, G. Czycholl, Phys. Rev. B **73**, 245327 (2006).
[2] N. Baer, S. Schulz, P. Gartner, S. Schuhmacher, G. Czycholl, and F. Jahnke, Phys. Rev. B **76**, 075310 (2007).
[3] M. Korkusinski, M. Zielinski, P. Hawrylak, J. Appl. Phys. **105**, 122406 (2009).
[4] M. Korkusinski, O. Voznyy, P. Hawrylak, P. Phys. Rev. B **82**, 245304 (2010).
[5] J. Megow, B. Röder, A. Kulesza, V. Bonacic-Koutecky, and V. May, Theodor Förster commemorative issue, ChemPhysChem, **12**, 645 (2011).
[6] Z. Lin, A. Franceschetti, and M. T. Lusk, ACS Nano **6**, 4029 (2012).
[7] C. Curutchet, A. Franceschetti, A. Zunger, G. D. Scholes, J. Phys. Chem. C 112, 13336 (2008).
[8] G. Wu, Z. Li, X. Zhang, and G. Lu, J. Phys. Chem. Lett. **5**, 2649 (2014).
[9] A. Troisi, Faraday Discuss. 163, 377 (2013).
[10] H. Ma and A. Troisi, Adv. Mater. 26, 6163 (2014).
[11] H. Tamura and I. Burghardt, J. Am. Chem. Soc. **135**, 16364 (2013).
[12] L. Han, X. Zhong, W. Liang, and Y. Zhao, J. Chem. Phys. **140**, 214107 (2014).
[13] J. C. Phillips, R. Braun, W. Wang, J. Gumbart, E. Tajkhorshid, E. Villa, C.

Chipot, R. D. Skeel, L. Kale, and K. Schulten, J. Comput. Chem. **26**, 1781 (2005) .
[14] N. A. Hill and U. Waghmare, Phys. Rev B **62**, 9902 (2000).
[15] Z. Zeng, C. S. Garoufalis, S. Baskoutas, and G. Bester, Phys. Rev. B **87**, 125302 (2013).
[16] M. Rohlfing and S. G. Louie, Phys. Rev. B **62**, 4927 (2000).
[17] V. May and O. Kühn, Charge and Energy Transfer Dynamics in Molecular Systems, Wiley-VCH, 2000, 2004, 2011.
[18] A. Kubas, F. Hoffmann, A. Heck, H. Oberhofer, M. Elstner, and J. Blumberger, J. Chem. Phys. **140**, 104105 (2014).
[19] S. Mukamel and D. Abramavicius, Chem. Rev. **104**, 2073 (2004).
[20] J. Megow, Y. Zelinskyy, B. Röder, A. Kulesza, D. Mitric, and V. May, Chem. Phys. Lett. **522**, 103 (2012).
[21] D. M. Eisele, S. Kirstein, J. Knoester, J. P. Rabe, D. A. Vanden Bout, Nature Nanotechnology **4**, 658 (2009).
[22] D. M. Eisele, C. W. Cone, E. A. Bloemsma, S. M. Vlaming, C. G. F. van der Kwaak, R. J. Silbey, M. G. Bawendi, J. Knoester, J. P. Rabe, D. A. Vanden Bout, Nature Chemistry **4**, 655 (2012).
[23] S. M. Vlaming, E. A. Bloemsma, M. L. Nietiadi, and J. Knoester, J. Chem. Phys. **134**, 114507 (2011).
[24] F. Haverkort, A. Stradomska, A. H. de Vries, and J. Knoester, J. Phys. Chem. A **118**, 1012 (2014).
[25] G. D. Scholes, C. Smyth, J. Chem. Phys. **140**, 110901 (2014).
[26] T. Fujita, J. C. Brookes, S. K. Saikin, and A. Aspuru-Guzik, J. Phys. Chem. Lett. **3**, 2357 (2012).
[27] J. M. Linnanto and E. I. Korppi-Tommola, J. Phys. Chem. B **117**, 11144 (2013).
[28] J. Huh, S. K. Saikin,; J. C. Brookes, S. Valleau, T. Fujita, and A. Aspuru-Guzik, J. Am. Chem. Soc. **136**, 2048 (2014).

3.3.2 Project-related publications

Published work

[P1] Y. Zelinskyy and V. May, “Photoinduced Switching of the Current through a Single Molecule: Effects of Surface Plasmon Excitations of the Leads”, Nano Lett. **12**, 446 (2012).
[P2] Y. Zelinskyy, Y. Zhang, and V. May, “A Supramolecular Complex Coupled to a Metal Nanoparticle: Computational Studies on the Optical Absorption”, J. Phys. Chem. A **116**, 11330 (2012).
[P3] Y. Zhang, Y. Zelinskyy, and V. May, “Plasmon Enhanced Single Molecule Electroluminescence”, J. Phys. Chem. C **116**, 25962 (2012).
[P4] Y. Zhang, Y. Zelinskyy, and V. May, “Time and Frequency Resolved Emission of Molecular Systems Coupled to a Metal Nanoparticle”, J. Nanophot. **6**, 063533 (2012).
[P5] G. Kyas, Y. Zelinskyy, Y. Zhang, and V. May, “Spatio-Temporal Excitation Energy Localization in a Supramolecular Complex Coupled to a Metal-Nanoparticle”, Ann. Phys. (Berlin) **525**, 189 (2013).
[P6] Y. Zelinskyy, Y. Zhang, and V. May, “Photoinduced Dynamics in a Molecule Metal Nanoparticle Complex: Mean-Field Approximation Versus Exact Treatment of the Interaction”, J. Chem. Phys. **138**, 114704 (2013).
[P7] Y. Zhang, Y. Zelinskyy, and V. May, “Plasmon Enhanced Electroluminescence of a Single Molecule: A Theoretical Study, Phys. Rev. B **88**, 155426 (2013).
[P8] L. Wang and V. May, “Plasmon Enhanced Heterogeneous Electron Transfer: A Model Study”, J. Phys. Chem. C **118**, 2812 (2014).
[P9] D. Ziemann and V. May, “Distant and Shape Dependent Excitation Energy Transfer in Nanohybrid Systems: Computations on a Pheophorbide-a CdSe Nanocrystals Complex”, J. Phys. Chem. Lett. **5**, 1203 (2014).
[010] Y. Zhang and V. May, “Plasmon-Enhanced Molecular Electroluminescence: Effects of Nonlinear Excitation and Molecular Cooperativity”, Phys. Rev. B **89**, 245441 (2014).

Unpublished work

[011] J. Megow, T. Körzdörfer, T. Renger, M. Sparenberg, S. Blumstengel, F. Henneberger, and V. May, ’’Calculating optical absorption spectra of thin polycrystalline films: Structural disorder and site-dependent molecular electronic polarization”, https://www.physik.hu-berlin.de/sfb951/publications
[012] J. Megow, M. Röhr, M. Schmidt am Busch, T. Renger, R. Mitric, S. Kirstein, J. Rabe, and V. May, ’’Understanding the exciton spectrum of double-walled tubular dye-aggregates: Importance of the excitation energy shift due to site-dependent electronic polarization”, https://www.physik.hu-berlin.de/sfb951/publications
[013] T. Plehn, D. Ziemann, J. Megow, and V. May, “Frenkel to Wannier-Mott Exciton Transition: Theory of FRET-Rates for a Tubular Dye Aggregate Coupled to a CdSe Nanocrystal”, https://www.physik.hu-berlin.de/sfb951/publications

3.4 Research plan

3.4.1 Sub-project 1: Charge transfer kinetics at the HIOS interface

If photoexcitation is applied to a semiconductor molecule interface charge transfer and charge separation is common. In particular project B7 (Neher) documented a number of respective processes in the first funding period. A detailed theoretical analysis is planned of these measurements as well as of future experiments, done also by B3 (Blumstengel) and B9 (Stähler). It is of particular interest for the future work that the semi-empirical models developed in the first funding period are ready for an application to a large interface model. This model is formed by a ZnO cluster which covers thousands of atoms and thus reaches an edge length somewhat below 10 nm. Such an extension also allows to place some hundreds of molecules (oligophenyls, perylene and naphthalene derivatives) to the surface. The subsequent work then comprises: (a) MD simulations of the molecular arrangement at the ZnO-surface to obtain a sufficient realistic geometry, (b) a reliable characterization of the excited and charge separated states of the ZnO molecule interface, (c) simulations of photoinduced interface electron-hole pair kinetics, and (d) computation of transient optical spectra. So, a description of photoinduced interface processes is reached with an atomic resolution but at a level of theory ready to arrive at a length scale of some tens of nm. In a first step a pure electronic model will be used. Later phonon coupling to the electrons and holes in ZnO as well as the influence of intramolecular vibrations in the molecular complex will be studied. After the development of a realistic model of all involved excited and charge separated states, the interrelation between the type of photoexcitation and the resulting excitation energy and charge transfer kinetics will be uncovered. At the same time it is necessary to highlight signatures of these kinetics in, for example, transient absorption spectra.

Noting the state of the art in this field, project work has to develop own models and methodologies to describe photoinduced charge separation for larger systems. This is of particular importance since only large systems offer the possibility to describe the transition from a correlated to an un-correlated motion of the electron and the hole near the interface. There is one recent first-principle study on a poly(3-hexylthiophene) ZnO interface which combines time-dependent DFT with nonadiabatic ab initio MD simulations [8]. Although of high accuracy both, the smallness of the considered interface part as well as the restriction to a 500 fs time interval indicate that such technique is not suited to describe charge separation at the interface nor to obtain related transient spectra. Indeed, the work of [9,10] addresses the problem of charge separation at an interface but concentrates on that between two types of molecular systems. Moreover energy spectra and DOS for charge transfer excitation are computed. Dynamical considerations are restricted to the computation of transition rates. The work of [11] (and earlier studies by the same authors) on an oligothiophene fullerene interface goes beyond such a description and studied the detailed dynamics of charge separation in a system with some hundreds of molecules. In particular, the coupling of the hole moving through the oligothiophene layers to molecular vibrations could be considered. The propagation of an electron-hole pair wavefunction to study charge separated motion in a molecular aggregate has been suggested in [12]. However, not any study concentrates on the computation of transient spectra like the frequency dispersed probe pulse absorption. Beside the requirements of the experimental partners B3 (Blumstengel), B7 (Neher), and B9 (Stähler), it is just this situation in literature which motivates the present project to concentrate on the computation of such types of transient spectra. And, all these studies are related to those of B12 (Knorr/Richter) on a macroscopic and periodic ZnO surface regularly decorated with molecules.

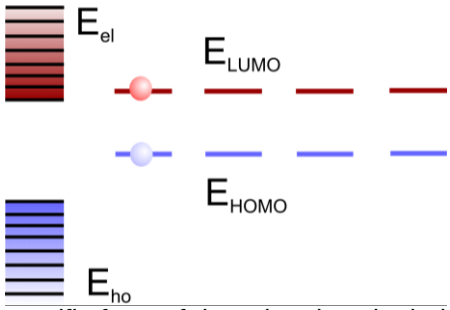

Figure 14: Electronic energy level scheme typical for oligophenyls attached to a ZnO surface. The ZnO cluster is represented by electron (conduction-band like) and hole (valence-band like) levels. The molecular states are restricted to the HOMO and LUMO level of every molecule placed here in a linear arrangement. Optical excitation of an electron-hole pair in the molecule close to the ZnO-surface has been assumed.

MD simulations: The actual structure of the semiconductor cluster, of the molecular complex, and of the interface is translated to a specific form of the related excited electronic states. All energy levels and couplings are determined by the atomic configuration. The tight-binding model used for the definition of single particle (electron and hole) states of the ZnO cluster (and of the CdSe cluster, see sub-project II) is usually defined for a regular arrangement of atoms. However, deviations due to surface reconstructions can become of interest and need to be considered. In the molecular complex, in contrary, Frenkel-exciton states are formed which are basically determined by the excitation energy transfer coupling (excitonic coupling). Its value depends rather directly on the mutual molecular position. A similar dependence applies for charge

separated states. It is therefore essential to calculate all these excited states in starting with a realistic structure. A reliable tool to generate the structure of a molecular complex placed on a semiconductor cluster is the performance of MD simulations. If carried out appropriately (so-called NPT-ensemble simulations) the thermally induced fluctuations around the equilibrium structure of the considered system are obtained (at a particular number of particles, at a particular pressure and at a particular temperature). Based on a longstanding application of the NAMD package [13] and the respective experiences which were gained by this, we continue to use this program. The work of A1 (Dzubiella), A4 (Heimel) and A7 (Klapp) within the first founding period indicated that standard force fields, like that of the well-known AMBER program package, have to be adopted to the specific features of the ZnO surface (decisive rule of the atomic centred partial charges) and the van der Waals coupling to the molecules. Accordingly, close collaboration will be carried out with A4 (Heimel) and A7 (Klapp/Dzubiella). But the interface structure necessary for subsequent computations will be determined by own MD simulations

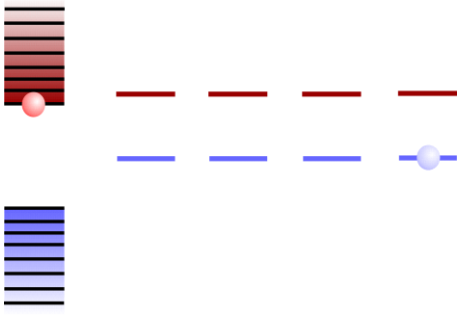

Figure 15: Electronic energy level scheme typical for oligothyophenes attached to a ZnO surface as in Fig. F but after charge separation at the interface.

Excited and charge separated states of the ZnO molecule interface: Fig. 4 displays the relevant electronic levels of a molecular-complex placed on a ZnO cluster, with the latter represented by electron (conduction-band like) and hole (valence-band like) levels. The molecular states are restricted to the HOMO and LUMO level of every molecule placed here in a linear arrangement. Optical excitation of an electron-hole pair in the molecule close to the ZnO-surface has been assumed. According to the drawn energy level scheme the system is ready to initiate electron injection into the ZnO cluster and hole motion in the molecular system (see Fig. 5). To become comparable with the experiment the simple electron-hole picture has to be improved. As long as no charge separation takes place we have to introduce Wannier-Mott-like excitons in the ZnO cluster and Frenkel-like exciton states in the molecular complex.

To obtain Wannier-Mott-like excitons (Coulomb correlated electron-hole pairs) of ZnO we use the expertise obtained in the first funding period by studying excited electronic states of a CdSe NC (cf. Ref. [P9]). Starting with a tight-binding description of ZnO as given in [14] (strain effects are discussed in [15]) electron and hole levels according to Fig. 4 can be computed. Surface reconstruction will be addressed, however, in a later stage of work. In a second step the Coulomb-interaction between the electron and hole of the considered pair has to be computed. If only a single pair is excited this corresponds to the trivial solution of the Bethe-Salpeter equation methodology of electron-hole pair propagation (for example [16]). Following quantum chemistry terminology the treatment is also known as the configuration interaction (CI) approach ([1-4]). As a result one obtains exciton energies E_α and expansion coefficients $C_\alpha(a,\bar{a})$ which describe the pairing of an electron (with quantum number a) and a hole (with quantum number $\bar{a}$).

Concerning Frenkel-like excitons of the oligophenyl complex the planed investigations are based on a longstanding expertise in the field (some remarks extending the subsequent description can be also found in the respective part of sub-project 2). The work starts with own quantum chemical studies. As in earlier work DFT and TD-DFT techniques as available in standard quantum chemical program packages will be used to carry out these computations. Here, excited state wave functions are obtained with a sufficient accuracy to deduce atomic centered partial transition charges and transition dipole moments. However, the excitation energy E_m (site energy of the Frenkel-exciton model referring to molecule m) has to be corrected to match the value known from experiment. The excitation energy transfer (excitonic) coupling J_{mn} between molecule m and n is essential for the Frenkel-exciton formation. It will be calculated beyond the dipole-dipole coupling in using the atomic centered partial transition charges (see, e.g., [17]). Diagonalization of the Hamilton matrix $\delta_{m,n}E_m + J_{mn}$ gives the exciton spectrum. It directly reflects the concrete arrangement of the molecule in the cluster via the J_{mn}. It also has to be proven if charge transfer contributions to the Frenkel-exciton levels are of some relevance. Moreover, we will check if the generalizations of the standard Frenkel-exciton approach as discussed in section 3.3.1 (site-dependent polarization) have to be applied here, too. In a final step the charge separated states with an electron in the ZnO cluster and a hole in the molecular system have to be characterized (hybrid charge transfer exciton and its decay, cf. Fig. 5).

To describe hole motion in the molecular system the use of an empty HOMO-level is insufficient. Instead the oxidized state of the oligophenyl with total energy E_{m+} has to be considered. The transfer coupling T_{mn} may

move the hole from site n to site m. Both sets of quantities E_{m+} and T_{mn} will be calculated, with the T_{mn} to be deduced by a so-called diabatization procedure (see the approach used in [11] and the recent overview on transfer couplings in [18]). When considering electron transfer from an excited molecule at the ZnO surface into the semiconductor we will not apply the mentioned diabatization procedure. Instead, a single molecule at the ZnO surface is studied in a model with respective transfer couplings incorporated. Then, these couplings are fixed by a comparison with ab-initio computations carried out in B11 (Draxl) for the same system. (This procedure will be also carried out when considering hole transfer from a ZnO electron-hole pair into a molecule at the interface). Finally, it is necessary to emphasize that the construction of the Hamiltonian covering all necessary interactions is an independent work since there is not any standard in literature within this respect.

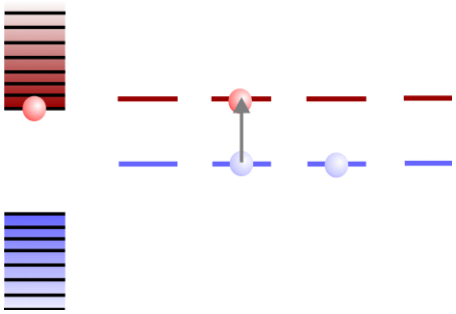

Figure 16: Transient absorption spectroscopy creates an initial electron-hole pair by the pump pulse (drawn in a spatial separated configuration). The subsequent probe pulse induces a second electron-hole pair (intramolecular excitation) which may interact with the first one.

Interface electron and hole kinetics: The properly defined excited and charge separated states at the molecule ZnO interface form the basis to study photoinduced dynamics. To initiate the dynamics and to later on correctly compute transient spectra optical excitation is included into the description via the standard term $-\vec{\mu}\vec{E}(t)$. The electronic transitions are considered by the dipole operator $\vec{\mu}$. It covers either the formation of Wannier-Mott-like excitons in ZnO or that of Frenkel-like exciton in the molecular complex. And, it has to be proven if transition dipole moments are large enough to also allow for the direct excitation of a charge transfer. The electric field-strength $\vec{E}(t)$ of the coupling expressions specifies the type of optical excitation (wavelength, intensity, duration).
To later on change to a more involved description we start with the following ansatz for the time-dependent wave function $|\psi(t)>=C_0(t)|0>+\sum_{a,\bar{a}}C_{a\bar{a}}(t)|a\bar{a}>+\sum_m C_m(t)|m>+\sum_{a,m}C_{am+}(t)|am+>$. It covers the coherent superposition of the interface electronic ground-state $|0>$ and all possible singly excited states. Those comprise electron-hole pair excitations $|a\bar{a}>$ in ZnO, intramolecular excitations $|m>$ in the molecular complex, and the charge transfer (charge separated) states $|am+>$ with an electron in the conduction band-like ZnO state a and a hole at molecule m. Since the related time-dependent Schrödinger-equation is solved including electron-hole Coulomb interaction, the dynamics represented by $|\psi(t)>$ cover a correlated motion of the electron and the hole. In particular, an initially photoexcited electron-hole pair in the ZnO cluster may be split into a remaining electron and a hole placed in a molecule positioned close to the interface. Concerning the ZnO cluster the structure of the Coulomb coupling is known [P9]. It is accounted for by the matrix elements $V_{a\bar{a},\bar{b}b}$. When describing Coulomb-interaction of the hole at molecule m and the electron transition density in ZnO, the matrix elements $V_{am,mb}$ have to be taken. They represent the essential quantities which control the persistence of a charge transition state as well as its decay in a charge separated state.
The description based on a time-dependent electron-hole pair expansion coefficient has the potential to characterize correlated charge motion. In order to distinguish between correlated and a (charge) separated motion, however, a methodology is necessary which also accounts for energy dissipation and dephasing. The standard approach would be the density matrix description of such a system. Now, the density matrix $\rho_{AB}(t)$ replaces the time-dependent expansion coefficients $C_A(t)$ (for a plausible notation the A,B replace the pair of quantum numbers referring to the electron and the hole; be aware that elements of type $\rho_{A0}(t)$ and $\rho_{00}(t)$ also appear). Since the number of density matrix elements is much larger than the number of expansion coefficients the description is limited to smaller ZnO-molecule systems. However, it is well established how to include into density matrix theory electron phonon (electron vibrational) interaction if the weak and intermediate coupling case is valid [17]. (Alternatively, there are different approaches known as the Monte Carlo wave function techniques which combine the determination of a time-dependent wave function with the consideration of dissipation. A recent variant can be found in [12].) We also indicate that the present description of single electron-hole pair dynamics can be rather directly related to CW-absorption spectra and also time-resolved of photoluminescence [17,P2,P4].

Transient optical spectra: As long as a single laser pulse is applied the study of the subsequent dynamics can be restricted to a single electron-hole pair. In a transient absorption measurement, however, the second pulse may create a further electron-hole pair. For example, a situation may be possible as drawn in Fig. 6. Here, the charge separated state with the electron in ZnO and the hole at a molecule is completed by an additional excitation of a further molecule (obviously, other types of excited states can be also formed). A proper description requires the consideration of all types of Coulomb-coupling among the two electron-hole pairs. Such a single and two electron-hole pair kinetic has to be related to the measured transient spectra. We will focus here on the frequency dispersed transient absorption what represents a standard quantity measured when ultrafast photoinduced dynamics needs an elucidation. Its computation is well-established in literature [19] and will not be repeated here (for a recent description see [20]).

3.4.2 Sub-project 2: Excitation energy transfer kinetics at the HIOS interface: Effects of metal nanoparticles

While in the first sub-project situations shall be considered where charge transfer at the HIOS interface may interfere with excitation energy transfer, this second sub-project concentrates on a hybrid system which exclusively displays excitation energy transfer. The system consist of a large tubular dye aggregate (TDA) formed by the isocyanine type molecule C8S3 and one or more CdTe nano-crystals (NCs) attached to it (cf. Fig. 7). It will be manufactured and characterized in A6 (Kirstein/Rabe). The TDA is composed by two walls of dye molecules, an inner and an outer one and has been already described in [21,22]. Moreover, first computations on the TDA exciton levels and on linear absorption spectra can be found in [23] (see also [24]). There, excitons were introduced by presuming a perfect, distortion free TDA structure with extended dipoles regularly arranged. Recently we suggested a novel TDA structure in Ref. [P12]. MD simulations have been used to proof the molecular structure of the TDA and to get data on thermal fluctuations. The electronic excitations are characterized on the basis of some own preliminary quantum chemical computations. To achieve a uniform description of energy transfer kinetics the earlier work of [P12,P13] shall be continued in this sub-project 2. Therefore, we need to merge different work done in the first funding period. A close comparison with future experimental findings of A6 (Kirstein/Rabe) will be also carried out. In [P9] we computed semiconductor NC electron-hole pair and exciton states and considered their coupling to a nearby placed single molecule. Frenkel-excitons have been introduced in [P2,P4,P5] (and their changed properties due to the coupling to a MNP could be investigated). Accordingly, the whole computations will represent a novel and exciting combination of Frenkel-like exciton dynamics in the TDA with the motion of Wannier-Mott-like excitons of a semiconductor NC. Preliminary work of [P13], furthermore, indicates that efficient energy transfer can be expected even in the sub-ns-range.
According to the planed experiments energy transfer in the TDA shall be probed by energy exchange between semiconductor NCs differently placed in the proximity of the TDA. So, a particular challenge of project work is the proper description of excitation energy transfer dynamics in a TDA with some hundreds of molecules (this goes definitely beyond the work of [P13] where only stationary exciton levels have been computed). Finally, the theory of molecule metal-nanoparticle coupling as developed in the first founding period will be used to make predictions on plasmon enhancement effects on the interplay among Frenkel-excitons and Wannier-Mott-excitons.

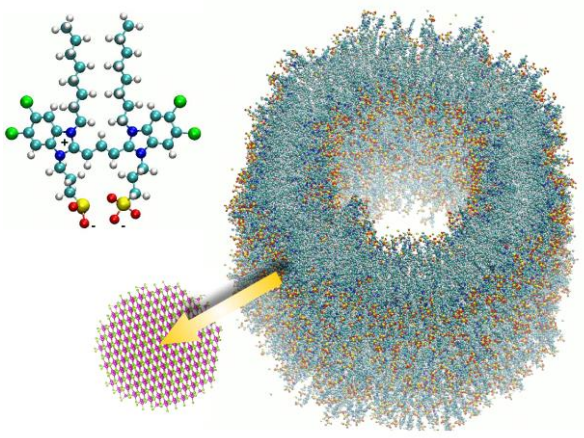

Figure 17: CdSe NC (lower left) placed in the proximity of a TDA formed by isocyanine type molecules C8S3 (upper left part). Excitation energy transfer from the TDA to the NC is indicated by the yellow arrow.

Frenkel-like excitons in the TDA: As already described in the presentation of sub-project 1 exciton levels and wave functions are determined in diagonalizing the respective Hamiltonian $\sum_{m,n} H_{mn} |\phi_m><\phi_n|$. The Hamiltonian matrix H_{mn} has the simple structure $\delta_{m,n}E_m + J_{mn}$. In its diagonal part it covers the so-called site energies E_m (excitation energy of molecule m). The off-diagonal part is formed by the excitonic coupling J_{mn} which resonantly transfers excitation energy from one dye molecule to the other. The ϕ_m are molecular product states with molecule m in the first excited state and all other molecules in the ground-state. The restriction to a single excited state per molecule becomes possible since for the considered cyanine dye C8S3 higher excited states are energetically sufficiently far away.

The excitonic coupling J_{mn} is determined by the electronic transition density $\rho_{eg}(\vec{x})$ (between ground and excited state) of molecule m and n [5,17]. For concrete computations the continuous charge densities are replaced by discrete atomic centered partial transition charges. While respective estimates of J_{mn} have been already used in [P12,P13], more improved computation of the molecular electronic ground and excited state wave functions will be undertaken to get reliable values for $\rho_{eg}(\vec{x})$ and the subsequently derived atomic centered transition charges. Since the J_{mn} depend on the position of the interacting molecules the determination of reliable values for the coupling matrix requires a realistic structure of the TDA. Respective MD simulations confirm the suggested novel structure of [P12] and generate thermal fluctuations with respect to the ideal (regular) arrangement of the dyes in the TDA. So, the approach offers an atomistic description of the energy transfer (excitonic) coupling. It also offers a very direct way to consider effects of disorder. However, the interest is also on an extension to the temporal change of the structure. This change and the subsequent change of the energy levels is of central importance in a mixed quantum classical description (see also below). To reproduce the characteristic line shape of the TDA optical absorption spectrum, it was essential to extend the standard Frenkel-exciton model as described in [P11,P12] (see also Section 3.2.1).

Dynamics of Frenkel-like excitons in the TDA: According to A6 (Kirstein/Rabe) the study of excitation energy kinetics in the TDA represents an essential part of the work. This aim has to be related to the enormous interest in literature to elucidate the type and pathway of electronic excitation energy transfer in huge molecular systems. It is of particular interest in view of the diversity of biological light harvesting antennae [25]. Recently, chlorosomes from green sulfur bacteria which cover thousands of pigment molecules have been theoretically investigated [26,27,28]. The planed work on the exciton motion in the TDA has some similarities with these studies.
To simulate exciton kinetics in molecular systems has a long tradition [17]. The most common approach is the use of Förster-type rates of energy transfer which allow to characterize the redistribution of local molecular excitation. It provides weak excitonic coupling and determines the temporal behavior of the probabilities $P_m(t)$ to have molecule m in its excited state. If the excitonic coupling is strong excitons appear as delocalized or partially delocalized states. These states $|\alpha>$ can be used to describe the kinetics as rate determined transitions among exciton states. Excitation energy transfer kinetics are characterized by probabilities $P_\alpha(t)$. Optical excitation may induce coherences. Correlations between different local states or different exciton levels as described in a density matrix theory become essential. Now the theory can be formulated either by $\rho_{mn}(t)$ or by $\rho_{\alpha\beta}(t)$.
The computations carried out in [P12,P13] are based on a TDA structure with nearly 1000 dye molecules. If the density matrix is defined in the site basis as $\rho_{mn}(t)$ (or if $\rho_{\alpha\beta}(t)$ is taken) we arrive at a matrix with 10^6 elements what may cause numerical problems when propagating up to a 10 ps or even larger time-interval and, moreover, carry out a disorder averaging. As well appreciated in literature the numerical effort is drastically reduced if methods are applied which are based on a propagation of a wave function, here the expansion coefficients $C_m(t)$, only. One may use so-called quantum jump or quantum diffusion techniques (cf. [12] and references therein), or more easily, a mixed quantum classical approach. Concerning the mixed quantum classical description planed work can be based on the extensive study of excitation energy transfer in tetrapyrrole-type molecules [5]. A somewhat similar approach has been used recently in [26]. Also here an ensemble average requires some hundreds of independent wave function propagations to result, for example, in acceptable averaged site-populations $<|C_m(t)|^2>$ [5].

Coupling of the TDA to NCs and MNPs: Excitation energy transfer coupling between NC excitons and a single molecular excitation has been investigated by us in [P9]. As in other cases it is given by the Coulomb interaction of NC exciton transition densities and the ground-state excited-state transition density $\rho_{eg}(\vec{x})$ of the molecule. If we change from a single molecule to the TDA, $\rho_{eg}(\vec{x})$ has to be replaced by a transition density into the TDA exciton levels. For concrete computations a discretization of the transition densities by defining atomic centred transition charge is achieved (cf. [5,P9,P13]).
In a complete density matrix description of the TDA-NC system, respective coupling matrix elements account for energy transfer between the TDA excitons and the NC excitations. Probabilities of having NC-excitons excited may characterize energy transfer into or from the TDA and can be used to determine time-resolved

photoluminescence of the energy acceptor NC. Choosing a mixed quantum classical description of the TDA we use expansion coefficients $C_m(t)$ which have been determined by using a fluctuating (time-dependent) Hamilton matrix $H_{mn}(t)$. (The latter is caused by the translation of TDA structure fluctuations into energy and coupling fluctuations.) If we include NC-exciton contributions in the state expansion and take the TDA-NC energy transfer coupling into account, energy injection from an NC into the TDA and the reverse process can be also accounted for in this mixed quantum-classical scheme. Coupling to a MNP will be described as done in [P2].

3.5 Role within the Collaborative Research Centre

Sub-project 1 was strongly motivated by the planed experiments in B3 (Blumstengel), B7 (Neher) and B9 (Stähler) on HIOS interface charge separation dynamics. So, our work will focus on the computation of transient spectra to support the interpretation of respective measurements. This is of basic importance since computations which could be used for that are not known from literature. The necessary input for such excited state quantum dynamics simulations concerns the atomistic and electronic structure of the ZnO oligophenyl interface. It will be made available in collaboration with A4 (Heimel), A7 (Klapp/Dzubiella) und B11 (Draxl). The work of A4 (Heimel) and A7 (Klapp/Dzubiella) is of importance for the planed own MD simulations of molecular complexes attached to a ZnO surface. We will profit from respective investigations on partial charges and redefined molecule-surface van der Waals interactions. Such knowledge is a prerequisite to generate sufficient realistic interface structures. As described earlier transfer integrals for hole motion in the surface attached molecular complex will be computed. However, the complex problem of the determination of charge transfer integrals valid for the separation of a Frenkel-exciton at the interface into a charge transfer state will be solved in collaboration with B11 (Draxl). All computations are related to those of B12 (Knorr/Richter) on a macroscopic and periodic ZnO surface regularly decorated with molecules. Assistance in quantum chemical calculations will be offered by A4 (Heimel) here and also for sub-project 2.
The work of **sub-project 2** aims at a simulation of experiments planed by A6 (Kirstein/Rabe). Our simulations on TDA excitation energy transfer dynamics may select experimental situations which are most suited for long range energy transfer detection (relative position of the donor and acceptor-NC at the TDA; NC shape and resulting excitation energy spectrum; etc.). At the same time, interpretation of experimental results are assisted in particular if they affected by structural and energetic disorder. The planed close collaboration should result in a development of simulation techniques which are appropriate to describe energy transfer in complexes with thousands of molecules. Finally, simulations on the influence of MNPs placed in the proximity of the NC-TDA complex should find out if plasmon enhancement effects my change the NC-TDA energy exchange. Respective suggestions for more involved experiments in A6 (Kirstein/Rabe) shall follow.

3.6 Delineation from other funded projects

The German-Israeli Foundation for Scientific Research and Development (GIF) supports the project “Time-resolved transport in molecular junctions: measurements and simulation”. The Israel partner is Yoram Selzer from Tel Aviv University, School of Chemistry. The work focuses on the formation of transient currents through a single molecule sandwiched by nano-electrodes.

3.7 Project funds

3.7.1 Previous funding

The project has been funded within the Collaborative Research Centre since 07/2011. Funds requested

Funding for	2015/2		2016		2017		2018		2019/1	
Staff	Quantity	Sum	Quantity	Sum	Quantity	Sum	Quantity	Sum	Quantity	Sum
PhD student, 75%	2	44.100	2	88.200	2	88.200	2	88.200	2	44.100
Total		44.100		88.200		88.200		88.200		44.100
Direct costs	Sum		Sum		Sum		Sum		Sum	
Small equipment, Software, Consumables	1.000		2.000		2.000		2.000		1.000	
Total	1.000		2.000		2.000		2.000		1.000	
Major research equipment	Sum		Sum		Sum		Sum		Sum	
Total	0		0		0		0		0	
Total	0		0		0		0		0	

(All figures in Euro)

3.7.2 Staff

	No.	Name, academic degree, position	Field of research	Department of university or non-university institution	Commitment in hours/week	Category	Funded through:
Available							
Research staff	1	Volkhard May, PD Dr. habil.	Theor. Phys.	HU Phys.	10		
Requested							
Research staff	2	Dirk Ziemann, M. Sci.	Theor. Phys.	HU Phys.			
	3	Thomas Plehn, M. Sci.	Theor. Phys.	HU Phys.			

Job description of staff (supported through available funds):
1) V. May: scientific and organisational leadership of then project
Job description of staff (requested):
2) D. Ziemann: PhD student with background in exciton theory of NCs. Future work concentrates on this part of both sub-projects and on effects of MNPs.
3) Th. Plehn: PhD student with background in charge transfer processes. Future work concentrates on MD simulations, interface dynamics, and computation of transient spectra.

3.7.3 Direct costs for the new funding period

	2015/2	2016	2017	2018	2019/1
Funds available	250	500	500	500	250
Funds requested	1.000	2.000	2.000	2.000	1.000

(All figures in Euro)

Consumables for 2015/2 and 2019/1

software, computer and office supplies	EUR	1.000

Consumables for 2015 - 2018

software, computer and office supplies	EUR	2.000

3.7.4 Major research equipment requested for the new funding period

No funding is requested.

3.7.5 Student assistants

No funding is requested.

3.1 About Project B7

3.1.1 **Title:** Charge Transfer and Charge Separation Across Hybrid Surfaces

3.1.2 **Research areas:** Condensed Matter Physics, Soft Matter Physics

3.1.3 Principal investigator(s)

Prof. Dr. Neher, Dieter (*21.06.1960, German),
Institut für Physik und Astronomie
Universität Potsdam
Karl-Liebknecht-Str.24-25
14476 Potsdam-Golm
Phone: +49 (0) 331 977 1265
Fax: +49 (0) 331 977 5615
E-mail: neher@uni-potsdam.de

3.1.4 Legal issues

This project includes

1.	research on human subjects or human material.	no
2.	clinical trials	no
3.	experiments involving vertebrates.	no
4.	experiments involving recombinant DNA.	no
5.	research involving human embryonic stem cells.	no
6.	research concerning the Convention on Biological Diversity.	no

3.2 Summary

This project aims at a detailed understanding of charge transfer and charge separation across hybrid ZnO/organic interfaces. The proposed work is stimulated by two recent achievements of the PI in the first funding period. Firstly, the PI succeeded to tune the work function of well-defined ZnO single crystal surfaces over a wide range, from 4.1-5.6 eV. This change caused a massive variation of unipolar currents across the hybrid interface, highlighting the large influence of the interface energetics on the injection current. Secondly, the work by the PI on organic bulk heterojunction solar cells revealed efficient split-up of thermalized charge transfer states into free charges, challenging the current view that charge carrier photogeneration must involve excited CT excitons. These studies will be now extended to morphological and electronically well-defined hybrid systems. In particular, we aim at the comprehensive characterization of the charge injection in samples with a homogeneous, possibly controllable, alignment of the organic semiconductor molecules on the inorganic surface. Being able to fine tune the work function of the inorganic surface will allow us to analyze how injection currents are affected by the energetic and structural properties of the hybrid interface. Secondly, we will perform a comprehensive investigation on the formation and split-up of hybrid CT excitons. In contrast to most organic donor-acceptor heterojunctions studied by now, hybrid heterojunctions are accessible to a detailed control of the interface properties. In particular, we want to address the question whether, and to which extend, excess energy (supplied by photons or heat) affects the probability of CT exciton split-up. The success of this work will largely depend on the ability to directly excite hybrid CT excitons, to control the energetics at the interface and to detect charge generation via hybrid CT-split-up with sufficient sensitivity. To this end, we will employ a recently acquired fs pump-probe setup, designed to capture the dynamics of excited species and mobile charges with high sensitivity and time resolution.

3.3 Project progress to date

3.3.1 Report and state of understanding

The main goal of work in the first funding period was to establish protocols for the preparation of hybrid devices with morphologically and energetically well defined hybrid interfaces and to use these devices for a comprehensive study of the efficiency of charge injection in relation to the energetics at the interface and in the bulk of the OSC. Despite the rapid commercialisation of hybrid organic/inorganic electronics for applications such as light emitting diodes, field-effect transistors or solar cells, the fundamental principles of charge injection into the active organic material is still little understood. One reason for this poor understanding is that interfaces used in previous studies were invariably rough and poorly defined, or that experiments were conducted with charge injection from the top electrode, with incontrollable and inaccessible interface energetics and morphology. A promising solution to this problem is to employ hybrid devices with inorganic bottom electrodes, as these can be prepared with high chemical and structural perfection. The development of an energetically as well as structurally well-defined electrode for an accurate investigation of the charge transfer at these hybrid interfaces was, therefore, a major objective of work performed in project B7.

3.3.1.1 Preparation of Morphological Well-Defined Zinc Oxide Surfaces with Tuneable Work Function

Zinc oxide (ZnO) was chosen because of the possibility to grow ZnO hydrothermally or by molecular beam epitaxy (MBE) in single-crystalline structures enabling the preparation of well-defined, very smooth surfaces. Also, while already being applied as a transparent electrode in inorganic optoelectronic devices, there is a growing interest to use ZnO as an electron-injection contact in hybrid LEDs [1] or as the cathode in hybrid photovoltaic (PV) devices [2]. Also, ZnO is now commonly employed as an electron-selective contact in unipolar diodes [3, 4], but quantitative data on the efficiency of electron injection and extraction across the ZnO/OSC interface is largely missing. Moreover, most of these devices employed ZnO electrodes which were structurally and energetically ill defined.

Known drawbacks of untreated ZnO are its moderate work function (WF), which causes injection barriers to almost all conventional organic semiconductors, a poor reproducibility of the WF due to the physisorption of contaminations and its poor chemical stability in an acid environment. An elegant way to alter the WF and, at the same time, passivate the surface is the attachment of a self-assembled monolayer (SAM) of polar molecules. At the beginning of the this CRC, various groups had successfully applied substituted benzylphosphonic acids (BPAs) to modify the surface properties of indium tin oxide (ITO) [5]. These molecules were shown to form stable bonds to the ITO surface. Moreover, the attachment of electron-donating or withdrawing groups allowed to alter the electric dipole moment and with that the substrate work function over a wide range. When applied to ZnO, however the appearance of etching effects during the immersion of the substrate into a solution of the BPAs turned out to be a major problem.

We were able to develop a protocol, which circumvent this problem, allowing for the first time for the preparation of flat and homogeneous ZnO substrates with widely tunable work function. Most importantly, this protocol involves the immersion of the ZnO in explicitly dried ethanol in an inert atmosphere, which guaranteed a very low concentration of water during the entire modification process.

Figure 1a summarizes the chemical structures of the used PAs. In addition to commercially available BPAs, we employed a new class of phosphonic acids based on pyrimidine, with the goal to further lower the WF of ZnO. Pyrimidine derivatives have already been discussed in literature as a means to alter the substrate WF and, therefore, the electron injection properties. As a representative of this promising class of PA-based molecules, the non-substituted pyrimidine PA (PyPA) was synthesized by the Hecht group (**A3**). For all molecules, static electric dipole moments were calculated by the Heimel group (**A4**). WFs measured by Kelvin Probe in inert atmosphere on SAM-modified single-crystalline ZnO-surfaces are collected in Figure 1a. The WF values span a range from 4.1 eV to almost 5.7 eV. Interestingly, we see an only little effect of the crystal orientation on the work function. Moreover, similar work function shifts are achieved for SAM-modified single-crystalline ZnO substrates grown by MBE in **A3** (*Henneberger*) or ZnO films prepared via a sol-gel process. The result that the work function of BPA-treated ZnO is independent of the choice of substrate is in agreement with recent work by N. Kedem et al., [6]. Figure 1a also shows that the work function of the PA-modified ZnO surface varies strictly with the molecular dipole moment of the head group. This is fully consistent with the prediction of the Helmholtz-equation, indicating that the molecular tilt angle and the surface coverage is either constant or it changes only gradually with the dipole moment.

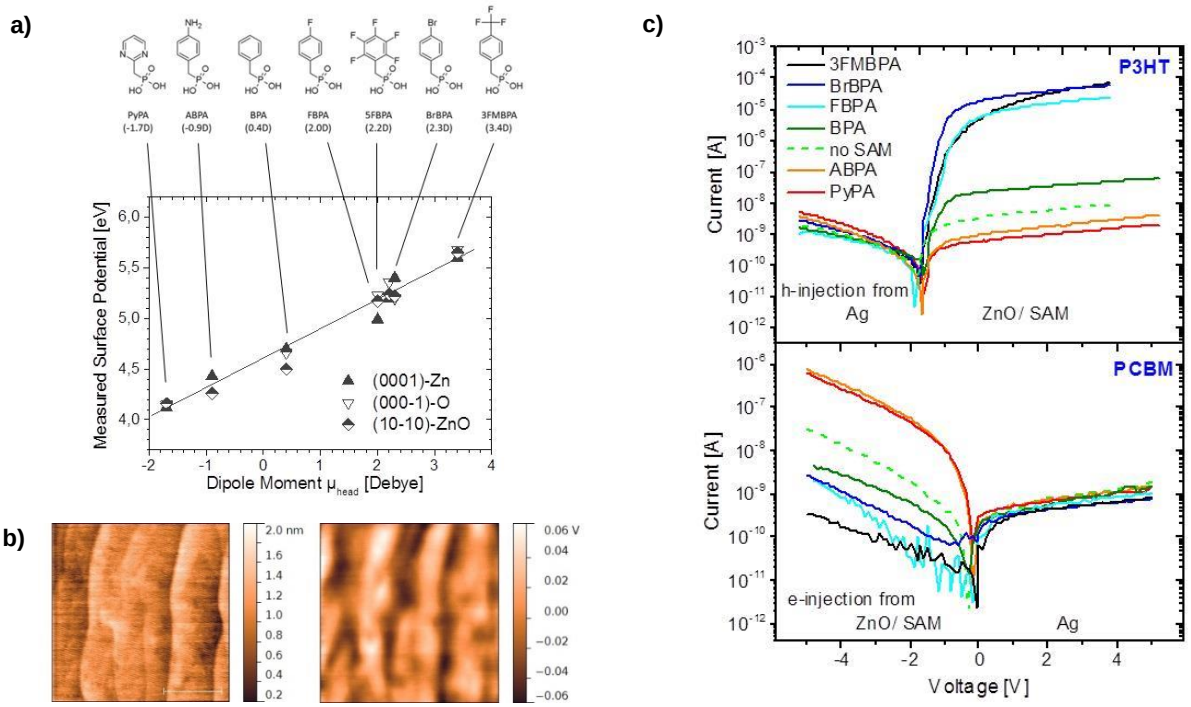

Figure 1. *(a) Chemical structures and acronyms of all applied phosphonic acids, with their respective dipole moments of the head group, μ_{head}, shown in the brackets. A negative sign indicates that the negative pole points towards the PA anchoring group. Also shown is the WF of different single-crystalline ZnO substrates plotted as a function of the head group dipole moment μ_{head}. All WF values were measured with the Kelvin Probe (KP) technique. The WF spans a range of up to almost 1.6 eV. (b) AFM height profile and SKPM image of 5FBPA on a (0001)-Zn-terminated single crystal. The AFM reveals the underlying terraced ZnO structure, indicating the absence of etching effects. The very weak variation of the surface voltage across the scanned area proves a homogeneous coverage of the ZnO surface with the SAM molecules. The scanned area is 3 x 3 μm^2. (c) J-V characteristics of single carrier devices in the stack ZnO/SAM/organic semiconductor/Ag with P3HT or PCBM. The only parameter varied is the WF of the ZnO due to the application of different SAMs. A voltage larger than zero means that a positive bias is applied to the bottom electrode [19].*

The high quality of the SAMs was proven by angle-dependent near-edge X-ray absorption fine structure (NEXAFS) spectroscopy, X-ray reflectivity (XRR) measurements, Kelvin Probe (KP), atomic force microscopy (AFM), and scanning Kelvin Probe microscopy (SKPM). AFM and SKPM measurements on 5FBPA-motified (0001) surfaces are exemplarily shown in Figure 1b. These measurements revealed a structurally well-defined surface with atomically-flat terraces and with very little spread of the work function. NEXAFS spectroscopy proved the existence of oriented aromatic rings at the ZnO surface with a preferential tilt angle of ~47° with respect to the interface, which fits perfectly the theoretical predictions on that system [7]. XRR measurements were performed in collaboration with **A9 (***Kowarik*) and revealed a coverage of the ZnO surface with about one molecular monolayer. The analysis of the slope in Fig. 1a results in a dense molecular packing of about 2 nm^{-2}, which is close to the theoretical maximum of 2.7 nm^{-3}. We conclude that well-defined, homogeneous monolayers of densely packed and oriented molecules have been formed in the ZnO surfaces. Such a full exploration of all relevant physical parameters determining the SAM quality is novel and outstanding in literature, and it has become possible only by the use of single crystalline surfaces and the development of a proper preparation protocol which avoids the commonly-observed etching effects.

3.3.1.2 Application of SAM-Modified Electrodes in Prototype Devices

Using such “electronic grade” SAMs with tunable WF enabled us to tune the efficiency of charge injection over an exceptionally wide range. In particular, the ability to raise the WF of ZnO to values exceeding 5.5 eV allowed us, for the first time, to use it as a hole-injecting contact. As proof of concept, hole- and electron-only devices with the modified ZnO as the injecting electrode and poly(3-hexylthiophene) (P3HT) or phenyl-C71-butyric acid methyl ester (PCBM), respectively, as transporting organic semiconductors were investigated. Within the two types of devices, the WF of the ZnO was continuously altered by using different SAMs. The results in Fig. 1c show a significant increase of the hole-only current when the WF of the ZnO approaches the HOMO onset of P3HT. Vice versa, for electron-only devices with PCBM, the unipolar current increased by several orders of magnitude with decreasing work function (decreasing barrier for electron injection). The data show that ZnO can be simply tuned from an electron-injecting to hole-injecting contact by choosing the right SAM-molecule. In both cases, a saturation of the current, when the ZnO WF exceeds (or drops below)

a certain value, indicates the transition from an injection-limited to a bulk-limited transport behavior. The large reduction of the unipolar currents for improper energy alignment indicates again the very high quality of the SAM.

Being able to tune the injection properties of ZnO over a wide range allowed us to prepare solar cells with modified ZnO either serving as the anode or the cathode. Figure 2 shows J-V curves of regular and inverted solar cells prepared on ITO/sol-gel ZnO. Reference devices were prepared on PEDOT:PSS (regular structure) or bare ZnO (inverted architecture). Both regular and inverted devices with modified ZnO electrodes compete with or even exceed the performance of the benchmark stack on ITO/PEDOT:PSS. The higher short circuit current of the optimized inverted device is most likely caused by a more ideal optical field profile [8]. These results highlight again the high quality and electronic grade of our SAM-modified ZnO electrodes. Our approach might not only allow to replace PEDOT:PSS in regular devices, but also opens new design possibilities for multi-junction solar cells with regular or inverted structures.

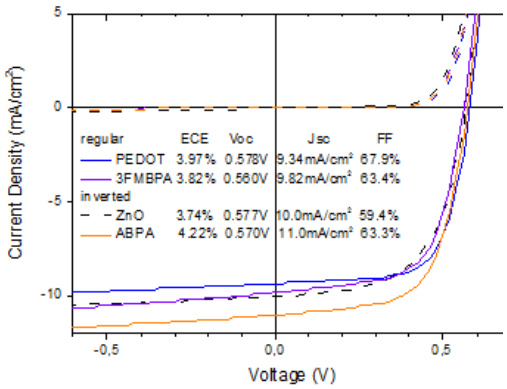

Figure 2: J-V characteristics of regular and inverted P3HT:PCBM solar cells. Regular cells were prepared either on PEDOT:PSS or on high workfunction ZnO treated with 3FMBPA. For inverted devices, the blend was coated either on bare ZnO or on ZnO covered with ABPA [21].

A close inspection of the J-V curves in Figure 2, however, displays a slightly smaller open circuit voltage (V_{oc}) of the devices prepared on modified ZnO substrates. While this might indicate a yet not-optimized energetics at the hybrid interface, we point out that the energetics in the P3HT:PCBM blend, and with that the achievable open circuit voltage, is highly sensitive to the actual blend morphology. Notably, altering the post-preparation treatment or the composition of this blend caused the energies of the LUMO- and HOMO-related transport states to vary by up to 0.3 eV [20]. Therefore, slightly different morphologies on the different substrate electrodes used here might as well account for the observed variation of V_{oc}.

3.3.1.3 Hybrid Charge Transfer Excitons with Tuneable Energy

During the course of the first funding period, the understanding of the energetics and dynamics of charge-transfer excitons (or charge-transfer states, CTSs) in either all-organic donor-acceptor solar cells or hybrid devices moved into the focus of research on excitonic photovoltaic devices. These excitons are proposed to act as the precursor to free charges. However, as electrons and holes forming the CTSs are in close proximity, several authors proposed that free charge generation must involve hot (vibronically and/or electronically excited) CT states. Evidence for this scenario came from recent fs pump-probe studies [9] and from quantum chemical simulations [10]. However, experiments performed under application-relevant illumination conditions by the Neher-group in close collaboration with Koen Vandewal (now TU Dresden) and Alberto Salleo (U Stanford) disproved this hypothesis [21, 22]. For all organic donor-acceptor blends studied by the consortium, the field dependence and efficiency of free-carrier generation was shown to be independent of whether or not the donor, the acceptor or the CT exciton was excited. It is concluded that charge generation in these all-organic systems involves a CT manifold coupled to the vibronically and electronically relaxed CT^1, without the need for excess electronic or vibrational energy. Though a conclusive explanation for this unique behaviour is still missing, efficient split-up of CT excitons may be assisted by the large structural heterogeneity of these donor-acceptor blends or the delocalisation of charge carriers on pure domains or the donor and acceptor component. In fact, high efficiencies in organic:fullerene devices has been related to the presence of pure fullerene clusters [11]. The situation is far less clear for hybrid inorganic/organic photovoltaic systems. Haeldemans et al. were able to resolve a sub-gap signal in the external quantum efficiency (EQE) spectrum of TiO2:P3HT solar cell and related this to the direct excitation of a hybrid charge transfer exciton (HCTE) [12] More recently an extra feature in the electroluminescence spectra of CdS:P3HT device, not present in the pure materials, was detected and associated to HCTE emission [13]. Some evidence for the existence of HCTEs at the ZnO/organic interface came from steady state PL studies on ZnO nanorod/P3HT heterojunctions, though the emission from these hybrid excitations was largely obscured by the stronger photoluminescence from P3HT [14]. Femtosecond optical pump-push photocurrent measurements performed by Vaynzof et al. [15] suggested that electron-hole pairs formed at the ZnO/organic interface are strongly bound. In agreement to this, recent theoretical work on the energetics and dynamics of excitations at the ZnO/P3HT interface stated that the presence of defects at the ZnO surface give rise to highly localized (perpendicular and parallel to the interface) HCTSs [16]. On the other

hand, theoretical and experimental work by Forrest and coworkers suggest a low binding energy of the hybrid charge transfer excitons [17].

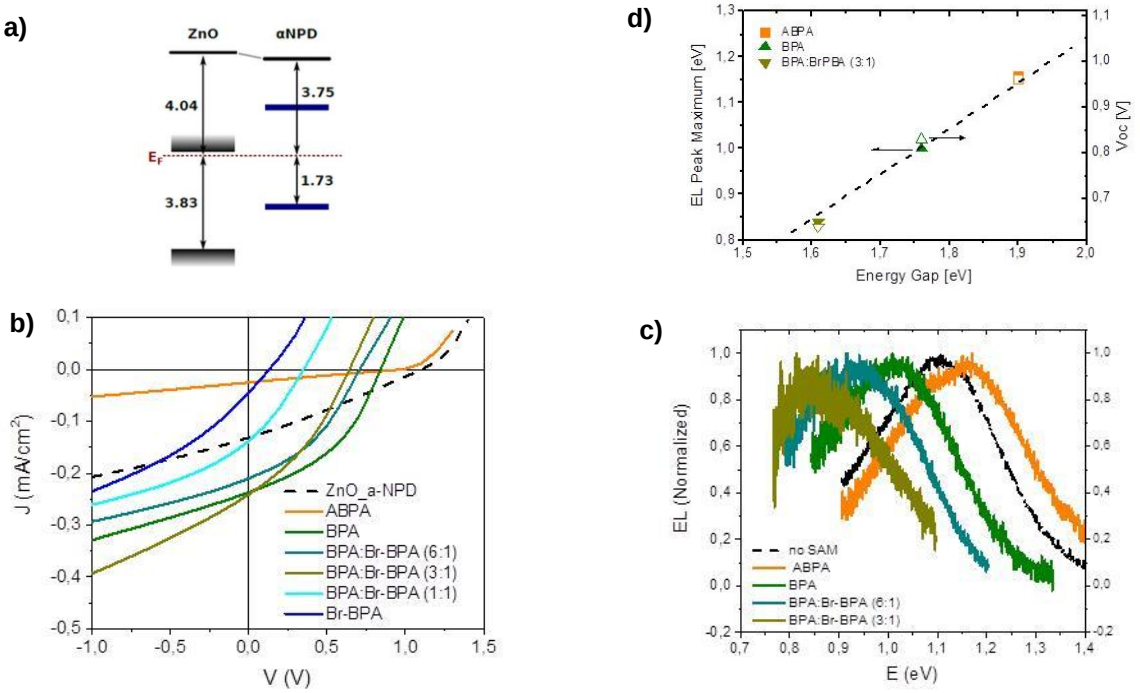

*Figure 3: (a) Energetics of the hybrid interface between ZnO and α-NPD. The band diagram is based on UPS experiments performed by **A8** (Koch) and literature values. (b) J-V characteristics of planar hybrid devices, with either untreated or SAM-modified ZnO, under simulated AM1.5G illumination. (c) Normalized EL spectra measured on planar hybrid devices, driven as a light emitting diode. Note that due to the limited spectral resolution of the used detector, no emission was seen when using pure BrBPA or a 1:1 mixture with BPA (d). Correlation between the EL emission maximum and the open circuit voltage with the energy gap between the ZnO CBM and the α-NPD HOMO onset. It is assumed that the CBM is 0.2 eV above E_F in the ZnO bulk [24].*

In a first attempt to unambiguously prove the existence of HCTEs at the ZnO/organic interface and its radiative coupling to the ground state, electroluminescence and photovoltaic properties of devices comprising a planar heterojunction between ZnO and some common hole-transporting molecules were studied. Figure 3 summarizes results on hybrid bilayer devices made of untreated or SAM-modified sol-gel processed ZnO and thermally-evaporated α-NPD. J-V curves shown in Figure 3b demonstrate that these devices act, as expected, as hybrid solar cells, though with poor performances. Increasing the ZnO work function by employing different SAM molecules results in a drastic decrease of the V_{oc}, from 1.06 V for the non-treated ZnO down to 0.12 V for ZnO fully covered with BrBPA. Importantly, for our devices with well-defined ZnO surfaces, a strict relation between the V_{oc} and the energy gap is observed, with a slope of nearly one. Previous work on hybrid devices with modified ZnO or ITO often displayed a sublinear change of V_{oc} with the substrate workfunction [e.g.18], which might point to an ill-defined interface. When driven as a light-emitting diode, these devices emit light in the NIR. Notably, the emission maximum changes in a linear fashion with the energy gap at the hybrid interface, ruling out bulk emission as the emitting species. Therefore, we attribute this emission to the radiative decay of HCTEs, involving charge transfer across the hybrid interface.

As demonstrated by others [6, 18], mixing of two different SAM molecules allows for fine tuning of the ZnO work function and with this of the energy gap. Our data show that mixing of two SAM molecules results in a gradual and continuous shift of the EL spectrum, without considerable broadening of the EL peak. The important result points to a certain degree of delocalization of the HCTE parallel to the hybrid interface, meaning that its energy is determined by a lateral average of the local work function variation of the modified ZnO surface. This finding is, at a first view, at variance with the simulation by Wu et al., which pointed to a strong localization of the hole in the HCTE at a molecular side. Cleary, a more detailed investigation on a variety of devices is needed to resolve the nature of excitations at the hybrid interface.

References

1. D. Kabra, L.P. Lu, M.H. Song, H.J. Snaith, R.H. Friend, Adv. Mater 22, 3194 (2010)
2. Y. Sun, J.H. seo, C.J. Takacs, J. Seifter, A.J. Heeger, Adv. Mater. 23, 1679 (2011)
3. S.-H. Liao, H.-J. Jhuo, Y.-S. Cheng, S.-A. Chen, Adv Mater. 25, 4766 (2013)
4. P. de Bruyn, A.H.P. can Rest, G.A.H. Wetzelaer, et al., Phys. Rev. Lett. 111, 186801 (2013)
5. P.J. Hotchkiss, S.C. Jones, S.A. Paniagua, A. Sharma, B. Kippelen et al., Acc. Chem. Res 45, 337 (2012)
6. N. Kedem, S. Blumstengel, F. Henneberger, H. Cohen et al., Phys. Chem. Chem. Phys. 16, 8310 (2014)
7. C. Wood, H. Li, P. Winget, J.-L. Brédas, J. Phys. Chem. C **116**, 19125 (2012)
8. S. Albrecht, S. Schäfer, I. lange, S. Yilmaz, I., Dumsch, S. Allard, U. Scherf, A. Hertwig, D. Neher, Org. Electr. 13, 615 (2012)
9. G. Grancini, M. Maiuri, D. Fazzi, A. Petrozza, H.-J. Egelhaaf, D. Brida et al., Nat. Mater. 12, 29 (2013)
10. A. Troisi, Faraday Discuss 163, 377 (2013)
11. (a) H. Tumara, I. Burghardt, J. Am. Chem. Soc. 135, 16364 (2013); (b) S. Delinas, A. Rao, A. Kumar, S.L. Smith, A.W. Chin, J. Clark et al., Science 343, 512 (2014)
12. I. Haeldermans, K. Vandewal, W. Oosterbaan, A. Gadisa, et al., Appl. Phys. Lett. 93, 223302 (2008)
13. N. Bansal, L.X. Reynolds, A. MacLachlan, T. Lutz, R.S. Ashraf et al., Sci. Rep. 3, 1531 (2013)
14. M.H. Cahn, J.Y. Chen, T.Y. Lin, Y.F. Chen, Appl. Phys. Lett. 100, 021912 (2012)
15. Y. Vaynzof , A.A. Bakulin, S. Gélinas, R.H. Friend, Phys. Rev. Lett. 108, 246605 (2012)
16. G. Wu, Z. Li, G. Lu, J. Phys. Chem. Lett. 5, 2649 (2014)
17. a) C.K. Renshaw, S.R. Forrest, Phys. Rev. B 90, 045302 (2014); (b) A. Panda, C.K. Renshaw, A. Oskooi, K. Lee, S.R. Forrest, Phys. Rev. B 90, 045303 (2014)
18. a) T. Brenner, G. Chen, E.P. Meinig, D.J. Baker, D.C. Olson et al., J. Mater. Chem. C 1, 5935 (2013), b) B.A. MacLeod, N.E. Horwitz, E.L. Ratcliff, J.L. Jenkins, N. R. Armstrong et al., J Phys. Chem Lett. 3, 1202 (2012)

3.3.2 Project-related publications

19. I. Lange, S. Reiter, M. Pätzel, A. Zykov, A. Nefedov, J. Hildebrandt, S. Hecht, S. Kowarik, C. Wöll, G. Heimel, D. Neher, „Tuning the Work Function of Polar Zinc Oxide Surfaces by Modified Phosphonic Acid Self-Assembled Monolayers", Adv. Funct. Mater. 10.1002/adfm.201401493, (2014)
20. I. Lange, J. Kniepert, P. Pingel, I. Dumsch, S. Allard, S. Janietz, U. Scherf, D. Neher, "Correlation between the Open Circuit Voltage and the Energetics of Organic Bulk Heterojunction Solar Cells", J. Phys. Chem. Lett. 4, 3865 (2013)
21. K. Vandewal, S. Albrecht, E.T. Hoke, K.R. Graham, J. Widmer, J.D. Douglas, M. Schubert, W.R. Mateker, J.T. Bloking, G.F. Burkhard, A. Sellinger, J.M.J. Fréchet, A. Amassian, M.K. Riede, M.D. McGehee, D. Neher, A. Salleo, "Efficient charge generation by relaxed charge-transfer states at organic interfaces", *Nat. Mater.* **13**, 63 (2014)
22. S. Albrecht, K. Vandewal, J.R. Tumbleston, F.S.U. Fischer, J.D. Douglas, J.M.J. Fréchet, S. Ludwigs, H. Ade, A. Salleo, D. Neher, "On the Efficiency of Charge Transfer State Splitting in Polymer:Fullerene Solar Cells", *Adv. Mater.* **26**, 2533 (2014)
23. S. Reiter, I. Lange, D. Neher, ZnO modified with Phenylphosphonates as Electron- and Hole-collecting Interlayers in Hybrid Solar Cells", in preparation for submission to the Appl. Phys. Lett.
24. F. Piersimoni, I. Lange, D. Neher, S. Blumstengel, F. Henneberger, Raphael Schlesinger, N. Koch, K. Vandewal, "Charge Carrier Generation and Emission from Charge Transfer Excitons at the Hybrid ZnO/organic Interface, in preparation for submission to the J. Phys. Chem. Lett.

3.4 Research plan

Research work to be performed during the second funding period will build on the knowledge gained by the Neher group and the partner in the CRC consortium during the past years and on the long standing experience of the Potsdam group on the study of charge carrier dynamics in excitonic solar cells. It aims at a conclusive, possibly quantitative, understanding of the transfer of charge, either being injected or photogenerated, across a morphological and energetically well-defined hybrid interface.

3.4.1. Transfer of injected charge across the ZnO/Organic interface

Though work performed by the Neher group and others showed that PA-modified ZnO is suited for efficient injection of electrons and holes into organic semiconductors, it is yet to be proven that, and under what conditions, ohmic conditions can be established at the hybrid interface. In fact, Wang and coworkers reported pronounced deviations from the ideal case of ohmic injection for α-NPD coated on several different

metal oxide electrodes [25]. With an ideal ohmic contact, the current through an electronic device is entirely limited by the transport of charge carriers through the bulk of the semiconductor. This condition is established if the electrode is able to supply a sufficient amount of charge at low, or ideally, zero electric field at the contact. It has, however, been acknowledged that due to the injection of charge at thermal equilibrium, a space charge layer forms in the OSC, causing band bending and shifting the electrode Fermi level back into the band gap of the semiconductor [26]. The situation is illustrated for the case of an OSC in contact with a high and low work function metal in Figure 4a and 4b, respectively. In combination with an applied forward bias, a situation is established where a virtual ohmic contact (defined by the point where the total electric field is zero) is formed within the OSC, but with the charge carrier density at this point being significantly smaller than at the contact. While this situation has been largely overlooked in the past, recent work incorporated band bending in the analysis of unipolar currents through OSCs [4]. This knowledge will serve as the basis for a comprehensive characterization and understanding of the energetic and injection properties of hybrid interfaces.

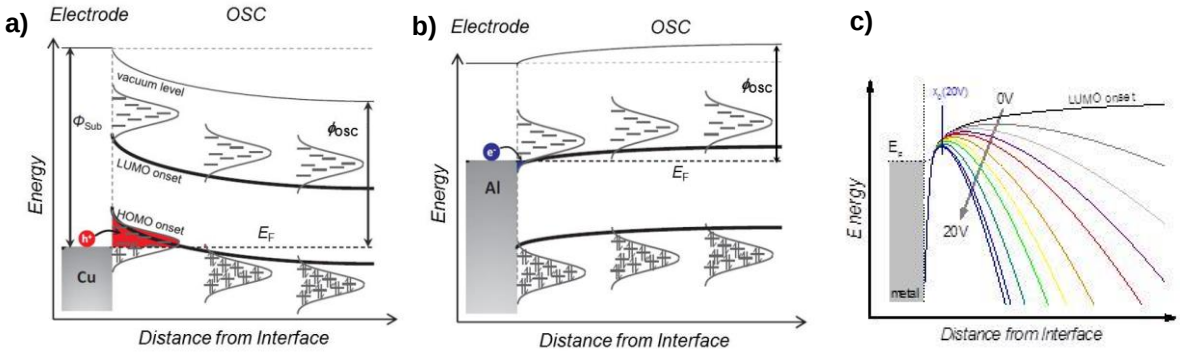

Figure 4: Scheme of the equilibrium energetics at the interface between an OSC and a high (a) or low (b) work function metal. (c) Scheme of the situation as is (b) but now with different electric fields being applied in forward direction.

3.4.1.1 Characterization of band bending on modified ZnO electrodes with variable work function.
For the characterization of the energetics at the hybrid interface, UPS experiments will be performed in collaboration with the **A8** (*Koch*), while Kelvin probe experiments will be applied to samples with thicker organic layers. Experimental data will be analyzed with an electrostatic model developed by Blakelesley et al. [26] and recently improved by the Koch group [27]. This analysis will allow us to access the energetics at the interface and the OSC density of states near the contact. Several COMs will be applied, differing in the position of the HOMO resp. LUMO band and in the degree of crystallinity. To extend the accessible work function range, novel pyrimidine-based SAMs will be developed in **A3** (Hecht) and tested as ZnO modifiers.

3.4.1.2 Measurements of unipolar currents in the diffusion and drift regime
JV-characteristics will be recorded on the same hybrid systems as used for the energetic characterization described above, with charge injection from the metal oxide. In the first period, experimental data will be analyzed with analytical expressions describing unipolar currents under diffusion-limited [4] and drift-limited [28] conditions. This analytical analysis will be complemented by one-dimensional drift-diffusion simulations, relying on an ongoing collaboration with Prof. J.A. Koster (U Groningen). By performing these studies as function of temperature, and using the knowledge gained on the energetics at the interface and bulk of the OSC, we will be in the position to conclude unambiguously, whether or not, and under which conditions, unipolar currents are injection- or bulk-limited. Also, if non-ohmic injection is established, these experiments will allow us to conclude on the origin of injecting-limited properties, be it the existence of an energy barrier at the interface or a tunneling barrier through the self-assembled molecular layer. In a final stage of this work, dynamic MC simulations are envisaged with the goal to include information about the microscopic structure at the heterojunction. These simulations will be performed in close collaboration with groups of Dr. Karin Zojer and Prof. Egbert Zojer at the TU Graz.

3.4.1.3 Energetics and unipolar currents with variable ZnO doping concentrations
Recent simulation work unambiguously proved that the potential profile across the hybrid interface and within the OSC bulk is sensitive to the doping concentration of the charge-injecting contact [29]. A particular prediction of this work was that with increasing doping concentration a larger fraction of the space-charge induced band bending will occur within the OSC, with important consequences for the heights and width of the apparent injection barrier. This issue will be treated by investigating the energetics and the injection efficiency of selected devices with different doping levels, in close collaboration with **A5** (*Henneberger*) and **A8** (*Koch*).

3.4.1.4 Unipolar currents with mixed SAMs

The ability to apply mixed molecular SAMs opens exciting new possibilities to study the mechanism of charge injection. Figure 5a and 5b depicts two different scenarios, one with the SAM formed by only one kind of molecule, the other employing a mixture of SAM molecules with different dipole moments. Work described above showed that mixtures of different SAM molecules can be used to continuously tune the "macroscopic" work function as well as the HCTE emission energy, indicating that the PAs forming the SAM mix at the molecular level. Given the local nature of charge injection, it is far from being clear whether injection will be dominated by the sites with the lowest local injection barrier or by an average interfacial energy. Therefore, by measuring unipolar currents with mixtures of different SAMs and at different mixing ratios, we aim at an understanding of the locality of injection. These experiments will be carried out first with COMs forming amorphous layers (e.g. α-NPD or derivatives of L4P-Sp3) where charges are expected to localize at the individual molecular sites, while later studies will be conducted on more ordered molecular layers, either formed upon evaporation of suited molecules (like 6T or pentacene), or by employing SAMs with covalently attached COMs to be supplied by the **A3** (*Hecht*). In order to gain access to the local variation of the work function of ZnO substrates carrying mixed SAMs, low temperature scanning tunneling spectroscopy will be conducted in **A2** (*Kumagai-Wolf*) on selected high quality samples.

3.4.1.5 Unipolar currents with switchable SAMs

Electrodes with injection properties tunable by external stimuli are highly attractive for the realization of sensing devices and memories, but also offer exciting opportunities for the study of charge injection and transport. We will, therefore, investigate unipolar devices comprising SAMs with photo-controllable build-in switches as designed by **A3** (*Hecht*) and **A4** (Heimel), Figure 5c. Experiments will be conducted where the surface density of "open" and "closed" switches is continuously tuned by light. It is envisaged that switching of the connecting group will affect the local energetics, allowing to fine-tune the injection current.

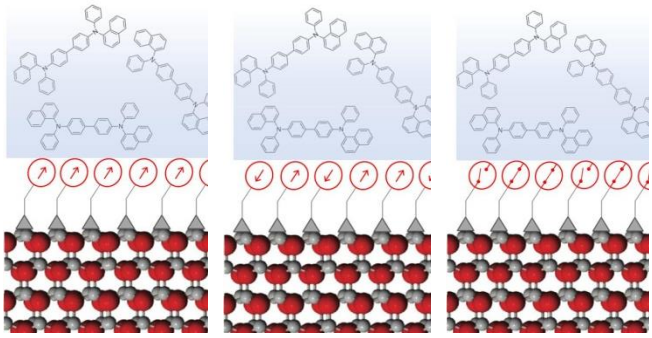

Figure 5 HIOS comprising SAMs with (left) all dipoles pointing the same direction, (middle) mixed layers of molecules with different dipole moments, (right) SAM molecules with build-in switches

3.4.1.6 Work function modification and charge injection properties of NiO

NiO has recently attracted considerable attention as a charge selective contact in organic and hybrid solar cells [30]. Being a p-type semiconductor with a VBM at 5.8 eV and a large bandgap of 3.7 eV, this metal oxide can be considered as the perfect p-analogue to ZnO. Initial work to be performed during this funding period will address the control of the NiO work function with appropriate SAMs as well as its function as hole-injecting contact with variable, possibly switchable work function.

3.4.2 Energetics and Dynamics of Hybrid Charge Transfer Excitations

Work by the Neher group in collaboration with partners as described above has provided solid evidence that electronically and vibronically relaxed CT state serves as the precursor to free charge carriers in all-organic bulk heterojunction donor-acceptor solar cells. In the course of this project, HIOS comprising ZnO and suitable electron-donating COMs will be employed as testbeds for elaborating this scenario for morphological and energetically well-defined hybrid heterojunctions. Thereby, we aim at resolving the ongoing controversial discussion on the nature of hybrid charge transfer excitons.

3.4.2.1 Absorption and emission properties of HCTEs in relation to interface energetics

Following the protocols described above, hybrid photovoltaic systems with planar type II heterojunctions will be formed by combining SAM-modified ZnO with suitable donor molecules (α-NPD, oligothiophenes, polythiophenes, derivatives of L4P-Sp3, pentacene) processed from vacuum. Information on the CT energy and the relaxation energy will be gained from the measurement of photocurrent and electroluminescence spectra, following the approach by [31]. By performing some of these measurements as a function of temperature, we will quantify the contribution of inhomogeneous broadening to the overall absorption and EL lineshape. These results will be related to the interface energetics to be investigated in **A8** (*Koch*). The study

will also involve the measurement of the quantum efficiency of electroluminescence to yield information on the efficiency of radiative and non-radiative relaxation pathways from vibronically and electronically relaxed HCTEs. Experiments will be performed on either unimolecular SAMs or on SAMs formed by PAs of different dipole moment, with the aim to address the lateral extension of the HCTE. At a later stage, studies will be extended to donors covalently attached to the SAM unit. These HIOS structures with covalently attached chromophores offer several benefits. Firstly, they exhibit a more regular arrangement and orientation of the electron-donating chromophores with regard to the ZnO surface structure. Secondly, these structures can be more accurately treated by quantum-chemical calculations (to be performed in **A4**, **B6** and **B11**), delivering information on the energetics and nature of the excitations at the hybrid interface. Finally, by performing emission experiments with different compositions of the organic donor layer (see Figure 6), we aim at an understanding of the degree of delocalization of the HTCE perpendicular to the hybrid interface.

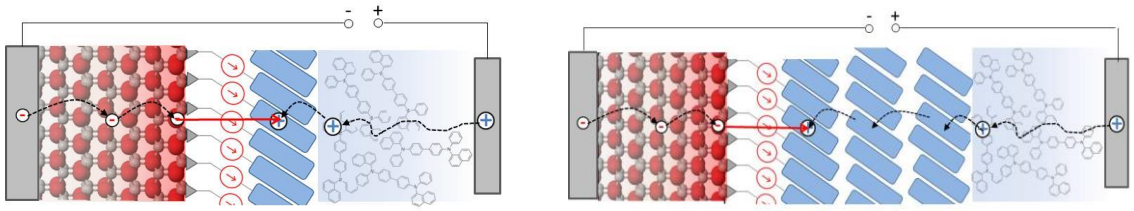

Figure 6: Schemes of devices to selectively address the emission of HCTE at the interface between ZnO and covalently-bonded chromophores. A disordered OSC of higher ionization energy is used to transmit holes to the chromophore-bearing SAM. By inserting additional layers of the same type of chromophore, we aim at addressing the influence of the local environment on the HCTE emission energy.

3.4.2.2 Efficiency of charge generation at the hybrid interface

With the knowledge of the HTCE energy from 3.4.2.1, efficiencies for free charge generation will be quantified as a function of electric field and temperature, using the setups established in the Neher group. By perform these experiments with different excitation energies, possibly with direct excitation of low energy HTCEs, with donor molecules of different HOMO and LUMO energies, and with differently modified ZnO surfaces, we will address some of the most urgent questions regarding charge carrier generation at hybrid interfaces:

- Does charge generation at hybrid interfaces (as for all-organic interfaces) involve relaxed CT excitons?
- Can we establish solid evidence for, or against, a higher degree of localization of HTCEs in comparison to CT excitons at all-organic type II heterojunctions, e.g. by analyzing the field and photon energy dependence of generation?
- What is the minimum energy offset at the hybrid interface to guarantee efficient charge generation?

3.4.2.3 Dynamics of excitations and charge generation at the hybrid interface

This will be the most challenging task of the second funding period, as it requires to apply pump-probe techniques to a planar interface, where the total number of hybrid excitations and generated free charge carriers is expected to be significant smaller than in classical bulk heterojunction devices. The Neher group is currently setting up a femtosecond pump-probe laser experiment, which combines different techniques to address the generation, recombination and extraction of free charge with high sensitivity and temporal resolution. Details about these techniques can be found in the **Methods** section. These studies will be complemented by time-resolved measurements by the CRC partners. In particular, time-resolved photoluminescence performed in **B3** (*Blumstengel*) will deliver information about the radiative decay kinetics of HCTEs upon photoexcitation. In a later stage of the project, samples with a monomolecular layer of suitable donor molecules, either physisorbed or covalently bonded to an atomically-flat ZnO substrate, will be subject to initial studies with 2PPE to be performed in **B9** (*Stähler*). This technique is unique as it allows to track the energetics of photoexcited electrons at the hybrid interface with high time resolution. Information on the dynamics of bound and free charges gained from these experiments will serve as the input for time-dependent quantum chemical calculations, which will be subject of work to be performed in **B6** and **B11**.

Additional References

25. Wang, M. G. Helander, M. T. Greiner, J. Qiu, Z. H. Lu, Phys. Rev. B 80, 235325 (2009)
26. I. Lange, J. C. Blakesley, J. Frisch, A. Vollmer, N. Koch, D. Neher, Phys. Rev. Lett. 106, 216402 (2011).
27. M. Oehzelt, N. Koch, G. Heimel, Nature Commun. 5, 4174 (2014)
28. H.T. Nicolai, M.M. Mandoc, P.W.M. Blom, Phys. Rev. B 83, 195204 (2011)
29. L. Ley, Y. Smets, C.I. Pakes, J. Ristein, Adv. Funct. Mater. 23, 794 (2013)
30. E.L. Ratcliff, A. Garcia, S.A. Paniagua, S.R. Cowam, A.J. Giordano et al., Adv. Energ. Mater. 3, 647 (2013)
31. K. Vandewal, K. Twingstedt, A. Gadisa, J.V. Manca, Phys. Rev. B 81, 125204 (2010)

Methods

Singly crystal ZnO substrates will be purchased, ZnO and NiO interlayers will be formed on ITO substrates with established sol-gel processes, epitaxially-grown ZnO substrates will be supplied by the CRC partners

Modification of the ZNO (NiO) surfaces will be performed according to the protocol developed by the Neher group during the first funding period. The energetics of the modified ZnO (NiO) surfaces will be studied by KP under inert gas atmosphere, SKPM, and with UPS/XPS by the Koch group.

COMs will deposited by thermal evaporation under HV conditions using an existing evaporation tool.

JV characterization will be performed under inert atmosphere conditions. For the measurement of *JV* curves as a function of temperature, an electrical probe station positioned in a vacuum chamber will be purchased.

Photovoltaic parameters will be measured in inert gas atmosphere with existing equipment.

EQE and EL spectra will be measured on encapsulated devices, either with equipment installed in Potsdam or at partner institutes (HU und TU Dresden).

The field dependence of generation will be measured as function of temperature and excitation energy with an existing transient photocurrent setup.

For the high resolution spectroscopy of the dynamics of neutral and charges excitations, we will use a femtosecond pump-probe laser experiments (funded by the DFG and the Land Brandenburg), which is currently being setup in the Neher group. This setup combines three different transient techniques:

- Transient photocurrent (TPC) and time-delayed collection field (TDCF) experiments: these are the most sensitive techniques as electrical currents can be measured with very high sensitivity. The time resolution of these experiments will be limited to ca. 1 ns. Experiments conducted with these techniques will deliver quantitative information about the amount and the fate of photogenerated free charge, possibly as a function of photon energy.
- Optical pump-push photocurrent probe has been invented by the Friend group and more recently applied to study the dynamics of photogenerated excitations at the organic-inorganic interface. It measures the change in the photocurrent by applying a short and intensive IR pulse shortly after photoexciting the sample. Thereby, any bound species will be excited to higher states, thus affecting the probability of spitting into free charge carriers. The technique is particularly suited to study the kinetics of bound HCTE with sub-ps resolution.
- Time-resolved electric-field-induced second harmonic generation (TREFISH): this is a relatively new technique invented to investigate the motion of free charge on a picosecond to nanosecond time scale. Being essentially background free, this method has the necessary sensitivity to study the dynamics of charge photogenerated at a planar heterojunction. Applied to organic BHJ solar cells, TREFISH has given strong evidence that photogeneration at type II heterojunctions generates hot charges with high transient mobilities, but the interpretation of the data is complicated by the complex morphology of such blends. Applying TREFISH to a hybrid structure with a more well-defined interface will enable us to develop a comprehensive picture of charge generation in HIOS.

3.5 Role within the Collaborative Research Centre

Experimental research work in **B7** will be performed in close collaboration with other partners of the CRC. SAM-molecules with different functionalities will be provided by **A3** (*Hecht*). Information on the electronic structure of these molecules (including static charge distribution and excited state properties) will be provided by **A4** (*Heimel*) and **B11** (*Draxl*). **Z1 (**Hecht) will supply COMs (in particular derivatives of L4P-Sp3) to be used as charge-transporting species in unipolar devices and as the electron-donating molecules in hybrid photovoltaic devices. ZnO layers with variable degree of doping will be prepared in **A5** (*Henneberger*). Experiments regarding the static energetics at the hybrid interface will be performed and analyzed together with **A8** (*Koch*). 2PPE experiments will be conducted in **B9** (*Stähler*) to study the energy and dynamics of photoexcited electrons. **B6** (May) and **B11** (*Draxl*) will perform time-dependent quantum chemical calculations regarding the energetics and dynamics of neutral and charged excitations at the hybrid interface. Information on the energetics of SAM-modified ZnO and NiO surfaces and on the efficiency of charge extraction will be shared with **B13 (***List-Kratochvil*) to optimize the performance of injection-type hybrid devices. All studies in **B7** will be close coordinated with **B3** (Blumstengel). In particular **B3** will perform studies on selected HIOS systems comprising epitaxially grown ZnO surfaces and COMs deposited under UHV conditions.

3.6 Delineation from other funded projects

The Neher group is a partner of the Helmholtz-Energie-Allianz Das Beste aus zwei Welten: „anorganische/organische Hybrid-Solarzellen und –Techniken für die Photovoltaik“. Work being performed in course of the project concerns hybrid solar cells comprising nanostructured ZnO in combination with solution-processable polymers. No work on SAM-modified planar ZnO nor on COMs deposited by thermal evaporation is conducted. Very recently, the DFG has provided funding for a project (NE 410/15-1, one PhD student) aiming at the understanding of role of charge transfer excitons in all-organic donor-acceptor solar cells. Though this project will use similar techniques to investigate the efficiency of free charge generation as function of excitation energy and temperature, it will exclusively study solution-processed all-organic systems.

3.7 Funding of the project

3.7.1 Previous funding

The project has been funded within the Collaborative Research Centre since July 2011

3.7.2 Funds requested

Funding for	2015/2		2016		2017		2018		2019/1	
Staff	Quantity	Sum	Quantity	Sum	Quantity	Sum	Quantity	Sum	Quantity	Sum
<category, percentage>										
PhD student, 75%	2	44.100	2	88.200	2	88.200	2	88.200	2	44.100
Total										
Direct costs	Sum		Sum		Sum		Sum		Sum	
Small equipment, Software, Consumables	7.500		15.000		15.000		15.000		7.500	
Other										
Total	7.500		15.000		15.000		15.000		7.500	
Major research equipment	Sum		Sum		Sum		Sum		Sum	
€ 10.000 - 50.000										
> € 50.000	100.000									
Total	100.000									
Total	151.600		103.200		103.200		103.200		51.600	

(All figures in Euro)

3.7.3 Staff

	No.	Name, academic degree, position	Field of research	Department of university or non-university institution	Commitment in hours/week	Category	Funded through:
Available							
Research staff	1	Dieter Neher, Prof. Dr., Group Leader	experim ental physics	Inst. Physics & Astronomy, University of Pots-dam	10		
	2	Frank Jaiser, Dr., Research Associate	experim ental physics	Inst. Physics & Astronomy, UP	15		
Non-research staff	3	Burkhard Stiller, Lab Engineer		Inst. Physics & Astronomy, UP	5		
	4	Andreas Horka, Tech. Assistant		Inst. Physics & Astronomy, UP	5		
	5	N.N. Mechanics		Inst. Physics & Astronomy, UP	5		
Requested							
Research staff	6	N.N. PhD student		Inst. Physics & Astronomy, UP		E13 75 %	
	7	N.N. PhD student		Inst. Physics & Astronomy, UP		E13 75 %	

Job description of staff (supported through available funds):

1 Prof. Dr. Dieter Neher: Group leader, supervisor of research.
2 Dr. Frank Jaiser: Research Associate, co-supervisor of experimental work, conducting laboratory work together with doctoral candidates 6 and 7, analysis of experimental data and development of new models and numerical simulations to describe injection currents.
3 Burkhard Stiller: Laboratory engineer, experimental assistance, particularly microscopy of film surfaces.
4 Andreas Horka: Technical assistant, maintenance of laboratories and equipment.
5 N.N.: Mechanic, maintenance of laboratories and building new laboratory equipment, e.g. new sample holders for different device sizes.

Job description of staff (requested):

6 N.N: The first doctoral candidate will study the transfer of injected charge across the hybrid interface. This will include the modification of ZnO and NiO substrates with SAMs, the characterisation of these surfaces with AFM and SKPM, evaporation of COMs, device fabrication and temperature-dependent J-V characterisation of unipolar devices. He/she will also study the energetics of the hybrid system by performing Kelvin probe measurements. He/she will analyse the experimental data using analytical equations and established drift-diffusion simulation tools. He/she will be involved in the modelling of charge transfer across the hybrid interface using dynamic MC simulations.

7 N.N: The second doctoral candidate will work on the transfer of photogenerated charge across the hybrid interface. Besides the preparation and standard characterisation of hybrid photovoltaic devices, this will include a detailed analysis of the charge generation and emission in relation to the interface energetics, using highly sensitive photocurrent and EL spectroscopy. In the later stage of the project, he/she will concentrate on the characterisation of the dynamic properties of charge generation and recombination, using the new femtosecond laser equipment in Potsdam and setups installed by the partners.

3.7.4 Direct costs for the new funding period

	2015/2	2016	2017	2018	2019/1
Funds available	3.000	6.000	6.000	6.000	6.000
Funds requested	7.500	15.000	15.000	15.000	7.500

(All figures in Euro)

Consumables for 2011/2 – 2015/1

Substrates, ZnO singly crystals from external suppliers, shadow mask sets for different sample sizes, small molecules, metals, optical and electrical components	EUR	60.000

3.7.5 Major research equipment requested for the new funding period

> € 50.000 for 2/2015

Measurement system for electrical characterization (diodes, transistors) as function of temperature	EUR	100.000

This equipment will comprise a computer-controlled micro-probe station placed in a vacuum chamber. The setup will be used for performing current-voltage measurements on unipolar hybrid devices as a function of temperature, ranging from ca. 100 K to 300 K. The analysis of these measurements will allow us to identify the nature of the injection processes (tunneling, thermionic emission), and to verify predictions from theory and simulations. The setup will be placed in an inert gas environment, allowing for the transfer of samples without exposure to air.

3.7.6 Student assistants

	2015/2	2016	2017	2018	2019/1
Quantity	0	0	0	0	0
Commitment in hours/week	0	0	0	0	0
Sum	0	0	0	0	0
Tasks					

3.1 About project B8

3.1.1 Title: Inorganic/organic core/shell GaN-based nanowire light-emitting diodes based on Förster resonant energy

3.1.2 Principal investigators

Prof. Dr., Riechert, Henning (*06.09.1953, German)
Paul-Drude-Institut für Festkörperelektronik (PDI)
Leibniz-Institut im Forschungsverbund Berlin e.V.
Hausvogteiplatz 5−7, 10117 Berlin
Phone: +49 (0)30 20377-365
Fax: +49 (0)30 20377-201
E-mail: riechert@pdi-berlin.de

Prof. Dr., Grahn, Holger Theodor (*14.04.1957, German)
Paul-Drude-Institut für Festkörperelektronik (PDI)
Leibniz-Institut im Forschungsverbund Berlin e.V.
Hausvogteiplatz 5−7, 10117 Berlin
Phone: +49 (0)30 20377-318
Fax: +49 (0)30 20377-257
E-mail: htgrahn@pdi-berlin.de

3.2 Project history

3.2.1 Report

The exciton transfer between inorganic and organic materials can become very efficient due to the non-radiative Förster resonant energy transfer (FRET) process. Achermann *et al.* [1] were one of the first to describe an approach for the indirect injection of electron-hole pairs from an electrically or optically pumped (In,Ga)N/GaN quantum well (QW) into highly monodisperse CdSe/ZnS core/shell nanocrystals (NCs) using the FRET process. The efficient dipole-dipole coupling of excitons in (In,Ga)N/GaN QW/polyfluorene semiconductor hybrid structures has been investigated by Itskos *et al.* [2]. The transfer mechanism was assigned to the FRET between the Wanner-Mott exciton donors in (In,Ga)N and Frenkel exciton acceptors in the polymer. They reported transfer efficiencies of up to 43% at 15 K. The dependence of the FRET rate on the distance R between the inorganic QW and the organic film indicated that a plane-plane interaction characterized by a R^{-2} dependence described their experimental results best. In a later review paper by the same group [3], they reported on the observation that the relative efficiency of the FRET process increases with increasing temperature. At 300 K, they reported that the FRET process becomes 20 times more efficient than the radiative transfer process. In order to decrease the distance between the inorganic light-emitting layer and the organic material, Chanyawadee *et al.* [4] have used a top-down approach. Holes penetrating through the active QWs are etched into conventional (In,Ga)N/GaN light-emitting diodes (LEDs) with a thick top p-contact layer. The holes are subsequently filled with colloidal NCs (acceptors) bringing them in close proximity to the active layers (donors). A 100% enhancement of the colloidal NC emission was demonstrated for this structure in comparison to a control structure, where the holes were not etched all the way into the QWs.

The central goal of this project was the realization of inorganic/organic core-shell nanowire (NW) LEDs based on the FRET process. In order to achieve this goal, the project was originally divided into three stages. In the first stage, the FRET process was to be investigated in planar (In,Ga)N/GaN layers by photoluminescence (PL) spectroscopy. In the second stage, these investigations were to be extended to (In,Ga)N/GaN NWs. In the third stage, the effect of the FRET process was to be studied for light emitting diodes based on (In,Ga)N/GaN NWs in a *p-i-n* configuration using electroluminescence spectroscopy. We believed that this bottom-up approach could result in superior device performance due to the better interface quality between the inorganic core and the organic shell than those reported in Ref. [4].

As a starting point, planar (In,Ga)N/GaN QW structures were prepared to investigate the FRET process in group-III nitrides. A series of single QW samples was grown by molecular beam epitaxy (MBE). The width of the single QW was kept constant (2.6 nm) and the capping layer thickness was varied between 0 and 30 nm to investigate the FRET process as a function of the distance from the QW to the organic layer deposited on top. These QW samples exhibit an intense PL line with similar linewidths as state-of-the-art (In,Ga)N QWs grown by molecular beam epitaxy. However, the samples also show a strong donor-acceptor-pair (DAP) PL band due to unintentional Mg doping (inevitable in our MBE systems because of prior experiments involving *p*-type doping with Mg), which spectrally overlaps in part with the QW-related PL line. The FRET process from the single QWs to SuperYellow 52 (polyphenylene vinylene, fabricated by Merck) was investigated by M. Eyer (project A5, Henneberger). Time-resolved PL (TRPL) experiments indicated nonradiative energy transfer with an efficiency of up to 55%. Nevertheless, due to the spectral overlap between the DAP and the single QW PL line, an unambiguous proof of FRET was not possible. Over the time of the project, we were not able to fabricate (In,Ga)N/GaN layers with a reduced DAP PL intensity. An Mg-free MBE system will not be in operation before the end of 2014. This is the first reason, why we decided to focus our efforts on the study of the FRET process in GaN NWs where, as result of the higher substrate temperature necessary to form these nanostructures, Mg is not incorporated during growth.

During the course of this project, Marquardt *et al.* [5] reported on the in-plane spatial separation of electrons and holes in the case of axial (In,Ga)N insertions in GaN NWs. The study, using continuum elasticity theory and an eight-band **k•p** formalism, revealed that electrons always localize at the center of the NWs, whereas the hole localization depends on the NW diameter, quantum disk thickness, and In content. For typical values of the NW diameter, quantum disk thickness, and In content, the holes were found to be localized close to the NW sidewall surfaces. This spatial separation of electrons and holes inhibits the formation of Wannier-Mott excitons in the QW. In addition, the localization of electrons and holes at potential minima caused by alloy inhomogeneities in the (In,Ga)N insertions also contribute to a reduction of the formation of Wannier-Mott excitons. These two phenomena will significantly reduce the efficiency of the FRET process in the inorganic/organic core-shell (In,Ga)N/GaN NW-based structures originally proposed in this work. This is the second reason for the shift of the focus of our research toward more promising nanostructures for the FRET process such as GaN/(Al,Ga)N NW heterostuctures and pure GaN NWs, where alloy fluctuations in the active region are not present.

For the fabrication of inorganic/organic core-shell NW-based structures, several preliminary growth studies of GaN and GaN/(Al,Ga)N NWs were performed. The aim of these studies was to gain control over the NW number density as well as to improve the crystal quality of the GaN NWs and GaN/(Al,Ga)N NW heterostructures. The former is crucial for a complete coverage of the NW sidewalls with an organic shell. We developed a two-step growth approach, where the nucleation and elongation stages during the formation of GaN NWs are separated. This growth approach enabled us to improve the control over the NW number density and prepare NW samples that can be easily covered with an organic shell by spin coating. Next, we explored the growth of GaN NWs under extreme growth conditions in terms of impinging fluxes and substrate temperatures. GaN NWs grown at high substrate temperatures were found to be free of strain on a macroscopic scale and of a structural perfection similar to that of state-of-the-art free-standing GaN layers. Therefore, these GaN NWs can constitute the basis for a potentially highly efficient FRET process in a hybrid inorganic/organic core-shell NW structure.

Simultaneously, the coverage of GaN NW ensembles with a polyfluorene (PFO) shell was optimized using the spin coating technique where the polymer is dissolved in a solvent (tetrahydrofuran, THF). It was found that the quality of the organic shell not only depends on the spin coating parameters, but also on the ambient conditions, i.e., temperature and humidity. Optimal and reproducible shell fabrication can only be achieved when the spin coating process is performed in a controlled nitrogen atmosphere. Thus, the organic shell fabrication using spin coating was performed in collaboration with R. Schlesinger (project A8, Koch). The group of Prof. Koch provided their nitrogen glove box and a spin coater for our experiments. The fabrication of organic shells by organic molecular beam deposition (OMBD), as a superior alternative to spin coating, was not possible because the chamber for the organic coating of NWs under vacuum has not been installed yet.

In search of FRET in inorganic/organic core-shell NW-based structures, we have investigated pure GaN and GaN/(Al,Ga)N NWs coated with PFO using TRPL. The measurements on GaN/(Al,Ga)N NWs showed that the lifetime of the QW transition of the GaN insertions was not affected by the organic shell. Thus, no indication of the FRET process has been observed in these structures. However, the pure GaN NW samples coated with PFO exhibited a clear reduction of the effective GaN PL lifetime. Nevertheless, an organic shell may already cause a reduction of the effective lifetime by introducing non-radiative interface recombination.

Unfortunately, due to the strong spatial inhomogeneities of the investigated samples, a detailed analysis in order to identify the non-radiative process was not possible yet. Therefore, detailed temperature- and excitation-dependent TRPL investigations of inorganic/organic core-shell structures of PFO on more homogeneous GaN NW ensembles are currently under way. Once we have shown conclusively that we can observe the FRET process in inorganic/organic core-shell GaN NW-based structures, we can proceed toward *p-i-n* and hybrid LED structures.

Since the beginning of this project, other groups have reported on the FRET process in hybrid structures using group-III nitride semiconductors. In 2013, Smith *et al.* [6] reported on the FRET process in top-down etched (In,Ga)N/GaN nanorods filled up with polyfluorene. This approach resembles very much the previous one by Chanyawadee *et al.* [4]. Due to the large diameter of the nanorods, typically around 220 nm, and the top-down approach, the consideration of the electron-hole separation in (In,Ga)N/GaN NWs [5] does not directly apply to this structure. Nevertheless, the separation between the WM exciton in the (In,Ga)N layer and the Frenkel exciton in the polymer shell exceeds the limits of the FRET process in most cases. At the international workshop on nitride semiconductors held in Wrocław in August 2014, Smith *et al.* [7] reported on the temperature dependence of the FRET process and efficiencies of about 40% at room temperature. The latter result was explained in terms of the enhanced exciton diffusion length at elevated temperatures. We believe that, although these results are quite promising, hybrid structures based on GaN NWs grown by molecular beam epitaxy could be more efficient once they are optimized for the FRET process. This expectation is primarily due to the higher quality of the inorganic/organic interface, but also due to the smaller NW diameter as well as their superior structural perfection.

The following problems have resulted in a delay and change of focus with respect to the original proposal:

- Due to the Mg contamination of all our MBE systems used for group-III nitrides, a strong DAP PL intensity could not be avoided in our planar QW structures. The strong DAP PL intensity makes it difficult to investigate the FRET process in such structures by TRPL.
- The report on the electron-hole-separation in (In,Ga)N insertions in GaN NWs [5] and a likely similar situation for GaN insertions in (Al,GaN) disks caused us to refocus toward pure GaN NWs.
- Since the one Ph. D. student supported by the project could only work on the growth of these structures, the manpower for the TRPL experiments was limited. Therefore, the TRPL experiments were performed in the beginning of the project in collaboration with project A5, which caused a less effective growth-analysis feedback than originally intended. In a later stage of the project, we employed a master student to perform the TRPL experiments in our institute. After the master student had been trained to conduct these experiments, the growth-analysis feedback improved.
- As neither a vacuum deposition chamber nor a nitrogen glove box was available for the deposition of the organic shells, these experiments had to be carried out in collaboration with project A8. Because of this reason, the number of experiments that could be performed toward an optimization of the organic shell was strongly limited and much more time consuming than originally intended.

During the course of this project, we collaborated with other several other subprojects of the CRC:

- A5 (Henneberger):
  - Investigation of our initial planar (In,Ga)N/GaN QWs structures using TRPL spectroscopy.
- A8 (Koch):
  - Utilization of their facilities and experience for the coating of our group-III nitride NWs with an organic shell by spin coating.
  - Investigation of the energy level alignment of F4TCNQ deposited on unintentionally *n*-doped and n^+-doped GaN films. We prepared the GaN layers for those studies.
- A9 (Kowarik):
  - Growth studies using in-situ x-ray measurements of organic films deposited on GaN layers. We provided unintentionally *n*-doped and n^+-doped GaN layers.
- A3 (Hecht)
  - Assistance and support through fruitful discussions for choosing suitable organics semiconductors and solvents for the organic shell fabrication.
- B5 (Kühn)
  - Growth of a planar GaN/(Al,Ga)N structure for surface exciton investigations on hybrid structures.

References
[1] M. Achermann, M. A. Petruska, S. Kos, D. L. Smith, D. D. Koleske, and V. I. Klimov, Nature **429**, 642 (2004).
[2] G. Itskos, G. Heliotis, P. G. Lagoudakis, J. Lupton, N. P. Barradas, E. Alves, S. Pereira, I. M. Watson, M. D. Dawson, J. Feldmann, R. Murray, and D. D. C. Bradley, Phys. Rev. B **76**, 035344 (2007).
[3] C. R. Belton, G. Itskos, G. Heliotis, P. N. Stavrinou, P. G. Lagoudakis, J. Lupton, S. Pereira, E. Gu, C. Griffin, B. Guilhabert, I. M. Watson, A. R. Mackintosh, R. A. Pethrick, J. Feldmann, R. Murray, M. D. Dawson, and D. D. C. Bradley, J. Phys. D: Appl. Phys. **41**, 094006 (2008).
[4] S. Chanyawadee, P. G. Lagoudakis, R. T. Harley, M. D. B. Charlton, D. V. Talapin, H. W. Huang, and C.-H. Lin, Adv. Mater. **22**, 602 (2010).
[5] O. Marquardt, C. Hauswald, M. Wölz, L. Geelhaar, and O. Brandt, Nano Lett. **13**, 3298 (2013).
[6] R. Smith, B. Liu, J. Bai, and T. Wang, Nano Lett. **13**, 3042 (2013).
[7] R. Smith, B. Liu, J. Bai, and T. Wang, International Workshop on Nitrides, TuOP21, Wroclaw (2014).

3.2.2 Project-related publications

a)

[1] O. Brandt, S. Fernández-Garrido, J. K. Zettler, E. Luna, U. Jahn, C. Chèze, and V. M. Kaganer, “Statistical analysis of the shape of one-dimensional nanostructures: determining the coalescence degree of spontaneously formed GaN nanowires”, Cryst. Growth Des. **14**, 2246 (2014).
[2] C. Hauswald, P. Corfdir, J. K. Zettler, V. M. Kaganer, K. K. Sabelfeld, S. Fernández-Garrido, T. Flissikowski, V. Consonni, T. Gotschke, H. T. Grahn, L. Geelhaar, and O. Brandt, “Origin of the nonradiative decay of bound excitons in GaN nanowires“, Phys. Rev. B **90**, 165304 (2014).
[3] P. Corfdir, J. K. Zettler, C. Hauswald, S. Fernández-Garrido, O. Brandt, and P. Lefebvre, “Sub-meV linewidth in GaN nanowire ensembles: absence of surface excitons due to the field-ionization of donors”, Phys. Rev. B, submitted (2014), arXiv:1407.4279.
[4] P. Corfdir, C. Hauswald, J. K. Zettler, T. Flissikowski, J. Lähnemann, S. Fernández-Garrido, L. Geelhaar, H. T. Grahn, and O. Brandt, “Stacking faults as quantum wells in nanowires: Density of states, oscillator strength and radiative efficiency”, Phys. Rev. B, submitted (2014), arXiv:1408.5263

3.3 Funding

The project will be completed by the end of the current funding period.

3.3.1 Project staff in the ending funding period

	No.	Name, academic degree, position	Field of research	Department of university or non-university institution	Commitment in hours/week	Category	Funded through:
Available							
Research staff	1	Timur Flissikowski, Dr., senior scientist	Semiconductor Physics	Semiconductor Spectroscopy	5		institute
	2	Sergio Fernández-Garrido, Dr., senior scientist	Materials Science	Epitaxy	5		institute
Non-research staff	3	Hans-Peter Schönherr		Epitaxy	5		institute
Requested							
Research staff	4	Johannes Zettler	Materials Science	Epitaxy		Ph. D.	
Non-research staff							

Job description of staff (supported through available funds):
1 Timur Flissikowski
Time-resolved photolumimescence spectroscopy of GaN and GaN/(Al,Ga)N nanowires

2 Sergio Fernández-Garrido,
MBE growth of (In,Ga)N/GaN quantum wells and GaN as well as GaN/(Al,Ga)N nanowires

Job description of staff (requested):
4 Johannes Zettler
MBE growth of (In,Ga)N/GaN quantum wells and GaN as well as GaN/(Al,Ga)N nanowires

3.1 About project B9

3.1.1 Title: Electronic structure and ultrafast carrier dynamics at hybrid inorganic/organic interfaces

3.1.2 Research areas: Surface science, condensed matter physics, ultrafast carrier dynamics at interfaces, time-resolved (non-) linear optical and photoelectron spectroscopy

3.1.3 Principal investigator

Dr. rer. nat. Stähler, Julia (*18.11.1978, deutsch)
Fritz-Haber-Institut der Max-Planck-Gesellschaft
Phone: +49 (0)30 8413 5125
Fax: +49 (0)8413 5375
E-mail: staehler@fhi-berlin.mpg.de

Do the above mentioned persons hold fixed-term positions? no
End date 31.12.2015
Further employment is planned until >30.06.2019

3.1.4 Legal issues

This project includes

1.	research on human subjects or human material.	no
	<If applicable:> A copy of the required approval of the responsible ethics committee is included with the proposal.	
2.	clinical trials	no
	<If applicable:> A copy of the studies' registration is included with the proposal.	
3.	experiments involving vertebrates.	no
4.	experiments involving recombinant DNA.	no
5.	research involving human embryonic stem cells.	no
	<If applicable:> Legal authorization has been obtained.	
6.	research concerning the Convention on Biological Diversity.	no

3.2 Summary

Any functionality of an inorganic/organic hybrid system is governed by the electronic levels and resonances at the interface. As illustrated in Fig. 1, these determine the efficiency of charge and Förster resonance energy transfer processes (CT & FRET), which occur on ultrafast timescales (femto- to picoseconds). This project uses femtosecond (fs) time-resolved (TR) optical and photoelectron spectroscopies to study the elementary processes of formation, transfer, and dissociation of excitons at *functional* HIOS interfaces in real time. These will be systematically varied in order to achieve thorough understanding about how the competition of CT and FRET can be manipulated and utilized for superior functionality of HIOS. Here, the interface will be altered by adsorption of different donor/acceptor molecules and docking groups that modify the surface dipole and level alignment. Furthermore, the role of interfacial charge density for the formation of hybrid charge transfer excitons (HCTE) and also the interfacial screening will be investigated. In a second step, the functional interface will be upgraded with a dipolar group in the organic molecules that is switchable by light. The resulting change of the level alignment (and thus electronic coupling) promises, for instance, the possibility to manipulate the emission properties of the HIOS on an ultrafast timescale using fs laser pulses. The ultrafast carrier and exciton dynamics will be monitored by a set of complementary techniques probing the timescales of (a) exciton formation, (b) relaxation (internal conversion/intersystem crossing), (c)

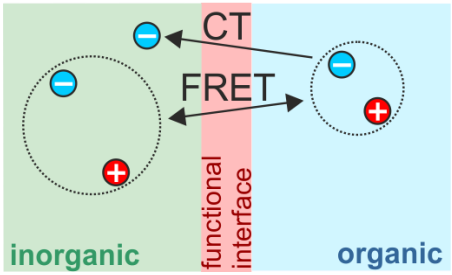

Fig. 1: The functional interface determines the balance of charge and energy transfer processes.

dissociation (interfacial/intermolecular), and (d) recombination (emissive/dark) by fs-TR linear optical spectroscopy (LOS), photoluminescence (PL), electronic sum frequency generation (eSFG), and two-photon photoelectron (2PPE) spectroscopy. The HIOS interfaces will be prepared in situ under ultrahigh vacuum (UHV) conditions and characterized by low-energy electron diffraction (LEED, inorganic substrate) and thermal desorption spectroscopy (TDS, organic film).

By systematic variation of the HIOS interface using (i) different inorganic semiconducting substrates (e.g., ZnO(10-10), ZnO(000-1)) and adjustment of their chemical potential by (ii) adsorption of donor/acceptor molecules (e.g., F4TCNQ, pyridine) as a buffer between the substrate and the optically active organic film (e.g., oligophenylenes, L4P), (iii) modification of the docking groups of the organic molecules (e.g. 5P-Py), or (iv) dipolar molecules that change their conformation by photoexcitation, the energy level alignment will be manipulated and thus the electronic and excitonic coupling modified. The combination of the set of powerful time-resolved techniques with different strengths (absolute vs. relative energies, bulk vs. surface/interface sensitivity) will enable the disentanglement of all elementary processes (a-d) and thus to a comprehensive picture of the electronic and excitonic coupling mechanisms at HIOS interfaces.

Our studies will be complemented by collaboration with the projects A3 (Hecht), A4 (Heimel), A8 (Koch), B4 (Körzdörfer/Scheffler/Rinke), B6 (May), B7 (Neher), Z1 (Hecht) (**energy level alignment**), A3 (Hecht), A10 (Tkatchenko/Scheffler), B3 (Blumstengel), B11 (Draxl), B12 (Knorr/Richter) (**charge transfer and exciton dynamics**), and A2 (Kumagai/Wolf), Z2 (Kowarik/Koch) (**structure and growth**).

3.3 Project progress to date

3.3.1 Report and state of understanding

The aim of this project is the characterization of the ultrafast quasiparticle dynamics at *functional interfaces* of organic and inorganic semiconductors using femtosecond time-resolved (TR) spectroscopic techniques. In particular, the alignment of energy levels and resonances for charge and energy transfer are in the focus of the research, respectively, and how they can be utilized to optimize functionality at HIOS interfaces. The following three main goals of this project were defined in the initial proposal for the whole course of the CRC:

A Determination of the occupied and unoccupied electronic structure of HIOS
B Investigation of the charge carrier and exciton dynamics at inorganic/ organic interfaces
C Understanding the electro-optical properties of more realistic HIOS

As discussed in the following, the results of the first funding period represent milestones towards the successful fulfillment of these goals. The focus lay here on the first goal (**A** control of energy level alignment), but also first results on the latter two will be presented. Naturally, this focus will, in the second funding period, be increasingly shifted towards **B** and **C** as outlined in section 3.4.

At the beginning of this CRC, only sparse information [1] of the unoccupied electronic structure of ZnO surfaces was available and even less was known about the carrier and exciton dynamics at these surfaces. This was partially caused by the bulk sensitivity of most ultrafast spectroscopic techniques. Analogously, most TR spectroscopic information on conjugated organic molecules (COMs) with HOMO-LUMO gaps in the UV was based on LOS or PL, both bulk sensitive and providing relative energies of electronic levels only and often just with picosecond time resolution. Using femtosecond TR 2PPE spectroscopy, linear and non-linear optical spectroscopy, this project is, in collaboration with other projects of the CRC and based on the results of the first funding period, contributing to a detailed understanding of the energy level alignment, electron and exciton dynamics as well as interfacial phenomena in HIOS, as outlined in the following.

Energy level alignment by work function modification
Adsorption of hydrogen onto ZnO surfaces strongly influences the electronic structure, because charge transfer modifies the surface dipole and can also lead to surface band bending. [2,3] As hydrogen is present under most experimental conditions, even under ultrahigh vacuum, it is crucial to systematically characterize its effect on the ZnO surface electronic structure. In the case of ZnO(10-10) and ZnO(000-1) (O-terminated), hydrogen exposure leads to a work function reduction and formation of a charge accumulation layer (CAL) at the surface, which is reflected in the build-up of density of states right below the Fermi energy E_F (cf. Fig.2a). This results from the donor character of H, which, when forming hydroxyl groups at the ZnO surfaces, locally pulls the potential downwards, causing the conduction band (CB) to cross E_F and reducing the work function. Continuous exposure of the ZnO(10-10) and ZnO(000-1) surface to hydrogen leads to a maximum reduction

of the sample work function by 0.7 eV and 1.4 eV, respectively, reflecting the larger number of oxygen sites at the polar surface. This work was done in close collaboration with B4(Knorr/Rinke/Scheffler) and the H/ZnO(10-10) results published in [8] and another paper, which is close to submission. Hydrogen adsorption on ZnO(000-1) will be subject of a forthcoming publication.
An even stronger reduction of the sample work function (up to 2.9 eV) can be achieved when adsorbing pyridine on the ZnO(10-10) surface (green markers). However, in contrast to hydrogen adsorption, this large change of work function is not mainly caused by charge transfer; density functional theory (DFT) calculations of B4 expose excellent agreement with our experiments (black triangles) and show that both, molecular and bonding dipole, dominate this work function change. The reduction of the work function down to only 1.6 eV is only possible due to the *negative* electron affinity of pyridine which prevents charge transfer and Fermi level pinning.

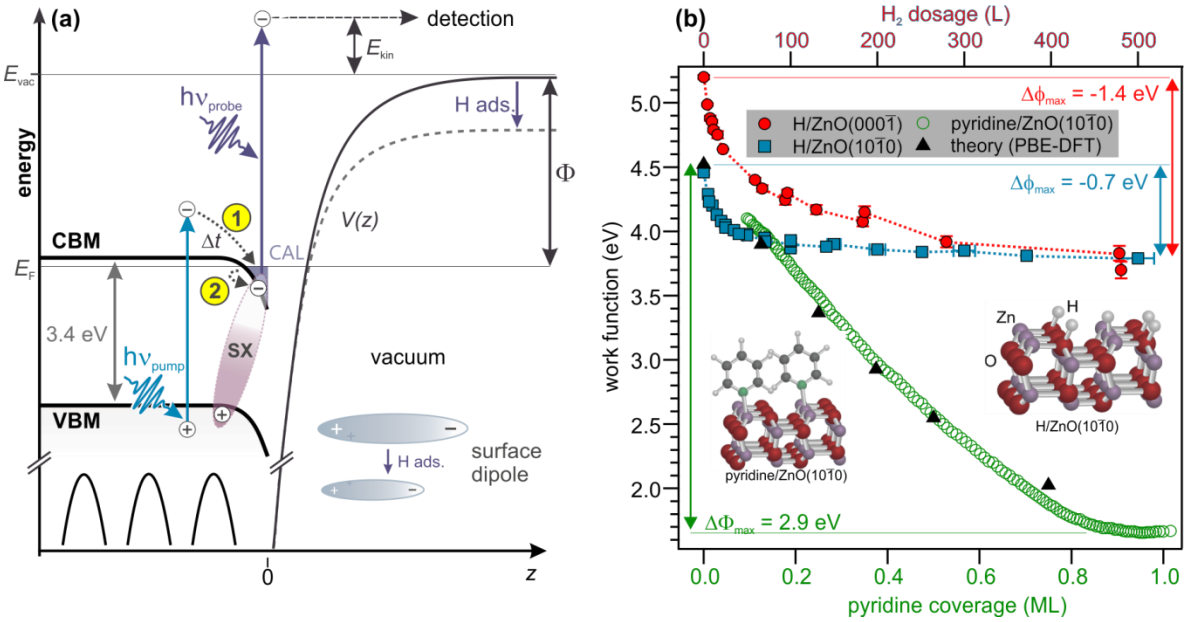

Fig. 2: a) Surface electronic structure of pristine and hydrogen-covered ZnO(10-10) and ZnO(000-1), pump-probe scheme for time-resolved 2PPE and non-equilibrium electron/exciton dynamics at ZnO surfaces after above gap excitation. b) Work function reduction through H and pyridine adsorption. (Data partially from [8,10], insets courtesy of B4.)

Ultrafast electron relaxation and exciton formation dynamics at ZnO surfaces

The ultrafast non-equilibrium dynamics at ZnO surfaces are monitored by TR 2PPE after above band gap excitation using h□$_{pump}$ as illustrated in Fig. 2a. A second, time-delayed probe pulse then photoemits the excited electrons close to E_F. The photoexcited dynamics are shown in the representative TR 2PPE measurement in Fig. 3a. The relaxation times of the excited electrons are shown in Fig. 3b and are on the order of 20-60 fs at high energies (above the bulk CB minimum). They do not depend on temperature, suggesting that the hot electrons mainly scatter with optical phonons. [4] Their relaxation proceeds even below the bulk conduction band bottom (dashed line) due to hydrogen-induced downward surface band bending (SBB) (process 1 in Fig. 2a).
Notably, below E_F, a pump-induced *increase* of 2PPE intensity is observed (Fig. 3a), i.e., below the energy which defines the highest occupied electronic state in equilibrium. Consequently, photoexcitation generates additional states below the Fermi level. This is due to the formation of sub surface-bound excitons (SX) (process 2 in Fig.2a), which can be suppressed by strong excitation close to the Mott density where the Coulomb interaction of the electron-hole pairs is reduced by the photoexcited e-h plasma and thus the exciton formation probability is diminished. [8]
The formation of SX occurs at least as fast as the observed rise time of PE intensity below E_F of 200 fs, however, these excitons are in a highly excited "hot" state that relaxes to the ground state on longer timescales. As the electron of the SX energetically lies below the Fermi level, nonradiative decay of this excitation is strongly suppressed: Dissociation of the exciton and separation of electron and hole in defect states within the band gap usually is a prominent non-radiative decay channel for excitons. It cannot occur here, as all resonant and lower-energy final states for the electron lie below E_F and are therefore occupied. The decay of SX population can thus only happen through electron-hole pair recombination going along with luminescence or Auger-type processes, which results in the high stability of this excited state. [13]

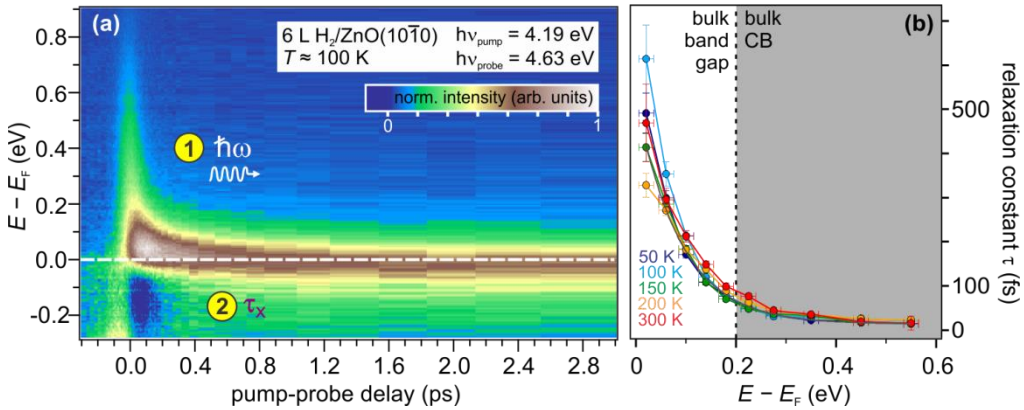

Fig. 3: a) Exemplary time-resolved 2PPE experiment of the electron relaxation (1) and surface exciton formation dynamics (2). b) Electron relaxation times are independent of temperature and slow down below the CB minimum. (Modified from Ref. [13].)

In the spirit of the long-time goal (**C** "more realistic" HIOS), the stability of the SX was tested in two ways. Firstly, the surface electronic properties were modified by variation of the hydrogen termination from 3 to 44 L (□□ = - 250 meV). This surface modification did not suppress, but *enhance* the SX signature. [13] Secondly, very recent experimental results unveil that the SX signature is even stable after sample exposure to air (still to be published). These results underline the technological potential of this sub surface (~1 nm) bound excitonic species for FRET applications at HIOS interfaces.

Impact of molecular vibrations on exciton relaxation pathways & strong intermolecular coupling

The first optically active molecule with a HOMO-LUMO gap on the order of the ZnO band gap investigated in B9 was 2,7-bis(biphenyl-4-yl-)2',7'-ditertbutyl-9,9'-spirobifluorene (SP6) [5-7], which is depicted in the inset of Fig. 4a. SP6 grows in amorphous layers on different substrates [5,16] and exhibits a maximum absorption at 3.6 eV [5] and emits strongest at 3.15 eV. Transient transmission spectroscopy of the excited state unveils different decay dynamics of the SP6 exciton, depending on the vibrational state of the molecule (cf. Fig. 4b). While excitons localized at molecules in the vibrational ground state diffuse to the HIOS interface and dissociate, excitons localized at vibrationally excited molecules in the S_1 state have too short diffusion lengths and couple with dark (triplet or charge transfer) states on 100 ps timescales, [15] which exhibit lifetimes on the order of 10 □s. First photoemission experiments furthermore indicate that the dark state strongly couples to other excitons in the film, leading to enhanced, stimulated photoemission independent of the laser excitation energy as shown by Fig.4c.

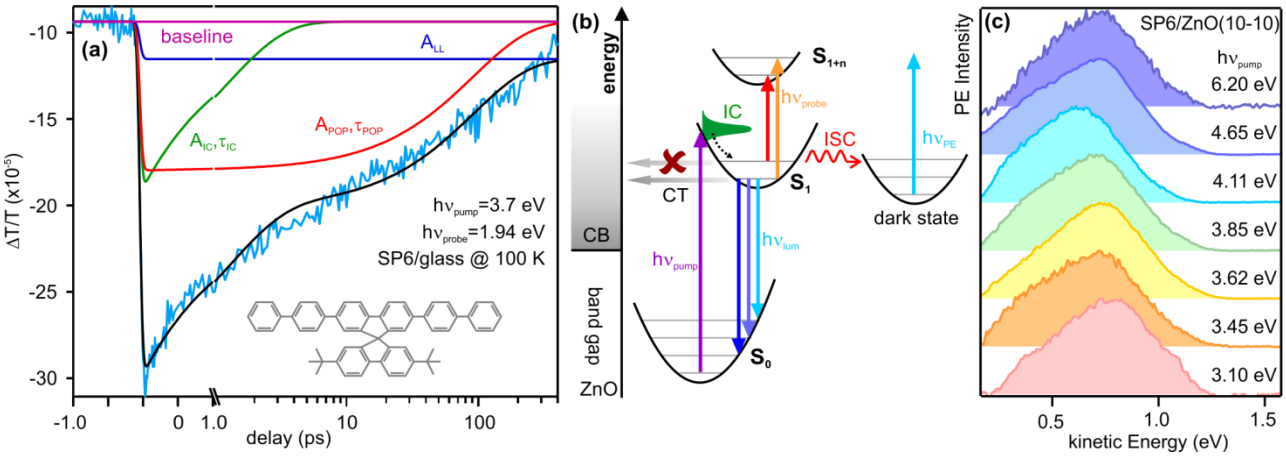

Fig. 4: a) Exemplary intensity trace of a TR excited state transmission experiment with phenomenological double exponential fit. b) Illustration of the involved processes after resonant excitation of SP6: internal conversion (IC), luminescence, diffusion-limited charge transfer (CT), and intersystem crossing (ISC) as probed by excited state transmission ($h\nu_{probe}$) and photoemission mediated by strong intermolecular coupling. c) Photon energy dependence of 2PPE from SP6/ZnO: Intermediate states should shift by □hv.

Charge transfer dynamics at HIOS interfaces

The influence of the energy level alignment on the interfacial dynamics is addressed in first experiments at the 5P-Py/ZnO(10-10) interface. Here, the polar pyridine end group binds the molecule to the ZnO surface and modifies the surface dipole as discussed above. At the same time, the 5P frontier molecular orbitals align accordingly. Using 2PPE, we are able to directly measure the absolute binding energy of the LUMO of the molecule. Furthermore, we make use of the charge accumulation layer at the ZnO surface by resonantly exciting electrons from the CAL into the LUMO, creating a transient negative ion of 5P-Py. A second, time-delayed laser pulse subsequently monitors the population decay of this excited state, which occurs through charge transfer from the molecule to the ZnO CB, which occurs on a 100 fs timescale.

Proof of principle: Femtosecond TR eSFG using white light supercontinuum

While linear optical spectroscopy is dominated by bulk contributions of photoexcited dynamics, photoelectron spectroscopy is, due to the finite mean free path of low-energy electrons in condensed matter, sensitive to only the first few nm of the samples. In order to selectively probe the dynamics at *buried* interfaces, we set up a TR-eSFG experiment that, because of the non-linearity of this technique, is surface and interface sensitive in otherwise centrosymmetric systems. Note that, contrary to vibrational SFG, which probes resonances in the IR, this setup is installed in order to probe *electronic* transitions in the visible and near UV and is thus complementary to TR-LOS and TR-PES. Furthermore, different to previous applications of this concept, the present experiment uses a white light supercontinuum for SFG in order to also achieve spectral resolution without the necessity of laser tuning. To our knowledge, this experimentally very challenging approach has not been realized so far; the time- and spectrally-dependent eSFG signal of ZnO after above band gap excitation shown in Fig. 5 thus represent the proof of principle of this technique. It will be further developed in the second funding period of the CRC in order to use its interface selectivity in HIOS.

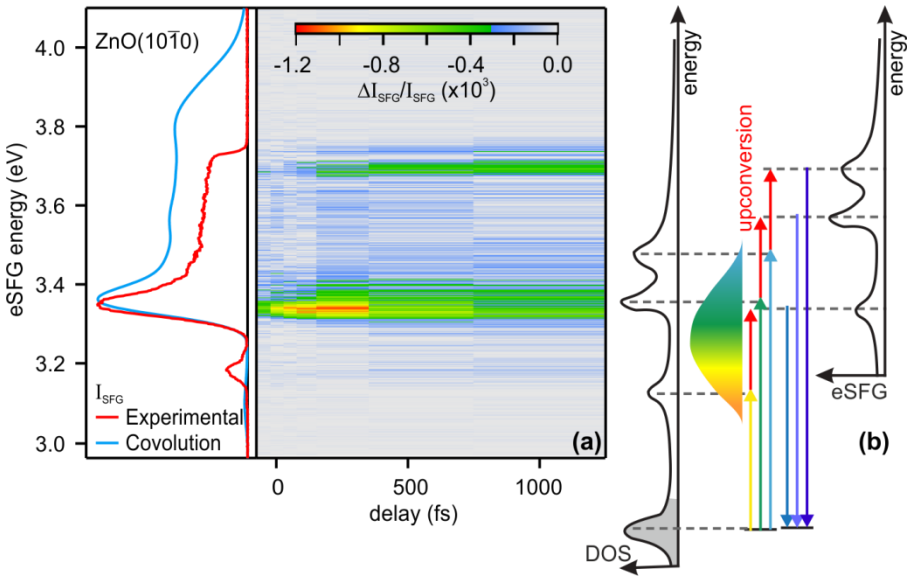

Fig. 5: a) Proof of principle of TR eSFG using a WL supercontinuum. b) Experimental scheme.

Summary

In conclusion, the first funding period has significantly improved our understanding of the microscopic mechanisms that determine the energy level alignment, the carrier and exciton dynamics at ZnO surfaces. On top of that, first very promising results on HIOS interfaces were achieved using TR photoemission and LOS. Together with the newly set up TR eSFG experiment and the planned TR PL setup, we will build on the above described results in order to characterize and exploit the properties of HIOS interfaces. A systematic, direct investigation of the ultrafast charge and energy transfer dynamics across well-defined inorganic/organic 2D interfaces is still lacking until today, despite the great interest and effort in the dynamics of related systems [e.g. 13-15]. The second funding period will therefore be devoted to the study of the *ultrafast dynamics* at HIOS interfaces (subject to conscious energy level alignment) with particular focus on HCTE and photo-switchable functional interfaces as discussed in the following.

References

[1] W. A. Tisdale, M. Muntwiler, D. J. Norris, E. S. Aydil, and X.-Y. Zhu, J. Phys. Chem. C **112**, 14682 (2008).
[2] K. Ozawa and K. Mase, Phys. Rev. B **81**, 205322 (2010).
[3] C. Wöll, Prog. Surf. Sci. **82**, 55 (2007).

[4] V. P. Zhukov, P. M. Echenique, and E. V. Chulkov, Phys. Rev. B **82**, 094302 (2010).
[5] S. Blumstengel, S. Sadofev, C. Xu, J. Puls, R. L. Johnson, H. Glowatzki, N. Koch, and F. Henneberger, Phys. Rev. B **77**, 085323, (2008).
[6] D. Schneider, T. Rabe, T. Riedl, T. Dobbertin, O. Werner et al., Appl. Phys. Lett. **84**, 4693 (2004).
[7] W. Kowalsky, T. Rabe, D. Schneider, H.-H. Johannes, C. Karnutsch, M. Gerken, U. Lemmer, J. Wang, T.Weimann, P. Hinze and T. Riedl, Proc. of SPIE **6008**, 60080Z, (2005).
[8] A. E. Jailaubekov, A. P. Willard, J. R. Tritsch, W.-L. Chan, N. Sai, R. Gearba, L. G. Kaake, K. J. Williams, K. Leung, P. J. Rossky, and X-Y. Zhu, Nat. Mat. **12**, 66 (2013)
[9] M. Marks, A. Schöll, and U. Höfer, J. Electr. Spectrosc. **195**, 263 (2014)
[10] G. Grancini, M. Maiuri, D. Fazzi, A. Petrozza, H-J. Egelhaaf, D. Brida, G. Cerullo and G. Lanzani, Nat. Mat. **12**, 29 (2013)
[11] C. K. Renshaw and S. R. Forrest, Phys. Rev. B **90**, 045302 (2014).
[12] A. Panda, C. K. Renshaw, A. Oskooi, K. Lee, and S. R. Forrest Phys. Rev. B **90**, 045303 (2014).

3.3.2 Project-related publications

a) Peer-reviewed publications

[13] J. C. Deinert, D. Wegkamp, M. Meyer, C. Richter, M. Wolf, and J. Stähler, Phys. Rev. Lett. **113**, 057602 (2014).
[14] D. Wegkamp, M. Meyer, C. Richter, M. Wolf, and J. Stähler, Appl. Phys. Lett. **103**, 151603 (2013).
[15] O. T. Hofmann, J.-C. Deinert, Y. Xu, P. Rinke, J. Stähler, M. Wolf, and M. Scheffler, J. Chem. Phys. **139**, 174701 (2013).
[16] J. Stähler, O. T. Hofmann, P. Rinke, S. Blumstengel, F. Henneberger, Y. Li, and T. F. Heinz, Chem. Phys. Lett. **584**, 74 (2013).

b) Other publications

[17] L. Foglia, L. Bogner, M. Wolf, J. Stähler, *Ultrafast exciton dynamics at the SP6/ZnO(10-10) interface,* in preparation for *J. Chem. Phys. ARXIV*

3.4 Research plan

3.4.1 Goals and work program

In order to achieve superior functionality of a HIOS interface, it is crucial to have knowledge about the energy level alignment of the inorganic and the organic semiconductor as well as about potential hybrid states (e.g. HCTE etc.) The resulting electronic and dipole-dipole coupling across the interfaces determines the charge and energy transfer between the constituents and can be measured by, e.g. probing the population dynamics in transiently occupied states. The choice of energy levels and the degree of coupling thus determine the ultrafast dynamics (cf. Fig. 6). In a first step, this project will, based on the thorough understanding achieved in the first funding period, systematically investigate this influence of energy level alignment on the ultrafast dynamics of charge and energy transfer in real time. Particular focus will lie here on the role of the (functional) interface in terms of work function tuning, surface band bending, and screening by interfacial charge density as outlined below. These results will serve as a fundament for the second step, where specifically designed molecules with photo-activatable dipole moments will be used to switch the interfacial coupling on an ultrafast timescale.

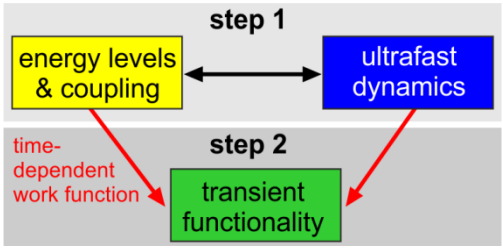

Fig. 6: Concept for the second funding period

Step 1: Interplay of energy level alignment and the ultrafast dynamics of CT & FRET

Figure 7 illustrates how we plan to manipulate the energy level alignment and thus the electronic coupling across the HIOS interface. The basic idea is to tune the properties of the interface such that it exhibits an own functionality. This will be achieved in three different ways:

(i) Modification of the surface dipole: By adsorption of hydrogen or different types of donor/acceptor molecules with and without internal dipole moment (e.g. pyridine or F4TCNQ), we modify the work

function and the SBB. This will be achieved by buffer layers between the inorganic and the organic semiconductor and through functional docking groups of the optically active COM.

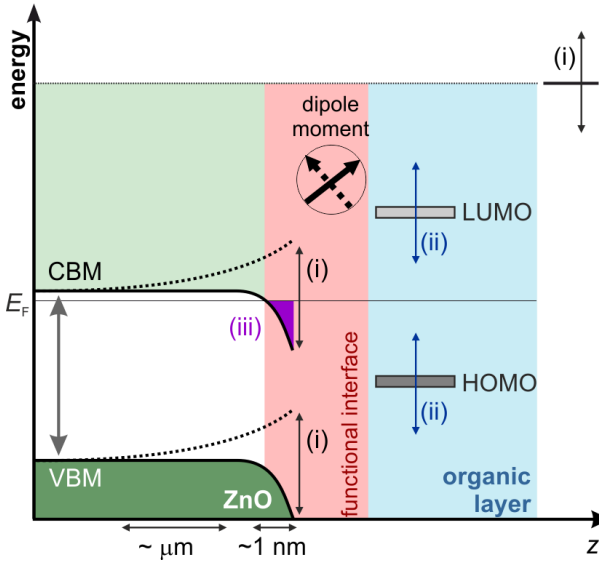

Fig. 7: Adjustment of energy levels at functional interfaces.

(ii) The alignment of the energy levels with respect to the vacuum level E_{vac}, i.e. the electron affinity and ionization potential, will be tuned chemically (collaboration with Z1 & A3). In combination with (i), this will allow, for instance, to quantify the influence of an interfacial barrier (upward SBB) on the CT compared to downward SBB with a *fixed energy* difference of LUMO and bulk CBM.

(iii) As outlined in 3.3, downward SBB can cause the formation of an interfacial charge accumulation layer. The charge density in this two-dimensional metal should strongly affect the electronic coupling between organic and inorganic semiconductor through screening of the Coulomb interaction and, therefore, also the formation probability of hybrid charge transfer excitons (HCTE).

These three approaches will enable to modify the *electronic* coupling across the HIOS interface whilst *energy* transfer (via, e.g. ZnO surface excitons discovered in the first funding period) will remain largely unaffected (constant distance). This control over the relative transfer probabilities should eventually make it possible to choose functional interfaces such that either energy transfer (for opto-electronic applications) or charge separation (for light harvesting applications) are optimized. The proposed studies will be coordinated with the projects A4 (Heimel), A8 (Koch), and B4 (Körzdörfer/Scheffler/Rinke), which will also investigate the influence of different anchor groups and/or buffer layers on the energy level alignment.
In the context of energy level alignment and its impact on interfacial CT, particular focus will lie on the formation and decay dynamics of hybrid CT excitons (with electron and hole localized at different sides of the interface). This species is suspected to be a precursor for heterogeneous CT [8-12] and exhibits distinct absorption and emission characteristics. These will be co-investigated in the projects B3 (Blumstengel) by TR-PL, B7 (Neher) by electro-luminescence and Kelvin probe, and theoretically by B6 (May) using semiempirical and quantumchemical calculations. First results (see section 3.2.1) on 5P-Py seem promising with regard to investigating the formation and decay dynamics of HCTE.

Step 2: Transient functionality at HIOS interfaces

The basic concept of this approach is to use dipolar organic molecules that change their conformation after photoexcitation and thereby change their dipole moment. These will be developed in project (A3 Hecht). Adsorption of such “dipolar switches” on the inorganic substrate will allow to change the work function of the HIOS by photoactivation using ultrashort laser pulses (cf. Fig. 8). This change of surface dipole will also modify the alignment of the energy levels. Based on the knowledge of the electronic coupling at different functional interfaces achieved in step 1, it will be possible to synthesize appropriate organic molecules such that their *electronic* coupling is significantly altered when the work function is switched by light (for details, see A3 Hecht).
Fig. 8 illustrates one (simplified) example for a *transiently functional* HIOS interface. Photoexcitation

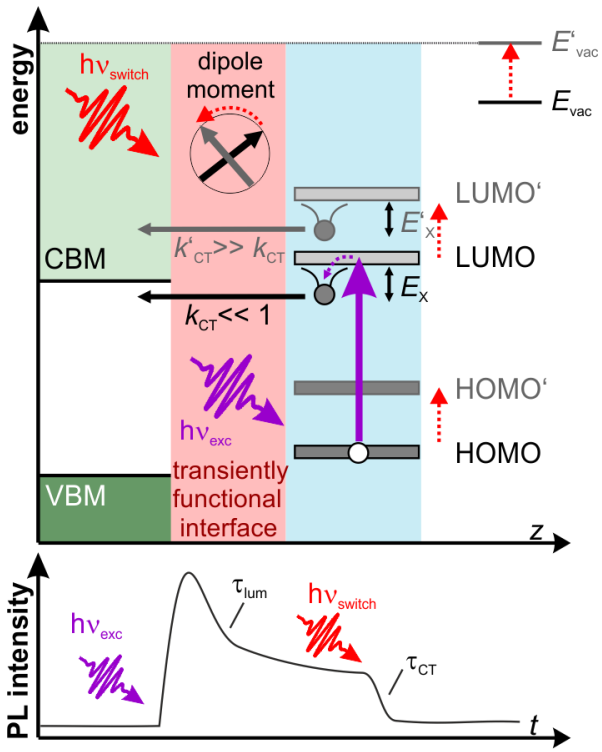

Fig. 8: Switching light emission by photoexctiation of transiently functional interfaces

($h\nu_{exc}$) creates excitons in the organic molecules, with the electronic level of the exciton energetically lying in the gap of the inorganic substrate (i.e. charge separation through electron transfer is suppressed). The excitons can radiatively recombine and the photoluminescence will decay on the characteristic timescale τ_{lum} (Fig. 8, bottom). Photoinduced switching of the molecular dipole moment ($h\nu_{switch}$) causes an upward shift of the vacuum level E_{vac} → E'_{vac}. Analogously, the electronic levels are shifted to higher energies (LUMO → LUMO'). This upward shift changes the resonance conditions of the excited electron, which can now directly transfer to the CB of the substrate. The photoinduced charge transfer rate k'_{CT} is much larger than the one of the ground state (k_{CT}). Thus, the exciton population will decay on the ultrafast timescales characteristic for charge transfer ($\tau_{CT} = 1/k'_{CT}$) and the photoluminescence of the molecules is *switched off by light*.

In summary, the proposed project will make use of (static and transient) energy level alignment, surface band bending, and charge accumulation layer at the interface of inorganic/organic semiconductors to understand and manipulate heterogeneous charge and energy transfer in HIOS. This will be achieved by combining several bulk-, surface-, and interface-sensitive fs TR spectroscopic techniques that are applied to a selection of appropriate HIOS systems as outlined in the following.

Year 1
- Charge transfer dynamics of 5P-Py/ZnO(10-10) as a function of hydrogen pre-adsorption (interfacial charge density) using TR 2PPE
- Complementary: CT dynamics of 5P molecules on top of pyridine/ZnO(10-10) using TR 2PPE
- Exciton dynamics in L4P/ZnO and glass substrates using TR LOS
- Characterization of angle dependence of TR eSFG of ZnO(10-10) to determine surface contributions
- Setup and first tests of TR PL using an upconversion scheme

Year 2
- Charge transfer dynamics of 3P-Py/ZnO(10-10) as a function of hydrogen pre-adsorption (interfacial charge density) using TR 2PPE
- Complementary: CT dynamics of 3P molecules on top of pyridine/ZnO(10-10) using TR 2PPE
- Charge transfer dynamics at L4P/ZnO interfaces using TR 2PPE as a function of hydrogen pre-adsoption
- Exciton dynamics of oligophenyl-Py molecules on ZnO and glass substrates using TR LOS and TR PL
- First TR eSFG experiments on HIOS interfaces

Year 3
- Characterization of the unoccupied electronic structure of F4TCNQ/ZnO using 2PPE as a function of hydrogen pre-adsorption
- Charge transfer dynamics of 5P and L4P layers on F4TCNQ/ZnO substrates using TR 2PPE
- Exciton dynamics using TR LOS, TR eSFG, and TR PL

Year 4
- Characterization of photoinduced work function switching using TR 2PPE
- Charge transfer dynamics of optically active dipolar switch molecules using TR 2PPE
- Exciton dynamics using TR LOS, TR eSFG, and TR PL

3.4.2 Methods

The electronic structure of the HIOS and the charge carrier/exciton dynamics will be investigated using femtosecond time- and angle-resolved 2PPE spectroscopy, time-resolved (linear and non-linear) optical spectroscopy and time-resolved photoluminescence (PL). Except for the latter, all techniques access the ultrafast dynamics by using fs-laser pulses in a pump-probe scheme as depicted in Fig. 9. A first laser pulse ($h\nu_{pump}$) creates non-equilibrium conditions in the sample that subsequently relax until equilibrium is re-established. These relaxation dynamics are then probed by a second, time-delayed fs-laser pulse ($h\nu_{probe}$). Variation of this time delay facilitates the observation of the femto- and picosecond evolution of the system in real time.
The 2PPE process is schematically illustrated in Fig. 2. $h\nu_{pump}$ excites electrons from below the Fermi level E_F (e.g. valence band electrons) into usually unoccupied states and launches processes such as hot electron relaxation or exciton formation. The population of these excited states is probed by photoionization of the sample using $h\nu_{probe}$. The kinetic energy and momentum of the photoelectrons comprises information about the absolute binding energies and dispersion of the unoccupied levels.
When measuring the transient transmission of the *excited state*, the pump pulse first excites non-equilibrium dynamics and the population of the transiently occupied states is probed using a white light super continuum

that provides spectral resolution as well as fs- time resolution when the pump-probe delay is varied (cf. Fig. 4). In the case of non-linear optical spectroscopy, we monitor the sum frequency that is generated in the sample (cf. Fig. 5). This is a second order process that happens in centrosymmetric materials only at the surface/interface. However, even in non-centrosymmetric media as ZnO, interface sensitivity can be reached when taking into account that bulk and surface susceptibility have different non-zero matrix elements, which makes them distinguishable.

Collection of the photoluminescence after excitation with the pump laser provides information about the emission properties of the sample. Femtosecond time resolution can be achieved by frequency mixing of the PL with another laser pulse ($h\nu_{gate}$) in a non-linear crystal (e.g. BBO) and detection of the up- (or down-) converted light.

Note that all TR spectroscopic techniques will be performed at nominally *the same* samples, which will be realized using the small, transportable UHV chamber developed during the first funding period. This will allow the sample preparation in the UHV system and transfer to the transport chamber under UHV conditions. Optical and PL experiments will then be performed directly in the transport chamber.

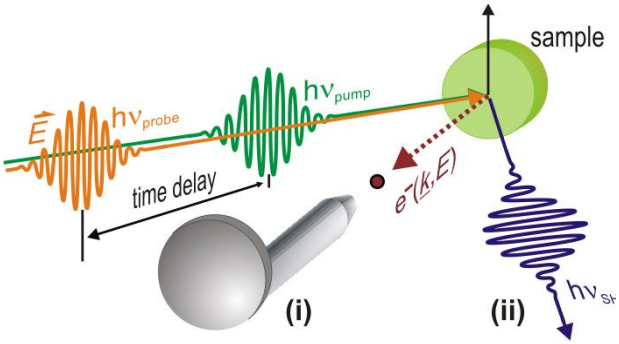

Fig. 9: Experimental scheme. A first fs-laser pulse ($h\nu_{pump}$) photoexcites the sample. The resulting non-equilibrium dynamics (see text) are monitored using a second, time-delayed laser pulse: (i) In 2PPE, photoelectrons are created that are analyzed regarding their kinetic energy and momentum parallel to the surface using a hemispherical analyzer. (ii) Detection of the second harmonic that is generated in the sample.

Sample preparation and characterization

The surface quality of our inorganic substrates will be checked using LEED, Auger electron spectroscopy (AES), and work function/electron affinity measurements using 2PPE. Depending on the sublimation temperature of the respective organic molecule under UHV conditions, we will either use our gas system and pinhole doser to deposit the organic compound onto the sample or a Knudsen cell for larger molecules. During deposition, the sample temperature can be controlled using a He-flow cryostat and resistive heating and the exposure monitored using a quartz microbalance. Furthermore, if desorption kinetics allow, the coverage can be determined by TPD (for $m < 300$).

Experimental setup

(i) *Optical setup:*
The fs-laser Ti:Sa system is set up in the laboratory and provides laser pulses (10-100 fs) over almost the whole frequency range between 0.22 and 6.2 eV (5500 - 200 nm). Prism compressors and high precision delay stages with retroreflectors are used for optimal time resolution. Beam paths to the 2PPE chamber are installed as well as the optical setups for linear and non-linear optical spectroscopy. The TR photoluminescence experiment is still to be set up.

(ii) *He-flow cryostat for non-linear optical spectroscopy:*
For optical experiments, the samples can be mounted in a He-flow cryostat that is equipped with a temperature controller which allows for experiments between 4 and 700 K. Experiments are performed under high vacuum conditions.

(iii) *Ultrahigh vacuum system for 2PPE spectroscopy:*
The UHV chamber is held at a base pressure below 10^{-10} mbar and equipped with various devices for sample characterization: LEED, AES, TPD/TDS using a QMS (quadrupole mass spectrometer). Furthermore, the sample holder is mounted to a temperature-controlled He-flow cryostat and can be moved using a four-axis manipulator. The chamber is equipped with a two-compartment gas system that allows for independent dosing of two different species, with a Knudsen cell for larger molecules, and with a quartz microbalance. For 2PPE spectroscopy, a hemispherical analyzer simultaneously detects kinetic energy and momentum of the photoelectrons.

3.5 Role within the Collaborative Research Centre

This project investigates the role of functional interfaces on the electronic structure as well as the carrier/exciton dynamics at HIOS interfaces using time- and angle-resolved 2PPE, non-linear optical spectroscopy, and TR photoluminescence. With this approach, it exhibits joint interests with several theoretical and experimental groups as outlined in the following.

Energy level alignment:

- A3 (Hecht): Development of suitable organic molecules for charge and energy transfer across functional HIOS interfaces
- A8 (Koch): Determination of the (occupied and unoccupied) energy level alignment in HIOS using electron donors or acceptors (e.g. F4TCNQ).
- B4 (Körzdörfer/Scheffler/Rinke) and A4 (Heimel): Determination of occupied and unoccupied electronic structure including work functions and charge densities (in particular the interplay of charge transfer and dipole moments) for the developement of functional HIOS interfaces.
- B6 (May): Computation of absorption spectra of nanostructured HIOS counterparts for comparison
- B7 (Neher): Energy level alignment for charge transfer and surface dipole measurements
- Z1 (Hecht): Oligophenylenes with pyridine endgroups, L4P

Charge transfer and exciton dynamics:

- A3 (Hecht): Development of photo-switchable dipolar organic molecules for transiently functional interfaces
- A10 (Tkatchenko/Scheffler): static and time-dependent electronic and vibrational properties of HIOS
- B3 (Blumstengel): Energy transfer at HIOS interfaces via dipole-dipole coupling
- B11 (Draxl): Non-equilibrium dynamics of excited states in HIOS
- B12 (Knorr/Richter): Ultrafast dynamics of electronic levels and lattice

Structure and growth:

- A2 (Kumagai/Wolf): Adsorption and electronic structure of selected HIOS
- Z2 (Kowarik/Koch): Determination of the growth conditions of the investigated samples

3.6 Delineation from other funded projects

The proposed project is not funded by the DFG or other sources and is clearly separated from other funded projects of the principal investigator. The PI's task in the EU project *Time dynamics and ContROl in naNOStructures for magnetic recording and energy applications (CRONOS)* (within FP7-NMP-2011-SMALL), ending in 05/2015, focusses on light-harvesting applications (not opto-electronics) and will end before the second funding period of this CRC would start.

3.7 Project funds

3.7.1 Previous funding

The project has been funded within the Collaborative Research Centre since 07/2011.

3.7.2 Funds requested

Funding for	2015/2		2016		2017		2018		2019/1	
Staff	Quantity	Sum	Quantity	Sum	Quantity	Sum	Quantity	Sum	Quantity	Sum
PhD student, 66%	2	44100	2	88200	2	88200	2	88200	2	44100
Total		44100		88200		88200		88200		44100
Direct costs	Sum		Sum		Sum		Sum		Sum	
Small equipment, Software, Consumables	5.000		10.000		10.000		10.000		5.000	
Other	-		-		-		-		-	
Total	5.000		10.000		10.000		10.000		5.000	
Major research equipment	Sum		Sum		Sum		Sum		Sum	
€ 10.000 - 50.000	-		-		-		-		-	
> € 50.000	-		-		-		-		-	
Total	-		-		-		-		-	
Total	49.100		98.200		98.200		98.200		49.100	

(All figures in Euro)

3.7.3 Staff

	No.	Name, academic degree, position	Field of research	Department of university or non-university institution	Commitment in hours/week	Category	Funded through:
Available							
Research staff	1	Stähler, Julia Dr., group leader	physics/ surf. science	FHI der MPG, physical chemistry	15		MPG
	2	Laura Foglia PhD student	physics/ surf. science	FHI der MPG, physical chemistry	40		MPG
Non-research staff	3	Lehnert, Joachim chem. engineer		FHI der MPG, physical chemistry	5		MPG
Requested							
Research staff	4	N.N. Ph.D. student	chemistry/ surf. science	FHI der MPG, physical chemistry		E13, 75%	
	5	N.N. Ph.D. student	physics/ surf. science	FHI der MPG, physical chemistry		E13, 75%	
Non-research staff							

Job description of staff (supported through available funds):

1. Dr. Julia Stähler (Principal investigator): Scientific coordination and organization of the project, instruction and supervision of the project staff, co-operation in experiments and data analysis, publishing.

2. Laura Foglia (PhD student): Performance of the TR eSFG experiment, data analysis, operation and support of the optical setup, publishing.

3. Dipl. Ing. Joachim Lehnert: Technical support of the experiments including design and manufacturing of new components, maintenance of equipment.

Job description of staff (requested):

This project aims at the comprehensive characterization of the energy levels, charge and energy transfer dynamics at HIOS interfaces. This requires application of a broad selection of sophisticated and experimentally challenging femtosecond time-resolved spectroscopic techniques as well as the operation of our UHV system for sample preparation and photoemission. These requirements are so diverse that they *have to* be distributed between at least three different PhD students (each of them undertaking one experiment: TR eSFG, TR 2PPE, TR LOS (incl. PL)). The students will undertake three scientifically overlapping studies, each of them performing complementary experiments to the other students' projects on the respective machines. One of these positions will be funded through available funds (see above).

4. N.N. (PhD student): Sample preparation (inorganic substrates & HIOS), operation and support of the laser and UHV system, TR 2PPE spectroscopy of electronic structure and dynamics, data analysis, publishing. The conduction of TR 2PPE studies is experimentally very challenging and requires the full attention of one PhD student.

5. N.N. (PhD student): sample preparation (inorganic substrates & HIOS), operation and support of the laser and UHV system, TR LOS of various HIOS systems and comparison to organic layers on inert substrates. Design, setup, and characterization of the TR PL experiment, data analysis, publishing. The diversity of these tasks require the full attention of one PhD student.

3.7.4 Direct costs for the new funding period

	2015/2	2016	2017	2018	2019/1
Funds available	10.000	20.000	20.000	20.000	10.000
Funds requested	5.000	10.000	10.000	10.000	5.000

(All figures in Euro)

Consumables for 2015/2

optical components & optomechanics	EUR	2000
small UHV parts	EUR	1000
chemicals for sample preparation & cleaning of optical components	EUR	500
molecules for adsorption	EUR	1500

Consumables for 2016

cf. 2015/2	EUR	10000

Consumables for 2017

cf. 2015/2	EUR	10000

Consumables for 2018

cf. 2015/2	EUR	10000

Consumables for 2019/1

cf. 2015/2	EUR	5000

3.7.5 Major research equipment requested for the new funding period

No funding for instrumentation is requested.

3.1 About project B10

3.1.1 Title: Theory of Active Hyperbolic Metamaterials and Spaser Action in HIOS

3.1.2 Research areas: Theoretical Physics, Photonics, Plasmonics, Optics

3.1.3 Principal investigator

Prof. Dr. Busch, Kurt (*12.01.1967, German)
Humboldt-Universität zu Berlin
Institut für Physik
AG Theoretische Optik & Photonik
Newtonstr. 15
12489 Berlin
Phone: +49 (0)30 2093 7892
Fax: +49 (0)30 2093 7643
E-mail: kurt.busch@physik.hu-berlin.de

Do the above mentioned persons hold fixed-term positions? no

3.2 Summary

The development of a comprehensive theoretical framework for the analysis of two prototypical hybrid plasmonic systems and corresponding applications in terms of functional elements and devices is suggested. First, Hyperbolic Metamaterials (HMMs), i.e., structures consisting of alternating layers of plasmonic and dielectric materials, promise novel dispersion relations and broad-band enhancements of the optical density of states. In turn, this leads to complex radiation dynamics of embedded active materials. The ultimate optical performance of HMMs is determined by nonlocal effects of the plasmonic constituents as well as the details of their microstructure. Such active HMMs represent ideal hybrid structures that can be fabricated by alternating layers of ordinary metals and/or doped transparent conductive oxide with layers of conjugated polymers or dielectric matrices with embedded conjugated molecules. Further, active HMMs as well as cavity and waveguiding structures derived from them lead to novel applications such as unusual light-matter coupling and unusual extraordinary optical transmission.
Second, the SPASER (Surface Plasmon Amplification by Stimulated Emission of Radiation) is a nano-scale generator of coherent plasmons. Therefore, SPASER action requires the simultaneous presence of a resonant plasmonic system and an optical gain medium. As a result, the SPASER properties strongly depend on the coherent interplay of optical fields and electronic excitations in both, the metal and the active material. Such systems can be realized via metal core/conjugated organic shell hybrid structures. In such systems, the higher-order multipolar modes associated with the plasmonic element play an important role.
In cooperation with experimental partners, this theoretical framework will be applied to investigate the complex radiation dynamics in and the modified optical properties of these two prototypical systems.

3.3 Project progress to date

Project B10 started as a late-comer to the CRC in January 2013. Therefore, in section 3.3 we report on the background of the project and the progress achieved so for. In section 3.4, we describe the research plan for the next funding period which – in view of the results obtained so far, the progress obtained of the collaborating projects within the CRC, and the arrival of new cooperating projects – is based on a significant adjustment and extension of the original proposal.

3.3.1 Report and state of understanding

Theory of Fluorescence in Hyperbolic Metamaterials

In their simplest version, Hyperbolic Metamaterials (HMMs) consist of stacks of alternating thin, i.e., sub-wavelength metallic and dielectric layers. To a first approximation, this composite system may be regarded as an effective anisotropic homogeneous system with one specific effective value of the permittivity perpendicular and another specific value of the permittivity parallel to the stacking direction. By properly selecting materials and adjusting the layer thicknesses and one can realize the hyperbolic medium regime when the different effective permittivities feature different signs. Consequently, HMMs [1] exhibit effective dispersion relations that, for fixed frequency, take on the form of hyperboloids in wave-vector space – in sharp contrast to the well-known ellipsoids associated with conventional optically anisotropic materials. As a result, HMMs allow the access to much larger ranges of wave-vectors and – originally under the name of indefinite materials [2] – they have been considered for applications in imaging and microscopy [3]. Perhaps even more interesting is the more recent realization that this large reach in wave-vector space together with the dispersive character of metals leads to a broadband "super-singularity" in the optical density of states of HMMs. This may be exploited in a number of ways. For instance, large enhancements in the spontaneous emission rates of active materials *in the vicinity* of HMMs have been observed [4,5], giant forces in nano-scale slot waveguides within HMMs [6], and "darker than black" absorption properties of HMMs with corrugated surfaces [7] have been suggested. This enhanced optical density of states may even be utilized to increase light-matter interaction on the single quantum-emitter level [8].
However, it has been suggested that some of these exciting properties might have to be reexamined. On the one hand, a recent theoretical work using the above model for HMMs has found the surprising result that spontaneous emission rates of quantum dot emitters located *inside* HMMs depend on the emitters' size and diverges formally as this size tends to zero [9]. The authors of [9] accommodate this result by invoking that their theory breaks down once the emitter size becomes smaller than the layer spacing so that inverse layer spacing provides a natural cut-off to the UV-divergent integrals. In a subsequent work [10], the same authors acknowledge that the effective medium approximation also underestimates the radiative decay rate due to the enhanced excitation of surface plasmon polaritons at the metal-dielectric interfaces inside HMMs. On the other hand, a recent theoretical work [11] has found rather unusual conditions under which the effective medium approximation may be applied to HMMs which are quite distinct from those that have been used in [9,10]. Further, for the thin metallic layers used in HMMs, the traditional (spatially local) Drude- and/or Drude-Lorentz model may not be directly applicable. Rather, one would expect that nonlocal effects become important and a recent theoretical work has shown that, within a nonlocal Drude model, the broadband "super singularity" in the density of states would become regularized [12].
The above discussion suggests that all physical mechanisms that exhibit a behavior significant wave-vector dependence can also significantly contribute to the optically properties of HMMs. These include the finite extent of the individual layers, the nonlocal characteristics of the constituent plasmonic material, and local field effects as the emitters are usually embedded within the dielectric layers. To the best of our knowledge, no systematic investigation of these mechanisms and their (due to multiple scattering effects non-additive) interplay has been carried out and the local field effects have been ignored altogether. Consequently, we have developed a comprehensive theory of fluorescence in layered HMMs of finite and infinite extent based on determining the exact electromagnetic Green's tensor and also accounting for the local-field effects within the so-called real-cavity model [P5]. Based on this, we have performed a systematic study of the emission rate enhancement relative to vacuum that is experienced by an electric-dipole emitter whose dipole moment is oriented orthogonal to the material interfaces of a HMM consisting of alternating silver and SiO_2 layers.
Fig. 1 depicts the results this study for infinitely extended systems and different material models for silver, specifically a simple (local) Drude model, a nonlocal (hydrodynamic) Drude model [12], and a description based on an approximate (and nonlocal) solution of the Boltzmann equation [13]. In addition, the results for a finite-sized (slab) geometry is depicted

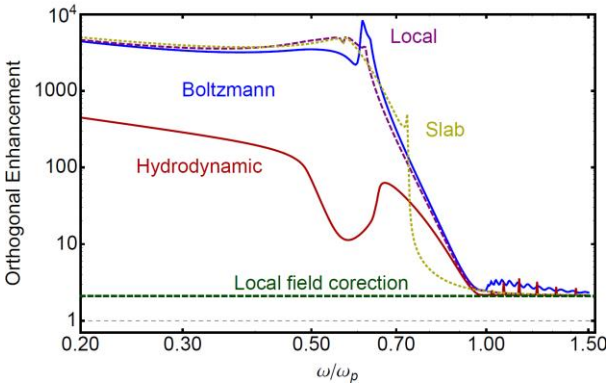

Fig. 1: Emission enhancement of a dipole emitter embedded into infinitely extended and finite-sized HMMs consisting of alternating layers of silver and SiO_2 (thicknesses 6.6 nm and 4.4 nm) for various plasmonic material models. The emitter's dipole moment is oriented orthogonal to the material interfaces). The curves labelled "Local", Hydrodynamic", and "Boltzmann" correspond to infinitely extended HMMs using different models for silver with the same plasma frequency and damping constants. The curve labelled "Slab" represents the results for a SiO2 layer sandwiched between two silver layers and using a local Drude model for silver. Adapted from Ref. [P5], see text for further details.

This slab geometry consists of a central dielectric layer that is sandwiched between two plasmonic layers described by the (local) Drude model. Obviously, the different material models lead to very different emission characteristics, both for frequencies above and below the plasma frequency ω_p. First, while for frequencies below the plasma frequency, the nonlocal Drude model shows the expected reduction in the emission enhancement relative to the local Drude model, the nonlocal Boltzmann model does not confirm this. At this point, we can only speculate about the origin of this difference but would like to note that in a recent work [14] a modification of the nonlocal Drude model has been suggested (albeit without detailed microscopic justification) in order to account for phenomena observed in plasmonic antenna systems with nano-gap structure. Second, for frequencies above the plasma frequency, the nonlocal models show characteristic resonances that are associated with the excitations of bulk plasmons in the metal – naturally, these bulk plasmons are absent in local models so that this constitutes a direct way of probing nonlocal material properties, if only plasmonic materials with sufficiently low plasma frequencies can be found.
Such plasmonic materials with low values of the plasma frequency do indeed exist in the form of highly-doped semiconductors. In fact, following the successful evaluation of this proposal B10 as a late proposal, project A5 has successfully started to develop highly-doped ZnO into a tunable plasmonic material with significantly improved figure-of-merit [15]. In addition, the researchers in project A5 have demonstrated unusual surface plasmon polariton waves at interfaces of highly-doped ZnO and ordinary metals [16]. Thus our results regarding the impact of the plasmonic material properties on emission characteristics in layered systems and the experimental progress in project A5 lead directly point to a number of very interesting research directions.

Semi-classical SPASER theory

Much the present interest in plasmonic nano-structures is based on their potential for overcoming a number of limitations associated with dielectric nano-structures in opto-electronic applications, for instance, by replacing optical excitations with mixed light-matter excitations that are confined on nano-meter scales near metal-dielectric interfaces. On the classical level, such so-called surface plasmon polariton waves (wave-like excitations running on flat interfaces) and particle plasmon polariton resonances (localized excitations in nano-particles) facilitate efficient information processing and short-distance information transmission. Furthermore, the corresponding quantized excitations lend themselves rather well to applications in quantum information processing [17], thus spawning the field of quantum plasmonics. Naturally, the realization of such plasmonic technologies requires a number of functional elements, notably efficient coherent plasmon polariton sources. This latter functionality is embodied in the concept of the so-called SPASER (Surface Plasmon Amplification by Stimulated Emission of Radiation) [18,19] and the related concept of the lasing SPASER [20]. Loosely speaking, the SPASER may be envisioned as a traditional laser where the optical resonator is replaced by a (spatially confined) plasmon resonance such that the optical gain material generates coherent plasmons rather than coherent photons. Similar to the traditional laser, the SPASER-threshold is determined by the balance of total losses (dissipation within the metal and leakage radiation from the particle to the far-field) and the total gain that originates from the interplay of optically active material with the plasmonic field enhancement.
From a theoretical point of view, one can conceive of semi-classical and fully quantum theoretical descriptions. In particular, a fully quantum-optical description is rather challenging since the quantization of the electromagnetic field in dispersive and dissipative open systems is far from trivial. One problem is that bona-fide modes (bound states) for dielectric or metallic particles do not exist – Mie resonances correspond to scattering states so that mode volumes and, subsequently, the light-matter coupling constants are ill-defined. Recent progress in defining so-called quasi-normal modes [21,22] indicates that this problem may eventually be overcome, albeit only dipolar modes have been considered so far. Another problem results

from the fact that the strongly dispersive and dissipative optical properties of metals implies that such quasi-normal modes, being associated with different frequencies, are not orthogonal anymore so that corresponding cross-coupling effects cannot be ignored. As a matter of fact, in conventional laser theory, the non-orthogonality of modes leads to an increased laser threshold due to additional noise effects. This is known as the Petermann excess-noise factor. Nevertheless, the vast majority of theoretical SPASER works either restrict themselves to treating only dipolar modes (either on a quasi-static [23] or electromagnetic [24] level) or to phenomenological parameters [25] that do not allow for quantitative predictions.
These theoretical considerations along with the need to provide predictive and interpretative support for experimental works within project B2 of the CRC have inspired us – in collaboration with the researchers from project B2 – to first formulate a semi-classical SPASER theory for spherical nano-particles. When constructing such a theory, we can rely on the rather well-understood analytical (Mie-type) solution of the radiative and non-radiative rates of a single dipole-emitter in the vicinity of a metal nano-particle [26,27]. In particular, for decreasing emitter-particle distances below the wavelength of light, higher-order multi-polar modes increasingly contribute to the non-radiative rate, eventually overcompensating field-enhanced gain amplification. This behavior essentially corresponds to the above-mentioned cross-coupling of different multi-polar modes on the level of rates. In contrast, the radiative rate is dominated by the dipolar mode.

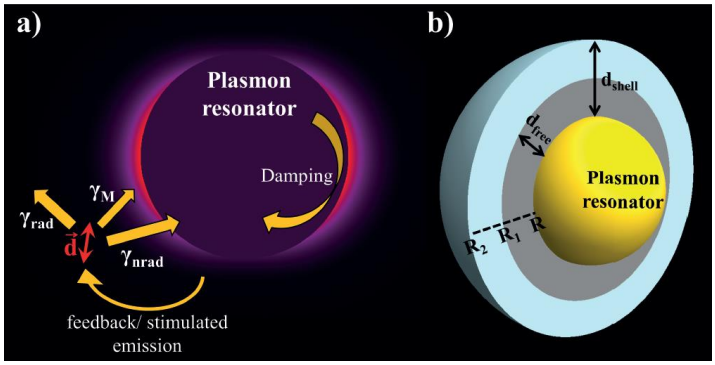

Fig. 2: Schemtatic of a core/shell plasmonic SPASER (right) and illustration of the different processes of an electric dipole emitter interacting with a plasmonic nano-particle. The emitter can radiatively decay by emission into the far field (γ_{rad}) and can non-radiatively decay into the different multi-polar plasmon resonances of the nano-particle. Here, part of the non-radiative decay goes into the plasmon mode targeted for spasing action (γ_M) and the off-resonant modes (γ_{rad}), all of which are subject to cross-coupling and damping. Adapted from Ref. [P3]; see text for details.

In fact, we have rearranged the different multi-polar contributions in order to formulate a multi-mode rate equation for each dipolar emitter (see Fig. 2). Upon averaging over a distribution (for instance, in a shell around the particle) and incorporation of a pump rate, we finally obtain a multi-mode laser rate equation that is capable of quantitatively describing the SPASER threshold (see Fig. 3) and associated phenomena such as the corresponding mode competition dynamics and the modulation bandwidth. Moreover, as our semi-classical SPASER theory for spherical particles builds on a fully electromagnetic description of the light field, we may straightforwardly generalize it to arbitrary particles by replacing the vector-spherical harmonics of the Mie theory by the above-mentioned numerically determined quasi-normal modes.
However, the most important result of our semi-classical SPASER theory may well be the insight that we can now determine the optimal location of fluorescent molecules in core-shell geometries as envisaged by our experimental collaborators in B2. These locations are determined by the balancing the field-enhanced gain with the total losses, both of which exhibit strong dependences on the molecule-particle separation. In fact, we can show that for a typical SPASER geometry of a gold sphere of 7 nm radius, a spacing layer of about 5 nm for the molecules to the sphere's surface, significantly improves the SPASER threshold relative to the naïve placement of the molecule directly at the surface (and assuming that charge transfer processes are obsent). Presently, our experimental collaborators in project B2 are fabricating such optimized SPASER configurations.

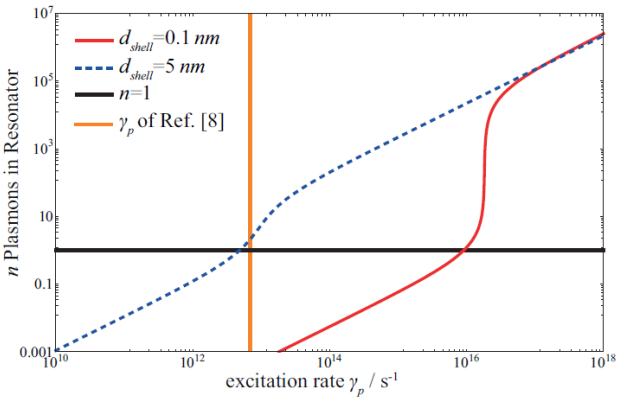

Fig. 3: Plasmon number in the resonator-mode of a spherical core/shell lasing SPASER with gain material in a shell with distance *d* from sphere surface as a function of pump rate (double-logarithmic plot). The solid red curve displays SPASER with almost no emitter-free spacing layer (d_{shell} = 0.1 nm), the dashed blue line a SPASER with a d_{shell} = 5 nm spacing layer between the emitters and sphere surface. The same density of emitters (slightly less total gain medium for the spaser with spacing layer) is used in both cases. The orange vertical line shows the excitation rate used by Noginov et al., the horizontal black line

indicates a spaser threshold value of one plasmon in the resonator-mode.

Clearly, our above SPASER theory can also be applied to ordinary hybrid nano-laser systems where the metal nano-particle is replaced by a low-loss dielectric nano-particle made, e.g., from high-index material. Such dielectric nano-particles support different modes than do metal nano-particles and it turns out that they offer novel pathways to realize low-threshold and truly nano-scopic lasers [P4]. In collaboration with our experimental collaborators in project B2, we have developed a corresponding design for a silicon-nano-particle laser that is presently being realized.

Preliminary work

At this point, we would also like to note that we have carried out a number of preliminary works that are not yet directly related to the HIOS but they nevertheless constitute important methodic advances on which much of the above-discussed work has been and much of our planned research will be based.
In particular, one of these works constitutes the design of an easy-to-fabricate photon-to-plasmon coupler that has been accomplished in collaboration with researchers from project B2 [P1]. These couplers are presently being fabricated and constitute an important element for future nano-plasmonic devices, notably plasmonic waveguide based SPASER systems.
In a second work, we have realized an efficient numerical method for computing the electromagnetic Green's tensor in complex nano-photonic systems and the subsequent determination of the fluorescence lifetime. The results of these computations have been compared with corresponding spatially resolved experimental data on the fluorescence lifetime of single quantum emitters interacting with a plasmonic system (obtained by researchers in project B2) and excellent agreement has been obtained [P2]. Consequently, we are very confident that our methodologies are capable of providing interpretative as well as predictive support for our experimental collaborators.

References

[169] A. Poddubny, I. Iorsh, P. Belov, and Y. Kivshar, Nat. Photon. **7**, 948 (2013).
[170] D.R. Smith and D. Schurig, Phys. Rev. Lett. 90, 077405 (2003).
[171] A. Salandrino and N. Engheta, Phys. Rev. B **74**, 075103 (2006).
[172] M.A. Noginov, H. Li, A. Barnakov, D. Dryden, G. Nataraj, G. Zhu, C.E. Bonner, M. Mavy, Z. Jacob, and E.E. Narimanov, Opt. Lett. **35**, 1863 (2010).
[173] J. Kim, V.P. Drachev, Z. Jacob, G.V. Naik, A. Boltasseva, E.E. Narimanov, and V.M. Shalaev, Opt. Express **20**, 8100 (2012).
[174] Y. He, S. He, J. Gao, and X. Yang, Opt. Express **20**, 22372 (2012)
[175] E.E. Narimanov, H. Li, A. Barnakov, T.U. Tumkur, and M.A. Noginov, arXiv:1109.5469v1.
[176] C.L. Cortes, W. Newman, S. Molevsky, and Z. Jacob, J. Opt. **14**, 063001 (2012).
[177] A.N. Poddubny, P.A. Belov, and Y.S. Kivshar, Phys. Rev. A **84**, 023807 (2011).
[178] I. Iorsh, A. Poddubny, A. Orlov, P. Belov, and Y.S. Kivshar, Phys. Lett. A **376**, 185 (2012).
[179] O. Kidwai, S.V. Zhukovsky, and J. Sipe, Opt. Lett. 36, 2530 (2011).
[180] W. Yan, M. Wubs, and N.A. Mortensen, Phys. Rev. B **86**, 205429 (2012).
[181] R. Fuchs and K.L. Kliewer, Phys. Rev. **185**, 905 (1969); see also W.E. Jones and R. Fuchs, Phys. Rev. **178**, 1201 (1978).
[182] N.A. Mortensen, S. Raza, M. Wubs, T. Søndergaard, and S.I. Bozhevolnyi, Nat. Commun. **5**, 3809 (2014).
[183] S. Sadofev, S. Kalusniak, P. Schäfer, and K. Henneberger, Appl. Phys. Lett. **102**, 181905 (2013).
[184] S. Kalusniak, S. Sadofev, and F. Henneberger, Phys. Rev. Lett. **112**, 137401 (2014).
[185] A.V. Akhimov, A. Mukherjee, C.L. Yu, D.E. Chang, A.S. Zibrov, P.R. Hemmer, H. Park, and M.D. Lukin, Nature **450**, 402 (2007).
[186] D.J. Bergman and M.I. Stockman, Phys. Rev. Lett. **90**, 027402 (2003).
[187] M.I. Stockman, J. Opt. **12**, 024004 (2010).
[188] N.I. Zheludev, S.L. Prosvirnin, N. Papasimakis, and V.A. Fedotov, Nat. Photon. **2**, 351 (2008).
[189] C. Sauvan, J.P. Hugonin, I.S. Maksymov, and P. Lalanne, Phys. Rev. Lett. **110**, 237401 (2013).
[190] P.T. Kristensen and S. Hughes, ACS Photonics **1**, 2 (2014).
[191] P. Ginzburg and A.V. Zayats, Opt. Express **21**, 2147 (2013).
[192] X.-L. Zhong and Z.-Y. Li, Phys. Rev. B **88**, 085101 (2013).
[193] V.M. Parfenyev and S.S. Vergeles, Opt. Express **22**, 13671 (2014).
[194] R. Ruppin, J. Chem. Phys. **76**, 1681 (1982).
[195] A. Moroz, Opt. Comm. **283**, 2277 (2010).
[196] A. Jüngerl, *Transport Equations for Semiconductors*, Springer Lecture Notes in Physics 773 (2009).
[197] X. Yang, J. Yao, J. Rho. X. Yin, and X. Zhang, Nat. Photon. **6**, 450 (2012).

[198] R. Walther, I. Carmeli, R. Scheider, D. Gerthsen, K. Busch, C. Matyssek, A. Shvarzman, T. Maniv, S. Richter, and H. Cohen, J. Phys. Chem. C **118**, 11043 (2014).
[199] A. Andryieuski, S.V. Zhukovsky, and A.V. Lavrinenko. Opt. Express **22**, 14975 (2014).
[200] S.A. Brown and B.J. Dalton, J. Mod. Opt. **49**, 1009 (2002).
[201] M.I. Mishchenko, G. Videen, V.A. Babenko, N.G. Khlebtsov, and T. Wriedt, J. Quant. Spectrosc. Radiat. Transfer **88**, 357 (2004).
[202] A. Lubatsch, J. Kroha, and K. Busch, Phys. Rev. B **71**, 184301 (2005).

3.3.2 Project-related publications

[P1] G. Kewes, A.W. Schell, R. Henze, R.S. Schönfeld, S. Burger, K. Busch, and O. Benson, “Design and numerical optimization of an easy-to-fabricate photon-to-plasmon-coupler for quantum plasmonics”, Appl. Phys. Lett. 102, 051104 (2013).
[P2] A.W. Schell, P. Engel, J.F.M. Werra, C. Wolff, K. Busch, and O. Benson, “Scanning single quantum emitter fluorescence lifetime imaging: Quantitative analysis of the local density of photonic states”, Nano Lett. **14**, 2623 (2014).
[P3] G. Kewes, R. Rodriguez-Oliveros, K. Höfner, A. Kuhlicke, O. Benson, and K. Busch, “Threshold Limitations of the SPASER”, arXiv:1408.7054
[P4] G. Kewes et al., “Silicon NanoLaser”, arXiv
[P5] F. Intravaia and K. Busch, “Theory of Fluorescence in Hyperbolic Metamaterials”, arXiv

3.4 Research plan

The objectives of this project are centered at developing a comprehensive theoretical understanding of the optical properties and modified radiation dynamics in hyperbolic metamaterials (subproject a)) and developing a fully quantum-optical theory of the SPASER (subproject b)).
Specifically, we plan to achieve the following objectives:

- Develop a **consistent model for the optical properties of hyperbolic metamaterials** with special emphasis on embedded active materials containing conjugated systems, including also defect structures such as indefinite cavities as well as disorder.
- Investigate and design **active hybrid hyperbolic metamaterials** that are based on doped transparent conductive oxides as the plasmonic constituents and conjugated systems as the active constitutents.
- Develop a **quantum theory of the SPASER** and apply them to systems comprising metal core/conjugated organic shell hybrid structures.
- Investigate **multiple scattering effects** for SPASER systems that comprise several metal core/conjugated organic shell hybrid structures

Below, further details for the two subprojects are provided.

Subproject a) – Theory of Active Hyperbolic Metamaterials in HIOS

As described in section 3.3.1, the naïve approach to the optical properties of layered hyperbolic metamaterials (HMMs) does not necessarily lead to useful results, notably when the radiation dynamics of embedded emitters is concerned. In addition, the optical properties of the plasmonic layers have to modelled with significant care. Therefore, we propose to utilize the results of the first funding period and to develop a comprehensive framework that allows one to address a number of shortcomings of the presently available descriptions. This framework will be utilized to provide interpretative and predictive support for the experimental works on HMMs in projects A5 and A11. The eventual goal here is the realization of novel functionalities such as nonlinear switches and so-called indefinite cavities in a reliable manner.

Task 1: Macroscopic Material Model for highly-doped ZnO

Within the macroscopic Maxwell equations, material properties are described through specific material models that usually are the result of an analysis and corresponding approximations of the underlying classical or quantum Boltzmann equations. For instance, within a classical Boltzmann equation approach, the so-called hydrodynamic scaling leads to the nonlocal Drude model for metals (which is often further

simplified to the local Drude model) and the so-called diffusive scaling leads to the (inherently nonlocal) drift-diffusion model for undoped and/or weakly doped semiconductors [28]. Furthermore, and as mentioned above, a recent work suggests adding a diffusive contribution to the nonlocal Drude model in order to account for the properties of plasmonic nano-gap structures, albeit without a microscopic justification.
The above-discussed novel plasmonic materials based on highly-doped semiconductors such as ZnO represent intermediate systems. On the one hand, their free-carrier concentration is considerably higher than what would be required for the diffusive scaling so that one would expect significantly stronger collective effects such as in the hydrodynamic regime while, on the other hand, their low plasma frequencies correspond to free carrier concentrations where screening will be less efficient, thus rendering local Drude-like approaches rather doubtful.
We thus propose to develop an appropriate material model for the nonlocal characteristics of highly-doped ZnO (and other highly-doped semiconductors) through an analysis of the Boltzmann equation that incorporates elements of the underlying bandstructure as described within in a k.p-theory approach for the bulk, albeit with a doping-modified Fermi energy. Further, the scattering through the doping centers shall be included as well as the creation of trapping centers near (rough) surfaces. In these developments, we shall also be inspired by similar developments of extended drift diffusion models that have been developed in different contexts for modeling the electronic properties of organic solar cells.
This model shall be compared with the results of corresponding ab-initio computations on doped ZnO that will carried out in project B11. Furthermore, we anticipate that this model will also shine some light onto a more microscopic justification of the above-mentioned diffusive correction to the hydrodynamic model of ordinary metals. Most importantly, this model will be applied to a number of HMM and related structures that are being pursued experimentally in project A5, such as those described in task 2.

Task 2: Optical Properties of and Active Materials in HMM Structures

In view of our work on the fluorescence in HMMs which is based on the electromagnetic Green's tensor of layered systems, the next step will be the analysis of the optical properties of various types of cavity and other "defect" structures. For instance, as HMMs allow for waves with extremely large wave vectors, the rather dramatic momentum mismatch between the HMM and air will lead to unusual total internal reflection effects. These can subsequently be employed to construct novel types of cavities with anomalous scaling laws regarding mode order (higher order modes can have lower energies) and size dependence. Such indefinite cavities [29] and their properties and applications are yet to be fully explored. Similar statements apply to waveguiding structures on the surface or written inside in HMMs.
For instance, the strongly modified electromagnetic mode structure within a lateral cavity (i.e., a defect layer sandwiched between two layered HMM) will facilitate very different coupling scenarios for optically active molecules embedded in the defect layer. By the same token, pores carved through a layered HMM along the stacking direction will provide a pathway for probing novel aspects of extraordinary optical transmission (EOT) by optical means and/or scanning transmission electron microscopic energy electron loss spectroscopy (STEM-EELS; for an example of EOT through hole in metal films, we refer to [30]). The STEM-EELS approach might even allow for probing novel aspects of quantum friction.
The theoretical analysis of the above (and further) optical properties of HMMs and embedded optically active molecules requires a precise knowledge of the electromagnetic Green's tensor of the modified HMM structures and can be constructed from the Green's tensor that we have recently obtained for the layered HMMs without defect structures [P5] (see also the discussion in section 3.3.1). Therefore, we plan to investigate the above-mentioned phenomena in close collaboration with our experimental partners in project A5 and A11. Specifically, the researchers in project A5 aim at the construction of novel coupling phenomena in layered HMMs where highly-doped ZnO serves as the plasmonic material. In a complementary approach, the researchers in project A11 aim at more traditional HMMs consisting of alternating layers of silver and SiO_2 (with embedded molecules serving as emitters) into which pores and more complex defects are written via focused ion beam milling.

Task 3: Role of Disorder in HMMs

Once the ideal structure has been characterized theoretically, it is important to understand the role of unintentional (e.g., due to imperfect fabrication processes) and/or intentional disorder. One aspect, the creation of trap states at interfaces has already been addressed in Task 1. Other types of disorder are related to fluctuating layer thicknesses or roughened layer interfaces. In particular, the randomly fluctuating layer systems constitute a novel type of (incoherent) random laser whose properties may sharply differ from those of ordinary systems (and may have some similarities with the three-dimensional "random SPASERs" that will be investigated within task 3 of subproject b)). By the same token, a recent theoretical work [31] has suggested that disordered HMMs containing roughened layers exhibit strongly enhanced absorption

characteristics relative to well-ordered HMMs with smooth layers.
Consequently, it is planned to elucidate the role of disorder on the various levels of description of HMMs that are being developed within the project (with or without nonlocal effects, photonic bandstructure etc.).

The corresponding research schedule within which the above tasks shall be completed, reads as follows:

Research Schedule Subproject a)								
Task	H2, 2015	H1, 2016	H2, 2016	H1, 2017	H2, 2017	H1, 2018	H2, 2018	H1, 2019
Task 1								
Task 2								
Task 3								

Subproject b) – Theory of SPASER Action in HIOS

While subproject a) is predominantly concerned with optical properties and incoherent processes in layered hybrid plasmonic systems, subproject b) is focusing on coherent effects including (i) a fully quantum-optical description of the individual SPASING unit and (ii) coherent multiple-scattering effects when several SPASING units are present. The vision here is to build on the above-described semi-classical multi-modal SPASER theory and to develop a quantum theoretical framework capable of describing SPASER and SPASER-like action for single molecule-decorated metal nano-particles. Furthermore, in order to allow for disentangling true SPASER effects from random-lasing-like, the semi-classical SPASER theory shall be extended to treat the multiple-scattering effects between different units. This comprehensive theory will allow will then be applied to specific systems such as those investigated within project B2 of the CRC.

Task 1: Quasi-normal Modes

The above-described semi-classical theory has been formulated for spherical nano-particles so that semi-analytical considerations regarding multi-polar modes and notably their contributions to the radiative and non-radiative rates become possible. This allows for testing the recently introduced concept of quasi-normal modes [21,22] which exhibit a complex-value effective mode volume and, for general particles, have to be determined numerically. Specifically, in Ref. [21], only the Fano factor for dipolar modes has been considered and the extension to the computation of higher-order modes has only been sketched. Nevertheless, for a spherical particle, we have successfully implemented the quasi-normal mode recipe of Ref. [21] to the dipolar vector-spherical harmonics. Upon computing this quasi-normal mode's contributions to the radiative and non-radiative rates of a dipole emitter via the effective complex volume we have been able to recover the well-known results of ordinary Mie theory mentioned above (see Fig. 4).

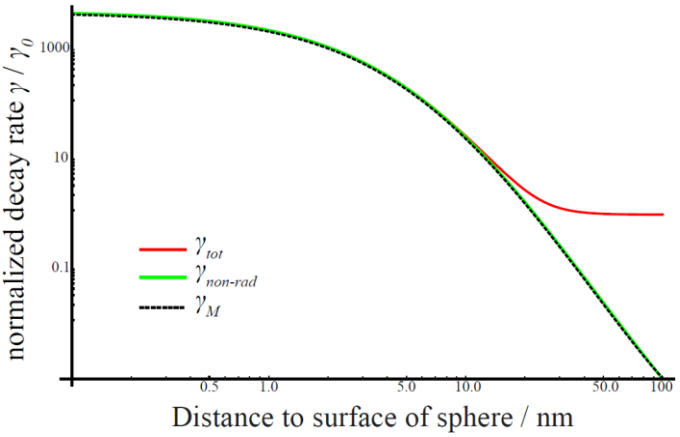

Fig. 4: Comparison of the dipolar contribution to the non-radiative rate of an electric dipole emitter interacting with a metal nano-particle. The results are obtained via standard Mie theory [26,27] (green line) and by the complex volume of numerically determined quasi-normal modes as suggested in Ref. [21] (black line). Both approaches deliver the same results.
Also shown (red line) is the total decay rate of the emitter, i.e., the sum of radiative rate and the dipolar contribution to the non-radiative decay rate. All rates are scaled to the radiative rate in the absence of the metal nano-particle.

This implies that we have now established a solid basis for bench-marking numerical computations and we can proceed to extend this approach to the higher-order quasi-normal modes and to complex-shaped nano-

particles. Besides their usefulness for semi-classical or fully quantum-optical descriptions (see task 2) of the various SPASER geometries considered in project B2, the results of these computations will also allow us to provide quantitative values of coupling constants for the mesoscopic Hamiltonians of light-matter interaction that are employed within projects B6 and B12 for various energy and excitation transfer processes in hybrid plasmonic systems. In addition, these quasi-normal modes in conjunction with the above-described semi-classical framework will facilitate the development of optimized designs for SPASER and nano-Laser geometries that are being pursed in project B2.

Task 2: Quantum-optical Theory of the SPASER

There are two interrelated routes to arrive at a quantum-optical description of the macroscopic electromagnetic field in an open systems that features dispersive and dissipative constituent materials such as is the case in a SPASER configuration.
The first route starts directly from the corresponding Green's tensors which, as described above, we have already successfully determined for plasmonic systems via numerical approaches. However, while this approach is thus quite feasible, it is technically involved and, most importantly, does not easily yield a mode-resolved physical picture similar to those we found highly informative within the semi-classical SPASER theory. Thus, in principle, we would prefer to work with an approach that corresponds to a generalization of the semi-classical approach discussed above.
This second route for a quantum-optical description of the macroscopic electromagnetic field starts from the observation that dissipation leads to a non-Hermitean problem so that not only the eigenmodes of the original system operator, i.e., the quasi-normal modes described in task 1 above, have to be considered, but that also the eigenmodes of the adjoint system operator have to be involved – when thinking in terms of a non-Hermitean system operator in matrix form this corresponds to considering left and right eigenvectors. The combined set of such eigenmodes of the system operator and its adjoint is generally referred to as a bi-orthogonal basis and it may be used to quantize the macroscopic electromagnetic field [32]. This bi-orthogonal basis would also directly implement the above-discussed non-orthogonality of the modes along with the Peterman excess-noise factor. The link to the Green's tensor approach is provided by the fact that the Green's tensor can explicitly be constructed as a sum over dyadic products of the corresponding pairs of basis functions of the bi-orthogonal basis.
Consequently, we will initially aim at constructing the bi-orthogonal basis for spherical particles in a semi-analytical fashion using the appropriate vector-spherical harmonics. On the one hand, the bi-orthogonal basis for spherical particles will serve as a valuable test-bed for the numerical construction of bi-orthogonal bases for complex geometries. On the other hand, this bi-orthogonal basis for spherical particles will allow for a fully quantitative quantum-optical analysis of a dipole emitter interacting with a metal sphere. In particular, this will allow us to determine any level shifts and changes in line shape of the emitter induced by the interaction with the spherical particle relative to the corresponding properties of the emitter embedded in a homogeneous environment – effects that are not considered (more precisely, in the case of level shifts taken for granted in form of the emission frequency being an input parameter) in the semi-classical rate description of Refs. [26,27]. Within the CRC such types of measurements can best be implemented by using well-defined plasmonic antennas carved out of perfectly crystalline gold flakes that are decorated with dye molecules embedded in silica shells, as is envisaged within a collaboration of the experimental projects A11 and B2. In turn, this would allow for further possibilities of testing the quality of bi-orthogonal basis of quasi-normal modes.
Using this bi-orthogonal basis, we will subsequently develop a full quantum-optical multi-modal description of hybrid SPASER systems that allows addressing issues such as the plasmon statistics and the SPASER □-factor that are not accessible within semi-classical approaches.

Task 3: Multiple scattering Effects

Analogous to the concept of random lasing, the treatment of multiple scattering effects in systems containing several individual SPASER units represents a fascinating topic. For instance, as many experimental systems based on core-shell-type systems consist of many individual SPASER units so that especially in Lasing-SPASER systems it is actually a non-trivial problem to distinguish between spasing action of individual units and random lasing brought about by the multiple-scattering effects associated with the metallic nano-particles. Conversely, multiple scattering effects may actually be useful for lowering the spasing thresholds, thus potentially realizing a random Lasing-SPASER.
We will address this challenge in two ways. First, for systems with a low number of spherical scatterers, we will utilize the multiple-scattering techniques such as the T-matrix method [33] that use expansions in vector-spherical harmonics that are centered about the individual sphere centers. These expansions are connected with each other through self-consistency arguments and have to be combined with the rate equation

descriptions for a number of emitters as already employed in our semi-classical SPASER theory. Taken together, this yields a numerically exact scheme where all parameters (sphere position and size, emitter position and dipole moment orientation) may be individually varied. However, such an approach is effectively limited to a moderate numbers of spheres and emitters – we estimate several tens to a few hundred spheres and several thousands of emitters. This numerically exact approach will provide us with insight on the characteristics of individual realizations of such "random SPASERs" and will serve as a reference for the second approach that is based on solving the Bethe-Salpeter transport equation for the averaged intensity. Such theories have already been formulated for dielectric systems with linear absorption and gain (e.g., see [34]) and shall now be extended to capture SPASER action.

The corresponding research schedule within which the above tasks shall be completed, reads as follows:

Research Schedule Subproject b)								
Task	H2, 2015	H1, 2016	H2, 2016	H1, 2017	H2, 2017	H1, 2018	H2, 2018	H1, 2019
Task 1								
Task 2								
Task 3								

3.5 Role within the Collaborative Research Centre

Collaboration with experimental projects:

- A5 (Henneberger): B10 provides detailed theoretical support for the hybrid layered structures based on highly-doped ZnO that are frabricated and measured within A5.
- A11 (Christiansen): B10 provides detailed theoretical support for the hybrid nanostructures that are fabricated within and measured within A11, incuding hyperbolic metamaterials and indefinite cavities with embedded fluorescent molecules.
- B2 (Ballauf/Benson/Lu): B10 provides design guidelines for hybrid spaser and nanolaser devices as well as for systems with several nanoparticles where multiple scattering effects are important. Through comparisons of measured data (B2) and computations (B10) a detailed characterization of the devices will be achieved.

Collaborations with theoretical projects:

- B6 (May): B10 provides quasi-normal mode properties of plasmonic nanoparticles and corresponding coupling constants for the density-matrix computations in B6. There will be a detailed exchange on directly interfacing the density-matrix methodologies of B6 with the Maxwell solvers of B10.
- B11 (Draxl): There will be a detailed comparison of the phenomenological material model for highly-doped ZnO required for the Maxwell solver developed in B10 with the results from corresponding microscopic computations for this material as they are performed in B11.
- B12 (Knorr/Richter): B10 provides quasi-normal mode properties of plasmonic nanoparticles and corresponding coupling constansts for the mesoscopic Hamiltionians considered in B12. There will be a detailed exchange between B10 and B12 regarding the methods for solving the Maxwell equations on the mesoscale for many emitters and multi-mode electromagnetic fields.

3.6 Delineation from other funded projects

There is no overlap with other projects that are already funded by or for which funding has been applied for from DFG or other funding agencies. Specifically, neither the theory of SPASER action nor the theory of active emitters in hyperbolic metamaterials are research themes within the presently funded projects of the applicant:

- 2012-2015: DFG-Research Grant "Tunable SERS": Together with the experimental groups of Prof. Wehrspohn (Halle) and Prof. Guldi (Erlangen), the feasibility of coinage and magneto-optically active metals for use in tunable surface-enhanced Raman spectroscopy settings is investigated.

- 2012-2015: DFG-Priority program 1391 “Ultrafast Nanooptics”, project “Hydrodynamic modeling of the ultrafast nonlinear response of metallic nanostructures”: The nonlinear response of a metallic nanoparticle is modeled by treating the free electrons as a plasma in confined that moves against an immobile background (jellium model) and solving the corresponding set of coupled Maxwell-Euler equations.
- 2014-2017: Einstein Foundation Grant “ActiPLAnt”: Together with the experimental groups of Prof. Benson (HU Berlin), Prof. Rapaport and Prof. Levy (both Hebrew University, Jerusalem, Israel) efficient single-photon sources and absorbers based on quantum dots and color-centers in nano-diamonds are investigated.

3.7 Project funds

3.7.1 Previous funding

The project has been funded within the Collaborative Research Centre since January 2013.

3.7.2 Funds requested

Funding for	2015/2		2016		2017		2018		2019/1	
Staff	Quantity	Sum	Quantity	Sum	Quantity	Sum	Quantity	Sum	Quantity	Sum
PhD student, 75%	2	44.100	2	88.200	2	88.200	2	88.200	2	44.100
Total		44.100		88.200		88.200		88.200		44.100
Direct costs	Sum		Sum		Sum		Sum		Sum	
Small equipment, Software, Consumables	1.000		2.000		2.000		2.000		1000	
Other	-		-		-		-		-	
Total	1.000		2000		2.000		2.000		1.000	
Total	45.100		90.200		90.200		90.200		45.100	

(All figures in Euro)

3.7.3 Staff

	No.	Name, academic degree, position	Field of research	Department of university or non-university institution	Commitment in hours/week	Category	Funded through:
Available							
Research staff	1.	Busch, Kurt, Dr. rer. nat., Prof.	Theoretical Optics & Photonics	Institut für Physik, HU Berlin	5h		Core support
	2.	Matyssek, Chrisitan, Dr. rer. nat.	Computational Photonis, Nano-Plasmonics	Institut für Physik, HU Berlin	10h		Core support
	3.	Intravaia, Francesco, Dr. rer. nat.	Quantum Optics, Fluctuation-induced Phenomena	Max-Born-Institut, Berlin	10h		Core support
Requested							
Research staff	1.	Höfner, Kathrin, M.Sc.		Institut für Physik, HU Berlin		Doctoral Researcher 75%	
	2.	Werra, Julia, Dipl.-Phys.		Institut für Physik, HU Berlin		Doctoral Researcher 75%	

Job description of staff (supported through available funds):
1. Prof. Dr. Kurt Busch
Scientific and organizational coordination of the project, exploration of the fundamental theoretical concepts, design of research programme and selection of methods, supervision of PhD students.
2. Dr. Christian Matyssek
Scientific and organizational coordination of the project, scientific support on numerical methods and multiple-scattering approaches in nano-photonic and nano-plasmonic systems, supervision of PhD students
3. Dr. Francesco Intravaia
Scientific and organizational coordination of the project, scientific support on the quantum description of light-matter interaction in nano-photonic and nano-plasmonic systems, supervision of PhD students

Job description of staff (requested):
1. M.Sc. Kathrin Höfner
Kathrin Höfner is a very talented student (Lise-Meitner Award 2014 for her Master thesis) who has been instrumental in the development of the semi-classical theory of the SPASER [P3] and will continue her successful work as a PhD student.
2. Dipl.-Phys. Julia Werra is a very talented student (Diploma with distinction) who has been instrumental in the method development of the numerical determination of Greens tensors in nano-plasmonic systems [P2] and will continue her successful work as a PhD student on optically active layered materials, notably hyperbolic metamaterials .

3.7.4 Direct costs for the new funding period

	2015/2	2016	2017	2018	2019/1
Funds available					
Funds requested	1.000	2.000	2.000	2.000	1.000

(All figures in Euro)

3.7.5 Major research equipment requested for the new funding period

€ 10.000 - 50.000: none
> € 50.000: none

3.7.6 Student assistants

	2015/2	2016	2017	2018	2019/1
Quantity	0	0	0	0	0
Commitment in hours/week	0	0	0	0	0
Sum	0	0	0	0	0
Tasks					

3.1 About project B 11

3.1.1 Title: Optoelectronic excitations at inorganic/organic interfaces: Role of vibrations and time scales

3.1.2 Research areas: condensed-matter theory, computational spectroscopy, inorganic/organic interfaces

3.1.3 Principal investigator

Prof. Dr. rer. nat. Dr. h.c. Claudia Draxl (*19.12.1959, Austrian)

Humboldt-Universität zu Berlin, Physics Department and IRIS Adlershof
Zum Großen Windkanal 6, D12489 Berlin
Phone: +49 (0)30 2093 66363
Fax: +49 (0)30 2093 66372
Email: claudia.draxl@physik.hu-berlin.de

Does the above mentioned person hold a permanent position? yes

3.1.4 Legal issues

This project includes

1.	research on human subjects or human material.	no
2.	clinical trials.	no
3.	experiments involving vertebrates.	no
4.	experiments involving recombinant DNA.	no
5.	research involving human embryonic stem cells.	no
6.	research concerning the Convention on Biological Diversity.	no

3.2 Summary

The second phase of the project is dedicated to the *ab initio* description of temperature-dependent exciton spectra of hybrid inorganic/organic interfaces by a combination of density-functional theory with many-body perturbation theory. The basis will be the outcome of the first funding period where electronic structure and optical spectra of various systems were investigated in detail, comprising single molecules, monolayers, and molecular crystals as well as ZnO bulk and surfaces. Method-wise we have analyzed in detail the *GW* self-energy in view of a possible basis-set dependence, in particular for various oxides. Concerning optical excitations, we confronted many-body perturbation theory to time-dependent density-functional theory (TDDFT) and constrained DFT. Evaluating various TDDFT kernels concerning their applicability to the HIOS systems, we consider them to be of limited practicability. Likewise, constrained DFT turned out problematic when using semi-local exchange-correlation functionals and to a large extent also require knowledge from the solution of the Bethe-Salpeter equation (BSE) of many-body perturbation theory (MBPT). Hence, overall this approach does not provide an efficient reliable alternative to the BSE.

Based on this experience, the method of choice for the coming period will be in most cases the BSE that we aim to extend towards inclusion of electron-phonon coupling to obtain temperature-dependent optical spectra. For the underlying band structure we will also account for vibrational-coupling in order to handle zero-point motion and temperature effects. At the same time, we will consider possible polarization effects since both give rise to band renormalization thus affecting the excitation spectra. We will identify the leading contributions, *i.e.*, those vibrations with the strongest coupling to the electronic system. Based on *GW*

calculations for prototypical systems, we are aiming to derive a model that allows us to predict the possible polarization-induced band-gap lowering of adsorbed molecules from the constituents' dielectric screening and the interfacial electronic structure.

Another focus of the project will be laid on the life times of excitations, a crucial parameter for the applicability of hybrid materials in devices. We will make use of MBPT by computing the imaginary part of the Green functions.

We will continue working with ZnO, but also consider Si and GaN on the inorganic side, while oligo-fluorines, substituted oligo-acenes and -phenylenes, and pyridine will be in the focus for the organic side.

Our investigations will be carried out in close collaboration with experimental projects **B3** (Blumstengel), **B5** (Neher), and **B9** (Stähler) dealing with optical spectroscopy. Together with **B3** (Blumstengel) we are aiming at identification of molecules leading to maximal hybridization of the exciton wavefunction. We will benefit from the structural investigations of **B4** (Körzdörfer/Scheffler/Rinke) and **A4** (Heimel) and surface/interface characterization by **A5** (Henneberger) and collaborate with **B4** (Körzdörfer/Scheffler/Rinke) on polaronic effects.

3.3 Project progress to date

3.3.1 Report and state of understanding

Hybrid materials pose severe challenges on modern *ab initio* theory on various levels. In fact, to fully understand hybrid materials and reach predictive power on a quantitative level, novel methodology is needed [P1]. In that sense, the first phase of the CRC was mostly dedicated to an in-depth evaluation of the theoretical methodology that we have in hand to describe opto-electronic properties of hybrid materials and their constituents. Confronting MBPT to TDDFT and constrained DFT, we have evaluated fore-front methodology for selected prototypical systems, in view of a robust and feasible description of excitonic spectra. Through MBPT we have reached in-depth insight into low-energy optical excitations in inorganic bulk and surfaces systems as well as molecules and their condensed phases, paving the way towards the understanding of hybrid systems.

On the molecular side, we have chosen a set of prototypical molecules, comprising oligo-thiophenes, quaterphenyl derivatives, and PTCDI. For the inorganic counterparts, we have worked on wurtzite ZnO and other oxides. First investigations of prototypical hybrid materials are in progress. In the following we briefly sketch the outcome of selected tasks:

Derivatives of quaterphenyl molecules

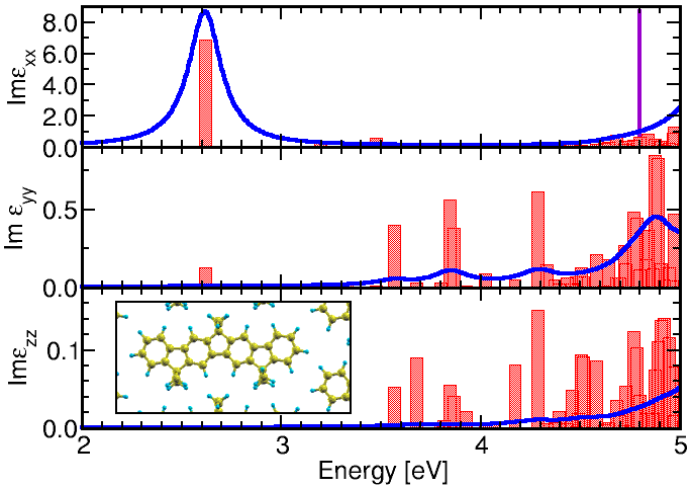

Fig. 1: Dielectric tensor components of a L4P monolayer (inset), along with the oscillator strength (in arbitrary units) of the calculated excitons (red bars). The x (y) direction corresponds to the long (short) molecular axis. The optical band gap calculated with BSE@GW is 2.61 eV. For comparison, the fundamental gap computed by GW is indicated by the purple line.

Employing *GW* and the Bethe-Salpeter equation, we have addressed three different ladder-type molecules, *i.e.*, ladder-quaterphenyl (L4P), 2Sp-L4Pb, and 3Sp-L4P, first investigating their optical spectra in the gas phase. We could determine the impact of different side groups on the lowest optical excitations. For the L4P, we also studied the changes introduced by polymerization and monolayer formation. Taking the latter as an

example, we find that both the DFT-LDA and the *GW* band gap are indirect, with values of 2.50 eV and 4.78 eV, respectively. The cartesian components of the imaginary part of the dielectric function are depicted in Fig. 1. The *xx* component shows an intense peak at the absorption onset, corresponding to a binding energy E_b of 2.21 eV of the lowest bound singlet exciton. Due to the packing of the molecules within the monolayer, E_b is reduced by 21% compared to the molecule in gas phase where a value of 2.8 eV is found. Due to anisotropy, the other two components exhibit substantially higher transition onsets and much lower oscillator strength. (G. Biddau and C. Draxl, in preparation)

Oligo-phenyls: from a monolayer to bulk in various phases

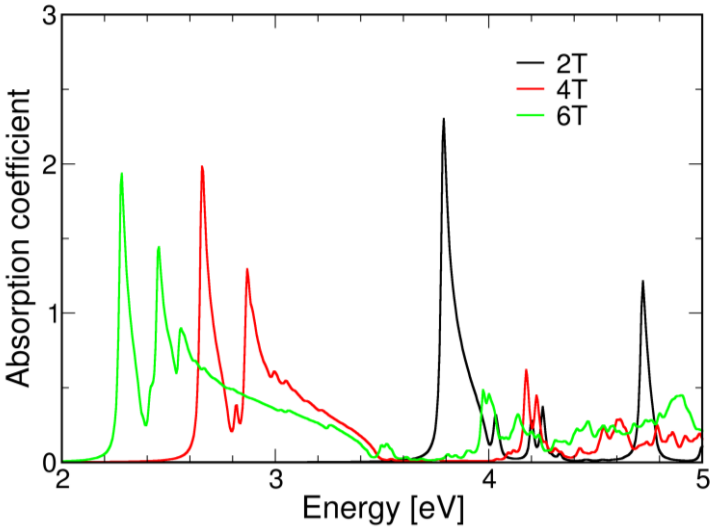

Fig. 2: Absorption coefficient of oligo-thiophenes of various lengths in the herringbone structure, considering polarization of light along the long molecular axis. The singlet exciton binding energy decreases with the molecular length from 0.85 eV for 2T to 0.48 eV for 4T, and 0.37 eV for 6T.

The absorption spectra of oligo-thiophenes (labeled *n*T, where *n* stands for the number of thiophene rings in the molecule) are depicted in Fig. 2, exhibiting the decrease in band gap and, hence, lowering of the absorption onset with increasing molecular length. Following the trend found for the oligo-acenes [1], also the singlet binding energy thereby decreases. (J. P. Echeverry and C. Draxl, preprint)

As a starting point towards a hybrid system consisting of a molecular layer on an inorganic counterpart, we are investigating the optical spectra of a flat-lying 6T monolayer as a function of intermolecular distance. Surprisingly at first glance, but in-line with experiments [2], the spectra exhibit a red-shift when the packing becomes denser. A detailed study of the reasons behind is currently performed.

In a combined experimental / theoretical study carried out in collaboration with project **A9** (Kowarik) we explore light being used as a control parameter in organic molecular beam deposition to grow thin 6T films of enhanced phase purity. It was experimentally demonstrated that 6T films deposited on KCl in dark environments exhibit a bimodal growth with phase coexistence of two polymorphs, while films grown under illumination with laser of 532 nm exhibit high phase purity, where the high-temperature phase growth is quenched. To understand the mechanism behind this optical control, our first-principles calculations complement x-ray, AFM, and optical absorption measurements to shed light on the mechanism [P2].

ZnO: from bulk to surfaces

Recent studies have highlighted intrinsic problems with the convergence of *GW* quasi-particle spectra with respect to the number of unoccupied states [3,4,5]. As a particularly challenging case, wurtzite ZnO has been heavily discussed in literature without a clear consensus on the final value of the *GW* band gap with the local-density approximation (LDA) as the starting point [6,7,8,4]. Thereby a most accurate description of the unoccupied states together with a physically motivated estimate of the number of unoccupied states turned out essential. Based on our *GW* implementation in the **exciting** code, we have readdressed this puzzle. We have developed a strategy how to use local orbitals for systematically improving the quality of the unoccupied part of the spectrum. This strategy in a combination with an extrapolation procedure to the converged limit of the correlation part of the self-energy was successfully applied to the quasi-particle spectra of ZnO and other oxides (A. Gulans, D. Nabok, and C. Draxl, in preparation).

Proceeding to ZnO surfaces, we have focused on the optical properties of the two polar surfaces, *i.e.*, the zinc-terminated ZnO(0001) and the oxygen-terminated ZnO(000-1) surface. These surfaces are far from being understood, and their structure including hydroxylation, vacancy formation, and reconstructions, have not been uniquely determined. Moreover, whatever stabilization mechanism is considered, the relaxation of the zinc-terminated slab has so far never been reproduced by any theoretical investigation. (Whether this is related to the relatively low number of layers taken into account in literature, needs to be further investigated.) Due to this uncertainty, we have considered different configurations according to the most prominent experimental findings. Our calculations of the corresponding optical spectra employing TDDFT shown in Fig. 3 are based on a slab geometry containing 12 bilayers, representing the thin-film regime where the system is still metallic [9,10]. The impact of hydrogenation is substantial, reflecting the distinct bonding situation. We conclude that for comparison with and understanding of experimental findings, information about possible hydrogenation will be also crucial for hybrid materials. (G. Biddau and C. Draxl, in preparation)

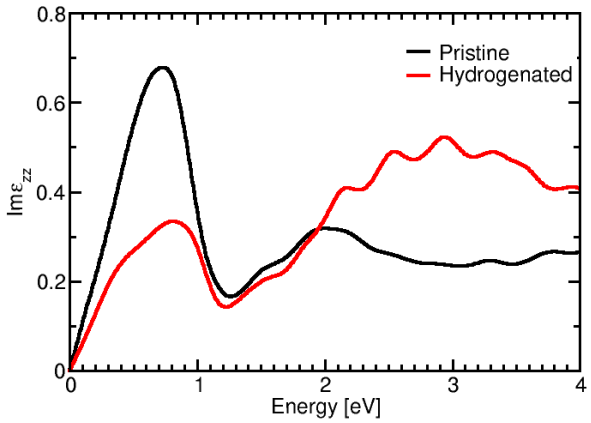

Fig. 3: Optical spectra of a ZnO slab with two polar surfaces, i.e., the zinc-terminated ZnO(0001) and the oxygen-terminated ZnO(000-1) surface without considering reconstruction. For comparison, the results for a slab with hydrogenation of the oxygen-terminated side is shown.

Work along these lines is being performed in collaboration with project **B9** (Stähler). Adopting the geometry of a 12-layer Zn(10-10) slab, exhibiting 1/3 hydrogen coverage as theoretically optimized in project **B4** (Knorr/ Rinke/Scheffler) [11], we are currently investigating the low-lying excitons in this system. Performing BSE calculations, we are aiming at theoretical insight into the experimentally observed ultrafast formation of a surface exciton [12], the outcome of two-photon photoelectron spectroscopy experiments performed in project **B9**.

Evaluation of methodology:

TDDFT in principle represents an alternative to the computationally much more involved *GW*/BSE approach. Thus, an exchange-correlation (xc) kernel of TDDFT that works equally well for molecules and solids, is an object of particular interest. Besides the *Nanoquanta* kernel derived from the BSE that comes with the same computational costs as BSE itself, the so-called bootstrap kernel [13] looked very promising at first glance. Analyzing bootstrap results in detail, we found, however, that trustful prediction of strongly bound electron-hole pairs using simple approximations is still impossible [P3].

In another study, we have confronted *GW*/BSE to TDDFT (in the adiabatic local-density approximation, ALDA) to learn to which extent one can rely on TDDFT when going from molecules in the gas phase to their condensed phases. TDDFT turned out useful for selected systems, in particular for small molecules as well as very weakly bound excitons (C. Cocchi and C. Draxl, in preparation). Overall, however, we conclude that TDDFT is of limited practicability for the systems studied in this project.

Another alternative to MBPT is provided by constrained DFT. For core excitations, this method is popular and known as the super-cell core-hole approach. Thereby an electron is removed from an atomic core and added to the valence band. This way, an electron-hole pair is built into the system in the self-consistency cycle, and thus is treated on the DFT level. This method is appealing due to its low computational cost, but also in view of the fact that it opens a perspective to include lattice relaxation effects in the excited state. Our attempts to exploit this procedure to treat excitonic effects in optical spectroscopy, so far did not lead to the desired success. The reasons are manifold, and we have demonstrated them with the example of rutile TiO_2: First, semi-local xc functionals are unable to lead to strong enough excitons binding, *i.e.,* electron-hole pairs turned out to be too delocalized compared to the BSE results. Similar findings had been reported for triplet excitons by Di Valentin and Selloni [14] suggesting the usage of hybrid xc functionals. Computing supercells

with hybrid functionals is computationally expensive and maybe even not feasible for HIOS systems, thus making this approach less attractive. Second, TiO_2 exhibits several low-lying excitations of low oscillator strength. To mimic excitations that give rise to the strong absorption features in this material, requires constraints that, in turn, require knowledge of the nature of the specific excitation(s). This means that a BSE calculation is needed to obtain this knowledge. Overall, we conclude that new ways have to be found to make such an approach working for the systems investigated in this project. We will tackle this problem, if time allows. Overall, we will mainly adopt the *GW*/BSE route for the next funding period.

Figure 4 depicts the optical spectra of rutile TiO_2 as obtained by different groups from *GW*/BSE with the PBE functional being the starting point of G_0W_0. The discrepancy between different results is striking and asks for clarification. Assuming well-converged data throughout, obviously the underlying approximations - be it pseudopotentials, the treatment of the dielectric screening at the *GW* or BSE level - can have dramatic effects. Here we also address the effect of the xc potential underlying the G_0W_0 approximation. The so-called starting-point dependence of G_0W_0 is a well-known problem. In other words, the perturbative treatment of the electron self-energy in the G_0W_0 approximation works best when the starting point, *i.e.*, the underlying Kohn-Sham system, is a good approximation to the quasi-particle band structure. This issue may be or is even expected to be valid for the BSE as well. Therefore, Fig. 4 contains our calculation using PBE0' (green line) for comparison. With PBE0' we mean that we use 25% exact exchange in the hybrid functional like in PBE0, but use the exact-exchange or optimized effective potential (OEP) to provide the exchange part of the functional. As the difference between the two green curves demonstrate, a starting-point-dependence is clearly evident. Other causes of discrepancy can be ruled out here, since both results have been obtained with the same code, and are based on the same level of accuracy and even the same ingredients. To highlight the most important sources of deviations, we have analyzed the impact of potential, Kohn-Sham eigenvalues and wavefunctions, self-energies, as well as matrix elements on the BSE results. (O. Turkina and C. Draxl, in preparation).

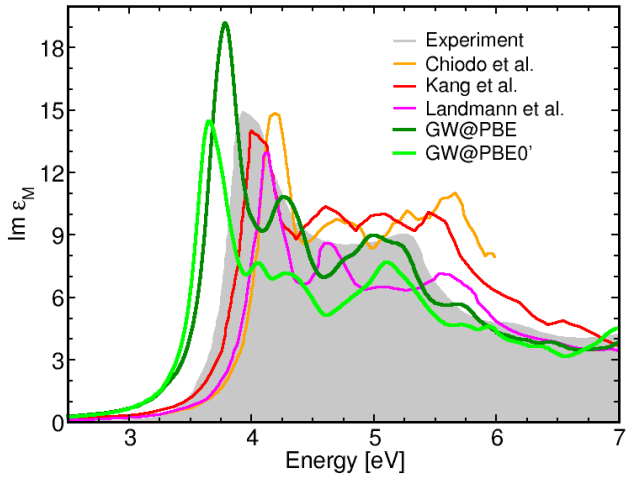

Fig. 4: Macroscopic dielectric function of rutile TiO_2 from GW/BSE with the PBE functional being the starting point as obtained by different groups and codes [15-17] in comparison to experiment [18]. Green lines represent own data. For comparison the spectra obtained with PBE0' is depicted.

Code development:

We have implemented the time-evolution algorithm [19] into the **exciting** code [95] to facilitate efficient calculation of optical spectra based on the BSE. The *GW* and BSE parts of the code have been substantially revised to allow for tackling hybrid materials. Concerning the ground state, in collaboration with the ETH Zürich and the Swiss Supercomputing Center a library was developed that allows for efficient computing of large systems. Currently the quasi-particle self-consistent *GW* method (*qp-GW*) [20] is implemented into **exciting**.

Hybrid systems

Investigations of the opto-electronic properties of PTCDI are currently performed analogously to the case of L4P, including various types of monolayers. First steps of including the ZnO surface have been made. This work is carried out in close collaboration with project **B3** (Blumstengel) dedicated to gain insight into measured optical spectra.
GW calculations of pyridine on the non-polar ZnO(10-10) surface are under investigation, adopting the slab geometry [11] of project **B4** (Knorr/Rinke/Scheffler).
Note that project **B11** had a shorter time frame due to later start of this sub-project (January 1, 2013) compared to the CRC as a whole.

References

[1] K. Hummer and C. Ambrosch-Draxl, Phys. Rev. B 71 081202(R) (2005).
[2] M. A. Loi, A. Mura, G. Bongiovanni, Q. Cai, C. Martin, H. R. Chandrasekhar, M. Chandrasekhar, W. Graupner, and F. Garnier, Phys. Rev. Lett. 86, 732 (2001).
[3] A. Schindlmayr, Phys. Rev. B 87, 075104 (2013).
[4] J. Klimeš, M. Kaltak, and G. Kresse, Phys. Rev. B 90, 075125 (2014).
[5] A. Gulans, J. Chem. Phys. 141, 164127 (2014).
[6] B.-C. Shih, et al., Phys. Rev. Lett. 105, 146401 (2010).
[7] M. Stankovski et al., Phys. Rev. B 84, 241201(R) (2011).
[8] C. C. Friedrich, M. C. Müller, and S. Blügel, Phys. Rev. B 83, 081101(R) (2011).
[9] J. Goniakowski, C. Noguera, and L. Giordano, Phys. Rev. Lett. 98 205701 (2007).
[10] C. Goniakowski, F. Finocchi, and C. Noguera, Rep. Prog. Phys. 71 016501 (2008).
[11] O.T. Hofmann, J.C. Deinert, Y. Xu, P. Rinke, J. Stähler, M. Wolf, and M. Scheffler, J. Chem. Phys. 139, 174701 (2013).
[12] J.-C. Deinert, D. Wegkamp, M. Meyer, C. Richter, M. Wolf, and J. Stähler, Phys. Rev. Lett. 113, 057602 (2014).
[13] S. Sharma, J. K. Dewhurst, A. Sanna, and E. K. U. Gross, Phys. Rev. Lett. 107, 186401 (2011).
[14] C. Di Valentin and A. Selloni, J. Phys. Chem. Lett. 2, 2223 (2011).
[15] L. Chiodo, J. M. García-Lastra, A. Iacomino, S. Ossicini, J. Zhao, H. Petek, and A. Rubio, Phys. Rev. B 82, 045207 (2010).
[16] W. Kang, and M. S. Hybertsen, Phys. Rev. B 82, 085203 (2010).
[17] M. Landmann, E. Rauls, W. G. Schmidt, J. Phys.: Condens. Matter 24, 195503 (2012).
[18] M. Cardona and G. Harbeke, Phys.Rev. 137, A1467(1965).
[19] W. G. Schmidt, S. Glutsch, P. H. Hahn, and F. Bechstedt, Phys. Rev. B 67, 085307 (2003).
[20] M. van Schilfgaarde, T. Kotani, and S.V. Faleev, Phys. Rev. B 74, 245125 (2006).
[21] M. Cardona and M. L. W. Thewalt, Rev. Mod. Phys. 77, 1173 (2005).
[22] D. A. da Silva Filho, E.-G. Kim, J.-L. Bredas, Adv. Mat. 17, 1072 (2005).
[23] A. Eiguren and C. Ambrosch-Draxl, Phys. Rev. Lett. 101, 036402 (2008).
[24] A. Eiguren, C. Ambrosch-Draxl, and P. M. Echenique, Phys. Rev. B 79, 245103 (2009).
[25] S. Engelsberg and J. R. Schrieffer, Phys. Rev. 131, 993 (1963).
[26] P. B. Allen and V. Heine, J. Phys. C 9, 2305 (1976).
[27] P. B. Allen, Phys. Rev. B 18, 5217 (1978).
[28] F. Giustino, M. L. Cohen, and S. G. Louie, Phys. Rev. B 76, 165108 (2007).
[29] F. Giustino , S. G. Louie, and M. L. Cohen, Phys. Rev. Lett. 105, 265501 (2010).
[30] E.Cannuccia and A.Marini, http: // arxiv.org/abs /1304.0072.
[31] X. Gonze, P. Boulanger, and M. Cote, Annalen der Physik 523, 168 (2011).
[32] A. Marini, Phys. Rev. Lett. 101, 106405 (2008).
[33] E. Cannuccia and A. Marini, Phys. Rev. Lett. 107, 255501 (2011).
[34] B. Arnaud, S. Lebègue and M. Alouani, Phys. Rev. B 71, 035308 (2005).

3.3.2 Project-related publications

[P1] C. Draxl, D. Nabok, and K. Hannewald, "Organic/inorganic hybrid materials: Challenges for ab initio methodology", Accounts of Chemical Research, (2014); DOI : 10.1021/ar500096q
[P2] L. Pithan, C. Cocchi, H. Zschiesche, C. Weber, A. Zykov, S. Bommel, S. J. Leake, P. Schäfer, C. Draxl, S. Kowarik, "Light controls polymorphism in thin films of sexithiophene", to be submitted to Crystal Growth & Design.
[P3] S. Botti, C. Draxl, L. Reining, S. Rigamonti, F. Sottile, and V. Veniard, "Estimating excitonic effects in the absorption spectra of solids: problems and insight from a guided iteration scheme", to be submitted to Phys. Rev. Lett.
[P4] A. Gulans, S. Kontur, C. Meisenbichler, D. Nabok, P. Pavone, S. Rigamonti, S. Sagmeister, U. Werner, and C. Draxl, **exciting**: a full-potential all-electron package implementing density-functional theory and many-body perturbation theory, J. Phys: Condens. Matter 26, 363202 (2014).
[P5] S.-A. Savu, G. Biddau, L. Pardini, R. Bula, H. F. Bettinger, C. Draxl, T. Chassé, M. B. Casu, "Influence of substrate-to-molecule charge transfer on the electronic structure of substituted pentacene nanorods" (submitted to Chemistry - A European Journal).

3.4 Research plan

Modern *ab initio* electronic-structure theory going beyond DFT can already provide substantial insight into electronic structure and optical excitations of hybrid materials. Nevertheless, there are challenges to be tackled. Figure 5 summarizes the major problem [P1]: It depicts the level alignment at an interface between an organic and an inorganic semiconductor. In the *real* case (middle), the HOMO (LUMO) resides in the organic (inorganic) side thus allowing for charge separation at the interface upon illumination by light. To the left and to the right, we see what can be expected from a *GW* calculation, while the outermost panels mimic the behavior of semi-local xc functionals. Semi-local DFT (just labelled GGA, as the particular flavor would not make any difference) could, through underestimation of both band gaps, lead to type I level alignment with both HOMO and LUMO sitting in the inorganic part. *GW* should generally do much better, widening the gaps on both sides. However, non-selfconsistent G_0W_0 still bears the risk of spurious charge transfer introduced by the underlying DFT level. Leaving this aside for a moment, there is another uncertainty coming into play here, namely zero-point vibration effects (ZPV). They typically lower the band gap - as much as 400 meV in diamond [21], and we can arguably expect this to be more pronounced in the organic side [22]. Thus, ignoring ZPV, even *GW* would give a *qualitatively* wrong picture, since it should *overestimate* the HOMO-LUMO distance. This worst-case scenario is sketched in the figure.

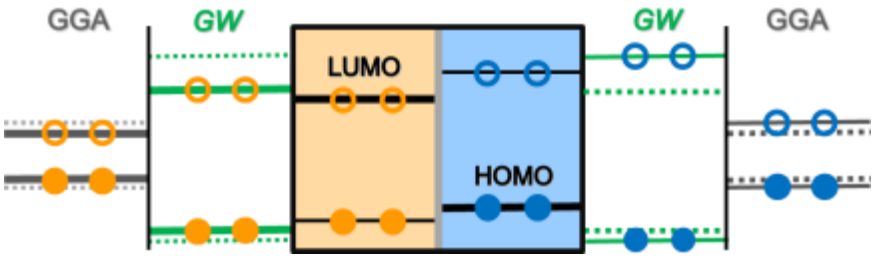

Fig. 5: Level alignment at an organic (blue) / inorganic (orange) interface. In the "real" case (middle), the HOMO (LUMO) resides in the organic (inorganic) side. For comparison, we see what can be expected from GW and DFT-GGA calculations. Dotted lines are guides to the eye.

We learn from this that the role of vibrations needs to be clarified, first on the band-structure level but naturally also in view of spectroscopy. This will help to understand polaronic effects including the impact of temperature, which is crucial for any application. Even more important for the question whether a hybrid material is useful for some device, requires consideration of excitation lifetimes and dynamics. We need to know not only the binding strength of electron-hole pairs and their spatial extension, but also the time scale of their formation and recombination. Likewise, *ab initio* approaches to exciton diffusion are totally lacking. In all these aspects, new grounds need to be broken, and project **B11** aims at solving some of these issues.

Based on the experience of the first funding period, the method of choice for the coming period will be in most cases the MBPT approach, combining *GW* and BSE that we aim to extend towards inclusion of electron-phonon coupling. That way, we will obtain temperature-dependent optical spectra. For the underlying band structure we will account for vibrational coupling as well, in order to treat zero-point motion and temperature effects. Another focus of the project will be laid on the life times of excitations, a crucial parameter for the usage of hybrid materials in devices. We will make use of MBPT by computing the imaginary part of the one- and twobody Green's functions.

A central goal of project **B11** is qualitative and quantitative insight into electron-hole pairs at HIOS interfaces that – at the same time – is a central goal of the overall CRC. In that sense, the key issues of the first funding period are still valid. These concern the question whether and when we find hybrid excitons at prototypical inorganic/organic interfaces. We ask about the binding energies of the low-lying electron-hole pairs and their character and spatial extension. We want to explore role of surface termination and orientation on the excitons' properties, and how hybrid excitons couple to vibrations and distortions.

The specific goals of **B11** in the second funding period are:

(i) finding and describing hybrid systems that exhibit hybrid charge transfer character
(ii) exploring the impact of vibrational coupling on the electronic and optical properties of hybrid materials
(iii) determining excitation lifetimes

Let us focus first on the electronic structure, leaving out vibrations for a moment. A critical task will still be the reliable alignment of electronic levels at the interface which is to date far from being settled. Typically, one would like to get along with a single-shot calculation, *i.e.*, the G_0W_0 approximation. This, however, is only possible if the underlying electron density does not suffer from spurious charge transfer at the interface, and the corresponding Kohn-Sham eigenvalues are not too far from their quasi-particle (QP) counterparts. This

condition to be fulfilled would, for organic materials, typically require a hybrid functional with an appreciable amount of exact exchange as the starting point, while for the inorganic component this amount would typically be smaller. Finding a compromise is a subtle issue. An alternative to this procedure is given by some self-consistent *GW*, allowing for a self-consistent update of the electron density. A promising scheme, in this context, is *qp-GW* [20] that is currently being implemented in **exciting** (see 3.3.1). Employing *GW*, in one or the other way, *i.e.*, either in terms of perturbation theory or self-consistent, bears the advantage of naturally including possible polarization effects that may even strongly affect the HOMO-LUMO gap of the molecular side. Based on such *GW* calculations for prototypical systems, we are aiming to derive a model that allows us to predict the possible polarization-induced band-gap lowering of adsorbed molecules from the constituents' dielectric screening and the interfacial electronic structure.

Proceeding to vibrational effects, we will make use of our experience that we have gained for different materials [23,24] by combining an approach by Engelsberg and Schrieffer [25] with *ab initio* methodology. More specific, the Dyson equation was solved with the electron-phonon interaction being the source of the self-energy. We note that in contrast to the *GW* approach also the imaginary part of the quasi-particle energies were determined. Thereby all ingredients, *i.e.*, electronic and vibrational properties as well as their coupling parameters were computed from DFT. Another route along the so-called HAC model (HAC stands for Heine, Allen, Cardona) [26,27,28] has been followed by other groups [28-30]. This method contains besides the self-energy term also the so-called Debye-Waller term. Also the non-diagonal Debye-Waller term has been included recently [31].

We point out here that the implementation and further development of these theoretical approaches is not part of this proposal. For this very involved work we are seeking funding for a postdoc elsewhere. We also note that a fully fletched application of this methodology will hardly be feasible for the hybrid materials under consideration or, at most, for rather small prototypical systems. Therefore, we will proceed in several steps. First, we will identify those vibrational modes that affect the electronic structure around the band gap most. These will be considered then for the renormalization of the electronic bands through the solution of the Dyson equation. Care must be taken though, since it has turned out that all modes contribute to the features in the spectral function [23]. Thus we will need to include the full information on the Eliashberg function in some way. The envisaged procedure here is to consider the corresponding phonon density of states or Eliashberg function from the pristine systems. For the calculations of phonons and their coupling strength we will make use of density-functional perturbation theory (DFTP, *linear-response for phonons*). Alternatively, we will apply a finite-displacement method which may well be more appropriate for complex systems like HIOS materials. For larges systems we will collaborate with project **B4** (Körzdörfer/ Scheffler/Rinke) where a similar scheme based on DFPT will be employed but using a different code (FHI-aims) that can handle larger unit cells efficiently. We will eventually adopt results from this project to combine them with our *GW* calculations and/or the optical spectra on top of this. Moreover, comparison of the different procedures will help to evaluate the approximate ones and identify the most efficient scheme to be used further on.

From the QP bands we will proceed to optical spectra including both excitonic and electron-phonon coupling. Solving the BSE starting from polaron states with QP energies as described before, corresponds to a treatment of exciton-phonon coupling similarly to that in Ref. [32] giving rise to zero-point vibrations, temperature-dependent absorption spectra, and phonon-induced excitation lifetimes. It incorporates individual scattering processes between phonons and electrons and holes, respectively, but also includes a coherent scattering term which allows for modification of electron-hole coupling and thus redistribution of oscillator strength. The latter, which dominates in the strong-coupling regime, is expected to be crucial for organic materials [33]. Also important for the organic side and as such for the hybrid materials, will be to go beyond the Tamm-Dancoff approximation in the BSE.

For a full assessment of excitation lifetimes [34], the imaginary parts of the Green functions will be implemented in the **exciting** code. This is an important piece of information to answer the question, how vibrations affect the absorption process, *i.e.*, atomic nuclei can be displaced from equilibrium before the excitation has decayed. Having also the lifetimes of polaronic excitations at hand, will give us insight in the experimental spectra measured by the spectroscopy groups. These tasks will require some development of methodology and coding.

Methods and codes: All work will be carried out with the **exciting** code. Its functionality is described in Ref. [P4]. In short, **exciting** is based on DFT, offering a variety of xc functionals including hybrid functionals based on Hartree-Fock as well as OEP. Using DFT as a starting point, charged and neutral electronic excitations are described in the framework of MBPT, comprising G_0W_0 and the BSE. TDFT is implemented with various xc kernels. Phonons are so far treated with a supercell approach, DFPT is currently being

implemented and available for the project in the second funding period. We note that owing to the complex systems, phonons will be treated on the DFT level. We will mainly rely on semi-local functionals, but consider hybrid functionals, depending on the findings of project **B4** (Körzdörfer/Scheffler/Rinke).

Materials: We will continue working with ZnO, but also consider Si and GaN on the inorganic side, while oligo-fluorines, substituted oligo-acenes and -phenylenes, and pyridine will be in the focus for the organic side. We will consider heterostructures as well as "thick" interfaces treated via slabs. At least 2 prototypical systems (Hyb1, Hyb2) will be identified together with projects **B3** (Blumstengel), **B5** (Neher), and **B9** (Stähler) in view of charge-transfer hybrid excitons at the beginning of the second funding period. Other two systems (Hyb3, Hyb4) will be identified together with **B4** (Körzdörfer/Scheffler/Rinke) in view of electron-vibrational coupling.

Work plan and time line:

PhD student 1 will focus on optical excitations by means of the Bethe-Salpeter equation with qp-*GW* as the basis. Several systems will be investigated in search of hybrid excitons exhibiting charge-transfer character. In the timeline below, only a minimum number of systems is given. The study of other systems will depend on the progress and insight during the runtime of the project. She will implement the calculation of the imaginary parts of the one-body and two-body Green function in **exciting** code to assess excitation lifetimes.

PhD student 2 will deal with all aspects of electron-phonon coupling in both the electronic and optical properties. He/she will implement the temperature-dependence in the BSE. Like for PhD 1, below only a minimum number of systems is given. The study of other systems will depend on the progress and insight during the runtime of the project.

1st year, PhD 1:
- Hyb1 hetero-structure (Hyb1-h) on the DFT level
- Constituents of Hyb1-h treated by *qp-GW* & BSE
- Implementation of the QP lifetimes (electronic contribution), application to small test systems

1st year, PhD 2:
- Hyb3 hetero-structure (Hyb3-h) on the DFT level, selected phonons
- Phonon self-energy of Hyb3-h

2nd year, PhD 1:
- Implementation of the QP lifetimes (continued)
- *qp-GW* & BSE including QP lifetimes for Hyb1-h
- Hyb1 slab (Hyb1-s) on the DFT level

2nd year, PhD 2:
- Phonon self-energy of Hyb3-h (continued); modelling of phonon full DOS
- Implementation of temperature-dependence in BSE

3rd year, PhD 1:
- *qp-GW* & BSE including QP lifetimes for Hyb1-s
- Hyb2-h and Hyb2-s on the DFT level
- *qp-GW* & BSE including QP lifetimes for Hyb2-h and Hyb2-s

3rd year, PhD 2:
- Combining phonon and electron self-energy of Hyb3-h
- Temperature-dependent optical spectra of Hyb3-h
- Hyb3 slab (Hyb3-s) on the DFT level including phonons
- Hyb4 hetero-structure (Hyb4-h) on the DFT level including phonons

4th year, PhD 1:
- *qp-GW* including phonon self-energy of Hyb3-h and Hyb3-s (together with PhD 2)

4th year, PhD 2:

- Combining phonon and electron self-energy of Hyb3-s and Hyb4-h
- Temperature-dependent optical spectra of Hyb-3-h and Hyb3-s including electronic lifetime effects (together with PhD 1)
- Temperature-dependent optical spectra of Hyb4-h

3.5 Role within the Collaborative Research Centre

Our investigations will be carried out in close collaboration with experiment performed in terms of optical spectroscopy in **B3** (Blumstengel), **B5** (Neher), and **B9** (Stähler). Together with **B3** (Blumstengel) we are aiming at identification of molecules leading to maximal hybridization of the exciton wavefunction. We will benefit from the structural investigations of **B4** (Körzdörfer/Scheffler/Rinke) and **A4** (Heimel) and surface/interface characterization by **A5** (Henneberger). For the phonon-driven renormalization of the electronic structure we will closely collaborate with project **B4** (Körzdörfer/Scheffler/Rinke).

3.6 Delineation from other funded projects

Does not apply.

3.7 Project funds

3.7.1 Previous funding

The project has been funded within the Collaborative Research Centre 951 HIOS since January 2013.

3.7.2 Funds requested

Funding for	2015/2		2016		2017		2018		2019/1	
Staff	Quantity	Sum	Quantity	Sum	Quantity	Sum	Quantity	Sum	Quantity	Sum
PhD student, 75%	2	44.100	2	88.200	2	88.200	2	88.200	2	44.100
Total		44.100		88.200		88.200		88.200		44.100
Direct costs	Sum		Sum		Sum		Sum		Sum	
Small equipment, Software, Consumables										
Other										
Total										
Major research equipment	Sum		Sum		Sum		Sum		Sum	
€ 10.000 - 50.000	50.000		0		0		0		0	
> € 50.000										
Total	50.000		0		0		0		0	
Total	94.100		88.200		88.200		88.200		44.100	

(All figures in Euro)

3.7.3 Staff

	No.	Name, academic degree, position	Field of research	Department of university or non-university institution	Commitment in hours/week	Category	Funded through:
Available							
Research staff	1	Claudia Draxl, Dr. rer. nat. Prof.	Theoret. physics, comput. materials science	Physics Department, HU Berlin	10		
	2	Pasquale Pavone, Dr. Privatdozent	electronic-structure, electron-phonon coupling	Physics Department, HU Berlin	8		
	3	Dmitrii Nabok Dr., Research assistant	many-body theory	Physics Department, HU Berlin	8		
	4	Andris Gulans Dr., Research assistant	comput. materials science	Physics Department, HU Berlin	8		
Non-research staff							
Requested							
Research staff	1	Olga Turkina, M. Sci.	many-body theory	Physics Department, HU Berlin		PhD student	
	2	N.N., M. Sci.	many-body theory	Physics Department, HU Berlin		PhD student	
Non-research staff							

Job description of staff (supported through available funds):

1. Claudia Draxl: Coordination of all organizational and scientific matters of the project, exploration and selection of concepts and methods, supervision of both PhD students.

4. Dimitrii Nabok: Supervision of PhD student 1, expertise in many-body perturbation theory (GW, BSE); expertise in organic/inorganic interfaces

3. Pasquale Pavone: Supervision of PhD student 2; coordination of method and code-development, expertise in electron-phonon coupling

4. Andris Gulans: Support of both PhD students in terms of DFT and MBPT; optimization of codes

Job description of staff (requested):

The proposed project involves a considerable workload that cannot be performed by a single PhD student. Therefore, two PhD students are requested.

1. Olga Turkina: The PhD student will focus on optical excitations by means of the Bethe-Salpeter equation with G_0W_0 and/or qp-*GW* as the basis. Several systems will be investigated in search of hybrid excitons exhibiting charge-transfer character. She will implement the calculation of the imaginary parts of the Green functions in the **exciting** code to assess excitation lifetimes.

2. NN: The PhD student will deal with all aspects of electron-phonon coupling in both the electronic and optical properties. She/he will implement the temperature-dependence of optical spectra in the **exciting** code.

3.7.4 Direct costs for the new funding period

No direct costs are requested. The used and further developed software **exciting** is developed in the group and free of charge.

3.7.5 Major research equipment requested for the new funding period

€ 10.000 - 50.000 for 2015/2

Computer Cluster	EUR	50.000

The **exciting** code is based on the LAPW method that is known for its high accuracy [P4] that comes at high computational costs. To allow for massively parallel and most efficient calculations, a library was developed in collaboration with the ETH Zürich and the Swiss Supercomputing Center within the framework of PRACE (Partnership for advanced computing in Europe). This library, called *SIRIUS*, now allows for computing large systems, and is particularly efficient by making use of modern hybrid architectures including GPUs and many-core CPUs. On the other hand, calculation of excited-state properties within the framework of MBPT requires large amounts of memory, even if computed highly parallel. Such nodes are not available neither in the computer facilities of the group nor in HPC centers. In order to investigate the systems of this project a compute-cluster shall be purchased that fulfill all these requirements. This cluster will be exclusively dedicated to the current project.

3.7.6 Student assistants

	2015/2	2016	2017	2018	2019/1
Quantity	1	1	1	1	1
Commitment in hours/week	10	10	10	10	10
Sum	3.000	6.000	6.000	6.000	3.000
Tasks	Testing of software; running benchmark calculations; developing visualization tools.				

3.1 About project B12

3.1.1 Title: Optical dynamics at organic/inorganic interfaces and in hybrid plasmonic nanostructures

3.1.2 Research areas: Theoretical Physics, Solid State Quantum Electronics, Optics

3.1.3 Principal investigators

Knorr, Andreas, Prof. Dr. rer. nat., 14.04.1965, German
Institut für Theoretische Physik
Technische Universität Berlin
Hardenbergstr. 36, EW 7-1,
10623 Berlin
Phone: +49 30 314 24255
Fax: +49 30 314 21130
E-Mail: andreas.knorr@physik.tu-berlin.de

Richter, Marten, Dr. rer. nat., 25.07.1980, German
Institut für Theoretische Physik
Technische Universität Berlin
Hardenbergstr. 36, EW 7-1,
10623 Berlin
E-Mail: marten.richter@tu-berlin.de

Do the above mentioned persons hold fixed-term positions?
yes

Marten Richter
End date 27.09.2018
Further employment is planned until 31.12.2019.

3.2 Summary

During the last funding period we jointly developed in B4 (Knorr/Scheffler/Rinke) a theory for the optical spectra and hybrid-coupling induced selection rules for the excitation transfer between ideally ordered semiconductor-molecule interfaces. Also, we addressed the photon emission dynamics of molecules coupled to metal nanostructures. Whereas ab initio calculations for semiconductor-molecule interfaces are continued in B4 (Körzdörfer/Rinke/Scheffler), two naturally evolving topics, labeled as (i) and (ii), for mesoscopically structured HIOS are continued in project B12 (Knorr/Richter):

(i) the simultaneous influence of hybrid-coupling, disorder and electron-phonon interaction on excitation transfer at (highly excited) **semiconductor-molecule interfaces** *on a mesoscopic spatial scale, as well as*
(ii) *the correlated emission and photon statistics of* **coupled molecule-plasmonic nanostructures** *for a variable (continuously increasing) number of non-identical emitters and varying coupling strength.*

These topics evolve directly from an interaction with experimental projects in the CRC and envision a central question for basic HIOS applications: How can the excitation transfer rates in HIOS be optimized for optoelectronic functions including external pumping, generation of optical gain and light emission?
(i) Semiconductor-molecule interfaces: The simultaneous influence of electron-phonon coupling and disorder is a fundamental question for transfer rates between the organic and inorganic part and determines in a non-trivial way the hybrid-coupling efficiency (Förster-, Dexter-transfer, tunneling). The following points impact the coupling: a) deviations from periodic arrangements, b) size/form of molecule domains and c) interaction with phonon modes. For optoelectronic functionality, external pumping is taken into account. For the semiconductor constituent we include excitation transfer from bound exciton states as well as from an excited electron-hole plasma. We aim at a comparison with experiments in projects B3 (Blumstengel) and B9

(Stähler). *Our goal is to optimize the excitation transfer rates between an externally pumped semiconductor (e.g. ZnO) coupled to light emitting organic molecules (e.g. ladder-type quarterphenyl).*

(ii) Coupled molecular-plasmonic nanostructures: The coupling of a variable number of molecular emitters to plasmons constitutes a fundamental question. We recently developed a numerically exact density matrix description from one up to hundreds of identical emitters coupled to a single plasmon mode. In experiments, deviations from this ideally ordered system with respect to the coupling strength and interaction with several plasmon modes will influence the dynamics. Taking into account these effects provides the basis to answer vital questions with respect to: a) conversion efficiency, b) threshold(less) behavior for nanolasers and quantum statistics, c) interference of light from different emitters. *Our theoretical approach is able to overcome typical mean field descriptions and thus allows for the description of quantum light emission from HIOS at a fundamental level.* To address specific experiments with different numbers of molecules and novel spasers concepts, proposed in B2 (Ballauf/Benson/Lu), large numbers of molecules and non-ideal arrangements are studied.

For both subprojects (i,ii) (see above) we use an exact or, if applicable, perturbative density matrix description (complementary to B6 (May)) starting from Hamiltonians valid on a mesoscopic spatial scale including ab initio material parameters/optical modes provided by B4 (Körzdörfer/Rinke/Scheffler) and B10 (Busch).

3.3 Research rationale

3.3.1 Current state of understanding and preliminary work

The potential and limits of HIOS critically depends on the coupling efficiency of functional states of its individual constituents, which directly influence transfer processes and -rates. One emerging field of HIOS is light emission by pumping one constituent (e.g. semiconductor/molecule) of the hybrid to transfer excitation and support light emission at the other constituent (molecule/metal).

a) <u>Coupling and optics of periodically arranged molecules on semiconductor surfaces</u>

Signatures of excitation transfer [1-5] from inorganic semiconductor to organic molecules can be observed in optical spectra and time resolved luminescence, if the coupling is strong compared to the intrinsic linewidth/temporal decay. So far, most calculations have been restricted to coupling of bound excitons with sharp spectral signatures and the low excitation limit [6]. One application envisioned is the electrical pumping of the semiconductor and the subsequent excitation transfer from the highly excited electron-hole plasma to optically active molecules with large oscillator strength.

Therefore, we developed HIOS Bloch-equations for a semiconductor layer (ZnO) dipole-dipole coupled to periodically arranged molecules (ladder-type quarterphenyl - L4P) [P1] (Fig. 1 a)). Parameters are calculated from ab-initio Coulomb-interaction (with B4 (Körzdörfer / Scheffler / Rinke)). *It turned out, that not only the type of coupling, but quasi momentum selection rules dominate the overall coupling strength in spectra and luminescence: In particular, the relation of the size of the Brillouin zones of the inorganic and organic part i.e. the number of semiconductor unit cells per molecule (molecular coverage) is important: The allowed momentum transfer channels for the excitation transfer (cf. Fig. 1 b)) depend significantly on the type of molecular coverage.*

Since a broader range of momentum transfer is allowed for lower molecular coverage, the excitation transfer mechanism at an ideally ordered interface is enhanced for lower molecular coverage. In Fig. 1 c), the coupling induced shift and broadening of the molecular HOMO-LUMO transition coupled to the electron-hole continuum is shown. Both increase with reduced molecular coverage due to the enhanced coupling channels. The broadening is a result of the hybridization of the continuum of the inorganic compound with the molecules.

Since the observed behavior is predicted for ideally ordered interfaces, investigation in the context of disorder is mandatory for explaining experimental spectra in HIOS and an extension to bound exciton states and high excitation phenomena will be targeted (see research program).

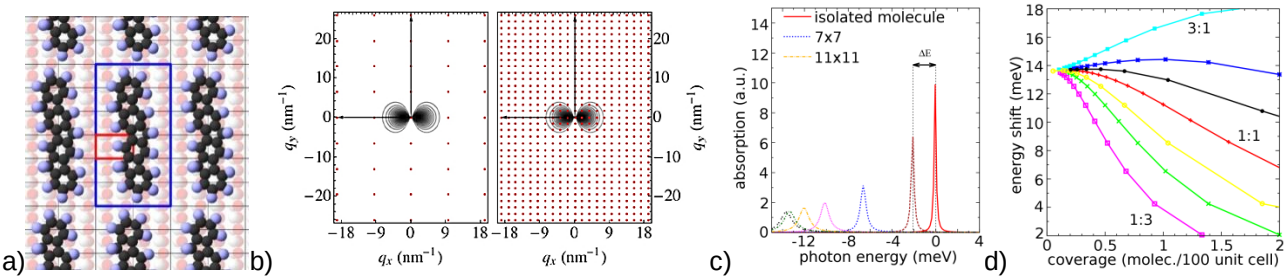

Figure 18 a) Spatial arrangement of the substrate (red) and molecular unit cell (blue) for L4P molecules on ZnO. b) Red dots indicate the allowed momentum transfer for different molecular surface coverage. Left: The extrema of the Coulomb-matrix elements (black) are missed for a 2x4 coverage, but reassembles for 10x16 (Right). c,d) The energy shift depends on the molecular coverage. Figures are taken from [P1].

b) A numerically exact solution of the N molecular emitters - metal nanostructure problem

A central question in hybrid plasmonic devices is to provide efficient gain for coherent plasmons to compensate for losses. A typical example includes the spaser [7, 8], which has been discussed controversially over the last years [9-12]. The spaser and other plasmon devices are in the focus of current research [13-17].

To analyze hybrids of metal nanoparticles and molecules, a description of many (N) quantum emitters and plasmon modes is necessary. We developed an exact expansion scheme [P10] for a system of N identical molecular emitters and a single plasmon (cf. Fig. 2 a) and Ref. [18]).

Within our fully quantized theory, we found that a spaser [7] is a threshold less device, and that although its realization is in principle possible, the required pump rates are unrealistically high, cf. Fig. 2 b), and that claims of experimental verification are questionable [8], in agreement with the simplified semi-classical description of Ref. [9]. However effective plasmon generation of designed statistics is still possible: *To explore the potential of hybrid molecule-metal structures for quantum light generation, a systematic study as a function of geometry and molecular coverage will be done jointly with B2 (Busch) (see research program).*

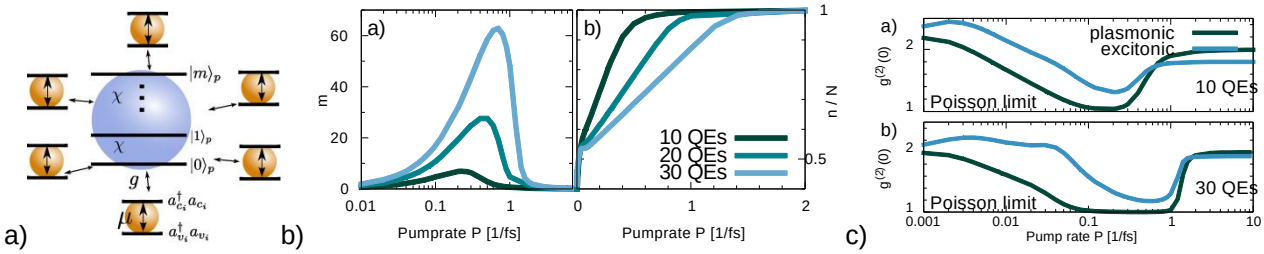

Figure 19 a) Several molecules coupled to a plasmon mode. b) The mean plasmon (a) and exciton (b) number as a function of the incoherent pump rate for different numbers of quantum emitters. c) The plasmonic and excitonic equal time second order correlation functions versus the pump rate for 10 (a) and 30 (b) quantum emitters [P10].

c) Excitation transfer in molecule-metal nanoplasmonic structures: Light emission statistics

Besides compensation of loss (b), in nano-plasmonic circuits, the control of the photon/plasmon emission statistics of hybrid plasmonic devices is of central importance [19, 20]: Sources for single, entangled and Poisson distributed plasmons are highly demanded for quantum information processing.

We performed a theoretical investigation of a system of two optically active molecular systems coupled to a single metal nanoparticle (MNP), cf. Fig. 3 a) [P2]: An enormous modification in the plasmon emission statistics (second order correlation function) can be induced by changing the dipole coupling strength between the molecular constituents (V_{12}), cf. Fig. 3 b): non-classical, bunched and Poissonian light can be extracted in the far field. The changes in the emission statistics are related to a modified Jaynes-Cummings-ladder formed by all three HIOS constituents. *We will focus on electrical pumping using the PPCE (photon-probability cluster expansion) technique [P9].*

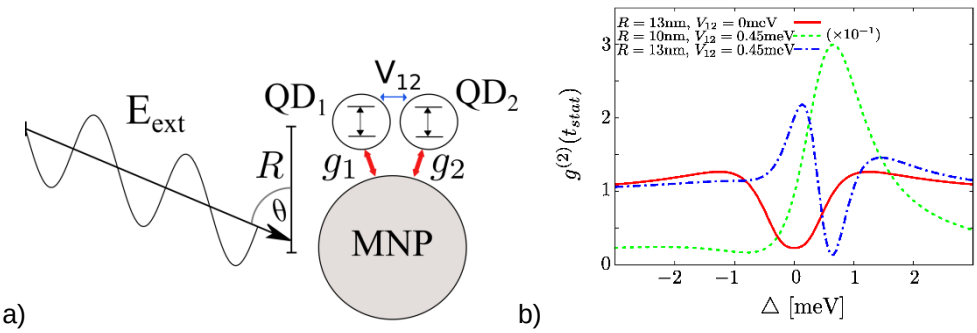

Figure 20 a) Two interacting molecules are coupled to a plasmon mode of a metal nanoparticle. b) Second order correlation function versus the detuning to the external optical field [P2].

d) Light scattering and secondary emission: Encoded information on hybrid coupling

For spherical metal nanoparticles the dipole mode dominates the light scattering [P3]. To study the information contained in the scattered light, we applied the theory (cf. Sections (b,c)) to time resolved fluorescence measurements of ensembles of quantum dots (QD) coupled to MNPs. For a realistic description two main aspects are important: First, since the ensemble fluorescence exhibits quantum

emission also from strongly coupled systems, no simple truncation of the equations of motion can be made. Second, the disorder ensemble average determines the relevant experimental signals.

We described the ensemble by calculating different coupling strengths between the QD and MNP (Fig. 4a). The observed and theoretically explained emission dynamics strongly depend on the coupling/distance, cf. Fig 4b,c). *This example illustrates the interplay of coupling and inhomogeneous broadening in disordered hybrids.*

e) Statistical ensembles averages and its impact to HIOS dipole couplings

In [P6] an effective numerical approach for the ensemble average was developed, providing access to properties like the homogeneous linewidth of excited excitons. Inhomogeneous broadening is caused by different dipole orientations and different transition energies. *Similar inhomogeneous distribution effects occur for the molecule-plasmon system as well as for molecules on the semiconductor surfaces.*

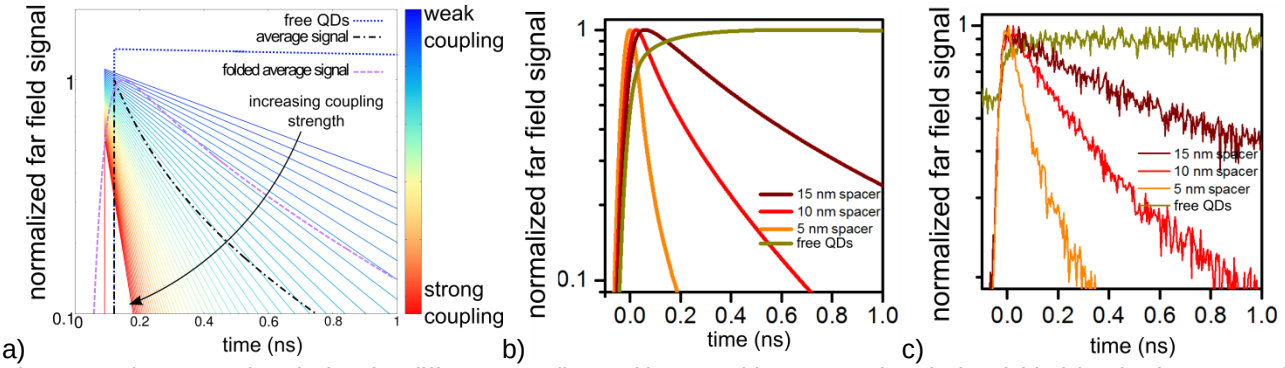

Figure 21 a) Temporal emission for different couplings. b) Ensemble averaged emission folded by the instrumental response. c) Measured fluorescence (H. Lange et al., Hamburg).

f) Two-dimensional coherent spectroscopy as a probe of interacting systems

A central information to optimize the coupling efficiency is knowledge on the character of the coupling, i.e. to judge whether Förster-, tunnel- or Dexter- transfer dominates. *In Sec 3.4 we show, that coherent spectroscopy is able to detect coupling effects* [P5] *and can be used to classify the interaction type between different HIOS constituents.*

References

[1] D. Basko, G.C. La Rocca, F. Bassani, and V.M. Agranovich. *Eur. Phys. J. B*, 8(3):353, 1999.
[2] N.-P. Wang, M. Rohlfing, P. Krüger, and J. Pollmann. *Phys. Rev. Lett.*, 92:216805, 2004.
[3] S. Blumstengel, S. Sadofev, C. Xu, J. Puls, and F. Henneberger. *Phys. Rev. Lett.*, 97:237401, 2006.
[4] G. Itskos, G. Heliotis, P. G. Lagoudakis, J. Lupton, N. P. Barradas, E. Alves, S. Pereira, I. M. Watson, M. D. Dawson, J. Feldmann, R. Murray, and D. D. C. Bradley. *Phys. Rev. B*, 76:035344, 2007.
[5] T. Liang, Y. Cui, J. Yu, W. Lin, Y. Yang, and G. Qian. *Thin Solid Films*, 544(0):407, 2013.
[6] V. M. Agranovich, D. M. Basko, G. C. La Rocca, and F. Bassani. *J. Phys.: Condens Matter*, 10(42):9369, 1998.
[7] D. J. Bergman and M. I. Stockman. *Phys. Rev. Lett.*, 90:027402, 2003.
[8] M. A. Noginov, G. Zhu, A. M. Belgrave, R. Bakker, V. M. Shalaev, E. E. Narimanov, S. Stout, E. Herz, T. Suteewong, and U. Wiesner. *Nature*, 460(7259):1110, 2009.
[9] J. B. Khurgin and G. Sun. *Nat Photon*, 8(6):468, 2014.
[10] J. B. Khurgin and G. Sun. *Opt. Express*, 20(14):15309, 2012.
[11] X.-L. Zhong and Z.-Y. Li. *Phys. Rev. B*, 88:085101, 2013.
[12] S.-Y. Liu, J. Li, F. Zhou, L. Gan, and Z.-Y. Li. *Opt. Lett.*, 36(7):1296, 2011.
[13] G. Kewes, A. W. Schell, R. Henze, R. S. Schönfeld, S. Burger, K. Busch, and O. Benson. *Appl. Phys. Lett.*, 102(5):051104, 2013.
[14] M. D. Brown, T. Suteewong, R. S. S. Kumar, V. D'Innocenzo, A. Petrozza, M. M. Lee, U. Wiesner, and H. J. Snaith. *Nano Letters*, 11(2):438, 2011.
[15] K. Suzuki, K. Kanisawa, C. Janer, S. Perraud, K. Takashina, T. Fujisawa, and Y. Hirayama. *Phys. Rev. Lett.*, 98:136802, 2007.
[16] P. Vasa, R. Pomraenke, G. Cirmi, E. De Re, W. Wang, S. Schwieger, D. Leipold, E. Runge, G. Cerullo, and C. Lienau. *ACS Nano*, 4(12):7559, 2010.
[17] Y. Zhang and V. May. *Phys. Rev. B*, 89:245441, 2014.
[18] M. Tavis and F. W. Cummings. *Phys. Rev.*, 170:379, 1968.
[19] B. Ding, C. Hrelescu, N. Arnold, G. Isic, and T. A. Klar. *Nano Lett.*, 13(2):378, 2013.
[20] N. Arnold, B. Ding, C. Hrelescu, and T. A. Klar. *Beilstein J. Nanotechnol.*, 4:974, 2013.
[21] M. Reichelt, T. Meier, S. W. Koch, and M. Rohlfing. *Phys. Rev. B*, 68:045330, 2003.

[22] N. Buecking, P. Kratzer, M. Scheffler, and A. Knorr. *Phys. Rev. B*, 77:233305, 2008.
[23] A. A. R. Neves, A. Camposeo, R. Cingolani, and D. Pisignano. *Adv. Funct. Mater.*, 18(5):751, 2008.
[24] T. U.-K. Dang, C. Weber, S. Eiser, A. Knorr, and M. Richter. *Phys. Rev. B*, 86:155306, 2012.
[25] D. L. Dexter. *J. Chem. Phys.*, 21(5):836, 1953.
[26] U. Jahn, M. Ramsteiner, R. Hey, H. T. Grahn, E. Runge, and R. Zimmermann. *Phys. Rev. B*, 56:R4387, 1997.
[27] A. Esser, E. Runge, R. Zimmermann, and W. Langbein. *Phys. Rev. B*, 62:8232, 2000.
[28] R. Zimmermann and E. Runge. *J. Lumin.*, (0):320, 1994.
[29] Y. Xu, O. T. Hofmann, R. Schlesinger, S. Winkler, J. Frisch, J. Niederhausen, A. Vollmer, S. Blumstengel, F. Henneberger, N. Koch, P. Rinke, and M. Scheffler. *Phys. Rev. Lett.*, 111:226802, 2013.
[30] P. Vasa, R. Pomraenke, G. Cirmi, E. De Re, W. Wang, S. Schwieger, D. Leipold, E. Runge, G. Cerullo, and C. Lienau. *ACS Nano*, 4(12):7559, 2010.
[31] S. Georg, J. Kabuss, I. M. Weidinger, D. H. Murgida, P. Hildebrandt, A. Knorr, and M. Richter. *Phys. Rev. E*, 81:046101, 2010.
[32] E. Waks and D. Sridharan. *Phys. Rev. A*, 82:043845, 2010.
[33] A. Ridolfo, O. Di Stefano, N. Fina, R. Saija, and S. Savasta. *Phys. Rev. Lett.*, 105:263601, 2010.
[34] M. E. Madjet, A. Abdurahman, and T. Renger. *J. Phys. Chem. B*, 110:17268, 2006.

3.3.2 Project-related publications

a) Peer-reviewed publications

[P1] Eike Verdenhalven, Andreas Knorr, Marten Richter, Bjoern Bieniek, and Patrick Rinke "Theory of optical excitations in dipole-coupled hybrid molecule-semiconductor layers: Coupling of a molecular resonance to semiconductor continuum states", Phys. Rev. B. **89**, 235314 (2014)
[P2] T. Sverre Theuerholz, Alexander Carmele, Marten Richter, and Andreas Knorr, "Influence of Förster interaction on light emission statistics in hybrid systems", Phys. Rev. B **87**, 245313 (2013)
[P3] Holger Lange, Beatriz H. Juárez, Adrian Carl, Marten Richter, Neus G. Bastús, Horst Weller, Christian Thomsen, Regine von Klitzing, and Andreas Knorr, *"Tunable Plasmon Coupling in Distance-Controlled Gold Nanoparticles"*,Langmuir **28**, 8862 (2012)
[P4] Marten Richter, Felix Schlosser, Mario Schoth, Sven Burger, Frank Schmidt, Andreas Knorr, and Shaul Mukamel *"Reconstruction of the wave functions of coupled nanoscopic emitters using a coherent optical technique"*, Phys. Rev. B 86, 085308 (2012)
[P5] Xingcan Dai, Marten Richter, Hebin Li, Alan D. Bristow, Cyril Falvo, Shaul Mukamel, and Steven T. Cundiff, *"Two-dimensional double-quantum spectra reveal collective resonances in an atomic vapor"*, Phys. Rev. Lett. 108, 193201 (2012)
[P6] Mario Schoth, Marten Richter, Andreas Knorr, and Thomas Renger, *"Line Narrowing of Excited-State Transitions in Nonlinear Polarization Spectroscopy"*, Phys. Rev. Lett. 108, 178104 (2012)
[P7] Shaul Mukamel and Marten Richter, *"Multidimensional phase-sensitive single-molecule spectroscopy with time-and-frequency-gated fluorescence detection"*, Phys. Rev. A 83, 013815 (2011)
[P8] E. Malic, C. Weber, M. Richter, V. Atalla, T. Klamroth, P. Saalfrank, S. Reich, and A. Knorr, *"Microscopic Model of the Optical Absorption of Carbon Nanotubes Functionalized with Molecular Spiropyran Photoswitches"*, Phys. Rev. Lett. 106, 097401 (2011)
[P9] Marten Richter, Alexander Carmele, Anna Sitek, and Andreas Knorr, *"Few-Photon Model of the Optical Emission of Semiconductor Quantum Dots"*, Phys. Rev. Lett. 103, 087407 (2009)
[P10] M. Richter, M. Gegg, T. S. Theuerholz and A. Knorr, *"Quantum statistics of a spaser: A numerically exact model study", with referees (Phys. Rev. B)*

3.4 Research plan

The investigations of the first funding period clearly show that for a realistic description of HIOS disorder effects in the molecular distribution at semiconductor surfaces and metallic nanostructures (varying coupling strength and spatial arrangement) are crucial to obtain a realistic description. Therefore, after the development of Bloch equations for ideal HIOS on mesoscopic length scales in the first funding period, we focus in the second funding period on the simultaneous influence of coupling, electron-phonon interaction and disorder, including also highly excited electron-hole plasmas. We discuss two subprojects (i) and (ii) individually:

(i) <u>Semiconductor-molecule interfaces:</u>

The understanding of the temporal and spectral dynamics of the excitation transfer at semiconductor-molecule interfaces is of central importance for future hybrid opto-electronic devices [4, 3]. *We aim to*

develop microscopic, ab-initio motivated models for the excitation transfer mechanisms in HIOS on a mesoscopic length scale. All occurring microscopic input for the dynamical description is parameterized input by ab-initio methods (from B4 Körzdörfer/Scheffler/Rinke). The dynamics of the excitation transfer, its spectroscopic signatures and HIOS device principles are calculated using density matrix techniques including the impact of disorder on mesoscopic length scales. *The combined approach of ab-initio (B4 Körzdörfer /Scheffler/ Rinke) and density matrix (B12 Knorr/Richter) theory enables a dynamical treatment of larger systems as compared to ab-initio methods alone [21, 22]. At the same time, we retain the microscopic foundation of the ab-initio treatment.* We address the following aspects:

a) Excitation transfer after optical/electrical pumping in HIOS devices: *Is it possible to optimize the transfer of inorganic, bound excitonic (and unbound electron-hole) excitation to molecular, light emitting transitions [4, 3] in the limit of a highly excited semiconductor?*

Depending on the external excitation (optical or electrical pumping) and resonance conditions, bound or continuum inorganic exciton states (both described by a combined ab-initio and density matrix approach) are relevant for the excitation transfer to the optical active molecules [1, 23]. Optimization of the excitation transfer to the molecular layer relies on the interplay of pump and relaxation processes [24]. *Of particular interest is the transfer of excitation/optical gain from a highly excited ZnO semiconductor (excitons and electron-hole plasma) to the organic molecules.*

b) Different types of Coulomb-coupling of a semiconductor layer (e.g. ZnO) and organic molecules (ladder-type quarterphenyl (L4P)): *Which type of coupling provides the most efficient excitation transfer and optimal HIOS device operation?*

The general Coulombmatrix V_{cd}^{ab} for molecule distributions on a mesoscopic spatial scale determine specific Förster-elements, monopole-monopole coupling and Dexter matrix- [25] as well as the tunneling matrix elements (cf. methods). In the density matrix the interaction elements account for excitation transfer and energy shifts. We developed a general density matrix description for these transfer processes which can also include charge transfer excitons. Independently, realistic parameters for the calculation of the interaction elements will be provided by B4 (Körzdörfer/Scheffler/Rinke). We clarify the overall structure of the Coulomb-interaction matrix for ideally ordered interfaces enforcing transfer selection rules and compare their impact on transfer rates.

To clarify the character of the Coulomb-coupling, we propose also individual spectroscopic fingerprints of Förster and Dexter transfer (Fig. 5 a)):

Förster coupling typically describes a dipole-dipole mediated exciton transfer which can either preserve or flip the spin state of the transferred exciton, determined by the mutual dipole orientation. Dexter interaction denotes a direct exchange of electrons not limited by the optical selection rules. In comparison to Förster coupling, Dexter coupling leads to a characteristic resonance line splitting in 2D coherent optical spectra [P4,P7] cf. Fig. 5 a,b). *Similar coupling identifying patterns are expected for a coupling between bound semiconductor excitons and molecular excitons.*

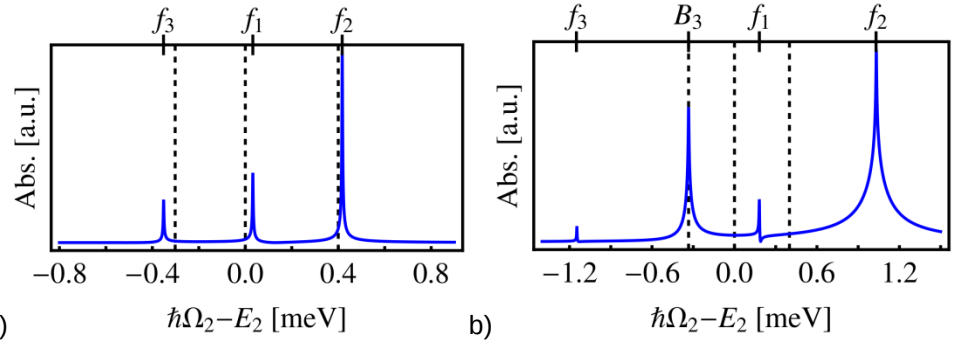

Figure 22 Two coupled spin degenerate two level systems in a spin preserving stacked geometry. a) Förster coupled system: Three two-exciton resonances. b) Dexter coupled system: Four two-exciton resonances.

c) Doping and Coulomb-screening at the HIOS interface: *How does doping, found to be important, modify the excitation transfer and the localization of hybrid excitons?*

Doping leads to spatial dependent random charge distributions. A solution of the electron-hole distribution in spatial domain results in the Schrödinger equation [26-28] $\left(-\frac{\hbar^2\Delta_e}{2m_e} - \frac{\hbar\Delta_h}{2m_h} + V_c(\vec{r}_e - \vec{r}_h) + V_{De}(\vec{r}_e) + V_{Dh}(\vec{r}_h) - E_\lambda\right)\psi_{e,h}(\vec{r}_e, \vec{r}_h) = 0$, where V_{Dh} is a random disorder potential whose magnitude can be obtained through space charges [29]. The occurring fields influence the exciton states and can be implemented in the density matrix dynamics for excitons and the electron-hole plasma.

d) Influence of electron-phonon coupling on excitation transfer processes: *To what extend does electron-phonon coupling break the excitation transfer selection rules at an ideal interface?*

The phonon system can balance energy and momentum in the course of the excitation transfer (absorption or emission of phonon): In particular, electron-phonon assisted transfer may relax the strict momentum selection rules, thus opening new channels for excitation transfer.

e) Disorder by phenomenological ensemble average: *To what extend is inhomogeneous broadening sufficient for describing disorder in CRC experiments and HIOS devices?*

The understanding of the selection rules [P1] under a realistic, disordered situation is mandatory to achieve an optimal coupling in real hybrid devices. This includes deviations from regular grids or small domains of regular arrangements. Both effects weaken the selection rules and therefore even may enhance the overall coupling strength. In the case of domains, the influence of form, size orientation and interfaces to other domains to the coupling will be analyzed. Our microscopic results will be compared to ab-initio ensemble averages from B4 (Körzdörfer/Scheffler/Rinke). We use similar methods as developed by us in Ref [P8] used to study the mutual influence of static molecular dipoles and carbon nanostructures excitons cf. Fig 6 a): The coupling channels for a regular arrangement and for specific quasi momenta are restricted (cf. Fig. 6 b)); a random distribution of the molecules leads to an opening of more interaction channels (cf. Fig 6 b)). *An analogous effect for organic molecules on inorganic layers will lead to dramatic changes in the coupling strength* [P1].

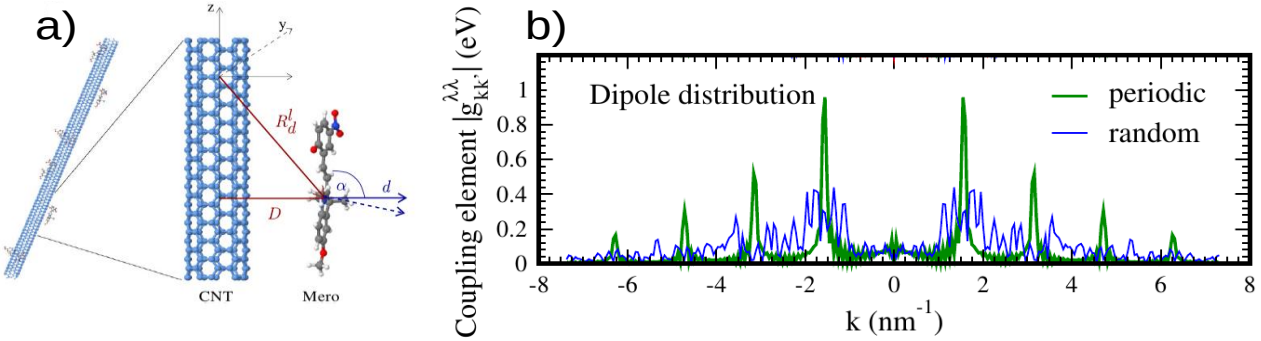

Figure 23 a) Merocyanine-functionalized exemplary (10,0) nanotube. b) nanotube-dipole matrix element as a function of the momentum transfer k: A random molecule distribution opens additional coupling channels.

f) Microscopic description of combined Coulomb-coupling, electron-phonon interaction and disorder interactions: *Do non-trivial processes of excitation-transfer/electron-phonon and disorder exist?*

Our goal is to develop first steps into a consistent approach of hybrid-coupling, electron-phonon interaction and disorder. Since interactions act simultaneously, the excitation transfer might be determined by combined higher order effects if the individual interaction strengths are comparable.

(ii) Coupled molecule-plasmonic nanostructures

Another type of hybrid materials for light generation are coupled molecule-plasmon systems [20, 30]. Due to strong losses in metals, the use of plasmonic nanostructures relies on efficient pump/gain mechanisms provided by their coupling to molecular or semiconductor nanostructures. *This subproject is focused on the description of the non-classical emission from molecule-plasmonic nanostructures as a function of the molecule density and spatial molecule arrangement*. We address the following questions:

a) Mechanism of molecule-plasmonic hybrid nanostructure coupling and their efficient external pumping: *To what extent can the plasmon generation be optimized?*

Our goal is to optimize the light emission from molecule-plasmonic nanostructures with respect to its use as quantum source of single, entangled and coherent plasmons. Surprisingly, we already found that changing Förster interaction between the molecules causes dramatic changes in the plasmon emission statistics. We aim at a systematic study of the emission statistics from non-classical, Poisson- or a thermal distribution by changing the average distance between the molecules.

b) Consistent study of light emission for increasing number of identical emitters: *How does quantum interference of few or many emitters (up to hundreds) determine the quantum light emission?*

The underlying model system of an optical mode coupled to several emitters is a basic model for many quantum optical processes. For this purpose, we have already developed a method for treating a single plasmon mode identically coupled to up to several hundreds of identical quantum emitters. *This has not been achieved before under open system conditions: Within the present solution, all quantum mechanical*

interference and correlation phenomena are taken into account including super radiance and lasing emission examples.

We will study the temporal dynamics as well as the steady state limit of the plasmonic and excitonic quantum correlations under external excitation. Since full access to the plasmon-molecule system all moments of the quantum statistics of the joint system are accessible, we aim at a detailed analysis of quantum statistics and all observables otherwise approximately calculated by mean field techniques. This also provides excellent possibilities to compare our results to many experiments carried out in B2 (Ballauf/Benson/Lu). Figure 7 provides a first example of our results.

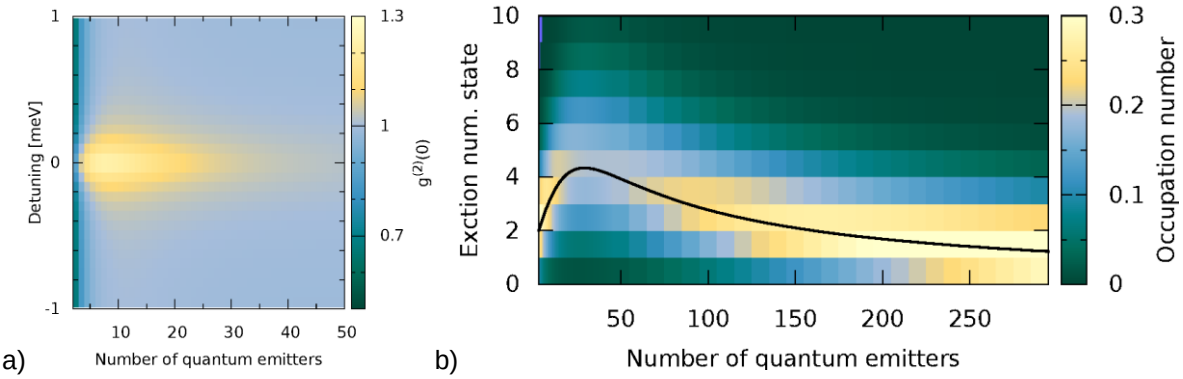

Figure 24 a) The plasmonic equal time second order correlation function for a coherently driven metal nanoparticle – quantum emitter hybrid. b) The corresponding exciton distribution in the resonant case.

c) Disorder in molecule-plasmonic nanostructures: *What is the influence of non-identical size and coupling of different molecules in the ensemble?*

In realistic nanostructures the size and arrangement of the metal nanoparticles and molecules varies from a mean value. A central question is, whether resonant molecules dominate the dynamics by their mutual collectivity, suppressing others. Inhomogeneous distribution of different energies and coupling strengths can change the qualitative behavior of observables from the distribution as compared identical molecules [31]. For averaging, we will apply a method recently developed by us [P6].

d) Extension to many plasmon modes: *Do different plasmon modes show mode competition?*

In most models [32, 33], only a single mode is considered (external excitation is polarized in only one direction). We apply our N-quantum emitter model to the many mode case to check on the validity of the single mode approximation, the modes are provided by B10 (Busch).

e) Spatial arrangement of multiple emitter types and metal nanoparticles: *How is the interplay of plasmon generation, propagation (spatially selective gain) and far field emission for plasmonic excitations manifested?*

For the explanation of a possible use of plasmonic components in nanostructured circuits, directional propagation and amplification is a central topic. We will study the spatial transfer of plasmons of specific statistics in nanostructured waveguides.

i) Methods for Semiconductor-molecule interfaces:

a) *External pumping:* To describe external pumping we apply optical dipole $(\vec{d})$ coupling for semiconductor/molecules $(a_\lambda, a_\lambda^\dagger)$:

$H_{e-l} = \sum_{\substack{\vec{k} \\ \lambda \neq \lambda'}} \vec{d}^{\vec{k}}_{\lambda,\lambda'} \vec{E}(t) a^\dagger_{\vec{k},\lambda} a_{\vec{k},\lambda'} + \sum_{\substack{A \neq B \\ \nu}} \vec{d}_{A_\nu,B_\nu} \vec{E}(t) a^\dagger_{A_\nu} a_{B_\nu}$ or an electron reservoir $(d_\lambda, d_\lambda^\dagger)$

$H_{el-res} = \sum_\lambda g d_\lambda a^\dagger_\lambda + h.a.$ in the Lindblad formalism $\mathcal{L}\rho = \frac{\gamma}{2}\left(2A\rho A^\dagger - \rho A^\dagger A - A^\dagger A \rho\right)$.

b) *Mesoscopic coupling:* To illustrate our approach to combine ab-initio parameters for the Coulomb-coupling with a density matrix theory on the mesoscopic scale, we describe the derivation of a Förster coupling a semiconductor - molecule interface: The general Coulomb matrix $V^{L_\nu \vec{k}}_{H_\nu \vec{k}_c} = \int d^3r \int d^3r' \psi^*_{L_\nu}(\vec{r}) \psi^*_{\vec{k}_\nu}(\vec{r}') V(\vec{r}-\vec{r}') \psi_{H_\nu}(\vec{r}) (\vec{r}') \psi_{\vec{k}'_c}(\vec{r})$ is reduced to dipole-dipole coupling $V^{L_\nu \vec{k} \nu}_{H_\nu \vec{k}+\vec{q} c} = \frac{1}{A}\frac{e_0^2}{2\varepsilon_0}\frac{e^{-|\vec{q}|\Delta z}}{|q|}\left[\begin{pmatrix} q_x \\ q_y \\ -i|q| \end{pmatrix} \cdot \vec{d}_{LH}\right]\left[\begin{pmatrix} q_x \\ q_y \\ -i|q| \end{pmatrix} \cdot \vec{d}^{\nu c}_{\vec{k},\vec{k}+\vec{q}}\right]$, where $\vec{q}$ is the reciprocal lattice vector, d_{LH} the dipole of the HOMO-LUMO transition, $d^{\nu c}_{\vec{k},\vec{k}'}$ are the semiconductor transition dipole moments and Δz is the distance between the layers:

$V^{L,\vec{k}v}_{H,\vec{k}+\vec{q}c}$ in dipole-dipole approximation reduces the coupling of ideal lattices to dipole elements $\vec{d}_{LH}$ and $\vec{d}^{vc}_{\vec{k}\vec{k}'}$ defined as integral over elementary cells of the lattice. Both can be calculated from ab-initio theory [B4].

The HIOS Bloch equations for the molecular polarization $\sigma^{\vec{l},\vec{l}'}_{HL}$ reads:

$$i\hbar\frac{d}{dt}\sigma^{\vec{l},\vec{l}'}_{HL} = (E_L - E_H)\,\sigma^{\vec{l},\vec{l}'}_{HL} + \vec{E}(t)\cdot\vec{d}_{LH}\left(\rho^{\vec{l}}_{H} - \rho^{\vec{l}'}_{L}\right)\delta_{\vec{l},\vec{l}'} + \frac{1}{A}\sum_{\vec{k}_1,\vec{k}_2}\sum_{\vec{G}} V^{L\vec{k}_1 v}_{H\vec{k}_2 c}\,\delta_{\vec{k}_1-\vec{k}_2+\vec{G},\vec{l}'-\vec{l}}\,\sigma^{\vec{k}_1,\vec{k}_2}_{vc}\left(\rho^{\vec{l}}_{H} - \rho^{\vec{l}'}_{L}\right).$$

One can clearly recognize selection rules including the lattice vectors in the Kronecker-symbol. Also, it is possible to improve the strict point dipole-dipole coupling by introducing transition partial charges. They resemble the Coulomb-potential of one constituent, observed by the other constituent [34]:

$$\phi_{ij}(\vec{r}) = \frac{1}{4\pi\varepsilon_0\varepsilon_r}\sum_j \frac{q_{ij}}{|\vec{r}-\vec{R}_j|} \approx \frac{1}{4\pi\varepsilon_0\varepsilon_r}\int d\vec{r}'\,\frac{\psi^*_i(\vec{r}')\psi_j(\vec{r}')}{|\vec{r}-\vec{r}'|}.$$

The advantage is besides the reduced data handling and computational effort, that a physical interpretation of the exchanged data is possible and extensions to larger geometries are possible without redoing the DFT calculation. For partial charges the first test calculations are currently carried out.

For couplings elements, where the wave function overlaps between the two systems are important, e.g. Dexter, charge transfer or tunnel coupling, we aim to fit the individual wave function/overlap to asymptotic model wave functions (or a set of wave functions) parameterized from ab-initio calculations (B4). Specific model wave function sets will be developed in the second funding period from typical quantum chemistry basis sets.

c) *Doping and screening:* In order to incorporate doping and screening at HIOS interfaces correctly, the vacuum Green function $\mathcal{G}(\vec{r},\vec{r}') = \frac{1}{4\pi\varepsilon_0}\frac{1}{|\vec{r}-\vec{r}'|}$ in Coulomb-coupling, which is in first approximation only modified through a constant background screening ε_r, is replaced by a more realistic Green function, obtained from the Poisson equation $\nabla_{\vec{r}}\,(\varepsilon(\vec{r})\,\nabla_{\vec{r}}\,\mathcal{G}(\vec{r},\vec{r}')) = -\delta(\vec{r}-\vec{r}')$. The resulting Coulomb-coupling elements incorporate a more realistic transfer dynamics.

d) *Electron-phonon interaction:* For the phonon modes we apply an analytical model construction of continuous media or spectral densities, coupling elements calculated by B4 (Körzdörfer/Scheffler/Rinke) $J^{(\omega)}_{\lambda\lambda'} = \sum_\alpha |g_{\lambda\lambda'}|^2\,\delta(\omega-\omega_\alpha)$. Both approaches allow to parameterize the electron-phonon interaction in a model Hamiltonian $H_{int,mem} = \sum_{\lambda,\lambda'} g^\alpha_{\lambda\lambda'} a^\dagger_\lambda a_{\lambda'} b^\dagger_\alpha + h.c.$. Afterwards correlation expansion to finite order or cumulant expansions (exact model solutions are rare) will be applied.

e) *Ensemble average:* For deviations from regular molecular arrangements we will treat deviations $\Delta\vec{R}_i$ with respect to the regular positions $\vec{R}_{0,i}$ as perturbation and calculate additional contributions perturbatively. For treating the domains we will do ensemble average of the electronic and optical dynamics with a finite number of molecules inside one domain on the substrate. The temporal dynamics of the experimental observables are then obtained by averaging over sufficient configurations. Another approach is to do selective summations in the HIOS Bloch-equations of motion such as coherent potential approximation or self-consistent Born approximation.

f) *Action of phonons and disorder:* We will attack this demanding problem with a correlation expansion approach of the density matrix, including disorder assisted density matrices or, alternatively using directly the disorder eigenstates. This allows to study interference perturbatively while including interactions at the same time. The simultaneous action of the HIOS constituents coupling, electron-phonon interaction and disorder leads to non-trivial operator equations in the Heisenberg- or density matrix equations: Many particle correlations are built up from simultaneous Coulomb coupling, electron-phonon interaction and disorder: If possible a Non-Markovian or otherwise a higher order Markovian calculation should be carried out for these processes. However, since the expected equation constitutes a huge challenge, a (self-consistent) second order Born approach is more likely.

ii) Methods for coupled molecular-plasmonic nanostructures

a) *Plasmon statistics:* As a start, the coupling between molecules and the plasmon modes are described within dipole approximation. The magnitudes of the coupling strengths are derived by phenomenological quantization [33]. The emission statistics of e.g. the plasmons is given by the second order correlation function $g^{(2)}(t) = \frac{\langle b^\dagger(t)b^\dagger(t)b(t)b(t)\rangle}{\langle b^\dagger(t)b(t)\rangle^2}$. Currently for optical pumping we are using only a two level system for the molecules and a pump rate (Lindblad term) and a number state basis for the numerical evaluation.

Depending on the molecule used in the CRC: Higher excited states can be included as well as electron-phonon coupling, based on DFT data from B4 (Körzdörfer/Scheffler/Rinke).

b) *Varying molecule coverage:* For treating few up to large numbers of molecules, we use symmetry relations in the density matrix and develop algorithms, which dynamically select the density matrix elements, which are significantly different from zero for achieving numerical convergence. For the algorithm the relevant ordering criteria are the number of excitations (excitons+plasmons).

c) *Disorder:* Few molecules can be treated by explicit calculation. However, for large emitter numbers deviations from typical coupling mean values cannot be treated by our method (cf. bullet b). Typically, mean field methods are used, however, there exist many situations where the statistics cannot be accurately described. If the deviations from the mean transition energy and mean coupling are small, the Hamiltonian can be split into $H_{av} = \bar{g} \sum_i a_{v_i}^\dagger a_{c_i} b^\dagger + h.c.$ describing the mean coupling and transitions and $H_{dev} = \sum_i \Delta g_i a_{v_i}^\dagger a_{c_i} b^\dagger + h.c.$ describing the deviations, with $\bar{g} = \sum_i g_i$ and $\Delta g_i = g_i - \bar{g}$. First we solve for the average interaction Hamiltonian $H_{av} = H - H_{dev}$, obtaining the full density matrix for average coupling. In a second step the density matrix ρ is split into the already solved part for averaged coupling and the deviations: $\rho = \rho_{av} + \Delta\rho$. The equation for $\Delta\rho$ reads $\partial_t \Delta\rho = -\frac{i}{\hbar}[H_{dev}, \rho_{av}] - \frac{i}{\hbar}[H_{av}, \Delta\rho] - \frac{i}{\hbar}[H_{dev}, \Delta\rho]$. Since it is not numerically possible to solve a deviation density matrix $\Delta\rho$ for large emitter numbers, we develop correlation expansion methods for $\Delta\rho$.

d) *Multiple plasmon modes:* Multiple plasmon dipole modes as well as higher modes like quadrupole modes can be important for certain geometries (e.g. metal nanoparticle dimer [P3]). Similarly, coupling several metal nanoparticles to molecules may be a setup important for HIOS. The generalization of the equations is straightforward, however the algorithms are computationally more expensive.

Additional to bound plasmon states also propagation of plasmons between e.g. two plasmon modes is important. These propagation effects may be handled in spatial-domain using spatially dependent plasmon operators in cooperation with B10 (Busch).

e) *Directional transfer:* For the creation of hybrid devices, it is possible to combine different types of molecules with (multiple) metal nanoparticles. Several different types of molecules may allow a directional excitation energy transfer like in photosynthetic light harvesting. Also the coupling strengths to the plasmon modes may be different, e.g. inside or outside of hotspots of the plasmon mode or for different relative orientations of the constituents. All these cases require a generalization to using more than one molecule type:

In order to achieve this we will sort the molecules in groups, where within each group the molecules have similar/identical coupling to the plasmon modes. A mean coupling will be assumed for each of the groups. The assumptions will be tested on full calculation of the few emitter case and for different grouping of the molecules and all different operating conditions.

3.5 Role within the Collaborative Research Centre

Collaboration with experimental projects:

- B12 (Knorr/Richter) applies a full quantum calculation of the emission of molecular-metal-hybrids investigated in B2 (Ballauff/Benson/Lu), including cooperation on optical modes with B10 (Busch).
- Results of B12 (Knorr/Richter) will be compared to experimental results of time resolved fluorescence and lifetimes of molecules located at semiconductor surfaces B3 (Blumstengel).
- Discussion, theoretical support to identify hybrid excitons in the experimental project B9 (Stähler).

Collaboration with theoretical projects:

- B4 (Körzdörfer/Scheffler/Rinke) provides ab-initio parameters (dipole moments, energy levels, partial charges and wavefunction overlap) for Bloch equations developed in B12 (Knorr/Richter).
- B10 (Busch) determines quasi normal modes of metal nanostructures, used to specify the parameters in the full quantum calculation of hybrid-quantum field interaction done in B12 (Knorr/Richter). Also, there will be an exchange of methods for the solution of Maxwell equations on the nanoscale.
- B6 (May) addresses transfer processes between molecules, nanocrystals and nanoplasmonic particles. Methods, geometry and spatial scale are complementary to B12 providing the basis for methodical exchange and cooperation.
- A7 (Klapp/Dzubiella) addresses the molecular arrangement on semiconductor surfaces, a collaboration on specific disorder realizations is planned.

3.6 Delineation from other funded projects of the principal investigators

There is no overlap with other, already supported DFG-projects, especially the focus on dynamics at hybrid interfaces and plasmonics for optoelectronic devices is not present in running projects:

- 2009–2018 DFG-Research Training Group RTG 1558: Nonlinear Collective Dynamics, project A4: The interplay of coherence and Brownian motion of colloidal quantum dots suspensions.
- 2009–2017: DFG-Collaborative Research Center CRC 658: Elementarprozesse in molekularen Schaltern an Oberflächen, project C5: Functionalized Carbon-nanostructures.This project deals with the unidirectional influence of the switching state of molecules on carbon-nanotubes.
- 2008-2015 : DFG-Collaborative Research Center CRC 787: Semiconductor Nanophotonics: project B1: Theory of photonic devices at the quantum-optical limit, application for third funding period until 2019 in preparation, focus is on selforganized GaAs/GaN quantum dot devices.
- 2011-2014: DFG-Collaborative Research Center CRC 910 Control of self-organizing nonlinear systems: project B1: Feedback control of photon statistics (approval pending for second period).

3.7 Project funds

3.7.1 Previous funding

This project is a continuation of the mesoscopic spacescale part of the previous project B4.

3.7.2 Funds requested

Funding for	2015/2		2016		2017		2018		2019/1	
Staff	Quantity	Sum	Quantity	Sum	Quantity	Sum	Quantity	Sum	Quantity	Sum
PhD student, 75%	2	44.100	2	88.200	2	88.200	2	88.200	2	44.100
Total		44.100		88.200		88.200		88.200		44.100
Direct costs	Sum		Sum		Sum		Sum		Sum	
Small equipment, Software, Consumables	1000		2000		2000		2000		1000	
Other	-		-		-		-		-	
Total	1000		2000		2000		2000		1000	
Total	45.100		90.200		90.200		90.200		45.100	

(All Figures in Euro)

3.7.3 Staff

	No.	Name, academic degree, position	Field of research	Department of university or non-university institution	Commit-ment in hours/week	Category	Funded through:
Available							
Research staff	1.	Knorr, Andreas, Dr. rer. nat., Prof.	Nonlinear optics and quantum electronics	Institut für Theo. Physik, TU Berlin	5h		Core support
	2.	Richter, Marten, Dr. rer. nat.	spectroscopy, quantum electronics, nanoplasmonics	Institut für Theo. Physik, TU Berlin	10h		Core support
	3.	Carmele, Alexander, Dr. rer. nat.	reservoir and quantum emission theory	Institut für Theo. Physik, TU Berlin	10h		Core support
Non-research staff	4.	Orlowski, Peter, Dipl.-Phys., system administrator		Institut für Theo. Physik, Technische Universität Berlin	5h		Core support
Requested							
Research staff	1.	Specht, Judith, M.Sc.		Institut für Theo. Physik, Technische Universität Berlin		Doctoral researcher 75%	
	2.	Gegg, Michael, M.Sc.		Institut für Theo. Physik, Technische Universität Berlin		Doctoral researcher 75%	

Job description of staff (supported through available funds):

1. Prof. Dr. rer. nat. Andreas Knorr

Scientific and organizational coordination of the project, exploration of the fundamental theoretical concepts and selection of methods, supervision of Ph.D. students.

2. Dr. rer. nat. Marten Richter

Scientific and organizational coordination of the project, development of new density matrix methods and coherent spectroscopy, supervision of Ph.D. students.

3. Dr. rer. nat. Alexander Carmele

Scientific support on methods of the quantum description of the light-matter interaction.

4. Dipl. Phys. Peter Orlowski

Administration of UNIX computers acquired within the CRC for numerical simulations.

Job description of staff (requested):

1. M.Sc. Judith Specht

Judith Specht is a very talented student with experience in spectroscopy of Dexter and Förster coupling. She will work on project (i), i.e. analytical and numerical work of molecule-semiconductor interfaces.

2. M.Sc. Michael Gegg

Michael Gegg is a very talented student with experience in the developed many emitter-metal nanoparticle hybrid [P10], he will continue his successful work as a PhD Student.

3.7.4 Direct costs

	2015/2	2016	2017	2018	2019/1
Funds available					
Funds requested	1000	2000	2000	2000	1000

(All Figures in Euro)

3.7.5 Major research equipment requested

€ 10.000 - 50.000 none
> € 50.000 none

3.7.6 Student assistants

	2015/2	2016	2017	2018	2019/1
Quantity	0	0	0	0	0
Commitment in hours/week	0	0	0	0	0
Sum	0	0	0	0	0
Tasks					

3.1 About project B13

3.1.1 Title: Monolithic inorganic/organic optoelectronic devices

3.1.2 Research areas: Device Physics

3.1.3 Principal investigator

Ao.Univ.-Prof. DI Dr techn. Emil J.W. List-Kratochvil (*8.11.1971, Austria)
NanoTecCenter Weiz Forschungsgesellschaft mbH, Franz-Pichler Strasse 32, A-8160 Weiz
Phone: +49 (0) 316 873 8000
Fax: +49 (0) 316 873 8060
E-mail: emil.list-kratochvil@ntc-weiz.at

Does the above mentioned person hold fixed-term positions? No

3.1.4 Legal issues

This project includes

1.	research on human subjects or human material.	No
	A copy of the required approval of the responsible ethics committee is included with the proposal.	No
2.	clinical trials	No
	A copy of the studies' registration is included with the proposal.	No
3.	experiments involving vertebrates.	No
4.	experiments involving recombinant DNA.	No
5.	research involving human embryonic stem cells.	No
	<If applicable:> Legal authorization has been obtained.	No
6.	research concerning the Convention on Biological Diversity.	No

3.2 Summary

To meet the demands for organic light emitting diode (OLEDs) in lighting applications the current R&D efforts are directed towards a) the development of novel more stable and more efficient emitter materials, b) cost effective large area based fabrication processes, and c) novel environmental stable anode and cathode materials. For inorganic light emitting diodes (LEDs) R&D efforts focus on d) improving external colour conversion efficiencies and colour quality, and e) the thermal management of LEDs to improve the overall efficiency and allow for high power LEDs with a luminous fux > 300 lm. Based on the expertise gained on optically pumped HIOS Förster-type resonant energy transfer (FRET) systems and HIOS based injection systems, two approaches to realize monolithic HIOS based optoelectronic devices so called hybrid LEDs (HyLEDs) have been envisaged: FRET-HYLEDs and INJECTION-HyLEDs. Both approaches are addressing many deficiencies identified for OLEDs and LEDs. In fact it is the general working hypothesis in this proposal that using HIOS in instead of focusing on solving the named deficiencies of LED and OLEDs or white light emitting OLEDs (WOLEDs) separately it is possible to realize HyLEDs giving the stability of inorganic devices, with high conversion efficiencies, high colour rendering index and the potential for high frequency modulation capability.

FRET-HyLEDs: A main deficiency of WOLED technology is the limited overall stability of the blue emitter. While for LEDs limitations due to external colour conversion and thermal management limitations are the main drawbacks. To overcome all of this limitations it is proposed to combine the inorganic LED technology with organic conversion or downshifting layers. However, instead of using external colour conversion, where the organic layer is deposited on-top of the LED dye we propose to embed the organic conversion layer in the inorganic LED structure. By this means it is possible to utilize a HIOS FRET system to pump the organic layer very efficiently. This is achieved by excitation of the organic layer via FRET from the LED or by direct carrier injection into the organic emissive layer. Such an approach is possible as has been jointly shown by Blumstengel (A3), Henneberger (A5), Koch (A8), Hecht (A3) using ladder-type oligo-phenyl based emitters

(LOPPs) on ZnO, which has been modified to attain type I energy level alignment achieving a optically pumped HIOS FRET system.

Injection-HyLEDs: Using HIOS based injection systems for HyLEDs will address mainly OLED related issues. HIOS based injection systems will address the quest for novel anode and cathode as well as HIL and EIL in OLEDs and will allow for using ZnO as universal electrode material in OLEDs also addressing the need for ITO free devices.

3.3 Research rationale

3.3.1 Current state of understanding and preliminary work

A) State of the Art

General motivation: More than 20% of the world's total electricity consumption is used for lighting applications and an estimate of 25% when including display and TV applications. [1] Therefore innovative, cost and energy effective solutions for lighting (and display) applications are in the focus of an on-going intense world wide and European effort in the field of photonics research and development activities (see European TP Photonics21 www.photonics.eu). Since the first discovery of bond fires by homo erectus 400.000 BC, lighting technologies have been developed stepwise from early oil pottery lamps, candle light and gas based lighting all through to today's used electricity based lighting systems including the tungsten filament lamp, fluorescent lamps and solid state lighting technologies. In particular organic light emitting diodes (OLED) as well as inorganic solid state lighting technologies (LED) are the most promising candidates for the lighting revolution of the 21st century with the potential to safe hundreds of GWh or millions tons of coal/year if put in place.

Deficiencies in OLED and LED devices: Despite the fact that both device technologies concepts, OLEDs and LEDs, are already established in the market there is an on-going R&D effort towards the improvement in performance of such devices with respect to an improved overall efficiency, emission colour stability, overall improved lifetime and most of all towards lower cost of fabrication to compete with the according figures for incandescent and fluorescent based lighting systems. (see Figure 1).

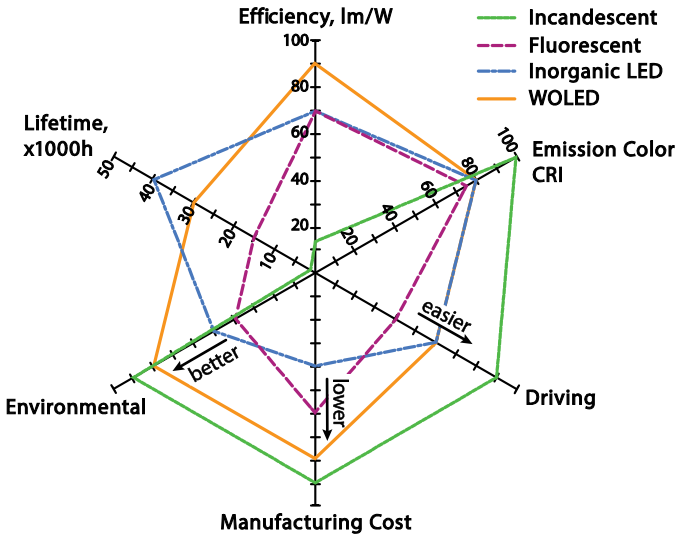

Figure 25. Semiquantitative comparison of the key performance parameters of white organic light emitting diodes (WOLED) relative to incandescent lamps, fluorescent tubes, and inorganic white LEDs. (taken and modified from Ref [2])

To meet the demands for OLEDs in lighting applications the current focus of research and development (R&D) efforts are mainly directed towards a) the development of novel more stable and more efficient emitter materials, b) cost effective large area based fabrication processes, and c) novel environmental stable anode

and cathode materials. In inorganic LEDs R&D efforts focus on d) improving external colour conversion efficiencies and colour quality, and e) the thermal management of LEDs to improve the overall efficiency and allow for high power LEDs with a luminous fux > 300 lm. Moreover there is a quest for LEDs allowing for higher modulation frequencies. As discussed in the following state of the art sections, many issues currently addressed in R&D for OLEDs as well as for inorganic LEDs may be jointly solved, when considering novel hybrid inorganic organic material systems (HIOS) as developed in the SFB in the first period, instead of addressing the deficiencies separately for OLED and LED technologies. Therefore it is proposed to utilize HIOSs in two general ways by I) realizing hybrid LEDs (HyLEDs) based on Förster Resonant Energy Transfer (FRET) as developed by Blumstengel (A3), Henneberger (A5), Koch (A8), and Hecht (A3) jointly addressing the deficiencies a), d), e), f) in **FRET-HyLED** and II) using newly developed HIOS based injection layers for OLEDs addressing the open issue c) and to a limited amount also b) in **INJECTION-HyLEDs**. Realizing such devices will allow for white light emitting HIOS based HyLEDs, which combine the efficiency of traditional inorganic LED solid state lighting with the ability of fast modulation further paving the way for wireless visible light communication applications (Li-Fi). [3]

State of the Art OLEDs and WOLEDs: Since the first demonstration of an efficient OLED by Tang et al. [4], several developments in the field of organic semiconductors led to the establishment of OLEDs as a competitive technology for lighting- and display applications. OLEDs may already be found in the displays of consumer products like smartphones as well as tablet PCs and companies such as Osram and Phillips are preparing white OLED panels for mass-market lighting applications at the time of writing. While many of the following arguments are also true for OLEDs to be used in display applications, given the focus of this proposal a clear focus is put on the state of the art of OLEDs for lighting applications so called white light emitting OLEDs, WOLEDs. In terms of lighting technology it can be stated that the basic performance of WOLEDs was significantly improved in recent years. This is partly due to drastically improved emitter material concepts, device architectures as well as effective photonic concepts boosting the out coupling efficiency, in such devices reaching highly efficient WOLEDs with efficiencies with up to 102 lm/W at 1000 cd/m^2 [4] and up to 124 lm/W at 1000 cd/m^2 for improved out coupling under lab conditions. [2]

In principle there are a number of different concepts used to realize WOLEDs covering the emission in the visible spectrum from 400nm to 800 nm, as depicted in Figure 2. In practice, in order to achieve white emission, mixtures of the three red, green, and blue (RGB) primary colours or two complementary colours are typically required. However, to ensure a high colour quality of lighting source i.e. a good colour rendering indices (CRI) the use of three colours is to be preferred.

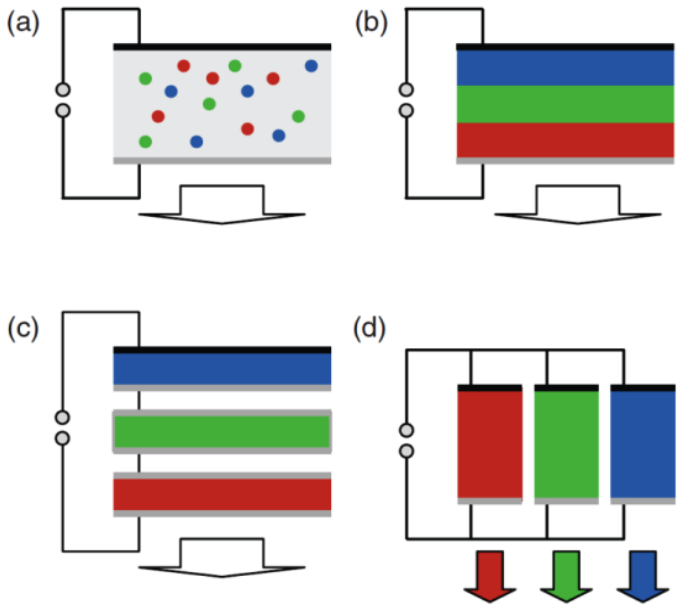

Figure 2: White light generation in OLEDs by means of a) internal color conversion using a blend of different blue, green, red emitting emitters b) a hetero structure comprising a stack of differently emitting materials c) a stack of individual vertically stacked OLEDs, and d) individual spatially separated OLEDs.

As depicted in Figure 2a, the simplest implementation of a WOLED is based in internal colour conversion using FRET and charge carrier trapping effects in a blend of several emitters in one emitting layer combining

blue or UV light emitting host materials doped with green and red emitting molecules. For efficient injection this combination is usually supported by additional electron or hole injecting layers at the electrodes, but there are also simple single-layer WOLED devices possible. Typically one uses phosphorescent materials as the green and red dopants and fluorescence as well as phosphorescent materials as the blue or UV emitting host. [5] The main challenge with this approach is to attain good colour stability for different brightness levels of the device since one has to balance FRET and carrier trapping based contributions from the guest molecules. As a second approach (Figure 2b) one uses a layered series of blue, green and red emitting layers. The challenge in this type of WOLED is mainly in the realization of a balanced emission from the different emitter layers, and thus in setting the desired emission colour. This problem is often addressed by the implementation of hole and electron blocking layer between the active layers requiring a more complex process flow. A third approach consists of stacking of complete OLEDs (Figure 2c) with different emission characteristics. This strategy aims to increase the power efficiency of WOLED: Instead of a maximum of one photon per injected charge carrier one obtains more photons per unit charge. The interconnection generally also leads to higher operating voltages. Using spatial multiplexing WOLEDs (Figure 2d) are realized fabricating red, green and blue emitting pixels. The general advantage of this method lies in the differential addressability of single-pixel, allowing for an active control of the colour temperature, while the main disadvantage of this method arises from the generally very complex manufacturing process of the WOLEDs. While all four approaches are being followed currently the best efficiencies are reported for WOLEDs using the configuration a) with a combination of blue, green and red phosphorescent emitters yielding a power efficacy of more than 102 lm/W at 1000 cd/m^2. [5]

a) Long-term stability: Despite these achievements long term stability of organic lighting devices does not yet meet market demands. This is because white light is a balanced blend of blue, green and red light. Regardless of the concept used this requires highly stable blue emitting materials. While intense research has led to well established active emitters (both small molecules and conjugated polymers) for the red and green spectral range with lifetimes of more than 350.000h for green emitting materials and 200.000h [4], up to date there is a still a quest for stable, highly efficient and easy to synthesise molecules emitting light in the deep blue wavelength range. Currently the lifetime of blue emitting materials is only found to be in the range of 20.000 h and 35.000h for fluorescent and phosphorescent materials, respectively [5]. Given the fact that an intrinsic problem of chemical instabilities due to an unbalanced interaction of excited states [7] and undesirable interactions of excited states with oxygen cause this limitation, this problem may only be solved on the molecular level by novel ground-breaking innovative molecular material design concepts and not by a specific technological device designs or any encapsulation technique.

b) Cost of large area fabrication: In general, the fabrication of an OLED involves the deposition of at least one organic layer on top of a transparent conductive oxide (TCO), typically indium tin oxide (ITO), which serves as the anode. The cathode is usually deposited under vacuum and consists of a low work function metal such as Ca or Ba bringing intrinsic instabilities due to their chemical reactivity. To date the existing procedures for the deposition of the organic layers are either based on vacuum sublimation of small molecules or on the deposition of conjugated polymers or soluble small molecules from solution. Contemporary OLED devices are built using vacuum sublimation techniques which, compared to wet chemical processes like spin- or dip-coating, roll-to-roll processing and inkjet printing, suffer from the need for sophisticated instruments, substantial material waste and low throughput. Additionally, in the case of OLED displays, pixilation via shadow masks limits the scalability and resolution of vacuum sublimation. Even though wet chemical processes present a significant advantage in terms of lower manufacturing costs, the performance of devices build this way still trail vacuum sublimated OLED devices. While the deposition aspect of large area fabrication will not be addressed in the following in detail it is worth noting that the use of ITO as transparent anode does have a huge impact on the total cost for large area devices. With this respect proper replacements, such as ZnO based electrodes developed in the SFB may have a huge impact on lowering cost for large area OLED devices.

c) Alternative electrodes and or hole and electron injection layers: In a conventional double-hetero OLED structure an organic emission layer (EML) is arranged between of an organic hole and electron transport layer (HTL and ETL) with ITO and a metal contact acting as the anode and cathode, respectively. As an alternative to organic ETL and HTL transport layers, a series of transition metal oxides (ZnO, NiO, MoO_3 etc.) have been tested to facilitate as injection layers as well as alternative to the anode and cathode materials used. As it has been studied within the SFB it is possible to tune the work-function of such transition metal oxides (ZnO) over a wide range using self assembled monolayers (SAMs) so that both electron and hole injection in OLEDs may be facilitated using the same material, which will clearly offer not only an advantage in processing but also a big advantage over the todays used cathode materials (Ca, Ba, etc.) which show inherent instabilities due to their inherent chemical reactivity.

State of the art inorganic LEDs: As a very rapid developing technology, white light emitting inorganic LEDs (WLEDs) based on inorganic semiconductor dyes and inorganic phosphor layers for solid-state lighting are also a very attractive technology. Following the concept of external colour conversion WLEDs are realised by the heterogeneous combination of an inorganic LED dye (in many cases GaN or InGaN based) and an external conversion layer consisting of one or more inorganic YAG based phosphor materials embedded in a transparent matrix.

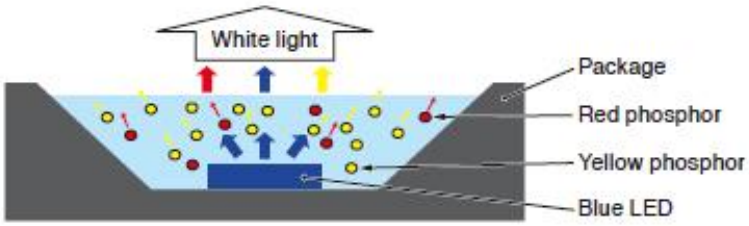

Figure 3: Conventional inorganic with light emitting diode LED using external color conversion green and red emitting containing phosphor embedded in matrix.

The power efficacy of WLEDs has surpassed that of linear florescent lamps (108 lm/W) and their colour quality has significantly improved. WLED for warm-white light with a colour temperature of 3500 K and a luminous efficacy of up to 118 lm/W have been reported. [6] As a result of this, WLEDs can already been found in the market and have been used in many lighting applications, traffic signal lights, backlight TV applications and portable light sources. However, also WLED technology is facing challenges, where the following two addressed in detail:

d) Limitations due to external colour conversion: The conversion efficiency of phosphors used in WLED technology is found to be in the range of 65%-67%. This is due to the fact that in WLED technology the down conversion of light from blue to green and red is realized by photon pumping from the inorganic dye and subsequent reabsorption in the phosphor. Furthermore the quantum yield of the most common todays used phosphor systems, such as Ce^{3+}:YAG systems is limited to ca. 70 %. [8] Achieving WLEDs with a high CRI index and a low emission colour variation for the emitting angle requires sophisticated and costly strategies for designing and realizing the external conversion layer, so that it is ensured that fro all optical pathways one finds the same conversion ratio between the blue light emitted by the dye and the yellow light emitted by the phosphor. Moreover given the long decay time of phosphors used the ability to modulate WLEDs with significant high frequencies is limited.

e) Thermal management issues: The overall external quantum efficacy of WLEDs is strongly depended on the operation temperature and it strongly deceases with increasing temperature. Therefore improvments in the thermal management of WLEDs have lead to drastic improvements in the overall external quantum efficacy. The thermal management of WLEDs is mainly achieved by placing the inorganic dye on a substrate, which acts as a heat-sink cooling the dye. However, this approach cannot be used to dissipate the heat in the conversion layer, which causes significant problems in high power devices for the luminous flux found to be > 300lm. Here heating in the conversion layer leads to significant losses and degradation effects. [8]

B) Preliminary work

No preliminary work was performed in this project since it did not exist in the first funding period. The realisation of HyLEDs as proposed in the proposal is triggered and to a large extent based on findings and results from the first SFB funding period. The essential basic scientific ideas and work to be further used for the proposed HyLEDs device research is based on following key findings in the SFB:

a) Blumstengel (A3), Henneberger (A5), Koch (A8), Hecht (A3) showed that Förster-type resonant energy transfer (FRET) is possible from an inorganic material (ZnO). It was demonstrated that ladder-type oligo-phenyl based emitters (LOPPs) on ZnO may be optically pumped when self assembled monolayers (SAMs) are used to attain type I energy level alignment to yield a HIOS FRET system.

b) Blumstengel (A3) and Henneberger (A5) have realized the growth of ZnO on organic layers, without harming the organic layer and attaining good conduction properties of the ZnO.

c) Koch (A8), Blumstengel (A3) and Henneberger (A5) as well as Neher (B7) have demonstrated that the workfunction of ZnO may be modified using phosphonate based SAMs to use ZnO as election as well as hole injection layer in OLEDs.

References:

[203] I.L. Azevedo, M.G. Morgan, and Fritz Morgan, Proceedings of the IEEE **97**, No. 3, March 2009.
[204] S. Reineke, F. Lindner, G. Schwartz, N. Seidler, K. Walzer, B. Lüssem, et al., Nature. **459**, 234 (2009).
[205] D. K Borah, et al. Journal on Wireless Communications and Networking, 2012:91, (2012)
[206] C. W. Tang, S. Van Slyke, Appl. Phys. Lett. **51**, 913 (1987).
[207] http://www.universaldisplay.com/, 7.10.2014.
[208] http://energy.gov/eere/ssl/solid-state-lighting, 7.10.2014, Manufacturing Roadmap Solid-State Lighting Research and Development
[209] M. Pope, C. E. Swenberg, New York: Oxford University Press (1998).
[210] C. Sommer, et al. Opt. Matter. **31,** 837 (2009)

3.3.2 Project-related publications

[211] J. Kofler, K. Schmoltner, A. Klug and E.J.W. List-Kratochvil ”Sensitive and robust electron beam lithography lift-off process using chemically amplified positive tone resist and PEDOT:PSS as a protective coating” J. of Micromech. and Microeng. **24**, 095010 (2014)
[212] R. Trattnig, L. Pevzner, M. Jäger, R. Schlesinger, M. V. Nardi, G. Ligorio, C. Christodoulou, N. Koch, M. Baumgarten, K. Müllen, and E. J.W. List, “Bright blue solution processed triple-layer polymer light emitting diodes realized by thermal layer stabilization and orthogonal solvents”, Adv. Funct. Mater., **23**, 4897 (2013)
[213] S. Nau, N. Schulte, S. Winkler, J. Frisch, A. Vollmer, N. Koch, S. Sax, E. J. W. List, ”Highly Efficient Color-Stable Deep-Blue Multilayer PLEDs: Preventing PEDOT: PSSInduced Interface Degradation”, Adv. Mater. **25**, 4420, (2013)
[214] E. J. W. List, N. Koch, “Focus Issue: Organic light-emitting diodes–status quo and current developments”, Opt.Exp. **19**, A1237, (2011)
[215] E. Fisslthaler, M. Sezen, H. Plank, A. Blumel, S. Sax, W. Grogger, and E. J. W. List, "Direct Sub-Micrometer-Patterning of Conjugated Polymers and Polymer Light-Emitting Devices by Electron Beam Lithography," Macromol Chem Physic **211**, 1402 (2010).
[216] S. Sax, N. Rugen-Penkalla, A. Neuhold, S. Schuh, E. Zojer, E. J. W. List, and K. Mullen, "Efficient Blue-Light-Emitting Polymer Heterostructure Devices: The Fabrication of Multilayer Structures from Orthogonal Solvents," Adv Mater **22**, 2087 (2010).
[217] S. Sax, E. Fisslthaler, S. Kappaun, C. Konrad, K. Waich, T. Mayr, C. Slugovc, I. Klimant, and E. J. W. List, "SensLED: An Electro-Optical Active Probe for Oxygen Determination," Adv Mater **21**, 3483 (2009)) also featured in Nature Photonics, 3, 439, (2009)
[218] M. Gaal, C. Gadermaier, H. Plank, E. Moderegger, A. Pogantsch, G. Leising, and E. J. W. List, "Imprined conjugated polymer laser," Adv Mater **15**, 1165 (2003).
[219] U. Scherf and E. J. W. List, "Semiconducting polyfluorenes - Towards reliable structure-property relationships," Adv Mater **14**, 477 (2002).
[220] S. Tasch, E. J. W. List, O. Ekstrom, W. Graupner, G. Leising, P. Schlichting, U. Rohr, Y. Geerts, U. Scherf, and K. Mullen, "Efficient white light-emitting diodes realized with new processable blends of conjugated polymers," Appl Phys Lett **71**, 2883 (1997).

3.4 Research plan

3.4.1 Issues to be addressed and goals

General hypothesis: The challenge to realize monolithic HIOS optoelectronic devices is that the realization of an ideal double hetero inorganic/organic/inorganic structures is hampered by the possibility to epitaxially grow high quality inorganic top layers on-top of the organic second layer to realize injection based devices in a sandwich configuration. Therefore two other approaches to realize monolithic HIOS based optoelectronic devices have been envisaged. Both approaches are addressing many deficiencies identified for OLEDs and LEDs in the section above. In fact it is the general working hypothesis that using HIOS in instead of focusing

on solving the named deficiencies of WOLED and WLEDs separately it is possible to realize HyLEDs giving the stability of inorganic devices, with high conversion efficiencies, high CRI and the potential for high frequency modulation capability.

FRET-HyLEDs: A main deficiency of WOLED technology is the limited overall stability of the blue emitter. While for WLEDs limitations due to external colour conversion and thermal management limitations are the main drawbacks. To overcome all of this limitations it is proposed to combine the inorganic LED technology with organic conversion or downshifting layers. However, instead of using external colour conversion, where the organic layer is deposited on-top of the LED dye we propose to embed the organic conversion layer in the inorganic LED structure. By this means it is possible to utilize a HIOS FRET system to pump the organic layer very efficiently. Such a FRET-HyLED will have the following advantages over WOLEDs and WLEDs addressing most of the listed deficiencies:

a) using FRET for pumping the organic layer is per definition more efficient than any photon pumping process as used in WLEDs

b) using FRET from a blue light emitting LED in a HyLED does help to overcome the limitation in lifetime in OLED due to the limitation of the blue emitter

c) placing the organic conversion layer inside the LED structure does overcome the angular dependency in the emission characteristics as found in WLEDs

d) placing the organic conversion layer inside the LED structure does allow for a fast modulation of the HyLED when using florescent organic emitters

e) placing the organic conversion layer inside the LED structure does allow for a good thermal management of the overall device, since the conversion layer is in good thermal contact with the LED dye.

The fabrication and investigation of hybrid emission FRET-HyLEDs will be done in close collaboration with Blumstengel (B3) and Henneberger (B5) and Koch (B8). Effectively, first proof of concept devices HyLED-Type I will be fabricated by Blumstengel (B3) based on using a commercial GaN structure and ladder-type oligo-phenyl based emitters (LOPPs) from Hecht (A3) as depicted in Figure 4 using organic emitter layers with a lateral dimension in the µm range using regular shadow masks. Note that the devices will be fabricated according to the process described in the section 3.3.2 Methods, where also a description of the fabrication of the nano-proximity shadow mask may be found.

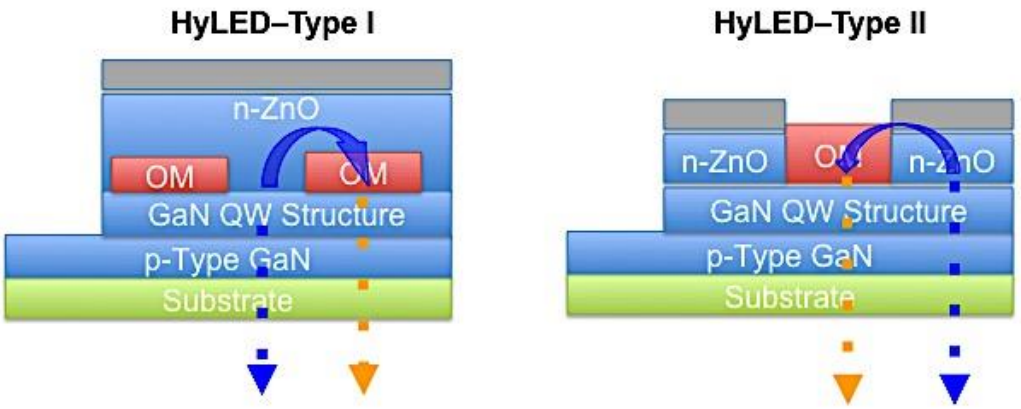

Figure 4: HyLED-Type I and II devices utilizing FRET (description see text)

Following first prove of concept studies undertaken jointly with the project Blumstengel (B3) using type I devices also type II devices will be fabricated and characterised. Both device concepts follow the same principle ie. FRET from the GaN quantum well structure to the organic emitter, but in case of the HyLED Type II there is no growth process of the ZnO on the organic emitter and the ZnO layer is structured. This second concept was chosen to address possible degradation processes during the ZnO growth on-top of the organic layer as well as a fall back scenario if the deposition of the organic materials using the nano-shadow mask may not lead to the desired resolution.

Questions to be addressed for FRET-HyLEDs:

a) determining the optimal device geometry for a maximised FRET: FRET is strongly distant dependent – therefore is a key requirement to minimize the distance between the origin of the emission in the GaN QW structure and the organic emission layer. This issue is addressed by using a so called nano-proximity shadow mask in the case of HyLED type I to deposited the organic layer from a PVD process. Alternatively the organic emitter may be structured directly using e-beam lithography. Such a process has been realized using ladder-type oligo-phenyl based emitters by the PI (see reference 16). As an alternative direct patterning of the inorganic device structure HyLED type II may be done by focused ion beam or e-beam lithography followed by subsequent deposition of the organic layer. Note that the organic layer may be deposited covering the entire device in this case, which should, however, not harm the functional principle since the organic layer is separated by a metallic layer from the rest of the device.

b) determining the a optimal FRET HIOS system for white light emission: Optimising the FRET HIOS for white light emission will be done by using appropriate green to orange light emitting organic molecules. Following first studies with commercially available green and orange emitters proper organic systems will be synthesised in the Hecht (Z1) project. Most probable perylene type emitters or ladder-type oligo-phenyl based emitters baring deliberately introduced ketonic groups will be used.

c) overall device performance: following the steps of optimised device geometry and optimised FRET HIOS for white light emission CRI and modulation speed will be optimised.

Injection-HyLEDs: Using HIOS based injection layers for HyLEDs will address mainly OLED related issues. Such Injection-HyLED will have the following advantages over conventionally fabricated OLEDs:

a) HIOS based injection layers will address the quest for novel anode and cathode as well as HIL and EIL in OLEDs (deficiency c)

b) HIOS based injection layers will to a limited amount also address deficiency b) since the targeted use of ZnO as universal electrode material in OLEDs also addressed the need for ITO free devices.

For the fabrication and investigation of injection HIOS based HyLEDs essentially the same approach described above will be followed with the sole difference that the lithographic structuring will be done in such a manner that a proper 50-200 nm gap is formed between the inorganic semiconductor forming the anode and cathode. Based on the findings from Koch (A8), Blumstengel (A3) and Henneberger (A5) as well as Neher (B7) the work-function of ZnO may be modified using phosphonate based SAMs to use ZnO as election as well as hole injection layer in OLEDs. To study the injection process and limitations of injection LOPP based emitters will be deposited in the gap/channel and energy level alignment issues will be addressed using SAMs in cooperation with Koch (B8). As an alternative using a classical sandwich device configuration will also be studied as depicted in Figure 5 entitled HyLED-Type IV.

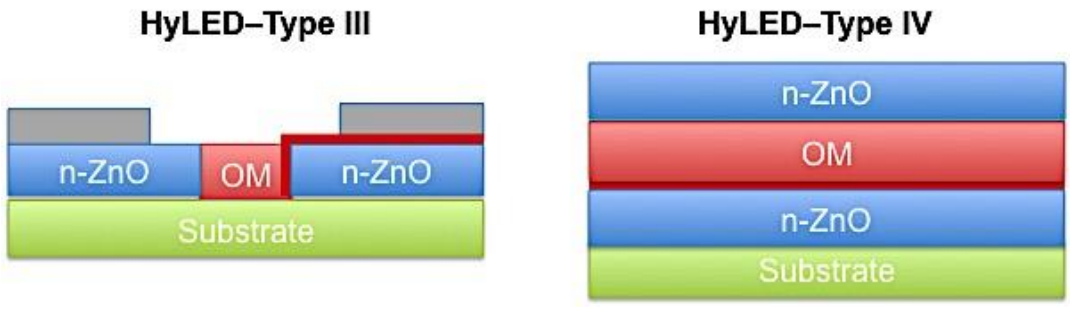

Figure 5: Injection HYLED-Type III and IV devices (description see text)

Questions to be addressed for Injection-HyLEDs:

a) determining the optimal device geometry to maximised injection of current: using Type III HyLEDs is the attempt to realize surface cell type OLEDs, which can be operated under high current densities. For this means the SAMs, effectively controlling the charge injection process will be chosens such, that a balanced hole and electron injection is secured, yielding an emission zone localized in the centre of the device. Besides the investigation with respect to all relevant parameters in this case we

also plan to include resonator structures at a later stage (eg. distributed feedback structures (DFB)) in the gap/channel region to test such configurations for LASER action. The DFB may be included in the substrate area or can also be inscribed in the organic layer. Both options will be tested based on imprint based fabrication processes (see ref. 16. For details).

b) realize fully transparent OLED based on all ZnO based electrodes: Type IV HyLEDs are fabricated with the aim to realize all transparent based on ZnO based air stable electrodes. This concept is addressing the pursuit to realize low cost simple to fabricate OLEDs.

c) investigate optically switchable SAMS from Hecht (A3) in Type IV HyLEDs: Hecht (A3) will develop optically addressable dipolar SAMs, which will allow for tuning the dipole moment by an optical stimulus. Such SAMS will be tested in prove of principle devices of Type IV HyLEDs. It is the aim to demonstrate the basic effect that the injection in the OLED may be locally controlled by an external light stimulus.

3.4.2 Methods

e-beam lithography: To structure the organic emitter in the HyLED type I device at a feature size below 20 nm nano-proximity shadow masks will be developed and used. Based on a regular PMMA e-beam resist process or a chemically amplified positive tone resist (see ref. 12 for further details) such a mask may be fabricated using e-beam lithography on PEDOT:PSS as release layer. First examples of such a nano-proximity shadow mask may be found in Figure 8. Based on the process available at NTC Weiz such masks will allow for feature sizes of below 20 nm and a size of 2x2 mm may be fabricated.

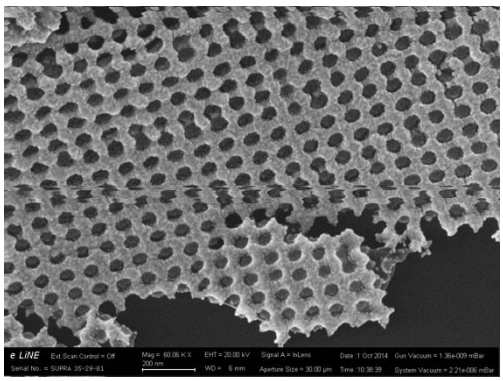

Figure 8: PMMA nano-proximity shadow mask with a dot size of ca. 35 nm.

Device Preparation and characterisation: HyLED Type I and II devices will be prepared by using commercial p-type GaN/GaN Quantum well structures, which are appropriately structured by photolithography and reactive ion etching (RIE) to allow for contacting of the p-type GaN. The deposition of the organic emitters will be done by physical vapour deposition (PVD) using a nano-proximity shadow mask, which will be developed in the project (see e-beam section below). The growth of n-ZnO will be preformed in project Blumstengel (A3). The deposition of SAMs to ensure for type I band-alignment of the organic emitter and the GaN QW will be done if necessary. Type I and II HyLEDs will be characterised for IV and electroluminescence behaviour. Particular attention will be given to determining the external quantum efficiency (EQE), the emission characteristics as a function of emission angle and the CRI.

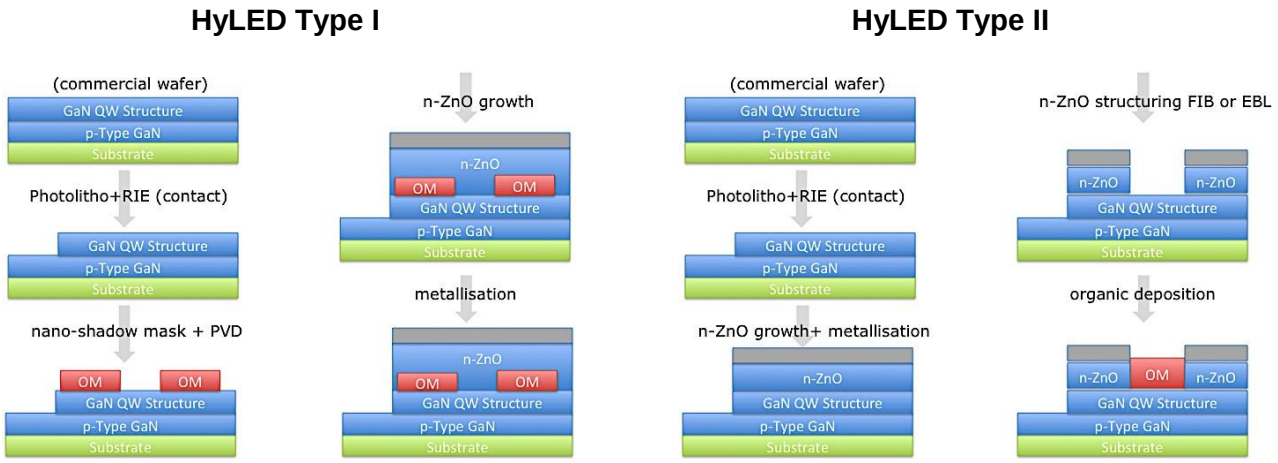

Figure 6: Preparation process for HyLEDs Type I & II (description see text)

HyLED Type III devices will be prepared by using n-type ZnO layers, which are appropriately structured by e-beam lithography to from the lateral gap in the device. The deposited SAMs will allow for using one electrode as the anode or hole injection electrode and the other one as the cathode or electron inject layer. Type III HyLEDs will be characterised for IV and electroluminescence behaviour. Particular attention will be given to study the charge injection processes in cooperation with (B3) Neher in addition to determining the external quantum efficiency (EQE).

HyLED Type IV devices will be prepared by using highly doped n-type ZnO layers, which are appropriately structured form making contacts. The deposited SAMs will allow for using the electrode as the cathode. After the deposition of the SAM an appropriate organic layer stack will be deposited. ZnO deposited on-top will also act as hole injection electrode yielding a transparent device. Type IV HyLEDs will be characterised for IV and electroluminescence behaviour. Particular attention will be given to study the charge inject process in addition to determining the external quantum efficiency (EQE).

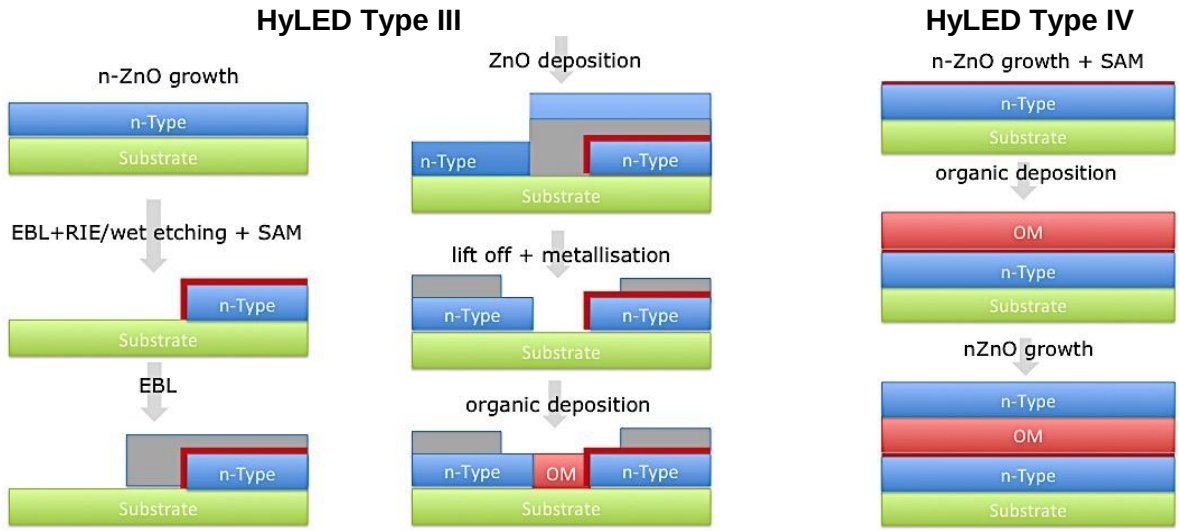

Figure 7: Preparation process for HyLEDs Type III & IV (description see text)

3.4.3 Work programme and timeline

The work program is divided into activities towards FRET-HyLEDs and Injection-HyLEDs. The overall effort in personal resources, which are 2 full time PhD students, will be split half-half with respect to the effort towards realizing the two different device types.

FRET-HyLEDs:

Y1 goal: realize a prove of concept HyLEDs Type I & II; **work to be done:** develop fabrication process for Type I & II devices; develop nano-proximity shadowmask process; Study the FRET for different HIOS
Y2 goal: determining the optimal device geometry for maximised FRET; **work to be done:** compare and optimize FRET in Type I & II devices; improve the fabrication process; study the FRET for different HIOS
Y3 goal: determining the a optimal FRET HIOS system for white light emission; **work to be done:** study the FRET for different HIOS and optimize for whilte light emission
Y4 goal and work to be done: improve overall device performance

Injection-HyLEDs:

Y1 goal: realize a prove of concept device based on HyLEDs Type III & IV**; work to be done:** develop basic fabrication process for Type III & IV devices;
Y2 goal and work to be done: determining the optimal device geometry in Type III HyLEDs
Y3 goal and work to be done: realize fully transparent OLED based on all ZnO based electrodes
Y4 goal and work to be done: investigate optically switchable SAMS from Hecht (A3) in Type IV HyLEDs

3.5 Role within the Collaborative Research Centre

Both topics FRET- and Injection-HyLEDs will be addressed in a concerted activity with B3 (Blumstengel) studying the inorganic components and characterizing the optical properties, respectively. Moreover the first prove of concept devices for FRET-HyLEDs will be jointly fabricated and characterized. A3 (Hecht) will be addressing modifying LOPP type emitters, SAM based molecular switches and provide tailor made preylene type emitters from (Z1). Moreover A5 (Henneberger), and B3 (Blumstengel) will perform the ZnO growth for both FRET- and Injection-HyLEDs. In collaboration with A8 (Koch) this project will studying and tuning the interface properties of SAM for modified electrodes in Injection-HyLEDs, while studying the injection process of carriers will be done jointly with B7 (Neher).

3.6 Delineation from other funded projects of the principal investigator

NTC Weiz GmbH is currently carrying out a number of projects from different funding agencies such as the EC (FP7 and H2020), the FFG and the FWF. Most projects are directed towards applied research activities with the focus on developing novel printing and coating technologies for electronics and photovoltaic industry. Currently the PI has one OLED related project focusing on the out-coupling improvement in OLEDs using plasmonic structures (PLASMOLED), which does not overlap with the proposal presented here.

3.7 Project funds

3.7.1 Previous funding

The PI has no previously funded project with the DFG.

3.7.2 Funds requested

Funding for	2015/2		2016		2017		2018		2019/1	
Staff	Quantity	Sum	Quantity	Sum	Quantity	Sum	Quantity	Sum	Quantity	Sum
PhD student, 75% FWF based	2	35.900	2	71.800	2	71.800	2	71.800	2	35.900
Total		35.900		71.800		71.800		71.800		35.900
Direct costs	Sum		Sum		Sum		Sum		Sum	
Small equipment, Software, Consumables	15.000		20.000		20.000		20.000		10.000	
Other	-		10.000		10.000		10.000		5.000	
Total	15.000		30.000		30.000		30.000		15.000	
Major research equipment	Sum		Sum		Sum		Sum		Sum	
€ 10.000 - 50.000	17.500		17.500		-		-		-	
> € 50.000	-		-		-		-		-	
Total	17.500		17.500		-		-		-	
Total	68.400		119.300		101.800		101.800		50.900	

(All figures in Euro)

3.7.3 Staff

	No.	Name, academic degree, position	Field of research	Department of university or non-university institution	Commitment in hours/week	Category	Funded through:
Available							
Research staff	1	List-Kratochvil	Physics	NTC Weiz GmbH	5h/week		Grund.
	2	Sebastian Nau	Physics	NTC Weiz GmbH	5h/week		Grund.
Non-research staff	-	-		-	-		-
Requested							
Research staff	3	N.N.	Physics	NTC Weiz GmbH		Student	
	4	N.N.	Physics	NTC Weiz GmbH		Student	
Non-research staff	-	-		-		-	

Job description of staff (supported through available funds):
1-Emil J.W. List-Kratochvil, scientific supervision of the project, supervision of the PhD students
2-Sebastian Nau, supervision of the students in the laboratory, assistance in writing scientific publications and discussion of results.

Job description of staff (requested):
3-N.N. Ph.D. Student – With a focus on FRET based HyLEDs, preparation and characterisation of devices
4-N.N. Ph.D. Student – With a focus on Injection based HyLEDs, preparation and characterisation of devices

3.7.4 Direct costs

	2015/2	2016	2017	2018	2019/1
Funds available	-	-	-	-	-
Funds requested	15.000	30.000	30.000	30.000	15.000

(All figures in Euro)

Note that NTC Weiz GmbH will provide the total laboratory infrastructure, the office place, PC and all running costs for equipment including maintenance of equipment. A detailed breakdown can no be given.

Consumables for 2015/2

Laboratory consumables: Substrates, Resist, GaN wafers, Metals (Au), organic semiconductors, other chemicals	EUR	15.000

Consumables for 2016-2019

Laboratory consumables: Substrates, Resist, GaN wafers, Metals (Au), organic semiconductors, other chemicals, cost for publishing in open access journals	EUR	20.000
Other, subcontracting work for on demand FIB preparation of devices; This work can only be done externally at Center for Electron Microscopy – TU Graz	EUR	10.000

Consumables for 2019/1

Laboratory consumables: Substrates, Resist, GaN wafers, Metals (Au), organic semiconductors, other chemicals, cost for publishing in open access journals	EUR	15.000

3.7.5 Major research equipment requested

€ 10.000 - 50.000 for 2015/2 and 2016

Measurement cell for the characterisation of HYLEDs outside the glove box, which include fibre optical feed-through (essential peace of equipment which does not exist in this form)	EUR	17.500
Second measurement cell for the characterisation of HYLEDs outside the glove box, which include fibre optical feed-through (	EUR	17.500

3.7.6 Student assistants

	2015/2	2016	2017	2018	2019/1
Quantity	0	0	0	0	0
Commitment in hours/week	-	-	-	-	-
Sum	-	-	-	-	-
Tasks	-				

3.1 About project Z1

3.1.1 Title: Custom-synthesis of conjugated organic molecules

3.1.2 Research areas: Molecular chemistry

3.1.3 Principal investigator

Prof. Stefan Hecht, Ph.D. (*06.01.1974, German)
Humboldt-Universität zu Berlin, Department of Chemistry (HU Chem)
Brook-Taylor-Str. 2, 12489 Berlin
Phone: +49 (0)30 2093 7365
Fax: +49 (0)30 2093 6940
E-mail: sh@chemie.hu-berlin.de

Does the above mentioned person hold a fixed-term position?
Yes

3.1.4 Legal issues

This project includes

1.	research on human subjects or human material.	no
	<If applicable:> A copy of the required approval of the responsible ethics committee is included with the proposal.	
2.	clinical trials	no
	<If applicable:> A copy of the studies' registration is included with the proposal.	
3.	experiments involving vertebrates.	no
4.	experiments involving recombinant DNA.	no
5.	research involving human embryonic stem cells.	no
	<If applicable:> Legal authorization has been obtained.	
6.	research concerning the Convention on Biological Diversity.	no

3.2 Summary

The central mission of this project will continue to be the preparation of specific conjugated organic molecules (COMs) for various projects within the CRC. For this purpose the present expertise in organic synthesis is used to supply research groups in project areas A and B with the optimal molecules for their experiments without the constraint of commercial availability. In this funding period, COMs that will primarily be targeted include:

Monomeric COMs: Various sterically shielded tetracyanoquinodimethane (TCNQs) acceptors and different triarylamine donors as well as differently substituted naphthalene and perylene diimides (NDIs and PDIs) for projects A8 (Koch), B3 (Blumstengel), and B7 (Neher),

Oligomeric COMs: Conjugated oligomers (and polymers) composed of the same repeat units in a symmetrical fashion, for example oligo(fluorene)s and oligo(thiophene)s for project A11 (Christiansen), and composed of alternating repeat units, for example oligo(*para*-phenylene-*alt*-thiophene)s for project B3 (Blumstengel) as well as oligo(*para*-phenylene)s substituted with terminal (polar) groups for projects B5 (Wörner/Elsässer) and B9 (Stähler),

Phosphonate COMs: Conjugated aromatic systems such as oligo(*para*-phenylene)s, poly(fluorene)s or dipolar phenyl moieties equipped with phosphonic or phosphoric acid substitution for projects A8 (Koch) and B7 (Neher).

Several projects in the CRC will utilize these custom-designed molecules. In the context of their actual experimental requirements, suitable COMs will be suggested to each project and synthesized, in case they

are commercially not available. All compounds to be prepared in Z1 have either been reported in the literature or similar molecules have previously been synthesized. Hence, for their synthesis standard organic chemistry procedures will be followed and the work will mostly be carried out by a laboratory technician under the supervision of the project leader.

3.3 Project progress to date

3.3.1 Report

Within the initial funding period the project has prepared a variety of COMs for projects in the CRC (Fig. 1).

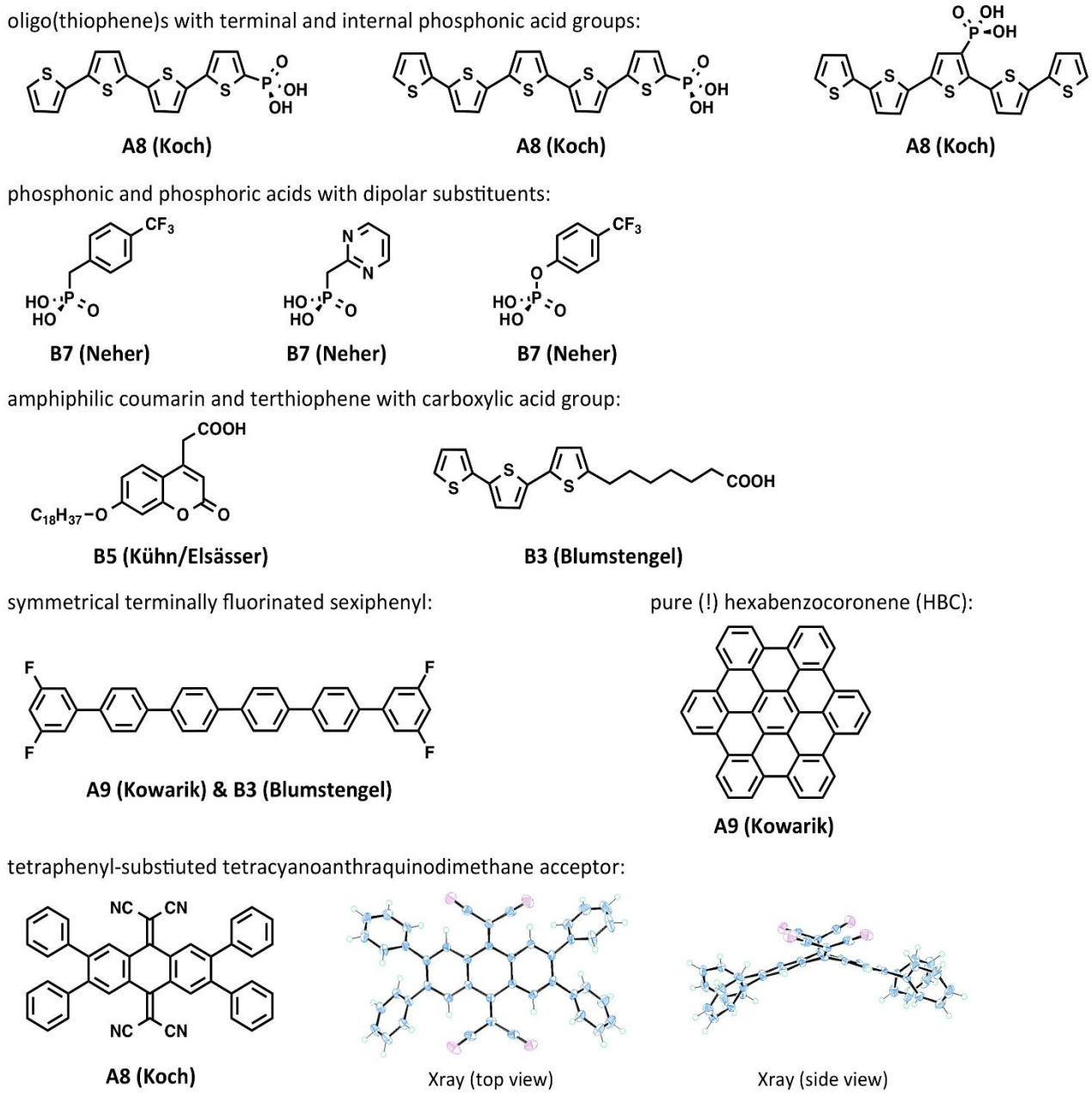

Fig. 1: COMs prepared in the initial funding period for various projects within the CRC. At the bottom not only the molecular formula is shown but also the molecular structure in the crystalline solid as obtained by single crystal Xray diffraction. More details can be found in refs. 1-3.

Work included the preparation of various thiophene oligomers with a differently placed phosphonic acid anchor group for A8 (Koch) as well as new phosphonic and phosphoric acid derivatives for B7 (Neher) [1]. In

addition, a symmetrical sexiphenyl derivative carrying a 3,5-difluorosubstitution pattern on both termini was prepared for A9 (Kowarik) and B3 (Blumstengel) [2]. Amphiphilic coumarin as well as a terthiophene derivatives carrying a carboxylic acid anchoring group for binding to ZnO were prepared for B5 (Kühn/Elsässer) [3] and B3 (Blumstengel). Furthermore, a very pure sample of hexabenzocoronene (HBC) was prepared for A9 (Kowarik) involving the use of our new gradient sublimation apparatus for final purification. Last but not least a tetraphenyl-substituted tetracyanoanthracene-quinodimethane (TCAQ) derivative was prepared for A8 (Koch). In this case, also single crystals were obtained for which the molecular structure could be determined by Xray diffraction (see Fig. 1, bottom right).

3.3.2 Project-related publications

[1] I. Lange, S. Reiter, M. Pätzel, A. Zykov, A. Nefedov, J. Hildebrand, S. Hecht, S. Kowarik, C. Wöll, G. Heimel, and D. Neher**,** "Tuning the work function of polar zinc oxide surfaces by modified phosphonic acid self-assembled monolayers", Adv. Funct. Mater., in press, DOI: 10.1002/adfm.201401493.

[2] M. Sparenberg, A. Zykov, P. Beyer, L. Pithan, C. Weber, Y. Garmshausen, F. Carla, S. Hecht, S. Blumstengel, F. Henneberger, and S. Kowarik: "Controlling the growth mode of para-sexiphenyl (6P) on ZnO by partial fluorination", Phys. Chem. Chem. Phys. accepted, DOI: 10.1039/c4cp04048a.

[3] S. Kuehn, S. Friede, S. Sadofev, S. Blumstengel, F. Henneberger, and T. Elsaesser, "Surface excitons on a ZnO (000-1) thin film", Appl. Phys. Lett. **103**, 191909 (2013).

Mehr wirklich erforderlich? Wenn ja, welcher Zusammenhang?

3.4 Project outline

3.4.1 Objectives

This project constitutes one central service project in the CRC, by which each "customer" project is provided with the molecule best suited to constructing and investigating a desired HIOS, regardless of its commercial availability. For this purpose, a variety of COMs, either known or related to published structures, will be synthesized in Z1. The following COMs will be prepared:

- *Monomeric COMs:* Various sterically shielded tetracyanoquinodimethane (TCNQs) acceptors and different triarylamine donors as well as differently substituted naphthalene and perylene diimides (NDIs and PDIs) for projects A8 (Koch), B3 (Blumstengel), and B7 (Neher) as depicted in Fig. 2:

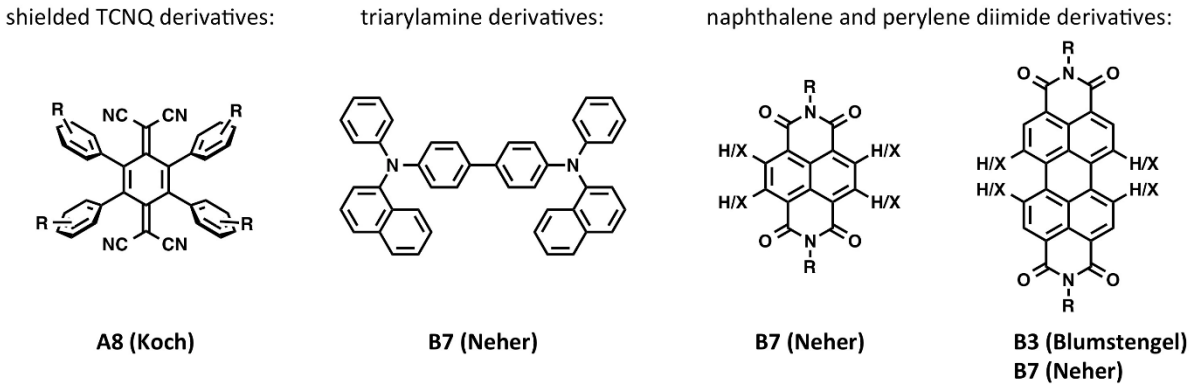

Fig. 2: Monomeric COMs to be prepared for various projects in the CRC.

- *Oligomeric COMs:* Conjugated oligomers (and polymers) composed of the same repeat units in a symmetrical fashion, for example oligo(fluorene)s and oligo(thiophene)s for project A11 (Christiansen), and composed of alternating repeat units, for example oligo(*para*-phenylene-*alt*-thiophene)s for project B3 (Blumstengel) as well as oligo(*para*-phenylene)s substituted with terminal (polar) groups for projects B5 (Wörner/Elsässer) and B9 (Stähler) as depicted in Fig. 3:

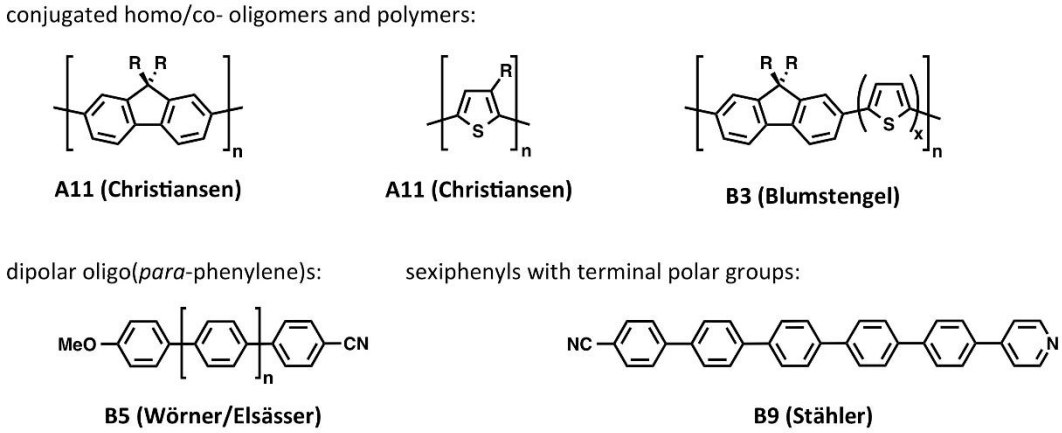

Fig. 3: Oligomeric COMs to be prepared for various projects in the CRC.

- *Phosphonate COMs:* Conjugated aromatic systems such as oligo(*para*-phenylene)s, poly(fluorene)s or dipolar phenyl moieties equipped with phosphonic or phosphoric acid substitution for projects A8 (Koch) and B7 (Neher) as depicted in Fig. 4:

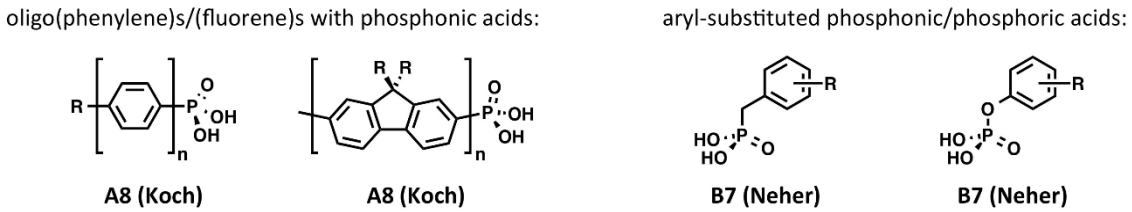

Fig. 4: Phosphonate COMs to be prepared for various projects in the CRC.

For the three COM classes depicted above, the preparation will follow mostly established synthetic routes as described in the given references (see below) or related literature. In some cases, procedures have to be suitably adapted. Specific examples of COMs prepared in Z1 are outlined in the following:

Monomeric COMs (Fig. 2) include tetraarylated TCNQ acceptors (synthesis of tetraphenyl derivative disclosed in patent [4]), dimeric triarylamine-based donors [5], as well as various substituted NDIs [6] and PDIs [7]).

Oligomeric COMs (Fig. 3) comprise various oligomers with chain-length up to approximately six aromatic moieties. These include: differently substituted difluorene and terfluorene (for published syntheses of 9,9'-dimethyl-difluorene and -terfluorene see [8]), oligo(thiophene)s [9], and alternating oligomers of them [10] as well as dipolar oligo(*para*-phenylene)s [11].

Phosphonate COMs (Fig. 4) include oligo(*para*-phenylene)s [11] and oligo(fluorene)s [8] as well as differently substituted aromatics carrying phosphonic acid groups [1] and also phosphoric acid groups [12].

3.4.2 Methods

Work in this project is devoted to the preparation of (mostly) known organic molecules via synthetic routes, which are either already established or are related to published procedures. Methods in this project include:

- organic synthesis (standard laboratory techniques),
- purification methods (column chromatography, recrystallization, gradient sublimation),
- structure elucidation in solution (nuclear magnetic resonance, mass spectrometry, among others],
- other characterization, such as thermal gravimetric analysis, differential scanning calorimetry, UV/vis spectroscopy, cyclic voltammetry, if required.

All of the above facilities and the technical infrastructure mandatory for successful operation of Z1 will be provided as core support from the group of the principle investigator. The amount of work for the diverse custom-syntheses requires the full time of one laboratory technician requested as auxiliary support.

3.4.3 Work plan

Work in this project can be classified according to the three different compounds classes. However, efforts will follow a priority basis dictated by the urgency of the need of the "customer" projects that will be communicated by the projects or, in case of conflict, by decision of the CRC managing board.

Additional References

[4] US Patent 3,408,367 (1968).
[5] Triarylamine
[6] F. Würthner et al., Chem. Eur. J. **8**, 4742 (2002) and C. Thalacker, C. Röger, F. Würthner, J. Org. Chem. **71**, 8098 (2006).
[7] PDIs
[8] B. Kobin et al., J. Mater. Chem. **22**, 4383 (2012).
[9] oligothiophenes
[10] oligo(fluorene-thiophene)s
[11] Y. Garmshausen et al., Org. Lett. **16**, 2838 (2014).
[12] Phosphoric acid groups

3.5 Role within the Collaborative Research Centre

The custom-synthesis project Z1 provides various research groups in project areas A and B with the organic materials needed for their experiments. In particular, there will be direct material service to the following projects:

- A8 (Koch): Monomeric and phosphonate COMs,
- A11 (Christiansen): Oligomeric COMs,
- B3 (Blumstengel): Monomeric and oligomeric COMs,
- B5 (Wörner/Elsässer): Oligomeric COMs,
- B7 (Neher): Monomeric and phosph(on)ate COMs,
- B9 (Stähler): Oligomeric COMs.

3.6 Delineation from other funded projects

No "service" project of the principle investigator is financed by any funding agency.

3.7 Project funds

3.7.1 Previous funding

The project has been funded within the Collaborative Research Centre since 07/2011.

3.7.2 Funds requested

Funding for	2015/2		2016		2017		2018		2019/1	
Staff	Quantity	Sum	Quantity	Sum	Quantity	Sum	Quantity	Sum	Quantity	Sum
Non-research staff, 100%	1	21.900	1	43.800	1	43.800	1	43.800	1	21.900
Total		21.900		43.800		43.800		43.800		21.900
Direct costs	Sum		Sum		Sum		Sum		Sum	
Consumables	3.000		6.000		6.000		6.000		3.000	
Other	-		-		-		-		-	
Total	3.000		6.000		6.000		6.000		3.000	
Major research equipment	Sum		Sum		Sum		Sum		Sum	
€ 10.000 - 50.000	-		-		-		-		-	
> € 50.000	-		-		-		-		-	
Total	-		-		-		-		-	
Total	24.900		49.800		49.800		49.800		24.900	

(All figures in Euro)

3.7.3 Staff

	No.	Name, academic degree, position	Field of research	Department of university or non-university institution	Commitment in hours/week	Category	Funded through:
Available							
Research staff	1	Hecht, Stefan, Prof.	Organic Chemistry	HU Chem	1		HUB
	2	Kobin, Björn, (Dr.)	Organic Chemistry	HU Chem	5		HUB
Non-research staff	3	Voigtländer, Daniela, Admin. Assistant		HU Chem	1		HUB
Requested							
Non-research staff	4	Hildebrandt, Jana, Chem-Technician	Organic Chemistry	HU Chem		100% E8	

Job description of staff (supported through available funds):

1) S. Hecht: Scientific and organisational management of the project.
2) B. Kobin: Primary supervision of laboratory technician, support with analytical methods.
3) D. Voigtländer: Administrative support (ordering/purchasing, accounting, contracting).

Job description of staff (auxiliary support):

4) J. Hildebrandt: The laboratory technician will prepare and purify the desired COMs. For this purpose, she will execute published synthetic procedures or develop adapted protocols. As a multitude of different compounds has to be prepared in multi-step syntheses, the laboratory technician will need to devote her full time for the diverse custom-syntheses. A crude estimation of on average, one complete synthetic step per day is ambitious when including compound purification and structure confirmation by analytical characterization. Hence, realistically a three-step synthesis of one derivative will take about one week providing the CRC with an estimated 4-5 new compounds per month. The staffing of the principle investigator's group includes only one laboratory technician, who has to support the work of more than a

dozen researchers (PhDs and postdocs) and who can therefore not be charged with additional responsibilities by the CRC.

3.7.4 Direct costs for the new funding period

	2015/2	2016	2017	2018	2019/1
Funds available	1.000	2.000	2.000	2.000	1.000
Funds requested	3.000	6.000	6.000	6.000	3.000

(All figures in Euro)

Consumables for 2015/2

Chemicals for syntheses	EUR	1250
Catalysts (Pd-complexes, ligands)	EUR	250
(Deuterated) solvents (NMR, UPLC, GPC)	EUR	500
Silica gel for column chromatography	EUR	500
Syringes, needles, septa	EUR	250
Glassware	EUR	250

Consumables for 2016, 2017, and 2018

Chemicals for syntheses	EUR	2500
Catalysts (Pd-complexes, ligands)	EUR	500
(Deuterated) solvents (NMR, UPLC, GPC)	EUR	1000
Silica gel for column chromatography	EUR	1000
Syringes, needles, septa	EUR	500
Glassware	EUR	500

Consumables for 2019/1

Chemicals for syntheses	EUR	1250
Catalysts (Pd-complexes, ligands)	EUR	250
(Deuterated) solvents (NMR, UPLC, GPC)	EUR	500
Silica gel for column chromatography	EUR	500
Syringes, needles, septa	EUR	250
Glassware	EUR	250

The consumables necessary for the synthetically working laboratory technician amount to 6000 Euro per year. These costs are associated primarily with the purchase of expensive fine chemicals and catalysts, as well as (deuterated) solvents and silica gel for chromatographic separations

3.7.5 Major research equipment requested for the new funding period

No funding for instrumentation is requested.

Z2 (Kowarik/Koch)

In Bearbeitung